



HAL
open science

Improving the cryo-resistance of a lactic acid bacterium by modulating fermentation and stabilization conditions: consequences on the properties of the lipid membrane

Maria de Lourdes Tovilla Coutino

► To cite this version:

Maria de Lourdes Tovilla Coutino. Improving the cryo-resistance of a lactic acid bacterium by modulating fermentation and stabilization conditions: consequences on the properties of the lipid membrane. Food and Nutrition. Université Paris-Saclay, 2022. English. NNT : 2022UPASB057 . tel-03942745

HAL Id: tel-03942745

<https://pastel.hal.science/tel-03942745>

Submitted on 17 Jan 2023

HAL is a multi-disciplinary open access archive for the deposit and dissemination of scientific research documents, whether they are published or not. The documents may come from teaching and research institutions in France or abroad, or from public or private research centers.

L'archive ouverte pluridisciplinaire **HAL**, est destinée au dépôt et à la diffusion de documents scientifiques de niveau recherche, publiés ou non, émanant des établissements d'enseignement et de recherche français ou étrangers, des laboratoires publics ou privés.

Improving the cryo-resistance of a lactic acid bacterium by modulating fermentation and stabilization conditions: consequences on the properties of the lipid membrane

Amélioration de la cryo-résistance d'une bactérie lactique en modulant les conditions de fermentation et de stabilisation : conséquences sur les propriétés de la membrane lipidique

Thèse de doctorat de l'université Paris-Saclay

Ecole doctorale n°581,
Agriculture, Alimentation, Biologie, Environnement, Santé (ABIES)
Spécialité de doctorat : Sciences des aliments et des bioproduits
Graduate School : Biosphera. Référent : AgroParisTech

Thèse préparée dans l'**UMR SayFood** (Université Paris-Saclay, INRAE, AgroParisTech) et l'**Institut Jean-Pierre Bourgin (IJPB)** (Université Paris-Saclay, INRAE, AgroParisTech), sous la direction de **Yann GOHON**, Maître de Conférences (HDR) et la co-direction de **Marie-Hélène ROPERS**, Chargée de Recherche (HDR)

Thèse soutenue à Paris-Saclay, le 22 septembre 2022, par

Maria de Lourdes TOVILLA COUTINO

Composition du Jury

Timothy VOGEL Professeur, Université Claude Bernard Lyon 1	Président
Claire BOURLIEU-LACANAL Chargée de Recherche, INRAE (centre Occitanie-Montpellier)	Rapporteur & Examinatrice
Jean-Marie PERRIER-CORNET Professeur, Institut Agro - Dijon	Rapporteur & Examineur
Eric DUBREUCQ Professeur, Institut Agro - Montpellier	Examineur
Marina CRETENET Maîtresse de Conférences, Université de Caen Normandie	Examinatrice
Yves LE-LOIR Directeur de recherche, INRAE (Bretagne-Normandie)	Examineur
Yann GOHON Maître de Conférences, AgroParisTech (Université Paris-Saclay)	Directeur de thèse
Marie-Hélène ROPERS Chargée de Recherche, INRAE (centre Pays de la Loire)	Co-Directrice de thèse

Titre : Amélioration de la cryo-résistance d'une bactérie lactique en modulant les conditions de fermentation et de stabilisation : conséquences sur les propriétés de la membrane lipidique

Mots clés : Bactéries lactiques, Congélation, Lyophilisation, Lipides membranaires

Résumé : Les Bactéries Lactiques (BL) sont largement utilisées pour produire une diversité d'aliments fermentés et fonctionnels. À l'échelle industrielle, les BL sont produites et stabilisées par congélation et lyophilisation. Selon les souches, ces procédés de cryopréservation conduisent à la dégradation plus ou moins importante de leurs propriétés fonctionnelles. Ainsi, certaines souches de BL, comme *L. bulgaricus* CFL1, restent inexploitées à l'échelle industrielle. Différentes stratégies existent pour limiter cette dégradation : la première consiste à modifier les conditions de fermentation mais au détriment de la quantité produite, la deuxième stratégie consiste à ajouter une solution de sucre.

Dans ce contexte, *L. bulgaricus* CFL1, une souche sensible à la cryoconservation, a été utilisée comme modèle de bactérie lactique. Ce travail de thèse visait à identifier les conditions d'amélioration de la résistance de *L. bulgaricus* CFL1, en mettant en œuvre les deux stratégies et en analysant leurs effets sur la membrane cellulaire, reconnue comme le site primaire de dommages. La première stratégie a consisté à optimiser les conditions de fermentation afin d'obtenir un compromis entre une bonne production de biomasse et une résistance élevée à la congélation et à la lyophilisation, à l'aide de l'optimisation multi objectif. Il en ressort qu'il n'y a pas de conditions de fermentation uniques pour satisfaire à la fois à l'exigence de biomasse et propriétés fonctionnelles mais que celles-ci doivent être adaptées au procédé de stabilisation choisie.

Chacune de ces conditions de fermentation a eu un impact sur les propriétés de la membrane lipidique, qui ont alors été reliées aux propriétés de cryopréservation de la bactérie. Pour la résistance à la congélation, ce sont les conditions de fermentation qui génèrent le plus d'acides gras insaturés et une membrane plus fluide qui sont bénéfiques. Pour la lyophilisation, les conditions favorisant la production d'acides gras cycliques contribuent significativement le maintien des propriétés fonctionnelles de *L. bulgaricus* CFL1.

La deuxième stratégie a impliqué la sélection d'une solution protectrice de sucre, parmi des molécules de glucose de différents degrés de polymérisation. Les résultats ont montré que le choix optimal du sucre dépendait des procédés de stabilisation.

Ce projet de thèse ouvre donc de nouvelles approches pour la production de BL: 1) en dehors des conditions optimales de production d'une bactérie, existent des conditions un peu moins productrices mais très bénéfiques pour le maintien de leurs propriétés biologiques. Ainsi, le choix du procédé de stabilisation est à réaliser en amont pour cibler les bonnes conditions de fermentation et la solution protectrice de sucre la mieux adaptée. 2) Favoriser la formation d'acides gras insaturés ou cycliques portés par les lipides membranaires contribuera à préserver la bactérie des dommages liés à la congélation et à la lyophilisation.

Title: Improving the cryo-resistance of a lactic acid bacterium by modulating fermentation and stabilization conditions: consequences on the properties of the lipid membrane

Keywords: Lactic acid bacteria, Freezing, Freeze-drying, Membrane lipids

Abstract: Lactic acid bacteria (LAB) are widely used to produce a variety of fermented and functional foods. On an industrial scale, LAB are produced and stabilized by freezing and freeze-drying. Depending on the strain, these cryopreservation processes lead to more or less significant degradation of their functional properties. Consequently, some LAB strains, such as *L. bulgaricus* CFL1, remain unexploited on an industrial scale. Different strategies exist to limit this degradation: the first consists of modifying the fermentation conditions at the expense of the quantity produced, and the second strategy consists of adding a sugar solution.

In this context, *L. bulgaricus* CFL1, a strain sensitive to cryopreservation, was used as a model lactic acid bacterium. This thesis aimed at identifying the fermentation condition that improved the resistance of *L. bulgaricus* CFL1 by implementing two strategies and analyzing their effects on the cell membrane, identified as the primary site of damage. The first strategy was to optimize the fermentation conditions to achieve a compromise between fair biomass production and high resistance to freezing and freeze-drying, using multi-objective optimization. No unique fermentation satisfied both the biomass and functional properties requirements. Fermentation conditions had to be adapted to the chosen stabilization process.

Each of these fermentation conditions impacted the lipid membrane's properties, which were then related to the cryopreservation properties of the bacteria. Here, the membrane characteristics depended on the stabilization process. For enhanced freezing resistance, fermentation conditions that generated more unsaturated fatty acids and a more fluid membrane were beneficial. For freeze-drying, conditions favoring cyclic fatty acid production contributed significantly to maintaining the functional properties of *L. bulgaricus* CFL1.

The second strategy involved the selection of a protective sugar solution among glucose molecules of different degrees of polymerization. The results showed that the optimal choice of sugar depended on the stabilization processes.

Therefore, this thesis project opens up new approaches for producing LAB: 1) outside the optimal production conditions of a bacterium, some conditions are slightly less productive but very beneficial for maintaining their functional properties. Thus, the choice of the stabilization process should be made upstream to target the appropriate fermentation conditions and protective sugar solution. 2) The formation of unsaturated or cyclic fatty acids in the membrane lipids will help preserve the bacterium from damage occurring during freezing and freeze-drying.

"We must keep moving. If you can't fly, run; if you can't run, walk; if you can't walk, crawl; but by all means keep moving"

(Martin Luther King Jr., 1960)

ACKNOWLEDGEMENTS

I want to thank Claire Bourlieu-Lacanal, a scientist at INRAE in Montpellier, and Jean-Marie Perrier-Cornet, professor at the Institute Agro Dijon, for accepting to be the reviewers of this thesis.

I would also like to thank Eric Dubreucq, professor at the Institute Agro Montpellier, Marina Cretenet, assistant professor at the University of Caen, Yves Le Loir, director of research at INRAE in Rennes, and Tim Vogel, professor at the University Claude Bernard Lyon for having accepted to be part of my thesis jury.

I would like to thank Catherine Bonazzi, director of the Food and Bioproducts Engineering Research Unit (UMR SayFood), and Christine Duvaux-Ponter, deputy director of the ED ABIES, for their support during the last months of my thesis. Thanks to you, I finished my thesis under the best conditions.

Many thanks to my two thesis directors: Marie-Hélène Ropers and Yann Gohon. I can say that I had two excellent people as supervisors. Thank you, Marie-Hélène, for your great human qualities and exemplary work ethic. I learned a lot from your enthusiasm, positive remarks, and ability to suggest new ways of working. Thanks, Yann, for your commitment as thesis director and for having transmitted to me some of your excellent knowledge in lipids biochemistry. Thank you for guiding me throughout my thesis.

I also had the opportunity to mentor one great student. Thanks to Justine Megalli for making such an essential contribution to this project.

I would especially like to thank the lab staff who helped me with my experiments and analysis. Many thanks to Jérôme Delettre (for my fermentation experiments, life bits of advice, and your splendid friendship), Anne-Claire Peron (for my experiments of lipids extractions, fractionation, and the GC-MS, and your beautiful friendship), Pascale Lieben (for my experiments in the FTIR), Brigitte Pollet (for my first experiments in the LC-MS/MS), Marie-Noëlle Leclercq Perlat (for my experiments of HPLC and your company during lunch), Sarrah Ghorbal (for my experiments of membrane fluidity), Cécile Willard (for you good mood and funny jokes). All of them shared their precious time and knowledge with me. I had this wonderful experience of working with all of them. Thanks also to Jérôme Bussiere and Frédéric Lecornue from the atelier for repairing and manufacturing the devices that I needed and helped me hold things that were bigger than my size.

Thanks to the SayFood agents with whom I was lucky enough to share the day-to-day: Catherine Béal (for your encouragement, kindness, and impressive humanity), Thomas Cattenoz (for your friendship, wisdom, and your support that are a treasure to me), Bruno Perret (for your friendship and our exciting discussions), and David Forest (for your big smile and good mood).

Many thanks to the SayFood agents with whom I shared charming moments with all of them: Claire Saulou, Violaine Athès, Marwen Moussa, Cristian Trélea, Caroline Pénicaud, Lucy Espinosa, Sophie Landaud, Sandra Helinck, Françoise Irlinger, Anne-So' Sarthou, Pascal

Bonnarme, Anne Saint-Eve, Vincent Mathieu, Christophe Monnet, Alice Danel. You are such great people.

Thanks, Laurence Fruchart and Thierry Feugnet, for always helping me with the administrative pieces.

Thanks to the DYSCOL team at the IJPB, you were my rock for the last months of my thesis. Your sympathy made the end of my thesis very peaceful: Thierry Chardot (for your kindness and support), Christelle, Sihem, Isabelle, Carine, Anne-Marie, Pierre, Nathan, and Frank.

Many thanks to the Ph.D. students and some of them already doctors with whom I was lucky to share good moments. Thank you to my dear friends latinos: Pedrito Arana and linda Karencita, for your tremendous help and sweetness. I am a blessed girl to have you as my friends. Thanks to the most beautiful girls outside and inside that I have ever met: Adeline Cortesi, Cynthia El Youseff, and Valentine Chartrel. You are just fantastic.

Special thanks to my amazing friends that were with me in the most challenging times. We could do it together, and we were there for each other: Amélie Girardeau and Juan Buceta. You are in my heart.

Thanks for your honesty and friendship. I do not have enough words to tell you how much I admire your strength and intelligence: Florence de Fouchécour and Julie Meneghel.

Thanks, Yohan, Mathieu, Audrey, Bastien, Carole, Rohit, and sweet Phuong (I will never forget your delicious food) for the excellent ambiance in the laboratory, the after-works, and your sympathy.

Now I would like to thank all the people who contributed to making my daily life outside the lab more pleasant and unforgettable: Catica Quesada Salas, Anne-Lise Boixel, Marie-Angèle Briand, Dieguiño, Aline Rault, Julie Bailly, petite Inès, and petit Théo.

*

I thank my family, Mamita Lulu, Muñequita Blanquita†, Manich Bris, and Hermano Cris. You have always been there for me and believed in me.

Finally, thanks to my husband Azariel for your unfailing daily support, advice, and curiosity about my work and life. I could not do it without you. Better times are ahead for us.

PUBLICATIONS AND COMMUNICATIONS

Articles in peer-reviewed journals

Tovilla-Coutiño, M.L., Passot, S., Trelea, I.C., Ropers, M.H., Fonseca, F., Gohon, Y (2022) Multi-objective optimization of frozen and freeze-dried *Lactobacillus delbrueckii* subsp. *bulgaricus* CFL1 production via the modification of fermentation conditions. Article submitted in *Journal of Applied Microbiology*.

Tovilla-Coutiño, M.L., Gohon, Y., Peron, A.C., Fonseca, F., Passot, S., Ropers, M.H. (2022) Deep analysis of membrane lipids of a lactic acid bacterium during mild-stressing growth conditions in relation with its resistance to freezing and freeze-drying. Article to be submitted.

Oral communications

Tovilla-Coutiño, M.L., Delettre, J., Passot, S., Gohon, Y., Ropers, M.H., Fonseca, F. Lipid membrane modification and survival of *L. bulgaricus* CFL1 in stabilization process is a response of an adaptation to environmental stress during fermentation. Microbial Stress (virtual) conference organized by the European Federation of Biotechnology. (16/11/2020-18/11/2020).

Gohon, Y., **Tovilla-Coutiño, M.L.**, Megalli, J., Fonseca, F., Passot, S., Ropers, M.H. Deciphering oligosaccharides – *L. bulgaricus* CFL1 membrane interactions upon freezing or drying, a preliminary study by FTIR. 3rd PREMIUM meeting, Barcelona (virtual) (19/04/2022-20/04/2022).

Poster presentations

Tovilla-Coutiño, M.L., Gohon, Y., Ropers, M.H., Ghorbal, S., Passot, S., Fonseca, F. Bacterial cell adaptation to environmental stress during fermentation improves cryo- and drying resistance: a focus on membrane properties. ABIES doctoral school. Winner of the best poster award. (06/05/2021-07/06/2021).

Tovilla-Coutiño, M.L., Passot, S., Peron, A.C., Ghorbal, S., Ropers, M.H., Gohon, Y., Fonseca, F. *L. bulgaricus* CFL1 lipid membrane's modulation and characterization: first step for developing lipid membrane models. Vibrational spectroscopy and biomimetic membranes for understanding protective mechanisms of oligosaccharides conference. ICFO, Barcelona, Spain (virtual), workshop PREMIUM. (05/10/2021).

Scientific vulgarization

Presenter at the AgroParisTech stand at the 2020 *Salon de l'Agriculture* in Paris.

ABBREVIATIONS AND SYMBOLS

ATCC	American Type Culture Collection
a_w	Water activity
C12:0	Dodecanoic acid (lauric acid)
C14:0	Tetradecanoic acid (myristic acid)
C15:0	Pentadecanoic acid
C16:0	Hexadecanoic acid (palmitic acid)
C16:1 trans 9	trans-hexadecenoic acid
C16:1 cis 9	cis-hexadecenoic acid (palmitoleic acid)
C17:0	Heptadecenoic acid
C18:0	Octadecanoic acid (stearic acid)
C18:1 cis 11	cis-11-octadecenoic acid
C18:1 cis 9	cis-9-octadecenoic acid (oleic acid)
C18:1 trans 9	trans-9-octadecenoic acid (elaidic acid)
C18:2 cis,cis-9,12	cis,cis-9,12-octadecadienoic acid (linoleic acid)
C19:0 cyc	cis-9,10-methyleneoctadecanoic acid (Dihydrosterculic acid)
C22:0	Docosanoic acid (Behenic acid)
CFA	Cyclic Fatty Acid
cFDA	Carboxyfluorescein diacetate
CFU	Colony Forming Unit
CL	Cardiolipin
CPA	Cryoprotective Agent
CSP	Cold-Shock Protein
DGDG	Diglycosyl diacylglycerol
DNA	Desoxyribonucleic Acid
DP	Degree of polymerization
DPH	1,6-diphényl-1,3,5-hexatriène
dt_{spe}	Loss of specific acidifying activity
EPS	Exopolysaccharide
F	Freezing
FA	Fatty Acid
FD	Freeze-drying
FTIR	Fourier Transform Infrared Spectroscopy
GC-MS	Gas Chromatography coupled to Mass Spectrometry
HPLC	High Pressure Liquid Chromatography
HPTLC	High-Performance Thin-Layer Chromatography
HSP	Heat-Shock Protein
INRAE	National Institute for Agricultural and Environmental Research

IR	Infrared
LAB	Lactic Acid Bacteria
LC-MS/MS	Liquid Chromatography with tandem mass spectrometry
M	molar ($\text{mol}\cdot\text{L}^{-1}$)
MCT	Mercury Cadmium Telluride
MGDG	Monoglycosyl diacylglycerol
mOsm	miliOsmole
MRS	Man, Rogosa and Sharpe broth for <i>Lactobacilli</i> growth medium
OD₆₀₀	Optical density at 600nm
OD₈₈₀	Optical density at 880nm
PE	Phosphatidylethanolamine
PG	Phosphatidylglycerol
PS	Phosphatidylserine
r	Fluorescence anisotropy
RNA	Ribonucleic Acid
S	Storage
SFA	Saturated Fatty Acid
subsp.	Subspecies
T	Temperature ($^{\circ}\text{C}$)
T_g	Glass transition temperature ($^{\circ}\text{C}$)
T_g'	T _g for maximally cryo-concentrated solutions ($^{\circ}\text{C}$)
T_g'_{extracellular}	Extracellular T _g ' ($^{\circ}\text{C}$)
T_g'_{intracellular}	Intracellular T _g ' ($^{\circ}\text{C}$)
T_m	Lipid membrane phase transition temperature during heating ($^{\circ}\text{C}$)
T_n	Water nucleation temperature ($^{\circ}\text{C}$)
t_{ΔpH0.7}	Acidifying activity
T_s	Lipid membrane phase transition temperature during cooling ($^{\circ}\text{C}$)
t_{spe}	Specific acidifying activity
UFA	Unsaturated Fatty Acid
δ	Infrared bending vibration modes
ν	Infrared stretching vibration modes

GENERAL TABLE OF CONTENTS

Aknowledgements	i
Publications and Communications	iii
Abbreviations and Symbols	v
General Table of Contents	vii
List of Figures	ix
List of Supplementary Figures	xi
List of Tables	xiii
List of Supplementary Tables	xiv
INTRODUCTION	1
1. LITERATURE REVIEW	5
1.1. Lactic acid bacteria composition and industrial applications	8
1.2. Production of lactic acid bacteria: stabilization and storage, critical steps that induce cell damages	24
1.3. Strategies to improve lactic acid bacteria resistance to the critical steps of their production: stabilization processes and storage	51
1.4. Conclusions and outlooks	76
2. OVERALL EXPERIMENTAL APPROACH	77
2.1. Choice of the lactic acid bacterium strain	78
2.2. Experimental strategies	78
3. MATERIALS AND METHODS	83
3.1. Production of concentrated <i>L. bulgaricus</i> CFL1	85
3.2. Stabilization processes and freeze-dried storage	90
3.3. Assessment of the functional properties of <i>L. bulgaricus</i> CFL1 at different production steps	92
3.4. Water content and temperature glass transition of the freeze-dried bacteria	95
3.5. Lipids composition of the <i>L. bulgaricus</i> CFL1 membrane	96
3.6. Biophysical properties of the <i>L. bulgaricus</i> CFL1 membrane: lipid phase transition temperature and membrane fluidity	105
3.7. Sugars effect on the resistance and membrane of <i>L. bulgaricus</i> CFL1	109
3.8. Statistical analysis	113
4. MULTI-OBJECTIVE OPTIMIZATION OF FROZEN AND FREEZE-DRIED <i>L. bulgaricus</i> CFL1	117
4.1. Preamble	119
4.2. Abstract	120
4.3. Introduction	121
4.4. Materials and methods	123
4.5. Results	131
4.6. Discussion	142
4.7. Supplementary Information	145
4.8. Prospects for this study	158
5. DEEP ANALYSIS OF MEMBRANE LIPIDS AND THEIR RELATIONSHIPS WITH <i>L. bulgaricus</i> CFL1 RESISTANCE TO FREEZING AND FREEZE-DRYING	161
5.1. Preamble	163
5.2. Abstract	164
5.3. Introduction	165
5.4. Materials and methods	167
5.5. Results	179
5.6. Discussion	200

5.7. Conclusion	203
5.8. Supplementary information	205
5.9. Prospects for this study	223
6. INFLUENCE OF SUGARS ON RESISTANCE AND THE MEMBRANE OF <i>L. bulgaricus</i> CFL1	225
6.1. Preamble	227
6.2. Introduction	227
6.3. Experimental approach	229
6.4. Results and discussion	235
6.5. Conclusion	252
6.6. Prospects for this study	252
CONCLUSIONS AND PROSPECTS	255
Conclusions	255
Prospects	260
BIBLIOGRAPHY	263
A. ANNEXES	297
A1. The updated list of the new genera in the family <i>Lactobacillaceae</i>	298
A2. Overview of the two LAB examples shown in Table 1.1 from family to species	299
A3. Media composition for the growth of lactic acid bacteria	300
A4. Glass transition temperature (T _g) of different freeze-dried protective suspensions	301
A5. Glass transition temperature of the maximally freeze-concentrated phase (T _g ') and collapse temperature (T _{coll}) of different sugar solutions used to freeze-dry lactic acid bacteria*	302
A6. Induced proteins description after applying the different stresses shown in Table 1.5	303

LIST OF FIGURES

Chapter 1 Literature review

Figure 1.1 Schematic representation of a lactic acid bacterium structure and composition.....	9
Figure 1.2 Schematic illustration of a Gram-positive cell wall and cytoplasmic membrane.....	11
Figure 1.3 Main membrane lipids in lactic acid bacteria.....	12
Figure 1.4 Schematic representation of different fatty acyl chain conformations found in lipids of lactic acid bacteria.....	15
Figure 1.5 Membrane fatty acid composition of three different LAB genera.....	16
Figure 1.6 Multi-step production of concentrated lactic acid bacteria.....	25
Figure 1.7 Schematic representation of a bacterial growth curve, indicating the different growth phases in bacteria.....	28
Figure 1.8 The main components of a freeze-dryer.....	31
Figure 1.9 pH decreases as a function of the time of <i>Lactobacillus delbrueckii</i> subsp. <i>bulgaricus</i> CFL1 before (light-blue curve) and after freezing (plum curve).....	33
Figure 1.10 Sucrose solution temperature profile and principal phenomena during freezing at slow cooling rate ($\leq 10^{\circ}\text{C}\cdot\text{min}^{-1}$).....	35
Figure 1.11 State diagram of a sucrose solution frozen at two different cooling rates.....	37
Figure 1.12 (A) The water phase diagram and (B) different state changes on a water phase diagram.....	38
Figure 1.13 Schematic representation of a frozen sample sublimation, placed on a shelf.....	39
Figure 1.14 Relationships among water activity (a_w) and water content (m, %)......	41
Figure 1.15 Schematic representation of the behavior of a lactic acid bacterium and its membrane as temperature decreases from growth conditions.....	43
Figure 1.16 Schematic representation of a membrane lipid transition from a disordered liquid-crystalline phase (L_{α}) to a rigid gel phase (L_{β}).....	44
Figure 1.17 Schematic illustration of membrane lateral phase separation upon cooling, causing protein aggregation.....	45
Figure 1.18 Schematic illustration of proposed mechanisms of membrane sugar-interactions.....	70
Figure 1.19 Overview of the vibration modes causing IR absorption, illustrated with water molecules.....	72
Figure 1.20 Absorption spectra of air-dried <i>Lactobacillus delbrueckii</i> subsp. <i>bulgaricus</i> CFL1.....	72

Chapter 2 Overall experimental approach

Figure 2.1 Schematic representation of the overall experimental approach implemented in the present thesis.....	79
--	----

Chapter 3 Materials and methods

Figure 3.1 Follow up of the growth of <i>L. bulgaricus</i> CFL1 from stock cultures for (A) a first preculture and (B) a second preculture.....	85
Figure 3.2 Curves that illustrate the addition in mL (gray line) and the consumption rate in $\text{g}\cdot\text{L}^{-1}\cdot\text{h}^{-1}$ (plum line) of a NaOH solution at 4.25 M.....	87
Figure 3.3 Schematic representation of harvest time normalization according to the maximum acidification rate and different growth phases of <i>L. bulgaricus</i> CFL1.....	88
Figure 3.4 Correlation between the 880 and 600 nm data.....	88
Figure 3.5 Schemes of the operating conditions set during the primary drying and the secondary drying stages of freeze-drying: shelf temperature and chamber pressure.....	91

Figure 3.6 Cinac® system.....	93
Figure 3.7 Schematic representation of concentrated <i>L. bulgaricus</i> CFL1 production and loss of specific acidifying activity during freezing, freeze-drying, and freeze-dried storage.....	94
Figure 3.8 Lipid extraction protocol to determine fatty acids composition for each harvest time.	97
Figure 3.9 Chromatogram example of <i>L. bulgaricus</i> CFL1 fatty acids profile.....	99
Figure 3.10 (A) Peak positions of $\nu_{sym}CH_2$ vibration bands arising from <i>L. bulgaricus</i> CFL1, plotted against their acquisition temperature.	107
Figure 3.11 Heatmap example of a specific lipid class.....	116
Chapter 4 Multi-objective optimization of frozen and freeze-dried <i>L. bulgaricus</i> CFL1	
Figure 4.1 Diagram of the experimental approach applied to assess the effect of fermentation parameters.....	124
Figure 4.2 Response surface representations of the effect of fermentation harvest time and temperature on the biomass productivity (P , in $g \cdot L^{-1} \cdot h^{-1}$) of <i>L. bulgaricus</i> CFL1 produced at (A) pH 5.8 and (B) pH 4.8.	133
Figure 4.3 Response surface representations of the effect of fermentation harvest time and temperature on the loss of specific acidifying activity.....	137
Figure 4.4 Pareto multi-objective optimization by maximizing the biomass productivity (high values of productivity, axis x) and minimizing the t_{spe} values were obtained after freezing or freeze-drying (axis y, corresponding to maximizing the t_{spe}) of <i>L. bulgaricus</i> CFL1.	140
Figure 4.5 Loss of specific acidifying activity during (A) freezing and (B) freeze-drying of <i>L. bulgaricus</i> CFL1 for fermentations carried out at uncontrolled pH.	159
Chapter 5 Deep analysis of membrane lipids and their relationships with <i>L. bulgaricus</i> CFL1 resistance to freezing and freeze-drying	
Figure 5.1 Diagram of the experimental approach used in this study and the main investigated lipid properties and composition of <i>L. bulgaricus</i> CFL1 membrane.....	167
Figure 5.2 The distribution in relative percentage of Saturated Fatty Acids (SFA), Unsaturated Fatty Acid (UFA) and Cyclic Fatty Acid, cycC19:0 (CFA) of the total lipids extracted from <i>L. bulgaricus</i> CFL1.	179
Figure 5.3 Ratios of the different groups of fatty acids in <i>L. bulgaricus</i> CFL1 cells: (A) UFA/SFA, (B) CFA/UFA, (C) CFA/SFA.....	181
Figure 5.4 Fatty acids content in different fractions of the total lipids extracted from <i>L. bulgaricus</i> CFL1 harvested at the stationary growth phase (t_{h3}) for the four fermentation conditions studied.....	183
Figure 5.5 The distribution in relative percentage of Saturated Fatty Acids (SFA), Unsaturated Fatty Acid (UFA) and Cyclic Fatty Acid, cycC19:0 (CFA) of the fractions obtained after fractionation of the total lipid extract of <i>L. bulgaricus</i> CFL1.	184
Figure 5.6 Heatmaps of monoglycosyldiacylglycerols (MGDG) found in f_1 for the four fermentation conditions studied. A, [42°C, pH 5.8]; B, [42°C, pH 4.8]; C, [37°C, pH 5.8]; and D, [37°C, pH 4.8].	188
Figure 5.7 Heatmaps of monoglycosyldiacylglycerols (MGDG) found in f_2 for the four fermentation conditions studied. A, [42°C, pH 5.8]; B, [42°C, pH 4.8]; C, [37°C, pH 5.8]; and D, [37°C, pH 4.8].	189
Figure 5.8 Heatmaps of diglycosyldiacylglycerols (DGDG) found in f_3 for the four fermentation conditions studied. A, [42°C, pH 5.8]; B, [42°C, pH 4.8]; C, [37°C, pH 5.8]; and D, [37°C, pH 4.8].	191
Figure 5.9 Heatmaps of phosphatidylglycerols (PG) found in f_4 for the four fermentation conditions studied. A, [42°C, pH 5.8]; B, [42°C, pH 4.8]; C, [37°C, pH 5.8]; and D, [37°C, pH 4.8].	193
Figure 5.10 Biophysical membrane properties of <i>L. bulgaricus</i> CFL1.....	195
Figure 5.11 Loss of the specific acidifying activity of <i>L. bulgaricus</i> CFL1 after (A) freezing ($dt_{spe} F$) and (B) freeze-drying ($dt_{spe} FD$) for the four studied fermentation conditions at different harvest times.	196

Figure 5.12 Principal component analyses of fatty acid content (SFA, UFA, CFA), lipid transition temperatures, membrane fluidity, and resistance to freezing and freeze-drying of *L. bulgaricus* CFL1 cells. 198

Chapter 6 Influence of sugars on resistance and the membrane of *L. bulgaricus* CFL1

Figure 6.1 Diagram of the experimental approach used in this study and the main investigated parameters..... 229

Figure 6.2 Resistance of *L. bulgaricus* CFL1 cells to freezing using different sugars. (A) The loss of acidifying activity ($dt_{\Delta pH 0.7}$ F), (B) survival, and (C) the loss of specific acidifying activity (dt_{spe} F). 236

Figure 6.3 Resistance of *L. bulgaricus* CFL1 cells to freeze-drying using different sugars. (A) The loss of acidifying activity ($dt_{\Delta pH 0.7}$ FD), (B) survival, and (C) the loss of specific acidifying activity (dt_{spe} FD). .. 239

Figure 6.4 Peak positions of the symmetric CH₂ stretching vibration band ($v_{sym}CH_2$) arising from hydrated *L. bulgaricus* CFL1 upon cooling (blue curves) and heating (red curves). 242

Figure 6.5 The first derivatives of the symmetric CH₂ stretching vibration band ($v_{sym}CH_2$) of *L. bulgaricus* CFL1 upon cooling (blue curves) and heating (red curves). 243

Figure 6.6 Schematical drawings of the various bilayer phases. 245

Figure 6.7 Peak positions of the symmetric CH₂ stretching vibration band ($v_{sym}CH_2$) arising from air-dried *L. bulgaricus* CFL1 upon heating (mustard curves). 246

Figure 6.8 The first derivatives of the symmetric CH₂ stretching vibration band ($v_{sym}CH_2$) arising from air-dried *L. bulgaricus* CFL1 upon heating (mustard curves). 247

Figure 6.9 Peak position of the asymmetric PO₂ stretching vibration band ($v_{asym}PO_2$) the asymmetric PO₂ stretching vibration band ($v_{asym}PO_2$) arising from hydrated *L. bulgaricus* CFL1 upon cooling (blue curves) and heating (red curves). 250

Figure 6.10 Peak position of the asymmetric PO₂ stretching vibration band ($v_{asym}PO_2$) arising from air-dried *L. bulgaricus* CFL1 upon heating (mustard curves). 251

LIST OF SUPPLEMENTARY FIGURES

Figure S4.1 (A) Growth curves based on optical density (OD) data at 880 nm; (B) Rate of NaOH consumption during fermentation ($dmNaOH/dt$, $g \cdot L^{-1} \cdot h^{-1}$); (C) Correlation between the 880 and 600 nm OD data: $OD_{600nm} = 1.63 \times (OD_{880nm})^2 + 1.45 \times (OD_{880nm})$ 153

Figure S4.2 Biomass productivity (P, in $g \cdot L^{-1} \cdot h^{-1}$) values predicted by the multiple linear regression model vs. the experimental biomass productivity values. 154

Figure S4.3 Initial specific acidifying activity (t_{spe} I, in $[\min (\log (CFU \cdot mL^{-1}))^{-1}]$) of *L. bulgaricus* CFL1 for the four combinations of fermentation conditions studied: [42°C, pH 5.8]; [42°C, pH 4.8]; [37°C, pH 5.8]; [37°C, pH 4.8] at three different harvest times. 154

Figure S4.4 Initial (A) acidifying activity ($t_{\Delta pH 0.7}$, in min) and (B) culturability ($CFU \cdot mL^{-1}$) of *L. bulgaricus* CFL1 for the four combinations of fermentation conditions studied: [42°C, pH 5.8]; [42°C, pH 4.8]; [37°C, pH 5.8]; [37°C, pH 4.8] at three different harvest times. 155

Figure S4.5 Loss of specific acidifying activity (dt_{spe} , in $[\min (\log (CFU \cdot mL^{-1}))^{-1}]$) values predicted by the multiple linear regression models vs. the experimental dt_{spe} values, for (A) freezing and (B) freeze-drying. 156

Figure S4.6 Loss of specific acidifying activity of *L. bulgaricus* CFL1 during freeze-dried storage for 15 days at 25°C (dt_{spe} S, in $[\min (\log (CFU \cdot mL^{-1}))^{-1}]$) for the four combinations of fermentation conditions studied: [42°C, pH 5.8]; [42°C, pH 4.8]; [37°C, pH 5.8]; [37°C, pH 4.8] at three different harvest times. Superscript letters represent significant differences between samples at a 95% confidence level. 157

Figure S5.1 Growth curves of *L. bulgaricus* CFL1 at four different fermentation conditions. [42°C, pH 5.8] is represented by a blue curve, [42°C, pH 4.8] by a light blue curve, [37°C, pH 5.8] by a brown curve, and [37°C, pH 4.8] by an orange curve. 211

Figure S5.2 Example of wavenumbers of the symmetric CH ₂ stretching peak ($v_{sym}CH_2$) versus temperature upon cooling and heating <i>L. bulgaricus</i> CFL1 cells grown at 42°C, pH5.8 and harvested at the stationary growth phase (t_{h3}).....	211
Figure S5.3 Lipid classes distribution of <i>L. bulgaricus</i> CFL1 harvested at the stationary growth phase (t_{h3}) for the four fermentation conditions studied: [42°C, pH 5.8], [42°C, pH 4.8], [37°C, pH 5.8], and [37°C, pH 4.8].	212
Figure S5.4 Lipid classes distribution of <i>L. bulgaricus</i> CFL1 harvested at the stationary growth phase (t_{h3}) for the four fermentation conditions studied: [42°C, pH 5.8], [42°C, pH 4.8], [37°C, pH 5.8], and [37°C, pH 4.8].	213
Figure S5.5 Lipid classes distribution of <i>L. bulgaricus</i> CFL1 harvested at the stationary growth phase (t_{h3}) for the four fermentation conditions studied: (a) [42°C, pH 5.8], (b) [42°C, pH 4.8], (c) [37°C, pH 5.8], and (d) [37°C, pH 4.8].	214
Figure S5.6 Triacylglycerols (TAG) of <i>L. bulgaricus</i> CFL1 membrane harvested at the stationary growth phase (t_{h3}) for the four fermentation conditions studied: A, [42°C, pH 5.8]; B, [42°C, pH 4.8]; C, [37°C, pH 5.8]; and D, [37°C, pH 4.8].	215
Figure S5.7 Monoglycodiacylglycerols (MGDG) of the <i>L. bulgaricus</i> CFL1 membrane harvested at the stationary growth phase (t_{h3}) for the four fermentation conditions studied: A, [42°C, pH 5.8]; B, [42°C, pH 4.8]; C, [37°C, pH 5.8]; and D, [37°C, pH 4.8].	216
Figure S5.8 Monoglycodiacylglycerols (MGDG) of the <i>L. bulgaricus</i> CFL1 membrane harvested at the stationary growth phase (t_{h3}) for the four fermentation conditions studied: A, [42°C, pH 5.8]; B, [42°C, pH 4.8]; C, [37°C, pH 5.8]; and D, [37°C, pH 4.8].	217
Figure S5.9 Diglycodiacylglycerols (DGDG) of the <i>L. bulgaricus</i> CFL1 membrane harvested at the stationary growth phase (t_{h3}) for the four fermentation conditions studied: A, [42°C, pH 5.8]; B, [42°C, pH 4.8]; C, [37°C, pH 5.8]; and D, [37°C, pH 4.8].	218
Figure S5.10 Diglycodiacylglycerols (DGDG) of the <i>L. bulgaricus</i> CFL1 membrane harvested at the stationary growth phase (t_{h3}) for the four fermentation conditions studied: A, [42°C, pH 5.8], B, [42°C, pH 4.8], C, [37°C, pH 5.8], and D, [37°C, pH 4.8].	219
Figure S5.11 Phosphatidylglycerols (PG) of the <i>L. bulgaricus</i> CFL1 membrane harvested at the stationary growth phase (t_{h3}) for the four fermentation conditions studied: A, [42°C, pH 5.8]; B, [42°C, pH 4.8]; C, [37°C, pH 5.8], and D, [37°C, pH 4.8].	220
Figure S5.12 Phosphatidylglycerols (PG) of the <i>L. bulgaricus</i> CFL1 membrane harvested at the stationary growth phase (t_{h3}) for the four fermentation conditions studied: A, [42°C, pH 5.8]; B, [42°C, pH 4.8]; C, [37°C, pH 5.8], and D, [37°C, pH 4.8].	221
Figure S5.13 Peak positions of the symmetric CH ₂ stretching vibration band ($v_{sym}CH_2$) arising from <i>L. bulgaricus</i> CFL1. Upon cooling (blue fitted curves) and heating (red fitted curves) for [42°C, pH 5.8], [42°C, pH 4.8] [37°C, pH 5.8], and [37°C, pH 4.8].	222

LIST OF TABLES

Chapter 1 Literature review

Table 1.1 Detailed taxonomic lineage of two different Lactic Acid Bacteria (LAB) down to the strain level.	9
Table 1.2 Chemical structure of different groups of phospholipids and glycolipids found in Lactic Acid Bacteria (LAB).....	13
Table 1.3 Some examples of Lactic Acid Bacteria (LAB) species used for different industrial applications.	20
Table 1.4 Lactic Acid Bacteria (LAB) adaptation mechanisms improving freezing, freeze-drying, and storage resistance by different stresses.....	54
Table 1.5 Studies on the influence of fermentation conditions on the freezing, freeze-drying, and storage resistance of Lactic Acid Bacteria (LAB) in the case of works carried out in a bioreactor.....	59
Table 1.6 Reported studies on the lipid cellular properties modifications that have been linked to Lactic Acid Bacteria (LAB) resistance to stabilization process and storage.	64
Table 1.7 Studies on the use of protective solutions that have been effective protectors for freezing, freeze-drying, and storage Lactic Acid Bacteria (LAB).	68

Chapter 3 Materials and Methods

Table 3.1 Different sugars at used to protect <i>L. bulgaricus</i> CFL1 cells.....	109
---	-----

Chapter 4 Multi-objective optimization of frozen and freeze-dried *L. bulgaricus* CFL1

Table 4.1 Multiple regression analysis of the biomass productivity (P , in $\text{g}\cdot\text{L}^{-1}\cdot\text{h}^{-1}$) of <i>L. bulgaricus</i> CFL1.	132
Table 4.2 Multiple regression analysis of the loss of specific acidifying activity of <i>L. bulgaricus</i> CFL1 during freezing ($dt_{\text{spe F}}$) and freeze-drying ($dt_{\text{spe FD}}$).	136

Chapter 5 Deep analysis of membrane lipids and their relationships with *L. bulgaricus* CFL1 resistance to freezing and freeze-drying

Table 5.1 Main lipids found after fractionation (f_1, f_2, f_3, f_4) the total lipid extract (LE) of <i>L. bulgaricus</i> CFL1.	187
---	-----

Chapter 6 Influence of sugars on resistance and the membrane of *L. bulgaricus* CFL1

Table 6.1 Physicochemical properties of different sugar solutions at 25% w/w (NaCl 0.9%).....	231
Table 6.2 Lipid phase transitions temperatures of hydrated (T_{cooling} and T_{heating}) <i>L. bulgaricus</i> CFL1 in the presence of different sugars.....	244
Table 6.3 Lipid phase transitions temperatures of Hydrated (H) and Air-Dried (AD) <i>L. bulgaricus</i> CFL1 upon heating.	247

LIST OF SUPPLEMENTARY TABLES

Table S4.1 Studies on the influence of fermentation conditions on the freezing, freeze-drying and storage resistance of lactic acid bacteria (LAB) in the case of experiments carried out in a bioreactor.	145
Table S4.2 Kinetic parameters characterizing <i>L. bulgaricus</i> CFL1 growth and acidifying activity, for fermentations carried out in MRS medium supplemented with glucose at different pH and temperatures.	147
Table S4.3 Multiple regression analysis of the initial specific acidifying activity (t_{spe} I) of <i>L. bulgaricus</i> CFL1.....	148
Table S4.4 Multiple regression analysis of the loss of acidifying activity ($dt_{\Delta pH 0.7}$) of <i>L. bulgaricus</i> CFL1 during each stabilization process (F: freezing; FD: freeze-drying; and S: freeze-dried storage).....	149
Table S4.5 Multiple regression analysis of the culturability loss ($dlog$ (CFU mL ⁻¹)) of <i>L. bulgaricus</i> CFL1 during each stabilization process (F: freezing; FD: freeze-drying; and S: freeze-dried storage).....	150
Table S4.6 Multiple regression analysis of the loss of specific acidifying activity of <i>L. bulgaricus</i> CFL1 during freeze-dried storage (dt_{spe} S).....	151
Table S4.7 Predictive capacity of the multiple regression models:	151
Table S4.8 Multiple regression analysis of the specific of acidifying activity (t_{spe}) of <i>L. bulgaricus</i> CFL1 after freezing (t_{spe} F), freeze-drying (t_{spe} FD) and freeze-dried storage (t_{spe} S).	152
Table S5.1 Comparison of extraction methods for fatty acid detection	205
Table S5.2 Detailed fatty acid composition of <i>L. bulgaricus</i> CFL1 for the fermentation conditions at different harvest times.....	206
Table S5.3 (A) Summary of lipid classes and species in <i>L. bulgaricus</i> CFL1 by LC-MS/MS in positive mode	207
Table S5.4 Pearson coefficients of significant relationships between fatty acid composition (UFA, SFA, CFA), lipid phase transition temperatures (T_s and T_m), anisotropy values, and resistance of <i>L. bulgaricus</i> CFL1 to freezing (dt_{spe} F) and freeze-drying (dt_{spe} FD).....	210

INTRODUCTION

Microorganisms have represented a crucial part of human nutrition since ancient times. Humans have used bacteria to help initiate many food production processes without even knowing their existence. After the invention of the microscope and the detection of microorganisms, we started to intentionally use bacteria to modify the taste and shelf life of food. Thus, humankind has benefited from the wide diversity of fermented food production.

Lactic Acid Bacteria (LAB) are a well-known group of bacteria that produce many fermented food products such as yogurts, cheeses, fermented meat, and vegetables. These bacteria give fermented food unique aromas and characteristic textures due to their metabolic ability to produce organic acids (e.g., lactic acid), organoleptic compounds, and gelling agents (e.g., exopolysaccharides). Among fermented foods, yogurt is one of the most widely consumed products. For instance, in France, the volume of yogurts and fermented kinds of milk sold in 2018 came close to 1 million tons. It generated almost 2 billion euros of turnover profit, according to SYNDIfrais (French National Dairy Manufacturers Union since 1978). Yogurt results from milk fermentation through protooperation of two LAB species (*Lactobacillus bulgaricus* and *Streptococcus thermophilus*).

LAB have also been associated with health benefits, i.e., probiotics. Some LAB strains have significantly prevented and treated rotavirus diarrhea, reduced irritable bowel syndrome symptoms, and corrected other gastrointestinal flora disorders (Ouweland 2019). These bacteria have been introduced into functional foods to be commercialized.

The worldwide adoption of fermented food in the daily diet and the awareness to maintain a healthy and wellness lifestyle have led to booming fermented food and probiotics markets. In 2019, the global fermented food market was valued at USD 565.09 billion, and Europe was the largest market actor. The global market is forecast to increase by 54% by 2027 (Emergen Research 2020). In the same year, the global probiotic market size for probiotics was valued at USD 48.88 billion, with the Asia Pacific being the largest market. The global market for probiotics is projected to increase by 93% by 2027 (Fortune Business insights 2020).

LAB used at the industrial scale are produced as easy-to-use preparations (starters) by a succession of different steps: fermentation, harvesting, concentration, the addition of a sterile protective solution, and long-term stabilization processes such as freezing and freeze-drying. The former steps expose cells to different stresses (thermal, osmotic, mechanical) in which the cell membrane of LAB has been identified as the primary site of degradation (Brennan et al. 1986; Castro et al. 1997; Girardeau et al. 2022; Chen et al. 2022). The stabilization processes also lead to the loss of LAB functional properties (viability, acidifying activity, among others). The degree of damage to these stabilization processes can be, however, significantly reduced by four different strategies: (i) changing operational parameters of the stabilization processes and storage: freezing kinetics, sublimation conditions during freeze-drying, and storage conditions (e.g., temperature and minimizing oxygen concentration) using a different fermentation condition from the optimal for growth; (ii) stressing LAB during growth or after harvesting (by heat, cold, and osmotic treatments); (iii) using a different fermentation condition than the one optimal for growth; and (iv) adding the adequate protective solution in concentrated LAB. The preservation of LAB can be maximized when all the mentioned strategies are well mastered. However, the wide diversity in LAB come with differences in cell structure (Fonseca et al. 2000; Dumont et al. 2004), that affect the sensitivity of some of them to stabilization processes and make them fail to be exploited at an industrial scale.

Lactobacillus delbrueckii subsp. *bulgaricus* CFL1 was previously purified and has been identified as highly sensitive to cryopreservation (Fonseca et al. 2000, 2001a; Meneguel et al. 2017). With the increased knowledge on cryopreservation, we questioned whether this kind of strain of industrial interest (for the yogurt production). This strain would be an excellent candidate for developing the improved cryo-resistance strategies.

In this context, the first research question was:

How to improve the cryo-resistance of a sensitive lactic acid bacterium by re-examining the existing strategies?

In this thesis, among the four strategies described above, the two were revisited and used to improve the resistance of a lactic acid bacteria bacterium to freezing and freeze-drying (strategies iii and iv). The remaining two were not considered because one of them (i) requires another complete investigation involving more study time (another thesis project could cover

this strategy). The second one implicates adding an extra step in the production chain, which would require into a high investment of time and energy.

The strategies reexamined in this thesis consisted of modifying the fermentation conditions from the one used for the optimal growth to enhance the resistance of a lactic acid bacterium to the stabilization processes. Another one involved identifying a suitable protector to stabilize this bacterium. A diversity of protectors is available to protect LAB. The most commonly used are sugar molecules because of their chemically innocuous nature. Sugars are carbohydrates with different Degrees of Polymerization (DP): from monosaccharides (DP1), disaccharides (DP2), trisaccharides (DP3), to polysaccharides (DP>10).

These two strategies lead to different responses on the membrane of LAB. First, LAB develop adaptation mechanisms to a new environment when different fermentation conditions are applied, especially using another condition from the optimal for growth. This bacteria adaptation generates a modulation in the lipid membrane, generally identified by the fatty acid composition. Second, the protective action of sugars is thought to occur at the surface of the cell membrane. Thus, a second research question was proposed in this thesis:

Do the modulation the membrane lipids and the membrane interaction with sugars explain the cryo-resistance improvement?

To answer both questions, the following objectives were developed in this thesis:

- Identifying the fermentation parameters that ensure efficient biomass production and resistance of a lactic acid bacterium to freezing and freeze-drying.
- Understanding the modulation of membrane lipid properties by different fermentation conditions and the implication of these properties in a lactic acid bacterium resistance.
- Assessing the influence of sugars with different degrees of polymerization on a lactic acid bacterium resistance and membrane.

The present manuscript is divided into six main chapters:

Chapter 1 presents the literature review focuses on three axes describing (i) the general features of a lactic acid bacterium and more detailed information about the industrial interest of LAB in different sectors; (ii) the industrial production of LAB, with particular attention to the stabilization processes; and (iii) the strategies implemented to improve the resistance of LAB to stabilization processes.

Chapter 2 explains the overall experimental approach used in the thesis.

In **Chapter 3**, the materials and methods are described, including the thoroughly detailed parameters to conduct and reproduce the research. Its purpose is not to be redundant with the "materials and methods" of Chapters 4, 5, and 6 but to give some complementary experimental information used during the thesis.

Chapters 4, 5, and 6 present the results and discussion to unfold the proposed objectives:

Chapter 4 introduces multi-objective optimization which is dedicated to identifying the fermentation parameters that enhance both biomass production and resistance to freezing and freeze-drying of a lactic acid bacterium model strain.

Chapter 5 targets a complete analysis of membrane lipids used in this thesis. Chapter 5 describes how a complete characterization of membrane lipids is essential to understanding the modulation of the membrane properties under different fermentation conditions.

Chapter 6 focuses on the influence of sugars with different polymerization degrees on freezing and freeze-drying resistance and the membrane.

Finally, a conclusion section summarizes the main findings of the present thesis and offers some perspectives for future research.

This thesis was funded by INRAE and is part of the European Union's Horizon H2020 staff exchange multidisciplinary program entitled PREMIUM (Preserving bacteria with oligosaccharides and eco-friendly processes). The PREMIUM project (N° 777657) was initiated in 2017 to propose innovative alternatives to companies for preserving LAB. It is devoted to studying and developing innovative strategies for the long-term preservation of lactic acid bacteria while considering product quality, process conditions, and environmental impact (www.inrae.fr/premium). Some of the innovative strategies include producing oligosaccharides such as Fructo-OligoSaccharides (FOS) and Galacto-OligoSaccharides (GOS) for protecting cells and developing novel preservation process, and evaluating the environmental impact of the whole system of production of microorganisms from the laboratory to the industrial scale.

The host academic partner of the PREMIUM project is located in the research group ProBioSSep (*Procédés microBiologiques, Stabilisation, Séparation*) in the INRAE, UMR SayFood (Food and Bioproduct Engineering), Thiverval-Grignon, France. This research team is specialized in different bioprocess topics, in which the optimization of microbial and stabilization processes is one of its expertise. Additionally, in the frame of the PREMIUM project, two other research laboratories in France were actively participating in accomplishing the objectives of the project. These are the Institute Jean Pierre Bourgin (IJPB) in Versailles and the UR BIA (*Biopolymères, Interactions, Assemblages*) in Nantes. This thesis work was carried out in the above three laboratories in France, and it benefited from the environment of the PREMIUM project.

Chapter 1

1. LITERATURE REVIEW

This chapter describes the current knowledge about the production of lactic acid bacteria, the most common stabilization processes: freezing and freeze-drying, and the strategies to preserve the functional properties of lactic acid bacteria from the production to the long-term storage. First, the lactic acid bacteria cell structure and the industrial applications of these bacteria are presented to position this research work. Then, the concentrated lactic acid bacteria production is summarized. This section highlights the stabilization process and storage to identify then steps where the LAB are negatively affected during these production steps. Finally, the present understanding of the alternatives to enhance lactic acid bacteria resistance to the stabilization process is reviewed to illustrate the gap in previous research that needs to be filled. Main conclusions are drawn at the end of each section, and some future directions are discussed at the end of this chapter.

SUMMARY OF THE CHAPTER

1. LITERATURE REVIEW	5
1.1. Lactic acid bacteria composition and industrial applications	8
1.1.1. Definition and taxonomy of Lactic Acid Bacteria	8
1.1.2. Lactic acid bacteria structure, composition and metabolism	9
1.1.2.1. The intracellular content	10
1.1.2.2. The cytoplasmic membrane	10
i. Membrane lipids	11
ii. Membrane proteins	16
1.1.2.3. The cell wall	17
i. Peptidoglycan	17
ii. Teichoic acids	17
iii. Cell-wall polysaccharides	18
iv. Cell wall proteins	18
1.1.2.4. Lactic acid bacteria metabolism	18
1.1.3. Industrial applications of lactic acid bacteria given their functional properties	19
1.1.3.1. The fermented food industry	20
1.1.3.2. The functional food industry	21
1.1.3.3. The chemical industry	22
1.2. Production of lactic acid bacteria: stabilization and storage, critical steps that induce cell damages	24
1.2.1. Multi-step production of lactic acid bacteria	24
1.2.1.1. Medium preparation and sterilization (steps ①-②)	24
1.2.1.2. Strain conditioning and inoculation (step ③)	26
1.2.1.3. Fermentation (step ④)	26
1.2.1.4. Cooling and harvest (step ⑤)	28
1.2.1.5. Concentration and protection (steps ⑥-⑨)	29
1.2.1.6. Stabilization: freezing or freeze-drying (steps ⑩ or ⑪)	30
i. Freezing	30
ii. Freeze-drying	30
1.2.1.7. Frozen and freeze-dried storages (step ⑫)	31
i. Frozen storage	31
ii. Freeze-dried storage	32
1.2.2. Stabilization and storage production steps affect the functional properties of lactic acid bacteria	32
1.2.2.1. Acidifying activity	33
1.2.2.2. Culturability	34
1.2.2.3. Viability	34
1.2.2.4. Other functional properties	34
1.2.3. Changes in the matrix of LAB suspensions during stabilization and storage	34
1.2.3.1. Freezing	35
i. The temperature decreases below 0°C	35
ii. Cryo-concentration	36
iii. The glass transition temperature	36
1.2.3.2. Frozen-storage	36
1.2.3.3. Freeze-drying	37
i. Freezing	37
ii. Primary drying or sublimation	38
iii. Secondary drying or desorption	40
1.2.3.4. Freeze-dried storage	40
1.2.4. Cellular damages during stabilization and storage	42
1.2.4.1. Cellular damages during freezing	42
i. Thermal stress: membrane phase transition and loss of enzymatic activities	44
i. Mechanical, osmotic and chemical stresses: cell dehydration and inactivation of proteins and nucleic acids ⁴⁵	45
ii. Intracellular and extracellular glass transitions	46
1.2.4.2. Cellular damages during frozen storage and thawing protocol	46
i. Frozen storage	46

ii. Thawing protocol	46
1.2.4.3. Cellular damages during freeze-drying	47
1.2.4.4. Cellular damages during freeze-dried storage and rehydration protocol	48
i. Freeze-dried storage: oxidation and non-enzymatic reactions	48
ii. Rehydration protocol	48
1.3. Strategies to improve lactic acid bacteria resistance to the critical steps of their production: stabilization processes and storage	51
1.3.1. Modification of freezing and freeze-drying operating parameters to enhance lactic acid bacteria resistance	51
1.3.1.1. The choice of cooling rate during freezing	51
1.3.1.2. Freeze-drying cycle	52
1.3.2. Stressful conditions to favor LAB resistance	53
1.3.3. Modulation of fermentation conditions to enhance lactic acid bacteria resistance	55
1.3.3.1. Fermentation parameters effect on LAB resistance	55
i. Supplementing the fermentation medium	55
ii. Fermentation temperature	56
iii. Fermentation pH	57
iv. Harvest time	57
1.3.3.2. Biophysical and biochemical properties of LAB membrane lipids are associated with stabilization and storage resistance	61
1.3.4. The addition of protective molecules	66
1.3.4.1. Protective molecules for LAB stabilization	66
1.3.4.2. Mechanisms of sugars to protect LAB	69
1.4. Conclusions and future directions	76

1.1. Lactic acid bacteria composition and industrial applications

1.1.1. Definition and taxonomy of Lactic Acid Bacteria

Lactic Acid Bacteria (LAB) are historically defined as a heterogeneous group of Gram-positive, non-spore-forming, catalase-negative, cytochrome-deficient, homo or heterofermentative, facultatively anaerobic, cocci, bacilli, or rod-shaped (Pot et al. 1994).

LAB had been consisted of six phylogenetic families: 1) *Aerococcaceae*, 2) *Carnobacteriaceae*, 3) *Enterococcaceae*, 4) *Lactobacillaceae*, 5) *Leuconostocaceae*, and 6) *Streptococcaceae* (Vandamme et al. 2014).

However, a recent taxonomic study has merged *Lactobacillaceae* and *Leuconostocaceae* into one family (*Lactobacillaceae*). Therefore, LAB have five phylogenetic families. Also, 23 new genera have been proposed for the family *Lactobacillaceae*, which already had the following genera: *Lactobacillus*, *Leuconostoc*, *Oenococcus*, *Weisella*, *Pediococcus*, *Convivina*, *Paralactobacillus* (Zheng et al. 2020).

In some cases, the LAB genus names have been changed. For example, *Lactobacillus plantarum*, *Lactobacillus reuteri*, and *Lactobacillus rhamnosus* are currently named as *Lactiplantibacillus plantarum*, *Limosilactobacillus reuteri*, and *Lacticaseibacillus rhamnosus*, respectively. The complete list of modified names can be found in the Annex A.1. This thesis uses the updated names to refer to different LAB genera.

In order to understand the taxonomic hierarchy of LAB cells, Table 1.1 shows the taxonomic classification of two LAB: *Lactobacillus delbrueckii* subsp. *bulgaricus* and *Streptococcus salivarius* subsp. *thermophilus*. Additionally, in the Annex A.2, a Table is presented to illustrate where these two LAB examples are taxonomically located from family to species.

LAB are mainly isolated from food but can also be isolated from intestinal and genital tracts of humans and animals, sewage, or plant materials. Their importance is mainly associated with their metabolic activity since these bacteria grow in foods using available sugar to produce organic acids and other metabolites. Their common occurrence in foods and utilization contribute to their natural acceptance as GRAS microorganisms (Generally Recognized As Safe) (Bintsis 2018). They are actively used for the fermentation of meat, vegetables, fruits, beverages, and dairy products. Also, some LAB strains are known to exert health benefits to the host; thus, food supplemented with LAB are called functional food (i.e., foods that positively affect health beyond their nutritional value).

Table 1.1 Detailed taxonomic lineage of two different Lactic Acid Bacteria (LAB) down to the strain level.

Taxonomic rank or level	<i>Lactobacillus delbrueckii</i> subsp. <i>bulgaricus</i>	<i>Streptococcus salivarius</i> subsp. <i>thermophilus</i>
Domain	Bacteria	Bacteria
Phylum	Firmicutes	Firmicutes
Class	Bacilli	Bacilli
Order	Lactobacillales	Lactobacillales
Family	<i>Lactobacillaceae</i>	<i>Streptococcaceae</i>
Genus	<i>Lactobacillus</i>	<i>Streptococcus</i>
Species	<i>Lactobacillus delbrueckii</i>	<i>Streptococcus salivarius</i>
Subspecies (subsp)	<i>Lactobacillus delbrueckii</i> subsp. <i>bulgaricus</i>	<i>Streptococcus salivarius</i> subsp. <i>thermophilus</i>
Strain <u>example</u>	<i>Lactobacillus delbrueckii</i> subsp. <i>bulgaricus</i> <u>CFL1</u> (Fonseca et al. 2000)	<i>Streptococcus salivarius</i> subsp. <i>thermophilus</i> <u>CNRZ1066</u> (Bolotin et al. 2004)
Short name in scientific literature	<i>Lactobacillus bulgaricus</i>	<i>Streptococcus thermophilus</i>

1.1.2. Lactic acid bacteria structure, composition and metabolism

LAB, as Gram-positive bacteria, structurally consist, from the interior to the exterior, of an intracellular content, where cytoplasm and genetic material are found; a cytoplasmic membrane, a fluid polar lipid bilayer that encloses the bacterial cytoplasm; and a cell wall, a highly-structured layer of great mechanical strength that encloses the cytoplasmic membrane (Figure 1.1).

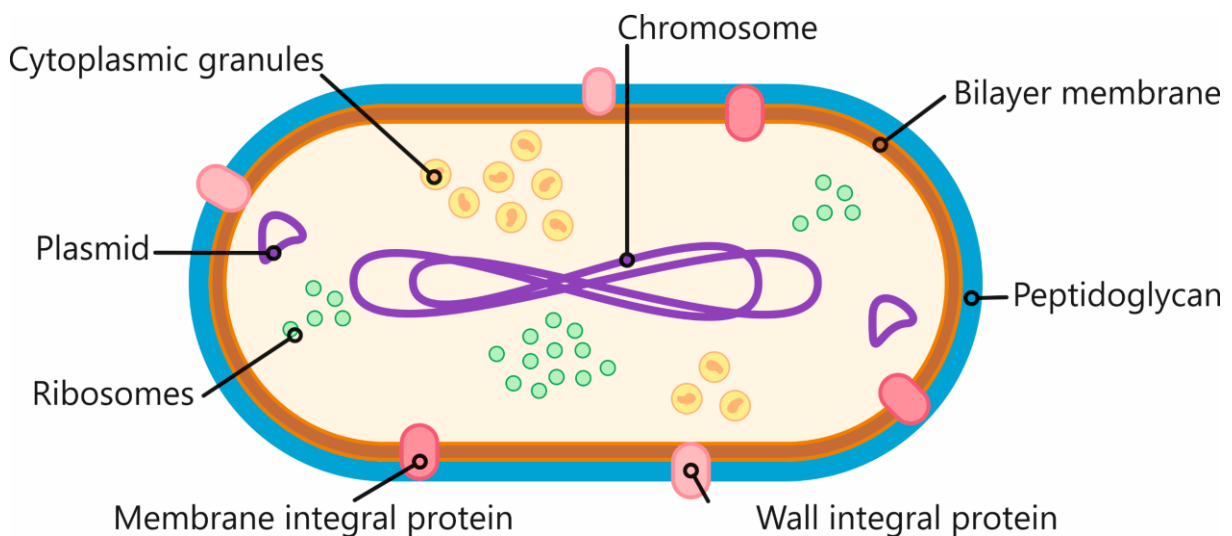


Figure 1.1 Schematic representation of a lactic acid bacterium structure and composition. Different components are not represented in the same scale. Adapted from Wu et al. 2014.

1.1.2.1. The intracellular content

The cytoplasm essentially represents the intracellular content. The cytoplasm is a gel-like matrix enclosed within the cytoplasmic membrane, which comprises, for example, water, proteins, lipids, nucleic acids, and inorganic salts. Most metabolic activities take place within the cytoplasm, and the following subcellular structures are located there: (i) ribosomes, (ii) cytoplasmic granules, and (iii) genome. The bacterial ribosome is a cytoplasmic nucleoprotein particle whose primary function is to process mRNA translation and protein synthesis. Cytoplasmic granules are storage granules that supply limited compounds in the bacteria environment (Zhou and Li 2015).

The genetic material can be found in chromosomes and plasmids. The genomes of LAB consist of single circular chromosomes and harbor plasmids with a length ranging from 1.3 to 3.35 Megabase pairs (Mbp).

Both circular chromosomes and harbor plasmids contain short DNA sequences and numerous pseudogenes (regions of the genome that contain defective copies of genes) (Goh and Klaenhammer 2009; Zhu et al. 2009; Vogel et al. 2011).

The guanine-cytosine (GC) content and the number of predicted protein-coding genes in LAB are other features to characterize the bacterial genome. In most LAB genomes, the GC content is less than 55% and the number of predicted genes ranges from 1700 to 2800 (Pridmore et al. 2004; Altermann et al. 2005; Makarova et al. 2006; Wassenaar and Lukjancenko 2014). For instance, the genome of the strain *Lactobacillus delbrueckii* subsp. *bulgaricus* CFL1 was sequenced by Meneghel et al. (2016). This genome is 1.8 Mbp in length, has a GC content of 49.8%, and is composed of 1882 predicted genes. These results were similar to the previously sequenced LAB, such as *Streptococcus thermophilus* CNRZ1066 (Bolotin et al. 2004), *Ligalactobacillus salivarius* UCC118 (Claesson et al. 2006), and *Oenococcus oeni* PSU-1 (Makarova et al. 2006).

1.1.2.2. The cytoplasmic membrane

The cytoplasmic membrane, usually called the cell membrane, forms a diffusion barrier and constitutes a physical barrier between the cytoplasm and the external medium (Konings 2002).

The cytoplasmic membrane is vital to numerous cell functions, including molecule diffusion, energy generation, cell division, and maintenance of electrochemical gradients (Dowhan 1997). The membrane structure is patchy, with segregated regions and domains constituted of lipids assembled and non-randomly distributed in a bilayer and membrane proteins with different structures (Engelman 2005). These proteins are tightly bound by hydrophobic forces and intercalated in the bilayer (integral or intrinsic membrane proteins) or loosely bound by electrostatic forces (peripheral or extrinsic membrane proteins) (Nicolson 2014) (Figure 1.2).

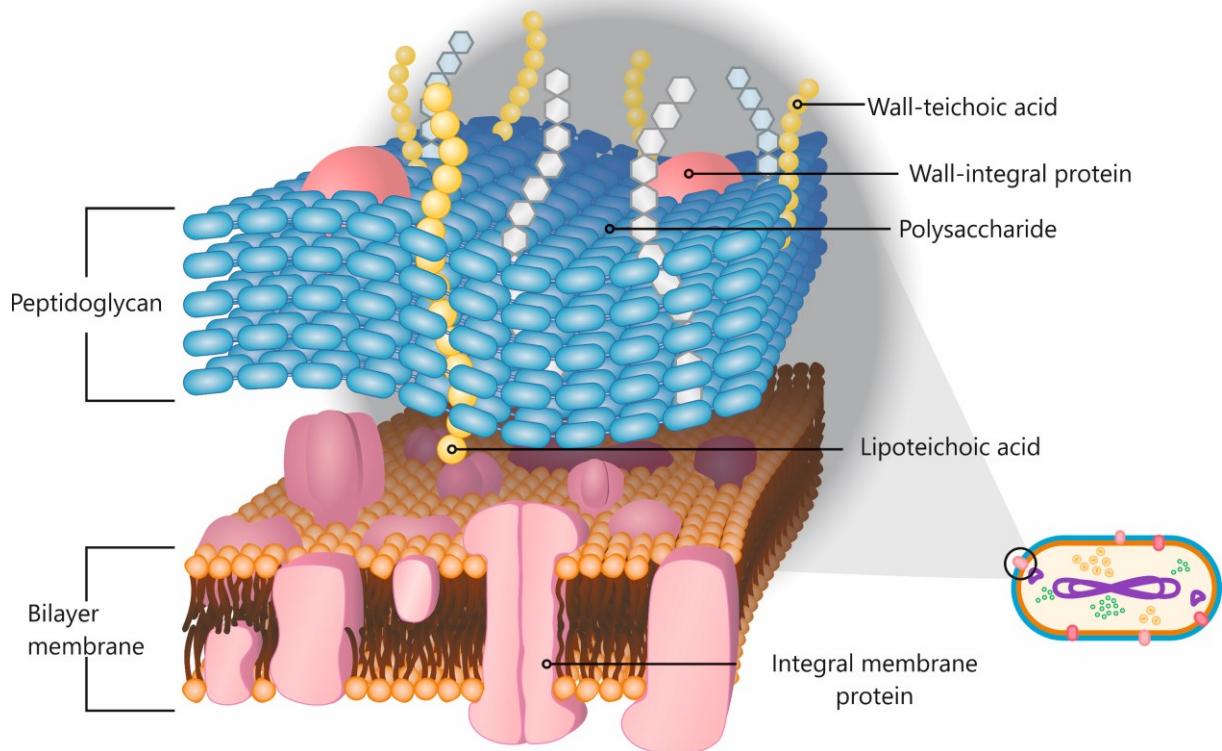


Figure 1.2 Schematic illustration of a Gram-positive cell wall and cytoplasmic membrane. Different components are not represented in the same scale. Adapted from Delcour et al. 1999 and Engelman 2005.

i. Membrane lipids

The classes of LAB membrane lipids that have been reported are the following: (1) phospholipids (also named glycerophospholipids) and (2) glycolipids (or named glyceroglycolipids).

Phospholipids contain a hydrophilic phosphate head group and two hydrophobic acyl chains (fatty acids) covalently bounded on a glycerol backbone. A phospholipid is often schematically represented, as shown in Figure 1.3. Phospholipids distinguish from each other according to the group fixed on the phosphate (and designated as "X" in Figure 1.3 (A)).

The structure of a glycolipid is also shown in Figure 1.3 (C). The glycolipids contain two hydrophobic acyl chains (fatty acids) bound to a glycerol backbone and have as a headgroup a carbohydrate portion containing one or more hexose moieties (Iwamori et al. 2011).

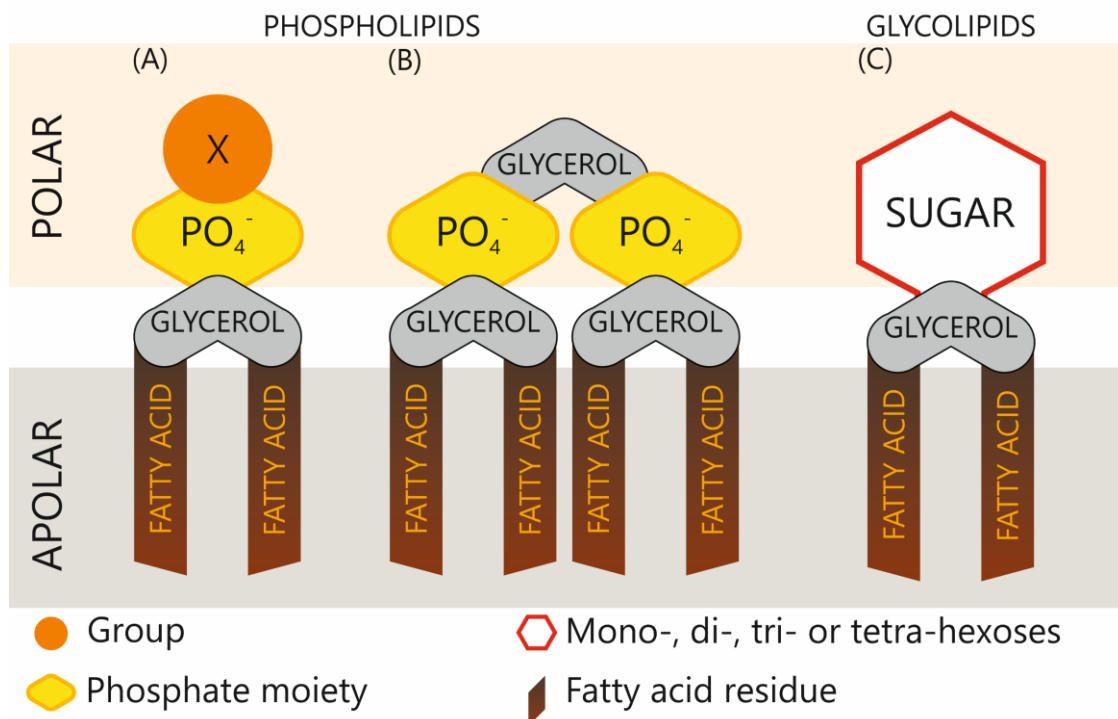


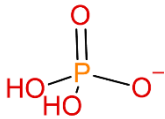
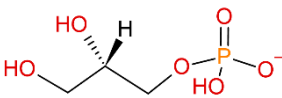
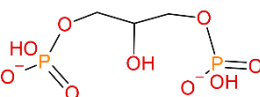
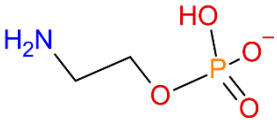
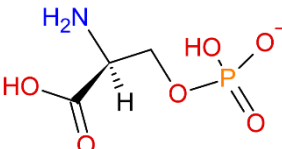
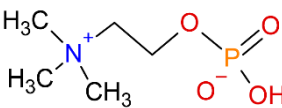
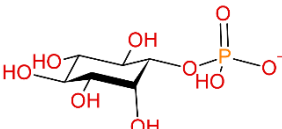
Figure 1.3 Main membrane lipids in lactic acid bacteria. (A) phospholipid, (B) cardiolipin (also a phospholipid), and (C) glycolipids. X or SUGAR is a chemical group described in Table 1.2. Adapted from Stillwell 2016.

Table 1.2 lists the thirteen studies that have reported, so far, the chemical structures of phospholipid families found in different LAB species (e.g., *Lactobacillus delbrueckii*, *Lactobacillus acidophilus*, *Lactobacillus helveticus*, *Lactococcus lactis*, *Lacticaseibacillus casei*, *Lactiplantibacillus plantarum*, *Leuconostoc mesenteroides*, *Oenococcus oeni* among others).

In the LAB membrane, nine studies in Table 1.2 reported the presence of phosphatidylglycerol (PG) and cardiolipin (CL), also referred to as diphosphatidylglycerol (Figure 1.3 (B)). (Exterkate et al. 1971; Fernández Murga et al. 2000; Gomez-Zavaglia 2000; Limonet et al. 2004; Machado et al. 2004; Calvano et al. 2011; Hansen et al. 2015a; Kato et al. 2019; Chamberlain et al. 2019). PG and CL maintain membrane permeability and fluidity due to their polar head geometries. These relevant roles of the two phospholipids in the membrane were observed in other Gram-positive bacteria than LAB, such as *Listeria monocytogenes* (Vadyvaloo et al. 2002); by molecular dynamics simulations (Murzyn et al. 2005); and lipid bilayers models (Unsay et al. 2013). Three studies have reported other phospholipids in the LAB lipid membrane, such as phosphatidylserine (PS), phosphatidylcholine (PC), and phosphatidylinositol (PI) (Table 1.2) (Drucker et al. 1995; Walczak-Skierska et al. 2020; Kim et al. 2020).

Also, in Table 1.2, the principal glycolipid structures found in LAB are presented. These are diacylglycerols (DG) bound to different hexoses such as galactose (Gal) or glucose (Glc) molecules. The hexoses of glycolipids are often covalently linked to a poly-glycerol phosphate backbone. This former is bound to lipoteichoic acids (LTA) (Shiraishi et al. 2016). LTA are anionic polymers that are anchored to the cell membrane heading to the cell wall (Figure 1.2).

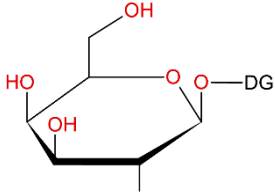
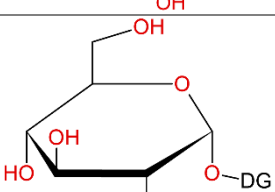
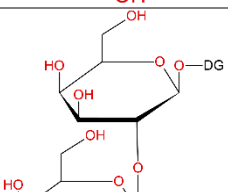
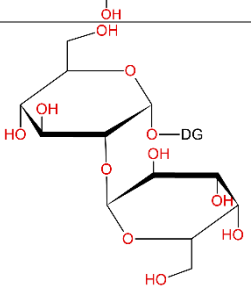
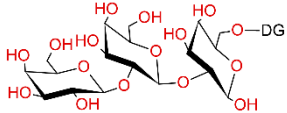
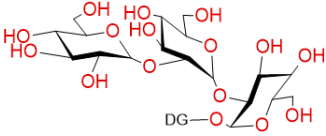
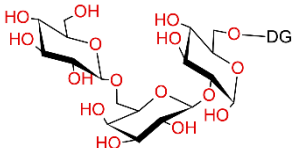
Table 1.2 Chemical structure of different groups of phospholipids and glycolipids found in Lactic Acid Bacteria (LAB).

Name of phospholipid	Group name	Chemical structure bound to phosphate group*	References
Phosphatidic acid (PA) and Lyso-PA	None		(Exterkate et al. 1971; Drucker et al. 1995; Hansen et al. 2015a; Kim et al. 2020)
Phosphatidyl glycerol (PG) and Lyso-PG	Glycerol		(Exterkate et al. 1971; Drucker et al. 1995; Fernández Murga et al. 2000; Gomez-Zavaglia 2000; Teixeira et al. 2002; Limonet et al. 2004; Machado et al. 2004; Calvano et al. 2011; Hansen et al. 2015a; Kato et al. 2019; Chamberlain et al. 2019; Walczak-Skierska et al. 2020; Kim et al. 2020)
Cardiolipin (CL)	Phosphatidylglycerol		(Exterkate et al. 1971; Fernández Murga et al. 2000; Gomez-Zavaglia 2000; Limonet et al. 2004; Machado et al. 2004; Calvano et al. 2011; Hansen et al. 2015a; Kato et al. 2019; Chamberlain et al. 2019)
Phosphatidyl ethanolamine (PE) and Lyso-PE	Ethanolamine		(Teixeira et al. 2002; Limonet et al. 2004; Walczak-Skierska et al. 2020; Kim et al. 2020)
Phosphatidyl serine (PS) and Lyso-PS	Serine		(Drucker et al. 1995; Walczak-Skierska et al. 2020; Kim et al. 2020)
Phosphatidyl choline (PC) and Lyso-PC	Choline		(Teixeira et al. 2002; Walczak-Skierska et al. 2020; Kim et al. 2020)
Phosphatidyl inositol (PI) and Lyso-PI	Inositol		(Walczak-Skierska et al. 2020; Kim et al. 2020)

Phospholipids

Lyso: Lysophospholipids are characterized by a single fatty acid chain and a polar head group; *Chemical structures of phosphate head (PO₄) linked to each group ("X" in Figure 1.3). Chemical structures adapted from LIPID MAPS® Structure Database (LMSD).

Table 1.2 (Continued) Chemical structure of different groups in phospholipids and glycolipids found in Lactic Acid Bacteria (LAB).

Name of glycolipid	Group name	Sugar chemical structures bound to glycerol*	References
β -D-Gal-diacylglycerol (MGDG)	One galactose molecule		(Kato et al. 2019)
α -D-Glc-diacylglycerol (MGlcDG)	One glucose molecule		(Machado et al. 2004; Iwamori et al. 2011; Sauvageau et al. 2012)
β -D-Gal(1 \rightarrow 2) β -D-Gal-diacylglycerol (DGDG)	Two galactose molecules		(Drucker et al. 1995; Fernández Murga et al. 2000, 2001; Calvano et al. 2011; Iwamori et al. 2011; Kato et al. 2019)
α -D-Gal(1 \rightarrow 2) α -D-Glc-diacylglycerol (GGlcDG)	Galactose and glucose		(Hözl and Dörmann 2007; Iwamori et al. 2011; Sauvageau et al. 2012)
β -D-Gal(1 \rightarrow 2) β -D-Gal(1 \rightarrow 2) β -D-Gal-diacylglycerol (TGDG)	Three galactose molecules		(Fernández Murga et al. 2000; Hansen et al. 2015a; Shiraishi et al. 2016; Kato et al. 2019)
α -D-Glc(1 \rightarrow 2) α -D-Glc(1 \rightarrow 2) α -D-Glc-diacylglycerol	Three glucose molecules		(Räisänen et al. 2007)
β -D-Glc(1 \rightarrow 6) α -D-Gal(1 \rightarrow 2) α -D-Glc-diacylglycerol	Glucose, galactose and glucose		(Nakano and Fischer 1978; Jang et al. 2011; Sauvageau et al. 2012; Jeong et al. 2015)

*Chemical structures of sugars linked to a glycerol ("SUGAR" in Figure 1.3). Abbreviation: DG, Diacyl Glycerol. Chemical structures adapted from LIPID MAPS® Structure Database (LMSD).

In the fatty acid nomenclature, the symbolic name C_x:_y refers to a fatty acid chain, where "x" is the number of carbons (C) in the fatty acid chain and "y" is the number of double bonds. Fatty

acids in LAB (the constituents of phospholipids and glycolipids) mainly have aliphatic chains from 10 to 22 carbons, involving saturated and unsaturated carbons. Some LAB contain cyclic fatty acids, assigned as cycCx:y (CFA) (Goldberg and Eschar 1977; Gomez-Zavaglia 2000; Girardeau et al. 2022). CFA are formed in situ via post-synthetic modification, which involves transferring a methyl group from S-adenosyl-L-methionine (AdoMet) to the double bond of unsaturated fatty acids in a phospholipid molecule (Grogan and Cronan 1997). Lastly, for some LAB membrane strains, branched fatty acids (BFA) have also been detected (Wang et al. 2011; Noda et al. 2020) (Figure 1.4).

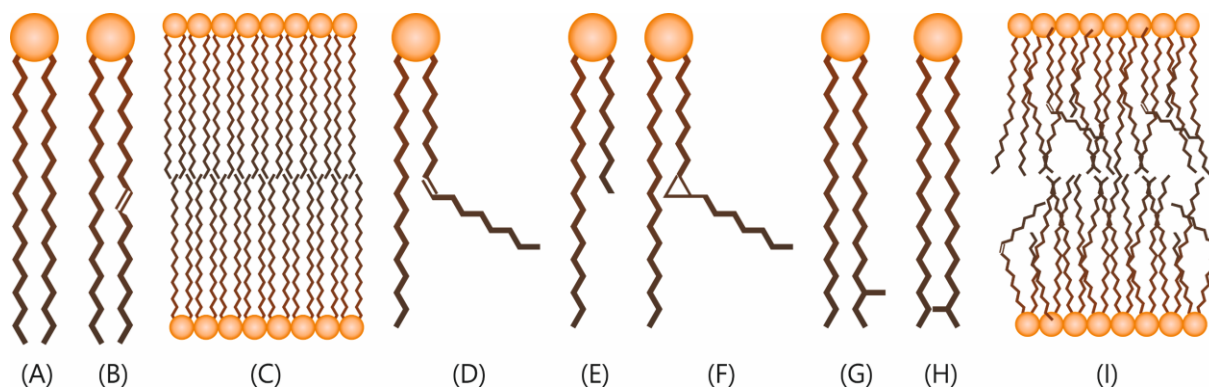


Figure 1.4 Schematic representation of different fatty acyl chain conformations found in lipids of lactic acid bacteria. (A, B, D, E, F, G, H) and their arrangements in the whole membrane ((C) and (I)). Orange circles and brown zigzag lines represent a polar head and fatty acid chains, respectively. (A) saturated fatty acid; (B) unsaturated fatty acid trans; (C) rigid fatty acid packing example; (D) unsaturated fatty acid cis; (E) chain length reduction; (F) cyclic fatty acid; (G) branched fatty acid ante-iso; (H) branched fatty acid iso; and (I) fluid fatty acid packing example. Adapted from Fonseca et al. 2019.

In lipid membranes, the fatty acyl chain structure and geometry govern the lipid's shape and the degree of lipid packing within the bilayer. Straight chains of saturated (Figure 1.4 (A)) and trans double bond (Figure 1.4 (B)) fatty acids facilitate the chain packing (Figure 1.4 (C)) compared to one cis double bond within the chain (Figure 1.4 (D)). Additionally, short-length chains (Figure 1.4 (E)), cyclic fatty acids (Figure 1.4 (F)), and iso-branched chains of fatty acids (Figure 1.4 (G, H)) contribute to bilayer disruption and a more fluid structure (Figure 1.4 (I)) (Diefenbach et al. 1992; Loffhagen et al. 2001; Denich et al. 2003; Poger and Mark 2015).

A recent review by Fonseca et al. (2019) summarized the most common fatty acids found in LAB. These are C10:0; C12:0, C14:0, C15:0, C16:0, C16:1, C17:1; C18:0, C18:1, C18:2, C20:0, C20:1; C22:0. The fatty acid content in LAB can vary among genera. For example, Figure 1.5 compares the fatty acid content of three different LAB genera: *Streptococcus thermophilus* CFS2, *Lactobacillus delbrueckii* susp. *bulgaricus* CFL1, and *Lactiplantibacillus plantarum* L1P-1 (Béal et al. 2001; Streit et al. 2008; E et al. 2021).

Fatty acids (FA) of 16 and 18 carbons (C16:0, C16:1, C18:0, C18:1) account for more than 50% of the total FA of the LAB membranes. Among the three LAB species, *Streptococcus thermophilus* CFS2 had the lowest CFA content. *Lactobacillus delbrueckii* susp. *bulgaricus* CFL1 had the highest C16:1, whereas C16:0 was the highest FA for *Lactiplantibacillus plantarum* L1P-

1. Additionally, the ratio of unsaturated fatty acid to saturated fatty acid (UFA/SFA) was different. *Lactobacillus delbrueckii* susp. *bulgaricus* CFL1 had the highest value (1.7), then *Streptococcus thermophilus* CFS2 (1.0), and finally *Lactiplantibacillus plantarum* L1P-1 (0.5).

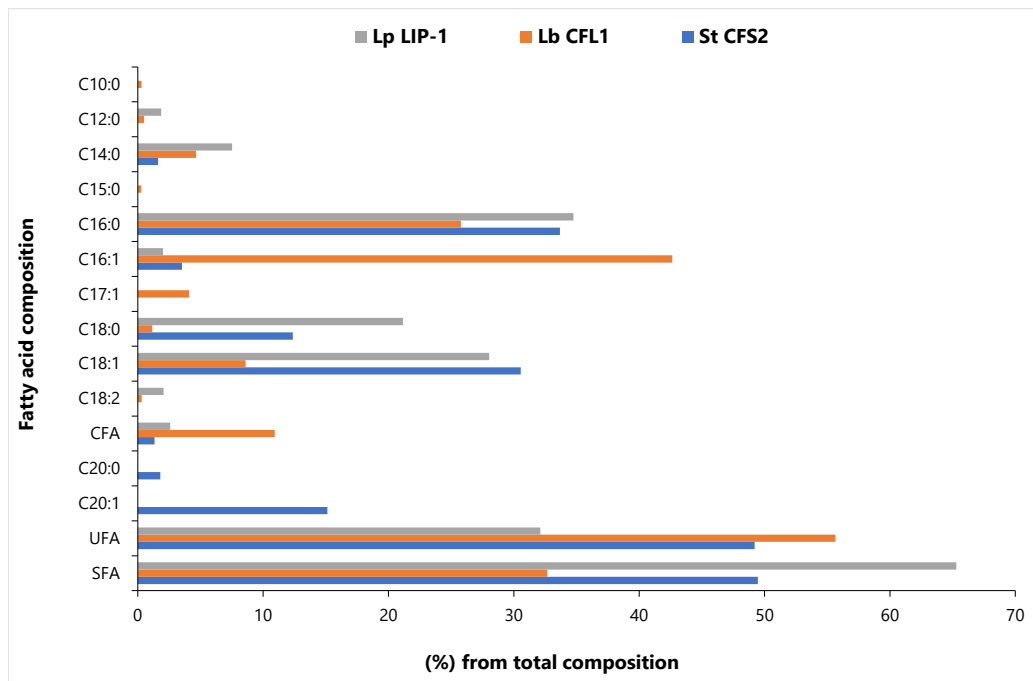


Figure 1.5 Membrane fatty acid composition of three different LAB genera. Abbreviations in the legend: Lp LIP-1, *Lactiplantibacillus plantarum* L1P-1 (E et al. 2021); Lb CFL1, *Lactobacillus delbrueckii* subsp. *bulgaricus* CFL1 (Streit et al. 2008); St CFS2, *Streptococcus thermophilus* CFS2 (Béal et al. 2001). Abbreviations in the Y axis: CFA, Cyclic Fatty Acid; UFA, Unsaturated Fatty Acid (without considering CFA); SFA, Saturated Fatty Acid.

The fatty acid composition in LAB can vary not only in LAB genera but also according to their growth conditions (further subsection 1.3.2, Table 1.6).

ii. Membrane proteins

Membrane proteins are bound to the membrane or anchored *via* several transmembrane domains and are involved in several cellular functions. These functions include various vital processes such as cell growth and division, cell integrity maintenance, energy transduction, and transmembrane transport mechanisms (Frelet-Barrand et al. 2010).

Membrane proteins are folded into either α -helix or β -sheet secondary structures. α -helices are formed by the consecutive joining of mostly non-polar amino acids in a range of 15-25 amino acids required to span the membrane bilayer. In contrast, β -sheet secondary structures are formed by alternate polar and non-polar amino acids. Polar amino acid side chains face the inner part of the protein, forming an aqueous channel. In contrast, the side chain of the non-polar amino acids faces the lipid bilayer (Santoni et al. 2000).

1.1.2.3. The cell wall

As Gram-positive bacteria, LAB have a thick cell wall (CW), illustrated previously in Figure 1.2. The cell wall is characterized by a (i) peptidoglycan layer, which functions as a scaffold for the attachment of other CW components such as (ii) teichoic acids, (iii) polysaccharides, and (iv) proteins (Chapot-Chartier and Kulakauskas 2014).

Far from being a static and rigid structure, the CW is highly dynamic. It is implicated in several essential cell functions, including cell division and shape. It is required to counteract turgor pressure (the force within the cell that pushes the plasma membrane against the cell wall). Moreover, as the outermost macrostructure of the bacterial cell, the CW is the primary sensory interface between the cell and the external environment (Martinez et al. 2020).

i. Peptidoglycan

Peptidoglycan is a complex macromolecule made of linear glycan chains cross-linked by short peptide chains. It is produced by extracellular polymerization of disaccharide-pentapeptide subunits synthesized in the cytoplasm. The resulting glycan chains consist of alternating N-acetylglucosamine (GlcNAc) and N-acetylmuramic acid (MurNAc) linked via β -1, 4 bonds. The peptidic chain is branched by its N-terminus on the lactyl group of MurNAc.

The peptidic chains vary in composition across LAB species. For example, in almost all bacterial cell walls, the most common sequence of a peptide chain is L-Ala- γ -D-Glu-X-D-Ala-D-Ala, where X represents a di-amino acid (Schleifer and Kandler 1972). This di-amino acid is often L-Lys, which is present in *Lactococcus lactis* and some LAB of the genus *Lactobacillus*. Conversely, other di-amino acids than L-lys can be found for different LAB, for example, mesodiaminopimelic and L-ornithine acids in *Lactiplantibacillus plantarum* and *Limosilactobacillus fermentum*, respectively (Delcour et al. 1999). Another variable feature among LAB species is the bridges linking peptides. It can be either directly between the two peptide chains, e.g., in *Lactiplantibacillus plantarum* (Bernard et al. 2011)) or through short inter-peptide bridges made of one D-amino acid, e.g., D-Asp or D-Asn in *Lactococcus lactis* (Courtin et al. 2006) and *Lacticaseibacillus casei* (Regulski et al. 2012).

ii. Teichoic acids

Teichoic acids are anionic polymers made of alditol-phosphate repeating units and are classified into two groups: wall teichoic acids (WTAs), covalently linked to peptidoglycan strands, and lipoteichoic acids (LTAs) that are anchored to the cytoplasmic membrane through a lipid anchor (i.e., glycolipid). Whereas LTAs are present in all LAB, WTAs are absent from certain LAB species such as *Lacticaseibacillus casei*, *Lacticaseibacillus rhamnosus*, and *Lactococcus lactis* (Vinogradov et al. 2018).

iii. Cell-wall polysaccharides

Polysaccharides (PS) are permanently attached to the cell wall. Some LAB can also produce exopolysaccharides (EPS), loosely attached to the cell surface. The difference is that cell wall polysaccharides must be extracted under harsh acid extract treatment. In contrast, EPS are released to the surrounding medium and can be "easily" purified from the culture supernatant. Cell-wall polysaccharides exhibit great diversity in sugar composition, linkage, branching, and substitution among LAB strains. For instance, 16 different strains of the species *Lacticaseibacillus casei* exhibited specific carbohydrate-binding proteins due to the heterogeneity of different sugar moieties: glucose (Glc), galactose (Gal), raffinose (Rha), N-Acetylglucosamine (GlcNAc), and N-Acetylgalactosamine (GalNAc) (Yasuda et al. 2011).

iv. Cell wall proteins

After proteins are synthesized in the cytoplasm, bacterial proteins are released outside the cytoplasmic membrane and retained in the cell envelope (Zhou et al. 2010). Secreted proteins can be covalently attached to the cell wall by sortase-mediated reactions or attached via (1) transmembrane anchors; (2) lipid anchors, and (3) different cell wall binding domains (Desvaux et al. 2006; Buist et al. 2006).

One remarkable family of cell wall proteins found in LAB is the mucus-binding proteins. These proteins contain mucus-binding domains (MUB or MucBP) that are essential in probiotics to facilitate mucosal colonization. Additionally, other functionally important proteins are the pilins, the structural components of pili. Pili are long filamentous structures that extend from the surfaces of various Gram-negative and Gram-positive bacteria. The pilus in LAB probiotics helps the adhesion and persistence of these bacteria in host's gut. *Lacticaseibacillus rhamnosus* GG cells have been found to contain multiple pili with lengths of up to 1 μm (Tripathi et al. 2012), while *Lactococcus lactis* produces thin pili that are relatively short (averaging 350 nm length) (Meyrand et al. 2013).

1.1.2.4. Lactic acid bacteria metabolism

LAB can be homofermenters bacteria, producing mainly lactic acid or heterofermenters, which, apart from lactic acid, produce a large variety of fermentation products such as acetic acid, ethanol, carbon dioxide, and formic acid. Some examples of homofermenters LAB are in the genera of *Lactococcus*, *Streptococcus*, *Pediococcus*, *Enterococcus*, and some species of *Lactobacillus* (e.g., *Lactobacillus delbrueckii* subsp. *bulgaricus*, *Lactobacillus acidophilus*, *Lactobacillus gasseri*, among others). For heterofermenters, these are *Leuconostoc*, *Oenococcus*, and certain *Lactobacillus* species (e.g., *Lactobacillus intestinalis*, *Lactobacillus jensenii*, *Lactobacillus psittaci*, among others) (Kleerebezem and Hugenholtz 2003).

Homofermentative LAB use the Embden-Meyerhoff-Parnas (EMP) pathway. Glucose, for example, is converted to lactic acid (per molecule of glucose consumed, two molecules of lactic acid are produced). Fructose-1,6-diphosphatase is the crucial enzyme in this pathway. Two

molecules of ATP are generated from one glucose molecule via substrate-level phosphorylation. Heterofermentative LAB use the phosphoketolase pathway (PKP). Using this pathway, LAB transform one molecule of glucose into one molecule of lactic acid, CO₂ and ethanol. Heterolactic fermentation results in a net gain of one molecule of ATP per molecule of glucose consumed (Endo and Dicks 2014).

Some LAB metabolize disaccharides such as cellobiose, lactose, maltose, melibiose, sucrose, among others. These sugars are transported across the cell membrane as free sugars or phosphorylated. Then, they are split into two monosaccharides or a monosaccharide and a monosaccharide phosphate. The products are metabolized via one of the pathways described above (EMP or PKP). Also, many LAB can metabolize pentoses, such as arabinose, ribose, xylose, and related carbohydrates such as gluconate. The compounds are generally transported into cells by permeases and metabolized by the phosphoketolase pathway (Kleerebezem and Hugenholtz 2003).

In addition to sugars, several LAB species can metabolize citrate, converting citrate into oxaloacetate and then into pyruvate and CO₂. Citrate fermentation by LAB leads to producing four-carbon compounds, such as diacetyl, acetoin, and butanediol, which have aromatic properties.

Some LAB can direct sugar metabolism toward the biosynthesis of exopolysaccharides. These long-chain polysaccharides can be loosely attached to the cell surface, forming capsules or secreting to their external environment. They are classified into homopolysaccharides consisting of one type of monosaccharide and heteropolysaccharides composed of different types of monosaccharides. Both groups are synthesized extracellularly by glycosyltransferase enzymes such as glucan or fructan sucrases (Mayo et al. 2010).

The proteolytic system and amino acid catabolism are also featuring the LAB metabolism. These bacteria have proteinases that hydrolyze proteins into peptides and peptidases that hydrolyze peptides into free amino acids. These amino acids are further used to generate volatile compounds responsible for the organoleptic properties (i.e., aroma profile) of fermented milk products (Savijoki et al. 2006).

1.1.3. Industrial applications of lactic acid bacteria, given their functional properties

As described above, LAB have vast metabolic characteristics; thus, these bacteria present different functional properties, which allow a broad range of industrial-scale applications. LAB are essentially used in the fermented food industry (as the primary sector), the functional food, and the chemical industry.

Table 1.3 presents these three-main industrial sectors, their applications, and a few LAB examples that have been reviewed. Note from Table 1.3 that the LAB often used in the fermented food industry are the genera of *Lactococcus*, *Streptococcus*, *Lactiplantibacillus*, and

Lactobacillus. Some LAB of the genus *Lactobacillus* and *Lacticaseibacillus* are also used in functional food production.

Table 1.3 Some examples of Lactic Acid Bacteria (LAB) species used for different industrial applications.

	LAB species	Industrial application	References
Fermented food industry	<i>Lactobacillus delbrueckii</i> and <i>Streptococcus thermophilus</i>	Yogurt production	(Granier et al. 2013; Nagaoka 2019)
	<i>Lactococcus lactis</i> , <i>Lactobacillus acidophilus</i> , <i>Lactobacillus helveticus</i> , and <i>Lactobacillus kefir</i>	Cheeses and fermented milk	(Wilkinson and LaPointe 2020)
	<i>Lactiplantibacillus plantarum</i> , <i>Lactobacillus curvatus</i> , <i>Lactobacillus acidophilus</i> , <i>Latilactobacillus sakei</i> , <i>Lacticaseibacillus casei</i> , <i>Lacticaseibacillus paracasei</i> , <i>Limosilactobacillus fermentum</i> , and <i>Fructilactobacillus sanfranciscensis</i>	Fermented vegetables and cereals	(Ashaolu and Reale 2020)
	<i>Lactiplantibacillus plantarum</i> , <i>Lactobacillus acidophilus</i> , <i>Latilactobacillus curvatus</i> , <i>Latilactobacillus sakei</i> , <i>Staphylococcus carnosus</i> , <i>Pediococcus pentosaceus</i>	Fermented meat	(Ojha et al. 2015)
	<i>Enterococcus faecium</i> , <i>Pediococcus damnosus</i> , <i>Weisella confusa</i> , <i>Levilactobacillus brevis</i> , <i>Leuconostoc mesenteroides</i> , <i>Lactiplantibacillus plantarum</i> , <i>Lacticaseibacillus casei</i> , <i>Lactobacillus suebicus</i> , and <i>Lactobacillus delbrueckii</i>	Food-fermented additives Exopolysaccharides	(Daba et al. 2021; Soumya and Nampoothiri 2021)
	<i>Enterococcus faecium</i> , <i>Lactococcus lactis</i> , <i>Streptococcus gallolyticus</i> , and <i>Pediococcus pentosaceus</i>	Food-fermented additives Bacteriocins	(Daba and Elkhateeb 2020; Hernández-González et al. 2021)
Functional food	<i>Lactobacillus delbrueckii</i> , <i>Lactobacillus gasseri</i> , <i>Lactobacillus acidophilus</i> , <i>Limosilactobacillus reuteri</i> , <i>Lactiplantibacillus plantarum</i> , <i>Lacticaseibacillus rhamnosus</i> , <i>Lacticaseibacillus casei</i> , <i>Lacticaseibacillus paracasei</i> , and <i>Leuconostoc mesenteroides</i>	Probiotics	(Evivie et al. 2017; Terpou et al. 2019)
Chemical industry	<i>Lacticaseibacillus rhamnosus</i> , <i>Lacticaseibacillus casei</i> , <i>Lactiplantibacillus plantarum</i> , <i>Lactococcus lactis</i> , <i>Amylolactobacillus amylophylus</i> , <i>Lactobacillus helveticus</i> , and <i>Lactobacillus delbrueckii</i>	Lactic acid production	(Alves de Oliveira et al. 2018; Abedi and Hashemi 2020)
	<i>Limosilactobacillus reuteri</i> , <i>Limosilactobacillus fermentum</i> , <i>Lentilactobacillus buchneri</i> , <i>Levilactobacillus brevis</i> , and <i>Lactococcus lactis</i>	Formic acid, acetic acid, propionic acid, butyric acid, succinic acid, and 3-hydroxy propionic acid	(Hatti-Kaul et al. 2018; Carvalho et al. 2021)

In the chemical industry, these latter genera (*Lactobacillus* and *Lacticaseibacillus*) are used to produce lactic acid. Other organic acids such as formic acid, acetic acid, propionic acid, butyric acid, succinic acid) are generally produced by *Limosilactobacillus*, *Lentilactobacillus*, *Levilactobacillus*, and *Lactococcus*.

The following paragraphs summarize each industrial sector (fermented food industry, functional food, and chemical industry), highlighting its main applications and economic relevance.

1.1.3.1. The fermented food industry

Fermented food is a significant part of human nutrition, dietary supply, and calorie intake. The fermented food includes five main applications, which consider the acidifying activity of LAB; i.e., their capacity to produce specific molecules, such as lactic acid:

- (i) Dairy products: fermented milk, dairy desserts, cheeses, cream, and yogurts
- (ii) Cereals and vegetables: sourdough, wheat, rice, green olives, cabbage, capers, and pickles.
- (iii) Fermented meat: sausages and goat meat.
- (iv) Food-fermented additives: exopolysaccharides.
- (v) Bacteriocins.

Among these applications, fermented dairy products have gained interest among consumers. Yogurt, for example, is one of the fastest-growing markets in the world of fermented food products. The global yogurt market is prognosticated to grow at a CAGR of 4.8% of CAGR by 2027 (Mordor intelligence, Yogurt market). The CAGR, the Compound Annual Growth Rate, is the mean annual growth rate of a product over a specific period longer than one year. The other fermented foods (dairy products, vegetables, cereals, and meat) use a large diversity of LAB, such as *Lactiplantibacillus plantarum*, *Lactobacillus curvatus*, *Lactobacillus acidophilus*, *Lactobacillus sakei*, among others (Table 1.3).

Some LAB species are known to produce exopolysaccharides (EPS). The role of EPS from LAB as gelling, thickeners, emulsifiers, stabilizers, water-binding, and viscosifying agents represents a tremendous interest in dairy and cereal-based products (Mårtensson et al. 2001; Katina et al. 2009; Lorusso et al. 2018).

Bacteriocins excreted by LAB (Table 1.3) are antimicrobial cationic and hydrophobic peptides used as food preservation ingredients. For instance, Nisin A (a commercial bacteriocin from LAB, BioSafe™) is added to some cheeses (e.g., cottage, feta) to prevent off-flavors and late blowing caused by clostridia (Chikindas et al. 2018).

1.1.3.2. The functional food industry

Functional food is referred to food that has been demonstrated to affect beneficially one or more target functions in the host, beyond the adequate nutritional effects and in a way that is relevant to either an improved state of health or reduction of risk of disease (Stein and Rodríguez-Cerezo 2008). In this context, functional food ingredients can be probiotic bacteria. Probiotics are "living microorganisms which, when administered in adequate amounts, confer a health benefit on the host" (Food and Health Agricultural Organization of the United Nations-World Health 2002). These bacteria should be viable and resistant to gastric acids and bile salts during their passage through the stomach, duodenum, and intestine.

Probiotics consumption in recent years has increased due to health care awareness of the global population. Thus, the economic development of this market segment has increased due to the rise in demand. The global probiotics market is projected to increase by 8.3% CAGR during 2021-2026 (Markets and Markets, Probiotics market).

The inclusion of probiotics in yogurts has been gaining popularity since it represents a practical way to consume them. The probiotic yogurt market, for example, is expected to increase by 6.3% CAGR through 2031 (Future market insights, Probiotic yogurt market).

These market tendencies lead to focus research studies on the design of carrier matrices and the selection of bacterial strains to enhance bacterial survival at each step of their production until their consumption (Champagne et al. 2005, 2018).

1.1.3.3. The chemical industry

Lactic acid is an organic acid with a hydroxyl group and asymmetric carbon. Lactic acid production via fermentation has several advantages over chemical syntheses, such as low-cost substrates, relatively lower temperatures, lower energy consumption, and better environmental concerns (John et al. 2007; Mussatto et al. 2008; Wang et al. 2015).

Lactic acid represents an interesting chemical compound for producing renewable plastic and biodegradable in industrial composting, i.e., polylactic acid (PLA). The PLA market is increased due to the increased consumption of biodegradable plastic packaging and is estimated to increase by 12.2% CAGR by 2026 (Markets and Markets, Polylactic Acid market).

In addition, LAB can produce organic acids such as formic acid, acetic acid, propionic acid, butyric acid, succinic acid, and 3-hydroxy propionic acid through glycerol metabolism. These molecules hold a strong potential as building blocks for the chemical industry (Hatti-Kaul et al. 2018; Carvalho et al. 2021).

Sum-up of section 1.1

Lactic acid bacteria composition and industrial applications

- Lactic Acid Bacteria (LAB) are a heterogeneous group of Gram-positive, and they can be homofermentative or heterofermentative.
- LAB consist of a cytoplasm where genetic material is found, a cytoplasmic membrane, and a cell wall.
- The primary lipid membranes in LAB are phospholipids and glycolipids. The most common phospholipids in LAB are phosphatidylglycerol (PG) and cardiolipin (CL). The principal glycolipid structures found in LAB are diacylglycerol (DG) bound to galactose (Gal) or glucose (Glc).
- The fatty acids in the LAB membrane often have aliphatic chains from 12 to 22 carbons, involving saturated and unsaturated carbons. The fatty acyl chain structure and geometry govern the lipid's shape and the degree of lipid packing within the bilayer.
- The membrane proteins are bound to the membrane or anchored via several transmembrane domains and are involved in several cellular functions. For example, cell growth, division, and integrity maintenance, among others.
- The cell wall is characterized by a peptidoglycan layer, which functions as a scaffold for attaching other components such as teichoic acids, polysaccharides, and proteins.
- LAB are used in a broad range of industrial-scale applications. These bacteria are essentially used in the fermented food industry (dairy, vegetables, meat, and food additives), the functional food industry (probiotics), and the chemical industry (lactic acid and polylactic acid production).

1.2. Production of lactic acid bacteria: stabilization and storage, critical steps that induce cell damages

Owing to the numerous industrial applications of LAB, particularly in the fermented and functional food sectors, industries have increased the production of LAB. These bacteria are commonly produced as highly concentrated cultures called starter cultures in a frozen or dried matrix. Starter cultures are used to inoculate any food matrix in order to provide the food products with chemical changes (e.g., metabolites production such as lactic acid or proteolytic activities) and sensorial qualities (e.g., flavor compounds and desired texture) (Medina-Pradas et al. 2017).

This section aims to give a general overview of the different steps involved in LAB production at both the lab and industrial scales. Then, the methods to determine the functional properties of LAB after their industrial production. Applying these methods is a systematic activity carried out to ensure the quality of the product (i.e., LAB's functional properties).

This section will focus on the two last steps of their production, stabilization and storage, responsible for LAB cell damage.

1.2.1. Multi-step production of lactic acid bacteria

The industrial production of concentrated lactic acid bacteria proceeds according to the main twelve steps described in the following subsections and Figure 1.6.

1.2.1.1. Medium preparation and sterilization (steps ①-②)

The choice of culture medium for LAB (step ①, Figure 1.6) is essential for getting a sufficient biomass concentration. It should always contain a carbon source (e.g., lactose, maltose, sucrose, glucose), nitrogen sources (e.g., yeast extracts, peptone, amino acids), vitamins, and mineral elements to enhance the bacterial growth (Snell 1945; Reuter 1985; Endo et al. 2019). In addition, the media must also have good solubility characteristics of their components and heat stability.

The composition of the medium is adapted to the particular nutritional needs of each strain. Carbohydrates such as lactose, glucose, and fructose are used indifferently as a carbon source for *Lactobacillus acidophilus*, *Lacticaseibacillus casei*, *Lactiplantibacillus plantarum*, and *Lactobacillus delbrueckii* subsp. *bulgaricus*. Some LAB of the *Lactococcus* genus can use sugars other than lactose, such as raffinose and mannitol (Batt 2014). Concerning vitamins, most LAB of the *Streptococcus* genus requires niacin, pantothenic acid, pyridoxine, biotin, and nitroflavin for growth. In contrast, LAB of the *Lactobacillus* genus only require niacin, pantothenic acid, and nitroflavin, with some of them also requiring cobalamin (Mäyrä-Mäkinen and Bigret 2004). The LAB cultures at the laboratory scale generally use the standard media of Man, Rogosa, and Sharpe, abbreviated to MRS (De Man et al. 1960) and the standard media M17 (Terzaghi and Sandine 1975).

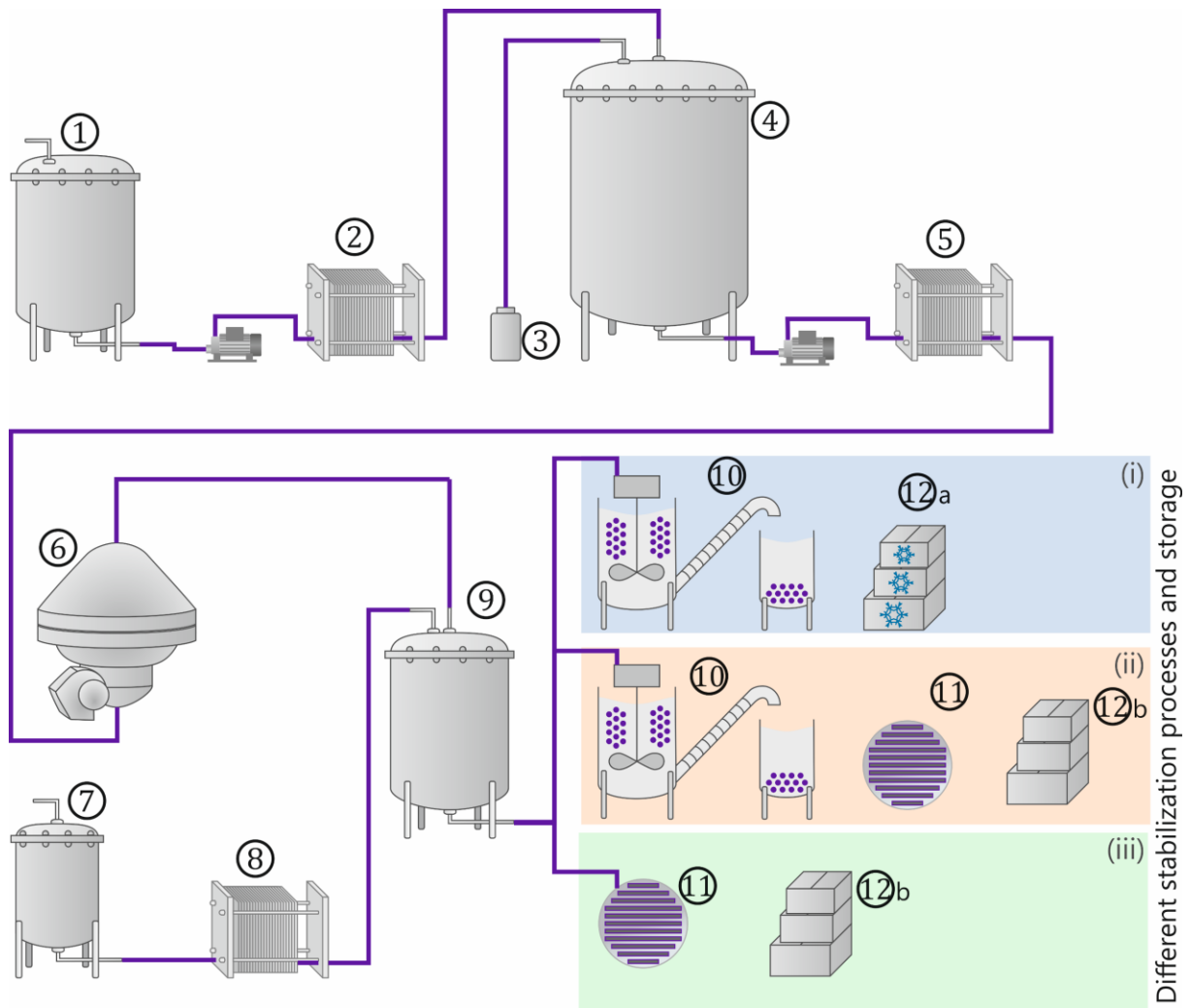


Figure 1.6 Multi-step production of concentrated lactic acid bacteria. ① Fermentation medium preparation; ② Fermentation medium sterilization; ③ Inoculation; ④ Fermentation at controlled temperature, pH, and stirring; ⑤ Cooling and harvest; ⑥ Concentration by centrifugation; ⑦ Protective solution preparation; ⑧ Protective medium sterilization; ⑨ Preparation of protected bacterial suspension. Three strategies to stabilize lactic acid bacteria suspensions are highlighted by colored transparent boxes: ⑩ Freezing by pellet granulation; ⑪ Freeze-drying; ⑫ Storage at (a) a negative temperature (frozen storage) and (b) a room or refrigerated temperature. Adapted from Béal et al. 2008; Chen and Hang 2019.

The MRS medium contains glucose, whereas the M17 medium contains lactose as a carbon source. Another difference between both media is the different vitamins and salt content (Annex A.3). MRS is often used for the genera *Lactobacillus*, *Lentilactobacillus*, *Lacticplantibacillus* and *Limosilactobacillus*. M17 is suitable for the growth of bacteria from the genera *Lactococcus*, *Pediococcus*, *Streptococcus*, among others (Fonseca et al. 2015; Hayek et al. 2019).

The LAB cultures at an industrial scale mostly use semisynthetic media whose ingredients are similar to MRS or M17 (Altaf et al. 2007; Hayek et al. 2013; Blajman et al. 2020). Also, media

based on milk and whey supplemented with salts and nitrogen sources are used to cultivate LAB on the large scale production (Macedo et al. 2002; Bulatović et al. 2014).

After culture medium preparation, the medium must undergo heat treatment to eliminate contaminating microorganisms (Figure 1.6 ②). This heat treatment is usually achieved by exposing the culture medium to an elevated temperature (between 110°C and 125°C) for a predetermined time. Also, filtration methods can be applied to sterilize the culture medium and avoid sugar caramelization, protein denaturation, and some vitamins inactivation (Walker 2014).

If a heat treatment is applied, the temperature and time combination must be optimized to eliminate the contaminating microorganisms without changing the culture media composition (Senz et al. 2019). The culture medium is then cooled to the fermentation temperature, and pH is adjusted to the optimal value for the LAB growth.

1.2.1.2. Strain conditioning and inoculation (step ③)

In the LAB stock collection of laboratories or industries, the LAB strains are usually frozen or freeze-dried. Thus, LAB should be reactivated to use them as inoculum for the fermentation step.

At the laboratory scale, before inoculation to Erlenmeyer flasks or lab-scale bioreactors, one or two precultures are prepared to reactivate the frozen/freeze-dried LAB stock. Precultures are often carried out at the same temperature and culture medium used during fermentation. At the industrial scale, specific nomenclature is used to define precultures. A first preculture is mother culture (obtained from industrial stock LAB collection). The second preculture is an intermediate working culture (Figure 1.6 ③). The volume of the intermediate working culture is higher than the mother culture to inoculate the appropriate cell concentration into the bioreactor (Chen and Hang 2019). Direct inoculation can also be carried out at an industrial scale by introducing frozen or freeze-dried concentrated bacteria into the bioreactor. This type of inoculation is known as direct-to-vat set cultures (Hutkins 2018).

1.2.1.3. Fermentation (step ④)

The objective of the fermentation step is to obtain the highest possible cell concentration and functional property according to the LAB application (e.g., acidifying activity for fermented dairy products) (Béal et al. 2008).

Fermentation is often carried out in an instrumented bioreactor (Figure 1.6 ④), either in batch or, in some cases, fed-batch or in a continuous process (Chen and Hang 2019). The fermentation is performed under controlled conditions of temperature, pH, and agitation at optimal conditions for the growth of the strain.

The growth is favored when the temperature is kept constant: the temperature is set before inoculation and controlled throughout the fermentation duration. The temperature is usually

set at the optimal value for cell growth. Studies have reported that optimal temperature for growth is genus-dependent (Vinderola et al. 2019). For example, the optimal temperature for mesophilic LAB is 20-30°C (e.g., *Lactococcus lactis* subsp. *lactis*, *Lactococcus lactis* subsp. *cremoris*, *Leuconostoc mesenteroides* subsp. *cremoris*, and *Leuconostoc lactis*). For thermophilic LAB, the optimal temperature is 35-45°C (e.g., *Streptococcus thermophilus*, *Lactobacillus delbrueckii* subsp. *bulgaricus*, *Lactobacillus acidophilus* and *Lactobacillus helveticus*) (Carminati et al. 2010).

The fermentation is generally performed at regulated pH. The pH is usually regulated either by adding an external neutralizer (e.g., hydroxide salts like ammonium, sodium, or potassium hydroxide) or by internal control through a neutralizing agent (e.g., sodium carbonate encapsulated in magnesium stearate) (Whitehead et al. 1993). Uncontrolled pH fermentations are seldom carried out for LAB starter productions due to a low biomass production obtained compared to LAB pH-regulated cultures (Cachon et al. 1998; Savoie et al. 2007). The pH choice is LAB genus dependent and, in some cases, strain-dependent. For example, the optimal pH for growth is 5.5-6.5 for *Streptococcus thermophilus*. The optimal pH is 6.5 for some LAB of the genus *Lactococcus*. LAB of the genus *Lactobacillus* usually grow best under slightly low controlled-pH conditions (pH 5.5-6.0) (Vinderola et al. 2019).

Although the temperature and pH set to the optimum for growth favor the cell biomass production, changing the optimum pH and temperature conditions may reduce the loss of LAB functional properties during the final steps of LAB production (freezing or freeze-drying and storage). This strategy is reviewed in subsection 1.3.3 (Table 1.5).

Stirring should be fair enough to maintain the homogeneity and facilitate temperature and pH control of the medium. High stirring speed is unnecessary since most LAB do not require oxygen to produce their intracellular energy. Some LAB, instead, are aero-tolerant bacteria, such as *Lactobacillus delbrueckii* subsp. *bulgaricus* and *Lactococcus lactis* subsp. *cremoris* (Marty-Teyssset et al. 2000; Duwat et al. 2001).

Directly monitoring of LAB growth is carried out by an optical density (Kiviharju et al. 2008) or electric conductivity probe (Arnoux et al. 2005). These probes are introduced into the bioreactor. Thus, the measurements can be done continuously and *in situ*.

Another indirect measurement to monitor LAB growth can be applied, for instance, gradually adding the neutralizing agent into the bioreactor to control the pH. This method can be performed online to monitor the growth, the concentration of the substrate, and the metabolites produced (Béal and Corrieu 1995).

In all cases, the LAB growth monitoring is carried out through a growth curve showing the cell concentration as a function of time. A growth curve exhibits distinct phases: the lag phase, the exponential phase, the deceleration phase, the stationary phase, and the death phase (Figure 1.7).

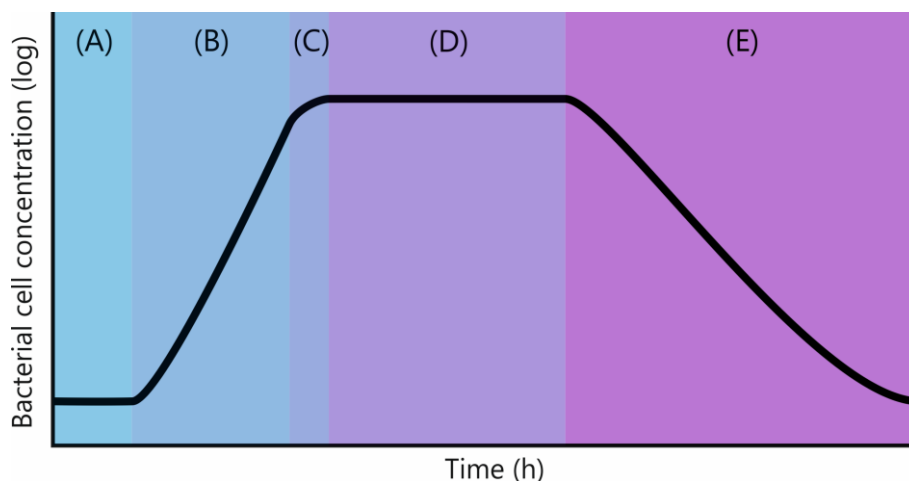


Figure 1.7 Schematic representation of a bacterial growth curve, indicating the different growth phases in bacteria. (A) the lag phase; (B) the exponential (log) phase; (C) the deceleration phase; (D) the stationary phase; (E) the death phase. Adapted from Garrison and Huigens 2017.

The initial phase is the lag phase, where the cells, newly inoculated in the fermentation medium, adjust their metabolism to their new environment. They are, thus, metabolically active, but no growth is observed. Cellular growth starts when the cells are ready to undertake all the biological reactions necessary for cell division. Then, the exponential or log phase comes. During this phase, the metabolic activity is at its highest and cell concentration doubles after each generation. Eventually, cells reach the stationary phase. During the stationary phase, the number of dividing cells equals the number of dying cells, thus resulting in no overall growth. The accumulation of metabolites such as lactic acid and the less available amount of substrate create unfavorable conditions for proper metabolic activity and directly provoke starvation or energy depletion, causing cell death (Konings et al. 1997).

1.2.1.4. Cooling and harvest (step ⑤)

When the fermentation is stopped to harvest, the culture medium is cooled to a temperature between 15°C and 20°C (Figure 1.6 ⑤). It is generally carried out with the help of a pump, which allows the passage of the fermented medium through a heat exchanger associated with an adapted cooling circuit. This cooling step slows down the metabolic activity and growth of the cells (Béal et al. 2008).

At the industrial scale, LAB are generally harvested in the stationary growth phase, where the highest cellular concentration is observed.

The harvest time has been reported to affect LAB's physiological state (e.g., cell size, acidifying activity, viability, among others) of LAB. For instance, small cell size and low specific acidifying activity were observed with an increase in the harvest time (from the exponential to stationary growth phase) for *Lactococcus lactis* subsp. *lactis* DGCC1212 (Hansen et al. 2016). Similarly, a decrease in acidifying activity was reported at increased harvest time for *Carnobacterium maltaromaticum* CNCM I 3298, when cells were cultivated at pH 9.5 (Girardeau et al. 2019).

Likewise, the harvest time affects LAB survival in the following production steps, stabilization and storage process. Further details are given in subsection 1.3.3, Table 1.5.

1.2.1.5. Concentration and protection (steps ⑥-⑨)

The concentration separates the bacterial cells from the culture medium to obtain the highest possible bacterial concentration in a reduced volume (Figure 1.6 ⑥). The concentration factors are between 10 and 40, allowing a cell concentration of 10^9 - 10^{11} CFU·mL⁻¹ (Colony Forming Unit, CFU) (Vinderola et al. 2019).

Centrifugation is the most widely used concentration method on an industrial scale because of the low viscosity of the medium. When LAB strains produce extracellular polysaccharides in a culture medium, the viscosity in the culture medium is increased. A high centrifugation speed is required in this condition to achieve the desired recovery (Mäyrä-Mäkinen and Bigret 2004).

Membrane separation technology (e.g., microfiltration, ultrafiltration) is a potential alternative to centrifugation methods but is less common at an industrial scale (Chen and Hang 2019).

Washing the bacterial pellet obtained after concentration is a common industrial and lab practice to neutralize the solution and remove the residual fermentation compounds. The washing solution most often contains mineral salts such as sodium, potassium phosphate, glycerophosphate, magnesium sulfate, or sodium chloride. The harvested, washed, and concentrated cells are suspended in protective solutions. These solutions reduce the detrimental effects of the next stabilization step (i.e., freezing or freeze-drying) and storage (Hubálek 2003). Protective solutions consist of concentrated solutions of molecules. These molecules have low volatility, are soluble in water, and have no toxic character. They are prepared and sterilized (Figure 1.6 ⑦ and ⑧) before being added and homogenized with LAB concentrates (Figure 1.6 ⑨). Some examples of protective molecules that have been used for LAB are the following: polyols (e.g., glycerol and sorbitol), sugars (e.g., sucrose and trehalose), dairy proteins (e.g., skim milk and whey protein), and polysaccharides (e.g., fructo-oligosaccharides, galacto-oligosaccharides, inulin, and maltodextrin) (Carvalho et al. 2004a). In subsection 1.3.3, the positive effect of these protectors and their mechanisms of protection to LAB cells are reviewed.

1.2.1.6. Stabilization: freezing or freeze-drying (steps ⑩ or ⑪)

This step aims at stabilizing LAB concentrated bacterial suspensions containing a protective solution for long periods while keeping their functional properties for further industrial applications.

The objective of stabilization process is to eliminate most of the available water in liquid form in order to stabilize the cell structures and limit biological reactions.

The most common methods used at an industrial scale are (i) freezing and (ii) freeze-drying. However, other methods such as spray-drying, vacuum drying, and fluidized bed drying are occasionally used to stabilize LAB. These methods employ higher temperatures than freezing or freeze-drying (up to 45°C) (Santivarangkna et al. 2007; Meng et al. 2008; Broeckx et al. 2016).

This subsection is dedicated to introducing general concepts of freezing and freeze-drying. A detailed description of the changes occurring in the matrix (surrounding medium) and in the LAB cells are presented in subsections 1.2.3 and 1.2.4.

i. Freezing

Bacterial suspensions are frozen under temperatures below 0°C (e.g., -50°C, -80°C, or -196°C) and cryo-preserved. At the laboratory scale, lab freezers that reach temperatures of -50°C or -80°C are used to freeze LAB suspensions. At the industrial scale, two manufacturing techniques have been reported to stabilize LAB concentrates (Santivarangkna et al. 2011): (1) Cryogenic granulation (Figure 1.6 ⑩): this method consists of distributing LAB suspensions into liquid nitrogen (-196°C) by a designed liquid dispenser, and the droplets freeze instantly into pellets after a few seconds. The pellets are then conveyed out of the immersion with a mesh-belt conveyor for preparing spherical or hemispherical particles. The diameter of particles prepared by cryogenic granulation is about 0.5–5 mm. Also, (2) freezing is carried out in industrial freezers (-50°C or -80°C), where frozen block LAB suspensions are dispensed in metal cans or plastic containers.

ii. Freeze-drying

This stabilization process is convenient when frozen transportation and storage at sub-zero temperatures are difficult. Freeze-drying is a preservation method based on a cold-drying process that consists of the dehydration of a frozen suspension by sublimation. A piece of freeze-dryer equipment is illustrated in Figure 1.8. It comprises a freeze-dryer drying chamber, shelves or drying trays, a condenser, and a vacuum pump. The samples are placed on shelves fitted into the freeze-dryer chamber. The shelves control and monitor the temperature of the samples (T_{shelf}) throughout the freeze-drying cycle.

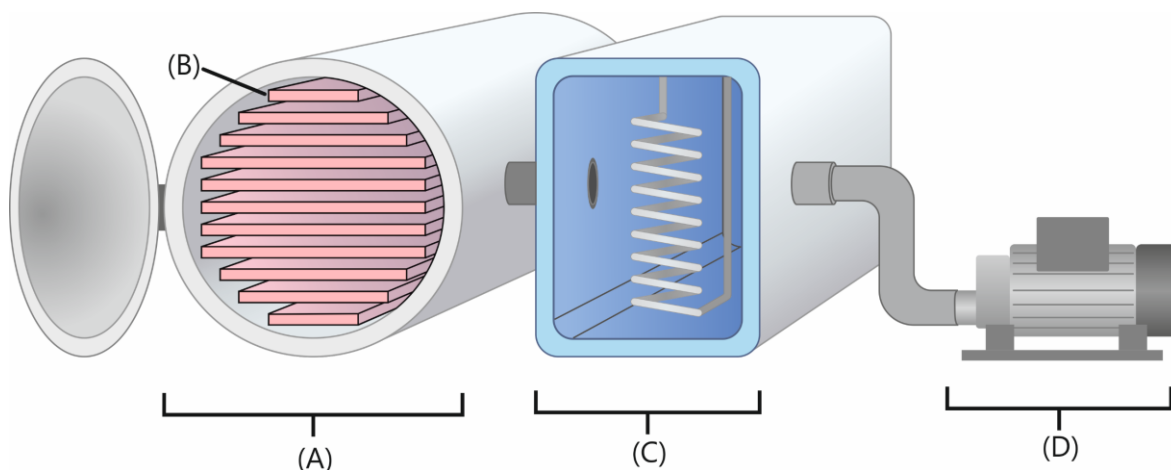


Figure 1.8 The main components of a freeze-dryer. (A) drying chamber; (B) shelves or drying trays; (C) condenser; and (D) vacuum pump. Adapted from Berk 2013.

A freeze-drying cycle involves three stages: (1) freezing, (2) primary drying (sublimation), and (3) secondary drying (desorption) (Figure 1.6 ⑪)

(1) Freezing can be carried out directly on the freeze-dryer shelf. The disadvantage of this method is that the freezing stage is part of the freeze-drying cycle, thus, increasing the usage time of the equipment and energy expenses (Adams 2007).

Samples may be frozen in a freezer or a cooling tunnel before transferring to the freeze-dryer for desiccation. As mentioned above, cryogenic granulation is another freezing method. In this case, pellets are placed into trays or flasks, and sublimation rates are typically very high because the thickness of the dry layer is restricted only by the pellet radius (Figure 1.6 ⑩). Freezing can also be carried out directly on the freeze-dryer shelf. In this case, samples must be transferred to the freeze-drier after precooling the shelves at -50°C (Fonseca et al. 2021).

(2) Primary drying or sublimation describes the process of removing all frozen water from the LAB suspension by sublimation. Finally, (3) the secondary drying or desorption is applied after the sublimation stage, in which the bound water in the sample is removed by desorption (Morgan and Vesey 2009).

1.2.1.7. Frozen and freeze-dried storages (step ⑫)

After the stabilization process, the storage and subsequent distribution of LAB are essential to commercializing these microorganisms.

i. Frozen storage

Frozen storage can be carried out at low (-50°C or 80°C in freezers) or ultra-low temperatures (-196°C in liquid nitrogen containers); in the latter case, cryo-preservation takes place in the liquid or the vapor phase of nitrogen (Santivarangkna et al. 2011).

In research laboratories, the frozen storage can be carried out in lab-scale freezers at -80°C or -50°C , according to the equipment availability. At the industrial scale, distribution and storage

temperatures at the producer, transporter, and the user are around -50°C (Figure 1.6 (12)a). Therefore, special attention must be paid to maintaining the cold chain (Béal et al. 2008).

ii. Freeze-dried storage

Some crucial factors must be considered to keep LAB survival for storing freeze-dried LAB. These factors are (1) the residual moisture content and water activity, (2) the atmospheric oxygen level, and (3) the storage temperature (Broeckx et al. 2016).

(1) After freeze-drying, the remaining water plays an essential role in LAB survival during storage. A good compromise must be found between reducing water activity and keeping a certain amount of water in the dehydrated LAB to keep a satisfactory survival rate. For example, Castro et al. (1995) reported higher survival rates of freeze-dried *Lactobacillus delbrueckii* subsp. *bulgaricus* NCFB 1489 after 40 days of storage when cells were stored at 11% than at 0% or 33% of moisture content. Also, Zayed and Roos (2004) observed an optimum moisture content for the storage freeze-dried *Ligilactobacillus salivarius* subsp. *salivarius* from 2.8 to 5.6%. Later, Kurtmann et al. (2009) demonstrated that freeze-dried storage stability of *Lactobacillus acidophilus* (La-5) depends on a water activity between 0.11-0.43.

(2) Different packaging strategies have been applied to avoid oxygen contact with cells. Decreasing oxygen permeability includes vacuum packaging, higher thickness plastic packaging with low oxygen permeability, multilayer packaging with selective permeability, and active packaging with incorporated oxygen scavengers (Miller et al. 2003a; da Cruz et al. 2007; Tripathi and Giri 2014). Another alternative to reduce the negative effect of oxygen is the addition of antioxidant molecules to the protective solution used to freeze-dry the bacteria (Kurtmann et al. 2009).

(3) The storage temperature of LAB strongly influences their shelf life. Refrigerated storage temperatures ($4-5^{\circ}\text{C}$) generally lead to the highest bacterial survival. For different freeze-dried LAB species, many studies have demonstrated better stability from two to six months at $4-5^{\circ}\text{C}$ compared to room temperatures ($20-30^{\circ}\text{C}$). This temperature range ($4-5^{\circ}\text{C}$) was shown to be beneficial for *Lactiplantibacillus plantarum* (Hongpattarakere et al. 2013; Lee et al. 2016; Savedboworn et al. 2019), *Latilactobacillus curvatus* (Gul et al. 2020a), *Streptococcus thermophilus* (Wang et al. 2004), and *Lactobacillus acidophilus* (Shu et al. 2018; Tang et al. 2020). In general, LAB can be stored at room temperatures for a short period (less than a month), or at refrigerated temperatures ($4-5^{\circ}\text{C}$) for a half year or at -20°C for 2-4 years of shelf life (Figure 1.6 (12)b) (Morgan and Vesey 2009).

1.2.2. Stabilization and storage production steps affect the functional properties of lactic acid bacteria

Before being used in a wide range of industrial applications, LAB suspensions should keep their initial functional properties following the stabilization and storage steps. These steps are critical since LAB cells are exposed to different stresses (further subsection 1.2.4).

The frozen or freeze-dried suspensions contain a combination of viable, injured, and dead cells in variable proportions. For several industrial applications, different methods are commonly used to evaluate the resistance of a global LAB population to freezing, freeze-drying, or storage.

These methods are applied to bacterial suspensions before each stabilization process (after fermentation: initial) and after each stabilization process and storage. Thus, the difference between after and before represents the loss of functional properties, including loss of acidifying activity, culturability, viability, and other technological properties. Each method is briefly summarized in the following subsections:

1.2.2.1. Acidifying activity

The central metabolism of lactic acid bacteria corresponds to the intracellular use of carbohydrates to synthesize lactic acid or other organic acids, together with ATP. The excretion of organic acids leads to a pH decrease in the medium. Acidifying activity corresponds to these microorganisms' capacity to decrease the pH of the medium. The more rapid the pH decrease, the higher the acidifying activity.

Different methods allow the quantification of this phenomenon, for instance, electric conductivity (Carvalho et al. 2003a) and substrate monitoring. The Cinac system (AMS Alliance, Frepillon, France) is the most used in fermented dairy companies to characterize the acidifying activity of a lactic acid bacterium strain. By continuously measuring the pH decrease, this system identifies specific descriptors, such as the time necessary to decrease a difference of pH ($t_{\Delta\text{pH}}$, in min) (Figure 1.9).

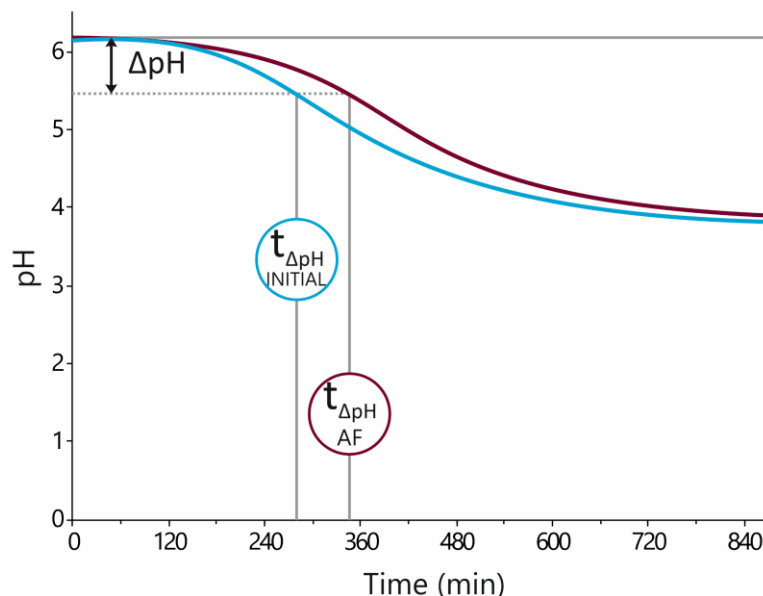


Figure 1.9 pH decreases as a function of the time of *Lactobacillus delbrueckii* subsp. *bulgaricus* CFL1 before (light-blue curve) and after freezing (plum curve). Abbreviations: $t_{\Delta\text{pH}}$ INITIAL and $t_{\Delta\text{pH}}$ AF, the time necessary to decrease a difference of pH (from 6.0 to 5.5) before stabilization process and after freezing, respectively. Adapted from Béal and Fonseca, 2015.

1.2.2.2. Culturability

It is the ability of bacteria to form colonies on agar plates. Culturability measurement (plate count in CFU·mL⁻¹) involves the spread of LAB suspension on an agar medium. Then, the plates are incubated under convenient growth conditions (temperature, anaerobiosis, duration). Subsequently, the number of colony-forming units is enumerated. Loss in culturability can be determined by comparing the plate counts after the stabilization process or storage to the initial cell count before stabilization. This method is often used to determine bacterial survival as a percentage (% survival) (Béal and Fonseca 2015).

1.2.2.3. Viability

Viability is quantified by combining fluorescent staining detected by fluorescent microscopy or flow cytometry. For this purpose, the fluorescent probe carboxyfluorescein diacetate (cFDA) is used. Its small size facilitates its entry into bacterial cells. cFDA is transformed into carboxyfluorescein (cF) by the enzymatic activity of cellular esterases; cFDA stained cells are considered active cells. Also, the combination of cFDA with propidium iodide probe (PI), a nucleic acid dye, can be used to identify the subpopulations in bacterial suspensions: viable (cFDA stained), injured and dead cells (PI stained) (Rault et al. 2007). From an economic point of view, the cost of the flow cytometry method and complex protocols remained relatively high, thus representing a drawback to its development and implementation in the industry.

1.2.2.4. Other functional properties

Other properties and metabolic activities than acidifying activity may be of particular interest depending on the industrial application of the lactic acid bacteria. Probiotic cells, for example, should exhibit resistance to gastrointestinal stress (low pH of gastric juice and bile salts presence) since these microorganisms display a beneficial effect on the health of the host's gastrointestinal tract. Resistance to gastrointestinal stress is generally determined by comparing culturability measurements before and after the stress. It is measured either in static conditions, e.g., by setting the cells in the presence of acidic conditions and bile salts at 37°C for about 1 hour or in dynamic conditions by using bioreactors that simulate digestion (Mainville et al. 2005; Sumeri et al. 2010; Madureira et al. 2011).

Some other technological properties include (i) flavoring and texturing properties measured by enzymatic activities of LAB and exopolysaccharides production; (ii) the production of CO₂ by heterofermentative lactic acid bacteria; and (iii) inhibitory activities by quantifying the production of bacteriocins (Béal et al. 2008).

1.2.3. Changes in the matrix of LAB suspensions during stabilization and storage

LAB suspensions and their constituents undergo a physical state change during the stabilization processes and storage, from a liquid state before the stabilization process to a solid state (frozen or dried).

A detailed description is given in this subsection to understand the significant transitions occurring in the LAB suspensions when they are frozen or freeze-dried.

1.2.3.1. Freezing

The physical transitions during freezing are schematically illustrated in Figure 1.10. It considers the freezing of a sucrose solution at 20% w/w as a function of time. Sucrose is widely used as a cryo-protectant at this concentration in LAB suspensions. Since LAB cells have a negligible influence on the physical behavior of the matrix following freezing (Fonseca et al. 2001b; Béal and Fonseca 2015), the cryo-protective solution can be used as a fair example to explain the events taking place during freezing. These events are summarized as three consecutive phases (Figure 1.10).

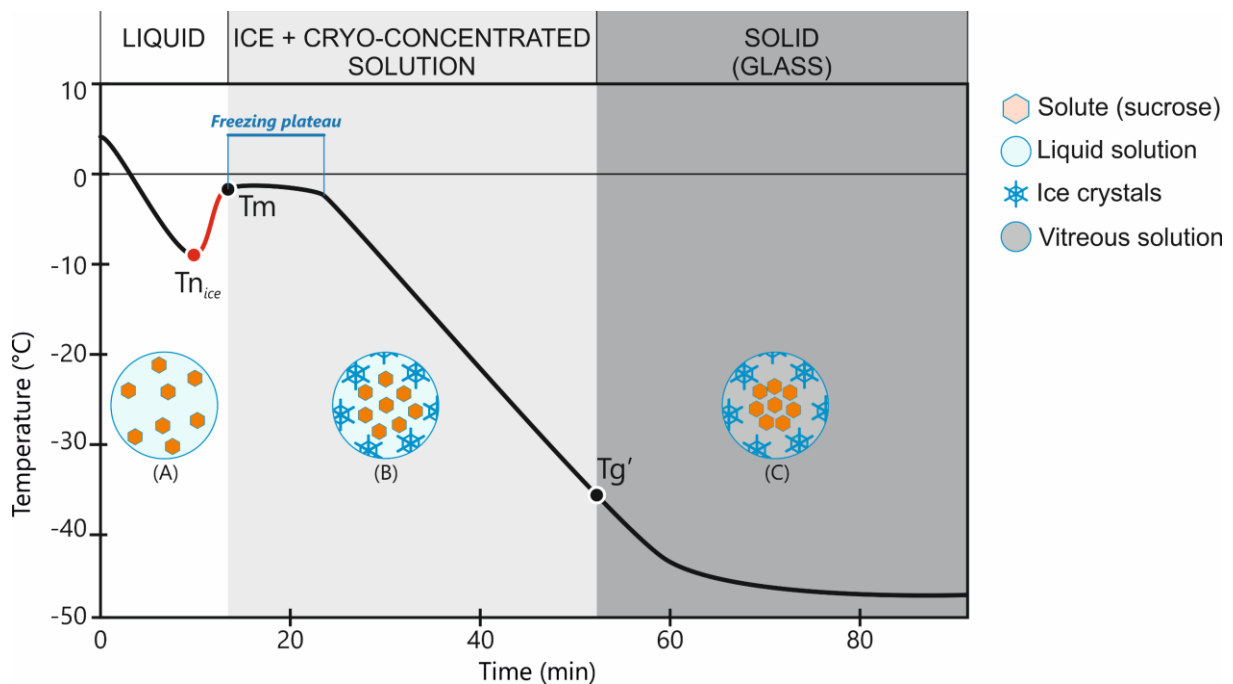


Figure 1.10 Sucrose solution temperature profile and principal phenomena during freezing at slow cooling rate ($\leq 10^{\circ}\text{C}\cdot\text{min}^{-1}$). The schematic representation of the physical state of sucrose solution is illustrated by (A) liquid, (B) cryo-concentrated, and (C) solid state. Abbreviations: T_n , nucleation temperature in $^{\circ}\text{C}$; T_m , ice melting temperature in $^{\circ}\text{C}$; $T_{g'}$, glass transition temperature at the maximally freeze-concentrated solution in $^{\circ}\text{C}$. Adapted from Béal and Fonseca 2015.

i. The temperature decreases below 0°C

A first phase is observed when the temperature decreases to subzero temperatures before ice nucleation (Figure 1.10 (A)). The temperature decrease ends when the first ice crystals appear at the nucleation temperature (T_n). When the ice forms, the exothermic nature of water crystallization results in a temperature solution increase up to the ice melting temperature (T_m). Then, a temperature plateau is observed (*Freezing plateau* in Figure 1.10), representing a metastable physical state where the constituents are kept in liquid form, slightly below the T_m .

ii. Cryo-concentration

As ice forms, the solute concentration of the unfrozen phase increases (Figure 1.10 (B)). The concomitant temperature decrease and solute concentration increase results in a rapid rise in the viscosity of the unfrozen phase. The same phenomenon has also been observed for a glycerol solution, a cryo-protectant medium used to stabilize LAB and different eukaryotic cells (Morris et al. 2006).

iii. The glass transition temperature

The remaining cryo-concentrated phase containing low water content (10-30% from the initial content) follows a glass transition from a viscous liquid to a glassy state. The glassy state is an amorphous-glass metastable state with solid-appearance characteristics, random molecular arrangements, and high viscosity (Figure 1.10 (C)).

The temperature where this transition occurs at the maximally freeze-concentrated solution is called the glass transition temperature (T_g'). In the glassy state, molecular motions become constrained. The glass transition temperature can be determined, for example, by using differential scanning calorimetry (DSC) equipment (Roos and Karel 1991) or Fourier transform infrared spectroscopy (Wolkers and Oldenhof 2021).

1.2.3.2. Frozen-storage

Frozen LAB suspensions' stability during frozen storage depends on the cooling rate applied to freeze this suspension (Fonseca et al. 2006).

In Figure 1.11, a state diagram is presented to illustrate the behavior of a sucrose solution at two different cooling rates. State diagrams provide helpful maps for observing the changes in glass transitions as a function of freeze-concentration.

On the one hand, the blue line in Figure 1.11 represents slow cooling rates (e.g., $<10^{\circ}\text{C}\cdot\text{min}^{-1}$). Slow cooling rates favor ice formation, leading to the maximal cryo-concentrated matrix (80% sucrose concentration). At this point, the glass transition temperature is at the maximally freeze-concentrated solution (T_g'). The T_g' value is approximate -44°C . The sucrose solution can then be stored and stable in a laboratory freezer (-80°C) or industrial freezer (-50°C) because both storage temperatures are below T_g' , corresponding to the glassy state. In this state, the suspensions remain stable since the diffusion of water molecules through the glassy matrix is greatly hindered by high viscosity (from 10^{12} to 10^{14} Pa-s).

On the other hand, the red line in Figure 1.11 represents a rapid cooling rate, i.e., by immersion in liquid nitrogen. This high cooling rate ($>100^{\circ}\text{C}\cdot\text{min}^{-1}$) results in the formation of ice uniformly since solution temperature rapidly drops at -196°C ; thus, a lower glass transition temperature is observed ($T_g \sim -140^{\circ}\text{C}$). Once the sucrose solution is frozen, the sample should be stored at a lower temperature than T_g ($<-140^{\circ}\text{C}$). For this case, if frozen storage is carried out at any other temperature above $T_g \sim -140^{\circ}\text{C}$, the sucrose solution may be found in a viscous liquid

state where ice recrystallization can occur. For example, if this sucrose solution (frozen by immersion in liquid nitrogen) were stored at -80°C (laboratory freezer) or -50°C (industrial freezer), i.e., above its glass transition temperature; the medium would cryo-concentrate during storage as ice formation continues (red dashed lines in Figure 1.11).

1.2.3.3. Freeze-drying

As previously mentioned, the freeze-drying stabilization process includes three main stages: the medium surrounding changes from liquid to frozen and then to a final dried state. These physical changes are detailed in the following paragraphs.

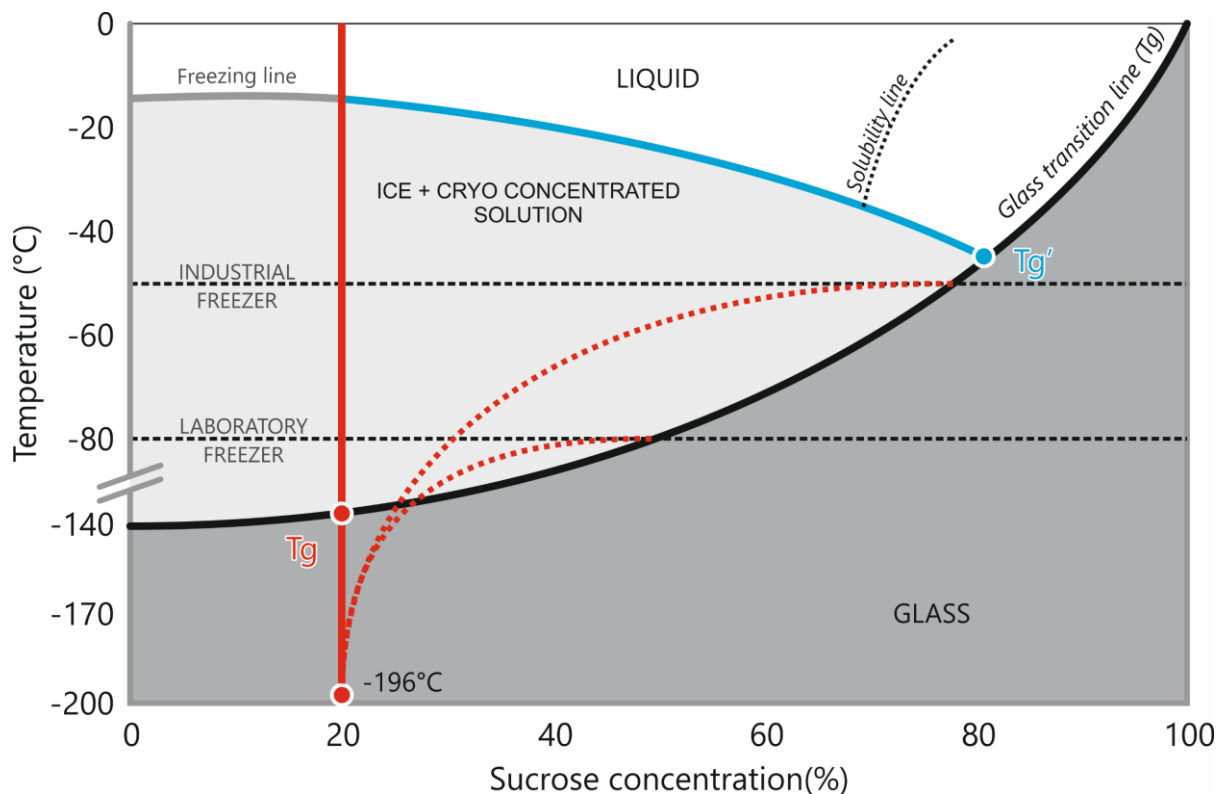


Figure 1.11 State diagram of a sucrose solution frozen at two different cooling rates. Slow cooling rate, $< 10^{\circ}\text{C}\cdot\text{min}^{-1}$ (blue line) and high cooling rate $> 100^{\circ}\text{C}\cdot\text{min}^{-1}$ (red line). Black line represents the glass transition line to determine the T_g . Red dashed lines illustrate the ice recrystallization of the sucrose solution, if it is stored in a laboratory and industrial freezer. Abbreviations: T_g , glass transition temperature in $^{\circ}\text{C}$; T_g' , glass transition temperature at the maximally freeze-concentrated solution in $^{\circ}\text{C}$. Adapted from Roos 2010.

i. Freezing

The freezing stage is the first freeze-drying process, which is crucial for the following primary drying (sublimation). According to the cooling rate applied, the ice crystals formed during freezing impact significantly the subsequent drying behavior, especially in the mass and heat transfer. The freezing stage also determines the morphology and distribution of the pores created during the ice crystal removal in the sublimation stage.

Fast cooling rates enhance the formation of numerous, tiny, randomly orientated ice crystals embedded in an amorphous matrix; as a result, the primary drying time is longer. In contrast, low cooling rates (e.g., $1.0\text{-}5.0^{\circ}\text{C}\cdot\text{min}^{-1}$) induce large contiguous ice crystals reducing the primary drying duration. In this case, the ice crystal removal by sublimation lead to a porous matrix (Adams 2007).

ii. Primary drying or sublimation

Figure 1.12 illustrates the three states of water (solid, liquid, and vapor). These three states coexist at the triple point (blue point in Figure 1.12 (A)). Under atmospheric conditions (101.32 kPa, Figure 1.12 (A)), liquid water is converted into vapor by increasing the temperature, a process defined as vaporization (Figure 1.12 (B)). At sub-atmospheric pressures (0.61 kPa, Figure 1.12 (A)), however, ice (solid) can be converted directly to vapor by sublimation (Figure 1.12 (B)) (Adams 2007).

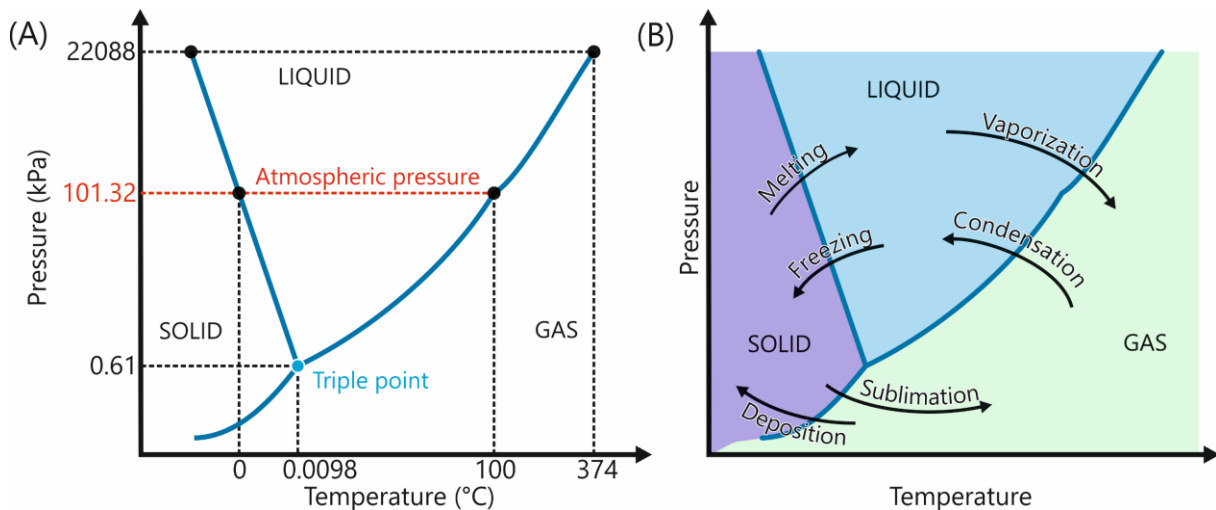


Figure 1.12 (A) The water phase diagram and (B) different state changes on a water phase diagram. The three phases of water meet at a triple point (blue point) where water can coexist in all three states in equilibrium. Red dashed line in (A) represents the atmospheric pressure. Adapted from Yu et al. 2011; Lopez-Quiroga et al. 2012.

The sublimation stage starts when the frozen LAB suspensions, placed inside the freeze-dryer chamber, are at a lower partial pressure of water than the triple point (blue point shown in Figure 1.12). This low pressure ensures the direct conversion of ice into water vapor. Values between 10-20 Pa (0.01-0.02 kPa) have been used to sublimate LAB (Fonseca et al. 2015; Wang et al. 2021).

Once the frozen sample in vials is under vacuum, the temperature of the frozen suspension is increased to speed up the primary drying process. The temperature increase is performed on the shelves containing the vials. Heat is conducted from the shelves through the vial base (Figure 1.13 red-orange arrows).

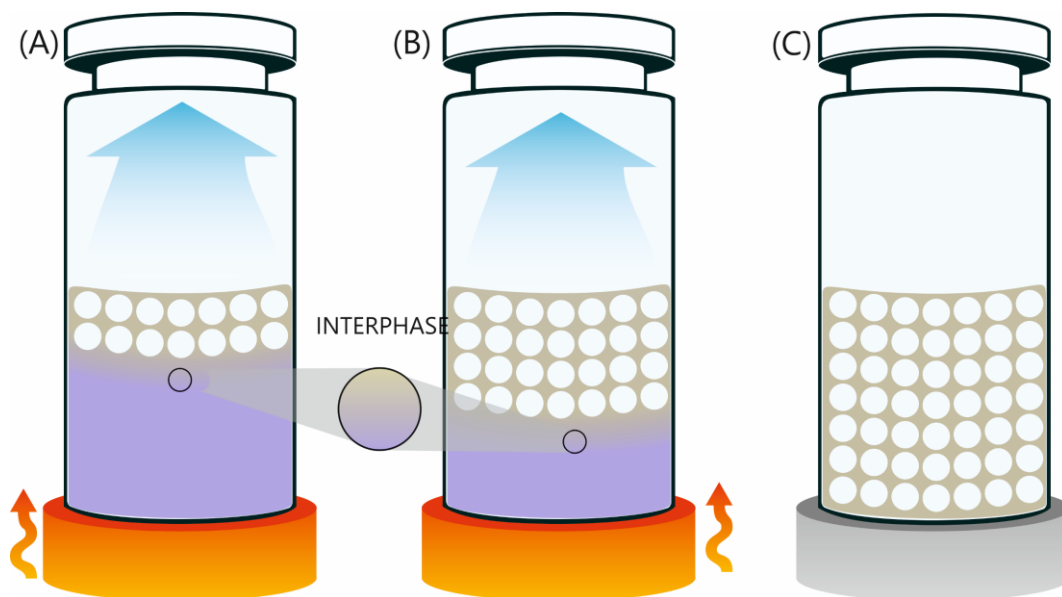


Figure 1.13 Schematic representation of a frozen sample sublimation, placed on a shelf. (A) The beginning of the sublimation: two zones are observed in the sample, frozen (purple color) and dry zone (gray color) with devoid ice crystals (empty circles). Both zones are separated by the sublimation front (interphase) and a light blue up-arrow indicates the water vapor. (B) The progression of the sublimation front (interphase). (C) The end of the sublimation stage, a porous and dried structure is observed in the sample. Red-orange arrows indicate the heat transfer from the shelf to the vial. Adapted from Vorhauer-Huget et al. 2020.

Two distinct zones separated by a narrow phase transition inside the vial can be observed: a frozen and a dry zone (Figure 1.13 (A)). The interface between the two zones is known as the sublimation front, where ice is converted into water vapor. As the sublimation stage progresses, the dry zone becomes devoid of ice crystals, and the sublimation front gradually lowers to the bottom of the frozen zone (Figure 1.13 (B)). Complete ice sublimation from the frozen sample results in an open, porous, dry structure where solutes are spatially arranged as in the original suspension (Figure 1.13 (C)) (Berk 2013).

During sublimation, the increase of sample temperature should be below the temperature at which a loss of the pore structure (collapsed sample) is observed. Collapsed dried samples generally have high residual water content and a longer reconstitution time.

The collapse temperature (T_{coll}), thus, defines the maximum allowable temperature increase for heating a sample (Pikal and Shah 1990).

Collapse temperature can be dynamically measured by direct microscopic observation in a stage at low temperature and low-pressure simulating freeze-drying conditions. T_{coll} is usually close to T_g' (the glass transition temperature of the maximally freeze-concentrated phase for amorphous structures). T_{coll} is about 1-3°C higher than T_g' (Merivaara et al. 2021). For instance, in the case of protective solutions, such as sucrose solution and sorbitol at 10%, their collapse temperatures are -32°C and -45°C, and their T_g' are -33°C and -48°C, respectively (Fonseca et al. 2004). The collapse temperature is higher when adding lactic acid bacteria to protective solutions. For example, *Lactobacillus delbrueckii* subsp. *bulgaricus* CFL1 and *Streptococcus*

thermophilus CFS2 exhibited at T_{coll} of -17°C and -24°C when cells were suspended in a protective solution containing fermented medium. This same protective solution without bacterial cells had a T_{coll} of -43°C and -49°C , respectively (Fonseca et al. 2004). Therefore, the presence of LAB cells and their organization in the dried matrix confers significant robustness to the freeze-dried suspension, allowing higher sublimation temperature during primary drying than the expected one for a protective solution.

iii. Secondary drying or desorption

Following sublimation, there is still an amount of bound water (20-30%) incompatible with the storage stability of freeze-dried samples. Desorption of bound water is achieved when the product is heated at moderate suprazero temperatures ($20-30^{\circ}\text{C}$) by increasing shelf temperature and reducing the vapor pressure inside the freeze-drying chamber. Secondary drying can be performed at elevated temperatures because the ice has been removed during the primary drying, and the risk of melting or collapsing is minimal (Merivaara et al. 2021).

Increasing the temperature gets rid of the remaining water from the sample. The freeze-drying process is completed when most of the water is removed, yielding a structurally stable dried product with preferably less than 12% of residual water (Bhushani and Anandharamakrishnan 2017).

1.2.3.4. Freeze-dried storage

Once the freeze-dried LAB suspension is under atmospheric pressure (101.32 kPa), it has a low water content combined with high porosity, providing the ability to rehydrate instantly.

During storage, the stability of bacteria depends mainly on the physical state of the matrix and the protective solution. The physical state of the amorphous matrix (sugar and cells) remains stable if the sample is stored under a lower temperature than the glass transition temperature (T_g). Above T_g , there is an exponential increase in molecular mobility and viscosity decrease, which govern non-enzymatic reactions (Jouppila and Roos 1994; Buera and Karel 1995; Roos 2004; Buera et al. 2005). In contrast to frozen storage, the values of T_g in freeze-dried samples are positive since the water was removed by desiccation.

Sugars solutions have been extensively used as protective solutions in freeze-dried LAB suspensions. These molecules are known to increase the glass transition temperatures. Cells are embedded in a highly viscous state matrix thanks to their glass-forming properties. The values of T_g vary according to the sugar (Annex A.4). Polysaccharides such as dextran and starch, for example, exhibit significant higher glass transition temperatures compared to sucrose and trehalose (200°C and 225°C vs. 62°C and 115°C).

The effect of the remaining water in the freeze-dried sample is another factor to consider for the stability of the amorphous matrix. Water may act as a plasticizer and decrease the freeze-dried samples' glass transition temperature (Passot et al. 2012).

To illustrate the relationships among water content, water activity, and glass transition temperature, an example is presented in Figure 1.14 for a freeze-dried *Lactobacillus delbrueckii* subsp. *bulgaricus* CFL1 suspension in the presence of sucrose at 20%.

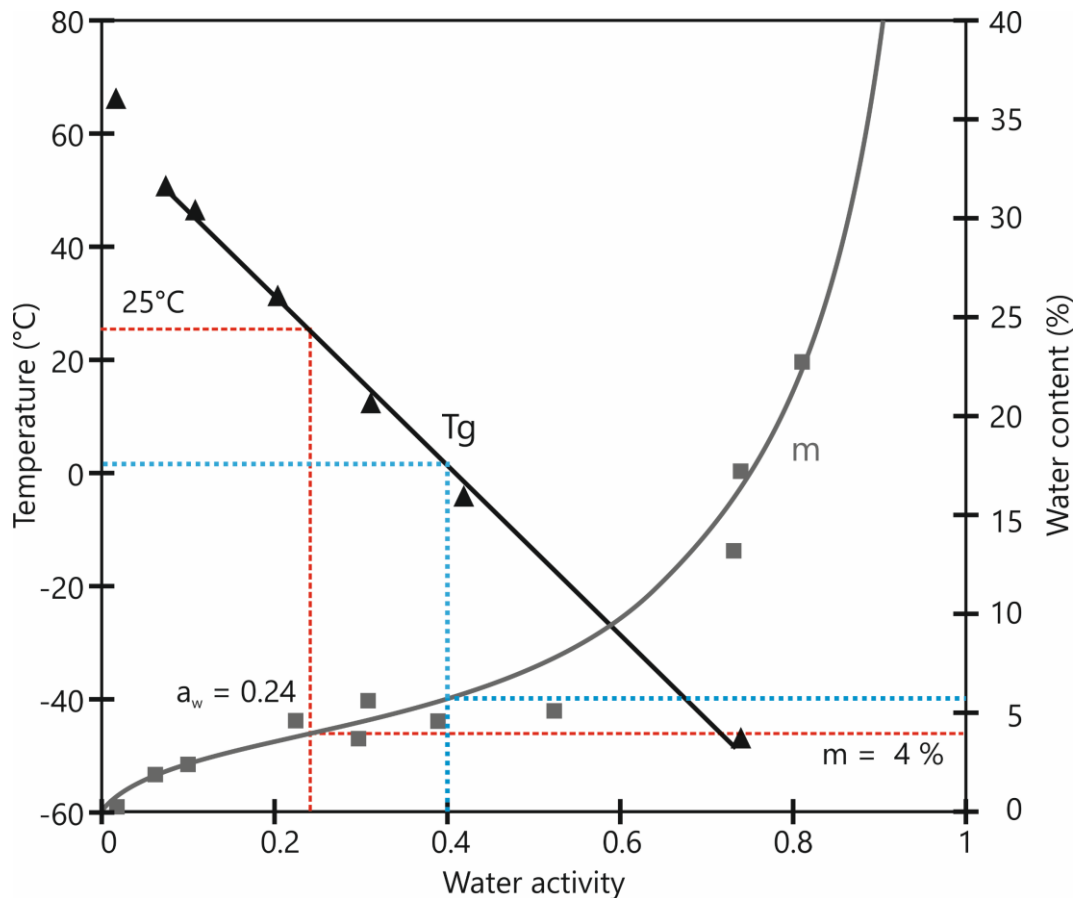


Figure 1.14 Relationships among water activity (a_w) and water content (m , %), as well as water activity (a_w) and glass transition temperature (T_g) °C (blue triangles) for a freeze-dried LAB bacterial suspension in a sucrose matrix. Red dashed lines indicate the location of the critical glass transition temperature, a_w , and m values when this sample is stored at 25°C. Adapted from Passot et al. 2012.

The glass transition temperatures (T_g , triangles in Figure 1.14) and the water content (squares in Figure 1.14) of the freeze-dried *L. bulgaricus* CFL1 are displayed as a function of water activity (a_w). The T_g decreased with water absorption of the matrix. The decrease was linear as water activity increased approximately from 0.1 to 0.7. If a freeze-dried sample had 0.24 of water activity and 4% of water content, the storage could be carried out at 25°C (room temperature), following the glass transition line (Figure 1.14, red dashed lines). If this same sample had, instead, a water activity of 0.40 and water content of 6%, the storage would be recommended to be at 0-1°C (Figure 1.14, light blue dashed lines). Using the relationships between water activity, water content, and glass transition temperature, the physical storage stability of the freeze-dried sample can be predicted.

1.2.4. Cellular damages during stabilization and storage

The physical changes of the LAB matrix suspension during freezing, freeze-drying or storage induce adverse effects on the bacteria cells. This subsection is addressed to explain the primary damages in LAB caused by both stabilization processes and storage.

1.2.4.1. Cellular damages during freezing

Cell damage following freezing depends on cooling rates. Based on observations on yeasts and Chinese hamster tissue-culture cells, Mazur et al. (1972) and Mazur (1977) proposed a widely accepted model of freezing injury to cells. The authors stated that high cooling rates ($>100^{\circ}\text{C}\cdot\text{min}^{-1}$) favor freezing injuries induced by intracellular ice formation. However, intracellular ice formation was not systematic as observed for prokaryotic cells such as *Escherichia coli* ATCC (Albrecht et al. 1973) and *Lactobacillus delbrueckii* subsp. *bulgaricus* CFL1 (Fonseca et al. 2006).

At low cooling rates ($<10^{\circ}\text{C}\cdot\text{min}^{-1}$), the freezing injuries are induced by ice concentration in the extracellular medium. Thus, an osmotic imbalance is generated between the extracellular and the intracellular compartment. Consequently, cell dehydration occurs.

The central cell damage during freezing is analyzed hereafter in the case of slow cooling rates since this cooling rate was used for this thesis. LAB cells suffer different stresses during freezing, leading to biochemical changes, cell deterioration, or cell death in the worst scenario. The following stresses occur during freezing: (i) thermal, (ii) mechanical, osmotic, and chemical. The cell membrane has been identified as the main target of degradation.

Figure 1.15 illustrates a schematic representation of the changes to which a lactic acid bacterium and its membrane are exposed as the temperature decreases. First, the bacterium is at growth temperature (T_{growth}); when temperature decreases, it encounters thermal stress in which membrane lipid phase transition and loss of enzymatic activities occur. Then, mechanical and osmotic stresses take place by the ice formation in the extracellular medium. Both stresses lead to cell dehydration. Cell dehydration ceases with the vitrification of the intracellular compartment. Cells, thus, become osmotically irresponsive to the extracellular compartment. Finally, the vitrification of the extracellular matrix occurs, and the bacterium is immobilized in a glassy state. More details are discussed in the following paragraphs after Figure 1.15.

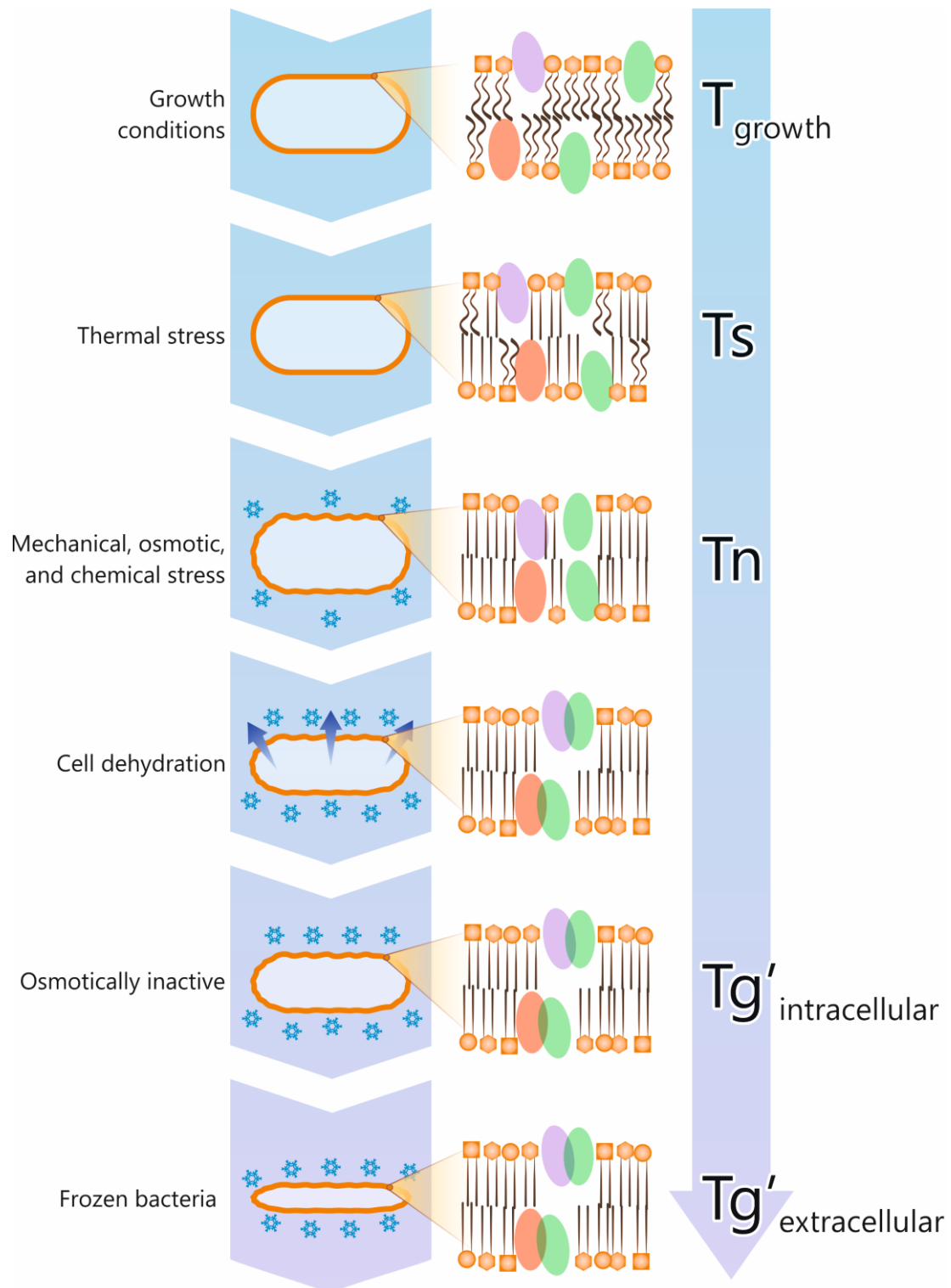


Figure 1.15 Schematic representation of the behavior of a lactic acid bacterium (left side) and its membrane (middle side) as temperature decreases from growth conditions (right side). It considers the major stresses occurring during freezing. Thermal stress when membrane lipid phase transition temperature occurs at T_s ; mechanical, osmotic, and chemical stresses when ice nucleation occurs at T_n ; intracellular glass transition of the cryo-protected bacterium at $T_g'_{\text{intracellular}}$; and glass transition of the extracellular matrix at $T_g'_{\text{extracellular}}$. Abbreviations: T_{growth} , the temperature of growth; T_s , lipid phase transition temperature during cooling; T_n , the temperature of ice nucleation; T_g' the glass transition temperature of the maximally freeze-concentrated phase. The lipid bilayer membrane is represented by different orange geometrical shapes and brown straight and curved lines. The vertical-colored ovals represent the membrane proteins. Adapted from Fonseca et al. 2016.

i. Thermal stress: membrane phase transition and loss of enzymatic activities

To understand the changes in the membrane when the temperature is decreased (thermal stress), Figures 1.16 and 1.17 are simultaneously used to schematize the main events taking place.

The consequence of lowering the temperature is the decreasing enzymatic activities of LAB cells. It occurs in several steps. In an initial step, membrane lipids are in a liquid crystalline phase (L_{α}) (Figure 1.16, left). In this phase (L_{α}), methyl groups of the lipid hydrocarbon chains (fatty acids) adopt *gauche* rotamers (Figure 1.16, bottom-left). Such conformation results in a laterally uncompressed bilayer with minimal van der Waals interactions among adjacent hydrocarbon chains. Therefore, liquid crystalline bilayers are characterized by a higher degree of disorder and fluidity. Proteins can be distributed well within the membranes (Figure 1.17 (A)).

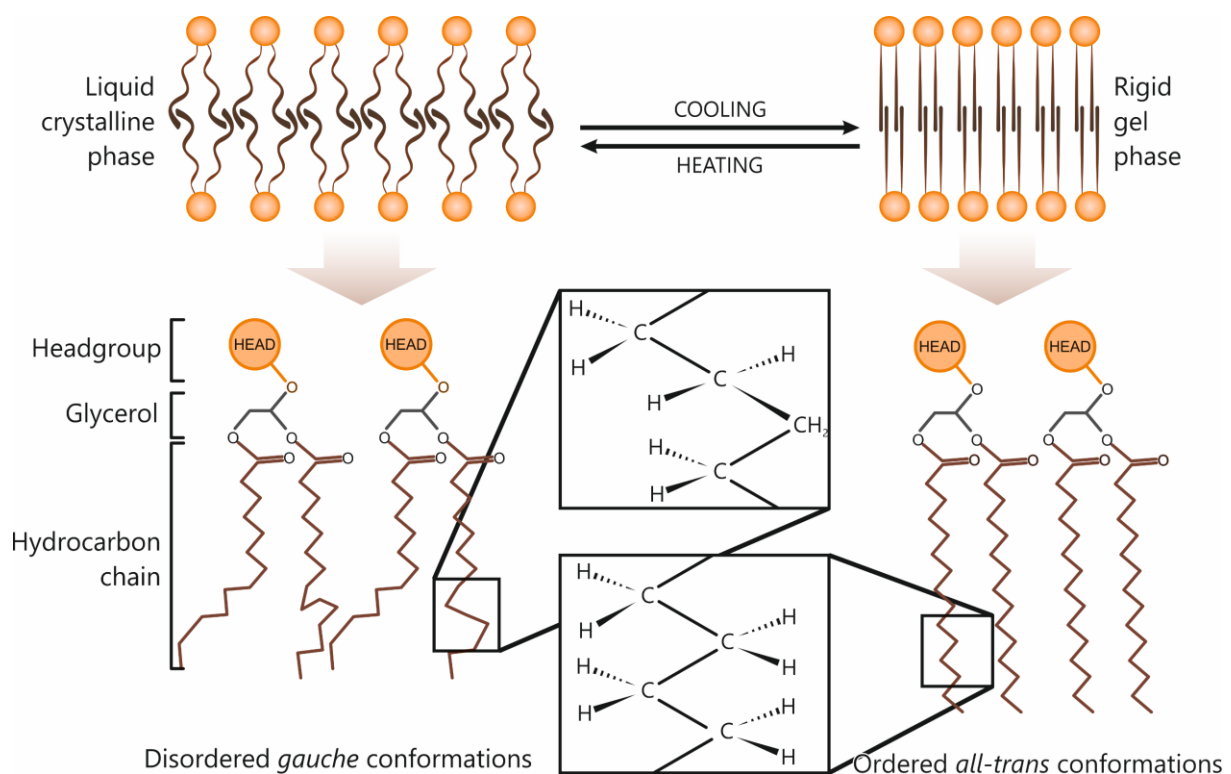


Figure 1.16 Schematic representation of a membrane lipid transition from a disordered liquid-crystalline phase (L_{α}) to rigid gel phase (L_{β}). Adapted from Borchman et al. 1991.

Cooling LAB cells alters this liquid-crystalline phase in their membrane since lipids undergo a phase transition from the liquid-crystalline phase (L_{α}) to a rigid gel phase (L_{β}) (Figure 1.16, right). (Denich et al. 2003; Mykytczuk et al. 2007). The temperature where this transition takes place is called solidification temperature (T_s). Most membrane fatty acids adopt straight all-trans conformations when the solidification temperature is reached (Figure 1.16, bottom-right). This densely packed state maximizes van der Waals interactions, forming highly ordered and rigid domains. Some lipids remain in a fluid state, resulting in the coexistence of fluid and rigid domains (Figure 1.17 (B)) (Beney and Gervais 2001; Le Guillou et al. 2016). The amount of fluid and rigid domains is related to the lipid composition of the LAB strain. In these conditions,

lateral phase separation between components (lipids and proteins) occurs within the membrane, inducing, in turn, increased membrane permeability and modifications of the protein-lipids interactions (Tablin et al. 2001). The exclusion of proteins from the rigid parts of the lipid membrane results in protein aggregation and eventually leads to their inactivation (Figure 1.17 (C)). The temperature decrease can also cause instability of hydrophobic interactions responsible for the denaturation of proteins and, more precisely, modifying their conformation (α -helix to β -sheet); thus, enzymatic activities get affected (Bischof et al. 2002).

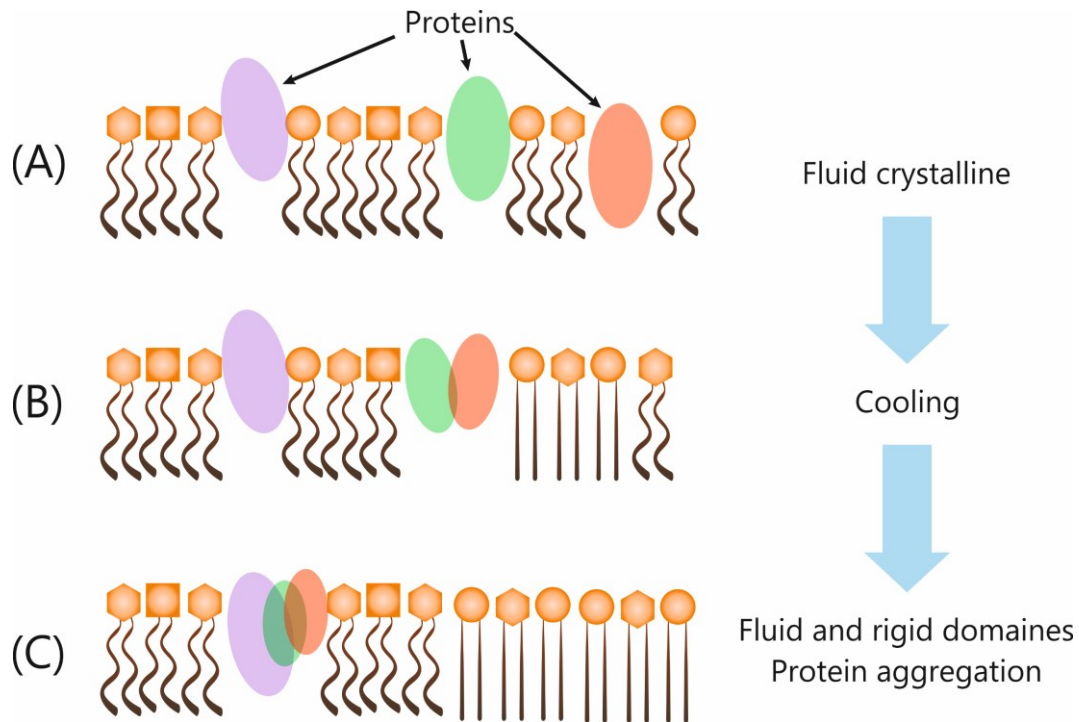


Figure 1.17 Schematic illustration of membrane lateral phase separation upon cooling, causing protein aggregation. (A) Liquid-crystalline phase of membrane lipids and well distribution of proteins; (B) coexistence of fluid and rigid domains; and (C) protein aggregation. Adapted from Tablin et al. 2001.

- i. Mechanical, osmotic and chemical stresses: cell dehydration and inactivation of proteins and nucleic acids

The formation of ice crystals outside the cells exerts mechanical stresses reducing cellular volume. Consequently, the destruction of the biological membrane and deformation of cell wall structure can be observed. In addition, the extracellular ice formation increases the external osmotic pressure, leading to changes in intracellular concentration. The external osmotic pressure induces a decreased cell volume by the passive exit of intracellular water, resulting in cell volume decreased. LAB cells are, thus, dehydrated and shrunken (Béal and Fonseca 2015).

Chemical changes may occur, such as the precipitation of salts, resulting in a modification of the intracellular pH and high electrolyte concentrations, causing the inactivation of macromolecules whose structure relies on non-covalent interactions (e.g., proteins and nucleic acids) (Béal and Fonseca 2015).

ii. Intracellular and extracellular glass transitions

The bacterial intracellular compartment is an aqueous environment that is highly crowded (Mourão et al. 2014). Following mechanical, osmotic, and chemical stresses, the diffusion rates of bacterial intracellular molecules decrease, and the macromolecule concentration may exceed, leading to a glassy state in the cytoplasm at a given temperature ($Tg'_{intracellular}$) (Mika et al. 2010). This glass state has the properties of a dense suspension of colloidal particles (colloid glass). A colloid glass behaves as a molecular sieve allowing the free passage of small molecules while restricting the diffusion of bigger ones (Mika et al. 2010; Sochacki et al. 2011; Mika and Poolman 2011).

The intracellular compartment of LAB then becomes "osmotically inactive", which means that it no longer responds to the increasing osmolarity of the extracellular matrix. The extracellular matrix continues to cryo-concentrate as more ice forms until, in turn, vitrifying at $Tg'_{extracellular}$ (glass transition temperature at the maximally freeze-concentrated solution, section 1.2.3.1).

$Tg'_{intracellular}$ is higher than $Tg'_{extracellular}$ (Figure 1.15) because the densely packed intracellular compartment with macromolecules causes a high viscosity medium inside the cell. For instance, Fonseca et al. (2016) reported $Tg'_{intracellular}$ and $Tg'_{extracellular}$ values for frozen *Lactobacillus delbrueckii* subsp. *bulgaricus* CFL1 cells in the presence of two different protective solutions (glycerol and sucrose). The authors reported a $Tg'_{intracellular}$ of $-[20-22]^{\circ}\text{C}$ vs. a $Tg'_{extracellular}$ of $-[48-99]^{\circ}\text{C}$.

1.2.4.2. Cellular damages during frozen storage and thawing protocol

i. Frozen storage

The oxidation of lipids and proteins can take place during high subzero temperature storage (e.g., -20°C). At -20°C , the addition of an antioxidant (e.g., sodium ascorbate or monosodium glutamate) in the protective medium is essential for limiting oxidation reactions (Fonseca et al. 2003).

ii. Thawing protocol

Ice recrystallization may occur during thawing, whereby large ice crystals increase in size at the expense of smaller ones (Briard et al. 2016). It is advisable to avoid this phenomenon since cells may be exposed to mechanical and osmotic stresses.

Therefore, it is crucial to define an adequate thawing protocol. When LAB are frozen at high cooling rates, thawing conditions consider high temperatures (40°C or 30°C) and short durations (10 min or 5 min) to guarantee high bacterial survival (Piatkiewicz and Mokrosinska 1995; Fonseca et al. 2001a).

Considering slow cooling rates to freeze LAB suspensions and other types of microorganisms such as eukaryotes, the conditions of thawing (temperature and duration) are similar to those

for high cooling rates (high temperatures and short duration) (Mazur 1966; Dumont et al. 2004; Kilbride and Meneghel 2021).

1.2.4.3. Cellular damages during freeze-drying

The freezing injuries have been previously described when slow cooling rates are applied (Figure 1.15). Hereafter, the main cellular damages induced by drying are discussed.

During the drying stages of the freeze-drying process, LAB cells are dried to low water content, causing some cell components such as DNA or RNA and proteins get affected. DNA must be fully hydrated to ensure its chemical stability. Thus, changes in the DNA hydration patterns during dehydration could affect several molecular processes (e.g., replication, transcription, and protein synthesis), disrupting the cellular functions (Potts 1994).

The damage in the DNA of *Lactiplantibacillus plantarum* LIP-1 was analyzed using Infrared Fourier transformed spectroscopy (FTIR). The D-phosphodiester bond symmetrical stretching vibration peak at 1080 cm^{-1} was used as an indicator of DNA synthesis. After freeze-drying *Lactiplantibacillus plantarum* LIP-1 cells, the intensity of this band was higher than for cells not freeze-dried (control), indicating that the synthesis of DNA was disrupted (Chen et al. 2022).

Drying also leads to protein denaturation due to removing hydrogen bonds between water and hydrophilic parts of the proteins, suggesting significant conformational protein changes (Hlaing et al. 2017). By using FTIR in air-dried *Lactobacillus delbrueckii* subsp. *bulgaricus* CFL1 suspensions, protein conformational changes have been detected by observing the spectra of the amide I around 1655 and 1635 cm^{-1} (Oldenhof et al. 2005).

Additionally, the LAB cell membrane has been detected as the main degradation target during drying. A loss in membrane integrity has been observed, resulting in leakage of aqueous contents of the intracellular LAB across the bilayer (Brennan et al. 1986).

An increase in the LAB membrane lipid phase transition temperature has been reported due to water removal following drying. Water interacts with the hydrophilic parts of the membrane (i.e., polar heads) by forming hydrogen bonds, thereby creating a hydration shell around the membrane. Water molecules act as a separator among the polar heads of the membrane lipids. When drying takes place, the packing density of the polar heads of the membrane increases, strengthening the van der Waals interactions between the carbon chains (Leslie et al. 1995), thus, increasing membrane lipid phase transition.

For example, the membrane lipid transition temperature (T_m) between hydrated and dried LAB cells increased from 4 to 20°C for *Lactiplantibacillus plantarum* P743 (Linders et al. 1997); from 35 to 40°C for *Lactobacillus delbrueckii* subsp. *bulgaricus* CFL1 cells (Oldenhof et al. 2005); and for *Lactobacillus helveticus* WS1032, from 37°C to 42°C (Santivarangkna et al. 2010).

1.2.4.4. Cellular damages during freeze-dried storage and rehydration protocol

After freeze-drying LAB suspensions, the factors to consider during the storage are the residual water content, the storage temperature, and the oxygen content (Broeckx et al. 2016). The latter has been identified as the main responsible for LAB degradation.

i. Freeze-dried storage: oxidation and non-enzymatic reactions

During storage, an adverse effect of oxygen has been widely observed on the survival and loss of functional properties of dried LAB. Oxygen toxicity is generally attributed to the formation of reactive oxygen species (ROS) such as superoxide anion ($O_2^{\cdot-}$), hydrogen peroxide (H_2O_2) and hydroxyl radical (OH^{\cdot}). These highly reactive oxygenated chemical species react with numerous cellular compounds. ROS are, therefore, the cause of irreversible damage such as (1) peroxidation and de-esterification of lipids which can lead to a modification of membrane fluidity (Borst et al. 2000); (2) denaturation of proteins, which can lead to inhibition of enzyme activity, and (3) damage to nucleic acids (Heckly and Quay 1981).

Additionally, it has been reported that the mono, di unsaturated fatty acids components of cell membranes were extremely sensitive to oxidation leading to a disruption of membrane structure and function. At 20°C, this lipid oxidation was observed for *Lactobacillus delbrueckii* subsp. *bulgaricus* NCFB 1489 lipid membrane. Consequently, the cell survival was minimum during the storage (Castro et al. 1995, 1996; Teixeira et al. 1996).

The non-enzymatic reactions (Maillard reactions) may also take place during storage. These reactions result from the interaction between the carbonyl groups of reducing sugars (e.g., the protective medium surrounding the cells) and the amine groups of proteins and nucleic acids of the bacterial cell. These reactions lead to pigments (melanoidins), aromatic compounds, and toxic molecules in the cells, such as hydroxymethylfurfural (Martins et al., 2001). For example, freeze-dried *Lactobacillus acidophilus* L-5 was stored at room temperature, and browning was observed as a result of non-enzymatic reactions due to the presence of hydroxymethylfurfural molecules (Kurtmann et al. 2009).

ii. Rehydration protocol

Rehydration is the final step for the revival of freeze-dried bacteria. This step includes submersion and homogenization of the freeze-dried sample in a rehydration medium.

Temperature, time, and rehydration medium significantly impact the proportion of bacteria restored to a functional or viable state (Dinkçi et al. 2019).

When cells are dehydrated, their membrane is in the gel state (L_{β}). The membrane can undergo the reverse phase transition from rigid gel to liquid crystalline phase upon rehydration at T_m (lipid phase transition temperature upon heating). Based on this assumption, the rehydration temperature should be higher than the T_m to guarantee that membrane lipids are found in the liquid crystalline phase (Santivarangkna et al. 2008). The rehydration temperature is usually

determined on an empirical basis by testing different temperatures without performing T_m measurements.

There are no universal rehydration conditions for all LAB. However, some tendencies can be identified. The optimum rehydration temperature in different LAB has been ranged between 20-35°C. The time to rehydrate LAB can be lower than one hour. A protective solution or fermentation medium is often used as a rehydration medium.

For example, it was recommended to rehydrate freeze-dried *Streptococcus* bacteria at 22°C for 5 or 22 min with a solution containing skim or sucrose (Sinha et al. 1982). Higher cell recovery was observed for other strains of the same LAB species (*Streptococcus*) when freeze-dried bacteria were rehydrated at 20°C with a peptone solution. Other sixteen LAB species showed a high recovery when freeze-dried cells were rehydrated at 32°C for 10 min with a solution containing peptone, tryptone, and meat extract (Wang et al. 2004).

Zhao and Zhang (2005) reported the following optimum rehydration conditions: room temperature for 15 min using a sucrose solution as a rehydration medium for *Levilactobacillus brevis*. At the same temperature (room temperature) for 20 min, *Oenococcus oeni* exhibited higher bacteria recovery when the fermentation medium was used than a sucrose solution as a rehydrated medium (Zhang et al. 2012). For *Lactiplantibacillus plantarum*, Lee et al. (2016) reported an adequate rehydration protocol at 25°C for less than one hour using a sorbitol solution.

Sum-up of section 1.2

Production of lactic acid bacteria: stabilization and storage, critical steps that induce cell damages

- LAB have many functional properties (e.g., acidifying activity, probiotic properties, viability, among others) that are used in many industrial applications.
- At industrial scale, LAB are produced by fermentation, then harvested and concentrated. After concentration, LAB are generally suspended in a protective solution to preserve them during the subsequent stabilization process.
- The most common stabilization processes to preserve LAB for long periods are freezing and freeze-drying.
- The stabilization process aims at eliminating most of the available water in liquid form to stabilize the cell structures and limit biological reactions.
- The freezing process involves lowering the temperature to subzero values (-80°C or -196°C). LAB can be then stored at -50°C (industrial freezers) or -80°C (laboratory freezers).
- The freeze-drying process involves three stages: freezing, primary drying (sublimation), and (3) secondary drying (desorption). It is a preservation method based on a cold-drying process that consists of the dehydration of a frozen suspension. A frozen suspension can be converted to vapour by sublimation at sub-atmospheric pressures (10–20 Pa). As a final stage, bound water in the sample is removed by desorption.
- The storage of a freeze-dried sample should consider the following essential factors: the residual moisture content, the atmospheric oxygen level, and the storage temperature.
- Freezing and freeze-drying induce thermal, mechanical, chemical, and osmotic stresses to LAB, leading to loss their functional properties.
- Both stabilization processes damage cellular structures such as lipids and proteins. The cell membrane has been identified as the main target of degradation.

1.3. Strategies to improve lactic acid bacteria resistance to the critical steps of their production: stabilization processes and storage

During freezing, freeze-drying and storage, LAB are exposed to several environmental stresses (thermal, osmotic, mechanical), which can induce cell damage, leading to loss of functional properties (e.g., culturability, viability, or acidifying activity). Therefore, LAB must be resistant to these adverse conditions.

The resistance of LAB means that these microorganisms are able to minimize their loss of functional properties (e.g., culturability and acidifying activity, subsection 1.2.2) after the subsequent stabilization process and storage.

This third part of the literature review focuses on the four known strategies to improve LAB resistance to the stabilization process and storage. The last two strategies reviewed in this section are in the frame of the research questions of this thesis.

1.3.1. Modification of freezing and freeze-drying operating parameters to enhance lactic acid bacteria resistance

An essential criterion for modifying the operating parameters is the feasibility of the equipment (freezer or freeze-dryer) to carry out these actions.

1.3.1.1. The choice of cooling rate during freezing

High ($>100^{\circ}\text{C}\cdot\text{min}^{-1}$) or low ($<10^{\circ}\text{C}\cdot\text{min}^{-1}$) cooling rate can be applied to freeze microorganisms. For freezing LAB, the literature shows that there is no consensus to prefer a fast or slow cooling rate for freezing LAB cells. Six studies proved that freezing at high cooling rates improves LAB survival compared to a slow cooling rate, against four for the reverse results. For high cooling rates these include the studies of Baumann and Reinbold (1966); Tsvetkov and Shishkova (1982); Morice et al. (1992); Fonseca et al. (2001a, 2006); Volkert et al. (2008). For low cooling rates, the works of Bâati et al. (2000); Péter and Reichart (2001); Schoug et al. (2006); Wang et al. (2019) are considered. In addition, one study reported no differences between high and slow cooling rates among eight different *Lactobacillus acidophilus* strains (Foschino et al. 1996). Even though there are more studies demonstrate that high cooling rates increase LAB survival, it is technically demanding because it involves a relatively higher cost of equipment to store LAB samples at very low temperatures (e.g., -196°C , section 1.2.3.2). Applying slow cooling rates allows reproducible freezing protocols for LAB and long-term storage at higher temperatures (e.g., -20°C or -40°C) (Fonseca et al. 2006).

1.3.1.2. Freeze-drying cycle

Long experiments are required to optimize the whole freeze-drying cycle. Parameters such as the freezing temperature and the optimization of the sublimation stage have been studied for LAB.

The choice of the freezing temperature (a compromise between ease sublimation and post-freeze-drying survival) appears to be LAB species-dependent, as shown by the following examples. Freezing different strains of *Lactiplantibacillus plantarum* at -20°C resulted in better post-freeze-drying survival compared to -40°C , -60°C , or -196°C (Wang et al. 2020). However, other LAB exhibited better survival at -43°C ; -65°C , or 196°C than at -20°C , such as *Lacticaseibacillus rhamnosus* GC (Pehkonen et al. 2008), *Oenococcus oeni* H-2 (Zhao and Zhang 2009), and *Liquorilactobacillus mali* (Polo et al. 2017), respectively.

Concerning the optimization of the sublimation time, shelf temperature and gas pressure during sublimation are the operating parameters that can be modified to shorten the sublimation time without reducing the LAB survival (Aragón-Rojas et al. 2019). For instance, the survival of freeze-dried *Lacticaseibacillus casei* ATCC 393TM was assessed when four gas pressures (10, 16, 21, and 27 Pa) and eight shelf temperatures (from 30°C to -45°C) were modified to reduce the sublimation time. The sublimation time was reduced by 40% without sacrificing bacteria survival by performing the sublimation at temperatures higher than the temperatures generally used for other freeze-dried microorganisms (0°C vs. -25°C) (Verlhac et al. 2020).

Another strategy to optimize the sublimation stage is measuring, before freeze-drying, two physical properties of LAB suspensions such as the T_{coll} (collapse temperature) and T_g' (the glass transition temperature of the maximally freeze-concentrated phase). These two temperatures can be measured using a freeze-drying microscope for T_{coll} and DSC (Differential Scanning Calorimetry) equipment for T_g' . LAB suspensions are generally formulated with a protective solution. The protective solution added to bacteria before freeze-drying affects the T_{coll} and T_g' .

Here is an example explaining how T_{coll} and T_g' measurements could help optimize the sublimation stage. During sublimation, frozen samples are heated at their maximum allowable sample temperature (T_{coll}). Higher temperatures than T_{coll} will lead to a collapsed structure. (loss of the pore structure in the freeze-dried sample). Thus, LAB suspensions should have a high T_{coll} to avoid this collapse phenomenon. One alternative is to increase the T_{coll} by using a protective solution that by itself has a high T_{coll} (Annex A.5) (Fonseca et al. 2021). Once the formulation is done (bacteria and protective medium), T_{coll} measurements can be carried out. In the case of not having the availability of a freeze-drying microscope to measure the T_{coll} , it could be readily determined by a simple measurement of T_g' since the difference between them is from one to three degrees. For instance, the T_{coll} and T_g' of a sucrose solution at 20% are -31°C and -33°C , respectively.

1.3.2. Stressful conditions to favor LAB resistance

Bacteria can be intentionally stressed to develop mechanisms to help them cope with the stresses that occur during the stabilization and storage processes. These intended stresses include heat, cold, osmotic, and acid treatments during a determined time in growth or once the cells have been harvested. Some of these stresses can be in a certain level severe because cells are exposed to lower temperatures of 5-15°C and a considerable NaCl concentration (7-30 g·L⁻¹) in the growth medium (Table 1.4).

Note that the studies in Table 1.4 were mainly cultivated in Erlenmeyer (13 out of 18). These 13 studies focused on understanding the biological responses of LAB after these treatments rather than enhancing a high biomass production.

Some of these biological responses are the induction of shock proteins such as heat shock proteins (HSPs) and cold shock proteins (CSPs) (Table 1.4). Both shock proteins act as molecular chaperones, assisting other proteins in folding correctly during or after synthesis and overcoming the protein aggregation (Kataridis et al. 2019).

Additionally, an increase in enzymatic activities involved in the LAB metabolism has been reported after heat stress. For example, the increase of enzymatic activities such as LDH, Na⁺, and K⁺ ATPase was observed for *Lactobacillus acidophilus* ATCC4356 (Zhen et al. 2020). Also, the increase of glycolytic enzymes was observed for *Lactocaseibacillus rhamnosus* HN001 (Prasad et al. 2003).

As shown in Table 1.4, osmotic stress is another way to alleviate further stress during the stabilization process. A sudden increase in the osmolarity of the LAB environment results in the movement of water from the cell to the outside, which causes a detrimental loss of cell turgor pressure and changes in the solute concentration (De Angelis and Gobbetti 2004). To retain water in the cell and maintain turgor pressure, LAB have systems for accumulating specific solutes, which do not interfere with the physiology of the intracellular cell volume. In response to osmotic stress, betaine accumulation has been observed, and it has been associated with better freeze-drying resistance (Louesdon et al. 2014) and drying process resistance (Kets et al. 1996). Lipids composition modulation is another adaptive mechanism that LAB have developed during hot, cold, and acid stresses (Broadbent and Lin 1999; Wang et al. 2005b; Streit et al. 2008)

Table 1.4 Lactic Acid Bacteria (LAB) adaptation mechanisms improving freezing, freeze-drying, and storage resistance by different stresses.

	LAB strains	Improved stabilization processes or storage resistance: stress conditions	Cellular modifications (adaptation) after stress conditions	Reference
Cold Stress (CS) and Heat Stress (HS)	<i>Lactococcus lactis</i> subsp. <i>lactis</i> (M392, M474, 712) and <i>Lactococcus lactis</i> subsp. <i>cremoris</i> (M392, M474, 712)	F: CS at 10°C for 2 h during growth, after NR growth phase	A gene homologous to the major cold shock protein exists in the <i>Lactococcus</i> strains	(Kim and Dunn 1997)
	<i>Lactococcus lactis</i> LL41-1	FS (100 days, 20°C): CS at 10°C for 5 h during growth, after NR growth phase	Induction of cold proteins NR-protein	(Kim et al. 1998)
	<i>Lactococcus lactis</i> subsp. <i>cremoris</i> MM160, MM310 and <i>Lactococcus lactis</i> subsp. <i>lactis</i> MM210 and FG2	F and FD: HS at 42°C for 25 minutes and CS at 10°C for 1, 2,3, and 4 h after harvesting, NR harvest time	Depending on the strain HS: (+) or (-) CFA and CS: (+) or (-) UFA/SFA Induction of shock proteins (Dnak and GroEL)	(Broadbent and Lin 1999)
	<i>Lactococcus lactis</i> subsp. <i>lactis</i> NZ9000	F cycles (1-4): CS at 10°C for 4 h during growth, after mid-EP	Induction of shock protein (CspE)	(Wouters et al. 2001)
	<i>Lactiplantibacillus plantarum</i> NC8 mutant	F: CS at 26°C for NR h, during growth, after mid-EP	Overproduction of CspP protein in SP culture	(Derzelle et al. 2003)
	<i>Lactocaseibacillus rhamnosus</i> HN001	S of fluid bed dried cells: HS at 50°C for 2 h after harvesting at SP	Induction of shock proteins (Dnak and GroEL) and glycolytic enzymes	(Prasad et al. 2003)
	<i>Lactobacillus acidophilus</i> RD758	F and FS (24 weeks, -20°C): CS at 26°C for 8 h, during growth then at 15°C, after the beginning of SP.	CS: (+) cyc C19:0 and UFA/SFA and (+) synthesis of specific proteins (ATP-dependent ClpP, pyruvate kinase and a putative glycoprotein endopeptidase)	(Wang et al. 2005b)*
	<i>Lactiplantibacillus plantarum</i> L67	F cycles (1-4), FD, and FDS (15, 30, and 60 days, 35°C): CS at 5°C for 6 hours after harvesting at mid-EP	Induction of cold shock-induced genes and cold-shock proteins (<i>cspL</i> , <i>cspP</i> , Hsp, and UspA)	(Song et al. 2014)
	<i>Lactococcus lactis</i> subsp. <i>lactis</i> SLT6	FD and FDS (10, 20, 30, 40, 50 days, 4°C, 15°C, 25°C, 37°C): HS at 45°C for 30 min after harvesting at the beginning of SP	NR measurements to assess cellular modifications	(Ziadi et al. 2005)*
	<i>Lactobacillus delbrueckii</i> subsp. <i>bulgaricus</i> ND02	FD: CS at 10°C for 2 h and HS at 37°C for 30 min after harvesting at EP	The expression of two cold shock-induced genes (<i>cspA</i> and <i>cspB</i>) and 6 heat shock-induced genes (<i>groES</i> , <i>hsp</i> , <i>hsp20</i> , <i>hsp40</i> , <i>hsp60</i> , and <i>hsp70</i>)	(Shao et al. 2014)
<i>Lactobacillus acidophilus</i> ATCC4356	FD: HS at 45°C for 30 min during growth, after harvesting at NR growth phase	(+) Enzymatic activities involved in energy metabolism (LDH, Na ⁺ , K ⁺ -ATPase) and glycogen biosynthetic pathway (glycosyltransferase, phosphoglucomutase, and UGPase). Induction of heat shock protein (Lo18)	(Zhen et al. 2020)	
<i>Lactobacillus acidophilus</i> ATCC4356	FD: HS at 45°C for 30 min during growth, after harvesting at NR growth phase	75 differentially expressed proteins (DEPs) were affected. These proteins were mainly related to acid metabolism, glycolysis, ABC transportation, transcription and translation.	(Liu et al. 2021)	
Osmotic stress	<i>Lactobacillus delbrueckii</i> subsp. <i>lactis</i> FAM-10991	FD: 25-30 g·L ⁻¹ of NaCl in the medium during growth after EP	No correlation was found between the autolytic activity of the bacterium and FD survival	(Koch et al. 2007)*
	<i>Lactocaseibacillus rhamnosus</i> OXY	FD: 29 g·L ⁻¹ of NaCl in the medium for 7 hours after harvesting, NR harvest time	Induction of shock proteins (GroEL, ClpB, Dnak, TF)	(Waako et al. 2013)
	<i>Lentilactobacillus buchneri</i> R1102	FD and FDS (3months, 25°C): 7.5 g·L ⁻¹ of KCl in the medium at the beginning of the fermentation	Relatively high intracellular betaine accumulation and high membrane fluidity	(Louesdon et al. 2014)*
	<i>Lactobacillus delbrueckii</i> subsp. <i>bulgaricus</i> ATCC11842	FD: 20 g·L ⁻¹ of NaCl in the medium for 2 hours during growth, after the end of EP.	Nine proteins were altered by NaCl stress (EF-G, GroEL, TS, IMPDH, LDH, UMPK, D-LDH, SlrB, Piridoxine 5)	(Li et al. 2014)
	<i>Lactobacillus delbrueckii</i> subsp. <i>bulgaricus</i> ATCC11842	FD: 20 g·L ⁻¹ of NaCl in the medium for 2 hours during growth, after the end of EP	(+) Enzymatic activities: phosphofructokinase, pyruvate kinase, and lactate dehydrogenase	(Li et al. 2015)
Acid stress	<i>Lactobacillus delbrueckii</i> subsp. <i>bulgaricus</i> CFL1	F and FS (3 months, -20°C): pH 5.25 for 30 min after harvesting at the SP	Slight decrease of UFA/SFA and CFA and 21 proteins changes by acidification were related to energy metabolism, protein and nucleotide synthesis	(Streit et al. 2008)*

F: Freezing; FS: Frozen Storage; FD: Freeze-Drying; FDS: Freeze-Dried Storage; S: storage; EP: the Exponential growth Phase; SP: the Stationary growth Phase; CS: Cold Stress; HS: Heat Stress; UFA: Unsaturated Fatty Acid; SFA: Saturated Fatty Acid; CFA: Cyclic Fatty Acid (cycC19:0); (+): increase; (-) decrease; NR: Not Reported.

*Studies in which LAB were grown in a bioreactor. Proteins characteristics are summarized in Annex A.6.

1.3.3. Modulation of fermentation conditions to enhance lactic acid bacteria resistance

Changes in the fermentation conditions are considered moderate mild-stressful conditions because they allow a progressive bacteria adaptation during growth. Due to these modifications, LAB cells develop adaptation mechanisms that help bacteria survive after the stabilization and storage processes.

1.3.3.1. Fermentation parameters effect on LAB resistance

Changes in the fermentation parameters such as (i) culture medium, (ii) temperature, (iii) pH, and (iv) harvest time have been reported to improve LAB resistance to freezing, freeze-drying, or storage. For example, the studies in Table 1.5 target LAB grown in a lab-bioreactor, in which conditions are close to LAB industrial production compared to an Erlenmeyer flask.

The studies in Table 1.5 are organized by fermentation parameter, stabilization process, and storage. First, freezing (F) and frozen storage (FS) are displayed, followed by freeze-drying (FD) and freeze-dried storage (FDS). Note that 13 out of 22 studies have assessed the effect of fermentation parameters on growth and LAB resistance. Six out of these 13 studies have demonstrated that LAB growing at a fermentation condition different from the optimum one for growth promotes LAB resistance (Li et al. 2009a; Ampatzoglou et al. 2010; Li et al. 2012; Liu et al. 2014; Shao et al. 2014; Velly et al. 2014). The explanations of LAB adaptation resulting from modifying one or two fermentation parameters from Table 1.5 are as follows.

i. Supplementing the fermentation medium

Six studies have supplemented the medium by adding sugars, proteins (e.g., yeast extract), or oleates (e.g., Tween 80, polysorbate 80, a molecule that could be hydrolyzed to oleic acid).

A supplemented fermentation medium appears to have a neutral or beneficial effect on LAB resistance. Three works reported no resistance improvement to freeze-drying and freeze-dried storage compared to the control medium (Champagne et al. 1991; Shao et al. 2014; Hansen et al. 2015b). The three remaining studies have revealed that supplementing the fermentation medium can improve freezing, freeze-drying, and storage resistance (Béal et al. 2001; Fonseca et al. 2001a; Li et al. 2012).

Growing LAB in Erlenmeyer, the resistance of bacteria to freezing and freeze-drying have also been observed. For freezing, different strains of *Lactobacillus delbrueckii* subsp. *bulgaricus* exhibited high survival when cultivated in a fermentation medium supplemented with sodium oleate (Smittle et al. 1974), as well as oleic acid and Tween 80 (Goldberg and Eschar 1977). Since then, LAB resistance has been associated with modifying fatty acid content in the LAB membrane. The specific changes in the fatty acid composition are further detailed and discussed in subsection 1.3.3.2, Table 1.6.

Concerning the freeze-drying process, *Lactobacillus delbrueckii* subsp. *bulgaricus* showed an increased freeze-dried resistance when calcium was added to the fermentation medium

(Wright and Klaenhammer 1983). For this same LAB species, a fermentation medium supplemented with sugars such as lactose or mannose enhanced LAB resistance to freeze-drying (Carvalho et al. 2003c, 2004b).

A more recent study reported that *Lactiplantibacillus plantarum* L1P-1 cells cultivated in a culture medium enriched with six buffer salts improved the freeze-drying survival rate. This strain promoted the expression of genes related to fatty acid metabolism and synthesis; particularly, an increase in unsaturated fatty acid content was observed (E et al. 2020).

Still considering the LAB growth at the Erlenmeyer scale, the growth of LAB in the MRS medium compared to another medium (e.g., whey-medium or gM17) has been reported to enhance higher resistance to freezing of *Lactobacillus delbrueckii* subsp. *bulgaricus* CFL1 (Gautier et al. 2013) and freeze-drying of *Lactococcus lactis* NCDO 712 and NZ9000 (Bodzen et al. 2021a). Both LAB species exhibited a high membrane fluidity when the MRS medium was used for their growth.

ii. Fermentation temperature

In light of the literature background (Table 1.5), three studies reported increased resistance to freezing and frozen storage of LAB due to low growth temperatures (Fernández Murga et al. 2000; Bâati et al. 2000; Wang et al. 2005a). Nevertheless, the adaptation mechanisms to low temperatures in LAB have not been systematically related to their resistance to freeze-drying or freeze-dried storage (Schoug et al. 2008; Zotta et al. 2013; Velly et al. 2014; Liu et al. 2014).

Studies of LAB cultivated in Erlenmeyer have provided insights about the adaptation mechanisms of these microorganisms to low growth temperature. *Latilactobacillus sakei* 23K grown at two different temperatures (4°C and 37°C) exhibited that, at low temperature, six proteins were affected: two were involved in the carbohydrate metabolism pathway and four were identified as stress proteins (Marceau et al. 2004). Recently, Liu et al. (2020) investigated the molecular mechanism involved in the cold adaptation during the growth of *Lactiplantibacillus plantarum* K25 at 10°C. They agreed that low temperatures affected the proteins required in this lactic acid bacterium's carbohydrate, amino acid, and fatty acid metabolism. In addition, the proteins related to DNA repair were up-regulated. Low temperature led to gene expression changes, and more protein biosynthesis was needed in response to cold stress.

iii. Fermentation pH

The pH effect during growth on stabilization processes resistance has been only assessed in combination with other fermentation factors (fermentation medium \times pH, temperature \times pH or harvest time \times pH). A pattern can be observed, low controlled pH has induced the resistance of *Limosilactobacillus reuteri* ATCC 55790 (Palmfeldt and Hahn-Hägerdal 2000a), *Streptococcus thermophilus* CFS2 (Béal et al. 2001), *Lactobacillus delbrueckii* subsp. *lactis* FAM 10991 (Koch et al. 2008), *Lactobacillus delbrueckii* subsp. *bulgaricus* L2 (Li et al. 2009a), *Lactobacillus delbrueckii* subsp. *bulgaricus* CFL1 (Rault et al. 2010), and *Lactobacillus delbrueckii* subsp. *bulgaricus* ND02 (Shao et al. 2014) (Table 1.5).

LAB inherently acidify their environment, self-imposing acid stress. Then, there is a need for these bacteria to respond to acidification to ensure physiological maintenance and rely on the involvement of multiple mechanisms to survive. The mechanisms that have been associated with stabilization process resistance include cell size reduction and cell morphology changes (Palmfeldt and Hahn-Hägerdal 2000; Koch et al. 2008; Shao et al. 2014), low acidifying activity after harvest and concentration (Rault et al. 2010), and fatty acids composition changes (Li et al. 2009a). The latter mechanism is presented and discussed in section 1.3.2.3, Table 1.6.

Likewise, studies that have been performed at uncontrolled pH in bioreactors (standard parameter in Erlenmeyer cultures) reported improved freezing and freeze-drying resistance (Lorca and Font de Valdez 2001; Koch et al. 2008). At uncontrolled pH, the accumulation of lactic acid in the medium leads to a progressive acid adaptation that could enhance LAB resistance to the stabilization processes. This adaptation is even favored when the initial pH set value is lower. For Erlenmeyer scale culture, for instance, the freeze-drying resistance was observed for *Oenococcus oeni* SD-2a at initial pH of 3.5 vs. pH 4.8 (Li et al. 2009b) and *Lactiplantibacillus plantarum* LIP-1 at initial pH 6.8 vs. pH 7.4 (E et al. 2021).

It is worth mentioning that uncontrolled pH is rarely used at an industrial scale to produce LAB. The accumulation of lactic acid slows down LAB growth rather than the depletion of nutrients.

iv. Harvest time

Six out of nine studies shown in Table 1.5 revealed the beneficial effect of harvesting LAB cells at the stationary growth phase to improve stabilization and storage resistance (Palmfeldt and Hahn-Hägerdal 2000; Rault et al. 2010; Ampatzoglou et al. 2010; Zotta et al. 2013; Velly et al. 2014, 2015). In addition, LAB that were cultured in Erlenmeyer have exhibited this same result. Increased freezing (Lorca and Font de Valdez 1999; Péter and Reichart 2001), freeze-drying (Schwab et al. 2007; Li et al. 2009b), and spray-drying (Corcoran et al. 2004) of harvested stationary-phase LAB have been previously reported. The stationary phase induces various physiological states within the bacteria due to carbon starvation and exhaustion of available carbon sources that trigger stress responses to allow survival of the bacterial population. Thus, LAB can overcome the adverse conditions occurring in the stabilization process.

To understand the metabolic behavior and stress responses of stationary-phase LAB, a few studies have compared cells harvested at exponential and stationary growth phases, using proteomic approach, without performing experiments on stabilization resistance. The reported results are the following:

(1) A ten-fold increase in synthesizing of the classic heat shock protein such as GroEL was observed when *Lactocaseibacillus rhamnosus* HN001 culture passed from the exponential growth phase to the stationary growth phase. Also, the levels of the glycolytic enzymes such as enolase and lactate dehydrogenase increased at least two-fold when the bacterial culture passed from the exponential to stationary growth phase (Prasad et al. 2003).

(2) For *Lactiplantibacillus plantarum* WCFS1, it was observed the strengthening of the cell membrane from the late-exponential to early-stationary growth phases based on a greater abundance of enzymes involved in fatty acid biosynthesis for the formation of phospholipids. In addition, proteins involved in cell wall structures, such as UDP-sugars and PBP-proteins, were increased in relative abundance for the stationary-growth phases; thus, this increase results in high membrane permeability and the alteration of the cell envelope composition (Cohen et al. 2006).

(3) Finally, two strains of *Lactiplantibacillus plantarum* (REB1 and MLBPL1) harvested at the exponential and stationary phase exhibited the metabolic potential involved for both growth phases. Exponential growth phase cells have an active metabolism creating a pool of metabolic enzymes for energy production and a pool of nucleotides for cell division. However, the bacteria metabolism in the stationary growth phase decreased the enzyme activities for metabolism and cell division was less favored; instead the production of proteins in biosynthetic pathways was observed (Koistinen et al. 2007).

Different alterations represent each growth phase in LAB in bacteria metabolism and in the production of different biological molecules to ensure growth. Consequently, harvesting LAB during a specific growth phase could affect their subsequent production steps (i.e., the stabilization process).

Table 1.5 Studies on the influence of fermentation conditions on the freezing, freeze-drying, and storage resistance of Lactic Acid Bacteria (LAB) in the case of works carried out in a bioreactor.

	LAB strains	Fermentation parameters studied	Fermentation parameter for optimal growth	Stabilization or storage resistance improvement: selected fermentation parameters	Reference
Fermentation medium and pH	<i>Lactobacillus delbrueckii</i> subsp. <i>bulgaricus</i> CFL1	F_m : Mild-whey medium vs. mild whey medium + Tween 80	NR	F : mild whey medium + Tween 80 FS (2 months, -20°C): No effect of culture medium	(Fonseca et al. 2001a)
	<i>Streptococcus thermophilus</i> CFS2	F_m : Mild-whey medium vs. mild whey medium + oleic acid (Tween 80) pH : 5.5, 5.6 or 6.5	NR	FS (2 months, -20°C): mild whey medium + oleic acid and pH 5.5	(Béal et al. 2001)
	<i>Lactobacillus delbrueckii</i> subsp. <i>bulgaricus</i> Y-12	F_m : Skim milk medium vs. whey-based medium with or without papain treatment	Skim milk medium	FD : No effect of culture medium	(Champagne et al. 1991)
	<i>Lactobacillus delbrueckii</i> subsp. <i>bulgaricus</i> L2	F_m : MRS + Tween 20, 40, 60, 80, peanut oil, olive oil or soybean oil and MRS + glucose, lactose, fructose, mannitol, sucrose, maltose, trehalose, dextrin or glycerol	MRS + Tween 80 or Peanut oil MRS + glucose or lactose	FD : MRS + soybean oil and MRS + sucrose	(Li et al. 2012)
	<i>Lactobacillus delbrueckii</i> subsp. <i>bulgaricus</i> ND02	F_m : MRS medium vs. MRS medium +2 or 4% of yeast extract pH : initial pH adjusted at 6.5, then pH : 5.1 vs. pH 5.7	MRS + 4% yeast extract pH 5.7	FD : MRS medium and pH 5.1	(Shao et al. 2014)
	<i>Lactobacillus acidophilus</i> La-5	F_m : MRS medium vs. MRS + Tween 20, linoleic acid or α -linoleic acid	NR	FDS (1, 2, 3, 6, 10 and 15 weeks, 30°C, 0% O ₂ or 21% O ₂) MRS medium	(Hansen et al. 2015b)
Temperature and pH	<i>Lactobacillus acidophilus</i> CRL 640	Temperature : 25°C, 30°C, 37°C or 40°C	NR	F : 25°C	(Fernández Murga et al. 2000)
	<i>Lactobacillus acidophilus</i> ATCC 4356	Temperature : (37°C for 9 h, then 22°C for 6 h) at pH 6.5 pH : (6.5 vs. uncontrolled) at 37°C	NR	F : 37°C for 9 h at pH 6.5 then 22°C for 6 h at pH 6.5	(Bâati et al. 2000)
	<i>Lactobacillus acidophilus</i> RD758	Temperature : (30°C, 37°C or 42°C) at pH 6.0 pH : (4.5, 5.0 or 6.0) at 37°C	NR	F and FS (3 months, -20°C): 30°C, pH 6.0 and 37°C, pH 5.0	(Wang et al. 2005a)
	<i>Lactobacillus acidophilus</i> CRL 639	pH : 6.0 vs. uncontrolled	NR	F and FD : uncontrolled pH	(Lorca and Font de Valdez 2001)
	<i>Loigolactobacillus coryniformis</i> Si3	First 12 h of culture at 34°C, pH5.5 and then for 6 h: Temperature : (26°C, 34°C or 42°C) at pH 5.5 pH : (6.5 vs. 4.5) at 34°C and 30°C, pH 4.5	34°C, pH 5.5	FD : 42°C, pH 5.5 and 34°C, pH 5.5	(Schoug et al. 2008)
	<i>Lactobacillus bulgaricus</i> L2	Temperature : 30°C, 35°C, 37°C or 39°C pH : 5.0, 5.5, 6.0 or 6.5	39°C, pH 5.0 and pH 5.5	FD : 30°C, pH 5.0	(Li et al. 2009a)
	<i>Limosilactobacillus reuteri</i> I5007	First 10 h of culture at 37°C, pH5.7 and then for 6 h: Temperature : (4°C, 27°C or 47°C) at pH 5.7 pH : (4.7, 5.7, or 6.7) at 37°C	37°C, pH 5.7	FD : 37°C, pH 6.7	(Liu et al. 2014)

F_m: Fermentation medium; **F**: Freezing; **FS**: Frozen Storage **FD**: Freeze-Drying; **FDS**: Freeze-Dried Storage; EP: the Exponential growth Phase; SP: the Stationary growth Phase; +: supplemented with; vs. versus; or: three or more comparisons; NR: Not Reported.

Table 1.5 (Continued) Studies on the influence of fermentation conditions on the freezing, freeze-drying, and storage resistance of Lactic Acid Bacteria (LAB) in the case of works carried out in a bioreactor.

	LAB strains	Studied fermentation parameters	Fermentation parameter for optimal growth	Stabilization or storage resistance improvement: selected fermentation parameters	Reference
Harvest time and pH	<i>Lactobacillus delbrueckii</i> subsp. <i>bulgaricus</i> CFL1	Harvest time: end EP vs. SP	NA	F and FS (2 months, -20°C): No effect of harvest time	(Fonseca et al. 2001a)
	<i>Lactobacillus delbrueckii</i> subsp. <i>bulgaricus</i> CFL1	Harvest time: EP, end EP, SP or late SP pH: 5.0, 6.0 or uncontrolled	SP and pH 5.0	F and FS (5 months, -20°C): pH 5.0, SP and late SP	(Rault et al. 2010)
	<i>Lentilactobacillus buchneri</i> R1102	Harvest time: EP vs. SP	NA	F: EP for acidifying activity	(Louesdon et al. 2015)
	<i>Limosilactobacillus reuteri</i> ATCC 55730	Harvest time: approximately 0 h, 2 h or 4 h of SP pH: 5.0 vs. 6.0	All harvest times pH 5.0 and pH 6.0	FD: 2h of SP and pH 5.0	(Palmfeldt and Hahn-Hägerdal, 2000)
	<i>Lactobacillus delbrueckii</i> subsp. <i>lactis</i> FAM 10991	Harvest time: beginning of SP, SP or end SP pH: 5.0, 5.5, 6.0 or uncontrolled	NR harvest time pH 5.0 and pH5.5	FD: No effect of harvest time pH 5.0 and uncontrolled pH	(Koch et al. 2008)
	<i>Lactocaseibacillus rhamnosus</i> GG	Harvest time: late EP, mid-SP or late SP pH: 6.8 vs. uncontrolled	Late SP and pH 6.8	FD: late SP and uncontrolled pH	(Ampatzoglou et al. 2010)
Temperature, pH, and harvest time	<i>Lactiplantibacillus plantarum</i> C17	Temperature: 25° vs. 35°C Harvest time: EP vs. SP	35°C and SP	FS and FDS (1month, -20°C) 35°C and SP	(Zotta et al. 2013)
	<i>Lactococcus lactis</i> subsp. <i>lactis</i> TOMSC161	Temperature: 22°C, 30°C, or 38°C pH: 5.6, 6.2 or 6.8 Harvest time: 0 h, 3 h or 6 h of SP	30°C, pH 6.8, 6h of SP	FD and FDS (1 and 3 months, 4°C or 25°C) FD: 32°C, pH 6.2, and 6 h of SP FDS: 1 and 3 months at 4°C	(Velly et al. 2014)
	<i>Lactococcus lactis</i> subsp. <i>lactis</i> TOMSC161	Temperature: 22°C vs. 30°C Harvest time: middle EP, late EP, early SP or late SP	NR	FD and FDS (3 months, 25°C) 30°C, late SP	(Velly et al. 2015)

F.m: Fermentation medium; **F:** Freezing; **FS:** Frozen Storage **FD:** Freeze-Drying; **FDS:** Freeze-Dried Storage; EP: the Exponential growth Phase; SP: the Stationary growth Phase; +: supplemented with; vs. versus; or: three or more comparisons; NR: Not Reported; NA: Not Applied.

1.3.3.2. Biophysical and biochemical properties of LAB membrane lipids are associated with stabilization and storage resistance

Researchers have long realized that different stresses (osmotic, acid heat treatments) and mild stresses (the modifications of fermentation conditions) generate active LAB cellular responses leading to changes in cellular constituents, especially the membrane lipids (Table 1.6). The cell membrane is the main target of freezing and freeze-drying injuries. Therefore, many studies have focused on characterizing membrane properties to explain the resistance of LAB to the stabilization processes and storage.

Table 1.6 summarizes the studies investigating lipid properties related to LAB resistance to freezing, freeze-drying, and storage. Different analytical methods have characterized these lipid properties:

- (i) Fatty acids composition and quantification by Gas Chromatography-Mass Spectrometry (GC-MS).
- (ii) Lipid classes composition by Thin Layer Chromatography and Liquid Chromatography coupled with tandem mass spectrometry (TLC and LC-MS/MS).
- (iii) Membrane fluidity by fluorescence anisotropy, in which a probe (DiPhenylHexatriene, DPH) is inserted in the lipid bilayer.
- (iv) Lipid phase transition temperatures, which can be measured *in situ* as a function of temperature, during cooling or heating by Fourier-Transform Infrared Spectroscopy (FT-IR).

Table 1.6 shows that most of the studies used the fatty acid composition to correlate the resistance of LAB to stabilization or storage. As a general pattern, the increase of the ratio UFA/SFA (unsaturated fatty acid/saturated fatty acids) or CFA content (cyclic fatty acid, cycC19:0) lead to higher resistance of LAB to stabilization and storage.

The increased of UFA/SFA was observed when the fermentation medium was supplemented with oleic acids or similar molecules (e.g., Tween 80) (Béal et al. 2001, Smittle et al. 1974, Goldberg and Eschar 1997). Also, when LAB were cultivated in uncontrolled pH conditions and low initial pH (Zhao et al. 2009; E et al. 2021). Likewise, CFA content was increased when LAB were exposed to different stresses such as cold shock, heat shock, and osmotic stresses (Broadbent and Lin 1999; Wang et al. 2005b; Louesdon et al. 2014). This CFA increase was associated with stabilization process and storage resistance of LAB.

There are some exceptions when two fermentation parameters are modified (e.g., Temperature and pH, Table 1.6). An increased UFA/SFA or CFA was not necessarily associated with LAB resistance. For instance, Schoug et al. (2008) reported a decrease in UFA/SFA and CFA for the freeze-drying resistance of *Loigolactobacillus coryniformis* Si3. Li et al. (2009a) did not observe

any relation between the freeze-drying resistance and UFA/SFA for *Lactobacillus delbrueckii* subsp. *bulgaricus* L2. Conversely, the freeze-drying resistance of *Lactococcus lactis* subsp. *lactis* TOMSC161 was positively correlated to a low UFA/SFA (Velly et al. 2015).

Table 1.6 also includes the few studies in which LAB membrane fluidity (Louesdon et al. 2014, 2015; Velly et al. 2015) and lipid phase transition temperatures (Gautier et al. 2013; Velly et al. 2015) were determined.

The UFA/SFA ratio can influence the membrane fluidity; unsaturated carbons in fatty acids affect the conformations of the acyl chains, limiting lipid packaging in the bilayer. Consequently, membrane fluidity is increased (Fonseca et al. 2019). A fluid membrane in LAB is preferred to overcome the different stresses during freezing (Passot et al. 2014; Louesdon et al. 2014) and freeze-drying (Bodzen et al. 2021a). Only one study demonstrated the opposite behavior in *Lactococcus lactis* (Velly et al. 2015); a rigid membrane was associated with increased freeze-dried resistance. The hypothesis provided by the authors implies that a rigid membrane could exert a higher mechanical resistance of the membrane when bound water is removed during the secondary stage of freeze-drying.

Concerning lipid phase transition temperatures, these are related to the saturation level of the fatty acids in the cytoplasmic membrane (Knothe and Dunn 2009). High freezing resistance was observed when low values of lipid phase transition temperatures during cooling (8°C vs. 22°C, Table 1.6). This low temperature was also related to high UFA/SFA ratio (1.6 vs. 0.5) (Gautier et al. 2013). Conversely, high freeze-dried resistance was not related to a lipid transition temperature during heating (Velly et al. 2015).

From the reviewed studies in Table 1.6, little is known about the effect of the different lipids in the LAB membrane. At the beginning of this chapter (Table 1.2), the different types of phospholipids and glycolipids found in LAB were described. Each polar head type is associated with many water molecules, tightly bound through hydrogen bonds (Luzardo et al. 2000). Phospholipids and glycolipids present different sizes and shapes that could affect the extent of the interfacial area between head groups and the distribution and packing in the membrane. Both lipids may eventually modulate membrane fluidity. Table 1.6 notes that only Fernández Murga et al. (2000) have deeply characterized the lipid classes of *Lactobacillus acidophilus* CRL640 membrane (neutral lipids, glycolipids, phospholipids). The authors revealed the relevance of glycolipids in membrane composition. A high ratio of (sugar/phosphorus) (4.4 vs. 1.8-1.9) was linked to an improved freezing resistance instead of a fatty acid composition.

The literature reviewed in Table 1.6 highlighted the need to use multiple analytical methods to gain insights into the membrane properties (biochemical and biophysical properties) with the stabilization process resistance.

Recent works evidenced the interest in performing complementary analytical methods to understand the link of membrane properties with the freezing resistance of different strains. Meneghel et al. (2017) and Girardeau et al. (2022) performed measurements of the fatty acid composition, membrane fluidity, and lipid transition temperatures for two or three strains exhibiting various levels of freeze-sensitivity: *Carnobacterium maltaromaticum* CNCM I-3298 (high resistant strain); *Lactobacillus delbrueckii* subsp. *bulgaricus* ATCC 11842 (medium resistant strain); and *Lactobacillus delbrueckii* subsp. *bulgaricus* CFL1 (low resistant strain). The authors showed a list of "membrane markers" associated with high freezing resistance: (i) a ratio of UFA/SFA above 1.5, CFA content higher than 20%, (ii) lipid phase transition temperature lower than 0°C, and (iii) high membrane fluidity at 0°C (0.20 vs. 0.24-0.28, anisotropy values).

Based on the conclusions of both authors (Meneghel et al. 2017; Girardeau et al. 2022) and the extensive literature on the topic (Table 1.6), some assumptions about the membrane properties (e.g., high UFA/SFA ratio or high CFA content, or high membrane fluidity...) can be applied for improved freezing and freeze-drying resistance. A comprehensive study is lacking to understand the role of the different lipids class in the resistance of LAB to the stabilization process.

Table 1.6 Reported studies on the lipid cellular properties modifications that have been linked to Lactic Acid Bacteria (LAB) resistance to stabilization process and storage.

LAB strain	Stabilization process: selected condition The conditions studied	Methods of analysis	Relation between resistance and lipid component modifications	Reference	
Fermentation medium and pH	<i>Lactobacillus bulgaricus</i> NCS1, NCS2, NCS3 and NCS4	F: control medium + sodium oleate Control medium (tryptone, yeast extract, lactose and Tween 20) + sodium oleate vs. this medium without sodium oleate	FA: GC-MS Lipid classes distribution: 1) neutral, 2) polar and 3) bound-hydrolyzed lipid by gravimetric analysis of total lipids and silicic acid chromatography	Mean of the four strains (+) UFA/SFA (1.1 vs. 0.7) and (+) CFA content (17% vs. 4%) for all the strains (+) polar lipid fraction for the strain NCS1 (55% vs. 25% or 26% of the other lipid fractions)	(Smittle et al. 1974)
	<i>Streptococcus lactis</i> and <i>Lactobacillus</i> subsp. A-12	F: Tomato juice this medium + Tween 80 Tomato juice medium + Tween 80 vs. Tomato juice medium	FA: GC-MS	<i>Streptococcus lactis</i> : (+) UFA/SFA (1.1 vs. 0.3) no effect on CFA <i>Lactobacillus</i> subsp. A-12: (+) UFA/SFA (1.2 vs. 0.6) and (+) CFA content (19% vs. 11%)	(Goldberg and Eschar 1977)
	<i>Streptococcus thermophilus</i> CFS2	F and FS (2 months, -20°C): whey medium + oleic acid whey medium + oleic acid vs. whey medium pH: 5.5 pH: 5.5, 5.6 or 6.5	FA: GC-MS	Whey medium + oleic acid: (+) UFA/SFA (1.4 vs. 1.0) and (+) CFA content (2% vs. 1%) pH 5.5: (+) UFA/SFA (1.4 vs. 0.9-1.1) and (+) CFA content (4% vs. 1-2%)	(Béal et al. 2001)
	<i>Lactobacillus delbrueckii</i> subsp. <i>bulgaricus</i> CFL1	F: MRS medium MRS medium vs. whey-based medium	FA: GC-MS MI: Propidium iodide (PI) by flow cytometry Lipid transition temperature during cooling (Ts): FT-IR	(+) UFA/SFA (1.6 vs. 0.5) and (+) CFA content (14% vs. 2%) (+) MI : low % of PI-stained cells (-) Ts (-8°C vs. 22°C)	(Gautier et al. 2013)
	<i>Lactobacillus delbrueckii</i> subsp. <i>bulgaricus</i> CFL1	F: MRS medium MRS medium vs. whey-based medium	MF: fluorescence anisotropy values, low values = (+) MF and synchrotron UV fluorescence microscopy	(+) MF at 0°C (0.12 vs. 0.25)* by synchrotron UV and (0.25 vs. 0.33)* by fluorescence anisotropy	(Passot et al. 2014)
	<i>Lactobacillus bulgaricus</i> L2	FD: MRS + soybean oil and MRS + sucrose MRS + Tween 20, 40, 60, 80, peanut oil, olive oil or soybean oil MRS + glucose, lactose, fructose, mannitol, sucrose, maltose, trehalose, dextrin or glycerol	FA: GC-MS	MRS + soybean: No effect either UFA/SFA (10 vs. 7-25) or CFA (2% vs. 0.3-3%) MRS + glucose: No effect on UFA/SFA (11 vs. 7-14) (+) trend CFA content (2.0-3.4% vs. 0.3-1.4)	(Li et al. 2012)
	<i>Lactobacillus acidophilus</i> La-5	FDS (1, 2, 3, 6, 10 and 15 weeks, 30°C, 0% O ₂ or 21% O ₂): MRS medium MRS medium vs. MRS + Tween 20, linoleic acid or α-linoleic acid	FA: GC-MS MI: leakage of lactate dehydrogenase	(-) UFA/SFA (5.2 vs. 5.5) and (+) CFA content (28% vs. 18%) (+) MI : (-) leakage activity (415 g·min ⁻¹ vs. 524 g·min ⁻¹)	(Hansen et al. 2015b)
	<i>Lactococcus lactis</i> NCDO 712 and NZ9000	FD: MRS medium gM17 medium vs. MRS medium	MF: fluorescence anisotropy values, low values = (+) MF	NCDO 712: (+) MF at 5°C (0.27 vs. 0.31) * NZ9000: (0.27 vs. 0.29) *	(Bodzen et al. 2021a)
	<i>Lactiplantibacillus plantarum</i> L1P-1	FD: MRS medium + 0.04 g·L ⁻¹ aspartate MRS medium vs. MRS medium + 0.04 g·L ⁻¹ aspartate	FA: GC-MS	(+) UFA/SFA (1.38 vs. 0.89) and (+) CFA content (10% vs. 7%)	(Chen et al. 2022)
	Uncontrolled pH	<i>Streptococci</i> strains (AC1, AC11, E8, ML1)	F: pH 6.0 pH 6.0 or uncontrolled pH	FA: GC-MS	Mean of three out four strains (AC1, AC11, ML1): (+) UFA/SFA (1.7 vs. 1.1) and (-) CFA (42% vs. 49%)
<i>Enococcus oeni</i> SD-2a		FD: pH 3.2 and pH 3.5, after uncontrolled pH Initial pH 3.2, pH 3.5, pH 4.0 or pH 4.8, after uncontrolled pH	FA: GC-MS	(+) UFA/SFA (2.2-2.0 vs. 1.5-1.7) and (+) CFA content (44-47% vs. 29-37%)	(Zhao et al. 2009)
<i>Enococcus oeni</i> SD-2a		FD: pH 3.5, after uncontrolled pH Initial pH 3.2, pH 3.5, pH 4.0 or pH 4.8, after uncontrolled pH in ATB medium	FA: GC-MS	No effect on UFA/SFA (0.63 vs. 0.67-0.94) (+) CFA content (48% vs. 31-45%)	(Li et al. 2009b)
<i>Lactiplantibacillus plantarum</i> L1P-1		FD: pH 6.8, after uncontrolled pH Initial pH 6.8 or pH 7.4, after uncontrolled pH	FA: GC-MS MI: β-galactosidase and Propidium Iodide (PI)	(+) UFA/SFA (0.6 vs. 0.5) and (+) CFA content (4% vs. 3%) (+) MI : low β-galactosidase activity low % of PI-stained cells	(E et al. 2021)

F: Freezing; FS: Frozen Storage; FD: Freeze-Drying; FDS: Freeze-Dried Storage; EP: the Exponential growth Phase; SP: the Stationary growth Phase; +: supplemented with; FA: Fatty Acids; GC-MS: Gas Chromatography-Mass Spectrometry; UFA: Unsaturated Fatty Acids; SFA: Saturated Fatty Acids; CFA: Cyclic Fatty Acid (cycC19:0); MF (bold or not bold): Membrane Fluidity; MI (bold or not bold): Membrane Integrity; Ts (bold or not bold): lipid transition temperature during cooling; (+): increase; (-): decrease; *: approximate values; vs.: versus; or: three or more comparisons; NR: Not Reported.

Table 1.6 (Continued) Reported studies on the lipid cellular properties modifications that have been linked to Lactic Acid Bacteria (LAB) resistance to stabilization process and storage.

	LAB strain	Stabilization process: selected condition Conditions evaluated	Methods of analysis	Relation between resistance and lipid component modifications	Reference
Temperature and pH	<i>Lactobacillus acidophilus</i> CRL 640	F: 25°C 25°C, 30°C, 37°C or 40°C	FA: GC-MS Lipid distribution fractions: phospholipids and glycolipids by TLC and FAB-MS	No effect on UFA/SFA (2.4 vs. 2.3-2.9), instead (+) C18:2 content (20% vs. 5-4%) (-) CFA content (6% vs. 10-17%), (+) ratio of glycolipids/phospholipids ratio (4.4 vs. 1.8-1.9)	(Fernández Murga et al. 2000)
	<i>Lactobacillus acidophilus</i> RD758	F and FS (3 months, -20°C): 30°C, pH 6.0 and 37°C, pH 5.0 Temperatures at pH 6.0: 30°C, 37°C or 42°C and pHs at 37°C: 4.5, 5.0 or 6.0	FA: GC-MS	(+) UFA/SFA (0.3 vs. 0.2) and (+) CFA content (11% vs. 5-7%) at 30°C, pH 6.0 (+) UFA/SFA (0.4 vs. 0.3-0.2) and (+) CFA content (12% vs. 8-11%) at 37°C, pH 5.0	(Wang et al. 2005a)
	<i>Loigolactobacillus coryniformis</i> Si3	FD: 42°C, pH 5.5 and 34°C, pH 5.5 First 12 h of culture at 34°C, pH 5.5 and then for 6 h, temperatures at pH 5.5: 26°C, 34°C or 42°C, pHs at 34°C: 6.5 vs. 4.5 and 30°C, pH 4.5	FA: GC-MS	No effect on UFA/SFA (1.2-1.6 vs. 1.5-3.0) No effect on CFA content (27-22% vs. 21-25%)	(Schoug et al. 2008)
	<i>Lactobacillus bulgaricus</i> L2	FD: 30°C, pH 5.0, 35°C, pH 5.5 and 39°C, pH 6.0 Temperatures: 30°C, 35°C, 37°C or 39°C and pHs: 5.0, 5.5, 6.0 or 6.5	FA: GC-MS	No effect on UFA/SFA (11.1 vs. 6.9-13.3) No effect on CFA (3-4% vs. 2-8%)	(Li et al. 2009a)
	<i>Limosilactobacillus reuteri</i> I5007	FD: 37°C, pH 6.7 First 10 h of culture at 37°C, pH 5.7 and then for 6h, Temperatures at pH 5.7: 4°C, 27°C or 47°C and pHs at 37°C: 4.7, 5.7 or 6.7	FA: GC-MS	(+) UFA/SFA (1.5 vs. 1.3-1.4) No effect on CFA (2% vs. 2%)	(Liu et al. 2014)
Harvest time	<i>Lactobacillus acidophilus</i> RD758	F and FS (2 months, -20°C): starved cells Not starved cells (1 h after the beginning of SP) vs. starved cells (18 h after the beginning of SP)	FA: GC-MS	(+) UFA/SFA (0.18 vs. 0.15), (+) BFA (9.8 vs. 1.8) (+) CFA content (2.2 vs. 1.6)	(Wang et al. 2011)
	<i>Lentilactobacillus buchneri</i> R1102	F: EP EP vs. SP	FA: GC-MS MF: fluorescence anisotropy values, low values = (+) MF	(+) UFA/SFA (0.8 vs. 0.4) and (-) CFA content (10% vs. 21%) (+) MF at 37°C (0.136 vs. 0.144)	(Louesdon et al. 2015)
	<i>Limosilactobacillus reuteri</i> TMW1.106	F, FD, FDS (14 days, room temperature): SP EP vs. SP	Membrane integrity: the dye exclusion assay Live/Dead BacLight® bacterial viability kit	(+) MI : F (80% vs. 30%) *, FD (35% vs. 5%) * and FDS (25% vs. 0%) * when fructo-oligosaccharide is used as the protective solution	(Schwab et al. 2007)
	<i>Oenococcus oeni</i> SD-2a	FD: early SP mid-EP vs. early SP	FA: GC-MS	Not possible to calculate UFA/SFA, instead (-) C18:1 cis 11 content (25% vs. 35%), (+) CFA content (35% vs. 23%)	(Li et al. 2009b)
Harvest time and temperature	<i>Lactococcus lactis</i> subsp. <i>lactis</i> TOMSC161	FD and FDS (3 months, 25°C): late SP, 30°C and 22°C Harvest times: mid EP, late EP, early SP, and late SP Temperatures: 22°C vs. 30°C	FA: GC-MS MF: fluorescence anisotropy values, low values = (+) MF Lipid transition temperature during heating (Tm): FT-IR	When temperatures are compared for late SP (-) UFA/SFA (0.06 vs. 0.11), (-) CFA content (34% vs. 35%), (+) Tm (17°C vs. 9°C) At increased harvest time and 30°C (+) CFA content (34-35% vs. 19-29%) (-) MF at 20°C, high anisotropy values (0.169 vs. 0.139-0.166), No effect on Tm (17°C vs. 9-18°C)	(Velly et al. 2015)
	<i>Lactococcus lactis</i> subsp. <i>lactis</i> MM210 and FG2 and <i>Lactococcus lactis</i> subsp. <i>cremoris</i> MM160, MM310	F and FD: (1) HS for MM210 and FG2. (2) CS for MM160 and MM310 HS (42°C for 25 min) or CS (10°C for 2 h) stress vs. No stress cells (30°C)	FA: GC-MS	(1) MM210, HS: (-) UFA/SFA (0.8 vs. 0.9-1.1) and (+) CFA (27% vs. 21-24%). FG2, HS: (-) UFA/SFA (0.5 vs. 0.7-1.1) and (+) CFA (21% vs. 11-12%) (2) MM160, CS: (+) UFA/SFA (1.2 vs. 0.8-1.0) and no effect on CFA content (18% vs. 16-24%). MM310, CS: (+) UFA/SFA (0.9 vs. 0.5-0.6) and (-) CFA content (13% vs. 15-21%)	(Broadbent and Lin 1999)
Cold Stress (CS) and Heat Stress (HS)	<i>Lactobacillus acidophilus</i> RD758	F and FS (24 weeks, at -20°C): CS at 26°C for 8 h, during growth then at 15°C, after the beginning of SP vs. 37°C, pH 6.0	FA: GC-MS	(+) UFA/SFA (0.22 vs. 0.18) and (+) CFA content (3.1% vs. 2.5%)	(Wang et al. 2005b)
	<i>Lentilactobacillus buchneri</i> R1102	FD and FDS (3months, 25°C): KCl at 7.5 g·L ⁻¹ in the beginning the fermentation Addition of KCl at 7.5 g·L ⁻¹ , 45 g·L ⁻¹ in the beginning the fermentation, 45 g·L ⁻¹ after the fermentation, beginning (7.5 g·L ⁻¹)-after fermentation (45 g·L ⁻¹) or not addition of KCl	FA: GC-MS MF: fluorescence anisotropy values, low values = (+) MF	No effect on UFA/SFA (0.85 vs. 0.73-0.91), no effect on CFA content (17% vs. 16-25%), no effect (+) MF at 37°C (0.133 vs. 0.136-0.162)	(Louesdon et al. 2014)
Acid stress	<i>Lactobacillus delbrueckii</i> subsp. <i>bulgaricus</i> CFL1	F and FS (3 months, -20°C): pH 5.25 for 30 min after harvesting at the SP vs. cells without acidification treatment	FA: GC-MS	(-) UFA/SFA (1.6 vs. 1.7) and (-) CFA content (9% vs. 11%)	(Streit et al. 2008)

F: Freezing; FS: Frozen Storage; FD: Freeze-Drying; FDS: Freeze-Dried Storage; EP: the Exponential growth Phase; SP: the Stationary growth Phase; +: supplemented with; FA: Fatty Acids; GC-MS: Gas Chromatography-Mass Spectrometry; UFA: Unsaturated Fatty Acids; SFA: Saturated Fatty Acids; CFA: Cyclic Fatty Acid (cycC19:0); MF (bold or not bold): Membrane Fluidity; MI (bold or not bold): Membrane Integrity; Ts or Tm (bold or not bold): lipid transition temperature during cooling or heating, respectively; (+): increase; (-): decrease; vs.: versus; or: three or more comparisons; NR: Not Reported.

1.3.4. The addition of protective molecules

1.3.4.1. Protective molecules for LAB stabilization

The composition of the solution used to protect cells during freezing or freeze-drying has been pointed out as another critical factor to address for stabilizing these bacteria. Protective molecules are crucial to preserving bacteria's functional properties. For the freezing process, an efficient protective molecule should provide cryo-protection to the cells. For freeze-drying, these molecules should be easily dried, improve stability during storage and ease rehydration.

Numerous protective solutions have been reported. These protective solutions contain the following molecules: polyols (glycerol and sorbitol), disaccharides (two monosaccharides), polysaccharides (long chains of monosaccharides), organic salts (sodium glutamate, sodium ascorbate), and skim milk.

Table 1.7 compares the efficiency of protective solutions at different concentrations to enhance LAB survival. First, disaccharides such as sucrose and trehalose have been identified as suitable protective molecules to improve LAB freezing and freeze-drying resistance. These two disaccharides have ensured higher LAB culturability (survival rate in %) compared to other molecules.

For both disaccharides, an increase of 24-35% in LAB survival has been reported compared to glycerol (Dimitrellou et al. 2016; Wang et al. 2019) ; 300% compared to sorbitol (Siaterlis et al. 2009); 10-24% compared to skim milk (Castro et al. 1997; Wang et al. 2019); 2-5% compared to lactose (De Giulio et al. 2005; Miao et al. 2008; Pehkonen et al. 2008); and 78-100% compared to polysaccharides (Strasser et al. 2009; Hongpattarakere et al. 2013).

For freeze-dried storage, the polysaccharides and disaccharides have been predominantly used to preserve LAB (Schwab et al. 2007; Reddy et al. 2009; Santos et al. 2014; Romano et al. 2016b; Tang et al. 2020). Then, the use of antioxidant molecules as protective solutions has been reported to favor LAB survival during storage since these molecules avoid oxidation reactions (Fonseca et al. 2003; Martos et al. 2007). Finally, skim milk solution has received special attention for protecting LAB cells (the last four studies presented in Table 1.7) or as a composite in a protective solution mix.

In the last decade, several studies have focused on finding new alternatives of protective solutions. One alternative consists of optimizing the concentrations of different molecules to be used in a single formulation. These protective formulations have used at least skim milk, sucrose, trehalose as their main components (Khoramnia et al. 2011; Jalali et al. 2012; Shu et al. 2018; Turuvekere Sadguruprasad and Basavaraj 2018; Archacka et al. 2019; Ren et al. 2019; Gul et al. 2020b, a).

Another alternative proposes using unconventional molecules to efficiently protect LAB at the same level as the regular protective molecules (trehalose, sucrose, or skim milk). For example, rice protein and fructo-oligosaccharide mix (Sayedboworn et al. 2019), mungbean (Sulabo et al. 2020), and micellar casein (Bodzen et al. 2021b).

In an environmentally friendly context, protective molecules such as fructo-oligosaccharides (FOS) and galacto-oligosaccharides (GOS) can be produced from food and agricultural wastes (chicory, sweet potatoes, banana or agave). Additionally FOS and GOS are known to exert prebiotic properties (compounds that act as food for the host microflora) (Tymczyszyn et al. 2011).

These molecules have received a significant interest since they have been identified to successfully protect LAB. For *Lactobacillus delbrueckii* subsp. *bulgaricus* CIDCA 333, minimal loss of culturability (about 0-0.5 log CFU·mL⁻¹) during storage (4°C, 20 days, 11% water content) was observed when bacteria were protected with FOS (Romano et al. 2016b) and GOS (Santos et al. 2014), compared to bacteria without protection.

Overall, selecting a protective solution will rely on the molecules' availability, cost, and proven efficacy for the LAB strain stabilization.

Table 1.7 Studies on the use of protective solutions that have been effective protectors for freezing, freeze-drying, and storage Lactic Acid Bacteria (LAB).

LAB strain	Stabilization process: the most effective protective solution Studied protectors and concentration	Reference
<i>Streptococcus lactis</i> INIA 12	FS (60 days, -20°C and -70°C): lactose 10% Lactose 10%, sucrose 10%, egg yolk 10%, supernatant 10%, glycerol 10% or GCGS solution at 10%	(Chavarri et al. 1988)
<i>Lactobacillus delbrueckii</i> subsp. <i>bulgaricus</i> NCFB 1489	F (-80°C) and FD : trehalose 5% Trehalose 5%, glycerol 9.8%, skim milk powder 11% or maltodextrin 11%	(Castro et al. 1997)
<i>Lactobacillus delbrueckii</i> subsp. <i>bulgaricus</i> DSM20081, <i>Lactobacillus acidophilus</i> DSM20079, and <i>Streptococcus salivarius</i> subsp. <i>thermophilus</i>	F (-80°C) and FD : trehalose for the three LAB strains Trehalose, maltose, sucrose, glucose or lactose at NR%	(De Giulio et al. 2005)
<i>Lactocaseibacillus rhamnosus</i> GG LGG	FD and FDS (41 days, 30°C): trehalose 20% Trehalose 20% or lactose 20%	(Pehkonen et al. 2008)
<i>Lactocaseibacillus rhamnosus</i> GG	F (-80°C) and FD : trehalose 15% Trehalose 15%, lactose 15%, maltose 15% or sucrose 15%	(Miao et al. 2008)
<i>Lactocaseibacillus rhamnosus</i> GG ATCC 53103 and <i>Lactiplantibacillus plantarum</i> NCIMB 8826	FD : sucrose 10% for GG ATCC 53103 and sucrose 5% for NCIMB 8826 Sucrose (1, 5 or 10%), trehalose (1, 5 or 10%) or sorbitol (1 or 5%)	(Siaterlis et al. 2009)
<i>Enterococcus faecium</i> IFA 045 and <i>Lactiplantibacillus plantarum</i> IFA 278	FD : no difference for IFA 045, trehalose 32% or sucrose 32% for IFA 278 FDS (6 months, 4°C and 22°C): trehalose 32% for IFA 045 and IFA 278 Glucose 32%, sucrose 32%, trehalose 32% or maltodextrin 32%	(Strasser et al. 2009)
<i>Limosilactobacillus reuteri</i> CICC6226	FD : trehalose 10% or skim milk 10% Trehalose 10%, skim milk 10%, trehalose 5%, or sucrose 15%	(Li et al. 2011)
<i>Lactiplantibacillus plantarum</i> TISTR 875	FD : sucrose 10% Sucrose 10%, FOS 10%, skim milk 10%, soy extract 10%, soy fiber 10%, mung extract 10%, mung fiberB 10%, corn extract 10% or corn fiber 10%	(Hongpattarakere et al. 2013)
Three strains of <i>Lactiplantibacillus plantarum</i> (UNQLp 133, UNQLp 65.3, UNQLp 155)	F (-20°C): sodium glutamate 2.5% for UNQLp 133 and UNQLp 155, sucrose 20% for UNQLp 65.3 FD : trehalose 20% for UNQLp 133, sodium glutamate 2.5% for UNQLp 65.3, and sucrose 20% for UNQLp 155 Sodium glutamate 2.5%, sucrose 20% or trehalose at 20%	(Bravo-Ferrada et al. 2015)
<i>Lactocaseibacillus casei</i> ATCC 393	FD : Trehalose 10% Trehalose 10%, glucose 10%, fructose 10%, lactose 10%, glycerol 10% or whey at 10% FDS (6 and 12 months, 4°C, on apple pieces or casein): lactose 10% for apple pieces and monosodium glutamate % for casein Lactose, monosodium glutamate, glucose, fructose, galactose, sucrose, maltose, trehalose, raffinose, starch, glycerol, sorbitol, monosodium glutamate, peptone, skim milk or whey, all of them at 10%	(Dimitrellou et al. 2016)
<i>Lactiplantibacillus plantarum</i> ST-III and <i>Lactocaseibacillus casei</i> LC2W	F (-80°C): sucrose 15% for ST-III and sucrose 10% for LC2W Sucrose (5, 10 or 15%), trehalose (5, 10 or 15%), glycerol (5, 10 or 15%) or skim milk 10%	(Wang et al. 2019)
Three strains of <i>Lactiplantibacillus plantarum</i> (AR113, WCFS1, AR307)	F (-40°C): sucrose 10% or trehalose 10% for AR113 and WCFS1; 5 protectants (among them sucrose and trehalose) for AR307 and FD : sucrose 10% or soy polysaccharide 10% for AR113; sucrose 10% and gum Arabic 1% for WCFS1; sucrose 10% or trehalose 10% for AR307. Sucrose 10%, trehalose 10%, sorbitol 10%, mannose 10%, mannitol 10%, soy polysaccharides (1 or 10%) or gum Arabic 1%	(Wang et al. 2021)
<i>Limosilactobacillus reuteri</i> TW1.106	FD and FDS (14 days, room temperature): FOS 7.5% FOS 7.5%, sucrose 7.5%, inulin 7.5% or skim milk 7.5%	(Schwab et al. 2007)
<i>Ligalactobacillus salivarius</i> CFR-2158, <i>Lactiplantibacillus plantarum</i> , <i>Pediococcus acidilactici</i>	FDS (60 days, 4°C): maltodextrin 20% for the three LAB strains Maltodextrin 20%, lactose 20% or skim milk 20%	(Reddy et al. 2009)
<i>Lactobacillus delbrueckii</i> subsp. <i>bulgaricus</i> CIDCA 333	FDS (7 and 21 days, 4°C, up to 80%RH): GOS Biotempo 20% GOS Biotempo 20%, GOS Cup Oligo H-70® 20% or lactulose 20%	(Santos et al. 2014)
<i>Lactobacillus delbrueckii</i> subsp. <i>bulgaricus</i> CIDCA 333	FD : sucrose, FOS 2.5 h, FOS 24 h at 20% and FDS (80 days, 4°C): FOS 2.5 h and commercial FOS 20% Sucrose 20%, FOS 2.5 h, FOS 2.5 h (pure), FOS 24 h, FOS 24 h (pure) or commercial FOS 20%	(Romano et al. 2016b)
<i>Lactobacillus acidophilus</i> FTDC 3081	FD : maltodextrin 5%, FDS (30 days, 4°C, 25°C and 40°C): sucrose 20% at 4°C, maltodextrin 5% at 25°C, and maltodextrin 10% at 40°C. Maltodextrin (5, 10 or 20%), corn starch (5, 10 or 20%), skim milk (5, 10 or 20%) or sucrose (5, 10 or 20%)	(Tang et al. 2020)

F: Freezing; **FS**: Frozen Storage **FD**: Freeze-Drying; **FDS**: Freeze-Dried Storage; FOS: fructo-oligosaccharides; GOS: galacto-oligosaccharides.

Table 1.7 (Continued) Studies on the use of protective solutions that have been effective protectors during Lactic Acid Bacteria (LAB) freezing, freeze-drying, and storage.

	LAB strain	Stabilization process: the most effective protective solution Studied protectors and concentration	Reference
Polyols	<i>Lactocaseibacillus rhamnosus</i> IMC 501® and <i>Lactocaseibacillus paracasei</i> IMC 502®	FDS (5 months, 4°C and room temperature): glycerol 10% at room temperature and all protectors at 4°C for both LAB stains Glycerol 10%, skim milk 10%, inulin 10%, dextrin 10%, sorbitol 10%, mannitol 10% or crystalline 10%	(Savini et al. 2010)
	<i>Lactocaseibacillus paracasei</i> subsp. <i>paracasei</i> F19	FDS (20, 40, 60, 80 days, 20°C): sorbitol Sorbitol, maltodextrin or trehalose at NR%	(Ambros et al. 2018)
Antioxidants	<i>Lactobacillus delbrueckii</i> subsp. <i>bulgaricus</i> CFL1	F (-20°C): betaine and FS (8 weeks, -20°C): sodium ascorbate 1% Sodium ascorbate 1%, betaine 12%, sucrose, trehalose, maltodextrin 10%, lactose 10%, maltose 10%, sodium glutamate 10%, glycerol 5%, supernatant 5.3%	(Fonseca et al. 2003)
	<i>Levilactobacillus brevis</i> and <i>Oenococcus oeni</i> H-2	FD : yeast extract 4% for <i>Levilactobacillus brevis</i> and sodium glutamate 2.5% for H-2 Yeast extract 4%, sucrose 10%, lactose 10%, trehalose 10%, maltose 10%, glucose 10%, fructose 10%, sodium glutamate 2.5%, sorbitol 5%, mannitol 5% or MGY medium 5%	(Zhao and Zhang 2005)
	<i>Lactobacillus delbrueckii</i> subsp. <i>bulgaricus</i> CRL 494	FD and FDS (3 months, 30°C): monosodium aspartate (5% or 10%) or glutamate (5% or 10%) Monosodium aspartate (1.25, 2.5, 5 or 10%) or monosodium glutamate (1.25, 2.5, 5 or 10%)	(Martos et al. 2007)
	<i>Lactobacillus acidophilus</i> JCM1132 ^T , <i>Limosilactobacillus reuteri</i> JCM1112 ^T , and <i>Lactocaseibacillus paracasei</i> subsp. <i>paracasei</i> JCM8130 ^T	FDS (4 weeks, 37°C): Cys for JCM1132 ^T , carnosine for JCM1112 ^T and JCM8130 ^T Antioxidant solutions: carnosine 20 mM, Cys 20 mM, GSH 20 mM or ascorbic acid 20 mM	(Mikajiri et al. 2021)
Skim milk	<i>Lactiplantibacillus plantarum</i> L ₄	F and FD : Nonfat milk at 8% or peptone at 5% Nonfat milk at 8%, peptone 5%, sucrose 5%, lactose 5% or sodium glutamate 1.5%	(Tsvetkov and Brankova 1983)
	<i>Lactocaseibacillus rhamnosus</i> CT1, GT1/1, OT1/3	F (-80°C): skim milk at 20% for the three strains Skim milk at 20%, MRS broth and glycerol at 20%, or skim milk + 0.5% glucose	(Succi et al. 2007)
	<i>Lactobacillus acidophilus</i> ATCC 4962	FD : skim milk 0.1% FDS (8 weeks, 5°C, 28°C and 40°C): skim milk 0.1% Skim milk, skim milk with malt extract, sorbitol, sucrose, glycerol, dextran or monosodium glutamate at 0.1% for all protective solutions	(Pyar and Peh 2011)
	<i>Limosilactobacillus fermentum</i> IAL 4541	FDS (30, 60, 90, 120, 210, and 365 days, room temperature): skim milk 10% + sodium glutamate skim milk 10%, skim milk + sodium glutamate 10%, trehalose 5% or sucrose 10%	(Stefanello et al. 2019)

F: Freezing; **FS**: Frozen Storage **FD**: Freeze-Drying; **FDS**: Freeze-Dried Storage; +: supplemented with

1.3.4.2. Mechanisms of sugars to protect LAB

As described above, adding a protective solution to LAB concentrates is considered a common strategy to keep the survival and functional properties of LAB after the stabilization process and subsequent storage. Sugars are preferable among the protective molecules because of their relatively low prices, chemically innocuous nature, and common use in the food industry (the primary sector where LAB are used). Sugars are actually used in patented protective solutions for starter producers such as Danisco® and Chris Hansen® (Corveleyn et al. 2010; Hollard et al. 2011).

Sugars have extensively studied and proven their effectiveness in protecting LAB during freezing, freeze-drying, and storage (previously seen in Table 1.7). When considering the cytoplasmic membrane, they have been considered non-penetrating Cryo-Protective Agents (non-penetrating-CPA). According to Hubálek (2003), these molecules cross (penetrate) the cell wall but not the cytoplasmic membrane. The protection mechanisms of sugars are based on the following hypothesis: water replacement and hydration forces (Figure 1.18).

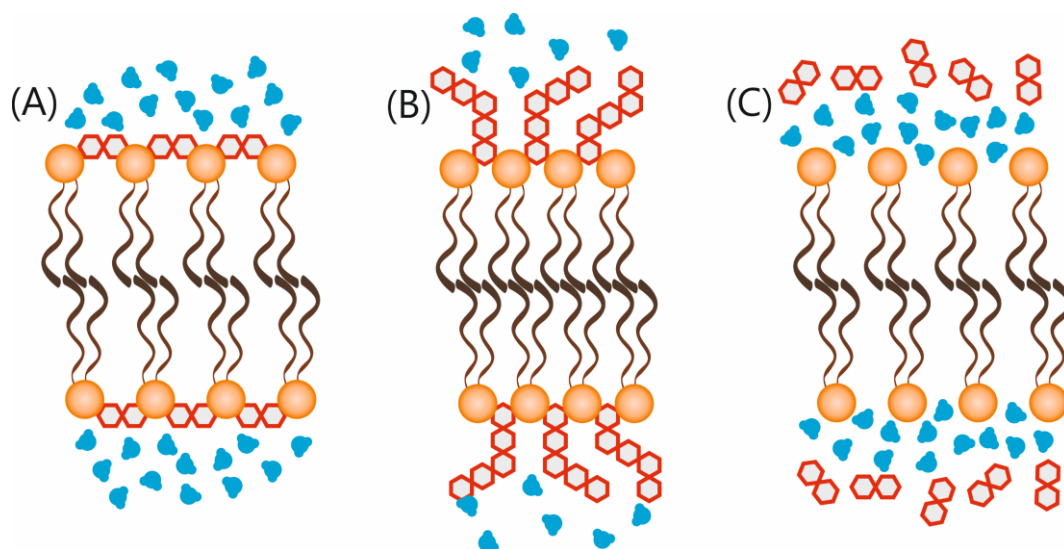


Figure 1.18 Schematic illustration of proposed mechanisms of membrane sugar-interactions. (A) and (B) water replacement by disaccharides and polysaccharides, respectively. (C) Hydration forces. Sugars are represented by hexagons with red outlines and water molecules are represented by blue circles.

When liquid water is removed due to freezing or freeze-drying, the water replacement hypothesis (Figure 1.18 (A)) postulates that sugars replace the water surrounding the polar head groups via the hydrogen bonds between hydroxyl groups of the sugars (OH) and the phosphate group in the polar head of the phospholipids. These hydrogen bonds allow the head groups to spread apart, decreasing van der Waals' interactions among the acyl chains of the phospholipid (preventing membrane acyl chains from coming closer to each other). Head group separation lowers the lipid phase transition temperature (Crowe et al. 1984, 1992; Crowe 2002).

Since the eighties, studies have suggested that sucrose and trehalose molecules replace the water around the polar head in the membrane. These observations have been performed on liposomes (Crowe et al. 1988), pollen cells (Crowe et al. 1989a; Hoekstra et al. 1992), yeast cells (Leslie et al. 1994), and *E.coli* and *Bacillus thuringiensis* bacteria (Leslie et al. 1995).

Inulin (a polysaccharide) interaction with lipid models has corroborated the water replacement hypothesis (Vereyken et al. 2003b). Despite its large molecule size, inulin may get inserted between headgroups of phospholipids and decrease the lipid phase transition temperature. The interaction of this polysaccharide was possible due to its structure flexibility (Figure 1.18 (B)). This hypothesis was based on comparing other polysaccharides such as dextran and glucan and analyzing their interaction with a lipid monolayer model. Cacula and Hinch (2006) also confirmed this observation by assessing three oligosaccharides of the same degree of polymerization in interaction with egg phosphatidylcholine liposomes.

Thus, the structural flexibility of each polysaccharide has an important interactional role in the phospholipids' polar heads.

The hydration forces hypothesis (Figure 1.18 (C)) suggests that sugars are preferentially excluded from the bilayer water interface and remain within the bulk solution. Sugars indirectly increase the interfacial free energy through osmotic imbalance that preserves the hydration shell surrounding phospholipid head groups (Yoon et al. 1998; Demé and Zemb 2000; Dhaliwal et al. 2019).

Aside from the two hypotheses (water replacement and hydration forces), the ability of the sugars (disaccharides and polysaccharides) to form a glassy allows that cells are found in a vitreous state (high viscosity and low molecular mobility). In this glassy state, molecular interactions are restricted (Slade and Levine 1994; Koster et al. 1994). It has been reported that vitrification complements these two interaction hypotheses (Crowe et al. 1996, 1998).

The two mechanisms of protection of the sugars have been studied using lipid models and applying different biophysical methods. For example, these include scattering methods (Garvey et al. 2013; Kent et al. 2015), anisotropy (Roy et al. 2016), mathematical simulations (Lee et al. 2005; Van Den Bogaart et al. 2007; Kapla et al. 2013; Stachura et al. 2019), nuclear magnetic resonance (Strauss et al. 1986; Moiset et al. 2014), and infrared spectroscopy.

Among the different biophysical methods, Fourier-transform infrared spectroscopy (FTIR) requires minimal sample handling, no need for exogenous probes, and the intact cells can be examined without lysis.

This method exploits the absorption of InfraRed (IR) radiation by molecular vibrations of specific groups in molecules. Vibration modes include stretching (ν) and bending (δ) of the chemical bond. Stretching modes involve a modification of the bond length symmetrically or asymmetrically. Bending modes involve a modification of the bond angle (or torsion angle) occurring in-plane (scissoring and wagging) or out-of-plane (twisting and rocking) (Davis et al. 2001) (Figure 1.19).

The interaction mechanisms between a sugar and membrane lipid can be elucidated by analyzing the shifts and intensity variations of the specific chemical structures of membrane lipids in the presence of sugars. For example, it has been observed that the position of the CH_2 symmetric ($\nu_{\text{sym}}\text{CH}_2$) stretching band (approximately 2850 cm^{-1}) arising from hydrocarbon chains of lipids, e.g., in phospholipids and glycolipids (Figure 1.20).

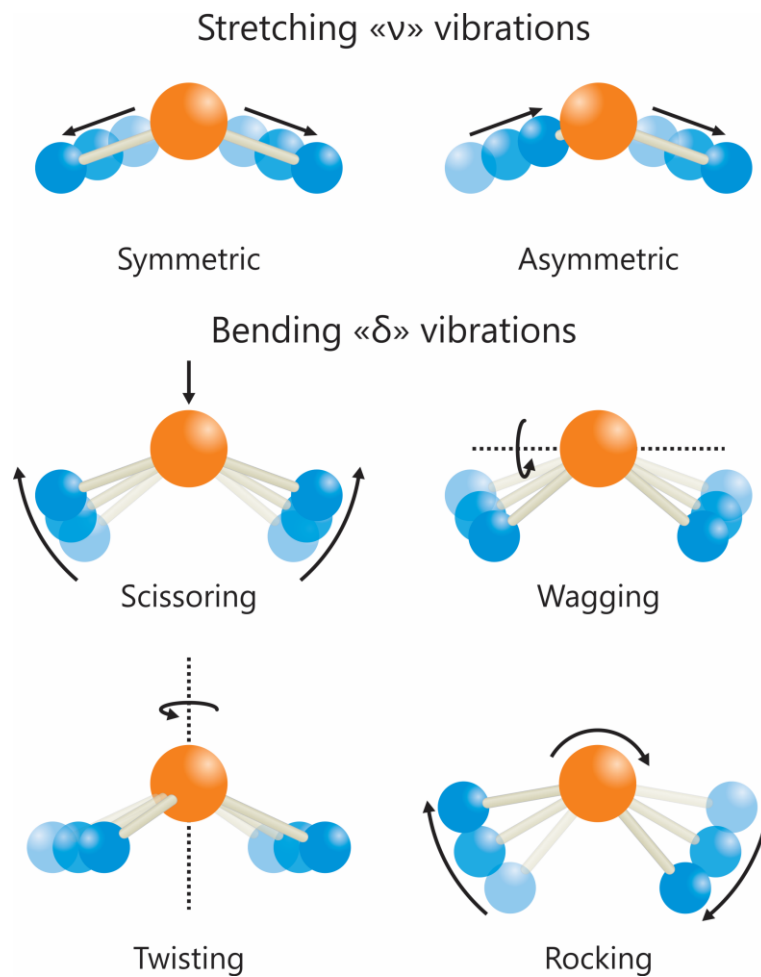


Figure 1.19 Overview of the vibration modes causing IR absorption, illustrated with water molecules. Adapted from (Chaplin 2022).

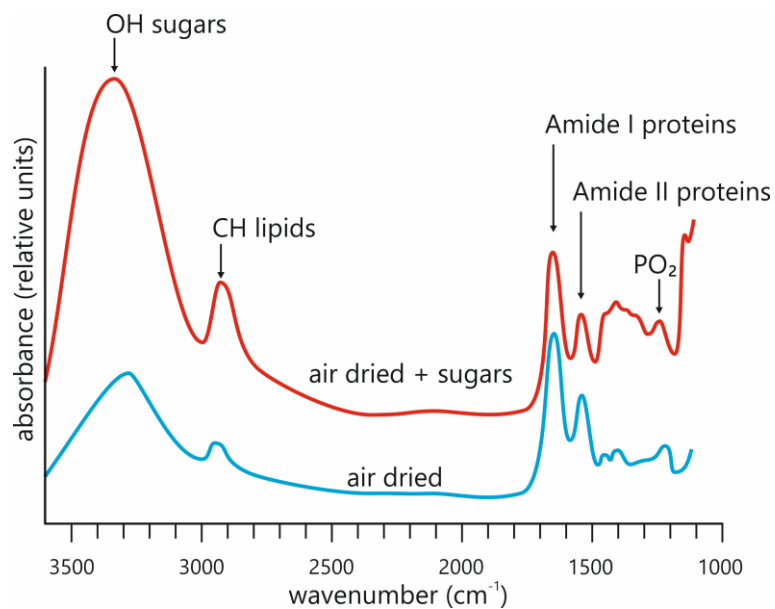


Figure 1.20 Absorption spectra of air-dried *Lactobacillus delbrueckii* subsp. *bulgaricus* CFL1. In the presence (red spectrum) and absence (blue spectrum) of a mixture of sucrose and maltose (5/5) at 20°C. Adapted from Oldenhof et al. 2005.

For lipid models, the asymmetric PO_2 stretching vibration band ($\nu_{\text{asym}}\text{PO}_2$) has also been analyzed (Hincha et al., 2003; Cacela and Hincha, 2006). This vibration band is located at approximately 1220 cm^{-1} and arises from the phosphate moiety of phospholipids head groups. Additionally, the Amide I and Amide II bands have been analyzed. These bands are located between $1700\text{-}1600\text{ cm}^{-1}$ and $1580\text{-}1510\text{ cm}^{-1}$, respectively. Amide I mainly result from the C=O stretching vibration and the N-H bending, whereas Amide II is from the C-N stretching vibrations of the protein backbone (Figure 1.20). Amide I and II vibration modes are hardly affected by the nature of the protein side-chain but are sensitive to protein secondary structures, especially the Amide I. Water is a strong IR light absorber. In particular, the H-O-H bending frequency at 1650 cm^{-1} occurs at the same position as the Amide I, thus interfering with the analysis of proteins in hydrated samples (Miller et al. 2003b).

FTIR has been used for studies on the effects or influences of chemical agents on the damage of cell components of Gram-negative bacteria such as *Escherichia coli* and *Pseudomonas aeruginosa* (Al-Qadiri et al. 2008). Additionally, four studies have analyzed small molecules' interaction with LAB by mainly monitoring the position ($\nu_{\text{sym}}\text{CH}_2$) in the presence of different molecules. These molecules include maltose (Linders et al. 1997), sucrose (Kilimann et al. 2006), skim milk and maltodextrin (Oldenhof et al. 2005), as well as sorbitol (Santivarangkna et al. 2010).

Sum-up of section 1.3

Strategies to improve lactic acid bacteria resistance to the critical steps of their production: stabilization processes and storage

- A low cooling rate during freezing is less technically demanding, and LAB cells can be stored at higher temperatures ($\leq -80^{\circ}\text{C}$).
- The reduction of the sublimation time can be achieved when the chamber pressure and shelf temperature are increased, provided that the LAB survival is not scarified.
- In bioreactor cultures, a supplemented fermentation medium with sugars or oleates has a neutral or beneficial effect on LAB resistance to freezing and freeze-drying.
- Low controlled pH has induced LAB resistance to freezing, freeze-dried or storage for different LAB species.
- LAB resistance can also be improved when LAB are exposed during growth or after harvesting to severe stress conditions for a determined time. Heat shock proteins (HSPs) and cold shock proteins (CSPs) are produced as a response adaptation mechanism.
- Most studies revealed the beneficial effect of harvesting LAB cells at the stationary growth phase to improve stabilization and storage resistance.
- The modifications of fermentation conditions and different stresses generate active LAB cellular responses leading to the modification of cellular constituents, especially the lipids composition.
- The increase of the ratio UFA/SFA or CFA usually enhances the resistance of LAB to stabilization and storage.
- Lipid phase transition temperatures and membrane fluidity have been related to the saturation level of the fatty acids in the cytoplasmic membrane. High freezing resistance has been related to low lipid phase transition temperatures. Conversely, high freeze-dried resistance has not linked to a lipid phase transition temperature.

Sum-up of section 1.3 (continued)

Strategies to improve lactic acid bacteria resistance to the critical steps of their production: stabilization processes and storage

- Only one study reported the relevance of glycolipids in membrane composition. A high ratio of sugar/phosphorus was associated with an improved freezing resistance instead of a fatty acid composition.
- The addition of a protective solution concentrated has been pointed out as another crucial factor in stabilizing LAB.
- Sugars, mainly sucrose and trehalose, have been identified as suitable protective molecules to improve LAB freezing and freeze-drying resistance.
- Minimal loss of LAB survival has been proved by using innovative protective molecules such as FOS and GOS.
- The protection mechanisms of sugars are based on the following hypothesis: water replacement and hydration forces.
- Sugars form a glassy matrix that cells are found in a vitreous state (high viscosity and low molecular mobility) where molecular interactions are restricted.
- Fourier-transform infrared spectroscopy (FTIR) requires minimal sample handling, and the intact cells can be examined among the different biophysical methods to examine sugars' interactions with the membrane.

1.4. Conclusions and future directions

The economic relevance of LAB relies on their multiple industrial applications, particularly in the worldwide production of fermented dairy products. Also, there is substantial evidence that the administration of some LAB genera (i.e., probiotics) promotes health benefits. Consequently, significant progress in LAB production has been made. Research efforts are mainly dedicated to preserving these microorganisms in the long term, using stabilization processes, such as freezing and freeze-drying. These processes, however, generate different stresses that lead to LAB degradation and loss of their functional proprieties. Stabilization processes induce cellular damage in proteins and lipids components of LAB; the cell membrane was identified as the main degradation target. Thus, various strategies have been proposed to improve LAB resistance to freezing or freeze-drying. One of them is to change the fermentation parameters to induce mild-stress so that LAB can develop adaptative mechanisms to help them cope with the stresses occurring during the stabilization processes. Culture medium, temperature, pH, and harvest time were identified as the crucial parameters to modify for improving LAB resistance. In general, the fermentation conditions that lead to this beneficial effect on LAB resistance differ from the optimal growth condition. According to the literature, it remains unclear if this strategy is suitable for LAB production on a large scale. In this case, not only resistant cells are required to stabilize, but also the production of a high cell concentration. Therefore, fully optimization seems necessary to find a compromise between both parameters (resistance and cell concentration).

As a consequence of changing the fermentation conditions of LAB, membrane lipid modulation has been observed and related to LAB resistance. For this reason, membrane characterization has primarily been carried out by determining the composition of fatty acids. A few studies performed measurements of membrane fluidity and lipid phase transition temperature. This first chapter revealed that lipid characterization does not consider the contribution of the different lipid classes present in the LAB membrane. A multi-analysis of membrane lipids in LAB could broaden the knowledge of the current information about membrane lipids' contribution to LAB resistance.

Finally, different protective molecules are available to stabilize LAB; they limit the detrimental effects of the stabilization processes, particularly sugars, which are widely used in all their structure types (disaccharides and polysaccharides). FT-IR appeared to be an adequate approach to elucidate the mechanisms of sugars.

Chapter 2

2. OVERALL EXPERIMENTAL APPROACH

This chapter presents the overall experimental strategy used in this thesis

SUMMARY OF THE CHAPTER

2. OVERALL EXPERIMENTAL APPROACH	77
2.1. Choice of the lactic acid bacterium strain	78
2.2. Experimental strategies	78
2.2.1. Multi-objective optimization of frozen and freeze-dried <i>L. bulgaricus</i> CFL1 (Chapter 4)	80
2.2.2. Deep analysis of membrane lipids and their relationships with <i>L. bulgaricus</i> CFL1 resistance to freezing and freeze-drying (Chapter 5)	81
2.2.3. Influence of sugars on resistance and the membrane of <i>L. bulgaricus</i> CFL1 (Chapter 6)	81

2.1. Choice of the lactic acid bacterium strain

Some lactic acid bacteria with interesting functional properties are not used at an industrial scale because they are not robust enough to withstand the stabilization processes. With the aim to revisit the strategies of production and stabilization of LAB, the current thesis focused on a model of cryo-sensitive lactic acid bacteria: *Lactobacillus delbrueckii* subsp. *bulgaricus* CFL1 (referred to as *L. bulgaricus* CFL1 in the following chapters). *L. bulgaricus* CFL1 belongs to the subspecies widely used in fermented dairy products, especially for yogurt production. The scientific relevance of this strain relies on its sensitivity to freezing, as reported in former studies (Fonseca et al. 2000; Rault et al. 2007; Meneghel et al. 2017).

2.2. Experimental strategies

Some elements of the literature review are provided to highlight the originality of this thesis. As mentioned in the general introduction, the present research work has three main objectives addressed in chapters 4, 5, and 6. The content and aim of each chapter are briefly explained to provide the overall experimental approach illustrated in Figure 2.1.

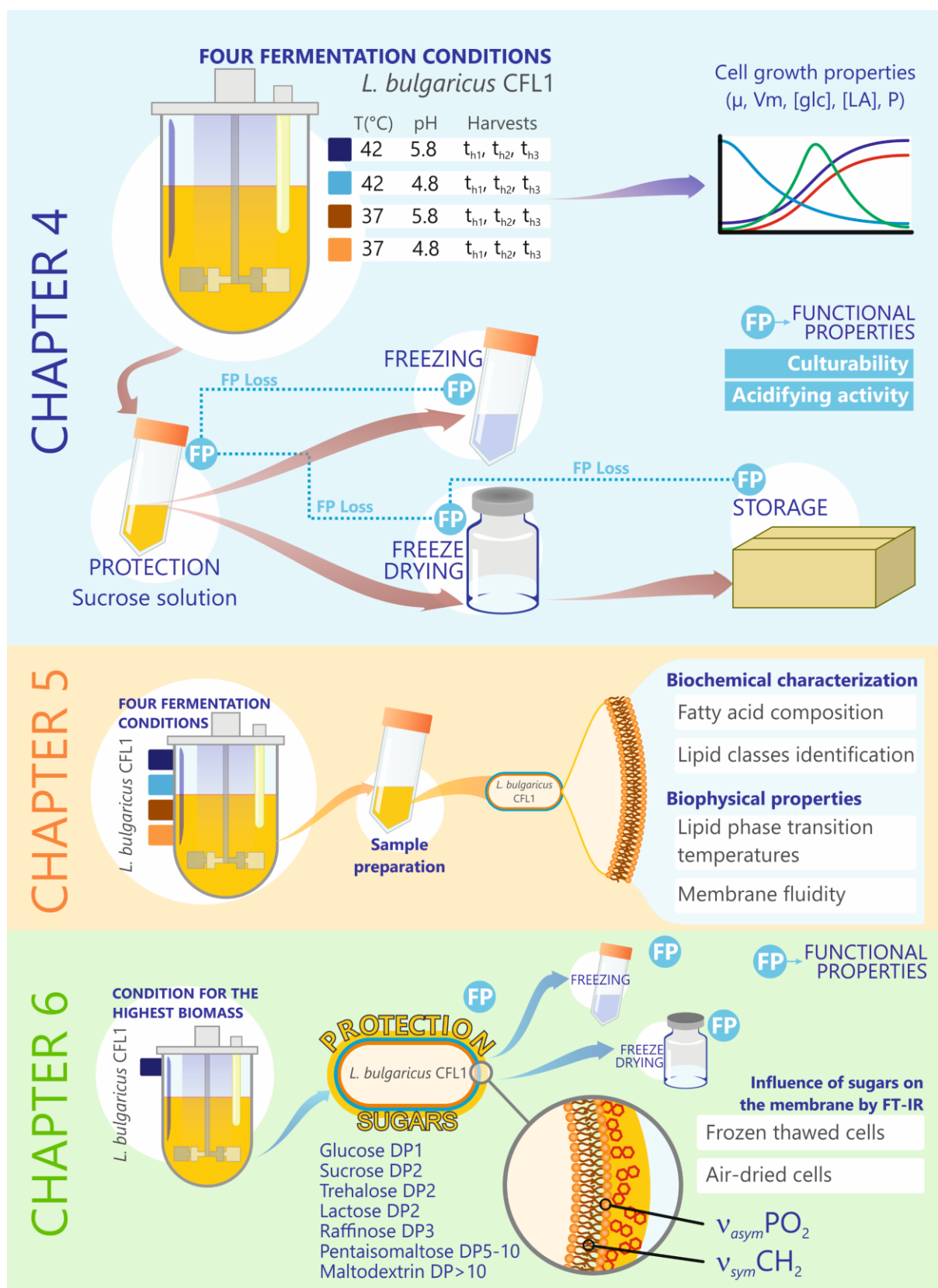


Figure 2.1 Schematic representation of the overall experimental approach implemented in the present thesis. Abbreviations: t_h , harvest time; μ , growth rate; V_m , maximal acidification rate; glc, glucose; LA, lactic acid; P, biomass productivity; DP, degree of polymerization; FTIR, Fourier Transform infrared spectroscopy; $\nu_{asym}PO_2$, asymmetric PO_2 stretching vibration band; $\nu_{sym}CH_2$, symmetric CH_2 stretching vibration band. Sugars molecules are represented by hexagons with red outline.

2.2.1. Multi-objective optimization of frozen and freeze-dried *L. bulgaricus* CFL1 (Chapter 4)

Literature review revealed that modifying LAB growth conditions during fermentation leads to resistant LAB to stabilization processes and storage. When LAB are cultivated at a different fermentation condition from the optimal one for growth, this new environment induce biological responses, that can help LAB withstand the subsequent stabilization processes. However, this new fermentation condition usually leads to lower concentrations of biomass ($\text{g}\cdot\text{L}^{-1}$ or $\text{CFU}\cdot\text{mL}^{-1}$). Producing large amounts of biomass at the industrial scale is necessary. Therefore, optimizing not only the biomass production but also the resistance of LAB to stabilization processes offers a solution to preserve the functional properties of LAB after the stabilization processes and storage.

L. bulgaricus CFL1 was grown at a lab-scale bioreactor in the culture medium MRS. This medium was previously identified to enhance the resistance of this strain to freezing (Gautier et al. 2013). Four different fermentation conditions were chosen, including two levels of temperature (42°C and 37°C) and pH (pH 5.8 and pH 4.8). The high level of temperature and pH (42°C and pH 5.8) were chosen to enhance growth according to previous studies using *L. bulgaricus* CFL1 (Streit et al. 2007; Rault et al. 2007) and different *L. bulgaricus* strains (Béal et al. 1989; Grobбен et al. 1995; Burgos-Rubio et al. 2000; Abbasalizadeh et al. 2015; Aghababaie et al. 2015). The low level of temperature and pH (37°C and pH 4.8) was selected to induce mild stress, allowing enough biomass production ($>1 \text{ g}\cdot\text{L}^{-1}$).

Bacterial cells were harvested according to the acidification rate in the culture medium (determined by adding a base solution to control the pH). The primary cell growth properties such as growth rate (μ), maximal acidification rate (V_m), substrate consumption (glc), lactic acid production (LA), and biomass productivity (P) were measured. V_m allowed a harvest time normalization (Rault et al. 2009), which corresponded to different growth phases: the exponential growth phase (t_{h1}), the deceleration growth phase (t_{h2}), and the stationary growth phase (t_{h3}).

The resistance of *L. bulgaricus* CFL1 cells was determined by the loss of their main functional properties: acidifying activity and culturability. Resistance to freezing, freeze-drying, and freeze-dried was determined per fermentation condition and harvest time. Multiple regression analysis and response surface method were used to assess the effect of these three fermentation parameters (temperature, pH, and harvest time) and their interactions on biomass production and resistance of *L. bulgaricus* CFL1. Moreover, a multi-objective optimization was implemented to predict the fermentation condition leading to increased resistance to freezing and freeze-drying with acceptable biomass production.

2.2.2. Deep analysis of membrane lipids and their relationships with *L. bulgaricus* CFL1 resistance to freezing and freeze-drying (Chapter 5)

In response to changing the fermentation conditions, LAB get adapted to this new induced environment by developing mechanisms. This adaptation is expected to increase resistance to the critical steps of their production (the stabilization process and storage). The different adaptation mechanisms in LAB include the modulation of their membrane. As the membrane serves as a barrier between the exterior and all intra-cellular materials, it is often considered the main target of injuries following the modification of environmental conditions. The literature review revealed that the composition in fatty acids has been mainly carried out and only a few studies have characterized biophysical membrane properties (including lipid phase transition temperatures and membrane fluidity). Thus, a larger study including a complete analysis of membrane properties is needed. For each fermentation condition and harvest time assessed in Chapter 4, a deep analysis of the membrane lipids of *L. bulgaricus* CFL1 was undertaken considering different membrane lipid properties (Figure 2.1):

- Biochemical characterization in which fatty acids composition and the identification of different lipid classes were determined.
- Biophysical properties included lipid phase transition temperatures and membrane fluidity.

Results were then discussed to elucidate the modulation of the membrane lipids under the different fermentation conditions and associate these properties of membrane lipids with *L. bulgaricus* CFL1 resistance to the most common stabilization processes: freezing and freeze-drying.

2.2.3. Influence of sugars on resistance and the membrane of *L. bulgaricus* CFL1 (Chapter 6)

The addition of protector solutions is a regular industrial practice for LAB production. Sugars molecules are the most used protectors. They are non-penetrating protectors, i.e., they diffuse through the cell wall but not to the cell membrane (Hubálek 2003). Therefore, the interaction of these molecules occurs mainly with the cell membrane.

In the frame of the European PREMIUM project (H2020-MSCA-RISE-2017, project n°777657), new alternatives of protectors were proposed to stabilize lactic acid bacteria: fructo-oligosaccharides (FOS) and galacto-oligosaccharides (GOS). FOS and GOS have demonstrated their prebiotic activity (compounds that induce the growth of probiotics) (Tavera-Quiroz et al. 2015; Romano et al. 2016a; Sosa et al. 2016). In addition, FOS and GOS can be produced from the hydrolysis of Agri-Resources waste in an eco-friendly context. These molecules are mixtures of oligosaccharides of different degrees of polymerization. Some sugars with different degrees of polymerization are frequently used in LAB stabilization without real understanding of the effect of the degree of polymerization.

Chapter 6 aims at investigating the influence of seven sugars with different degrees of polymerization on *L. bulgaricus* CFL1's resistance to freezing and freeze-drying and the *L. bulgaricus* CFL1 membrane.

A fermentation condition was selected among the four conditions previously assessed in Chapter 4 (42°C, pH 5.8, t_{h3}) since this fermentation condition produced enough biomass concentration to protect cells with the seven sugars.

The efficiency of each sugar to protect *L. bulgaricus* CFL1 cells was determined by measuring the loss of their functional properties during freezing and freeze-drying in the same manner as previously in Chapter 4.

The Fourier-transform infrared spectroscopy (FTIR) was chosen in this part of the thesis to elucidate the effect of the sugars on the membrane of *L. bulgaricus* CFL1. This technique has been used for elucidating sugars interactions with intact whole LAB cells (Linders et al. 1997; Oldenhof et al. 2005; Santivarangkna et al. 2010). The FTIR was used in frozen and air-dried *L. bulgaricus* CFL1 cells to explore the vibrational bands of the fatty acids ($\nu_{sym}CH_2$) in the membrane lipids like phospholipids and glycolipids, as well as the headgroup phosphate stretching vibrations ($\nu_{asym}PO_2$).

Chapter 3

3. MATERIALS AND METHODS

This chapter presents the detailed description of the materials and methods used for this thesis.

SUMMARY OF THE CHAPTER

3. MATERIALS AND METHODS	83
3.1. Production of concentrated <i>Lactobacillus delbrueckii</i> subsp. <i>bulgaricus</i> CFL1	85
3.1.1. Bacterial strain conditioning	85
3.1.2. Precultures	85
3.1.3. <i>Lactobacillus delbrueckii</i> subsp. <i>bulgaricus</i> CFL1 batch fermentation	86
3.1.3.1. Equipment	86
3.1.3.2. Culture medium and inoculation to start fermentation	86
3.1.3.3. Fermentation parameters	86
3.1.4. Harvesting	87
3.1.5. Measurements carried out throughout fermentation	87
3.1.5.1. Cell growth by optical density	87
3.1.5.2. Cell concentration by dry cell weight	89
3.1.5.3. Substrate consumption and metabolite production	89
3.2. Stabilization processes and freeze-dried storage	90
3.2.1. Concentration and protection	90
3.2.2. Freezing	90
3.2.3. Freeze-drying and freeze-dried storage	90
3.3. Assessment of <i>Lactobacillus delbrueckii</i> subsp. <i>bulgaricus</i> CFL1 functional properties at different production steps	92
3.3.1. Acidifying activity	92
3.3.2. Culturability	93
3.3.3. Specific acidifying activity and loss of specific acidifying activity	93

3.4. Water content and temperature glass transition of the freeze-dried bacteria	95
3.4.1. Water content measurements	95
3.4.2. Glass transition (T _g) measurements	95
3.5. Lipid composition of <i>Lactobacillus delbrueckii</i> subsp. <i>bulgaricus</i> CFL1	96
3.5.1. Fatty acid composition and quantification by Gas Chromatography-Mass Spectrometry (GC-MS)	96
3.5.1.1. Lipid extraction from <i>L. bulgaricus</i> CFL1 cells for fatty acid determination	96
3.5.1.2. Sample preparation for GC-MS analysis	97
3.5.1.3. GC-MS: equipment and configuration	98
3.5.1.4. Fatty Acid (FA) composition and quantification	98
3.5.2. Lipid classes identification	99
3.5.2.1. Total lipid extraction for lipid classes identification	99
3.5.2.2. Total lipid extract fractionation by solid-phase extraction (SPE)	100
3.5.2.3. Sample preparation for analysis	101
3.5.2.4. Fatty acids determination per lipid class	101
3.5.2.5. HPTLC: equipment and configuration	101
3.5.2.6. Lipid classes identification by different revelations in HPTLC plates	101
3.5.3. Lipid classes determination by liquid chromatography with tandem mass spectrometry (LC-MS/MS)	102
3.5.3.1. Sample preparation for analysis	102
3.5.3.2. LC-MS/MS: equipment and configuration	102
3.5.3.3. Lipids data processing	103
3.6. Biophysical properties of <i>Lactobacillus delbrueckii</i> subsp. <i>bulgaricus</i> CFL1 membrane: lipid phase transition temperature and membrane fluidity	105
3.6.1. Bacterial sample preparation	105
3.6.2. FTIR: equipment and configuration	105
3.6.3. FTIR: spectra acquisition and analysis	105
3.6.4. Fluorescence anisotropy by flow cytometry	108
3.7. Sugars effect on <i>Lactobacillus delbrueckii</i> subsp. <i>bulgaricus</i> CFL1 membrane	109
3.7.1. Bacterial sample preparation	109
3.7.2. Physicochemical properties of sugars	110
3.7.3. Protection efficiency of different sugars during freezing and freeze-drying	110
3.7.4. Sugars effect on <i>L. bulgaricus</i> CFL1 membrane by Fourier transform infrared (FTIR)	110
3.7.4.1. Hydrated cells	110
3.7.4.2. Air-dried cells	111
3.7.4.3. FTIR study	111
3.8. Statistical analysis	113
3.8.1. Factorial design experiment	113
3.8.2. Stepwise linear regression and response surface method	114
3.8.3. ANOVA tests	114
3.8.4. Pearson's correlation coefficient	114
3.8.5. Principal Component Analysis (PCA)	115
3.8.6. Clustering analysis for different lipids	116

3.1. Production of concentrated *L. bulgaricus* CFL1

(cf. Chapters 4, 5, and 6)

3.1.1. Bacterial strain conditioning

Stock cultures of *L. bulgaricus* CFL1 were stored at -80°C in Man, Rogosa, and Sharpe broth (MRS, Biokar, Diagnostics, Beauvais, France) supplemented with 15% (w/w) glycerol (VWR, Leuven, Belgium). Cell reactivation was performed by thawing 1 mL of stock culture in a 42°C water bath for 5 min.

3.1.2. Precultures

Reactivated bacterial suspensions were precultured twice in MRS broth (Biokar, Diagnostics, Beauvais, France) before being used to inoculate the bioreactor.

The medium was sterilized at 121°C for 20 min. Sixty milliliters of the sterilized medium were inoculated with 300 μL of thawed stock culture and incubated at 42°C for 12 h, corresponding to an optical density at 600 nm of approximately 4.5 ($\ln [\text{OD}_{600\text{nm}}/\text{OD}_{600\text{nm}}(t=0)] = 4.9$). Figure 3.1 (A) shows that this incubation duration permitted reaching the stationary growth phase.

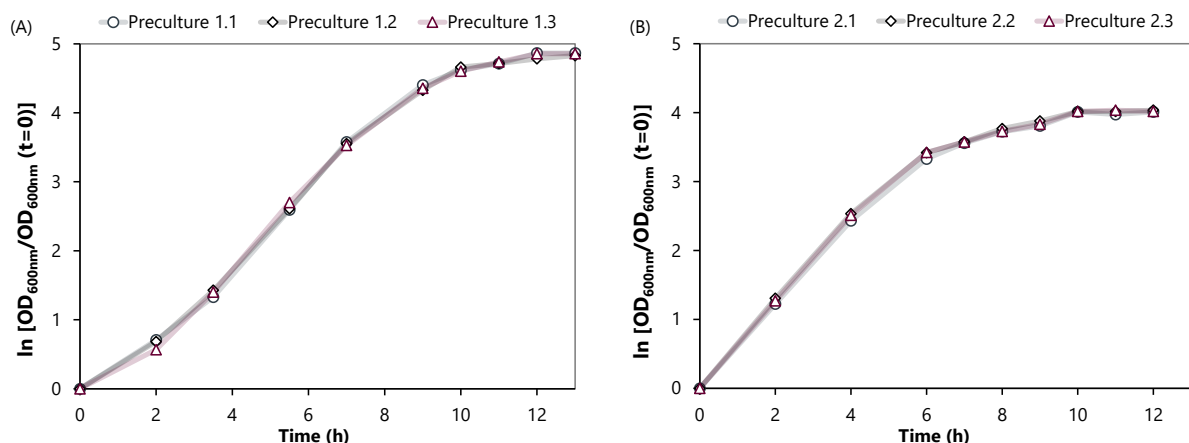


Figure 3.1 Follow up of the growth of *L. bulgaricus* CFL1 from stock cultures for (A) a first preculture and (B) a second preculture. The illustrated results are from three independent biological replicates.

Then, 1.5 milliliters of the resulting first preculture was transferred into 60 mL of the sterilized MRS to start the second preculture with an optical density at 600 nm of 0.1. This second preculture was incubated at 42°C for ten hours. For this second preculture, the incubation duration also permitted reaching the stationary growth phase (Figure 3.1 (B): $\ln [\text{OD}_{600\text{nm}}/\text{OD}_{600\text{nm}}(t=0)] = 4.0$). No stirring was applied for both precultures due to the material disponibility for carrying out the precultures experiments. The whole resulting second preculture was used to inoculate the bioreactor.

3.1.3. *Lactobacillus delbrueckii* subsp. *bulgaricus* CFL1 batch fermentation

3.1.3.1. Equipment

Fermentations were carried out in a Biostat® A plus 5 L bioreactor (Sartorius, Biostat® A plus, Melsungen, Germany) without any air inlet. The bioreactor was equipped with: a stirring motor, a temperature probe, a sterilizable pH probe (Easyferm K8 325, Hamilton; Bonaduz, Switzerland), and an optical density probe (880 nm infra-red probe, Excell210; CellID, Roquemaure, France).

3.1.3.2. Culture medium and inoculation to start fermentation

The culture medium was composed of MRS broth (MRS, Biokar, Diagnostics, Beauvais, France) supplemented with 20 g·L⁻¹ D-glucose (VWR, Leuven, Belgium). The culture medium sterilization was carried out by filtration through 0.22 µm polyethersulfone (Stericap PLUS, Millipore Express®, Merck, KGaA, Darmstadt, Germany). Filtration was chosen to avoid the Maillard reactions that occur for thermal sterilization. Then, the culture medium was introduced into a 4 L working volume bioreactor previously sterilized at 121°C for 20 min (Sartorius, Biostat® A plus, Melsungen, Germany).

The inoculation was performed at an initial optical density of 0.1 (OD_{600nm}), corresponding to approximately 4×10⁵ CFU·mL⁻¹. An agitation speed of 100 rpm was applied to ensure culture homogenization. Each fermentation condition was carried out at least in three independent replicates.

3.1.3.3. Fermentation parameters

The temperature and pH were set and maintained at two different values, for the temperature at 42°C or 37°C, for pH at 5.8 or pH 4.8. These two parameters were adjusted before inoculation and controlled throughout the fermentation by SartoriusBioPAT software (SARTORIUS®, Göttingen, Germany).

The temperature was regulated by a heating mantle and cold-water circulation in a sheath inside the bioreactor. The pH was regulated using a peristaltic pump by adding a 4.25 M NaOH solution (VWR, Leuven, Belgium). The consumption rate of NaOH (dm_{NaOH}/dt , in g·L⁻¹·h⁻¹) was calculated with SartoriusBioPAT software (SARTORIUS®, Göttingen, Germany). The consumption rate of NaOH was used to determine the maximum acidification rate (V_m in g·L⁻¹·h⁻¹) (Figure 3.2).

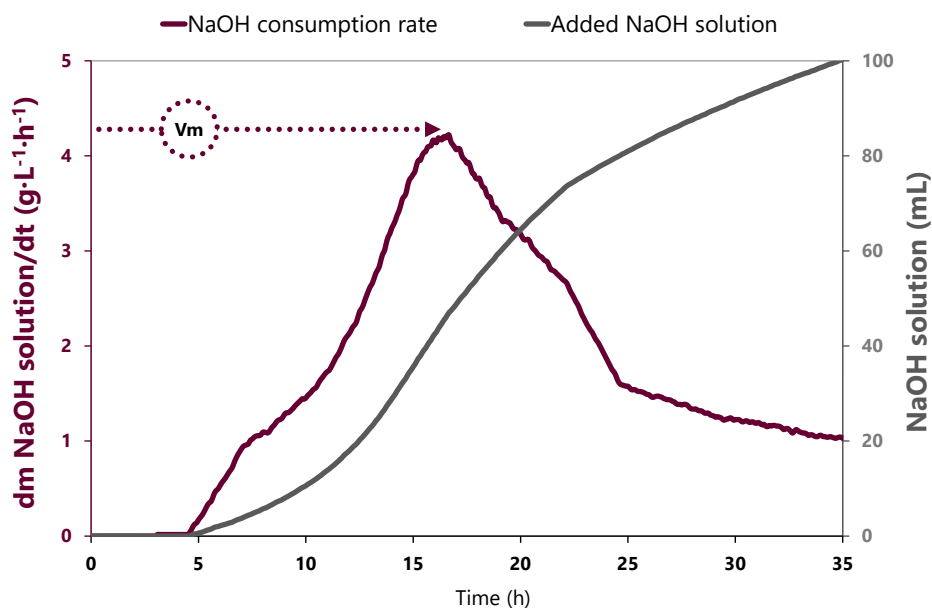


Figure 3.2 Curves that illustrate the addition in mL (gray line) and the consumption rate in $\text{g}\cdot\text{L}^{-1}\cdot\text{h}^{-1}$ (plum line) of a NaOH solution at 4.25 M. The curves are the result of the growth of *L. bulgaricus* CFL1 at [42°C, pH 5.8]. Abbreviation: V_m , the maximal volume of NaOH solution required to neutralize the acidification of the medium (the maximal acidification rate).

3.1.4. Harvesting

Bacterial cell samples were taken from the bioreactor at different harvest times for each couple of fermentation temperatures and pHs. According to the acidification rate (the consumption rate of NaOH), three groups of harvest times were defined (t_{h1} , t_{h2} and t_{h3} are illustrated in Figure 3.3). They were normalized and expressed as a function of the time necessary (t_{vm} , in hours) to reach V_m , considered reference time ($V_m: t_m = 0$ h). This normalization aims to obtain cells in a similar biological state (Rault et al. 2008, 2009).

Therefore, harvested samples were indicated as intervals, corresponding to different growth phases (Figure 3.3):

- (i) The mid-exponential growth phase (t_{h1} : -10 to -1.0 h from V_m)
- (ii) The deceleration growth phase (t_{h2} : -1.0 to +2.0 h from V_m)
- (iii) The stationary growth phase (t_{h3} : +2.2 to +10 h from V_m)

3.1.5. Measurements carried out throughout fermentation

3.1.5.1. Cell growth by optical density

Cell growth was monitored by an infra-red probe (Excell 210; CellID, Roque-maure, France) inserted in the bioreactor, measuring absorbance continuously at 880 nm (data acquisition every 5 minutes). In order to compare the specific growth rate to literature values, optical density was also measured ex-situ at 600 nm every two or three hours throughout the growth (Spectrophotometer VWR, UV-6300PC, Leuven, Belgium). A correlation was proposed between the 880 and 600 nm absorbance measurements (Figure 3.4).

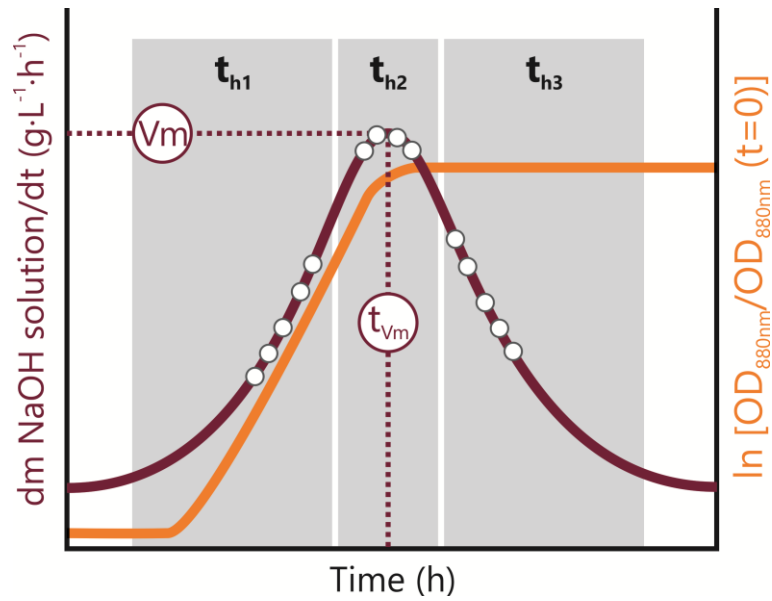


Figure 3.3 Schematic representation of harvest time normalization according to the maximum acidification rate and different growth phases of *L. bulgaricus* CFL1. t_{h1} , the mid-exponential growth phase; t_{h2} , the deceleration growth phase; and t_{h3} , the stationary growth phase. Abbreviations: V_m , the maximum volume of NaOH solution required to neutralize the acidification of the medium (the maximum acidification rate); t_{V_m} , the time necessary to reach V_m .

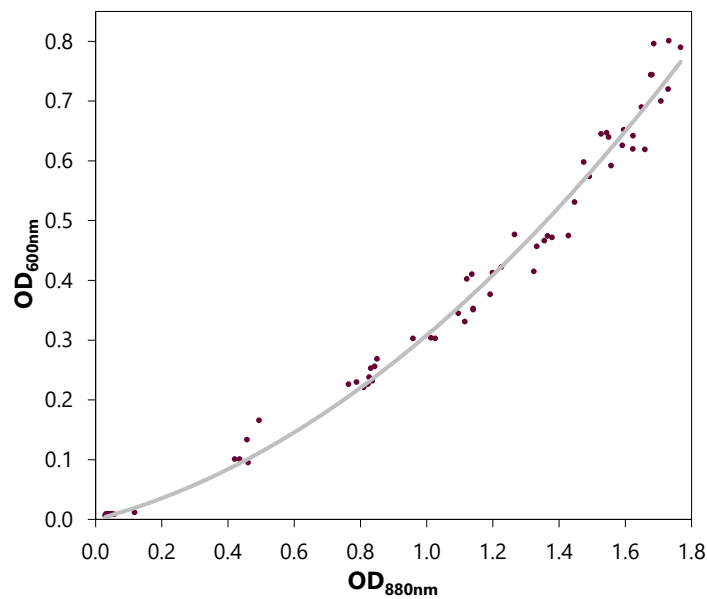


Figure 3.4 Correlation between the 880 and 600 nm data. $OD_{600nm} = 1.63 \times (OD_{880nm})^2 + 1.45 \times (OD_{880nm})$. The corresponding coefficient of determination ($R^2 = 0.988$) indicates the accuracy of the correlation.

The specific growth rate (μ , in h^{-1}) and lag phase duration (lag in h) were calculated according to the modified Gompertz equation (Zwietering et al. 1990), (Equation 3.1) at 880 and 600 nm:

$$\ln \left(\frac{OD_{880 \text{ nm or } 600 \text{ nm}}}{OD_{880 \text{ nm or } 600 \text{ nm}}} \right) = A \exp \left\{ -\exp \left[\frac{\mu \cdot \exp(1)}{A} \cdot (lag - t) + 1 \right] \right\} \quad (3.1)$$

Where A is the asymptote of the growth curve, μ is the specific growth rate in h^{-1} , lag is the lag phase duration in hours, and t is the time in hours per optical cell density measurement ($\text{OD}_{880\text{nm}}$ or $\text{OD}_{600\text{nm}}$).

3.1.5.2. Cell concentration by dry cell weight

The dry cell weight (DCW, in $\text{g}\cdot\text{L}^{-1}$) was determined by filtering 10 mL of culture sample through 0.20 μm hydrophilic polyethersulfone (PES) (Supor[®], PALL Biotech, Saint-Germain-en-Laye, France). The filters were previously dried at 80°C for 24 h. Filters containing culture samples were also dried under the same conditions (80°C, 24 h). The dry cell weight measurements were carried out using three independent filters after inoculating the bioreactor ($t = 0$) and at each harvest time (t_{h1} , t_{h2} , and t_{h3}).

Biomass productivity (P in $\text{g}\cdot\text{L}^{-1}\cdot\text{h}^{-1}$) was calculated according to the following equation:

$$P = \frac{\text{DCW (at } t = t_{hi}) - \text{DCW (at } t = 0_{\text{after inoculation}})}{t_{hi}} \quad (3.2)$$

3.1.5.3. Substrate consumption and metabolite production

Glucose and lactic acid concentrations were quantified per harvest time (t_{h1} , t_{h2} , and t_{h3}). The aim was to establish the fermentation profile of *L. bulgaricus* CFL1 (i.e., homolactic pathway) and verify no carbon source depletion.

Each harvested sample was centrifuged at 16 000 g , 4°C for 10 min, and the supernatant was filtered through a 0.20 μm polytetrafluoroethylene (PTFE) filter (CHROMAFIL[®] Xtra PA, Düren, Germany). Then, the supernatant samples were frozen at -80°C until analysis.

Substrate consumption and metabolite production were quantified using high-performance liquid chromatography (HPLC, Waters Associates, Millipore; Molsheim, France), coupled with a Refractive Index Detector (Waters, Milford, MA, USA). Analyses were made using a cation exchange column (Aminex Ion Exclusion HPX-87 300 X 7.8 mm; Biorad, Richmond, VA, USA) at 35°C. The mobile phase was 0.005 $\text{mol}\cdot\text{L}^{-1}$ H_2SO_4 , and a flow rate set at 0.6 $\text{mL}\cdot\text{min}^{-1}$ (LC-6A pump; Shimadzu, Courtaboeuf, France).

The results were recorded and processed by Millenium software (Waters Associates Millipore; Molsheim, France). The compounds were identified by their retention time. The concentrations were calculated from a calibration curve with reference solutions containing the molecules to be quantified: glucose and lactic acid (Merck, Sigma-Aldrich, Darmstadt, Germany). Quantifications were performed in duplicate. The results were expressed in $\text{g}\cdot\text{L}^{-1}$.

3.2. Stabilization processes and freeze-dried storage

(cf. Chapter 4, 5, and 6)

3.2.1. Concentration and protection

Harvested cell suspensions were concentrated by centrifugation at 11 500 *g* for 10 min at 4°C (Avanti® J-E centrifuge; Beckman Coulter, Fullerton, CA, USA). The resulting cell pellets were then re-suspended in the protective solution at a ratio of 1:2 (1 g of concentrated cells for 2 g of the protective solution). The protective solution was composed of 20% (w/w) of sucrose (VWR, Leuven, Belgium), previously sterilized at 121°C for 20 min. Sucrose is widely used to protect *L. bulgaricus* strains during both stabilization processes (Passot et al. 2012; Gautier et al. 2013; Romano et al. 2016).

3.2.2. Freezing

One milliliter of protected cell suspensions was distributed in cryo-tubes (Sarstedt, Nümbrecht, Germany) for freezing experiments and then frozen to -80°C in a laboratory freezer at a cooling rate of approximately 3°C·min⁻¹ (Freezer Froilabo, BM 1000, Meyzieu, France). Frozen cell samples were stored at -80°C for less than 24 h until analysis.

3.2.3. Freeze-drying and freeze-dried storage

Moderate operating conditions for freeze-drying were chosen due to the sensitivity of the biological products, i.e., bacterial suspensions.

Five-milliliter vials (Verretubex, Nogent-Le-Roi, France) containing one milliliter of frozen samples (-80°C, 3°C·min⁻¹) were transferred to a pre-cooled shelf at -50°C in a REVO pilot-scale freeze-dryer (Millrock Technology, Kingston, New York, USA). After a holding step of 1.5 h at -50°C, the chamber pressure was decreased to 10 Pa, and the shelf temperature was increased from -50°C to -20°C at a heating rate of 0.25°C·min⁻¹ to initiate sublimation. The shelf temperature at the end of ice sublimation was assessed by comparative pressure measurement (Pirani gauge versus capacitance manometer) (Passot et al. 2009) This pressure measurement ensured the absence of remaining ice inside the product.

After 40 h of sublimation (primary drying), the shelf step was increased to 25°C at a heating rate of 0.25°C·min⁻¹. After ten hours of desorption (secondary drying step), the vacuum was broken by injecting air into the drying chamber (Figure 3.5).

The vials were then removed from the freeze-dryer to be manually capped by inserting a rubber stopper. The vials were packed in multi-layer aluminum bags. The bags were hermetically closed using a vacuum sealer (Bernhardt, Wimille, France).

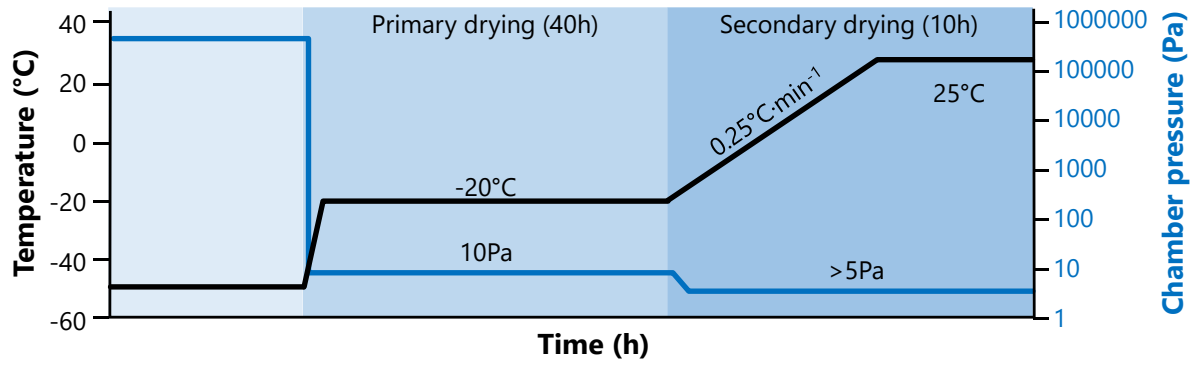


Figure 3.5 Schemes of the operating conditions set during the primary drying and the secondary drying stages of freeze-drying: shelf temperature and chamber pressure.

The bags for freeze-dried samples were stored at -80°C until the functional and physical properties were measured. The bags for storage experiments were immediately introduced into a controlled-temperature chamber at 25°C for 15 days.

3.3. Assessment of the functional properties of *L. bulgaricus* CFL1 at different production steps

(cf. Chapter 4, 5, and 6)

Acidifying activity and culturability were the functional properties measured for protected bacterial suspensions before the stabilization process (after concentration and protection: initial), after freezing, freeze-drying, and freeze-dried storage. For the frozen samples, bacterial suspensions were thawed at 42°C for 5 min in a water bath. For freeze-dried and freeze-dried storage samples, they were rehydrated in 1 mL skim milk solution (100 g·L⁻¹) at 42°C. This solution was prepared using milk powder (EPI-Ingredient, Ancenis, France) and heat-treated at 110°C for 20 min. These mild-thermal treatment conditions were chosen to minimize undesired contaminations and avoid sugar caramelization in the milk solution. Then, samples were stirred at room temperature for 5 min.

The temperature at 42°C was selected for thawing and rehydrating samples since it was the parameter for measuring the acidifying activity and culturability.

3.3.1. Acidifying activity

The Cinac system (AMS Alliance, Frépillon, France) was used to evaluate the acidifying activity of the concentrated-protected bacterial suspensions.

Three 150 mL-flasks contained 100 mL filled volume of a heat-treated (110°C for 20 min) skim milk solution at 100 g·L⁻¹ (EPI-Ingredient, Ancenis, France). The flasks were introduced into the water bath-Cinac until reaching the temperature of 42°C (Figure 3.6 (A)). Each flask was inoculated with 100 µL of the bacterial suspension. The pH was continuously measured by the Cinac system and led to the calculation of the time necessary ($t_{V_m-Cinac}$, in min) to reach the maximum acidification rate in the inoculated skim milk solution ($V_m-Cinac$, dpH/dt in pH·min⁻¹) (Spinnler and Corrieu 1989) (Figure 3.6 (B)). This time corresponds to obtaining a decrease of 0.7 pH units ($t_{\Delta pH 0.7}$, in min) and makes it possible to eliminate the initial variations in pH. The descriptor $t_{\Delta pH 0.7}$ was used to characterize the acidifying activity of *L. bulgaricus* CFL1 bacterial suspensions (Figure 3.6 (C)). The higher the $t_{\Delta pH 0.7}$ value, the lower the acidifying activity was observed.

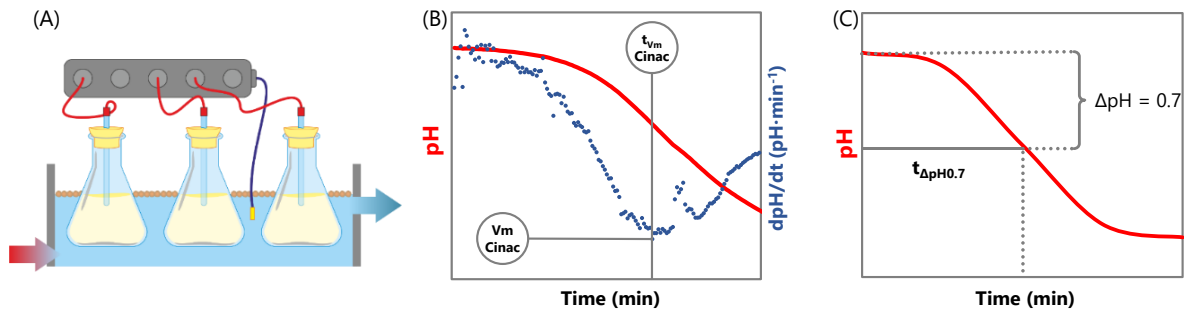


Figure 3.6 Cinac® system. (A) Schematic illustration of the Cinac® system, (B) pH change as a function of the time (orange line) and acidification rate as a function of the time (orange asterisks), and (C) pH change as a function of the time to calculate the $t_{\Delta\text{pH}0.7}$ descriptor. Abbreviations: $V_m\text{-Cinac}$, the maximum acidification rate in the inoculated skim milk solution; $t_{V_m\text{-Cinac}}$, the time necessary to reach $V_m\text{-Cinac}$; ΔpH , a decrease of 0.7 pH units; $t_{\Delta\text{pH}0.7}$, the time necessary to obtain a decrease of 0.7 pH units.

3.3.2. Culturability

The agar plate count method determined the bacterial cell concentration of concentrated-protected bacterial suspensions. Bacterial suspensions were serially diluted in 10 mL of NaCl solution at $9 \text{ g}\cdot\text{L}^{-1}$ (VWR, Leuven, Belgium). After homogenizing the bacterial dilutions, the last two dilutions were taken to plate on Petri dishes containing MRS Agar (Biokar Diagnostics, Paris, France). Three plates were used per dilution and were anaerobically incubated at 42°C for 48 h. Colony counting was assisted by a colony counter equipment (IUL's DOT-Colony Counter, Barcelona, Spain). Three plates containing 30 and 300 colony forming units (CFU) were kept for cell concentration determination. The cell count was expressed in $\text{CFU}\cdot\text{mL}^{-1}$.

3.3.3. Specific acidifying activity and loss of specific acidifying activity

The specific acidifying activity (t_{spe} , in $[\text{min} (\log (\text{CFU}\cdot\text{mL}^{-1}))^{-1}]$), was defined as the ratio of $t_{\Delta\text{pH}0.7}$ (in min) to the corresponding log of cell concentration ($\log(\text{CFU}\cdot\text{mL}^{-1})$) (Streit et al. 2007).

Therefore, t_{spe} gives a meaningful measurement of lactic acid bacteria's functional property, including acidifying activity and culturability.

The specific acidifying activity of protected bacterial suspensions was measured before the stabilization processes (initial, $t_{\text{spe I}}$), after freezing ($t_{\text{spe F}}$), freeze-drying ($t_{\text{spe FD}}$), and 15 days of storage at 25°C ($t_{\text{spe S}}$). Thus, the loss was the result of the following equations (Equations 3.3-3.5):

$$dt_{\text{spe F (Freezing)}} = t_{\text{spe after Freezing}} - t_{\text{spe I (Initial specific acidifying activity)}} \quad (3.3)$$

$$dt_{\text{spe FD (Freeze-Drying)}} = t_{\text{spe after Freeze-Drying}} - t_{\text{spe I (Initial specific acidifying activity)}} \quad (3.4)$$

$$dt_{\text{spe S (freeze-dried Storage)}} = t_{\text{spe after freeze-dried Storage}} - t_{\text{spe after Freeze-Drying}} \quad (3.5)$$

The determination of t_{spe} loss (dt_{spe}) during each stabilization process and freeze-dried storage is illustrated in Figure 3.7.

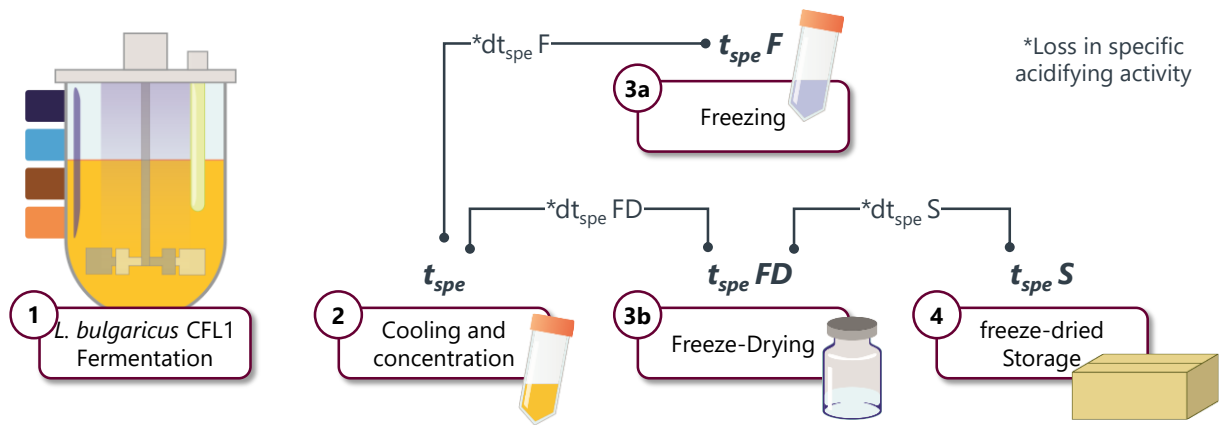


Figure 3.7 Schematic representation of concentrated *L. bulgaricus* CFL1 production and loss of specific acidifying activity during freezing, freeze-drying, and freeze-dried storage. Abbreviations: $t_{spe} F$, specific acidifying activity after freezing; $t_{spe} FD$, specific acidifying activity after freeze-drying; $t_{spe} S$, specific acidifying activity after freeze-dried storage; $dt_{spe} F$, loss in specific acidifying activity during freezing; $dt_{spe} FD$, loss in specific acidifying activity during freeze-drying; $dt_{spe} S$, loss in specific acidifying activity during freeze-dried storage.

3.4. Water content and temperature glass transition of the freeze-dried bacteria

3.4.1. Water content measurements

The water content (moisture content) of freeze-dried bacterial suspensions was measured three times per sample by the Karl Fisher titration method using a Metrohm KF 756 apparatus (Herisau, Switzerland). At least 20 mg of powder (initial mass of the sample, m_0) was mixed with 2 mL of dried methanol (Hydranal, Sigma Aldrich; St. Louis, MO, USA) and weighed again to obtain the mass of the solvent introduced (m_{solvent}). The sample was vortexed for 2 minutes and then decanted for 10 minutes. To determine the sample's water content, approximately 0.8 mL of this solution's liquid phase (m_{liquid}) is injected into the apparatus with a syringe to determine the mass of water (m_{KF}). Similarly, one milliliter of pure methanol (m'_{liquid}) is subjected to the same protocol to determine the mass of water (m_{blank}) present in the methanol before dissolution.

Once these two analyses have been carried out, the moisture content in the product (RH in %) is given by the following relationship:

$$\text{RH} = \frac{\frac{m_{\text{KF}}}{m_{\text{liquid}}} - A_0 \times m_{\text{solvent}}}{m_0} \quad (3.6)$$

$$\text{Where } A_0 = \frac{m_{\text{blank}}}{m'_{\text{liquid}}}$$

3.4.2. Glass transition (T_g) measurements

Glass transition temperature (T_g) was performed as described by Velly et al. (2015). Briefly, T_g measurements were carried out using a power compensation Differential Scanning Calorimetry (DSC) (Pyris 1, PerkinElmer LLC; Norwalk, CT, USA) equipped with a mechanical cooling system (Intracooler 1P, PerkinElmer). Temperature calibration was done using cyclohexane and indium (melting points at 6.5 and 156.6°C, respectively). Approximately 15 mg of each freeze-dried sample was placed in 50 μL PerkinElmer DSC sealed aluminum pans. An empty pan was used as a reference. Linear cooling and heating rates of 10°C·min⁻¹ were applied. The T_g of the freeze-dried samples was determined as the midpoint temperature of the heat flow step associated with glass transition with respect to the ASTM Standard Method, E1356-91. Results were obtained from at least three replicates.

3.5. Lipids composition of the *L. bulgaricus* CFL1 membrane

(cf. Chapter 5)

To analyze the lipids of the *L. bulgaricus* CFL1 membrane, lipids extraction was performed. Then, a portion of the lipid extract of *L. bulgaricus* CFL1 was fractionated to obtain different fractions that corresponded exclusively to membrane lipids. Before and after fractionation, the lipids were characterized by their fatty acid composition and their different lipids classes (e.g., phospholipids, glycolipids, triacylglycerols, among others). Fatty acids and lipid classes were determined for *L. bulgaricus* CFL1 cells cultivated in the four fermentation conditions (42°C, pH5.8; 42°C, pH4.8; 37°C, pH5.8; and 37°C, pH 4.8). For fatty acids determination, the three harvest times (t_{h1} , t_{h2} , and t_{h3}) were analyzed, whereas for lipid classes, only samples at t_{h3} .

Harvested bacterial cells were concentrated by centrifugation at 11 500 *g*, for 10 min, at 4°C (Avanti® J-E centrifuge; Beckman Coulter, Fullerton, CA). Then, the samples were washed twice with 20 mL of NaCl solution at 0.9% w/w (VWR, Leuven, Belgium) by centrifuging at 12 900 *g*, 4°C, for 10 min (Eppendorf® Centrifuge 5804 R – Benchtop, Hamburg Germany) and removing the supernatant. The resulting bacterial pellet was suspended in a 0.9% NaCl solution with the following ratio: 1 g of concentrated cells for 1 g of 0.9% NaCl solution. For fatty acid determination (subsection 3.5.1), the bacterial suspension was aliquoted at two milliliters in cryo-tubes (Sarstedt, Nümbrecht, Germany). For lipid classes identification (subsection 3.5.2), the bacterial suspension was aliquoted at 20 mL volume in centrifuge tubes (Corning® 50 mL centrifuge tubes, Arizona, USA). Samples were kept frozen at -80°C until lipid extraction.

3.5.1. Fatty acid composition and quantification by Gas Chromatography-Mass Spectrometry (GC-MS)

3.5.1.1. Lipid extraction for fatty acid determination

The lipids of *L. bulgaricus* CFL1 cells (before fractionation) were extracted according to the Folch procedure (Folch et al. 1957) with some modifications provided by Walczak-Skierska et al. (2020). The Folch method was chosen due to the low biomass amount (< 500 mg) available for each harvest time (t_{h1} , t_{h2} and t_{h3}) and to perform 12 samples in a run (a more significant sample number). The extraction was performed from three independent replicates.

For each extraction, two milliliters of bacterial cell suspension were thawed at 42°C for 10 minutes in a water bath and centrifuged at 12 900 *g*, 4°C, for 10 min (Eppendorf® Centrifuge 5804 R – Benchtop, Hamburg, Germany). The supernatant was removed, and the bacterial pellet was washed twice with two milliliters of 0.9% NaCl solution by centrifuging under the same conditions (12 900 *g*, 4°C, for 10 min) and removing the supernatant.

Lipids were extracted directly from the wet cells without drying to limit the modification of membrane lipids during the extraction (Kates 2010). For this purpose, one hundred milligrams

of wet bacterial pellet were introduced into a five-millilitre Eppendorf tube (Eppendorf Tubes-Microtube® for solvents, Hamburg, Germany). Then, 3.6 mL of chloroform (CHCl_3)-methanol (CH_3OH) (2:1, v/v) were added (Figure 3.8 ①). The suspension was vortexed and sonicated in a water bath (Elmasonic S 30 /H, 50 Hz, Aubagne, France) at room temperature for ten minutes (Figure 3.8 ②). After sonication, 0.85 mL of 0.9% NaCl solution was added (Figure 3.8 ③). The mixture was shaken for ten minutes on a rotary shaker (Rotary shaker SB2/SB3-STUART, Evreux, France) (Figure 3.8 ④) and centrifuged (12 900 g , 20°C, for 15 min) (Figure 3.8 ⑤). After centrifugation, two layers were observed: (i) upper layer (aqueous phase), (ii) lower layer (organic phase), and bacterial pellet (bottom of the tube) (Figure 3.8 ⑥). Carefully with the help of a Pasteur pipette, the lower layer was removed and transferred into a four-milliliter glass tube (NAFVSM, Nijmegen, Netherlands) (Figure 3.8 ⑦). Then, 0.85 mL of CHCl_3 were added into the Eppendorf tube containing the upper layer and the bacterial pellet (Figure 3.8 ⑧). Once again, the sample was shaken on the rotary shaker for ten minutes and centrifuged (12 900 g , 20°C, for 15 min) to collect the lower phase and incorporate it into the four-milliliter glass tube (Figure 3.8 ⑨). The collected lower layer contained the lipid extract. This lipid extract was dried using a vacuum-rotary evaporator (Refrigerated Vapor Trap: RVT5105, ThermoFisher, MA, USA) (Figure 3.8 ⑩).

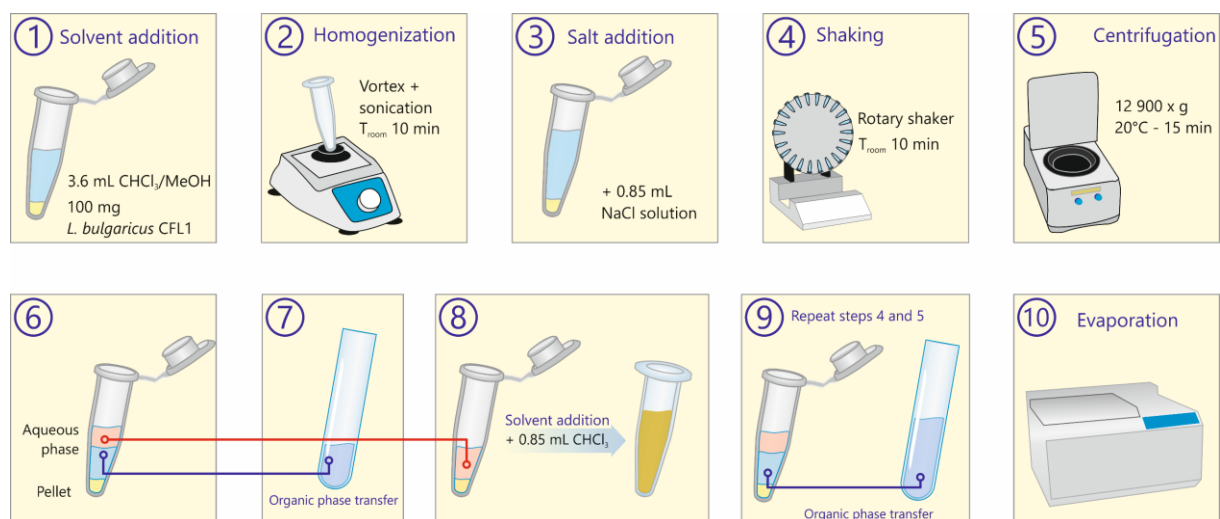


Figure 3.8 Lipid extraction protocol to determine fatty acids composition for each harvest time.

3.5.1.2. Sample preparation for GC-MS analysis

The dried extracted lipid samples were re-suspended in 150 μL of CHCl_3 . After samples were vortexed, 50 μL of the lipid suspension were transferred to GC-MS vials, adding 25 μL of an internal standard solution, C9:0 (Merck, Sigma-Aldrich, Darmstadt, Germany). This standard solution was at 0.44 $\text{mg}\cdot\text{mL}^{-1}$ in CHCl_3 .

Then, 50 μL of the methylation reagent, trimethyl sulfonium hydroxide (TMSH, Merck, Sigma-Aldrich, Darmstadt, Germany) were added to the lipid suspension. This reagent is adapted to different lipid classes in microbial samples (Pflaster et al. 2014).

3.5.1.3. GC-MS: equipment and configuration

Fatty acid analysis was carried out using a Hewlett-Packard 6890 gas chromatograph (GMI; Ramsey, MI, USA) equipped with a capillary column packed with 70% cyanopropyl polyphenylene-siloxane BPX70 (length 60 m, internal diameter 0.25 mm, coating thickness 0.25 μm ; SGE Analytical Science Pty Ltd.; Victoria, Australia), coupled to a mass selective detector (5973; Agilent Technologies, Avondale, PA, USA).

The carrier gas was helium at 1.2 $\text{mL}\cdot\text{min}^{-1}$, and the column pressure was 1.3×10^5 Pa. Injection of 1 μL of the vial was done split-less at an injector temperature of 250°C. The oven temperature was held for 1 min at 35°C and then increased from 35 to 100°C at 40°C $\cdot\text{min}^{-1}$, held for 1 min at 100°C and then increased from 100 to 130°C at 5°C $\cdot\text{min}^{-1}$, followed by an increase from 130 to 180°C at 1.5°C $\cdot\text{min}^{-1}$ and finally from 180 to 240°C at 5°C $\cdot\text{min}^{-1}$. The transfer line temperature was set at 280°C. The MS source temperature and MS Quad were set at 230°C and 150, respectively.

3.5.1.4. Fatty Acid (FA) composition and quantification

Identification of the FA methyl esters extracted from bacterial samples was carried out by comparing their retention time to those of the known commercial standards solutions: C12:0, C14:0, C15:0, C16:0, C16:1 trans9; C16:1 cis 9, C17:0, C18:0, C18:1 trans9; C18:1 cis9, C18:2 cis9, cis12, C18:2 cis 9, trans 11, C20:0, C22:0 (Merck, Sigma-Aldrich, Darmstadt, Germany), and cyc C19:0 (Larodan AB, Solna, Sweden). These standards were prepared in CHCl_3 and then stored at -20°C until use. FA identification was also confirmed by the mass selective detector at a scan rate of 3.14 scans $\cdot\text{s}^{-1}$, with data collected in the range of 33 to 500 amu. The mass spectra of the FA methyl esters were compared with the Wiley data bank, NIST 2020. L (Hewlett-Packard, Gaithersburg, MD, USA) data bank.

Quantification of the FA was calculated using external calibration curves performed with serial dilutions of commercial standards. The area of each peak was related to the internal standard (C9:0) peak to avoid the variability related to the differences in injected volume.

The fatty acid contents were expressed as a percentage of the total amount of extracted fatty acids. Results were expressed as relative percentages over total extracted FA.

In Figure 3.9, a chromatogram is exhibited to show an example of the FA profile of *L. bulgaricus* CFL1. Each peak represents a fatty acid in the sample, eluted at different retention times according to the fatty acid chain. Approximately from 9.5 (C9:0, internal standard), then 15.3 (C10:0) to 49.7 (C22:0) min.

From the relative fatty acid percentages, different ratios were calculated:

- (i) Unsaturated Fatty Acid content/Saturated Fatty Acid content (UFA/SFA).
- (ii) Cyclic Fatty Acid content/Unsaturated Fatty Acid content (CFA/UFA).

(iii) Cyclic Fatty Acid content/Saturated Fatty Acid content (CFA/SFA).

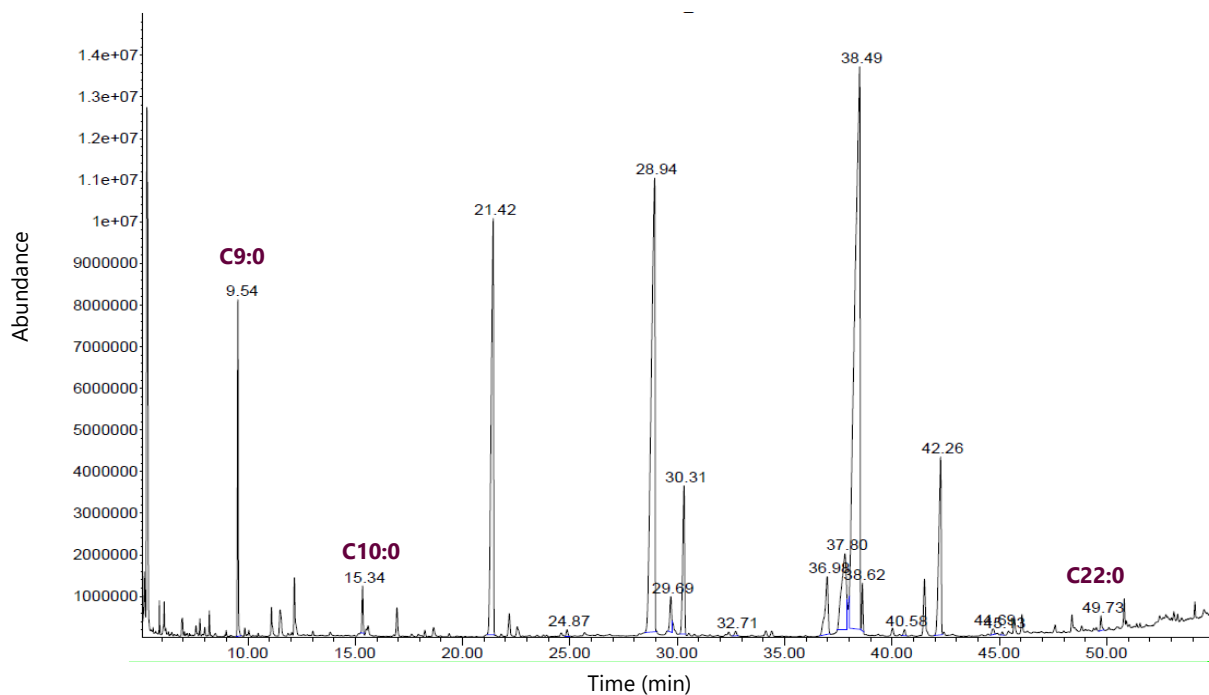


Figure 3.9 Chromatogram example of *L. bulgaricus* CFL1 fatty acids profile. Each peak represents a fatty acid in the sample which were eluted at different retention time according to the fatty acid chain.

3.5.2. Lipid classes identification

The different lipid classes in *L. bulgaricus* CFL1 were determined for the cells harvested at the stationary growth phase (t_{h3}). This harvest time represents the highest biomass concentration for the four fermentation conditions ([42°C, pH5.8]; [42°C, pH4.8]; [37°C, pH5.8]; and [37°C, pH 4.8]). A high biomass concentration was necessary because the total lipid extract (LE) was further fractionated. The fractionation was performed by eluting different solvents using a solid-phase separation (SPE) column.

3.5.2.1. Total lipid extraction for lipid classes identification

The total lipids of *L. bulgaricus* CFL1 were extracted according to the Bligh-Dyer procedure (Bligh and Dyer 1959). A comparison was made between the Folch and Bligh–Dyer methods by FA determination. There was no difference in FA composition and quantification between both methods for at least three independent samples (Chapter 5, Table S5.1). The Bligh-Dyer extraction procedure was chosen in this case because of the high biomass available to perform the extraction and the few numbers of samples per fermentation condition ($n=6$) to perform lipid extractions. The extraction was carried out from two independent biological replicates.

For each extraction, 20 mL of bacterial cell suspension were thawed at 42°C for 15 minutes in a water bath and centrifuged at 12 900 g , 4°C, for 10 min. The supernatant was removed, and the bacterial pellet was washed twice with 20 mL of 0.9% NaCl solution by centrifuging under the same conditions (12 900 g , 4°C, for 10 min) and removing the supernatant.

One gram of wet bacterial pellet was transferred to a first 50 mL-glass tube (Pyrex®, screw cap, Merck, Darmstadt, Germany). Then, 0.2 mL of 0.9% NaCl solution and 3.75 mL of chloroform (CHCl₃)-methanol (CH₃OH) (1:2, v/v) were added. The suspension was shaken on a rotary shaker for three hours (Rotary shaker SB2/SB3-STUART, Evreux, France). After centrifugation at 515 *g*, 20°C, for 10 min (Eppendorf® Centrifuge 5804 R – Benchtop, Hamburg, Germany), the supernatant was transferred to a second 50 mL-glass tube. Five milliliters of 0.9% NaCl solution and five milliliters of CHCl₃ were added into this second 50 mL-glass tube, which contained the recovered supernatant. After vortexing and centrifuging (515 *g*, 20°C, for 15 min) the sample, two layers were observed: an upper layer and a lower layer, the former containing the total lipid extract of bacterial cells. The organic solvent was removed under vacuum using a rotary evaporator (Refrigerated Vapor Trap: RVT5105, ThermoFisher, MA, USA). The obtained total lipid extract (LE) was weighed, diluted in one milliliter of chloroform, and stored at -20°C for further analysis.

3.5.2.2. Total lipid extract fractionation by Solid-Phase Extraction (SPE)

About 850 µL of lipid extract (LE) were fractionated into different solvents to favor the elution of different lipids. A total lipid extract of about 2.6 ± 2 mg/mL in chloroform was loaded to a silica SPE column (SPE-PAK silica classic cartridge, 2 mL, Waters Corporation, Milford, MA, USA), previously conditioned with 20 mL of methanol, then washed with 20 mL of chloroform. After the addition of different solvents into the SPE column, the following fractions were, thus, obtained:

f₁-chloroform fraction: lipids were eluted after adding 20 mL of chloroform (CHCl₃).

f₂- chloroform-acetone fraction: lipids were eluted after adding 20 mL of chloroform-acetone (50:50, v/v).

f₃-acetone fraction: lipids were eluted after adding 20 mL of acetone (CH₃COCH₃).

f₄-methanol fraction: the phospholipids were finally eluted with 20 mL of methanol (CH₃OH).

Solvents were evaporated from all fractions under vacuum using a rotary evaporator (Refrigerated Vapor Trap: RVT5105, ThermoFisher, MA, USA). The dried lipid fractions were diluted in one milliliter of chloroform and stored at -20°C until use.

3.5.2.3. Sample preparation for analysis

The lipid suspension of LE and each fraction obtained after SPE separation (f_1 , f_2 , f_3 , and f_4) were then transferred to two different GC-MS vials: one for FA identification and quantification by GC-MS and the other one for lipid classes' identification by High Performance Thin Layer Chromatography (HPTLC).

3.5.2.4. Fatty acids determination per lipid class

Fatty acids identification and quantification for LE and each fraction obtained after SPE separation (f_1 , f_2 , f_3 , and f_4) were carried out as described in subsections 3.5.1.2, 3.5.1.3, and 3.5.1.4.

3.5.2.5. HPTLC: equipment and configuration

HPTLC was performed on 10 cm × 20 cm dried glass-backed Silica Gel 60 HPTLC plates (HPTLC plates, Merck, Darmstadt, Germany). Plates were heated at 180°C for 30 minutes to minimize the background staining and remove water traces.

In a fume hood, about 20 µg of each lipid sample (LE, f_1 , f_2 , f_3 , and f_4) and lipid standards in chloroform were deposited automatically at 0.1 cm·s⁻¹ using a 25 µL solvent pipette. Each band was 0.6 cm long and 0.87 cm apart from each other (CAMAG® Automatic HPTLC Sampler III (ATS3), Chromacim SAS, Moirans, France).

Development was carried out at room temperature in a sealable HPTLC glass chamber (CAMAG® ADC2, Automatic Developing Chamber, Chromacim SAS, Moirans, France). Chloroform-methanol-propanol-2-KCl at 0.25%-Triethylamine (TEA) (30:9:25:6:18, v/v/v/v/v) was used as the developing solvent.

3.5.2.6. Lipid classes identification by different revelations in HPTLC plates

The presence of different lipids in the LE and each fraction (f_1 , f_2 , f_3 , and f_4) were revealed by dipping HPTLC plates in different reagents:

(i) Copper sulphate (CuSO₄): phosphoric acid (H₃PO₄): sulfuric acid (H₂SO₄) (10:4:4, v/v/v) reagent for non-specific revelation (Fewster et al. 1969). Then, HPTLC plates were heated at 140°C for 30 min.

(ii) Alpha-naphthol reagent for glycolipids (Wang and Benning 2011). Then, HPTLC plates were heated at 100°C for 5 min.

(iii) Ninhydrin reagent for lipids containing free amino groups (Hecht 1966). HPTLC plates were heated at 100°C for 3 min.

In all cases, the separated bands of the lipid sample were compared with the standard bands. Lipid were identified by comparing the relative Retention factor (R_f) values of the samples with those of standards. The standards included FA: C16:0 and C18:1. Phospholipids: PE,

phosphatidylethanolamine; PG, phosphatidylglycerol; CL, cardiolipin; PA, phosphatidic acid. Glycolipids: MGDG, monogalactosyldiacylglycerol and DGDG, digalactosylglycerol (Merck, Sigma-Aldrich, Darmstadt, Germany). Lipids were also identified because of their reactivity to alpha-naphthol and ninhydrin reagents.

3.5.3. Lipid classes determination by liquid chromatography with tandem mass spectrometry (LC-MS/MS)

3.5.3.1. Sample preparation for analysis

LE extract (LE) and fractions (f_1 , f_2 , f_3 , and f_4) samples were dried in a SpeedVac vacuum concentrator (o/n) (SP Genevac EZ-2, PA, USA) and resuspended in 250 μ L of a mixture of acetonitrile: isopropanol (7/3) ULC/MS grade (Biosolve, Chimie, Dieuze, France).

3.5.3.2. LC-MS/MS: equipment and configuration

After vortexing the samples, they were injected (5 μ L of the sample) into a liquid chromatography system (UltiMate 3000 UHPLC System, Thermo-Fisher, MA, USA) coupled to a quadrupole time of flight mass spectrometer (Q-ToF Impact II Bruker Daltonics, Bremen, Germany).

An EC 100/2 Nucleoshell Phenyl-Hexyl column (length 100 mm, internal diameter 2 mm, particle size 2.7 μ m; Macherey-Nagel, Düren, Germany) was used for chromatographic separation. The mobile phases used for the chromatographic separation were composed of two different solvents:

(A) H₂O + 1% ammonium formate in H₂O + 0.1% formic acid.

(B) Acetonitrile: isopropanol (7:3) + 1% of 10 mM ammonium formate in H₂O + 0.1% formic acid.

The flow rate was 400 μ L \cdot min⁻¹ and the following gradient was used (from (i) to (iv)):

(i) 45% of A for 1 min, followed by a linear gradient from 45% A to 30% A from 1 to 2 min.

(ii) A linear gradient from 30% A to 15% A from 2 to 7 min, a linear gradient from 15% A to 10% A from 7 to 15 min

(iii) A linear gradient from 10% A to 6% A from 15 to 19 min, a linear gradient from 6% A to 2% A from 19 to 26 min.

(iv) 0% of A was held until 40 min, followed by a linear gradient from 0% A to 45% A from 40.1 to 45 min (45 min total run time).

For mass spectrometer analysis, data analysis was performed in positive and negative Electrospray Ionization (ESI) modes. Two ionization modes were used to ionize different polar functions in the lipid's structures, thus maximizing lipids identification.

The following parameters were used for ESI: capillary voltage, 4.5 kV; nebulizer gas flow, 2.1 bar; dry gas flow, 6 L·min⁻¹; drying gas in the heated electrospray source temperature, 200°C. Samples were analyzed at 8 Hz with a mass range of 100–1700 *m/z*. Stepping acquisition parameters were created to improve the fragmentation profile with a collision RF from 200 to 700 Vpp, a transfer time from 150 μs, and collision energy from 20 to 40 eV. Each cycle included an MS full scan and 5 MS/MS CID on the 5 main ions of the previous MS spectrum.

3.5.3.3. Lipids data processing

The data processing was performed from *.d* data files (Bruker Daltonics, Bremen, Germany). These files were converted to *.mzXML* format using the MSConvert software (ProteoWizard package 3.0 (Chambers et al. 2012)). *mzXML* data processing, mass detection, chromatogram building, deconvolution, samples alignment and data export were performed using MZmine 2.53 software (Pluskal et al. 2010) for both positive and negative data files. The ADAP chromatogram builder (Myers et al. 2017) method was used with a minimum group size of scan 3, a group intensity threshold of 1000, a minimum highest intensity of 1000, and *m/z* tolerance of 2 ppm. Deconvolution was performed with the ADAP wavelets algorithm using the following settings: S/N threshold 10, peak duration range = 0.01–2 min of Retention Time (RT) wavelet range 0.01–0.2 min. MS² scans were paired using an *m/z* tolerance range of 0.05 Da and RT tolerance of 0.5 min. Then, the isotopic peak grouper algorithm was used with an *m/z* tolerance of 2 ppm and RT tolerance of 0.2 min. All the peaks were filtered using a feature list row filter keeping only peaks with the MS² scan. The alignment of samples was performed using the join aligner with an *m/z* tolerance of 2 ppm, a weight for *m/z* and RT at 1.0 min, And a retention time tolerance of 0.2 min.

For lipids identification (annotation), the first research in the library of Mzmine was done. This library contains an identification module and custom database, currently including 93 annotations (RT and *m/z*) in positive and negative modes, with RT tolerance of 0.2 min and *m/z* tolerance of 0.005 Da. Then, molecular networking of lipidomic data and lipid annotation by MS² spectral libraries were performed.

Molecular networking was generated by the MetGem software (Olivon et al. 2018) using the *.mgf* and *.csv* files obtained with MZmine 2.53 analysis. The molecular network was optimized for the ESI+ and ESI- datasets and different cosines similarity score thresholds were tested. ESI- and ESI+ molecular networks were generated using cosine score thresholds of 0.7 and 0.65, respectively.

Lipid annotations were performed in different consecutive steps. First, the ESI- and ESI+ metabolomic data used for molecular network analyses were searched against the available MS² spectral libraries (Massbank NA, GNPS Public Spectral Library, NIST14 Tandem, NIH Natural Product, Lipid Blast, and User database of the platform), with absolute *m/z* tolerance

of 0.02; 4 minimum matched peaks and minimal cosine score of 0.65. Second, in the different clusters of the molecular network, the database search result was validated using the different specific fragments and neutral loss for the different lipid classes with their MS^2 spectrum (Lipid Class-Specific Fragments - Lipidomics-Standards-Initiative (LSI)). If the database search result was validated, annotation of other features was performed by stepwise comparison from the valid lipid metabolite. Finally, for the cluster of molecular networks that had no database search result, Sirius 4software was used, which provides a fast computational approach for molecular structure identification (Dührkop et al. 2019).

3.6. Biophysical properties of the *L. bulgaricus* CFL1 membrane: lipid phase transition temperature and membrane fluidity

(c.f. Chapter 5)

The lipid phase transition temperature of *L. bulgaricus* CFL1 cells was determined by Fourier Transformed InfraRed spectroscopy (FTIR). This method involves monitoring the symmetric CH₂ stretching vibration absorbance band positions (Crowe et al. 1989b). Membrane fluidity was determined by fluoresce anisotropy. Fluorescent lipid soluble membrane probes are used as biomarkers of membrane lipid structure and motion. The degree of polarization of the fluorescent probe is generally characterized by the anisotropy (r), which decreases when cell membrane fluidity increases (Mykytczuk et al. 2007).

3.6.1. Bacterial sample preparation

Harvested bacterial cells (t_{h1} , t_{h2} , and t_{h3}) of the four evaluated fermentation conditions ([42°C, pH5.8]; [42°C, pH4.8]; [37°C, pH5.8]; and [37°C, pH 4.8]) were concentrated by centrifugation at 11 500 g , 4°C for 10 min (Avanti® J-E centrifuge; Beckman Coulter, Fullerton, CA). The resulting cell pellets were then re-suspended in the protective solution at a ratio of 1:2 (1 g of concentrated cells for 2 g of the protective solution). The protective solution was composed of 20% (w/w) of sucrose (VWR, Leuven, Belgium), previously sterilized at 121°C for 20 min. The bacterial suspension was aliquoted at two milliliters volume in cryo-tubes (Sarstedt, Nümbrecht, Germany). Bacterial samples were kept frozen at -80°C until FTIR and anisotropy analysis.

3.6.2. FTIR: equipment and configuration

Measurements were carried out in a transmission mode using a Nicolet Magna 750 FTIR spectrometer (Thermo Fisher Scientific; Madison, WI, USA) equipped with a mercury/cadmium/telluric (MCT) detector and a variable temperature stage (Specac Ltd.; Orpington, Kent, UK) (Gautier et al. 2013). The optical bench was continuously purged with dry air (Balston; Haverhill, MA, USA) to remove the spectral contribution of water vapor.

3.6.3. FTIR: spectra acquisition and analysis

Omnic software (version 7.1, Thermo Fisher Scientific; Madison, WI, USA) was used for spectra acquisition: 32 co-added scans were collected every 45 s with a resolution of 4 cm^{-1} (approximately one scan·°C⁻¹ by stepped temperature ramping) in the mid-IR region from 4000 to 900 cm^{-1} .

Before recording the infrared absorption spectra of *L. bulgaricus* CFL1 cells, background spectra were recorded (mid-IR region 4000 to 900 cm^{-1}) at room temperature. For background acquisition, two clean (70% ethanol) CaF₂ windows were mounted in the sample holder. The sample area was thoroughly flushed with dry to avoid the contribution of water vapor and CO₂ to the background.

Then, the bacterial cell suspension was thawed at 42°C for 5 min in a water bath and centrifuged at 12 900 *g*, 4°C, for 10 min (Eppendorf® Centrifuge 5804 R – Benchtop, Hamburg, Germany). At room temperature, the supernatant was removed. A small amount of the resulting cell pellet was tightly sandwiched between two calcium fluoride (CaF₂) windows (ISP Optics; Riga, Latvia). The infrared spectra acquisition (mid-IR region 4000 to 900 cm⁻¹) of *L. bulgaricus* CFL1 was performed upon cooling from 50°C to -50°C and heating from -50°C to 50°C. The temperature was decreased by pouring liquid nitrogen into the cell holder at a rate of 2°C·min⁻¹. A thermocouple inserted in a hole very close to the sample ensured an accurate cooling rate. During heating, the temperature was increased by the automatic system of the equipment at the same rate (2°C·min⁻¹).

The spectral analysis focused on the peak position of $\nu_{sym}CH_2$ arising from the lipid acyl chains of the membrane, located around 2850 cm⁻¹ (Crowe et al. 1989b; Mantsch and McElhaney 1991). A house-developed ASpiR software (Infrared Spectra Acquisition and Processing, INRAE; Thiverval-Grignon, France) was used for analyzing each spectrum. The peak position in each spectrum was determined using their second-order derivative and smoothed according to a seven-point Savitsky-Golay algorithm. Wavenumbers peaks of $\nu_{sym}CH_2$ were then plotted against the temperature at which they were measured.

For this study, we were focused on determining the main phase transition from liquid crystalline to rigid gel phase upon cooling and viceversa upon heating. For this reason, the $\nu_{sym}CH_2$ peak positions versus temperature plots from *L. bulgaricus* CFL1 samples were fitted with a curve based on an asymmetric sigmoid transition model.

The first-order derivative of this model was calculated to determine the lipid phase transition temperatures using the maximum of these first-order derivatives upon cooling (*T_s* in °C, lipid solidification) from 50°C down to -50°C and heating (*T_m* in °C, lipid melting) from -50°C to 50°C (Figure 3.10 (A)). Additionally, the peak positions of the O-H libration combined with the band of water (ν_{H_2O}) located around 2200 cm⁻¹ were simultaneously monitored to determine ice nucleation temperatures (*T_n*) (Wolkers et al. 2007). (Figure 3.10 (B)). The temperature dependence of these specific infrared bands reveals information about conformational and phase changes for acyl chains and water molecules (Crowe et al. 1989b).

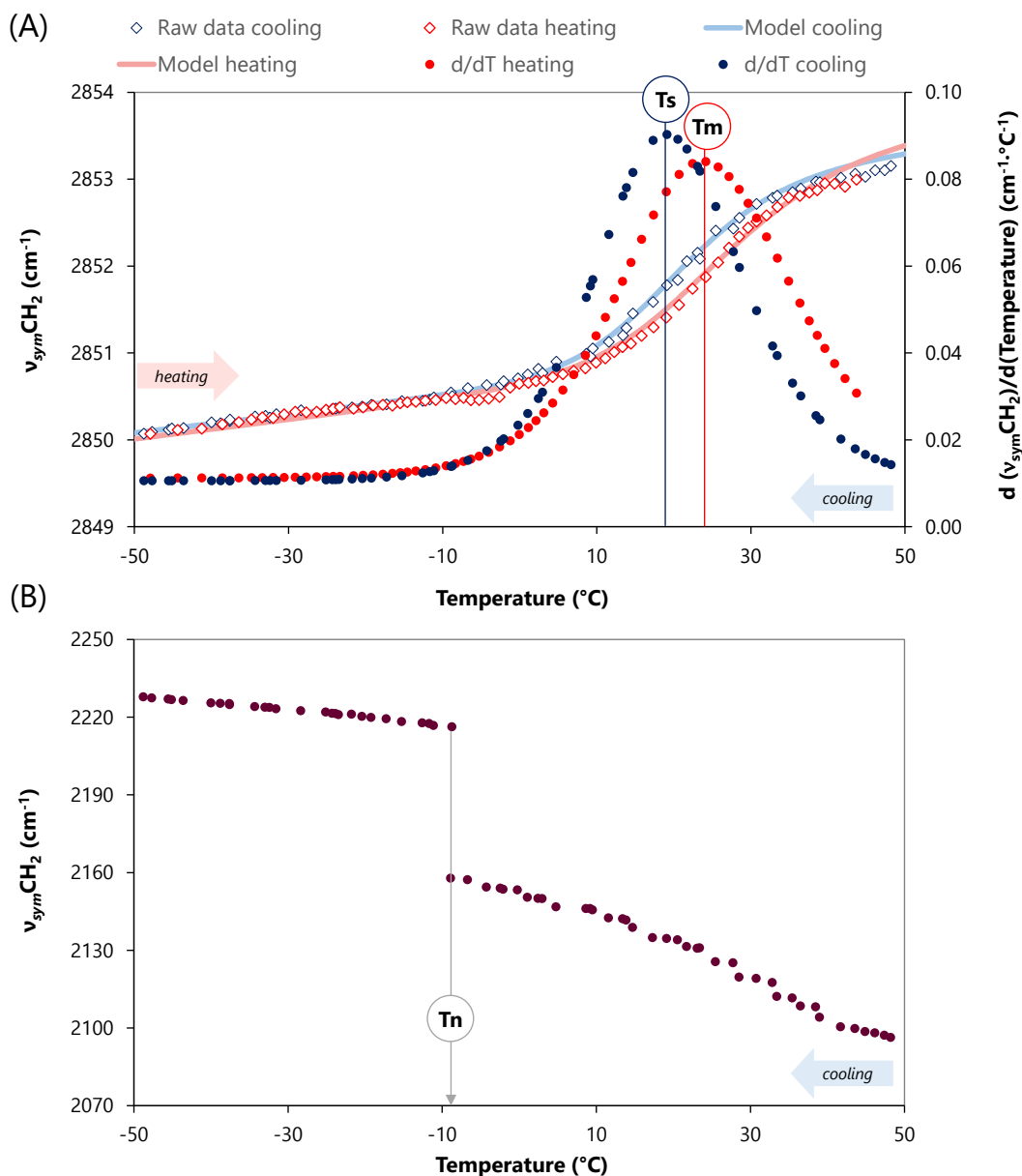


Figure 3.10 (A) Peak positions of $\nu_{sym}CH_2$ vibration bands arising from *L. bulgaricus* CFL1, plotted against their acquisition temperature. Raw data (empty blue and red diamonds) were fitted with a curve based on an asymmetric sigmoid transition function model. The maximum of the first derivative of the fitted curve was used to determine the lipid phase transitions temperatures during cooling (T_s) and heating (T_m). (B) Peak position and shape of the O-H libration and the combination of the bending band of water (νH_2O), as a function of temperature. The upshift from approximately 2160 to 2220 cm⁻¹ during cooling, determines the water nucleation temperature (T_n).

3.6.4. Fluorescence anisotropy by flow cytometry

The protected bacterial cell suspensions were thawed at 42°C for 5 min in a water bath and centrifuged at 12 900 *g*, 4°C, for 10 min (Eppendorf® Centrifuge 5804 R – Benchtop, Hamburg, Germany). After removing the supernatant, the bacterial pellet was suspended in morpholine ethane sulfonic acid (MES) buffer (Merck, Sigma-Aldrich, Darmstadt, Germany) and adjusted to 10⁷ cells·mL⁻¹. Then, bacteria were washed twice with this same buffer (MES) and resuspended in 2 mL of MES buffer adjusted at pH 5.5 with KOH at 30% (VWR, Leuven, Belgium). Then, 5 µL of DPH solution (6 mM in DMSO) (Merck, Sigma-Aldrich, Darmstadt, Germany) was added to 1 mL of the cell suspension to obtain a final DPH concentration of 30 µM.

The cell suspension was vigorously stirred for 1 min and centrifuged (14 000 *g*, 20°C, for 90 s). The pellet obtained was resuspended in 2 mL of the MES buffer, pH 5.5, and used immediately for fluorescence polarization measurements. Fluorescence polarization was determined by using a flow cytometer (CyFlow Space cytometer, Sysmex-Partec, Villepinte, France). The flow cytometer was equipped with a vertically polarized UV laser that emits at 488 nm a half-wave retarder plate (rotating polarizer) to depolarize the excited light, as well as parallel and perpendicular polarizers just prior to entering the two photomultiplier tubes. The measurement was performed at 20°C with emission wavelengths at 375 nm. The fluorescence anisotropy (*r*) was calculated according to the following equation:

$$r = \frac{I_{//} - I_{\perp}}{I_{//} + 2I_{\perp}} \quad (3.8)$$

Where *I*_{//} and *I*_⊥ are the polarized light intensities emitted in the parallel and perpendicular directions with respect to the excitation beam of light, respectively.

3.7. Sugars effect on the resistance and membrane of *L. bulgaricus* CFL1

(cf. Chapter 6)

3.7.1. Bacterial sample preparation

L. bulgaricus CFL1 cells cultivated at [42°C, pH 5.8] were harvested at the stationary growth phase (t_{h3}). Bacterial cells were concentrated by centrifugation at 11 500 *g*, 4°C for 10 min (Avanti® J-E centrifuge; Beckman Coulter, Fullerton, CA). The resulting cell pellets were resuspended in seven different protective solutions at a ratio of 1:2 (1 g of concentrated cells for 2 g of the protective solution). The sugars in this study were selected because they have a different degree of polymerization (monomeric units in a macromolecule) and their commercial availability for this study (Table 3.1). Besides, most of them were identified as effective protectors to stabilize lactic acid bacteria during freezing and freeze-drying (Carvalho et al. 2002; Schoug et al. 2006; Pehkonen et al. 2008; Bravo-Ferrada et al. 2015; Ambros et al. 2018) They are also the basic structures of the oligoaccharides currently use in the European project PREMIUM.

Each protective solution was prepared at 25% (w/w) in a saline water (NaCl 0.9%) and previously sterilized at 121°C for 20 min. Two milliliters of bacterial suspension were aliquoted in cryotubes (Sarstedt, Nümbrecht, Germany). Samples were kept frozen at -80°C until functional properties measurements and FTIR analysis.

Table 3.1 Different sugars at used to protect *L. bulgaricus* CFL1 cells

Code	Sugar (DP)	Molar mass (g·mol ⁻¹)	Supplier details
G	Glucose (DP1)	180.1	VWR, Leuven, Belgium
S	Sucrose (DP2)	342.3	VWR, Leuven, Belgium
T	Trehalose (DP2)	342.3	Merck, Sigma-Aldrich, Darmstadt, Germany
L	Lactose (DP2)	342.3	Merck, Sigma-Aldrich, Darmstadt, Germany
R	Raffinose (DP3)	504.4	Merck, Sigma-Aldrich, Darmstadt, Germany
P	Pentaisomaltose (DP 5-10)	~850-1750	PentaiHibe® Pharmacosmos, Holbaek, Denmark
M	Maltodextrin (DP~17)	~2700	Glucidex®6, Roquette Frères ; Lestrem, France

Abbreviations: DP, Degree of Polymerization

3.7.2. Physicochemical properties of sugars

The physicochemical properties measurements for the seven sugar solutions were pH, osmolarity, and viscosity. These measurements were carried out for three independent sugar solutions.

The pH of each sugar solution was measured by a pH meter MU 6100 L (pH-phenomena, VWR collection, Leuven, Belgium). Osmolarities were determined using a Roebeling osmometer (Type 13, Löser Messtechnik; Berlin, Germany). The viscosity was measured at 20°C and 0°C by a rheometer equipped with a cone plate (CP50, 32 mm in diameter) (Anton Paar, MCR 301, Graz, Austria). The temperature was controlled through a thermostatic bath (Julabo, Seelbach, Germany) by circulating a mixture of ethylene glycol and water in the outer jacket of the cylinder.

3.7.3. Protection efficiency of different sugars during freezing and freeze-drying

To determine the protection efficiency of each sugar in Table 3.1, the acidifying activity (subsection 3.3.1) and culturability (subsection 3.3.2) of *L. bulgaricus* CFL1 cells were determined. Both (acidifying activity and culturability) were measured before (initial) and after freezing (F) and freeze-drying (FD). Then, the loss of acidifying activity (Equation 3.9), the culturability (Equation 3.10), and the loss of specific acidifying (Equation 3.11) were calculated as follows:

$$dt_{\Delta\text{pH}0.7} \text{ F or FD} = t_{\Delta\text{pH}0.7} \text{ F or FD} - t_{\Delta\text{pH}0.7} \text{ I (Initial)} \quad (3.9)$$

$$\text{F or FD survival rate (\%)} = \frac{\text{Culturability (CFU}\cdot\text{mL}^{-1})_{\text{After F or FD}}}{\text{Culturability (CFU}\cdot\text{mL}^{-1})_{\text{Initial}}} \quad (3.10)$$

$$dt_{\text{spe}} \text{ F or FD} = t_{\text{spe}} \text{ F or FD} - t_{\text{spe}} \text{ I (Initial)} \quad (3.11)$$

3.7.4. Sugars effect on *L. bulgaricus* CFL1 membrane by Fourier transform infrared (FTIR)

The interaction of *L. bulgaricus* CFL1 cells with the different sugars studied was analyzed at two different physical states of bacterial cells: (i) hydrated cells (frozen-thawed cells) and (ii) air-dried cells (dried cells, water absence). The purpose was to assess the influence of the water when sugars are present in bacteria suspensions.

3.7.4.1. Hydrated cells

After producing bacterial suspensions (subsection 3.6.1), bacterial samples were thawed at 42°C for 5 min in a water bath and centrifuged at 12 900 *g*, 4°C, for 10 min (Eppendorf® Centrifuge 5804 R – Benchtop, Hamburg Germany). At room temperature, the supernatant was removed. A small amount of the resulting cell pellet was tightly sandwiched between two calcium fluoride (CaF₂) windows (ISP Optics; Riga, Latvia) to be analyzed in the FTIR equipment. Infrared absorption spectra were recorded during cooling from 50°C to -50°C.

3.7.4.2. Air-dried cells

Also, bacterial cell suspensions were prepared as described in subsection 3.6.1. They were thawed at 42°C for 5 min in a water bath and centrifuged (12 900 *g*, 4°C, for 10 min).

The supernatant was removed, then ten microliters of the cell/sugar suspensions were spread on a calcium fluoride (CaF₂) window and air-dried for 24 hours. Air-drying was done in a desiccator continuously flushed with less than 3% RH dry air. This air-drying method led to a residual water content of 0.022 ± 0.005 g H₂O per g dry weight (measurement determined by gravimetric analysis) (Oldenhof et al. 2005). Once the sample was dried at room temperature, it was tightly sandwiched with another calcium fluoride (CaF₂) window to be analyzed in the FTIR equipment. Infrared absorption spectra were recorded during heating from -50°C to 75°C.

3.7.4.3. FTIR study

The measures of IR spectra on both physical states of *L. bulgaricus* CFL1 cells (frozen-thawed and air-dried cells) were performed on a Nicolet Magna FTIR spectrometer (Thermo Fisher Scientific; Madison, WI, USA) as described in section 3.6.2.

Omnic software (version 7.1, Thermo Fisher Scientific; Madison, WI, USA) was used for spectra acquisition: 32 co-added scans were collected every 45 s with a resolution of 4 cm⁻¹ (approximately one scan·°C⁻¹ by stepped temperature ramping) in the mid-IR region from 4000 to 900 cm⁻¹ (see also section 3.6.3)

Peak positions of three different functional groups were determined by analyzing the spectra of samples using a house-developed ASplR software (Infrared Spectra Acquisition and Processing, INRAE; Thiverval-Grignon, France). For this purpose, the specific peak locations from each spectrum were obtained by calculating the second-order derivatives of each spectrum. The second derivatives were then smoothed according to a 9-point Savitsky-Golay algorithm. The obtained peak frequencies were then plotted against the temperature at which they were measured.

The first peak position studied was the symmetric CH₂ stretching vibration band ($\nu_{sym}CH_2$) located around 2850 cm⁻¹ arising from lipid acyl chains (Crowe et al. 1989b; Mantsch and McElhaney 1991). The temperature dependence of $\nu_{sym}CH_2$ reveals information about conformational and phase changes of acyl chains. The position of this peak allowed us to determine the membrane lipid phase transition. In this case (contrary to what has been explained in section 3.6.3), the $\nu_{sym}CH_2$ plots without applying any fitted model arising from used to calculate the first derivatives. The maximums of the first derivative curves were taken as the membrane lipid phase transition temperatures: $T_{cooling}$ (upon cooling, in °C) and $T_{heating}$ (upon heating).

The second peak positions analyzed were the O-H libration and a bending combination band of water (νH_2O) located around 2200 cm⁻¹. Both were simultaneously monitored to determine

ice nucleation temperatures (T_n) (Wolkers et al. 2007). Finally, the asymmetric PO_2 stretching vibration band ($\nu_{\text{asym}}\text{PO}_2$) positions were examined. This vibration band is located at approximately 1220 cm^{-1} . It represents a sensor for head group hydration (in the membrane), leading to a shift of its frequency (Fringeli and Günthard 1981).

3.8. Statistical analysis

Results in Chapters 4, 5, and 6 are given as mean \pm sample standard deviation of at least three independent biological cultures.

3.8.1. Factorial design experiment

(cf. Chapter 4 and 5)

A full factorial design $2 \times 2 \times 3$ was performed to evaluate the effect of fermentation parameters pH (2), temperature (2), and harvest time (3) on the following response variables:

(i) Biomass productivity (P, in $\text{g}\cdot\text{L}^{-1}\cdot\text{h}^{-1}$).

(ii) Metabolite production and substrate consumption: lactic acid concentration ($\text{g}\cdot\text{L}^{-1}$) and glucose concentration ($\text{g}\cdot\text{L}^{-1}$).

(iii) Functional properties: acidifying activity ($t_{\Delta\text{pH}0.7}$, in min), culturability ($\text{CFU}\cdot\text{mL}^{-1}$), and specific acidifying activity (t_{spe} , in $[\text{min} (\log (\text{CFU mL}^{-1}))^{-1}]$) for all steps of *L. bulgaricus* CFL1 production process, after:

(1) Fermentation (initial): $t_{\Delta\text{pH}0.7 I}$ in min; culturability ($\text{CFU}\cdot\text{mL}^{-1}$); and $t_{\text{spe I}}$, $[\text{min} (\log (\text{CFU mL}^{-1}))^{-1}]$.

(2) Freezing: $t_{\Delta\text{pH}0.7 F}$, in min; culturability ($\text{CFU}\cdot\text{mL}^{-1} F$); and $t_{\text{spe F}}$, $[\text{min} (\log (\text{CFU mL}^{-1}))^{-1}]$.

(3) Freeze-drying: $t_{\Delta\text{pH}0.7 FD}$, in min; culturability ($\text{CFU}\cdot\text{mL}^{-1} FD$); and $t_{\text{spe FD}}$, $[\text{min} (\log (\text{CFU mL}^{-1}))^{-1}]$.

(4) Freeze-dried storage: $t_{\Delta\text{pH}0.7 S}$, in min; culturability ($\text{CFU}\cdot\text{mL}^{-1} S$); and $t_{\text{spe S}}$, $[\text{min} (\log (\text{CFU mL}^{-1}))^{-1}]$.

(iv) Loss of functional properties (Equations 3.3-3.5): loss of the specific acidifying activity during freezing ($dt_{\text{spe F}}$, $[\text{min} (\log (\text{CFU mL}^{-1}))^{-1}]$), freeze-drying ($dt_{\text{spe FD}}$, $[\text{min} (\log (\text{CFU mL}^{-1}))^{-1}]$), and freeze-dried storage ($dt_{\text{spe S}}$, $[\text{min} (\log (\text{CFU mL}^{-1}))^{-1}]$)

(v) Lipid transition temperatures during cooling (T_s) and heating (T_m), as well as, water nucleation (T_n) (Temperatures, $^{\circ}\text{C}$).

(vi) Membrane fluidity (anisotropy values, r)

(vii) Fatty acid composition of *L. bulgaricus* CFL1 cells (Relative %).

3.8.2. Stepwise linear regression and response surface method

(c.f. Chapter 4)

Stepwise descending multiple regression analyses were performed to quantify the effect of independent variables (pH (X_1), temperature (X_2), and harvest time (X_3)) on the response variables (i), (iii), and (iv) of 3.7.1. These analyses were performed using the MATLAB R2014b software equipped with the Statistics Toolbox (The Mathworks, Inc., Natick, MA). The applied regression model was a second-order polynomial with interactions of the following form:

$$Y = \beta_0 + \beta_1 X_1 + \beta_2 X_2 + \beta_3 X_3 + \beta_{33} X_3^2 + \beta_{12} X_1 X_2 + \beta_{13} X_1 X_3 + \beta_{23} X_2 X_3 + \beta_{123} X_1 X_2 X_3 \quad (3.12)$$

Where β_0 , β_i , β_{ii} and β_{ij} are respectively the intercept, linear, and interaction coefficients. X_1 , X_2 , and X_3 are, respectively, pH, temperature, and harvest time. A quadratic coefficient is applied for harvest time since it has three levels (t_{h1} , t_{h2} , and t_{h3}), compared to pH (5.8 and 4.8) and temperature (42°C and 37°C) with only two levels.

The adequacy of the model was assessed by its coefficient of determination (R^2), a measurement of the percentage of total data variance explained by the model.

Stepwise regression is a method of fitting regression models in which an automatic procedure carries out the choice of predictive variables. Regression was initially performed with the complete model. Parameters (independent variables) not significantly different from zero at a 0.05 level were iteratively removed from the model (i.e., set to exactly zero), starting with the one exhibiting the highest coefficient of variation.

Response surface plots were generated from the fitted polynomial equations (Equation 3.8) to visualize the relationships between the responses and independent variables.

3.8.3. ANOVA tests

(c.f. Chapter 4, 5 and 6)

The one-way analysis of variance (ANOVA) and the post-hoc Tukey HSD were used to determine whether there are any statistically significant differences among the means of the four fermentation conditions and the three harvest times. Tests were performed using XLSTAT 2020.5 (Addinsoft, Paris, France). Significance levels of 95% (P -value < 0.05) were considered.

3.8.4. Pearson's correlation coefficient

(c.f. Chapter 5)

A Pearson's correlation coefficient test was performed to link the biophysical lipid properties (lipid transition temperatures, membrane fluidity) and biochemical characterization (fatty acids composition) to freezing and freeze-drying resistance of *L. bulgaricus* CFL1.

The Pearson correlation coefficient test is a normalization of the covariance by the product of the standard deviations of the variables. It measures the degree and direction of the relationship between the two variables (Hoffman 2019).

The coefficients generated from Pearson's correlation test measure the strength of the linear relationship between two variables, giving a value between -1 and $+1$. The higher the absolute value of the correlation coefficient (R) between two variables was, the stronger the linear relationship between the two variables was. The following variables were considered for this analysis: Saturated Fatty Acids (SFA), Unsaturated Fatty Acids (UFA), Unsaturated Fatty Acid-to-Saturated Fatty Acid ratio (UFA/SFA), membrane fluidity (the fluorescence anisotropy, r), the lipid transition temperatures (T_s and T_m), and the specific acidifying activity losses during freezing ($dt_{spe} F$) and freeze-drying ($dt_{spe} FD$). This test was carried out using XLSTAT 2020.5 (Addinsoft, Paris, France). The significance of the results was assessed at a 95% confidence level (P -value <0.05).

3.8.5. Principal Component Analysis (PCA)

(*cf.* Chapter 5)

PCA was also carried out to establish associations among the biophysical lipid properties (lipid transition temperatures, membrane fluidity) and biochemical characterization (fatty acids composition), as well as *L. bulgaricus* CFL1 resistance (XLSTAT 2020.5, Addinsoft, Paris, France).

Principal component analysis (PCA) simplifies the complexity of high-dimensional data while retaining trends and patterns by transforming the data into fewer dimensions.

PCA reduces data by geometrically projecting them onto lower dimensions called principal components (PCs), intending to find the best data summary using a limited number of PCs.

First, the variables representing the most significant variance are grouped to form the first axis. The second axis represents the following most significant variance until all the data's variance is represented. The analysis of the eigenvalues of each axis allows identifying the number of axes needed to explain the variance of the data. Once the axes have been chosen, the variables are positioned in a two-dimensional space according to the behavior of their variance concerning the axes in question. When variables are represented by two points close to each other, it means that they behave similarly. Second, individuals are positioned with the variables.

When examining the results of PCA, the position of the variables and the individuals in relation to the axes were analyzed to explain the differences in behavior observed. Before analyzing the results, it was identified the majority axis explained by each variable and individuals.

3.8.6. Clustering analysis for different lipids class

Heatmaps and hierarchical clustering analysis were used to analyze the different lipids classes in the *L. bulgaricus* CFL1 membrane. Both analyses were conducted by the open-source software MultiExperiment Viewer (MeV, version 4.9.0, Dana–Farber Cancer Institute, MA). The statistical significance was set at P -value < 0.05.

A heatmap uses a matrix layout with color and shading to show the relationships between two categories of values. This graphical representation helped visualize the relative abundance of each lipid class identified (with its corresponding fatty acid chains) within the samples (subsection 3.5.3: LE, f_1 , f_2 , f_3 , and f_4).

A normalized peak area determined the relative abundance of each lipid class. An example of a heatmap is shown in Figure 3.11. Columns represent the samples being compared, and rows represent a lipid class with its corresponding FA.

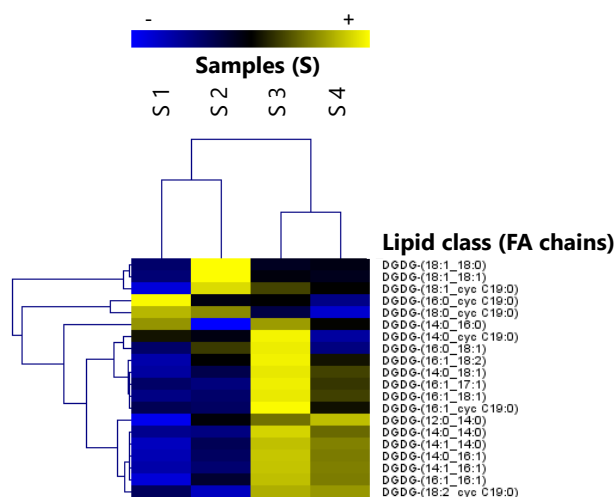


Figure 3.11 Heatmap example of a specific lipid class. Abbreviation: DGDG, diglycosyldiacylglycerol; FA, Fatty Acids; -, low relative abundance; +, high relative abundance.

The normalization of each peak is carried as follows:

$$\text{Normalized peak value} = \frac{(\text{Peak area} - \text{Mean Peak area}(\text{row}))}{\text{standard deviation Peak area}(\text{row})} \quad (3.13)$$

The color gradient sets from the lowest relative abundance (blue color) to the highest relative abundance (bright yellow). It also shows mid-range relative abundance (dark color). The hierarchical clustering is displayed as a dendrogram (Figure 3.11). The hierarchical clustering grouped similar peak areas of the samples by using Pearson correlation as a distance function.

Chapter 4

4. MULTI-OBJECTIVE OPTIMIZATION OF FROZEN AND FREEZE-DRIED *L. bulgaricus* CFL1

Before using LAB in various industrial applications, these bacteria are produced by fermentation. Then, they are concentrated and stabilized by freezing or freeze-drying. Both processes have the objective of preserving their functionality in the long term. Stabilization processes induce, however, different types of stresses (Chapter 1, subsection 1.2). Among the different approaches proposed to help bacteria overcome such stresses, the preparation of bacterial cells during the fermentation processes is one of them.

This chapter, thus, revisits this strategy in order to propose an innovative alternative to optimize different steps of the production process: fermentation, stabilization processes (freezing and freeze-drying), and freeze-dried storage

SUMMARY OF THE CHAPTER

4. MULTI-OBJECTIVE OPTIMIZATION OF FROZEN AND FREEZE-DRIED

<i>L. bulgaricus</i> CFL1	117
4.1. Preamble	119
4.2. Abstract	120
4.3. Introduction	121
4.4. Materials and methods	123
4.4.1. Starter production and stabilization processes	123
4.4.1.1. Strain and inoculum preparation	123
4.4.1.2. Fermentation	125
4.4.1.3. Concentration, protection, and freezing	126
4.4.1.4. Freeze-drying and freeze-dried storage	126
4.4.2. Cell growth and metabolite production during fermentation	126
4.4.2.1. Cell growth kinetics and biomass productivity measurements	126
4.4.2.2. Substrate and metabolite analysis	127
4.4.3. Functional properties of starters	127
4.4.3.1. Acidifying activity	128
4.4.3.2. Culturability	128
4.4.3.3. Specific acidifying activity and loss of specific acidifying activity	128
4.4.4. Water content and glass transition temperature measurements	128
4.4.5. Statistical analysis	129
4.4.5.1. Experimental design	129
4.4.5.2. Stepwise descending multiple regression analyses	129
4.4.5.3. Complementary statistical analysis	130
4.5. Results	131
4.5.1. Fermentation kinetics and biomass productivity	131
4.5.2. Initial functional properties of <i>L. bulgaricus</i> CFL1	134
4.5.3. Effects of fermentation parameters (pH, temperature, and harvest time) on the loss of specific acidifying activity after freezing, freeze-drying, and freeze-dried storage	135
4.5.3.1. Freezing	136
4.5.3.2. Freeze-drying	137
4.5.3.3. Freeze-dried storage	138
4.5.4. Predictive accuracy of the multiple regression models	138
4.5.5. Multi-objective optimization, Pareto front approach, to produce frozen and freeze-dried <i>L. bulgaricus</i> CFL1 cells	139
4.6. Discussion	142
4.7. Supplementary Information	145
4.7.1. Supplementary Tables	145
4.7.2. Supplementary Figures	153
4.8. Prospects for this study	158

4.1. Preamble

This chapter was written as an article format including a material and methods section adapted to publication. The reading of the experimental section can be skipped for those who read Chapter 3.

Supplementary information available in Chapter 3 Materials and methods

Chapter 4: subsection	Chapter 3: section or subsection
4.4.1 Starter production and stabilization processes	3.1 Production of concentrated <i>L. bulgaricus</i> CFL1 3.2. Stabilization processes and freeze-dried storage
4.4.2. Cell growth and metabolite production during fermentation	3.1.5 Measurements carried out throughout fermentation
4.4.3. Functional properties of starters	3.3. Assessment of the functional properties of <i>L. bulgaricus</i> CFL1 at different production steps
4.4.4. Water content and glass transition temperature measurements	3.4. Water content and temperature glass transition of the freeze-dried bacteria
4.4.5. Statistical analysis	3.8.1. Factorial design experiment 3.8.2. Stepwise linear regression and response surface method 3.8.3. ANOVA tests

Article submitted in *Journal of Applied Microbiology*

Multi-objective optimization of frozen and freeze-dried *Lactobacillus delbrueckii* subsp. *bulgaricus* CFL1 production via the modification of fermentation conditions.

Maria de L. Tovilla-Coutiño^{1,3}, Stéphanie Passot¹, Ioan-Cristian Trelea¹, Marie-Hélène Ropers², Fernanda Fonseca¹, Yann Gohon^{3*},

¹Université Paris-Saclay, INRAE, AgroParisTech, UMR SayFood, 91120 Palaiseau, France

²INRAE, UR1268 Biopolymères Interactions Assemblages, 44300 Nantes, France

³Université Paris-Saclay, INRAE, AgroParisTech, Institut Jean-Pierre Bourgin (IJPB), 78000 Versailles, France

*Corresponding author: Yann Gohon, Université Paris-Saclay, INRAE, AgroParisTech, Institut Jean-Pierre Bourgin (IJPB), 78000 Versailles, France.

E-mail: yann.gohon@inrae.fr

4.2. Abstract

Aim: This study investigates the individual and combined effects of fermentation parameters for improving cell biomass productivity and the resistance to freezing, freeze-drying, and freeze-dried storage of *Lactobacillus delbrueckii* subsp. *bulgaricus* CFL1.

Methods and Results: Cells were cultivated at different temperatures (42°C and 37°C) and pHs (5.8 and 4.8) and were harvested at mid-exponential, deceleration, and stationary growth phases. Acidifying activity and culturability were measured after fermentation, freezing, freeze-drying, and freeze-dried storage. Multiple regression analyses were performed to identify the effects of fermentation parameters on the specific acidifying activity losses and generate the corresponding 3D response surfaces. After each stabilization process, a multi-objective decision approach was applied to optimize biomass productivity and specific acidifying activity. The temperature positively influenced biomass productivity, whereas low pH during growth reduced the loss of specific acidifying activity after freezing and freeze-drying. Furthermore, freeze-drying resistance was favored by increased harvest time.

Conclusions: Productivity, freezing, and freeze-drying resistances of *Lactobacillus delbrueckii* subsp. *bulgaricus* CFL1 were differentially affected by the fermentation parameters studied. When cells were grown at 42°C, pH 4.8, and harvested at the deceleration phase, a compromise was reached using Pareto fronts to optimize biomass productivity and functional properties.

Significance and Impact of the study: Setting up predictive models for optimizing fermentation conditions is an efficient approach to guiding starter production and to modulating the resistance to freezing and freeze-drying.

Keywords: lactic acid bacteria; fermentation; freezing; freeze-drying; functional properties; multiple regression analysis; multi-objective optimization.

4.3. Introduction

Lactobacillus delbrueckii subsp. *bulgaricus* (*L. bulgaricus*) is a lactic acid bacteria that undoubtedly presents an economic interest, given its worldwide application in yogurt production (Van De Guchte et al. 2006). Additionally, some strains of *L. bulgaricus* have been used as probiotic cultures, exerting health benefits (Jain et al. 2004; Guha et al. 2019).

L. bulgaricus, as well as many lactic acid bacteria (LAB), are commercialized as ready-to-be-used products by food companies. The manufacturing process involves producing bacterial concentrates via fermentation, followed by centrifugation. Stabilization techniques are then applied to increase the shelf life of highly concentrated bacteria.

Freezing and freeze-drying are the most currently used techniques for stabilizing lactic acid bacteria. Freeze-drying offers the advantages of low storage, transportation costs, and easy handling compared to freezing. In addition, it has been recently demonstrated that for the long-term preservation of *L. bulgaricus*, the freeze-dried form is more eco-friendly than freezing (Pénicaud et al. 2018).

Freezing induces ice crystal formation and cryo-concentration of solutes with bacteria packed into the frozen concentrated matrix. Cryo-concentration leads to osmotic stress and cell dehydration, considered to be the primary source of cryoinjury of *L. bulgaricus* (Meneghel et al. 2017). Freeze-drying involves freezing the aqueous solution containing bacterial cells, followed by primary drying to sublimate ice and secondary drying to remove bound water by desorption. The removal of bound water may cause irreversible changes in the physical state of cell membrane lipids and the structure of sensitive proteins (Brennan et al. 1986; Castro et al. 1997).

Considering the harsh conditions to which these bacteria are subjected, their stabilization processes and subsequent storage provoke environmental stresses, leading to the loss of essential cell functionalities. Some strategies have been applied to limit cellular injuries and improve functional recovery, such as (i) controlling stabilization operating conditions (Fonseca et al. 2001a; Zayed and Roos 2004; Fonseca et al. 2006; Kurtmann et al. 2009; Aragón-Rojas et al. 2019; Verlhac et al. 2020), (ii) stressing LAB by heat, cold, and acid treatments, (iii) adding protective molecules (Fonseca et al. 2003, 2016; Carvalho et al. 2003b; Otero et al. 2007; Juárez-Tomás et al. 2009), and (iv) modulating fermentation parameters.

Modifying the fermentation conditions can induce cell-active responses to cope with the environmental stresses encountered during the stabilization processes. Table S4.1 summarizes the studies that report biological adaptation following cell growth carried out in a bioreactor for bacteria of the *Lactobacillus* genus (including *L. bulgaricus*) and other LAB. When specifically considering *L. bulgaricus*, only two studies have focused on the freezing process (Fonseca et al. 2001a; Rault et al. 2010), and four on freeze-drying (Champagne et al. 1991; Li et al. 2009a,

2012; Shao et al. 2014). Studies on storage stability in the freeze-dried state are also scarce (Zotta et al. 2013; Velly et al. 2014; Hansen et al. 2015b). Nevertheless, one can note that the fermentation conditions that induce resistant cells to stabilization processes and storage often differ from those that favor LAB growth. To optimize these conflicting criteria, a compromise must be found. Multiple objective optimization is an approach dedicated to modeling and fine-tuning the parameters in such situations (Khorram et al. 2014). Establishing Pareto fronts consists in determining the set of all efficient solutions to the problem. Our objective here is to apply this concept to optimize the fermentation parameters that produce sufficient biomass and provide sufficient resistance to stabilization processes. We selected a lactic acid bacterium: *L. bulgaricus* CFL1, that belongs to a LAB species widely used in fermented dairy products, such as the yogurt production, and represents a typical bacterium model for sensitive *L. bulgaricus* strains to freezing (Fonseca et al. 2000, 2001a; Meneghel et al. 2017). The experimental conditions were chosen in order to (i) modulate the biomass production and (ii) modulate the resistance (effect of pH, temperature, and harvest time).

Data are first analyzed through a response surface methodology to identify the effect of fermentation parameters on the functional properties of cells (acidifying activity and bacterial culturability) at different steps of the production process: fermentation, freezing, freeze-drying, and freeze-dried storage. Then, a multi-objective optimization, including bacterial cell biomass productivity and resistance to stabilization processes, is proposed in order to define the best possible compromise between a selected criterion.

4.4. Materials and methods

The experimental approach for the production and stabilization of *Lactobacillus delbrueckii* subsp. *bulgaricus* CFL1 (*L. bulgaricus* CFL1) cell concentrates as well as the main parameters investigated in this study are summarized in Figure 4.1. All measurements were performed on at least three independent bacterial cultures. The steps corresponding to Figure 4.1 are explained in the sections below.

4.4.1. Starter production and stabilization processes

4.4.1.1. Strain and inoculum preparation

L. bulgaricus CFL1 (CIRM-BIA; Rennes, France) was used in this study. Bacterial cells were stored at -80°C in Man, Rogosa and Sharpe broth (MRS, Biokar, Diagnostics, Beauvais, France), supplemented with 15% (w/w) glycerol (VWR, Leuven, Belgium). Before inoculating of the bioreactor, inocula were first precultured twice at 42°C in 60 mL of sterilized MRS medium (121°C , 20 min) without agitation. In the first preculture, 60 mL of sterilized medium was inoculated with 300 μL of stock culture and incubated for 12 hours until reaching the stationary phase, corresponding to an optical density at 600 nm ($\text{OD}_{600\text{nm}}$) of approximately 4.5. Then, 1.5 mL of the resulting first preculture was used to inoculate the second preculture in order to begin with an optical density ($\text{OD}_{600\text{nm}}$) of 0.1. This second preculture contained the same amount of medium (60 mL) and was incubated for 10 hours until reaching the stationary growth phase ($\text{OD}_{600\text{nm}} \sim 5.5$). The whole resulting second preculture was used to inoculate a 5.0 L bioreactor (Figure 4.1(A)).

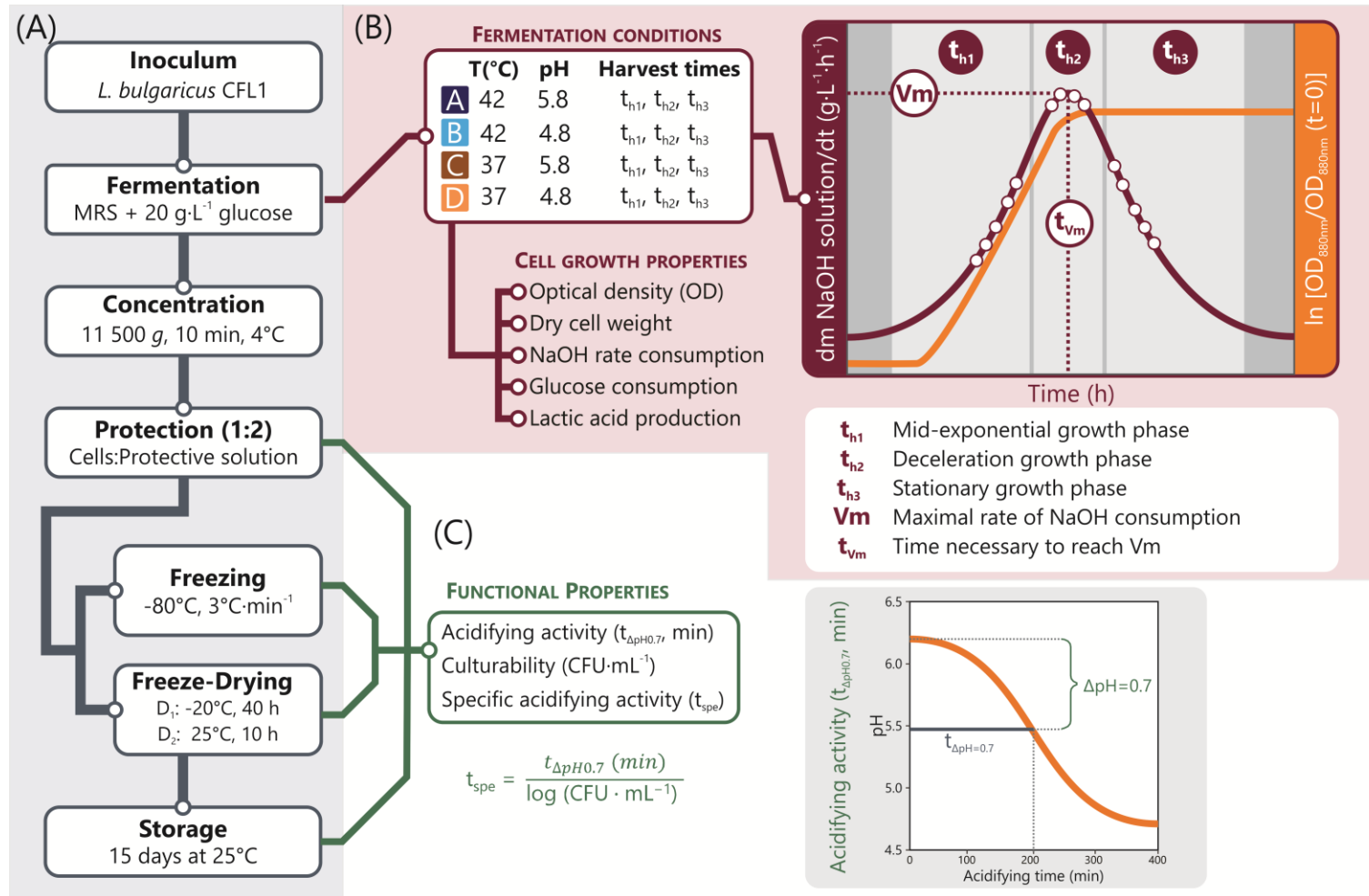


Figure 4.1 Diagram of the experimental approach applied to assess the effect of fermentation parameters (pH, temperature, and harvest time) on the loss of specific acidifying activity of *L. bulgaricus* CFL1 after freezing, freeze-drying and freeze-dried storage. (A) Starter production process; (B) Fermentation parameters: pH and temperature values, harvest times and cell growth properties measured throughout fermentation; (C) Functional properties of *L. bulgaricus* CFL1 cells measured after Concentration-Protection, Freezing, Freeze-Drying, and freeze-dried Storage. D₁, primary drying; D₂, secondary drying.

4.4.1.2. Fermentation

The culture medium was composed of MRS broth (Biokar, Diagnostics, Beauvais, France) supplemented with 20 g·L⁻¹ D-glucose (VWR, Leuven, Belgium). The culture medium was supplemented to avoid starvation stress caused by the depletion of the carbon sourced after reaching the stationary growth phase. After filtering through a 0.22-µm polyethersulfone filter (Stericap PLUS, Millipore Express[®], Merck KGaA, Darmstadt, Germany), four liters of medium were introduced into a 4.0 L working volume bioreactor (Sartorius, Biostat[®] A plus, Melsungen, Germany). The inoculation was performed at an initial optical density of 0.1 (OD_{600nm}), corresponding to a concentration of approximately 4 × 10⁴ CFU mL⁻¹. Stirring was set at 100 rpm to ensure homogenization.

To create a reasonable range of moderately stressful conditions that would induce changes in the functional properties while still permitting adequate cell growth. The temperature and pH were set at different values according to the experimental design (Figure 4.1 (B)). These levels of the fermentation parameters were chosen according to previous studies using *L. bulgaricus* CFL1 (Streit et al. 2007; Rault et al. 2010) and different *L. bulgaricus* strains. For example, the temperature was fixed at either 37°C or 42°C, and the pH was set at either 4.8 or 5.8. The optimal conditions to enhance growth were reported at 40°C, pH 5.2 to 6.0 for different *L. bulgaricus* strains (Béal et al. 1989; Grobbsen et al. 1995; Burgos-Rubio et al. 2000; Abbasalizadeh et al. 2015; Aghababaie et al. 2015). Therefore, the values of temperature and pH in this study were below to the optimal growth conditions reported for *L. bulgaricus*.

The pH and temperature were adjusted before inoculation and controlled throughout the fermentation. The pH was controlled by the automatic addition of 4.25 mol·L⁻¹ NaOH solution (VWR, Leuven, Belgium) to the bioreactor. The addition of NaOH solution was monitored throughout fermentation using SartoriusBioPAT software (SARTORIUS[®], Göttingen, Germany), allowing the calculation of the consumption rate (dm_{NaOH}/dt , in g·L⁻¹ of culture medium h⁻¹). The time, after inoculation, (t_{vm} , in h) necessary to reach the maximal rate of NaOH consumption (V_m , in g·L⁻¹·h⁻¹), corresponding to the maximal acidification rate, was considered as the reference time (0 h) for quantitatively defining the harvest times (t_{hi}) and identifying the different bacterial growth phases (Figure 4.1(B)).

For each couple of fermentation temperatures and pH, cell samples were taken from the bioreactor at three ranges of harvest times, corresponding to three growth phases:

t_{h1} , the mid-exponential growth phase (-10 to -1.0 h from t_{vm})

t_{h2} , the deceleration growth phase (-1.0 to +2.0 h from t_{vm})

t_{h3} , the stationary growth phase (+2.0 to +10 h from t_{vm})

4.4.1.3. Concentration, protection, and freezing

Harvested cells were concentrated by centrifugation (Avanti® J-E centrifuge; Beckman Coulter, Fullerton, CA, USA) at 11,500 *g* for 10 min at 4°C. The resulting cell pellets were then re-suspended in the protective solution at a ratio of 1:2 (1 g of concentrated cells for 2 g of the protective solution) before freezing and freeze-drying (Figure 4.1(A)). The protective solution was composed of 20% (w/w) sucrose (VWR, Leuven, Belgium) and was previously sterilized at 121°C for 20 min. One milliliter of the protected cell suspensions was distributed in cryo-tubes (Sarstedt, Nümbrecht, Germany) for freezing experiments and in five-milliliter vials (Verretubex, Nogent-Le-Roi, France) for freeze-drying trials. All samples were frozen at -80°C (freezing rate = 3°C·min⁻¹).

4.4.1.4. Freeze-drying and freeze-dried storage

Five-milliliter vials containing one milliliter of frozen samples (-80°C, 3°C·min⁻¹) were transferred to a pre-cooled shelf at -50°C in a REVO pilot-scale freeze-dryer (Millrock Technology, Kingston, NY, USA). After a holding step of 1.5 h at -50°C, the chamber pressure was decreased to 10 Pa, and the shelf temperature was increased from -50°C to -20°C at a heating rate of 0.25°C min⁻¹ to initiate sublimation. The end of ice sublimation (ensuring the absence of remaining ice inside the product) was assessed by comparative pressure measurement (Pirani gauge vs. capacitance manometer) (Passot et al. 2009). After 40 h of sublimation (primary drying), the shelf temperature was increased to 25°C at a heating rate of 0.25°C·min⁻¹. After 10 h of desorption (secondary drying step), the vacuum was broken by injecting air into the drying chamber. The vials were then taken out of the freeze-dryer, manually capped by inserting a rubber stopper and packed in multi-layer aluminum bags. The bags were hermetically closed using a vacuum sealer (Bernhardt, Wimille, France). For freeze-dried samples, bags were stored at -80°C for less than one week until the functional properties and residual water content were measured. For freeze-dried storage samples, bags were immediately stored at 25°C for 15 days.

4.4.2. Cell growth and metabolite production during fermentation

4.4.2.1. Cell growth kinetics and biomass productivity measurements

Cell growth was monitored by an infrared probe (Excell 210, CellID, Roquemaure, France) inserted into the bioreactor that continuously measured absorbance at 880 nm (data acquisition every 5 minutes) (Figure S4.1(A)). The specific growth rate (μ , in h⁻¹) and lag growth phase duration (*lag* in h) were calculated according to the modified Gompertz equation (Zwietering et al. 1990), (Equation 4.1):

$$y = \ln \left(\frac{OD}{OD_{at\ inoculation}} \right) = A \exp \left\{ -\exp \left[\frac{\mu \cdot \exp(1)}{A} (lag - t) + 1 \right] \right\} \quad (4.1)$$

where OD is the absorbance value at 880 or 600 nm, A is the asymptote value of the growth curve (absorbance value), μ is the specific growth rate in h^{-1} , and t and lag are the time and the lag growth phase duration, respectively, in hours.

A correlation was established between the absorbance measurement at 880 and 600 nm (Figure S4.1 (C)). The absorbance values measured at 880 nm were thus converted to absorbance values at 600 nm (Figure S4.1(D)), and the kinetic parameters at 880 and 600 nm were calculated using the Equation 4.1.

The dry cell weight in the bioreactor (DCW, in $\text{g}\cdot\text{L}^{-1}$) was determined by filtering 10 mL of culture sample through 0.20- μm hydrophilic polyethersulfone (PES). The filters (Supor[®], PALL Biotech, Saint-Germain-en-Laye, France) were previously dried at 80°C for 24 h. Then, filters containing biomass samples were dried under the same conditions (80°C, 24 h). The measurements were carried out in triplicate after inoculation of the bioreactor ($t = 0$) and at each harvest time.

Biomass productivity (P in $\text{g}\cdot\text{L}^{-1}\text{h}^{-1}$) was calculated using the following equation:

$$P = \frac{\text{DCW (at } t = t_{hi}) - \text{DCW (at } t = 0_{\text{after inoculation}})}{t_{hi}} \quad (4.2)$$

Where t_{hi} corresponds to each harvest time.

4.4.2.2. Substrate and metabolite analysis

For each harvested sample, glucose and lactic acid concentrations were quantified in duplicate using high-performance liquid chromatography (HPLC) (Waters Associates, Millipore; Molsheim, France), coupled with a Refractive Index detector (Waters, Milford, MA, USA). Before HPLC analysis, each sample was centrifuged at 16,000 g for 10 min at 4°C, and the supernatant was filtered through a 0.20 μm polytetrafluoroethylene (PTFE) filter (CHROMAFIL[®] Xtra PA, Düren, Germany). Analyses were made using a cation exchange column (Aminex Ion Exclusion HPX-87 300 X 7.8 mm; Biorad, Richmond, VA, USA) at 35°C. The mobile phase was 0.005 $\text{mol}\cdot\text{L}^{-1}$ H_2SO_4 and the flow rate was set at 0.6 $\text{mL}\cdot\text{min}^{-1}$ (LC-6A pump; Shimadzu, Courtaboeuf, France).

4.4.3. Functional properties of starters

The functional properties considered for this study were the acidifying activity and culturability of *L. bulgaricus* CFL1 cells. These properties were measured at different process steps: after cells were concentrated and protected (initial), after freezing, freeze-drying (stabilization process), and after 15 days of freeze-dried storage at 25°C. (Figure 4.1 (C)).

Frozen cell samples were thawed at 42°C for 5 min in a water bath before measuring the acidifying activity and culturability. Freeze-dried samples were first rehydrated in 1 mL of skim milk solution (100 $\text{g}\cdot\text{L}^{-1}$, EPI-Ingredient, Ancenis, France) at 42°C, previously heat-treated at 110°C for 20 min, and stirred for 5 min at room temperature.

4.4.3.1. Acidifying activity

The Cinac system (AMS Alliance, Frépillon, France) was used to evaluate the acidifying activity of the bacterial suspensions. The acidifying activity was measured in triplicate at 42°C in 100 g·L⁻¹ skim milk solution (EPI-Ingredient, Ancenis, France). Reconstituted skim milk solution was heat-treated at 110°C for 20 min in 150-mL flasks containing 100 mL filled volume. Each flask was inoculated with 100 µL of the bacterial suspension. The pH was continuously measured by the Cinac system and used to determine the time necessary to obtain a decrease of 0.7 pH units ($t_{\Delta\text{pH}0.7}$, in min). The descriptor, $t_{\Delta\text{pH}0.7}$, was used to characterize the acidifying activity of bacterial suspensions. The lower the value of the $t_{\Delta\text{pH}0.7}$ descriptor was, the greater the acidifying activity was observed.

4.4.3.2. Culturability

The cell concentration of bacterial suspensions was measured using the agar plate count method. Cell suspensions were serially diluted in saline water (NaCl, 9%), then plated on MRS Agar (Biokar Diagnostics, Paris, France) and anaerobically incubated at 42°C for 48 h. The cell count was expressed in CFU·mL⁻¹. Only plates containing between 30 and 300 colonies were considered for cell concentration calculation (in CFU·mL⁻¹). The measurements of plate count were performed in triplicate.

4.4.3.3. Specific acidifying activity and loss of specific acidifying activity

The specific acidifying activity (t_{spe}), in [min (log (CFU·mL⁻¹))⁻¹], was defined as the ratio of $t_{\Delta\text{pH}0.7}$ (min) to the corresponding log of cell concentration (CFU·mL⁻¹) (Streit et al. 2007). Therefore, t_{spe} provides a meaningful measurement of the functional properties of lactic acid bacteria, including acidifying activity and culturability.

The specific acidifying activity was thus determined after fermentation, concentration, and protection of bacterial cells (initial, $t_{\text{spe I}}$), after freezing ($t_{\text{spe F}}$), after freeze-drying ($t_{\text{spe FD}}$), and after 15 days of storage at 25°C ($t_{\text{spe S}}$).

After each stabilization process and freeze-dried storage, the determination of t_{spe} loss (dt_{spe}) was calculated using the following equations (Equation 4.3-4.5):

$$dt_{\text{spe F (Freezing)}} = t_{\text{spe after Freezing}} - t_{\text{spe I (Initial specific acidifying activity)}} \quad (4.3)$$

$$dt_{\text{spe FD (Freeze-Drying)}} = t_{\text{spe after Freeze-Drying}} - t_{\text{spe I (Initial specific acidifying activity)}} \quad (4.4)$$

$$dt_{\text{spe S (freeze-dried Storage)}} = t_{\text{spe after freeze-dried Storage}} - t_{\text{spe after Freeze-Drying}} \quad (4.5)$$

4.4.4. Water content and glass transition temperature measurements

The water content of freeze-dried samples was measured by the Karl Fisher titration method using a Metrohom KF 756 apparatus (Herisau, Switzerland). At least 20 mg of powder was mixed with 2 mL of dried methanol and titrated with Riedel-de Haen reagent (Seelze, Germany) until the endpoint was reached.

Glass transition temperature (T_g) was performed as described by Velly et al. (2015). Briefly, T_g measurements were carried out using a power compensation Differential Scanning Calorimetry (DSC) (Pyris 1, PerkinElmer LLC; Norwalk, CT, USA) equipped with a mechanical cooling system (Intracooler 1P, PerkinElmer). Temperature calibration was done using cyclohexane and indium (melting points at 6.5 and 156.6°C, respectively). Approximately 15 mg of each freeze-dried sample was placed in 50 µL PerkinElmer DSC sealed aluminum pans, and an empty pan was used as a reference. Linear cooling and heating rates of 10°C·min⁻¹ were applied. The T_g of the freeze-dried samples was determined as the midpoint temperature of the heat flow step associated with glass transition with respect to the ASTM Standard Method, E1356-91. Results were obtained from at least three replicates.

4.4.5. Statistical analysis

4.4.5.1. Experimental design

A full factorial design (2 × 2 × 3) was used to investigate the effect of fermentation parameters (pH, temperature, and harvest time) on different responses: (i) biomass productivity; (ii) initial specific acidifying activity after fermentation when cells were concentrated and protected (t_{spe I}), and (iii) the loss of specific acidifying activity after freezing (dt_{spe F}), freeze-drying (dt_{spe FD}) and freeze-dried storage (dt_{spe S}).

4.4.5.2. Stepwise descending multiple regression analyses

Two independent variables were coded at a low level (-1) and a high level (+1) for pH and temperature. The harvest time was recalculated for each fermentation trial by taking the time necessary to reach the maximal rate of NaOH consumption (t_{vm} in hours) as the reference time, corresponding to 0 h on a new time scale. The range from -10 h (low level, coded as -1) to +10 h (high level, coded as +1) was considered to code this variable.

Stepwise descending multiple regression analyses were performed to quantify the effects of three independent variables (coded pH (X₁), coded temperature (X₂), and coded harvest time (X₃)) on each response variable (Productivity, t_{spe I}, dt_{spe F}, dt_{spe FD}, dt_{spe S}) using MATLAB[®] R2014b software (The MathWorks Inc, Natick, MA, USA) equipped with the Statistics Toolbox.

Measurement units are different between the three culture parameters (pH in pH units, temperature in °C, and harvest time in hours on a new time scale regarding t_{vm}). To rank the influence of the culture variables on the response variables, coded variables were used in the stepwise descending regression analyses, thus setting the coefficients to the same scale.

The applied regression model was a second-order polynomial with interactions of the following form:

$$Y = \beta_0 + \beta_1 X_1 + \beta_2 X_2 + \beta_3 X_3 + \beta_{33} X_3^2 + \beta_{12} X_1 X_2 + \beta_{13} X_1 X_3 + \beta_{23} X_2 X_3 + \beta_{123} X_1 X_2 X_3 \quad (4.6)$$

where β_0 , β_i , β_{ii} and β_{ij} are the intercept, linear, quadratic, and interaction coefficients, respectively. X_1 , X_2 and X_3 are fermentation pH, temperature and harvest time, respectively.

Stepwise descending multiple regression iteratively removed the parameters not significantly different from zero at P -value ≤ 0.05 from the model.

The adjusted coefficient of determination (Adjusted R^2) assessed the adequacy of the model. R^2 measures the percentage of total data variance explained by each model. The criterion for accepting a mathematical model was to exhibit an $R^2 \geq 70\%$, which explains 70% of the response (dependent) variable variability. Response surface plots were generated from the fitted polynomial equations (Equation 4.6) in order to visualize the relationships between the responses and independent variables.

Multiple regression analysis allowed us to obtain a linear model for predicting the specific acidifying activity (t_{spe}) after freezing and freeze-drying within the experimental domain. These models were crucial to calculate a Pareto front by a multi-objective numerical optimization technique (NSGA II, MATLAB® R2014b software). In this plot, each point corresponded to one fermentation condition and one harvest time within the experimental design (Temperature, pH, t_{hi}). These points were plotted according to biomass productivity (X-axis) and t_{spe} (Y-axis). This technique was applied to determine the set of fermentation conditions that lead to the best possible compromises between biomass production (productivity) and the minor loss of t_{spe} after the stabilization processes. In the framework of the Pareto optimization, the best possible compromise is obtained when both criteria cannot be improved simultaneously, i.e., improving one necessarily degrades the other.

4.4.5.3. Complementary statistical analysis

The one-way analysis of variance (ANOVA) and post-hoc Tukey HSD were performed using XLSTAT 2020.5 (Addinsoft, Paris, France) to evaluate the effect of each independent variable (pH, temperature and harvest time) on the growth kinetic parameters (lag growth phase duration, specific growth rate, maximal rate of NaOH consumption (V_m), time to reach V_m (t_{vm}), concentrations of lactic acid and residual glucose), as well as on the functional properties of bacterial suspensions (acidifying activity, culturability, and specific acidifying activity).

A significance level of 95% (P -value ≤ 0.05) was considered. Such complementary tests were particularly useful to analyze results when multiple regression models were not adequate to describe the effect of fermentation conditions on response variables (functional properties of bacterial suspensions).

4.5. Results

4.5.1. Fermentation kinetics and biomass productivity

Bacterial growth (optical density) and the acidification rate (NaOH consumption rate) curves of *L. bulgaricus* CFL1 are presented in the Supplementary information for the four fermentation conditions of pH and temperature (Figs. S4.1 (A) and S1 (B), respectively). The curves correspond to means and the associated Standard Deviations (SD) of at least three biological replicates per condition. Culture reproducibility was considered satisfactory since the SD/median ratio was lower than 20% for the fermentation conditions evaluated.

The four parameters describing the growth kinetics that were calculated using the curves in Figure S4.1 (A, B, D) are summarized in Table S4.2: the lag growth phase duration (lag), the specific growth rate (μ), the maximal value of the NaOH consumption rate (V_m), and the time associated with the V_m value (t_{V_m} , time necessary in hours to reach V_m). The total lactic acid (LA) production and the residual glucose concentration (glc) measured at the stationary growth phase harvest (t_{h3} , the latest harvest time) are also included in Table S4.2.

Regardless of the fermentation conditions, HPLC measurements confirmed that there was still glucose content in the fermentation medium for the latest harvest time. Therefore, there was no additional stress due to carbon source depletion.

Concerning the lag growth phase durations, the shortest ones were observed for fermentations at 42°C (pH 5.8: 0.28 h and pH 4.8: 1.31 h). The most prolonged durations were observed for fermentations at 37°C. Thus, the lag growth phase duration in the bioreactor depended on the temperature used in the precultures (42°C).

Specific growth rates (μ) and the maximal NaOH consumption rates (V_m) were about twice higher at 42°C than at 37°C. The time to reach V_m (t_{V_m}) was about 10 hours less at 42°C ($t_{V_m} = 16.5$ and 16.8 h) than the t_{V_m} values observed at 37°C ($t_{V_m} = 24.4$ and 28.8 h). This result suggests that bacterial growth and lactic acid production are enhanced at high fermentation temperatures. In contrast, when two fermentation conditions at the same temperature are compared, the pH appeared to have no significant effect on *L. bulgaricus* CFL1 for most of the kinetic growth parameters (μ , V_m , LA, gluc of Table S4.2).

The final amount of biomass is another crucial variable to be considered in LAB production. Biomass productivity (P , $\text{g}\cdot\text{L}^{-1}\cdot\text{h}^{-1}$) was thus calculated (Equation 4.2) for all the fermentation conditions studied at each harvest time. The experimental values of productivity varied between 0.15 and 0.45 $\text{g}\cdot\text{L}^{-1}\cdot\text{h}^{-1}$. A stepwise multiple regression analysis was performed to quantify the linear (X_i), interactive ($X_i \times X_j$), and quadratic (X_i^2) effects of the three independent fermentation variables (pH, temperature, and harvest time) on biomass productivity. The coefficients (β_i) of the multiple regression (Equation 4.6) and the P -value of each model variable are presented in Table 4.1. This model also explains 84% of biomass productivity variability

according to the coefficient of determination (R^2) of the multiple regression, thus satisfactorily representing this response variable. Furthermore, in Figure S4.2, the predicted values calculated by the multiple regression model vs. experimental values were plotted, showing the accuracy of the model.

Table 4.1 Multiple regression analysis of the biomass productivity (P , in $\text{g}\cdot\text{L}^{-1}\cdot\text{h}^{-1}$) of *L. bulgaricus* CFL1. Cells were harvested at increasing harvest times during fermentations carried out at different pHs and temperatures. (X_1 : fermentation pH; X_2 : fermentation temperature (T); X_3 : harvest time) (Equation 4.6).

Term	Estimated Coefficient (β_i)	95% confidence interval		P-value
		Min	Max	
Intercept	0.29 (β_0)	0.27	0.30	3.7×10^{-51}
X_1 (pH)	0.02 (β_1)	0.01	0.03	2.3×10^{-03}
X_2 (T)	0.07 (β_2)	0.06	0.08	6.1×10^{-21}
X_3^2 (harvest time ²)	-0.06 (β_3)	-0.10	-0.03	1.0×10^{-03}
$X_1 X_2$ (pH \times T)	0.01 (β_{12})	0.00	0.02	1.3×10^{-02}
Adjusted $R^2 = 84\%$ RMSE = $0.04 \text{ g}\cdot\text{L}^{-1}\cdot\text{h}^{-1}$				

R^2 : coefficient of determination; RMSE: standard deviation of the residuals. Only the independent variables with a P-value lower than 0.05 were retained by the stepwise regression analysis.

The most significant effect on the response variable (biomass productivity in Table 4.1) was found at a high absolute value of β_i coefficients: the biomass productivity (P , in $\text{g}\cdot\text{L}^{-1}\cdot\text{h}^{-1}$) was mainly influenced by the linear effect of the temperature and the quadratic effect of harvest time, followed by the pH and the interactive effect of pH and temperature.

The response surfaces generated with the biomass productivity (P) model (Figure 4.2) show the conjugated effect of temperature and harvest time on the biomass productivity at the two pHs (Figure 4.2 (A) pH 5.8) and (Figure 4.2 (B) pH 4.8). The values of the harvest times were normalized by considering the reference ($t_h = 0$ in Figure 4.2) at the moment of the maximal NaOH consumption rate (t_{vm}) (see Figure 4.1 (B)).

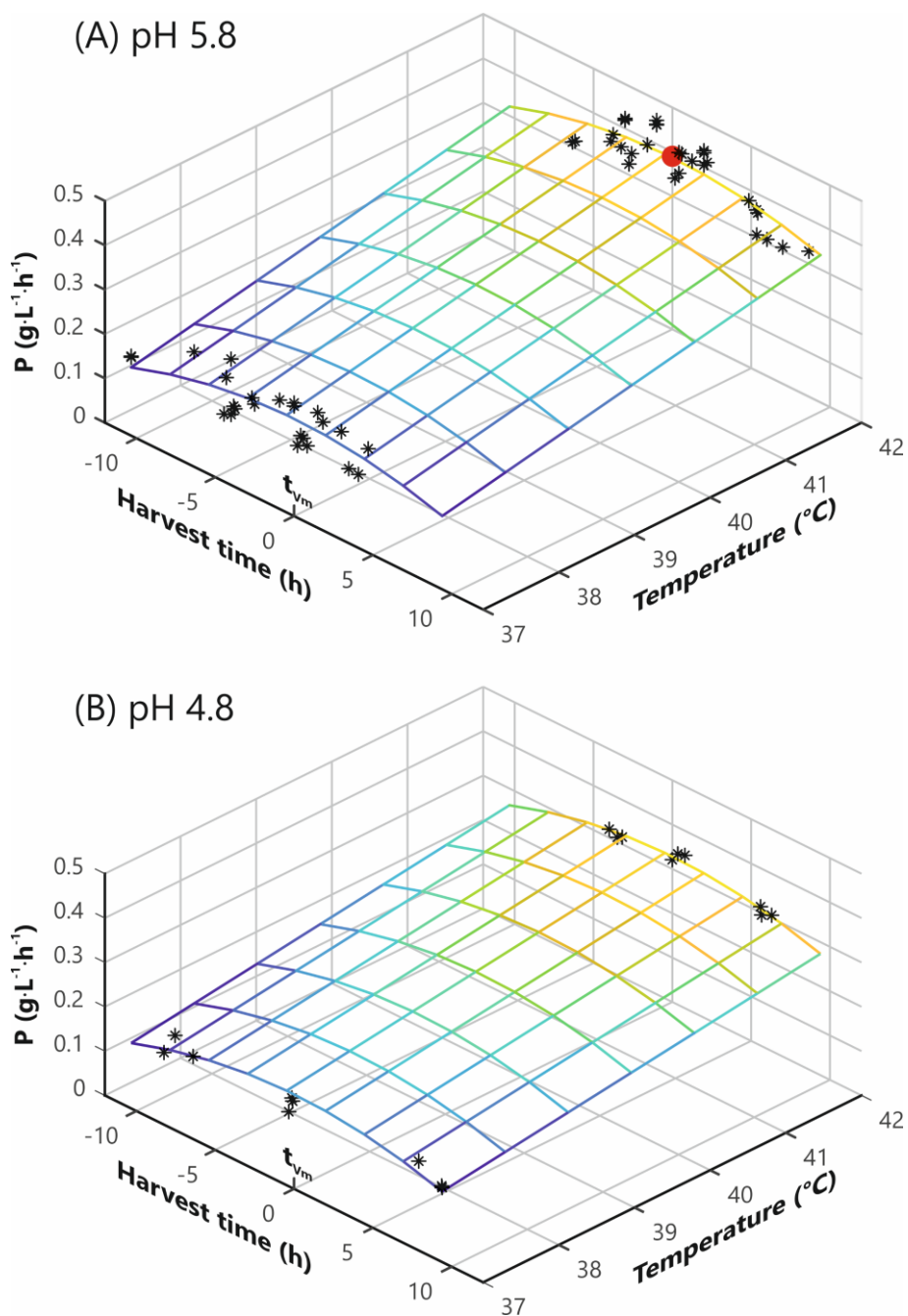


Figure 4.2 Response surface representations of the effect of fermentation harvest time and temperature on the biomass productivity (P , in $\text{g}\cdot\text{L}^{-1}\cdot\text{h}^{-1}$) of *L. bulgaricus* CFL1 produced at (A) pH 5.8 and (B) pH 4.8. Asterisks represent the experimental data points used in the model at the given pH. The red dot on the mesh of (A) pH 5.8, represents the maximal biomass productivity predicted by the biomass productivity multiple regression model. t_{vm} : the time necessary to reach the maximal rate of the NaOH consumption.

A high fermentation temperature (42°C) positively affected biomass productivity ($\beta_2 = 0.07$). Increasing the culture temperature from 37°C to 42°C resulted in an increase in productivity of approximately 70% at pH 5.8 (from 0.24 to $0.41 \text{ g}\cdot\text{L}^{-1}\cdot\text{h}^{-1}$ at pH 5.8, and from 0.20 to $0.34 \text{ g}\cdot\text{L}^{-1}\cdot\text{h}^{-1}$ at pH 4.8), for cells harvested at the deceleration growth phase (t_{h2} , -1.0 to 2.0 hours). For this same harvest time (t_{h2}), the pH effect ($\beta_1 = 0.02$) was observed when comparing two fermentation conditions at the same temperature. At 42°C , the biomass productivity was 0.07

$\text{g}\cdot\text{L}^{-1}\cdot\text{h}^{-1}$ higher at pH 5.8 than at pH 4.8 (0.34 vs. 0.41 $\text{g}\cdot\text{L}^{-1}\cdot\text{h}^{-1}$). At 37°C, the pH effect was less pronounced; an increase in biomass productivity of about 0.04 $\text{g}\cdot\text{L}^{-1}\cdot\text{h}^{-1}$ was observed at pH 5.8 compared to pH 4.8 (0.20 vs. 0.24 $\text{g}\cdot\text{L}^{-1}\cdot\text{h}^{-1}$). The fact that the pH effect was more pronounced at 42°C than at 37°C revealed the interaction between the temperature and pH ($\beta_{12} = 0.01$).

The negative quadratic effect of harvest time ($\beta_3 = -0.06$) explains the concave shapes of the response surfaces at both pH values studied (Figure 4.2). Cells harvested at the deceleration growth phase exhibited the highest productivity values regardless of pH and temperature. The multiple regression model predicted maximal biomass productivity of 0.39 $\text{g}\cdot\text{L}^{-1}\cdot\text{h}^{-1}$ at [42°C, pH 5.8], and cells harvested at 0.4 h after t_{vm} . This condition is represented by a red dot in Figure 4.2 (A).

4.5.2. Initial functional properties of *L. bulgaricus* CFL1

The acidifying activity and the number of culturable cells are the main functional and technological properties of lactic acid bacteria and were measured for all fermentation conditions examined in this study. The specific acidifying activity (t_{spe}), calculated as the ratio of the acidifying activity ($t_{\Delta\text{pH}0.7}$, in min) and the log of the concentrated-protected bacterial suspension (culturability in $\text{CFU}\cdot\text{mL}^{-1}$), made it possible to combine two experimental measurements in a single descriptor to characterize the biological activity of *L. bulgaricus* before the stabilization processes (initial, t_{spe} I) (Streit et al. 2007).

Stepwise multiple regression analysis was performed to determine the effect of the fermentation parameters (pH, temperature and harvest time) on t_{spe} I (Table S4.3) and predict t_{spe} I within the fermentation conditions studied. However, the poor coefficient of determination obtained ($R^2 = 51\%$) limited the analysis of this response variable by its corresponding multiple regression model. This low coefficient of determination value suggests that the factors considered in the model explain a small part of the experimental data variations (t_{spe} I in this case).

Therefore, boxplot representations and statistical analyses were performed. The harvest times were grouped into three categories (t_{h1} , t_{h2} , and t_{h3}). The effect of fermentation parameters on t_{spe} I (Figure S4.3), $t_{\Delta\text{pH}0.7}$, and culturability (Figure S4.4) can be observed.

For a given set of fermentation conditions (temperature and pH), the t_{spe} I values (Figure S4.3) were similar to those of the acidifying activity ($t_{\Delta\text{pH}0.7}$) (Figure S4.4 (A)). In contrast, the culturability values evolved in the opposite sense (Figure S4.4 (B)). For a given fermentation condition, an increase of the t_{spe} I and $t_{\Delta\text{pH}0.7}$ values (decrease of acidifying activity) is associated with a decrease in culturability.

The t_{spe} I values ranged between 20 and 45 [$\text{min} (\log (\text{CFU}\cdot\text{mL}^{-1}))^{-1}$] and were affected by the three fermentation parameters studied: pH, temperature, and harvest time.

The lowest $t_{\text{spe I}}$ values (21 to 25 [min (log (CFU·mL⁻¹))⁻¹]; Figure S4.3), corresponding to the highest specific acidifying activities, were observed at pH 4.8, regardless of the fermentation temperature, for cells harvested at the mid-exponential (t_{h1}) and the deceleration (t_{h2}) growth phases. Conversely, cells harvested in the stationary growth phase (t_{h3}) exhibited significantly higher $t_{\text{spe I}}$ values (P -value ≤ 0.05) when fermentation was performed at 42°C compared to cells cultivated at 37°C.

4.5.3. Effects of fermentation parameters (pH, temperature, and harvest time) on the loss of specific acidifying activity after freezing, freeze-drying, and freeze-dried storage

The specific acidifying activity of *L. bulgaricus* CFL1 was determined after freezing, freeze-drying, and two weeks of freeze-dried storage at 25°C to calculate the loss of specific acidifying activity (dt_{spe}) after each stabilization process and freeze-dried storage (Equation 4.3, 4.4, and 4.5). The lower the dt_{spe} values followed a process, the lower the biological activity degradation was and the higher the resistance of *L. bulgaricus* CFL1 to the process.

Similarly, as biomass productivity, a stepwise multiple regression analysis allowed the quantification of the linear, quadratic, and interactive effects of the three independent fermentation variables (pH, temperature, and harvest time) on the loss of specific acidifying activity after freezing ($dt_{\text{spe F}}$), freeze-drying ($dt_{\text{spe FD}}$), and freeze-dried storage ($dt_{\text{spe S}}$). We also determined the models corresponding to the loss of acidifying activity ($dt_{\Delta\text{pH}0.7}$; Table S4.4) and of log CFU·mL⁻¹ (dlog (CFU·mL⁻¹); Table S4.5).

The multiple regression models for $dt_{\text{spe F}}$ and $dt_{\text{spe FD}}$ had an acceptable value of $R^2 \geq 70\%$ (Table 4.2), indicating a fair representation of the loss of specific acidifying activity after freezing and freeze-drying within the experimental domain of this study. The accuracy of the model is shown in Figure S4.5 in the form of a plot of predicted values calculated by the multiple regression models vs. experimental values. A low value of the determination coefficient was observed ($R^2 = 49\%$; Table S4.6) for the loss of specific acidifying activity after freeze-dried storage ($dt_{\text{spe S}}$). Consequently, $dt_{\text{spe S}}$ was not adequately represented by the stepwise multiple regression analysis. Each stabilization process (freezing and freeze-drying) and freeze-dried storage is described separately in the following subsections.

Table 4.2 Multiple regression analysis of the loss of specific acidifying activity of *L. bulgaricus* CFL1 during freezing (dt_{spe} F) and freeze-drying (dt_{spe} FD). Cells were harvested at increasing harvest times during fermentations carried out at different pHs and and temperatures. (X_1 : fermentation pH; X_2 : fermentation temperature (T); X_3 : harvest time) (Equation 4.6).

dt_{spe} F					dt_{spe} FD				
Term	Estimated coefficient (β_i)	95% confidence interval		P-value	Term	Estimated coefficient (β_i)	95% confidence interval		P-value
		Min	Max				Min	Max	
Intercept	6.6 (β_0)	5.8	7.4	1.2×10^{-22}	Intercept	49.9 (β_0)	47.1	52.6	5.0×10^{-33}
X_1 (pH)	4.3 (β_1)	3.6	5.1	2.7×10^{-15}	X_1 (pH)	10.0 (β_1)	7.2	12.7	5.4×10^{-09}
$X_1 X_2$ (pH \times T)	1.4 (β_{12})	0.6	2.1	4.8×10^{-04}	X_3 (harvest time)	-17.2 (β_3)	-22.6	-11.9	8.6×10^{-08}
					$X_1 X_2$ (pH \times T)	-2.7 (β_{12})	-5.4	-0.01	4.9×10^{-02}
					$X_1 X_3$ (pH \times harvest time)	-8.0 (β_{13})	-13.3	-2.6	4.7×10^{-03}
Adjusted $R^2 = 70\%$					Adjusted $R^2 = 74\%$				
RMSE = 2.7 [$\min(\log(\text{CFU} \cdot \text{mL}^{-1}))^{-1}$]					RMSE = 8.8 [$\min(\log(\text{CFU} \cdot \text{mL}^{-1}))^{-1}$]				

R^2 : coefficient of determination; RMSE: standard deviation of the residuals. Only the independent variables with a P-value lower than 0.05 were retained by the stepwise regression analysis.

4.5.3.1. Freezing

Fermentation pH ($\beta_1 = 4.3$) and the interaction between pH and temperature ($\beta_{12} = 1.4$) had the most significant effects on the loss of specific acidifying activity after freezing (Table 4.2, dt_{spe} F), whereas the harvest time had no influence. Response surface representations for the two pH values (Figure 4.3 (A) and (B)) illustrate the pH effect. For instance, at 42°C, bacterial cells displayed lower dt_{spe} F values at pH 4.8 than at pH 5.8, regardless of the harvest time. Consequently, bacterial cells cultivated at low pHs exhibited a significant increase in freezing resistance (low dt_{spe} F values).

The interaction between pH and temperature was also significant ($\beta_{12} = 1.4$). At pH 4.8, a decrease of 46% in dt_{spe} values was observed when the temperature increased from 37°C to 42°C (from 2.6 to 1.4 [$\min(\log(\text{CFU} \cdot \text{mL}^{-1}))^{-1}$]). Conversely, at pH 5.8, increasing the temperature resulted in a two-fold increase of dt_{spe} values (from 6.8 to 14.2 [$\min(\log(\text{CFU} \cdot \text{mL}^{-1}))^{-1}$]).

The minimum loss of specific acidifying activity of 0.8 [min (log (CFU·mL⁻¹))⁻¹] after freezing was identified at [42°C, pH 4.8], regardless of harvest time, and indicated by a succession of red dots on the surface representation (Figure 4.3 (B)).

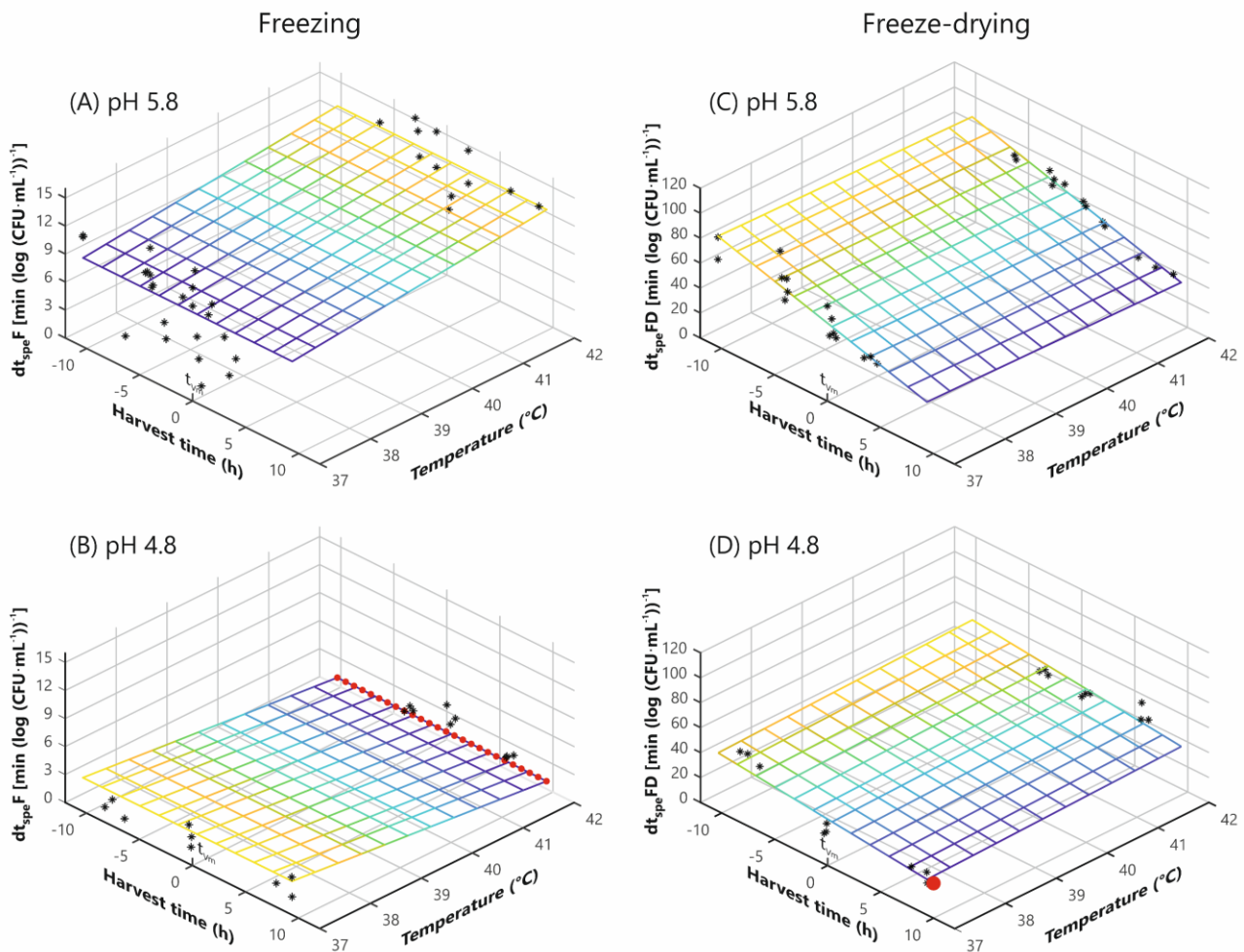


Figure 4.3 Response surface representations of the effect of fermentation harvest time and temperature on the loss of specific acidifying activity (dt_{spe} , in [min (log (CFU·mL⁻¹))⁻¹] of *L. bulgaricus* CFL1 during freezing (dt_{spe} F) at (A) pH 5.8, and (B) pH 4.8 and after freeze-drying (dt_{spe} FD) at (C) pH 5.8, and (D) pH 4.8. Asterisks represent the experimental data points used in the model at the given pH. The succession of red dots on the mesh of (B) pH 4.8 and the red dot on the mesh of (D) pH 4.8 represent the minimum loss of dt_{spe} predicted by the dt_{spe} F and the dt_{spe} FD multiple regression model, respectively. t_{vm} : the time necessary to reach the maximal rate of the NaOH consumption.

4.5.3.2. Freeze-drying

In Table 4.2, harvest time had the greatest effect on dt_{spe} FD. The negative sign of the harvest time coefficient ($\beta_3 = -17.2$) indicates that low values of dt_{spe} correspond to low specific acidifying activity losses after freeze-drying, resulting from harvest time increase. Response surface representations (Figure 4.3 (C) and (D)) permitted the visualization of the decrease of dt_{spe} FD values when cells were harvested at increasing harvest time for both pHs (5.8 and 4.8). For example, increasing the harvest time from the mid-exponential to the stationary growth

phase (from -6 h to 7 h) resulted in a decrease of dt_{spe} FD values of 39% for the fermentation conditions at [42°C, pH 5.8] (from 66 to 40 [min (log (CFU·mL⁻¹))⁻¹]).

The fermentation pH also influenced the loss of specific acidifying activity ($\beta_1 = 10.0$). Lower dt_{spe} FD values were observed at pH 4.8 than at pH 5.8. For instance, when analyzing cells cultivated at 37°C and harvested at the stationary growth phase (2 to 10 h from t_{vm}), dt_{spe} FD values were reduced (from 50 to 32 [min (log (CFU·mL⁻¹))⁻¹]) when the pH was decreased from 5.8 to 4.8. The same tendency was observed at 42°C (from 40 to 37 [min (log (CFU·mL⁻¹))⁻¹]).

The conjugated effect of pH and harvest time ($\beta_{13} = -8.0$; Figure 4.3 (C) and Figure 4.3 (D)) can be observed at 42°C. Cells grown at pH 5.8 and harvested at increased harvest time (from -10 to 10 h) led to a 39% decrease in dt_{spe} FD values (from 66 to 40 [min (log (CFU·mL⁻¹))⁻¹]) compared to 20% at pH 4.8 (from 46 to 37 [min (log (CFU·mL⁻¹))⁻¹]).

The slight interaction between pH and temperature ($\beta_{12} = -2.7$) can be visualized when cells were harvested at the stationary growth phase (+2.0 to +10 h from t_{vm}) and when the temperature increased from 37°C to 42°C. At pH 4.8, dt_{spe} FD values increased by 16% (from 32 to 37 [min (log (CFU·mL⁻¹))⁻¹]), whereas at pH 5.8, dt_{spe} FD values decreased by 20% (from 50 to 40 [min (log (CFU·mL⁻¹))⁻¹]).

The minimum loss of specific acidifying activity during freeze-drying was observed at 37°C, pH 4.8, and in cells harvested at the stationary growth phase (dt_{spe} FD = 29.0 [min (log (CFU·mL⁻¹))⁻¹], red dot on the surface representation in Figure 4.3 (D)).

Regardless of the fermentation conditions applied, the residual water content of the freeze-dried samples was lower than 3%. The glass transition temperature of the freeze-dried samples was about 50.4°C, a higher temperature than the one used for storing the samples.

4.5.3.3. Freeze-dried storage

Due to the low R^2 value for the multiple regression analysis of $dt_{spe}S$, the effects of fermentation parameters (pH, temperature, and harvest time) on $dt_{spe}S$ were solely visualized on boxplots in Figure S4.6. Two levels of $dt_{spe}S$ values were observed. A low level that includes the fermentation conditions carried out at 37°C (except for t_{h3}), where the smallest $dt_{spe}S$ values (the highest resistance to freeze-dried storage) were exhibited when cells were cultivated at [42°C, pH 4.8]. In contrast, the high level of $dt_{spe}S$ values was mainly obtained for the fermentation condition at 42°C, pH 5.8. without significant effect on the harvest time.

4.5.4. Predictive accuracy of the multiple regression models

The relevance and the predictive capacity of the models of biomass productivity (P), loss of specific acidifying activity during freezing ($dt_{spe}F$), and freeze-drying ($dt_{spe}FD$) were validated by carrying out two independent biological replicates at fermentation conditions located at the center of the experimental range: 39°C and pH 5.3. Cells were harvested at different harvest times: the deceleration growth phase ($t_{h2} = 0.6$ h and 1.0 h) and the stationary growth phase

($t_{h3} = 4.9$ and 5.2 h). The experimental results were compared with the values predicted by the multiple regression models for P , $dt_{spe} F$, and $dt_{spe} FD$ (Table S4.7).

Most of the measured values (nine out of 12) were in good agreement with the predicted ones, within less than one residual standard deviation for the corresponding model. Concerning biological replicate number two, the experimental productivity values at t_{h3} and $dt_{spe} F$ at t_{h2} and t_{h3} were higher than the predicted values. However, all measurements fell within two residual standard deviations of the predicted values, which roughly correspond to the 95% confidence interval. Model predictions were thus validated within the expected accuracy range.

4.5.5. Multi-objective optimization, Pareto front approach, to produce frozen and freeze-dried *L. bulgaricus* CFL1 cells

A Pareto front was constructed to optimize the production of frozen and freeze-dried *L. bulgaricus* cells (Figure 4.4). Pareto fronts are helpful tools for solving a multi-objective optimization problem. This tool searches for the best compromise solution, minimizing or maximizing responses. In this study, we considered as responses variables the biomass productivity (P , in $g \cdot L^{-1} \cdot h^{-1}$) and the functional properties of cells (acidifying activity and the number of culturable cells) after freezing and freeze-drying. The functional properties were expressed by the descriptor t_{spe} , i.e., the specific acidifying activity (t_{spe} , in $[\min(\log(CFU \cdot mL^{-1}))^{-1}]$).

By using multiple regression models, the biomass productivity, the initial t_{spe} ($t_{spe} I$), the t_{spe} after freezing ($t_{spe} F$), freeze-drying ($t_{spe} FD$), and freeze-dried storage ($t_{spe} S$) were calculated for the range of the studied fermentation parameters. According to the coefficient of determination (R^2), the multiple regression models explained only 51% of $t_{spe} I$ (Table S4.3) and 57% of $t_{spe} S$ (Table S4.8). In contrast, $t_{spe} F$ and $t_{spe} FD$ presented an $R^2 \geq 70\%$ (Table S4.8). For this reason, further analysis only deals with freezing and freeze-drying.

Two Pareto fronts are displayed in Figure 4.4 (blue symbols for $t_{spe} F$ and red ones for $t_{spe} FD$). Both resulted from a numerical optimization by considering different pH, temperature, and harvest time combinations within the experimental domain of this study. Note that increasing biomass productivity decreased specific acidifying activity (increasing $t_{spe} F$ and $t_{spe} FD$ values) and vice versa. In Figure 4.4, three main sections were delimited by the domain in which fair biomass productivity was observed (0.31 - $0.33 g \cdot L^{-1} \cdot h^{-1}$). The other two sections corresponded to the extreme values of the productivity range. Additionally, the $t_{spe} I$ values were also plotted to visualize the loss of specific acidifying activity after freezing ($dt_{spe} F$) and freeze-drying ($dt_{spe} FD$) (empty green circle in Figure 4.4).

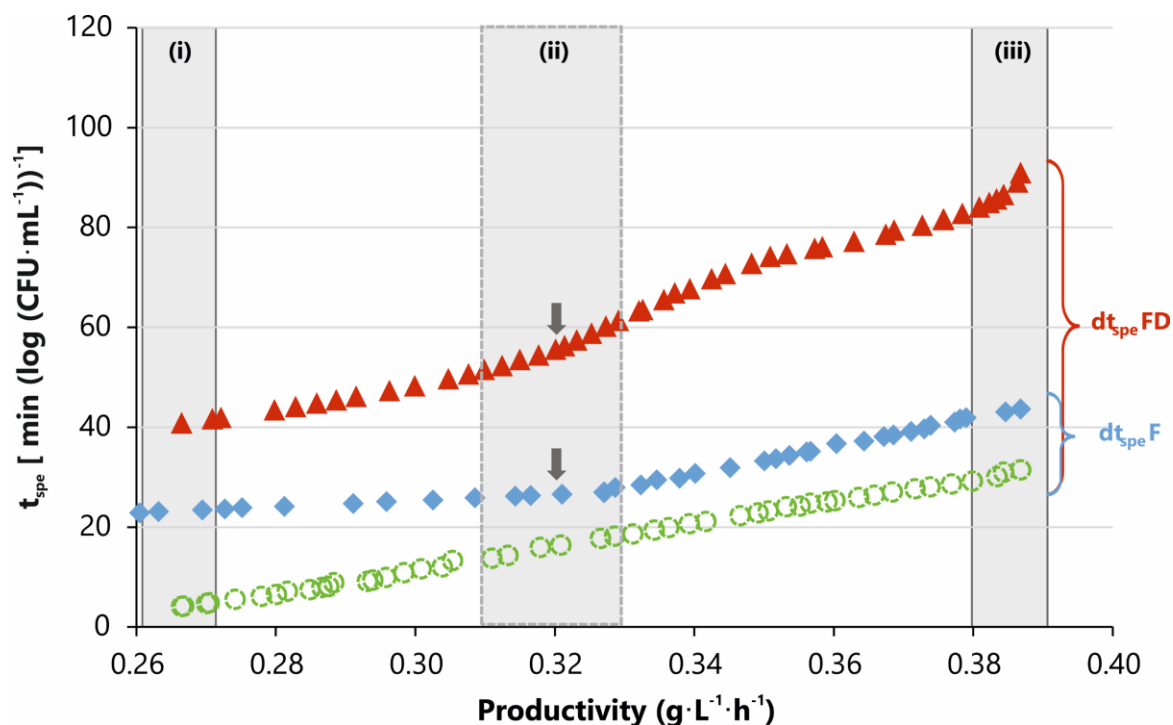


Figure 4.4 Pareto multi-objective optimization by maximizing the biomass productivity (high values of productivity, axis x) and minimizing the t_{spe} values were obtained after freezing or freeze-drying (axis y, corresponding to maximizing the t_{spe}) of *L. bulgaricus* CFL1. t_{spe} (specific acidifying activity) is defined as the ratio of $t_{\Delta pH 0.7}$ (min) to the corresponding log of cell concentration ($CFU \cdot mL^{-1}$); $t_{\Delta pH 0.7}$ corresponds to the time necessary to obtain a decrease of 0.7 pH units (Cinac system). The values of t_{spe} were indicated after concentration and protection (empty green circle:○); after freezing (blue diamond:◆); and after freeze-drying (red triangle:▲). Section (i) represents the minimum biomass productivity and the lowest t_{spe} values (42°C, pH 4.8, t_{h1}). Section (ii) is delimited by dotted lines, representing the compromise between the biomass productivity and t_{spe} . The fermentation condition (42°C, pH 4.8, t_{h2}) leading to this compromise is indicated by full gray arrows for curves after freezing and freeze-drying. Section (iii) represents the maximum biomass productivity and the highest t_{spe} values (42°C, pH 5.8, t_{h3}). Abbreviations: $dt_{spe} F$: loss of specific acidifying activity after freezing; and $dt_{spe} FD$: loss of specific acidifying activity after freeze-drying.

Section (i): The highest specific acidifying activity

Low t_{spe} values after freezing and freeze-drying were observed along with unfavorable biomass productivity (0.26-0.27 $g \cdot L^{-1} \cdot h^{-1}$). These data corresponded to cells cultivated at [42°C, pH 4.8], and harvested at the deceleration growth phase ($t_{h2} = -1.7$ h). *L. bulgaricus* CFL1 exhibited high specific acidifying activity (low t_{spe} values) following freezing, $t_{spe} = 24$ [$\text{min} (\log (CFU \cdot mL^{-1}))^{-1}$]. Following freeze-drying, $t_{spe} = 41$ [$\text{min} (\log (CFU \cdot mL^{-1}))^{-1}$] was observed for cells cultured at [42°C, pH 4.8], and harvested at the mid-exponential growth phase ($t_{h1} = -10$ h).

Section (ii): Balanced performance

This section represented a compromise between fair biomass productivity (0.31-0.33 $g \cdot L^{-1} \cdot h^{-1}$) and a good specific acidifying activity. In this section, a limited degradation of *L. bulgaricus* CFL1 specific acidifying activity (t_{spe}) after freezing and freeze-drying was observed. Cells cultivated at 42°C, pH 4.8, and harvested at the deceleration growth phase ($t_{h2} = -1.5$ h)

exhibited fair specific acidifying activity (relatively low t_{spe} values) following freezing ($t_{spe} = 27$ [min (log (CFU·mL⁻¹))⁻¹] and freeze-drying ($t_{spe} = 56$ [min (log (CFU·mL⁻¹))⁻¹]). Both results correspond to the reasonable productivity of 0.32 g·L⁻¹·h⁻¹ (full gray arrows in Figure 4.4).

Section (iii) The highest biomass productivity

Biomass productivity values between 0.38-0.39 g·L⁻¹·h⁻¹ were reached, sacrificing the specific acidifying activity after freezing ($t_{spe} = 44$ [min (log (CFU·mL⁻¹))⁻¹]) and freeze-drying ($t_{spe} = 91$ [min (log (CFU·mL⁻¹))⁻¹]). For the highest biomass productivity, cells grown at [42°C, pH 5.8], and harvested at the stationary growth phase ($t_{h3} = 7.0$ h) represented this case.

4.6. Discussion

We performed a complete study to identify the most influential fermentation parameters affecting the functional properties at each process stage of *L. bulgaricus* CFL1. In a second step, using multiple regression analysis, we modeled the bacteria biomass productivity and the loss of their main functional properties (i.e., acidifying activity and culturability) after freezing and freeze-drying.

After freezing and freeze-drying, the functional properties of LAB get affected. Our results showed that *L. bulgaricus* CFL1 cells exhibited losses of their functional properties (dt_{spe}). Lower losses were observed after freezing than freeze-drying (1-14 [$\text{min} \cdot (\log(\text{CFU mL}^{-1}))^{-1}$]) vs. (29-77 [$\text{min} \cdot (\log(\text{CFU mL}^{-1}))^{-1}$]). During freezing (at a low cooling rate), the extracellular ice forms and grows, leading to the cryo-concentration of the extracellular medium without intracellular ice formation (Fonseca et al. 2006). The cryo-concentration of the extracellular medium induces water efflux from the intracellular compartment, which, in turn, results in cell dehydration and cell volume reduction. Additionally, the mechanical constraints applied to the bacterial membrane following cell contraction lead to membrane leakage and loss of membrane integrity (Gautier et al. 2013).

Following freeze-drying, the bacterial cells are exposed to the osmotic stress provoked by the previous freezing step and additional mechanical stress due to removing the unfrozen water during the desorption step. Hydrogen bonds between water and cellular constituents such as membrane phospholipids and membrane proteins are broken, thus destabilizing bacterial cell membranes (Brennan et al. 1986; Lievens et al. 1994; Castro et al. 1997; Hlaing et al. 2017).

Multiple regression analysis helped us understand the main and the interaction effects of fermentation parameters (pH \times temperature and/or pH \times harvest time) on the resistance of *L. bulgaricus* CFL1. This combined effect is the result of studying three parameters simultaneously, which has been scarcely investigated for optimizing frozen or freeze-dried LAB (Table S4.1).

Our results showed that the pH was the most influential fermentation parameter on dt_{spe} for both stabilization processes. Notably, the low pH (pH 4.8) minimized the loss of specific acidifying activity during freezing and freeze-drying. Similar results were previously reported for *L. bulgaricus*. When *L. bulgaricus* cells were cultivated at low pH, bacteria improved their resistance to freezing (Rault et al. 2010) and freeze-drying (Shao et al. 2014).

For the freeze-drying process, the harvest time was another parameter that exclusively influenced the loss of the specific acidifying activity of *L. bulgaricus* CFL1. Low dt_{spe} FD values (high resistance to freeze-drying) were observed when the harvest time was increased. To our knowledge, no study had reported the effect of harvest time on the freeze-drying resistance of *L. bulgaricus*. However, some studies confirmed our results for other LAB cells. The increase

in harvest time improved freeze-drying resistance (Palmfeldt and Hahn-Hägerdal 2000; Schwab et al. 2007; Li et al. 2009b; Velly et al. 2015).

In this study, we showed that depending on the stabilization strategy, the fermentation parameters that affected the resistance were different: pH for freezing and pH and harvest time for freeze-drying.

Concerning the resistance to dried storage, the loss of specific acidifying activity of *L. bulgaricus* CFL1 following dried storage at 25°C (dt_{spe} S) appeared to be weakly influenced by the fermentation conditions applied in this study. Therefore, other factors during the storage step may have a more substantial effect than the fermentation conditions. For instance, several degradation reactions may occur during storage, either controlled by diffusion, such as the Maillard reaction or not controlled by diffusion, such as oxidation (Buera and Karel 1995; Lievonen et al. 1998; Kurtmann et al. 2009).

The water content and Tg of our freeze-dried samples confirmed that they were kept in a glassy state throughout storage. Consequently, the molecular mobility and the diffusion-controlled degradation reactions were limited by embedding bacteria in a solid glassy matrix (Higl et al. 2007; Passot et al. 2012). Thus, degradation reactions controlled by diffusion were not responsible for the dt_{spe} S observed in this study. The loss of acidifying activity of *L. bulgaricus* CFL1 after storage (dt_{spe} S) at 25°C could be attributed to oxidation reactions (Teixeira et al. 1996; Kurtmann et al. 2009; Ying et al. 2011) since no antioxidants were included in the protective solution.

L. bulgaricus CFL1 strain exhibited the highest losses after freezing and freeze-drying when cells were cultivated at the fermentation condition, which enhanced high growth rate values, substrate consumption, and biomass concentration (42°C, pH 5.8). Some studies agreed with our findings: different LAB species growing under their optimal fermentation condition led to higher loss of their functional properties (or less survival) after the following stabilization processes (Palmfeldt and Hahn-Hägerdal 2000; Li et al. 2009a; Li et al. 2012; Shao et al. 2014; Liu et al. 2014). This can be understood by the fact that when bacteria are grown at their optimal fermentation condition, their enzymes function at their maximal activity, thus enhancing their metabolism and growth (Sharma et al. 2020).

Industrial production of lactic acid bacteria requires the maximization of the quantity of biomass and the preservation of their functional properties after the stabilization processes (freezing or freeze-drying) and the subsequent storage. Aside from determining the effect of fermentation parameters on each stage of the production of lactic acid bacteria, we proposed a universal approach consisting of a Pareto front as a complementary tool to the 3D response surfaces for optimizing frozen and freeze-dried starter culture production. This tool made it possible to select the suitable fermentation condition: 42°C, pH 4.8, t_{h2} , which allows a balanced performance between both criteria, fair biomass production and reasonable specific acidifying

activity (t_{spe}) after freezing and freeze-drying. Providing a set of data is available, this methodology can be applied to any bacteria to determine the best fermentation condition tested.

In conclusion, the approaches used in this study, multi-regression analysis and Pareto front, are a breakthrough in determining the best solution to stabilize other lactic acid bacteria for two reasons. First, the multi-regression analysis allowed us to determine multivariate parameters' single and combined effects and provide models to predict different response variables. Second, the Pareto Front examined the essential criteria for LAB concentrate production, such as biomass productivity and the functional properties of bacteria that need to be preserved after the most common stabilization processes. Optimizing the fermentation conditions could help produce LAB at lower costs and time.

We speculate from the present results that *L. bulgaricus* CFL1 could have developed adaptive mechanisms to promote active biological responses under conditions other than optimal for growth (e.g., membrane lipids modification, expression of stress proteins, and changes in the morphology). These biological responses help LAB resist stressful environments induced during freezing or freeze-drying (Papadimitriou et al. 2016; Fonseca et al. 2019; Gao et al. 2021). Therefore, further work is needed to understand the cellular mechanisms responsible for improving bacterial resistance to the stabilization processes. For instance, an integrative approach can be used, which combines a lipid membrane composition (lipid classes and fatty acids) and membrane fluidity.

Acknowledgments

This work received funding from the European Union's Horizon 2020 research and innovation program under grant agreement No. 777657. The authors thank Jérôme Delettre for his technical support and Dr. Marie-Noëlle Leclercq-Perlat for the HPLC analyses.

Conflict of interest

No conflict of interest declared.

Authors contributions

Conceptualization and investigation, MLTC, SP, FF; experiments, MLTC; formal analysis SP, FF, ICT, MLTC; data curation and statistical treatment, ICT, MLTC, FF; writing, review and editing MLTC, FF, SP, ICT, MHR, YG; supervision, FF, SP, MHR, YG; funding acquisition SP and FF. All authors provided critical feedback.

Data availability

The datasets generated and/or analyzed during the current study are available in the Data INRAE repository at <https://doi.org/10.15454/FZHIE0>.

4.7. Supplementary Information

4.7.1. Supplementary Tables

Table S4.1 Studies on the influence of fermentation conditions on the freezing, freeze-drying and storage resistance of lactic acid bacteria (LAB) in the case of experiments carried out in a bioreactor.

	Strains	Studied fermentation conditions	Optimal growth conditions	Stabilization process: protective media	Optimal fermentation conditions for stabilization resistance	Reference
<i>L. bulgaricus</i> strains	<i>Lactobacillus delbrueckii</i> subsp. <i>bulgaricus</i> CFL1	Harvest time (end EP or SP)	42°C, pH 5.5	F and FS (2 months at -20°C): glycerol	42°C, pH 5.5 No effect of harvest time	(Fonseca et al. 2001a)
	<i>Lactobacillus delbrueckii</i> subsp. <i>bulgaricus</i> CFL1	pH (5.0, 6.0, or uncontrolled) Harvest time (EP, end EP, SP, or late SP)	42°C, pH 5.0, SP	F and FS (5 months at -20°C): culture supernatant	pH 5.0, SP and late SP	(Rault et al. 2010)
	<i>Lactobacillus delbrueckii</i> subsp. <i>bulgaricus</i> Y-12	Culture medium (Skim milk medium or whey-based medium, with or without papain treatment)	44°C, pH 5.7, skim milk	FD : skim milk, sucrose, casein, ascorbic acid mix	No effect of culture medium	(Champagne et al. 1991)
	<i>Lactobacillus bulgaricus</i> L2	Temperature (30°C, 35°C, 37°C, or 39°C) pH (5.0, 5.5, 6.0, or 6.5)	39°C, pH 5.0 or 5.5	FD : skim milk, sucrose and glycerol mix	30°C, pH 5.0	(Li et al. 2009a)
	<i>Lactobacillus bulgaricus</i> L2	Culture medium (MRS supplemented with 1 g l ⁻¹ of Tween 20, 40, 60, 80, peanut oil, olive oil or soybean oil and MRS supplemented with 20 g l ⁻¹ of glucose, lactose, fructose, mannitol, sucrose, maltose, trehalose, dextrin or glycerol)	39°C, pH 5.5, MRS supplemented with Tween 80 or glucose	FD : skim milk, sucrose, glycerol mix	MRS supplemented with soybean oil and MRS supplemented with sucrose	(Li et al. 2012)
	<i>Lactobacillus delbrueckii</i> subsp. <i>bulgaricus</i> ND02	Initial pH adjusted at pH 6.5, then pH (5.1 or 5.7) at 0% yeast extract MRS Culture medium (MRS supplemented with 0%, 2% or 4% yeast extract) at pH 5.7	37°C, pH 5.7, MRS supplemented with 4%	FD : skim milk and sodium glutamate mix	pH 5.1 and 0% yeast extract in MRS	(Shao et al. 2014)
<i>Lactobacillus</i> species strains other than <i>L. bulgaricus</i>	<i>Lactobacillus acidophilus</i> ATCC 4356	Temperature (37°C for 9 h, then 22°C for 6 h) at pH 6.5 pH (6.5 or uncontrolled) at 37°C	NR	F : no protective medium	37°C for 9 h, then 22°C for 6 h at pH 6.5	(Bâati et al. 2000)
	<i>Lactobacillus acidophilus</i> CRL 640	Temperature (25°C, 30°C, 37°C, or 40°C)	NR	F : distilled water	25°C	(Fernández Murga et al. 2000)
	<i>Lactobacillus acidophilus</i> CRL 639	pH (6.0 or uncontrolled)	37°C, Uncontrolled pH	F : MRS broth at pH 3.0 FD : NaCl solution	Uncontrolled pH	(Lorca and Font de Valdez 2001)
	<i>Lactobacillus acidophilus</i> RD758	Temperature (30°C, 37°C, or 42°C) at pH 6.0 pH (4.5, 5.0, or 6.0) at 37°C and 30°C, pH 5.0	37°C, pH 6.0	F and FS (3 months at -20°C): culture supernatant	30°C, pH 6.0 or 5.0, 37°C, pH 5.0	(Wang et al. 2005a)
	<i>Lactobacillus delbrueckii</i> subsp. <i>lactis</i> FAM 10991	pH (5.0, 5.5, 6.0, or uncontrolled) Harvest time (beginning of SP, SP, or end of SP)	37°C, pH 5.5, NR harvest time	FD : dextran and glycerol mix	pH 5.0 and uncontrolled pH, No effect of harvest time	(Koch et al. 2008)
	<i>Lactobacillus acidophilus</i> La-5	Culture medium (MRS medium or MRS supplemented with Tween 20, linoleic acid or α -linolenic acid)	NR	FDS (1, 2, 3, 6, 10 and 15 weeks, 30°C, 0% O ₂ or 21% O ₂): sucrose	MRS medium for storage 1, 2, 3, 6, 10 and 15 weeks, 30°C, 0% O ₂	(Hansen et al. 2015b)

EP: the exponential growth phase; SP: the stationary growth phase; F: freezing; FS: frozen storage; FD: freeze-drying; FDS: freeze-dried storage; NR: not reported. The new classification of LAB has been used for updating the name of the bacteria (Zheng et al. 2020).

Table S4.1 (Continued) Studies on the influence of fermentation conditions on the freezing, freeze-drying and storage resistance of lactic acid bacteria (LAB) in the case of experiments carried out in a bioreactor.

Strains	Studied fermentation conditions	Optimal growth conditions	Stabilization process: protective media	Optimal fermentation conditions for stabilization resistance	Reference
<i>Limosilactobacillus reuteri</i> ATCC 55730	pH (5.0 or 6.0) Harvest time (approximately 0 h, 2 h or 4 h of SP)	pH 6.0, all harvest times	FD: skim milk	pH 5.0, 2h of SP	(Palmfeldt and Hahn-Hägerdal 2000)
<i>Streptococcus thermophilus</i> CFS2	Culture medium (Mild-whey medium or mild whey medium supplemented with oleic acid) pH (5.5, 5.6 or 6.5)	NR	F and FS (2 months, -20°C): glycerol	Mild whey medium supplemented with oleic acid and pH 5.5	(Beal et al. 2001)
<i>Loigolactobacillus coryniformis</i> Si3	First 12 h of culture at 34°C, pH5.5 and then for 6h: Temperature (26°C, 34°C, or 42°C) at pH 5.5 pH (6.5 or 4.5) at 34°C and 30°C, pH 4.5	34°C, pH 5.5	FD: skim milk and sucrose mix	42°C, pH 5.5 and 34°C, pH 5.5	(Schoug et al. 2008)
<i>Lactiplantibacillus plantarum</i> C17	Temperature (25° or 35°C) Harvest time (EP or SP)	35°C, SP	FS and FDS (3 months at -20°C): skim milk, ascorbic acid and glycerol mix	35°C, SP, for storage 3 months at -20°C	(Zotta et al. 2013)
<i>Limosilactobacillus reuteri</i> I5007	First 10 h of culture at 37°C, pH5.7 and then for 6 h: Temperature (4°C, 27°C, or 47°C) at pH 5.7 pH (4.7, 5.7 or 6.7) at 37°C	37°C, pH 5.7	FD: soybean protein isolate, trehalose, and sorbitol mix	37°C, pH 6.7	(Liu et al. 2014)
<i>Lactococcus lactis</i> subsp. <i>lactis</i> TOMSC161	Temperature (22°C, 30°C or 38°C) pH (5.6, 6.2 or 6.8) Harvest time (0 h, 3 h or 6 h of SP)	30°C, pH 6.2, 0h of SP	FD and FDS (1 and 3 months at 4°C or 25°C): sucrose and maltodextrin mix	FD: 32°C, pH 6.2, and 6 h of SP FDS: 1 and 3 months at 4°C	(Velly et al. 2014)
<i>Lentilactobacillus buchneri</i> R1102	Harvest time (EP or SP)	NR	F: no protective medium	EP for acidifying activity	(Louesdon et al. 2015)
<i>Limosilactobacillus reuteri</i> DSM 17938	Temperature (32°C or 37°C) The starting pH was 6.5, and then pH control was kept: pH (4.5, 5.5 or 6.5)	37°C, pH 5.5 or 6.5	FD: sucrose	No effect of temperature pH 6.5	(Hernández et al. 2019)

LAB other than *Lactobacillus*

EP: the exponential growth phase; SP: the stationary growth phase; F: freezing; FS: frozen storage; FD: freeze-drying; FDS: freeze-dried storage; NR: not reported. The new classification of LAB has been used for updating the name of the bacteria (Zheng et al. 2020).

Table S4.2 Kinetic parameters characterizing *L. bulgaricus* CFL1 growth and acidifying activity, for fermentations carried out in MRS medium supplemented with glucose at different pH and temperatures.

Parameter	Culture conditions			
	[42°C pH 5.8]	[42°C pH 4.8]	[37°C pH 5.8]	[37°C pH 4.8]
lag (h)	0.28±0.08 ^a	1.31±0.28 ^b	1.33±0.17 ^b	1.95±0.12 ^c
	0.64±0.12 ^a	1.70±0.36 ^b	1.83±0.46 ^b	2.53±0.41 ^c
μ (h ⁻¹)	0.31±0.04 ^b	0.29±0.04 ^b	0.14±0.02 ^a	0.18±0.05 ^a
	0.37±0.04 ^b	0.35±0.08 ^b	0.16±0.01 ^a	0.21±0.06 ^a
V _m (g·L ⁻¹ ·h ⁻¹)	5.84±0.58 ^b	4.22±0.03 ^b	1.99±0.96 ^a	1.58±0.69 ^a
t _{vm} (h)	16.8±0.25 ^b	16.5±0.05 ^b	28.8±3.55 ^d	24.4±3.00 ^c
LA (g·L ⁻¹)	22.8±3.24 ^b	19.9±3.15 ^b	14.5±5.04 ^a	13.5±5.04 ^a
gluc (g·L ⁻¹)	12.8±1.98 ^a	16.4±1.29 ^{ab}	17.2±4.76 ^{ab}	19.4±6.27 ^b

lag: lag growth phase duration from the OD_{800nm} data (first row values), and from the OD_{600nm} data obtained using the correlation of Figure S4.1 (C) (second row values).

μ : specific growth rate from the OD_{800nm} data (first row values), and from the OD_{600nm} data obtained using the correlation of Figure S4.1 (C) (second row values).

V_m: the maximal rate of the NaOH consumption in g NaOH/liter of culture medium/hours.

t_{vm}: the time necessary to reach V_m.

LA: lactic acid concentration; gluc: residual glucose concentration. LA and gluc values correspond to samples harvested in the stationary growth phase.

Values are the median of at least three independent biological replicates with the corresponding inter quartile range values in parentheses. Superscript letters represent significant differences among fermentation conditions at a 95% confidence level.

Table S4.3 Multiple regression analysis of the initial specific acidifying activity ($t_{spe I}$) of *L. bulgaricus* CFL1. Cells were harvested at increasing harvest times during fermentations carried out at different pH and temperatures (X_1 : fermentation pH; X_2 : fermentation temperature (T); X_3 : harvest time) (Equation 4.6).

Term	$t_{spe I}$			
	Estimated coefficient (β_i)	95% confidence interval		P-value
		Min	Max	
Intercept	26.2 (β_0)	24.8	27.6	4.8×10^{-40}
X_1 (pH)	3.5 (β_1)	2.3	4.6	1.0×10^{-07}
X_2 (T)	1.8 (β_2)	0.8	2.8	5.3×10^{-04}
X_3 (harvest time)	4.3 (β_3)	1.9	6.6	6.7×10^{-04}
X_3^2 (harvest time ²)	6.6 (β_{33})	2.2	11.1	4.1×10^{-03}
$X_1 X_3$ (pH \times harvest time)	-3.2 (β_{13})	-5.7	-0.6	1.5×10^{-02}
$X_2 X_3$ (T \times harvest time)	2.7 (β_{23})	0.3	5.1	3.1×10^{-02}
$X_1 X_2 X_3$ (pH \times T \times harvest time)	-3.7 (β_{123})	-6.2	-1.3	3.5×10^{-03}
Adjusted $R^2 = 51\%$				
RMSE = 3.7 [min (log (CFU·mL ⁻¹)) ⁻¹]				

R^2 : coefficient of determination; RMSE: standard deviation of the residuals.

Table S4.4 Multiple regression analysis of the loss of acidifying activity ($dt_{\Delta pH0.7}$) of *L. bulgaricus* CFL1 during each stabilization process (F: freezing; FD: freeze-drying; and S: freeze-dried storage). Cells were harvested at increasing harvest times during fermentations carried out at different pHs and temperatures (X_1 : fermentation pH; X_2 : fermentation temperature (T); X_3 : harvest time) (Equation 4.6).

$dt_{\Delta pH0.7}$ F					$dt_{\Delta pH0.7}$ FD					$dt_{\Delta pH0.7}$ S				
Term	Estimated coefficient (β_i)	95% confidence interval	P-value		Term	Estimated coefficient (β_i)	95% confidence interval	P-value		Term	Estimated coefficient (β_i)	95% confidence interval	P-value	
			Min	Max				Min	Max				Min	Max
Intercept	56.5 (β_0)	48.2	64.7	1.1×10^{-01}	Intercept	359.0 (β_0)	341.5	376.6	4.5×10^{-35}	Intercept	122.6 (β_0)	108.6	136.6	1.1×10^{-19}
X_1 (pH)	40.2 (β_1)	32.0	48.4	4.4×10^{-04}	X_1 (pH)	68.6 (β_1)	50.9	86.3	1.2×10^{-09}	X_3 (harvest time)	53.1 (β_3)	25.9	80.2	3.3×10^{-04}
$X_1 X_2$ (pH \times T)	13.2 (β_{12})	5.5	20.8	9.7×10^{-14}	X_3 (harvest time)	-141.4 (β_3)	-176.2	-106.5	3.5×10^{-10}	$X_1 X_2 X_3$ (pH \times T \times harvest time)	87.5 (β_{123})	59.8	115.2	1.8×10^{-07}
					$X_1 X_3$ (pH \times harvest time)	-45.6 (β_{13})	-81.3	-9.9	1.4×10^{-02}					
					$X_1 X_2 X_3$ (pH \times T \times harvest time)	-45.6 (β_{123})	-82.0	-9.2	1.5×10^{-02}					
Adjusted R ² = 64% RMSE = 29.0 min					Adjusted R ² = 79% RMSE = 56.7 min					Adjusted R ² = 59% RMSE = 42.8 min				

R²: coefficient of determination; RMSE: standard deviation of the residuals.

Table S4.5 Multiple regression analysis of the culturability loss ($\text{dlog (CFU mL}^{-1}\text{)}$) of *L. bulgaricus* CFL1 during each stabilization process (F: freezing; FD: freeze-drying; and S: freeze-dried storage). Cells were harvested at increasing harvest times during fermentations carried out at different pH and temperatures (X1: fermentation pH X2: fermentation temperature (T); X3: harvest time) (Equation 4.6).

$\text{dlog (CFU}\cdot\text{mL}^{-1}\text{) F}$					$\text{dlog (CFU}\cdot\text{mL}^{-1}\text{) FD}$					$\text{dlog (CFU}\cdot\text{mL}^{-1}\text{) S}$				
Term	Estimated coefficient (β_i)	95% confidence interval		P-value	Term	Estimated coefficient (β_i)	95% confidence interval		P-value	Term	Estimated coefficient (β_i)	95% confidence interval		P-value
		Min	Max				Min	Max				Min	Max	
Intercept	0.2 (β_0)	0.2	0.3	4.1×10^{-13}	Intercept	1.5 (β_0)	1.4	1.6	6.4×10^{-30}	Intercept	1.3 (β_0)	1.2	1.5	4.4×10^{-19}
X ₁ X ₂ (pH x T)	0.1 (β_{12})	0.0	0.1	4.9×10^{-02}	X ₁ (pH)	0.1 (β_1)	0.0	0.2	3.1×10^{-02}	X ₂ (T)	0.5 (β_2)	0.4	0.6	9.2×10^{-10}
X ₁ X ₃ (pH x harvest time)	0.1 (β_{13})	0.0	0.3	2.2×10^{-02}	X ₂ (T)	-0.1 (β_2)	-0.2	0.0	1.1×10^{-02}	X ₃ (harvest time)	-0.7 (β_3)	-1.0	-0.5	1.1×10^{-06}
X ₁ X ₂ X ₃ (pH x T x harvest time)	0.1 (β_{123})	0.0	0.2	4.2×10^{-02}	X ₁ X ₂ (pH x T)	-0.2 (β_{12})	-0.3	-0.1	9.4×10^{-05}	X ₃ ² (harvest time ²)	0.8 (β_{33})	0.4	1.2	3.0×10^{-04}
					X ₁ X ₃ (pH x harvest time)	-0.3 (β_{13})	-0.5	-0.1	3.2×10^{-03}	X ₁ X ₂ (pH x T)	0.5 (β_{12})	0.3	0.6	1.5×10^{-09}
					X ₂ X ₃ (T x harvest time)	0.3 (β_{23})	0.1	0.5	7.9×10^{-04}	X ₁ X ₃ (pH x harvest time)	0.6 (β_{13})	0.4	0.9	2.5×10^{-06}
										X ₂ X ₃ (T x harvest time)	-0.7 (β_{23})	-0.9	-0.4	2.4×10^{-06}
Adjusted R ² = 15% RMSE = 0.19 log (CFU·mL ⁻¹)					Adjusted R ² = 61% RMSE = 0.30 log (CFU·mL ⁻¹)					Adjusted R ² = 87% RMSE = 0.28 log (CFU·mL ⁻¹)				

R²: coefficient of determination; RMSE: standard deviation of the residuals

Table S4.6 Multiple regression analysis of the loss of specific acidifying activity of *L. bulgaricus* CFL1 during freeze-dried storage ($dt_{spe} S$). Cells were harvested at increasing harvest times during fermentations carried out at different pH and temperatures (X_1 : fermentation pH; X_2 : fermentation temperature (T); X_3 : harvest time) (Equation 4.6).

$dt_{spe} S$				
Term	Estimated coefficient (β_i)	95% confidence interval		P-value
		Min	Max	
Intercept	32.3 (β_0)	29.1	35.4	6.2×10^{-21}
$X_1 X_2$ (pH \times T)	4.2 (β_{12})	1.0	7.5	1.1×10^{-02}
$X_1 X_3$ (pH \times harvest time)	10.8 (β_{13})	3.8	17.7	3.5×10^{-03}
$X_1 X_2 X_3$ (pH \times T \times harvest time)	16.1 (β_{123})	9.2	23.0	3.5×10^{-05}
Adjusted $R^2 = 49\%$ RMSE = 9.2 [min (log (CFU·mL ⁻¹)) ⁻¹]				

R^2 : coefficient of determination; RMSE: standard deviation of the residuals

Table S4.7 Predictive capacity of the multiple regression models: P (biomass productivity), $dt_{spe} F$ and $dt_{spe} FD$ (loss of specific acidifying activity during freezing and freeze-drying, respectively) by comparing predicted and the experimental values of two fermentations carried out at 39°C, pH 5.3 and different harvest times.

Biological replicate	Harvest times (h) t_{h2} or t_{h3}	P (g L ⁻¹ ·h ⁻¹)		$dt_{spe} F$ [min (log (CFU·mL ⁻¹)) ⁻¹]		$dt_{spe} FD$ [min (log (CFU·mL ⁻¹)) ⁻¹]	
		Predicted \pm RMSE	Experimental	Predicted \pm RMSE	Experimental	Predicted \pm RMSE	Experimental
1	0.6 t_{h2}	0.27 \pm 0.04	0.28	6.6 \pm 2.7	6.5	48.8 \pm 8.8	48.8
2	1.0 t_{h2}	0.27 \pm 0.04	0.27	6.6 \pm 2.7	10.4	48.1 \pm 8.8	47.6
1	4.9 t_{h3}	0.26 \pm 0.04	0.23	6.6 \pm 2.7	6.3	41.4 \pm 8.8	46.5
2	5.2 t_{h3}	0.26 \pm 0.04	0.33	6.6 \pm 2.7	9.7	40.9 \pm 8.8	40.9

RMSE: standard deviation of the residuals

Table S4.8 Multiple regression analysis of the specific of acidifying activity (t_{spe}) of *L. bulgaricus* CFL1 after freezing (t_{spe} F), freeze-drying (t_{spe} FD) and freeze-dried storage (t_{spe} S). Cells were harvested at increasing harvest times during fermentations carried out at different pHs and temperatures (X_1 : fermentation pH; X_2 : fermentation temperature (T); X_3 : harvest time) (Equation 4.6).

t_{spe} F					t_{spe} FD					t_{spe} S				
Term	Estimated coefficient (β_i)	95% confidence interval		P-value	Term	Estimated coefficient (β_i)	95% confidence interval		P-value	Term	Estimated coefficient (β_i)	95% confidence interval		P-value
		Min	Max				Min	Max				Min	Max	
Intercept	31.9 (β_0)	30.0	33.8	1.8×10^{-36}	Intercept	77.4 (β_0)	74.4	80.4	2.7×10^{-38}	Intercept	102.6 (β_0)	97.1	108.2	7.2×10^{-30}
X_1 (pH)	8.2 (β_1)	6.7	9.8	1.3×10^{-14}	X_1 (pH)	13.5 (β_{11})	10.4	16.5	3.5×10^{-11}	X_1 (pH)	12.5 (β_{21})	8.3	16.8	7.0×10^{-7}
X_2 (T)	3.5 (β_2)	2.1	5.0	1.0×10^{-5}	X_3 (harvest time)	-9.2 (β_{13})	-15.5	-3.0	4.9×10^{-03}	X_3 (harvest time)	-8.2 (β_{33})	-16.4	-0.06	4.8×10^{-2}
X_3 (harvest time)	3.6 (β_3)	0.6	6.7	2.1×10^{-2}	$X_1 X_3$ (pH x harvest time)	-14.6 (β_{13})	-20.9	-8.3	3.0×10^{-05}	X_3^2 (harvest time ²)	24.0 (β_{33})	10.2	37.8	1.1×10^{-3}
X_3^2 (harvest time ²)	12.1 (β_{33})	7.0	17.2	1.6×10^{-5}	$X_2 X_3$ (T x harvest time)	9.8 (β_{23})	3.6	16.1	2.9×10^{-03}					
					$X_2 X_3$ (T x harvest time)	0.3 (β_{23})	0.1	0.5	7.9×10^{-04}					
					$X_1 X_2 X_3$ (pH x T x harvest time)	-8.0 (β_{123})	-14.3	-1.7	1.4×10^{-02}					
Adjusted R ² = 70% RMSE = 5.1 [min (log (CFU·mL ⁻¹)) ⁻¹]					Adjusted R ² = 76% RMSE = 9.7 [min (log (CFU·mL ⁻¹)) ⁻¹]					Adjusted R ² = 57% RMSE = 12.8 [min (log (CFU·mL ⁻¹)) ⁻¹]				

R²: coefficient of determination; RMSE: standard deviation of the residuals

4.7.2. Supplementary Figures

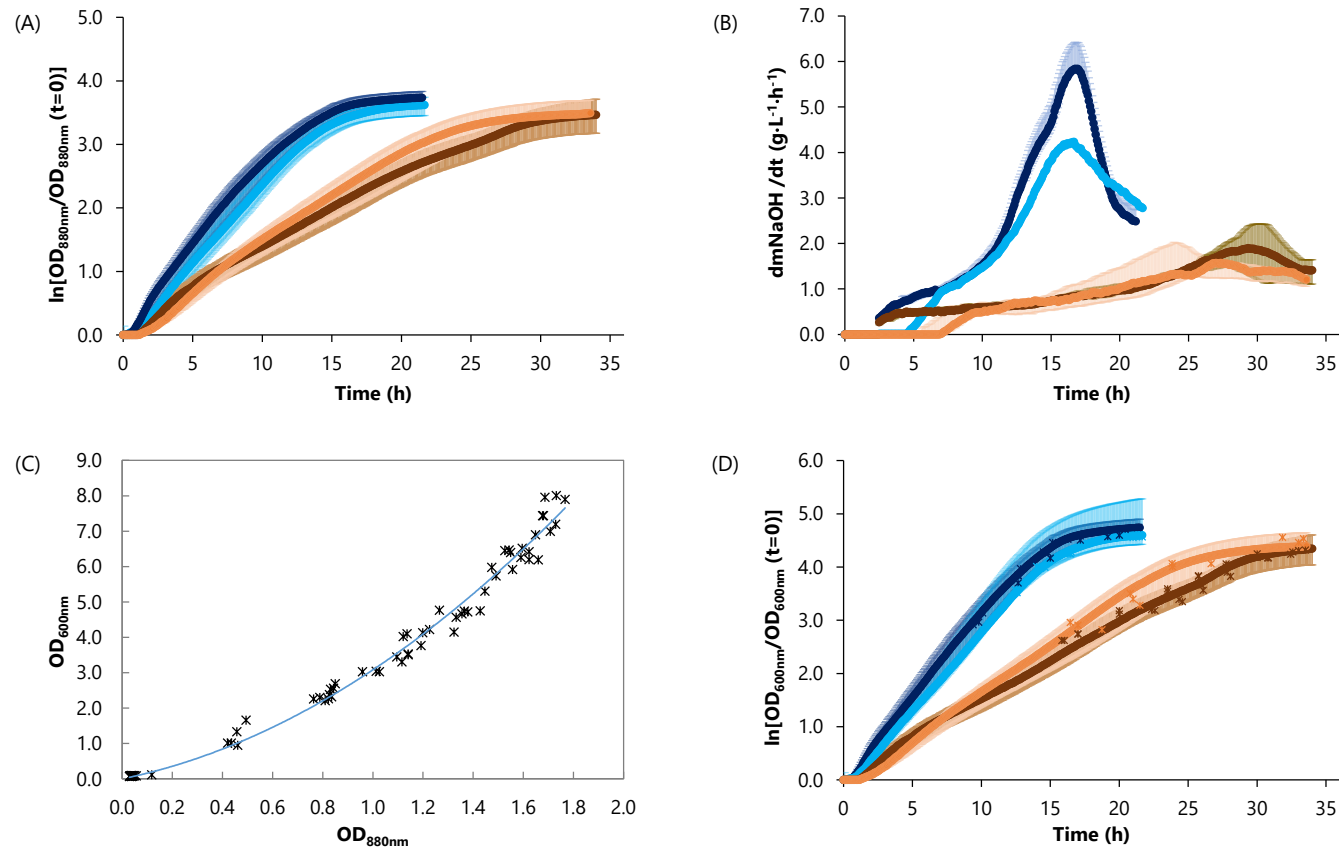


Figure S4.1 (A) Growth curves based on optical density (OD) data at 880 nm; (B) Rate of NaOH consumption during fermentation (dmNaOH/dt , $\text{g}\cdot\text{L}^{-1}\cdot\text{h}^{-1}$); (C) Correlation between the 880 and 600 nm OD data: $\text{OD}_{600\text{nm}} = 1.63 \times (\text{OD}_{880\text{nm}})^2 + 1.45 \times (\text{OD}_{880\text{nm}})$. The corresponding coefficient of determination ($R^2 = 0.988$) indicates the accuracy of the correlation; (D) Growth curves from the correlation shown in (C), asterisks represent the experimental data points at 600 nm. Growth and NaOH consumption rate curves of *L. bulgaricus* CFL1 correspond to the fermentation conditions: [42°C, pH 5.8] (blue curves: ●); [42°C, pH 4.8] (light blue curves: ●); [37°C, pH 5.8] (brown curves: ●); [37°C, pH 4.8] (orange curves: ●). Results are the means of at least three independent biological replicates. Standard deviation values are represented as a shaded area per fermentation condition.

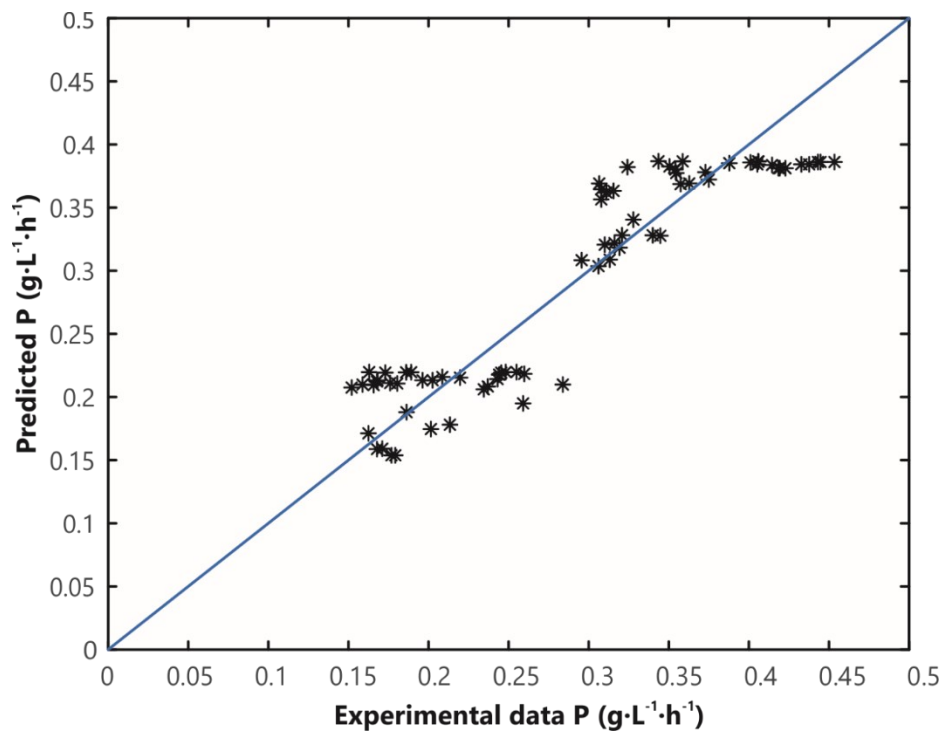


Figure S4.2 Biomass productivity (P , in $\text{g}\cdot\text{L}^{-1}\cdot\text{h}^{-1}$) values predicted by the multiple linear regression model vs. the experimental biomass productivity values. The corresponding coefficient of determination (adjusted $R^2 = 84\%$) indicates the accuracy of the model in the range of the studied fermentation conditions.

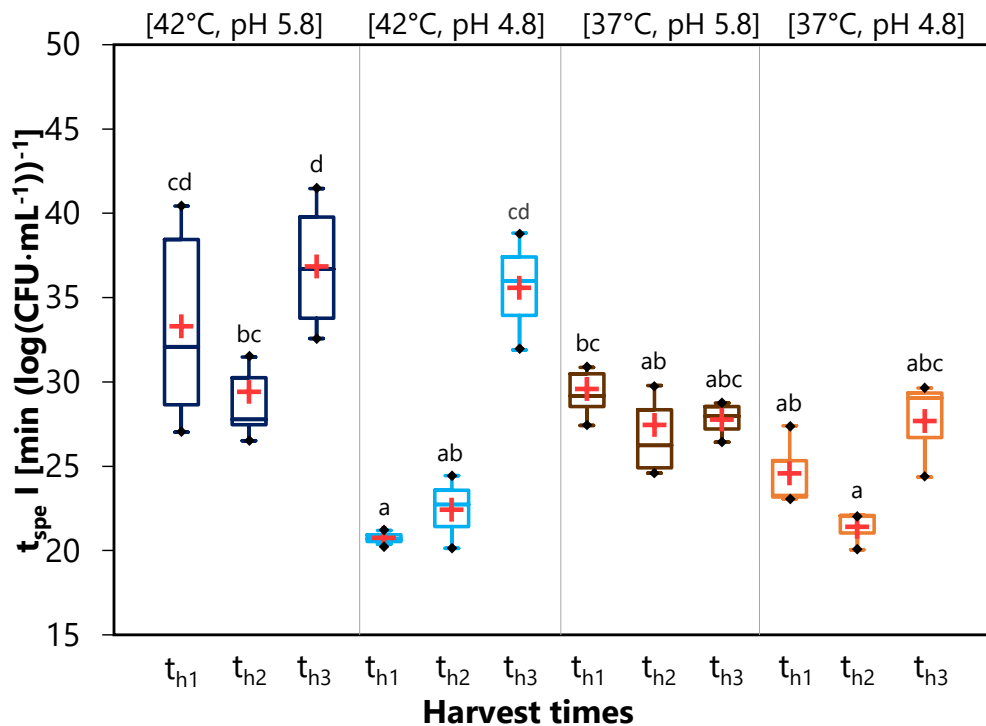


Figure S4.3 Initial specific acidifying activity ($t_{\text{spe } I}$, in $[\text{min} (\log(\text{CFU}\cdot\text{mL}^{-1}))^{-1}]$) of *L. bulgaricus* CFL1 for the four combinations of fermentation conditions studied: [42°C, pH 5.8]; [42°C, pH 4.8]; [37°C, pH 5.8]; [37°C, pH 4.8] at three different harvest times. t_{h1} : mid-exponential growth phase; t_{h2} : deceleration growth phase; t_{h3} : stationary growth phase. The boxplots (median = line in the middle of the box and mean = red cross) are the result of at least three independent biological replicates. Superscript letters represent significant differences between samples at a 95% confidence level.

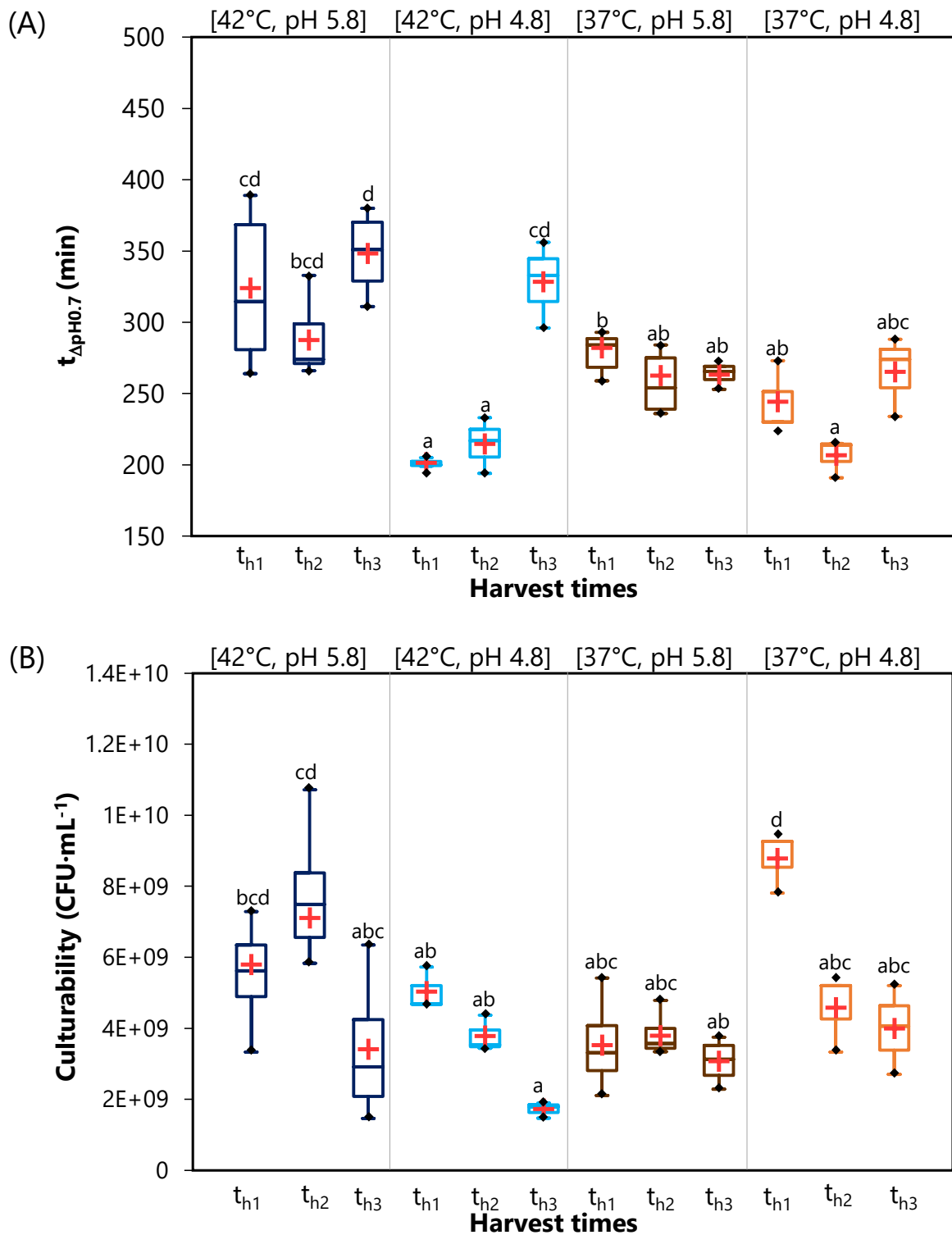


Figure S4.4 Initial (A) acidifying activity ($t_{\Delta\text{pH}0.7}$, in min) and (B) culturability ($\text{CFU}\cdot\text{mL}^{-1}$) of *L. bulgaricus* CFL1 for the four combinations of fermentation conditions studied: [42°C, pH 5.8]; [42°C, pH 4.8]; [37°C, pH 5.8]; [37°C, pH 4.8] at three different harvest times. t_{h1} : mid-exponential growth phase; t_{h2} : deceleration growth phase; t_{h3} : stationary growth phase. The boxplots (median = line in the middle of the box and mean = red cross) were obtained from at least three independent biological replicates. Superscript letters represent significant differences between samples at a 95% confidence level.

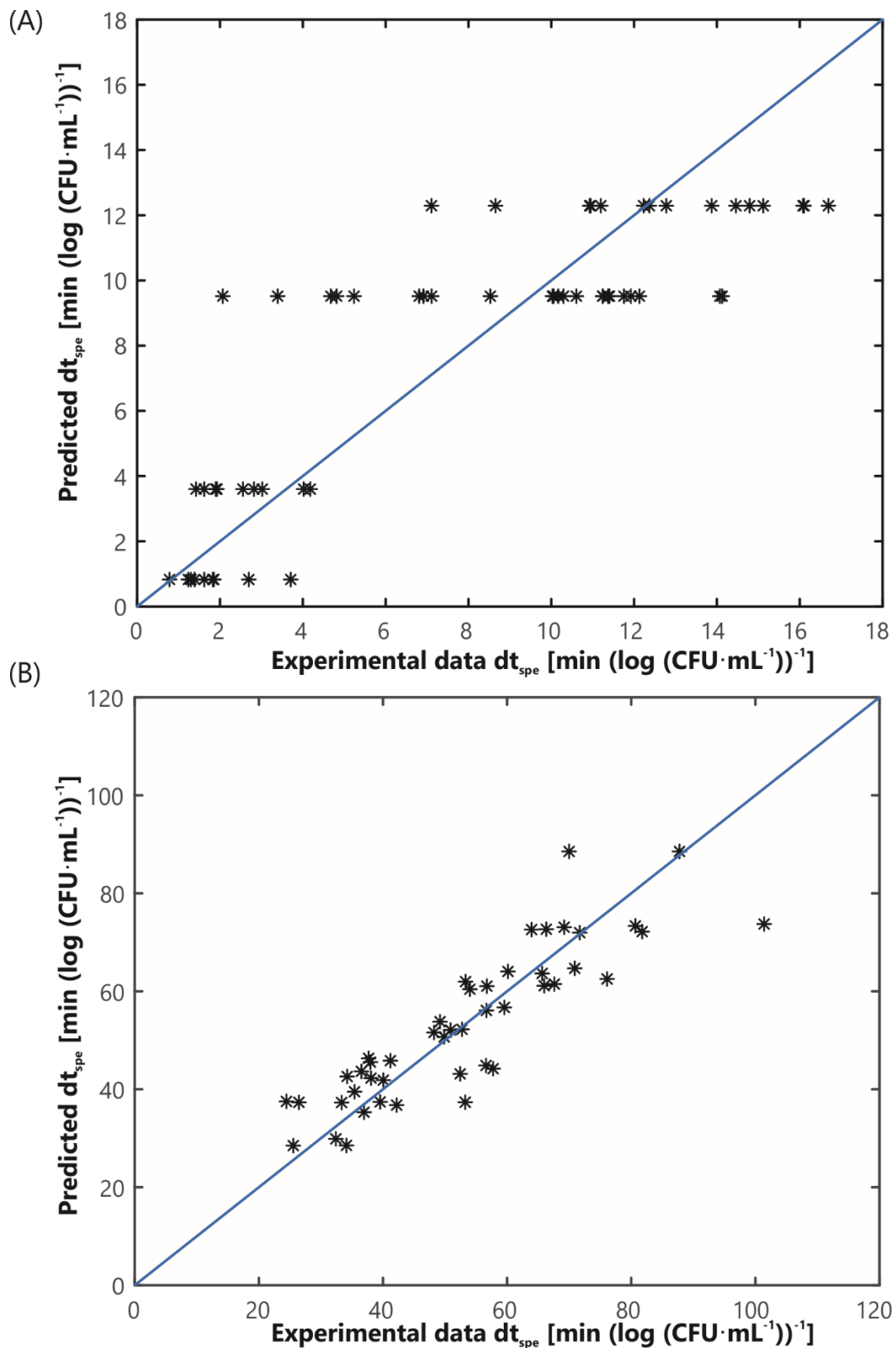


Figure S4.5 Loss of specific acidifying activity (dt_{spe} , in $[\text{min} (\log (\text{CFU} \cdot \text{mL}^{-1}))^{-1}]$) values predicted by the multiple linear regression models vs. the experimental dt_{spe} values, for (A) freezing and (B) freeze-drying. The corresponding coefficients of determination (adjusted $R^2 = 70\%$ and 74% , respectively) indicate the accuracy of both models.

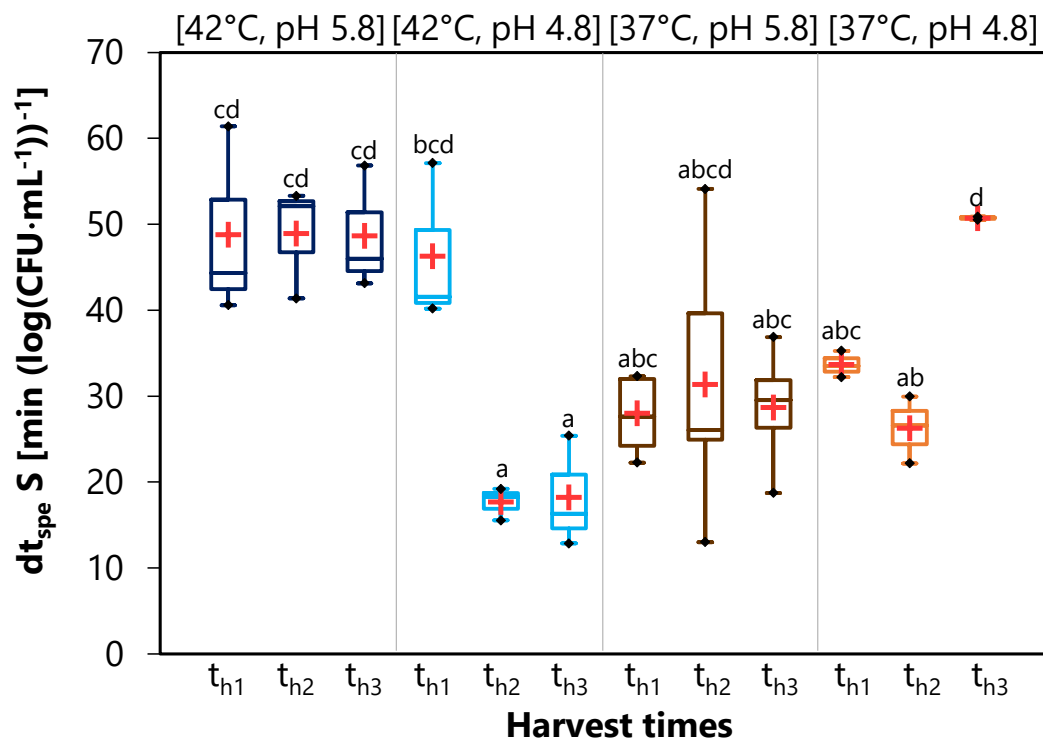


Figure S4.6 Loss of specific acidifying activity of *L. bulgaricus* CFL1 during freeze-dried storage for 15 days at 25°C ($dt_{spe} S$, in $[\text{min} (\log (\text{CFU}\cdot\text{mL}^{-1}))^{-1}]$) for the four combinations of fermentation conditions studied: [42°C, pH 5.8]; [42°C, pH 4.8]; [37°C, pH 5.8]; [37°C, pH 4.8] at three different harvest times. t_{h1} : mid-exponential growth phase; t_{h2} : deceleration growth phase; t_{h3} : stationary growth phase. The boxplots (median = line in the middle of the box and mean = red cross) are the result of at least three independent biological replicates. Superscript letters represent significant differences between samples at a 95% confidence level.

4.8. Prospects for this study

- Changing the fermentation medium to modulate the resistance of *L. bulgaricus* CFL1 to freezing and freeze-drying.

The parameters studied in the first part of the results of Chapter 4 were only focused on temperature, pH, and growth phase. The MRS culture medium (known as a laboratory medium) was used in the thesis. However, the MRS medium is characterized by its high cost, hampering it from being used on an industrial scale. The most common media used at an industrial scale are formulated or whey medium. MRS medium was previously reported as a culture medium that improved freezing resistance over a whey medium for *L. bulgaricus* CFL1 (Gautier et al. 2013).

Some studies have reported media formulation close to MRS for producing LAB. For instance, a formulated medium was developed to produce *Lactiplantibacillus plantarum* and *Lactocaseibacillus rhamnosus* cells. This medium consisted primarily of the key ingredients of a commercial MRS (glucose, yeast extract, and vegetable-derived peptone. Its ingredients were non-animal derived components, thus more affordable to be used on an industrial scale. The formulated medium guaranteed a comparable freeze-drying survival as the commercial MRS broth (Siaterlis et al. 2009).

A more recent study reported using a house-formulated MRS with a similar composition to commercial MRS to produce different LAB and stabilize them by spray-drying. The formulated MRS used low ingredient costs (by local providers), and its cost was four times lower than the commercial MRS (2.45 USD/L vs. 11.13 USD/L). Biomass production and spray-drying resistance were not different when formulated MRS and the commercial MRS broth were compared (Blajman et al. 2020).

Using a more affordable culture medium similar to MRS would make the approach presented in this thesis more robust toward an immediate industrial application.

- Extending the range of the experimental design to a lower controlled pH value

The results in Chapter 4 showed that low controlled pH enhanced *L. bulgaricus* CFL1 resistance to freezing and freeze-drying. During the thesis, experiments (lacking biological repetitions) were also carried out at uncontrolled pH for the two temperatures studied (42°C, uncontrolled pH and 37°C, uncontrolled pH) (Figure 4.5). At uncontrolled pH, bacteria acidify the culture medium as the growth progresses.

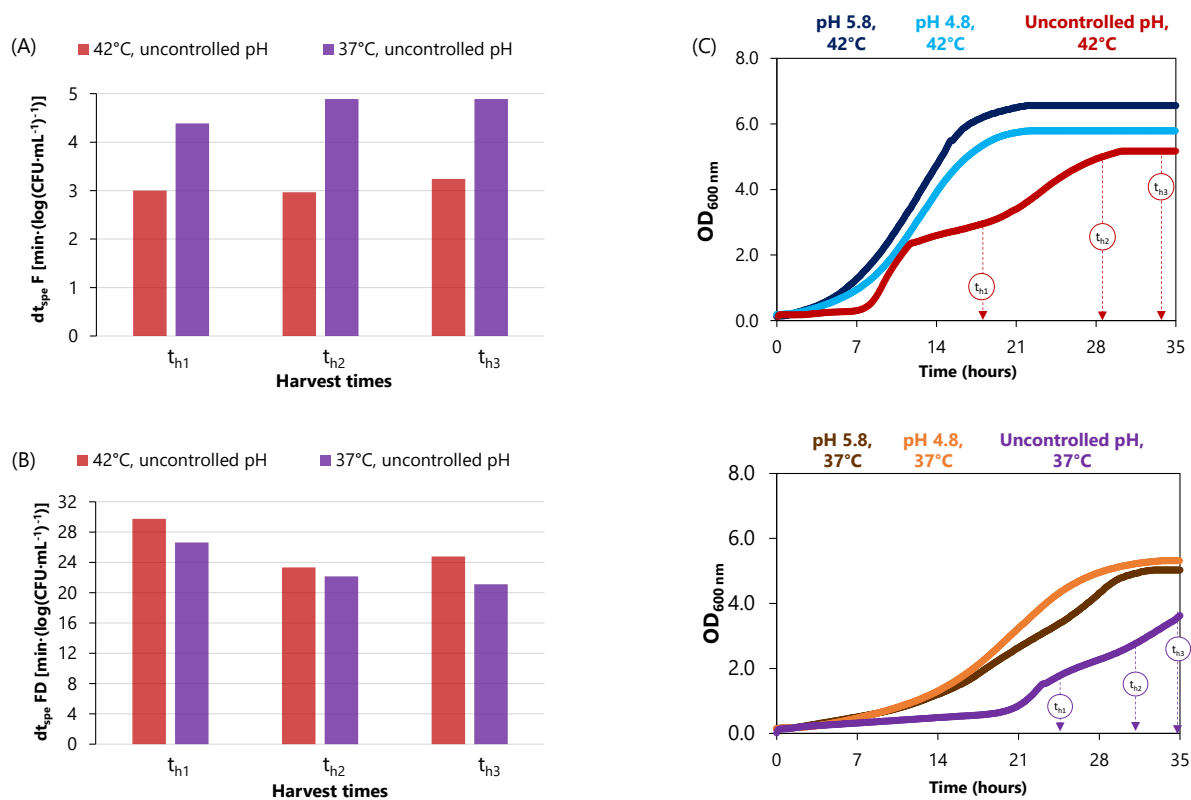


Figure 4.5 Loss of specific acidifying activity during (A) freezing and (B) freeze-drying of *L. bulgaricus* CFL1 for fermentations carried out at uncontrolled pH. Cells were cultivated at two fermentation conditions: 42°C, uncontrolled pH and 37°C, uncontrolled pH. (C) The growth of uncontrolled fermentations was compared to the fermentation conditions carried out at controlled pH.

At uncontrolled pH, the freezing resistance of *L. bulgaricus* CFL1 was slight lower or similar (42°C: 3 [min·(log (CFU·mL⁻¹))⁻¹] and 37°C: 4.5-5 [min·(log (CFU·mL⁻¹))⁻¹]) than the ones obtained at controlled pH 4.8 (42°C: 1-3 [min·(log (CFU·mL⁻¹))⁻¹] and 37°C: 2-3 [min·(log (CFU·mL⁻¹))⁻¹]).

For freeze-drying resistance, *L. bulgaricus* CFL1 cells exhibited an increased resistance of 17% when bacteria were harvested at the deceleration (t_{h2}) and the stationary phase (t_{h3}). In the growth phase, where cells were harvested, the pH of the medium dropped to a value of 4.5.

Therefore, the range of the experimental design used in Chapter 4 would be worth expanding to a lower controlled pH than pH 4.8. Controlled pH would be suitable since, at uncontrolled pH, the growth is slower (Figure 4.5 (C)).

Regarding values higher than the highest level used in this thesis (pH 5.8), the resistance to freezing might not be improved. A previous study on *L. bulgaricus* CFL1 confirmed this assumption (Rault et al. 2009)

Take-home messages

Chapter 4: Multi-objective optimization of frozen and freeze-dried *L. bulgaricus* CFL1

- This study led to the development of predictive models for producing and stabilizing *L. bulgaricus* CFL1.
- The growth of *L. bulgaricus* CFL1 was enhanced when cells were cultivated at [42°C, pH 5.8].
- The improvement of the freezing resistance of *L. bulgaricus* CFL1 was achieved when cells were cultivated at pH 4.8.
- The freeze-drying resistance of *L. bulgaricus* CFL1 was enhanced when cells were cultivated at pH 4.8 and harvested at the stationary growth phase (t_{h3}).
- The range of fermentation parameters applied did not affect the freeze-dried storage resistance of *L. bulgaricus* CFL1.
- The Pareto front was a helpful tool for finding the balance performance (compromise) between fair biomass production and resistance of *L. bulgaricus* CFL1 to freezing and freeze-drying.
- The fermentation condition representing this balance performance was [42°C, pH 4.8], and harvest at the deceleration phase (t_{h2}).

Chapter 5

5. DEEP ANALYSIS OF MEMBRANE LIPIDS AND THEIR RELATIONSHIPS WITH *L. bulgaricus* CFL1 RESISTANCE TO FREEZING AND FREEZE-DRYING

In Chapter 4, *L. bulgaricus* CFL1 was cultivated in four fermentation conditions and harvested at increasing harvest times (t_{h1} , t_{h2} , and t_{h3}). The purpose was to identify the effect of fermentation temperature, pH, and harvest time on the resistance of *L. bulgaricus* CFL1 to freezing and freeze-drying. To understand the bacteria adaptation at the molecular level, we investigated the effect of these fermentation parameters on the composition and biophysical properties of the membrane lipids. Then, the composition and properties of the membrane were related to the resistance of *L. bulgaricus* CFL1 to both stabilization processes.

SUMMARY OF THE CHAPTER

5. DEEP ANALYSIS OF MEMBRANE LIPIDS AND THEIR RELATIONSHIPS WITH <i>L. bulgaricus</i> CFL1 RESISTANCE TO FREEZING AND FREEZE-DRYING	161
5.1. Preamble	163
5.2. Abstract	164
5.3. Introduction	165
5.4. Materials and methods	167
5.4.1. Bacterial strain and growth conditions	167
5.4.1.1. Strain and inoculum preparation	167
5.4.1.2. Fermentation	168
5.4.1.3. Harvest, concentration and bacterial suspensions	168
5.4.2. Biochemical characterization of membrane lipids	169
5.4.2.1. Fatty acids determination of the total lipid extract at t_{h1} , t_{h2} , and t_{h3}	169
5.4.2.2. Lipid classes determination of the total lipid extract at t_{h3}	170
i. Lipid extraction and fractionation	171
ii. Fatty acids determination for LE, f_1 , f_2 , f_3 , and f_4	172
iii. Lipid classes identification by HPTLC analysis	172
iv. Lipid classes identification by LC-MS/MS	173
5.4.3. Biophysical properties of <i>L. bulgaricus</i> CFL1 membrane lipids	174
5.4.3.1. Temperatures of lipid phase transition by Fourier Transformed Infrared (FTIR) spectroscopy	174
5.4.3.2. Membrane fluidity by fluorescence anisotropy	175
5.4.4. Freezing and freeze-drying protocols	176
5.4.5. Resistance of <i>L. bulgaricus</i> CFL1 cells by their loss of functional properties	176
5.4.6. Statistical analysis	177
5.4.6.1. Differences among fermentation conditions and harvest times	178
5.4.6.2. Clustering analysis for lipid classes	178
5.4.6.3. Correlation of Pearson and Principal Component Analysis (PCA)	178
5.5. Results	179
5.5.1. Membrane lipid compositions of <i>L. bulgaricus</i> CFL1 for the four fermentation conditions	179
5.5.1.1. Fatty acids composition of the total lipid extract (LE) at t_{h1} , t_{h2} , t_{h3}	179
5.5.1.2. Lipid composition at t_{h3}	182
i. Lipid fractionation	182
ii. Fatty acid composition of each fraction at t_{h3}	183
iii. Identification of lipid classes of each fraction at t_{h3} by HPTLC	185
iv. Lipid classes of each fraction at t_{h3} by LC-MS/MS	186
5.5.2. Lipid phase transitions and membrane fluidity	194
5.5.3. Resistance of <i>L. bulgaricus</i> CFL1 to freezing and freeze-drying at four different fermentation conditions and harvest times	195
5.5.4. Relationships between membrane lipid characteristics and the two stabilization processes	197
5.6. Discussion	200
5.6.1. Fermentation conditions affect fatty acid composition at different harvest times	200
5.6.2. Fermentation conditions effect on membrane lipids: analysis of lipids fractions	201
5.6.3. Biophysical properties of membrane lipids	201
5.6.4. The resistance to freezing and freeze-drying and the link with the membrane	202
5.7. Conclusion	203
5.8. Supplementary information	205
5.8.1. Supplementary Tables	205
5.8.2. Supplementary Figures	211
5.9. Prospects for this study	223

5.1. Preamble

This chapter was written in an article format, including a material and methods section adapted to publication. The reading of the experimental section can be skipped for those who read Chapter 3. Also, the results of the resistance to freezing and freeze-drying of *L. bulgaricus* CFL1 from Chapter 4 are here presented in a different format and briefly explained to meet the objectives of the present chapter.

Supplementary information available in Chapter 3 Materials and methods

Chapter 5: subsection	Chapter 3: section or subsection
5.4.1. Bacterial strain and growth conditions	3.1. Production of concentrated <i>L. bulgaricus</i> CFL1
5.4.2. Biochemical characterization of membrane lipids	3.5. Lipid composition of the <i>L. bulgaricus</i> CFL1 membrane
5.4.3. Biophysical properties of <i>L. bulgaricus</i> CFL1 membrane lipids	3.6. Biophysical properties of the <i>L. bulgaricus</i> CFL1 membrane: lipid phase transition temperature and membrane fluidity
5.4.4. Freezing and freeze-drying protocols	3.2. Stabilization processes and freeze-dried storage
5.4.5. Resistance of <i>L. bulgaricus</i> CFL1 cells by their loss of functional properties	3.3. Assessment of the functional properties of <i>L. bulgaricus</i> CFL1 at different production steps
5.4.6. Statistical analysis	3.8.3. ANOVA tests
	3.8.4. Pearson's correlation coefficient
	3.8.5. Principal Component Analysis (PCA)
	3.8.6. Clustering analysis for different lipids

Deep analysis of membrane lipids of a lactic acid bacterium during mild-stressing growth conditions in relation with its resistance to freezing and freeze-drying

Maria de L. Tovilla-Coutiño^{1,3}, Yann Gohon³, Anne-Claire Peron¹, Fernanda Fonseca¹, Stéphanie Passot¹, Marie-Hélène Ropers^{2*}

¹Université Paris-Saclay, INRAE, AgroParisTech, UMR SayFood, 91120 Palaiseau, France

²INRAE, UR1268 Biopolymères Interactions Assemblages, 44300 Nantes, France

³Université Paris-Saclay, INRAE, AgroParisTech, Institut Jean-Pierre Bourgin (IJPB), 78000 Versailles, France

*Corresponding author:

Marie-Hélène Ropers, UR1268 Biopolymères Interactions Assemblages, 44300 Nantes, France

E-mail: marie-helene.ropers@inrae.fr

5.2. Abstract

Lactic acid bacteria (LAB) are renowned for their crucial role in the health of humans as functional foods and their essential industrial applications in fermented foods. During production and stabilization, these bacteria are exposed to adverse environmental conditions. To withstand the stresses occurring during the stabilization, they develop active responses such as the modulation of the lipid membrane composition. Due to the few studies on understanding the relationships between lipid composition and resistance, a global view of adaptation for different fermentation conditions has never been done. This study thus aimed at investigating the effect of fermentation parameters on *L. bulgaricus* CFL1 membrane lipids and the link of these properties on the cell resistance to freezing and freeze-drying. To achieve this aim, first, bacteria were grown at four different fermentation conditions, including two different temperatures (42°C and 37°C) and pHs (5.8 and 4.8). Cells were harvested at different growth phases (from the middle exponential to the stationary growth phase). Then, deep characterization of membrane lipids modulation was performed for the harvested bacteria. It was considered not only the classic fatty acid composition or biophysical properties such as membrane fluidity or lipid phase transition temperatures but also a complete lipid composition (including phospholipids and glycolipids) of *L. bulgaricus* CFL1. Finally, bacterial membrane lipids alterations were related to the resistance of cells to freezing and freeze-drying. Low fermentation temperature (37°C) or pH (pH 4.8) induced the production of unsaturated fatty acids, leading to a fluid membrane and lipid phase transition at zero or subzero temperatures. Low fermentation pH induced a high relative abundance of some glycolipids in the membrane. High temperature and pH fermentation (42°C, pH 5.8) led to the lowest relative abundance of some glycolipids.

The membrane lipid modulation was related differently to freezing and freeze-drying resistance. *L. bulgaricus* CFL1 with unsaturated fatty acids and a fluid membrane render cells resistant to freezing. In contrast, a high amount of cyclic fatty acids was related to freeze-drying. This study contributes to new knowledge on the membrane changes induced by different fermentation conditions and their relation to the most common process to preserve lactic acid bacteria.

5.3. Introduction

Lactic Acid Bacteria (LAB) are widely used in the food industry to manufacture a diversity of fermented products (García-Burgos et al. 2020; Ashaolu and Reale 2020). Some strains have even gained interest because they promote health benefits, i.e., probiotics (Eviwie et al. 2017; Terpou et al. 2019). These bacteria are industrially produced in several steps, including fermentation, concentration, and stabilization.

The last step aims at preserving LAB for long-term shelf life. The most common processes to stabilize LAB are freezing and freeze-drying. Nevertheless, these processes reduce the functional properties of LAB, such as their acidifying activity and survival, since both stabilization processes induce stresses (thermal, osmotic, and mechanical) (Béal and Fonseca 2015; Fonseca et al. 2021). Together with the cell wall, the cell membrane has been identified as the main target of degradation because it represents the barrier of the cell to the potentially stressful environment induced by freezing and freeze-drying (Brennan et al. 1986; Hlaing et al. 2017; Girardeau et al. 2022).

Changing fermentation parameters such as culture medium, temperature, pH, and harvest time has been shown to modulate cell membrane (Fonseca et al. 2019). The most common modulation of membrane properties includes the modification of the fatty acid composition, consisting in altering the saturated degree, cis/trans isomerization, and cyclopropanation of the acyl chains (Smittle et al. 1974; Goldberg and Eschar 1977; Béal et al. 2001; Wang et al. 2005a; Li et al. 2009a, 2012; Zhao et al. 2009; Liu et al. 2014; Velly et al. 2015; Louesdon et al. 2015; E et al. 2021). Accordingly, the temperatures of melting and solidification (crystallization) of lipids are shifted either to higher or lower values. When fermentation conditions are modified, the membrane fluidity and the lipid phase transition temperatures are the underlying membrane properties that can also be altered (Gautier et al. 2013; Passot et al. 2014; Meneghel et al. 2017; Bodzen et al. 2021a). All these membrane changes were thought to help bacteria withstand the subsequent stabilization processes such as freezing or freeze-drying. However, the studies that have assessed the influence of LAB growth conditions on the lipid membrane have not yet allowed the drawing up of a clear view of the effects of fermentation parameters on the membrane lipids properties. Indeed, the influence of different lipid classes on LAB resistance has been only and scarcely investigated for freezing (Smittle et al. 1974; Fernández Murga et al. 2000). In addition, membrane fluidity may be affected not only by the membrane fatty acids but also by different lipids such as phospholipids and glycolipids.

In this context, we first investigated how the lipid composition and biophysical properties of a sensitive freeze-thaw strain, *L. bulgaricus* CFL1, were modulated by cultivating the bacteria in four different fermentation conditions. Cells were harvested at three different growth phases. The membrane lipids were characterized by a thoroughly analytical approach for lipids, including a fine biochemical characterization (i.e., fatty acids and lipid classes present in the

membrane), lipid phase transition temperatures, and membrane fluidity. In a second step, these results were analyzed to correlate them with the resistance of the bacterium to freezing and freeze-drying.

5.4. Materials and methods

The experimental approach and various methods used for this study are shown in Figure 5.1. All measurements came from at least three independent bacterial cultures.

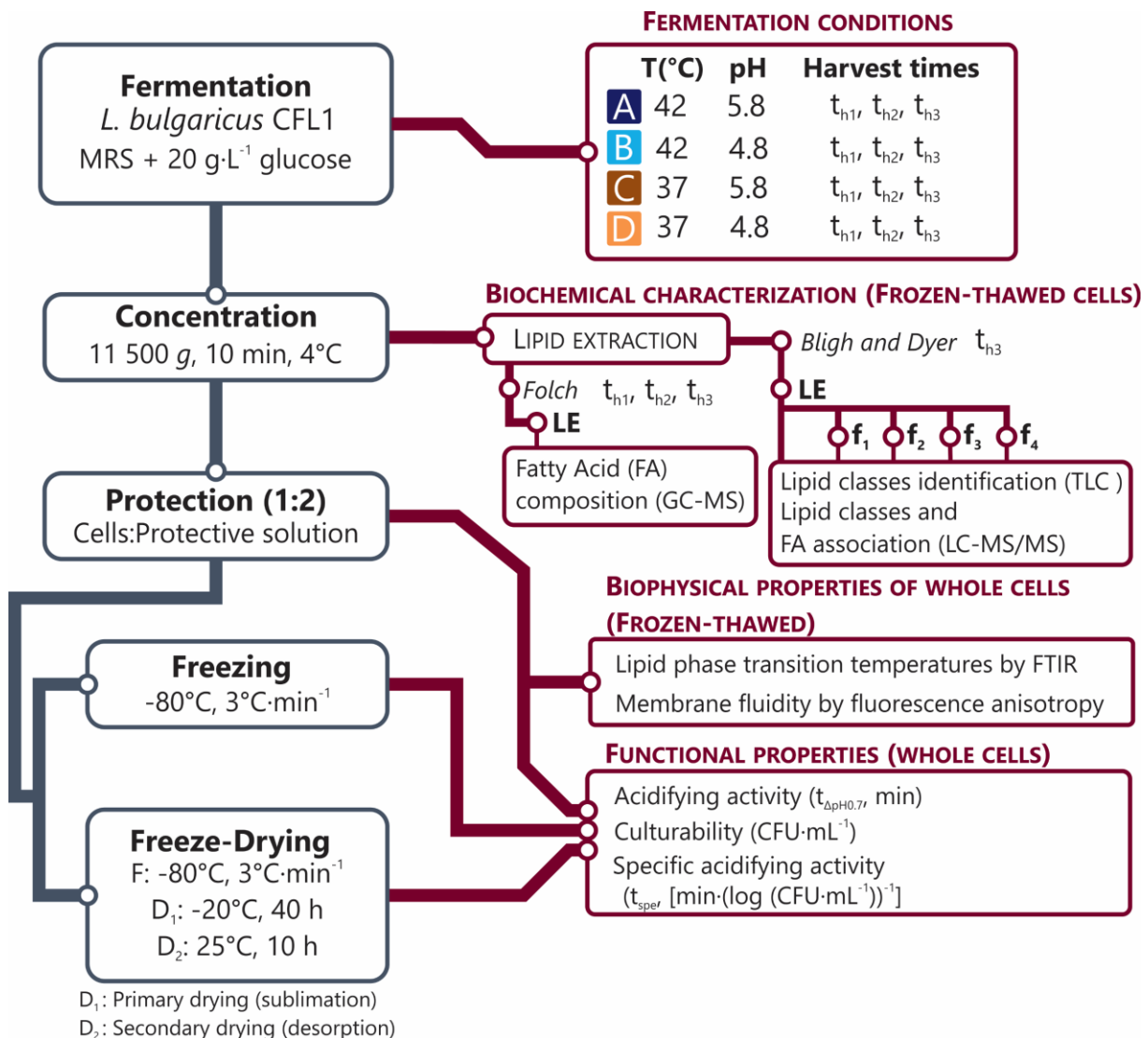


Figure 5.1 Diagram of the experimental approach used in this study and the main investigated lipid properties and composition of *L. bulgaricus* CFL1 membrane. The four fermentation conditions studied are indicated by a blue square for [42°C, pH 5.8], a light blue square for [42°C, pH 4.8], a brown square for [37°C, pH 5.8], and orange square for [37°C, pH 4.8]. Color and letter codes are used for the figures in the results section. Abbreviations: LE, Lipid Extract; f_1 , f_2 , f_3 , f_4 the lipid fractions obtained after fractionation of LE; F, Freezing; FD, Freeze-Drying

5.4.1. Bacterial strain and growth conditions

5.4.1.1. Strain and inoculum preparation

Lactobacillus delbrueckii subsp. *bulgaricus* CFL1 (*L. bulgaricus* CFL1) (CIRM-BIA; Rennes, France) was the strain selected for this study due to its sensitivity to freezing (Fonseca et al. 2000; Meneghel et al. 2017). Frozen aliquots of *L. bulgaricus* CFL1 cells were stored at -80°C in Man Rogosa and Sharpe (MRS) medium supplemented with 15% (w/w) glycerol (VWR, Leuven,

Belgium). 300 μL of a frozen aliquot were first precultured in 60 mL of MRS medium at 42°C for 12 hours without agitation. The MRS medium was previously sterilized at 121°C for 20 minutes. Then 1.5 mL of this first preculture were inoculated to a second preculture containing the same amount of sterilized MRS medium (60 mL). This second preculture was incubated at 42°C for 10 hours without agitation. Bacterial cells were in the stationary growth phase for both precultures. The whole volume of the second preculture was used to inoculate the bioreactor.

5.4.1.2. Fermentation

The culture medium was composed of MRS supplemented with 20 $\text{g}\cdot\text{L}^{-1}$ D-glucose (VWR, Leuven, Belgium). This medium was sterilized by filtering it through a 0.22 μm polyethersulfone membrane (Stericap PLUS, Millipore Express®, Merck, KGaA, Darmstadt, Germany). Then, the culture medium was introduced into a 4-L working volume bioreactor (Biostat® A plus 5 L bioreactor Sartorius, Biostat® A plus, Melsungen, Germany). The temperature and pH were set before inoculation and controlled throughout the growth (SartoriusBioPAT software, SARTORIUS®, Göttingen, Germany). Two different levels of temperature and pH were selected, leading to the following four fermentation conditions: [42°C, pH 5.8]; [42°C, pH 4.8]; [37°C, pH 5.8]; and [37°C, pH 4.8]. From these four fermentation conditions, [42°C, pH 5.8] has been previously identified as the optimal condition for the growth of *L. bulgaricus* CFL1 (Chapter 4, article n°1).

The pH control was carried out by adding NaOH solution at 4.25 M (VWR, Leuven, Belgium) into the bioreactor. Stirring was applied at 100 rpm to homogenize the culture medium. The inoculation was performed at an initial concentration of about 0.1 optical density at 600 nm ($\text{OD}_{600\text{nm}}$), corresponding to $\sim 4 \times 10^5$ $\text{CFU}\cdot\text{mL}^{-1}$. In situ, cell growth was monitored every five minutes by an optical density probe inserted into the bioreactor at 880 nm ($\text{OD}_{880\text{nm}}$) (880 nm infra-red probe, Excell210; CellID, Roquemaure, France). The natural logarithm of each $\text{OD}_{880\text{nm}}$ measurement ($\ln [\text{OD}_{880\text{nm}}/\text{OD}_{880\text{nm}} \text{ at } t=0 \text{ h}]$) allowed defining the growth phases per fermentation condition (Figure S5.1).

5.4.1.3. Harvest, concentration and bacterial suspensions

For each fermentation condition, bacterial cells were harvested at three different harvest times according to the following growth phases: the mid-exponential growth phase, t_{h1} ; the deceleration growth phase, t_{h2} ; and the stationary growth phase, t_{h3} (Figure S5.1).

The cell suspensions were then concentrated by centrifugation at 11 500 g for 10 minutes at 4°C (Avanti® J-E centrifuge; Beckman Coulter, Fullerton, CA). The resulting cell pellets were aliquoted to be suspended in two different solutions for (i) lipids analysis or (ii) functional and membrane biophysical properties.

For lipids analysis, bacterial cells were washed twice and suspended in a saline solution with the following ratio: 1 g of concentrated cells for 1 g of 0.9% w/w sterilized saline solution (NaCl, VWR, Leuven, Belgium. Sterilization cycle: 121°C for 20 min).

For functional properties measurements (before and after freezing and freeze-drying), as well as biophysical properties, bacterial cells were suspended at a ratio of 1:2 (1 g of concentrated cells for 2 g of the protective solution). The protective solution was composed of 20% (w/w) of sucrose (VWR, Leuven, Belgium) and was previously sterilized at 121°C for 20 min.

5.4.2. Biochemical characterization of membrane lipids

To analyze the lipids of the membrane of *L. bulgaricus* CFL1, the total lipids present in *L. bulgaricus* CFL1 cells were extracted. Then a portion of them was fractionated to obtain different fractions that correspond exclusively to membrane lipids. Before and after fractionation, lipids were characterized by their fatty acid composition and their different lipids classes (e.g., phospholipids, glycolipids, triglycerides, among others).

Lipids extraction, fractionation, and determination are described in the following subsections.

5.4.2.1. Fatty acids determination of the total lipid extract at t_{h1} , t_{h2} , and t_{h3}

The Fatty Acids (FA) of *L. bulgaricus* CFL1 were determined from the four fermentation conditions and the three harvest times. Frozen bacterial cell suspensions were thawed at 42°C for 10 minutes in a water bath and centrifuged at 12 900 *g* for 10 min at 4°C (Eppendorf® Centrifuge 5804 R – Benchtop, Hamburg; Germany). The supernatant was removed, and the bacterial pellet was washed twice with NaCl solution at 0.9% w/w (VWR, Leuven, Belgium) by centrifuging under the same conditions.

The total lipids of *L. bulgaricus* CFL1 cells were extracted according to the Folch procedure (Folch et al. 1957) with some modifications provided by (Walczak-Skierska et al. 2020). This method was chosen because it was adapted to the available quantity of cell biomass for each harvest time (<500 mg).

Briefly, one hundred milligrams of wet bacterial pellet were introduced into a five-milliliter Eppendorf tube (Eppendorf Tubes-Microtube® for solvents, Hamburg; Germany). Then, 3.6 mL of chloroform (CHCl₃)-methanol (CH₃OH) (2:1, v/v) were added. The suspension was vortexed and sonicated in a water bath (Elmasonic S 30 /H, 50 Hz, Aubagne, France) at room temperature for ten minutes. After sonication, 0.85 mL of 0.9% NaCl solution was added. The mixture was shaken for ten minutes on a rotary shaker (Rotary shaker SB2/SB3-STUART, Evreux, France) and centrifuged (12 900 *g*, 20°C, for 15 min). After centrifugation, three layers were observed: (i) upper layer (not organic phase), (ii) lower layer (organic phase), and (iii) bacterial pellet (bottom of the tube). The lower layer was transferred into a four-milliliter glass tube (NAFVSM, Nijmegen, Netherlands). Then, 0.85 mL of CHCl₃ were added into the Eppendorf tube containing the upper layer and the bacterial pellet. Once again, the sample was shaken on the

rotary shaker for ten minutes and centrifuged (12 900 *g*, 20°C, for 15 min). This step was performed to collect the lower phase and incorporate it into the four-milliliter glass tube. The collected lower layer contained the lipid extract. This lipid extract was dried using a vacuum-rotary evaporator (Refrigerated Vapor Trap: RVT5105, ThermoFisher, MA, USA).

The dried extracted lipid samples were re-suspended in 150 μL of CHCl_3 . After vortexing, 50 μL of the lipid suspension were transferred to GC-MS vials. Then, in each vial, it was added 25 μL of an internal standard solution. The standard solution was the FA C9:0 (Merck, Sigma-Aldrich, Darmstadt, Germany) at 0.44 $\text{mg}\cdot\text{mL}^{-1}$ in CHCl_3 . Samples were derivatized by adding 50 μL of the trimethyl sulfonium hydroxide reagent (TMSH, Merck, Sigma-Aldrich, Darmstadt, Germany).

FA analysis was carried out using a Hewlett-Packard 6890 gas chromatograph (GMI, Ramsey, MI, USA) equipped with a capillary column packed with 70% cyanopropyl polyphenylene-siloxane BPX70 (length 60 m, internal diameter 0.25 mm, coating thickness 0.25 μm ; SGE Analytical Science Pty Ltd.; Victoria, Australia), coupled to a mass selective detector (5973; Agilent Technologies, Avondale, PA, USA).

The carrier gas was helium at 1.2 $\text{mL}\cdot\text{min}^{-1}$, and the column pressure was 1.3×10^5 Pa. Injection of 1 μL of the vial was done split-less at an injector temperature of 250°C. The oven temperature was held first for 1 min at 35°C and then increased from 35 to 100°C at 40°C $\cdot\text{min}^{-1}$. Then, it held for 1 min at 100°C and then raised from 100 to 130°C at 5°C $\cdot\text{min}^{-1}$, followed by an increase from 130 to 180°C at 1.5°C $\cdot\text{min}^{-1}$. Finally, from 180 to 240°C at 5°C $\cdot\text{min}^{-1}$. The transfer line temperature was set at 280°C. The MS source temperature and MS Quad were set at 230°C and 150°C, respectively.

FA were first identified by comparison of their retention times with those of known standards (Merck, Sigma-Aldrich, Darmstadt, Germany), and this identification was confirmed using the mass selective detector at a scan rate of 3.14 scans $\cdot\text{s}^{-1}$, with data collected in the range of 33 to 500 amu. The mass spectra of the FA were compared with the Wiley data bank, NIST 2020. L (Hewlett-Packard, Gaithersburg, MD, USA). The quantification of FA was calculated on target ions using external calibration performed with serial dilutions of commercial standards of fatty acids methylated with TMSH (Merck, Sigma-Aldrich, Darmstadt, Germany) and C9:0 as the internal standard. Results were expressed as relative percentages of each fatty acid, standing for the sum of the absolute concentrations of all the fatty acids in the sample.

5.4.2.2. Lipid classes determination of the total lipid extract at t_{h3}

The different lipid classes present in the *L. bulgaricus* CFL1 membrane were identified for only the cells harvested at the highest biomass concentration (t_{h3}). Indeed, a high biomass concentration was necessary because the total lipid extract (LE) was further fractionated. The different lipid classes were identified by High-Performance Thin Layer Chromatography

(HPTLC) and by Liquid Chromatography-Tandem Mass spectrometry (LC-MS/MS). The former was useful to associate fatty acid chains with each lipid class.

i. Lipid extraction and fractionation

The total lipids of *L. bulgaricus* CFL1 were extracted according to the Bligh-Dyer procedure (Bligh and Dyer 1959). A comparison was made between the Folch and Bligh-Dyer method by FA determination. There was no difference in FA composition and quantification between both methods for at least three independent samples (Table S5.1). The Bligh-Dyer extraction procedure was chosen in this case because of the few samples per fermentation condition and the high quantity of cell biomass available to perform lipid extractions (three independent cultures for the harvest time at t_{h3}).

For each extraction, 20 mL of bacterial cell suspension were thawed at 42°C for 15 minutes in a water bath and centrifuged at 12 900 *g*, 4°C, for 10 min. The supernatant was removed, and the bacterial pellet was washed twice with 20 mL of 0.9% NaCl solution by centrifuging under the same conditions (12 900 *g*, 4°C, for 10 min) and removing the supernatant.

First, one gram of wet bacterial pellet was transferred to a first 50 mL-glass tube (Pyrex®, screw cap, Merck, Darmstadt, Germany). Then, 0.2 mL of 0.9% NaCl solution and 3.75 mL of chloroform (CHCl₃)-methanol (CH₃OH) (1:2, v/v) were added. The suspension was shaken on a rotary shaker at room temperature for three hours (Rotary shaker SB2/SB3-STUART, Evreux, France). After centrifugation at 515 *g*, 20°C, for 10 min (Eppendorf® Centrifuge 5804 R – Benchtop, Hamburg, Germany), the supernatant was transferred to a second 50 mL-glass tube. Five milliliters of 0.9% NaCl solution and five milliliters of CHCl₃ were added into this second 50 mL-glass tube, which contained the recovered supernatant. After the samples were vortexed and centrifuged (515 *g*, 20°C, for 15 min), two layers were observed: an upper layer and a lower layer, the former containing the total lipid extract of bacterial cells. The organic solvent was removed under vacuum using a rotary evaporator (Refrigerated Vapor Trap: RVT5105, ThermoFisher, MA, USA). The obtained total lipid extract (LE) was diluted in one milliliter of chloroform and stored at -20°C for further analysis.

About 850 µL of the total lipid extract in chloroform was loaded to a silica SPE (Solid Phase Extraction) column (SPE-PAK silica classic cartridge, 2 mL, Waters Corporation, Milford, MA, USA). The SPE column was previously conditioned with 20 mL of methanol and then washed with 20 mL of chloroform. After the addition of different solvents into the SPE column, the following fractions were obtained:

f₁, chloroform fraction: lipids were eluted after adding 20 mL of chloroform (CHCl₃).

f₂, chloroform-acetone fraction: lipids were eluted after adding 20 mL of chloroform-acetone (50:50, v/v).

f₃, acetone fraction: lipids were eluted after adding 20 mL of acetone (CH₃COCH₃).

f₄, methanol fraction: the phospholipids were finally eluted with 20 mL of methanol (CH₃OH).

Solvents were evaporated from all fractions under vacuum using a rotary evaporator (Refrigerated Vapor Trap: RVT5105, ThermoFisher, MA, USA). The dried lipid fractions were diluted in chloroform and stored at -20°C until use.

ii. Fatty acids determination for LE, f₁, f₂, f₃, and f₄

For the LE (before fractionation) and f₁, f₂, f₃, and f₄ (after fractionation by SPE column), the fatty acids were determined as described in subsection 5.4.2.1.

iii. Lipid classes identification by HPTLC analysis

HPTLC was performed on 10 cm × 20 cm dried glass-backed Silica Gel 60 HPTLC plates (HPTLC plates, Merck, Darmstadt, Germany). Plates were heated at 180°C for 30 min to minimize the background staining and to get rid of water traces.

In a fume hood, about 20 µg of each lipid sample (LE, f₁, f₂, f₃, and f₄) and lipid standards in chloroform were deposited automatically into 0.6 cm large bands at 0.1 cm·s⁻¹ and 0.87 cm apart from each other using a 25 µL solvent pipette (CAMAG® Automatic HPTLC Sampler III (ATS3), Chromacim SAS, Moirans, France).

Development was carried out at room temperature in a sealable HPTLC glass chamber (CAMAG® ADC2, Automatic Developing Chamber, Chromacim SAS, Moirans, France). Chloroform-methanol-propanol-2-KCl at 0.25%-Triethylamine (TEA) (30:9:25:6:18, v/v/v/v/v) was used as the developing solvent. The presence of different lipids in the LE and each fraction (f₁, f₂, f₃, and f₄) were revealed by dipping HPTLC plates in different reagents:

- (1) Copper sulphate (CuSO₄): phosphoric acid (H₃PO₄): sulfuric acid (H₂SO₄) (10:4:4, v/v/v) reagent for non-specific revelation (Fewster et al. 1969). Then, HPTLC plates were heated at 140°C for 30 min.
- (2) Alpha-naphthol reagent for glycolipids specific revelation (Wang and Benning 2011). Then, HPTLC plates were heated at 100°C for 5 min.
- (3) Ninhydrin reagent for lipids containing free amino groups (Hecht 1966). Then, HPTLC plates were heated at 100°C for 3 min.

The separated bands of the lipid samples (LE, f₁, f₂, f₃, and f₄) were compared with the standard bands. Neutral and phospholipids were identified by comparing the Retention factor (R_f) values of the samples with those of standards: FA: C16:0 and C18:1. Phospholipids: PE, phosphatidylethanolamine; PG, phosphatidylglycerol; CL, cardiolipin; PA, phosphatidic acid. Glycolipids: MGDG, monogalactosyldiacylglycerol and DGDG, digalactosyldiacylglycerol (Merck, Sigma-Aldrich, Darmstadt, Germany). Also, lipids were identified because of their reactivity to alpha-naphthol and ninhydrin reagents.

iv. Lipid classes identification by LC-MS/MS

The dried total lipid extract (LE) and lipid fractions issued from SPE fractionation (f_1 , f_2 , f_3 , f_4) were resuspended in 250 μL of a mixture of acetonitrile: isopropanol (7/3) ULC/MS grade (Biosolve, Chimie, Dieuze, France). After vortexing, the samples were injected (5 μL of the sample) into a liquid chromatography system (UltiMate 3000 UHPLC System, Thermo-Fisher, MA, USA) coupled to a quadrupole time of flight mass spectrometer (Q-ToF Impact II Bruker Daltonics, Bremen, Germany).

An EC 100/2 Nucleoshell Phenyl-Hexyl column (length 100 mm, internal diameter 2 mm, particle size 2.7 μm ; Macherey-Nagel, Düren, Germany) was used for chromatographic separation. The mobile phases used for the chromatographic separation were: (A) H_2O + 1% ammonium formate in H_2O + 0.1% formic acid; and (B) Acetonitrile: isopropanol (7:3) + 1% of 10 mM ammonium formate in H_2O + 0.1% formic acid. The flow rate was 400 $\mu\text{L}\cdot\text{min}^{-1}$. The following gradient was used: 45% of A for 1 min, followed by a linear gradient from 45% A to 30% A from 1 to 2 min, then a linear gradient from 30% A to 15% A from 2 to 7 min, a linear gradient from 15% A to 10% A from 7 to 15 min, a linear gradient from 10% A to 6% A from 15 to 19 min, a linear gradient from 6% A to 2% A from 19 to 26 min. 0% of A was held until 40 min, followed by a linear gradient from 0% A to 45% A from 40.1 to 45 min (45 min total run time).

For mass spectrometer analysis, data was performed in positive and negative ESI modes, using the following parameters: capillary voltage, 4.5 kV; nebulizer gas flow, 2.1 bar; dry gas flow, 6 $\text{L}\cdot\text{min}^{-1}$; drying gas in the heated electrospray source temperature, 200°C. Samples were analyzed at 8 Hz with a mass range of 100–1700 m/z . Stepping acquisition parameters were created to improve the fragmentation profile with a collision RF from 200 to 700 Vpp, a transfer time from 150 μs , and collision energy from 20 to 40 eV. Each cycle included an MS full scan and 5 MS/MS CID on the 5 primary ions of the previous MS spectrum.

The data processing was performed from *.d* data files (Bruker Daltonics, Bremen, Germany). These files were converted to *.mzXML* format using the MSConvert software (ProteoWizard package 3.0 (Chambers et al. 2012)). *mzXML* data processing, mass detection, chromatogram building, deconvolution, samples alignment, and data export were performed using the MZmine 2.53 software (Pluskal et al. 2010) for both positive and negative data files. The ADAP chromatogram builder (Myers et al. 2017) method was used with a minimum group size of scan 3, a group intensity threshold of 1000, a minimum highest intensity of 1000, and m/z tolerance of 2 ppm. Deconvolution was performed with the ADAP wavelets algorithm using the following settings: S/N threshold 10, peak duration range = 0.01–2 min of Retention Time (RT) wavelet range 0.01–0.2 min. MS^2 scans were paired using an m/z tolerance range of 0.05 Da and RT tolerance of 0.5 min. Then, the isotopic peak grouper algorithm was used with an m/z tolerance of 2 ppm and RT tolerance of 0.2 min. All the peaks were filtered using a feature list

row filter keeping only peaks with the MS² scan. The alignment of samples was performed using the join aligner with an m/z tolerance of 2 ppm, a weight for m/z and RT at 1.0 min, And a retention time tolerance of 0.2 min.

For lipids identification (annotation), the first research in the library of Mzmine was done. This library contains an identification module and custom database, currently including 93 annotations (RT and m/z) in positive mode and negative mode, with RT tolerance of 0.2 min and m/z tolerance of 0.005 Da. Then, molecular networking of lipidomic data and lipid annotation by MS² spectral libraries were performed.

Molecular networking was generated by the MetGem software (Olivon et al. 2018) using the .mgf and .csv files obtained from MZmine 2.53 analysis. The molecular network was optimized for the ESI+ and ESI- datasets and different cosines cosine similarity score thresholds were tested. ESI- and ESI+ molecular networks were generated using cosine score thresholds of 0.7 and 0.65, respectively.

Lipid annotations were performed in different consecutive steps. First, the ESI- and ESI+ metabolomic data used for molecular network analyses were searched against the available MS² spectral libraries (Massbank NA, GNPS Public Spectral Library, NIST14 Tandem, NIH Natural Product, Lipid Blast, and User database of the platform), with absolute m/z tolerance of 0.02; 4 minimum matched peaks and minimal cosine score of 0.65. Second, in the different clusters of the molecular network, the result of the database search was validated using the different specific fragments and neutral loss for the different lipid class with their MS² spectrum (Lipid-Class-Specific Fragments - Lipidomics-Standards-Initiative (LSI)). If the database search result was validated, annotation of other features was performed by stepwise comparison from the valid lipid metabolite. Finally, for the cluster of molecular networks that had no database search result, Sirius software was used. This software provides a computational approach for molecular structure databases (Dührkop et al. 2019).

5.4.3. Biophysical properties of *L. bulgaricus* CFL1 membrane lipids

5.4.3.1. Temperatures of lipid phase transition by Fourier Transformed Infrared (FTIR) spectroscopy

The lipid transition temperature of *L. bulgaricus* CFL1 cells was determined using FTIR spectroscopy by monitoring the absorbance band positions of the symmetric CH₂ stretching vibration band ($\nu_{sym}CH_2$) arising from the lipid acyl chains of the membrane, located around 2850 cm⁻¹ (Crowe et al. 1989b; Mantsch and McElhaney 1991).

From each fermentation condition and harvest time, protected bacterial suspensions were thawed at 42°C for 5 min in a water bath and centrifuged at 12 900 *g*, 4°C, for 10 min (Eppendorf® Centrifuge 5804 R – Benchtop, Hamburg, Germany). At room temperature, the

supernatant was removed, and the small amount of the resulting cell pellet was tightly sandwiched between two calcium fluoride (CaF₂) windows (ISP Optics; Riga, Latvia).

Infrared absorption measurements were carried out in a transmission mode using a Nicolet Magna 750 FTIR spectrometer (Thermo Fisher Scientific; Madison, WI, USA) equipped with a narrow band mercury/cadmium/telluride (MCT) infrared detector and a Specac variable temperature cell holder cooled by liquid nitrogen (Specac, Ltd., Orpington, Kent, UK).

L. bulgaricus CFL1 cell pellet was cooled from 50°C to -50°C at a rate of 2°C·min⁻¹ and then heated from -50°C to 50°C at the same rate. The temperature of the sample was recorded separately using an extra thermocouple that was located close to the sample. The optical bench was continuously purged with dry air (Balston; Haverhill, MA, USA).

Omic software (version 7.1, Thermo Fisher Scientific; Madison, WI, USA) was used for spectra acquisition: 32 co-added scans were collected every 45 s with a resolution of 4 cm⁻¹ (approximately one scan/°C by stepped temperature ramping) in the mid-IR region from 4000 to 900 cm⁻¹. Spectral analyses were performed according to Meneghel et al. (2017). Briefly, the ASplR house-developed software (Infrared Spectra Acquisition and Processing, INRAE; Thiverval-Grignon, France) was used to analyze each spectrum. The peak position in each spectrum was determined using their second-order derivative and smoothed according to a seven-point Savitsky-Golay algorithm. Wavenumbers peaks of $\nu_{sym}CH_2$ were then plotted against the temperature at which they were measured. The $\nu_{sym}CH_2$ peak position versus temperature plots arising from *L. bulgaricus* CFL1 samples were fitted with a curve based on an asymmetric sigmoid transition model. The first-order derivative of the fitted curves was calculated. Lipid phase transition temperatures were determined using the maximum of these first-order derivatives upon cooling (T_s in °C, lipid solidification) from 50°C down to -50°C and heating (T_m in °C, lipid melting) from -50°C to 50°C (Figure S5.2).

5.4.3.2. Membrane fluidity by fluorescence anisotropy

Membrane fluidity was evaluated on protected frozen-thawed cells by measuring the degree of polarization of the fluorescent probe 1,6-diphenyl-1,3,5-hexatriene (DPH). This fluorescence probe has hydrophobic properties that allow the molecule to be inserted into the lipid membrane of the cells.

Fluorescence anisotropy was measured according to the method developed by Bouix and Ghorbal (2017). Briefly, bacterial suspension adjusted to 10⁷ cells·mL⁻¹ was washed twice with morpholine ethane sulfonic acid (MES) buffer (Merck, Sigma-Aldrich, Darmstadt, Germany), and resuspended in 2 mL of MES buffer adjusted at pH 5.5 with KOH at 30% (VWR, Leuven, Belgium). Then, 5 µL of DPH solution (6 mM in DMSO) (Merck, Sigma-Aldrich, Darmstadt, Germany) was added to 1 mL of the cell suspension to obtain a final DPH concentration of 30 µM.

The cell suspension was vigorously stirred for 1 min and centrifuged (14 000 *g*, 20°C, for 90 s), and the pellet obtained was resuspended in 2 mL of the MES buffer, pH 5.5, and used immediately for fluorescence polarization measurements. Fluorescence polarization was determined by using a flow cytometer (CyFlow Space cytometer, Sysmex-Partec, Villepinte, France) equipped with a vertically polarized UV laser that emits at 488 nm a half-wave retarder plate (rotating polarizer) to depolarize the excited light, if necessary, and parallel and perpendicular polarizers just prior to entering the two photomultiplier tubes. The measurement was performed at 20°C with emission wavelengths at 375 nm. The fluorescence anisotropy (*r*) was calculated according to the following equation:

$$r = \frac{I_{//} - I_{\perp}}{I_{//} + 2I_{\perp}} \quad (5.1)$$

Where $I_{//}$ and I_{\perp} are the polarized light intensities emitted in the parallel and perpendicular directions with respect to the excitation beam of light, respectively.

5.4.4. Freezing and freeze-drying protocols

The protected bacterial suspension was aliquoted in cryo-tubes (Sarstedt, Nümbrecht, Germany) with a volume of one milliliter before freezing. Then, the samples were frozen at -80°C, at a freezing rate of 3°C·min⁻¹ (Freezer Froilabo, BM 1000, Meyzieu, France).

For freeze-drying, this same protected cell suspension was also aliquoted in five-milliliter vials (Verretubex, Nogent-Le-Roi, France) containing one milliliter of cell suspension. Then samples were frozen under the above-described conditions (-80°C, 3°C·min⁻¹). Frozen samples were transferred to a pre-cooled shelf at -50°C in a REVO pilot-scale freeze-dryer (Millrock Technology, Kingston, New York, USA). After a holding step of 1.5 hours at -50°C, the chamber pressure was decreased to 10 Pa, and the shelf temperature was increased from -50°C to -20°C at a heating rate of 0.25°C·min⁻¹ to initiate sublimation. After 40 hours of sublimation (primary drying), the shelf step was increased to 25°C at a heating rate of 0.25°C·min⁻¹. After ten hours of desorption (secondary drying step), the vacuum was broken by injecting air into the drying chamber. The vials were then taken out of the freeze-dryer to be manually capped by inserting a rubber stopper. The vials were packed in multi-layer aluminum bags, and the bags were hermetically closed using a vacuum sealer (Bernhardt, Wimille, France).

5.4.5. Resistance of *L. bulgaricus* CFL1 cells by their loss of functional properties

The resistance of *L. bulgaricus* CFL1 cells was determined by their loss of acidifying activity and culturability after the stabilization process. These functional properties were measured for protected bacterial suspensions before (initial) and after freezing and freeze-drying.

For frozen bacterial suspensions, they were thawed at 42°C for 5 min in a water bath. For freeze-dried samples, they were rehydrated in 1 mL skim milk solution (100 g·L⁻¹) at 42°C. This

solution was prepared using milk powder (EPI-Ingredient, Ancenis, France) and heat-treated at 110°C for 20 min; then, samples were stirred at room temperature for 5 min.

The acidifying activity of the protected bacterial suspension was measured by the Cinac system (AMS Alliance, Frepillon, France). One hundred microliters of protected bacterial suspension were inoculated and incubated at 42°C in 100 mL of skim milk solution at 100 g·L⁻¹ (EPI-Ingredient, Ancenis, France). This skim milk solution that was previously heat-treated at 110°C for 20 min. The pH of the inoculated skim milk solution was continuously measured by the Cinac system and determined the time necessary to obtain a decrease of 0.7 pH units ($t_{\Delta\text{pH}0.7}$, in minutes). The descriptor $t_{\Delta\text{pH}0.7}$ was used to characterize the acidifying activity of protected bacterial suspensions. The higher the $t_{\Delta\text{pH}0.7}$ value was, the lower the acidifying activity was observed. The measurements per sample were performed in triplicate.

The culturability was determined using the agar plate count method. One hundred microliters of protected bacterial suspension were serially diluted in saline water (NaCl 0.9% w/w) and plated onto MRS agar (Biokar Diagnostics, Paris, France). Plates were anaerobically incubated at 42°C for 48 h. Plate counts between 30 and 300 colony-forming units (CFU) were kept to determine bacterial cell concentration. The bacterial cell count was expressed in CFU·mL⁻¹. The measurements per sample were performed in triplicate.

The specific acidifying activity (t_{spe}), thus, is defined as the ratio of acidifying activity ($t_{\Delta\text{pH}0.7}$) in minutes to the corresponding log of cell concentration in CFU·mL⁻¹ (Streit et al. 2007) (Equation 5.2).

$$t_{\text{spe}} = \frac{t_{\Delta\text{pH}0.7}(\text{minutes})}{\log(\text{CFU} \cdot \text{mL}^{-1})} \quad (5.2)$$

The specific acidifying activity as mentioned above was determined before (initial, $t_{\text{spe}I}$), after freezing ($t_{\text{spe}F}$), and freeze-drying ($t_{\text{spe}FD}$). Therefore, the loss of specific acidifying (dt_{spe}) per stabilization process was calculated as the following equations (Equations 5.3 and 5.4):

$$dt_{\text{spe}F} (\text{Freezing}) = t_{\text{spe}F} - t_{\text{spe}I} \quad (5.3)$$

$$dt_{\text{spe}FD} (\text{Freeze-Drying}) = t_{\text{spe}FD} - t_{\text{spe}I} \quad (5.4)$$

5.4.6. Statistical analysis

For the loss of functional properties, biophysical properties (lipid phase transition temperatures and membrane fluidity), and fatty acid composition of the total lipid extract (LE), the fermentations were carried out three times per fermentation condition (three independent biological replicates). Data were the result of the mean and standard deviation of the biological replicates. Statistical analyses were performed for these results.

For lipid class identification and fatty acid composition of each fraction, two independent biological replicates were used per fermentation condition.

5.4.6.1. Differences among fermentation conditions and harvest times

One-way analyses of variance (ANOVA) were used to determine the significant differences in the means of each fermentation condition and harvest times for the following measurements: (i) fatty acids composition of the total lipid extract (LE), (ii) biophysical properties of lipids (lipid phase transition temperatures and membrane fluidity), and (iii) *L. bulgaricus* CFL1 resistance (the loss of functional properties). Significance levels of 95 % (P -value < 0.05) were considered. ANOVA test followed by a post-hoc Tukey (HSD) test were performed (XLSTAT 2020.5, Addinsoft, Paris, France).

5.4.6.2. Clustering analysis for lipid classes

Heatmaps and hierarchical clustering analysis were used to analyze the abundance of the different lipids in the *L. bulgaricus* CFL1 membrane. Both analyses were performed by the open-source software MultiExperiment Viewer (MeV, version 4.9.0, Dana–Farber Cancer Institute, MA). The statistical significance was set at P -value < 0.05.

Heatmaps were generated for each lipid class (e.g., phospholipids or glycolipids). In a heatmap, each row represents the peak area of the lipid identified (a lipid with its corresponding fatty acid chains). In a row, the blue and yellow boxes are the least and the most abundant lipids (respectively) among the samples. The data from each row were normalized by subtracting the mean (row) from each peak area and dividing the standard deviation (row). The hierarchical clustering grouped similar peak areas of the samples by using a Pearson correlation as a distance function.

5.4.6.3. Correlation of Pearson and Principal Component Analysis (PCA)

To link the biochemical characterization and biophysical properties of membrane lipids to freezing and freeze-drying resistance of *L. bulgaricus* CFL1, a Pearson correlation and PCA analysis were carried out (XLSTAT 2020.5, Addinsoft, Paris, France).

The following variables were considered for the Pearson correlation and PCA: Saturated Fatty Acids (SFA), Unsaturated Fatty Acids (UFA), membrane fluidity (by fluorescence anisotropy, r), lipid transition temperatures (T_s and T_m), and the losses of specific acidifying activity during freezing (dt_{spe} F) and freeze-drying (dt_{spe} FD). The significance of the results was assessed at a 95% confidence level (P -value < 0.05).

5.5. Results

5.5.1. Membrane lipid compositions of *L. bulgaricus* CFL1 for the four fermentation conditions

5.5.1.1. Fatty acids composition of the total lipid extract (LE) at t_{h1} , t_{h2} , t_{h3}

In Table S5.2, the relative percentages of the Fatty Acid (FA) composition per fermentation condition at each harvest time (t_{h1} , t_{h2} , t_{h3}) are presented. Lipid extraction was performed similarly for *L. bulgaricus* CFL1 cells produced from the four fermentation conditions. No difference in FA concentration was found ($2.6 \pm 0.2 \text{ mg}\cdot\text{mL}^{-1}$, Folch method).

A total of fifteen fatty acids were identified in *L. bulgaricus* CFL1, in which six FA represented more than 90% of the total FA composition. These were C14:0, C16:0, C16:1 cis-9; C18:1 cis-9; C18:2 cis9, trans 11 and cycC19:0. For the sake of clarity and an easy comparison with literature data, we grouped lipids into three categories (Figure 5.2): Saturated Fatty Acids (SFA), Unsaturated Fatty Acids (UFA), and Cyclic Fatty Acid (CFA).

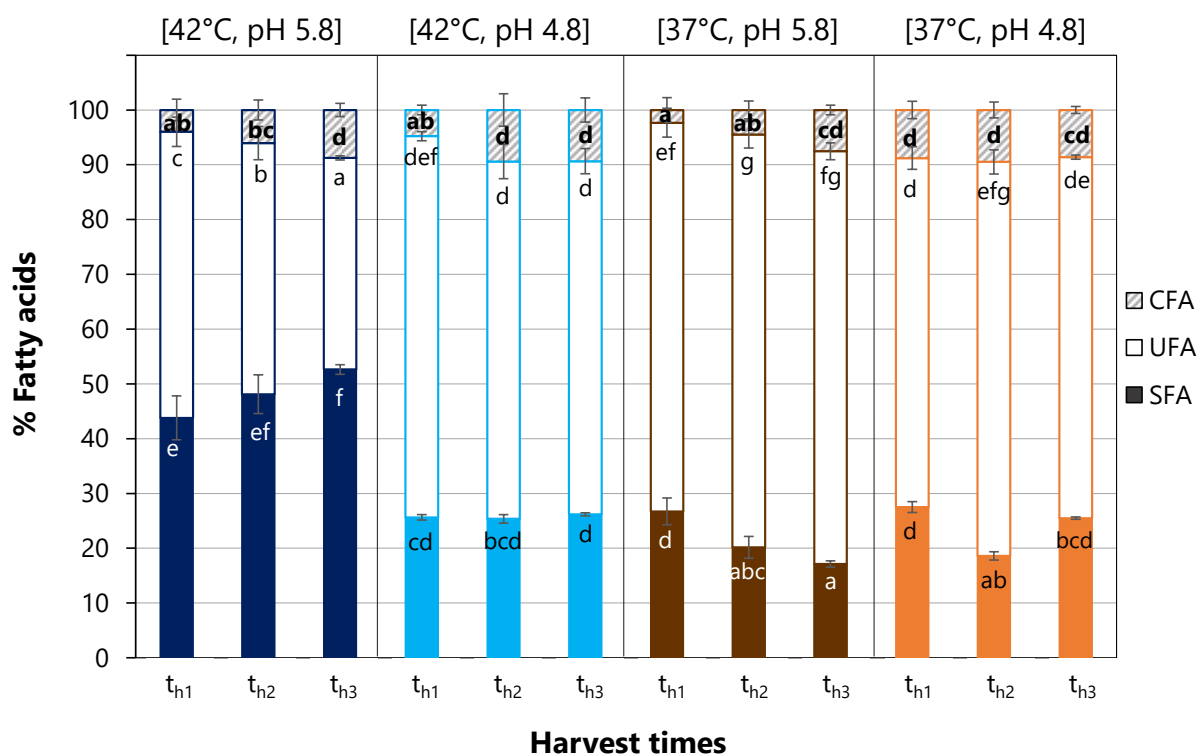


Figure 5.2 The distribution in relative percentage of Saturated Fatty Acids (SFA), Unsaturated Fatty Acid (UFA) and Cyclic Fatty Acid, cycC19:0 (CFA) of the total lipids extracted from *L. bulgaricus* CFL1. Cells were cultivated at four fermentation conditions and harvested at different harvest times. t_{h1} : mid-exponential growth phase; t_{h2} : deceleration growth phase; t_{h3} : stationary growth phase. Values are the mean of at least three independent biological replicates. Letters represent significant differences among fermentation conditions and harvest times at a 95% confidence level.

SFA include C12:0, C14:0, C15:0, C16:0, C17:0, C18:0, C22:0. UFA encompass C16:1 trans 9, C16:1 cis 9, C18:1 trans 9, C18:1 cis 9, C18:1 cis 11, C18:2 cis 9 cis 12, C18:2 cis 9 trans 11. CFA corresponds to cyc C19:0.

The saturated fatty acids (SFA) consisted of >70% of C14:0 and C16:0. In comparison, the unsaturated fatty acids (UFA) were represented by more than 60% of C16:1 cis-9 and C18:1 cis-9. The cyclic fatty acid (CFA) content ranged between 2-10%.

Figure 5.2 shows at least a two-fold increase in SFA content when *L. bulgaricus* CFL1 cells were grown at [42°C, pH 5.8], compared to the three other fermentation conditions (44-53% vs. 17-28%). At pH 5.8, low fermentation temperature significantly affected the UFA content of *L. bulgaricus* CFL1. Regardless of harvest time, bacteria exhibited higher UFA content when cells were grown at 37°C than at 42°C (about 37-92% of increase). At pH 4.8, the effect of growth temperature on UFA was not significant.

For three out of four fermentation conditions ([42°C, pH 5.8], [42°C, pH 4.8], and [37°C, pH 5.8]), the harvest time had a significant effect on CFA. For the fermentations carried out at pH 5.8, a progressive increase of CFA content was observed according to the increment of the harvest time (from t_{h1} , then t_{h2} , to t_{h3}).

The results from Table S5.2 also led to the calculations of the ratios UFA/SFA (Figure 5.3 (A)), CFA/UFA (Figure 5.3 (B)), and CFA/SFA (Figure 5.3 (C)).

Three levels of the UFA/SFA values were observed (Figure 5.3 (A)). A first low level was displayed for cells cultivated at [42°C, pH 5.8] (UFA/SFA = 0.7-1.2). Then, an intermediate level of UFA/SFA was shown for the fermentation condition at 42°C, pH 4.8 (UFA/SFA = 2.5-2.7), and some harvest times of [37°C, pH 5.8] (UFA/SFA = 2.7, t_{h1}) and [37°C, pH 4.8] (UFA/SFA = 2.3, t_{h1} and 2.6, t_{h3}). Finally, *L. bulgaricus* CFL1 exhibited the highest ratio UFA/SFA for bacteria harvested at t_{h2} and grown at 37°C (regardless of pH), as well as at t_{h3} at [37°C, pH 5.8].

Concerning the ratio CFA/UFA (Figure 5.3 (B)), it was significantly affected by the harvest time, temperature, and pH. For instance, the lowest CFA/UFA ratio resulted from the low CFA content in the bacteria harvested at t_{h1} (2-5%) and cultivated in the two fermentation conditions carried out at [42°C, pH 4.8] and at [37°C, pH 5.8]. Intermediate CFA/UFA values (CFA/UFA = 0.10-0.15) were obtained for the four fermentation conditions at different harvest times: t_{h2} for [42°C, pH 5.8], t_{h2} and t_{h3} for [42°C, pH 4.8], t_{h3} for [37°C, pH 5.8], and all the harvest times for [37°C, pH 4.8]. The highest CFA/UFA ratio (CFA/UFA = 0.22) was only observed for t_{h3} at [42°C, pH 5.8] since this fermentation condition led to the lowest UFA (39%) and relative high CFA content (9%).

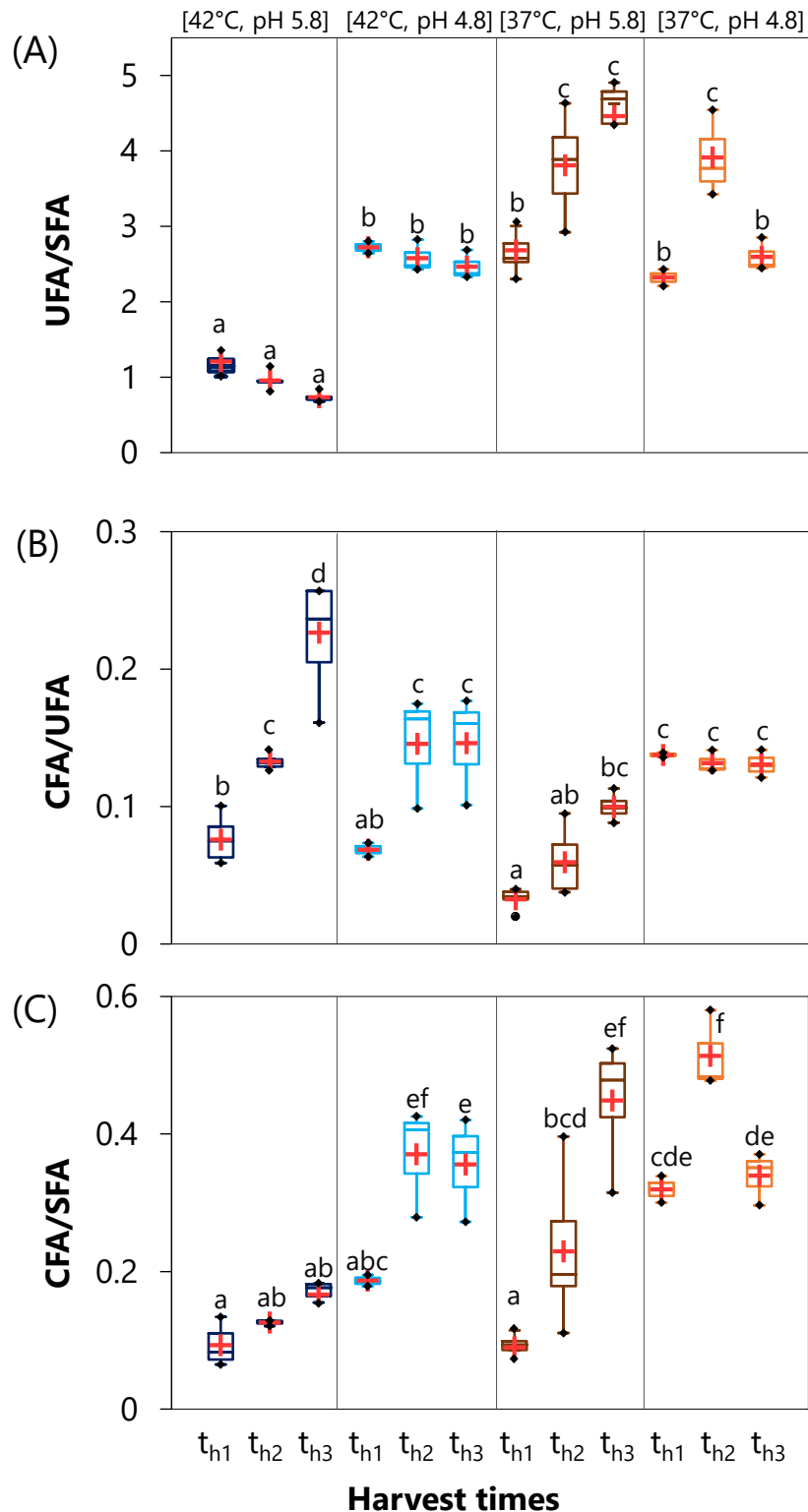


Figure 5.3 Ratios of the different groups of fatty acids in *L. bulgaricus* CFL1 cells: (A) UFA/SFA, (B) CFA/UFA, (C) CFA/SFA. Cells were cultivated at four fermentation conditions and harvested at different harvest times. t_{h1} : mid-exponential growth phase; t_{h2} : deceleration growth phase; t_{h3} : stationary growth phase. The boxplots (mean = red cross and median = line in the middle of the box) come from at least three independent biological replicates. Superscript letters represent significant differences between samples at a 95% confidence level.

When analyzing the CFA/SFA ratio (Figure 5.3 (C)), this ratio was different according to the fermentation condition. For [42°C, pH 5.8] and regardless of harvest time, this fermentation condition led to the lowest ratio (CFA/SFA = 0.09-0.16) due to the predominant content of SFA. The highest ratio (CFA/SFA = 0.36-0.51) was obtained by the three remaining fermentation conditions: [42°C, pH 4.8], [37°C, pH 5.8], and [37°C, pH 4.8]) at t_{h3} , in which CFA and low SFA content were observed.

5.5.1.2. Lipid composition at t_{h3}

i. Lipid fractionation

For each fermentation condition, *L. bulgaricus* CFL1 cells harvested at the stationary growth phase (t_{h3}) gave sufficient biomass, allowing a complete characterization of the bacterial lipids, particularly membrane lipids. A pool of samples harvested at t_{h3} in the same growth conditions were produced and analyzed by complementary methods.

Each total lipid extract per fermentation condition had the same fatty acid concentration ($2.5 \pm 0.2 \text{ mg}\cdot\text{mL}^{-1}$, Bligh and Dyer method). This total lipid extract was fractionated using an SPE column and different solvents, giving four different fractions per condition (f_1 , f_2 , f_3 , and f_4), corresponding to lipids with different polarities.

The fractions were further analyzed to determine their Fatty Acids (FA) composition by GC-MS and their lipid classes by HPTLC and LC/MS-MS. The latter method allowed a fine identification and the repartition of fatty acid chains on each lipid class.

For each fermentation condition harvested at t_{h3} , the FA content in the four fractions is illustrated in Figure 5.4. Each fermentation condition had the same content in fatty acid per fraction: 39-41% of the fatty acid content is in f_1 (chloroform fraction), the remaining 58-62% is distributed in f_2 (chloroform-acetone fraction) in a low proportion (9-11%) and in similar proportions for f_3 (acetone fraction) (21-25%) and f_4 (methanol fraction) (27-32%).

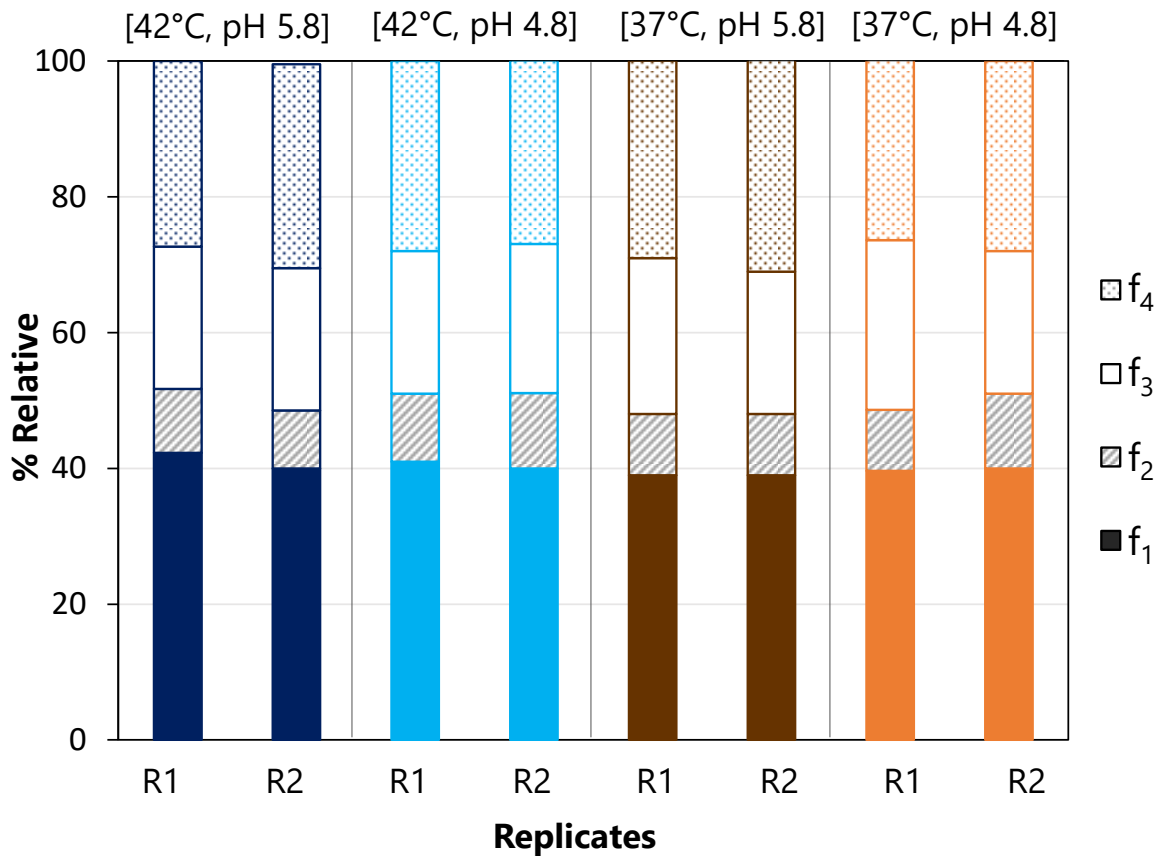


Figure 5.4 Fatty acids content in different fractions of the total lipids extracted from *L. bulgaricus* CFL1 harvested at the stationary growth phase (t_{h3}) for the four fermentation conditions studied. Each lipid extract was fractionated by the elution of different solvents: f_1 , chloroform; f_2 , chloroform-acetone (50/50); f_3 , acetone; and f_4 , methanol. Two independent biological replicates are represented by R1 (Replicate 1) and R2 (Replicate 2).

When comparing the four fermentation conditions, minor variations in fatty acid distribution per fraction were within the fluctuations of the biological replicates. These results suggest that the relative concentration of fatty acid in each fraction was constant, whatever the fermentation condition.

ii. Fatty acid composition of each fraction at t_{h3}

Although the total concentration of fatty acids was unchanged. Figure 5.5 allows us to examine the distribution of fatty acids into three categories according to the fractions by fermentation condition.

Figure 5.5 shows the SFA, UFA, and CFA contents per fraction. For each fermentation condition, the four different fractions were compared to the total lipid extract (LE). We obtained similar profiles of the fatty distribution as those previously reported in Figure 5.2.

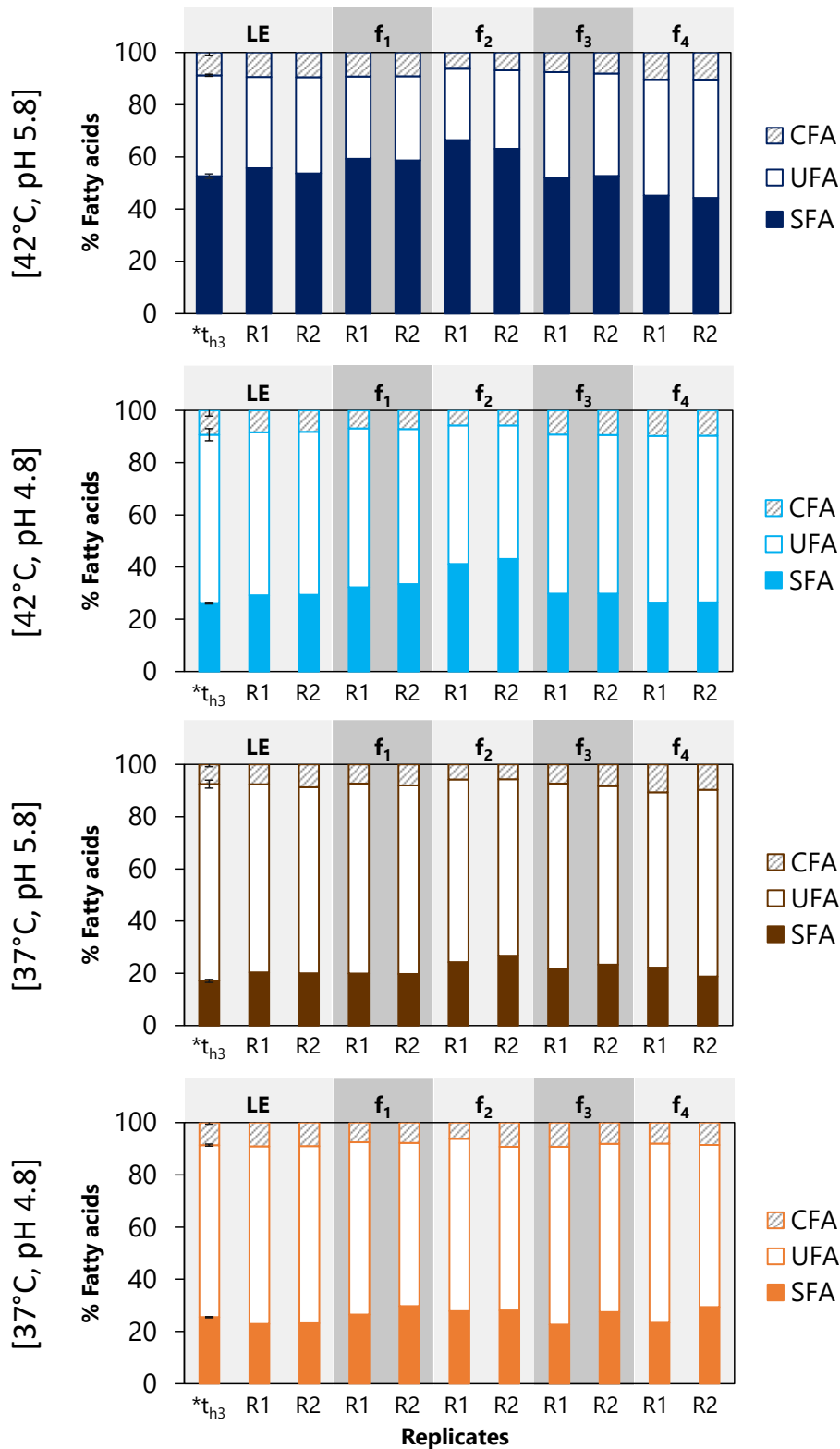


Figure 5.5 The distribution in relative percentage of Saturated Fatty Acids (SFA), Unsaturated Fatty Acid (UFA) and Cyclic Fatty Acid, cycC19:0 (CFA) of the fractions obtained after fractionation of the total lipid extract of *L. bulgaricus* CFL1. Cells were cultivated at four fermentation conditions and harvested at the stationary growth phase (t_{h3}). $*t_{h3}$, FA results showed in Figure 5.2. Each lipid extract was fractionated by the elution of different solvents: f_1 , chloroform; f_2 , chloroform-acetone (50/50); f_3 , acetone; and f_4 , methanol. Two independent biological replicates are represented by R1 (Replicate 1) and R2 (Replicate 2).

Regardless of fractions, the SFA content was the highest for the cells grown at [42°C, pH 5.8] (45-59%). In contrast, the UFA content was predominant for the fermentation conditions performed at 37°C (64-73%). Concerning the CFA content, the four fermentation conditions led to values between 6-10%.

When analyzing the four fractions per fermentation condition, the composition of the fraction f_1 is relatively similar to the composition of the LE. For the fermentations carried out at 42°C, the profile of other fractions (f_2 , f_3 , and f_4) was different with respect to LE. The fraction f_2 , for both fermentations at 42°C, exhibited the highest SFA content (pH 5.8: 65% and pH 4.8: 42%) and the lowest UFA content (pH 5.8: 29% and pH 4.8: 52%). Conversely, f_3 and f_4 showed an SFA decrease with a concomitant increase of UFA. Additionally, from f_2 to f_4 , an increase in CFA was observed (pH 5.8: from 7% to 11% and pH 4.8: from 6% to 10%) while the polarities of lipids increased in these fractions.

For the two fermentations carried out at 37°C (Figure 5.5), variations in the SFA, UFA, and CFA contents showed no prominent differences among f_1 , f_2 , f_3 , and f_4 .

At 42°C, fraction f_2 was always richer in SFA, and fraction f_4 was less rich in SFA. At 37°C, this effect was less marked and the distribution remained similar for all fractions.

iii. Identification of lipid classes of each fraction at t_{h3} by HPTLC

A first global identification of lipid classes was carried out by HPTLC. The same profile was observed regardless of the fermentation conditions (Figure S5.3). Ten lined spots on the fraction LE were distributed into the subsequent fractions. The bands on the top of the plate were mainly found in f_1 and f_2 , while the bands on the bottom were observed in f_3 and f_4 . The R_f of the fraction samples was compared with different phospholipids and glycolipids standards. In addition, plates were colored by specific dipping solutions: α -naphthol to reveal glycolipids and ninhydrin to reveal phospholipids with an amine group (Phosphatidylethanolamine, PE or phosphatidylserine, PS).

According to the R_f of the lipid standards (Figure S5.3), LE and f_1 in the four fermentation conditions contained mainly triglycerides (Figure S5.3, band n°1, $R_f = 0.90$).

The specific dipping solutions allowed identifying glycolipids primarily in the fractions f_1 , f_2 , f_3 , and in the bottom of the plate for f_4 (Figure S5.4). There was a shift in the R_f between the two reference glycolipids (standards) monogalactosyldiacylglycerol, MGDG, ($R_f = 0.60$) and galactosyldiacylglycerols, DGDG, ($R_f = 0.29$) and the glycolipids found in the fractions f_1 , f_2 , and f_3 . For example, f_1 and f_2 had a glycolipid band at $R_f = 0.70$ (Figure S5.4, band n°2), upper to the reference compound MGDG, whereas f_3 had a glycolipid band observed at $R_f = 0.42$ (Figure S5.4, band n°6), upper to the reference compound DGDG. These results indicate that the glycolipids identified in the fractions of our samples had different fatty acid chains from C18:3 found in the reference samples.

The bands observed at the bottom of the plate (Figure S5.4: bands n°8, 9, and 10) were not identified by the glycolipids' standards at our disposal. We speculate that these glycolipids had fatty acid chains below carbon number C18.

In f_4 , the phospholipid identified was phosphatidylglycerol (PG) (Figure S5.3, band n°4, $R_f = 0.58$) and possibly Cardiolipin (CL) or the free fatty acid C18:1 (Figure S5.3, band n°3 $R_f = 0.63$). The ninhydrin dipping solution revealed the absence of PE and PS in all fractions (Figure S5.5).

iv. Lipid classes of each fraction at t_{h3} by LC-MS/MS

GC-MS and HPTLC provided separate information on the lipid composition of *L. bulgaricus* CFL1. The first method allowed the determination of the fatty acid chains, and the second one a first identification of lipid classes. LC-MS/MS analysis was performed to complete the description by associating fatty acid chains to lipid classes such as diacylglycerols (DAG), triacylglycerols (TAG), monoglycodiacylglycerols (MGDG) diglycodiacylglycerols (DGDG), and phosphatidylglycerols (PG) (Table S5.3).

To determine in which fraction a lipid class is more predominant than in another, heat maps were used; these representations enabled us to visualize the relative abundance of each lipid class by the peak areas (from Figure S5.6 to Figure S5.12). The heatmap within each fermentation contains five columns and several rows. The columns represent the LE and four fractions obtained (per fermentation condition). Each row corresponds to a specific lipid class with its fatty acid chains. The two types of ionizations (positive and negative) are displayed in Figures S5.6 to S5.12. The positive ionization in mass spectrometry involves the formation of positive ions, whereas the negative ionization forms negatively charged ions. Some molecules are more sensitive to one of these ionizations (Schiller et al. 2004). Thus, looking into both ionizations provided a broad lipids identification.

For each fraction, the results observed in HPTLC were confirmed and identical lipids were found per fermentation condition: PG, glycolipids such as MGDG and DGDG (the hexose moieties were not identified), and TAG. Additionally, PE and PS were not identified by LC-MS/MS. Based on the HPTLC and LC-MS/MS results, the composition of each fraction is summarized in Table 5.1.

Table 5.1 Main lipids found after fractionation (f_1, f_2, f_3, f_4) the total lipid extract (LE) of *L. bulgaricus* CFL1. Cells were harvested at the stationary growth phase (t_{h3}).

Fraction	TAG	MGDG	DGDG	PG	Supplementary Figures
f_1	+	+	-	-	S5.6, S5.7 and S5.8
f_2	+/-	+	-	-	S5.6, S5.7 and S5.8
f_3	-	-	+	-	S5.9 and S5.10
f_4	-	-	-	+	S5.11 and S5.12

Abbreviations: TAG, triacylglycerol; MGDG, monoglycodiacylglycerols; DGDG, diglycodiacylglycerols; PG, phosphatidylglycerols; (+), higher relative abundance; (-), lower relative abundance.

From the information provided in Table 5.1, we focused on membrane lipids (glycolipids and phospholipids). Heatmaps were again used to represent the relative abundance of membrane lipids for each fermentation condition. The columns represent a specific fraction, and each row depicts a lipid class with its fatty acid chains. The purpose was to compare the relative abundance of a membrane lipid among the four fermentation conditions. For reasons of clarity, one biological replicate is represented in the following heatmaps figures (from Figure 5.6 to Figure 5.9).

(1) Glycolipids: monoglycodiacylglycerols, MGDG (Figure 5.6)

In Figure 5.6, MGDG (primarily found in f_1) are shown at both ionization modes (ESI + and ESI -). For both ionization modes, the heatmaps profile of MGDG was identical, indicating no bias due to ionization. The fermentation conditions were clustered according to the pH (pH 5.8: A_ f_1 and C_ f_1 ; pH 4.8: B_ f_1 and D_ f_1).

The FA found in MGDG corresponded to the main FA determined by GC-MS, namely: C12:0, C14:0, C16:0, C16:1, C18:0, C18:1, C18:2, and CFA. The fermentation condition [42°C, pH 5.8] (A_ f_1) induced a membrane containing MGDG enriched with saturated chains (C14:0 and C16:0), two and three monounsaturated chains (C18:1), and two CFA chains. On the contrary, at [37°C, pH 5.8] (C_ f_1), MGDG contained chains with 18 carbons, most of which were mono or di unsaturated. At low pH ([42°C, pH 4.8], B_ f_1 and [37°C, pH 4.8], D_ f_1), the MGDG exhibited a diversity of saturated and unsaturated fatty acids (C10:0, C12:0, C14:0, C16:0, C18:0, C18:1, and C18:2).

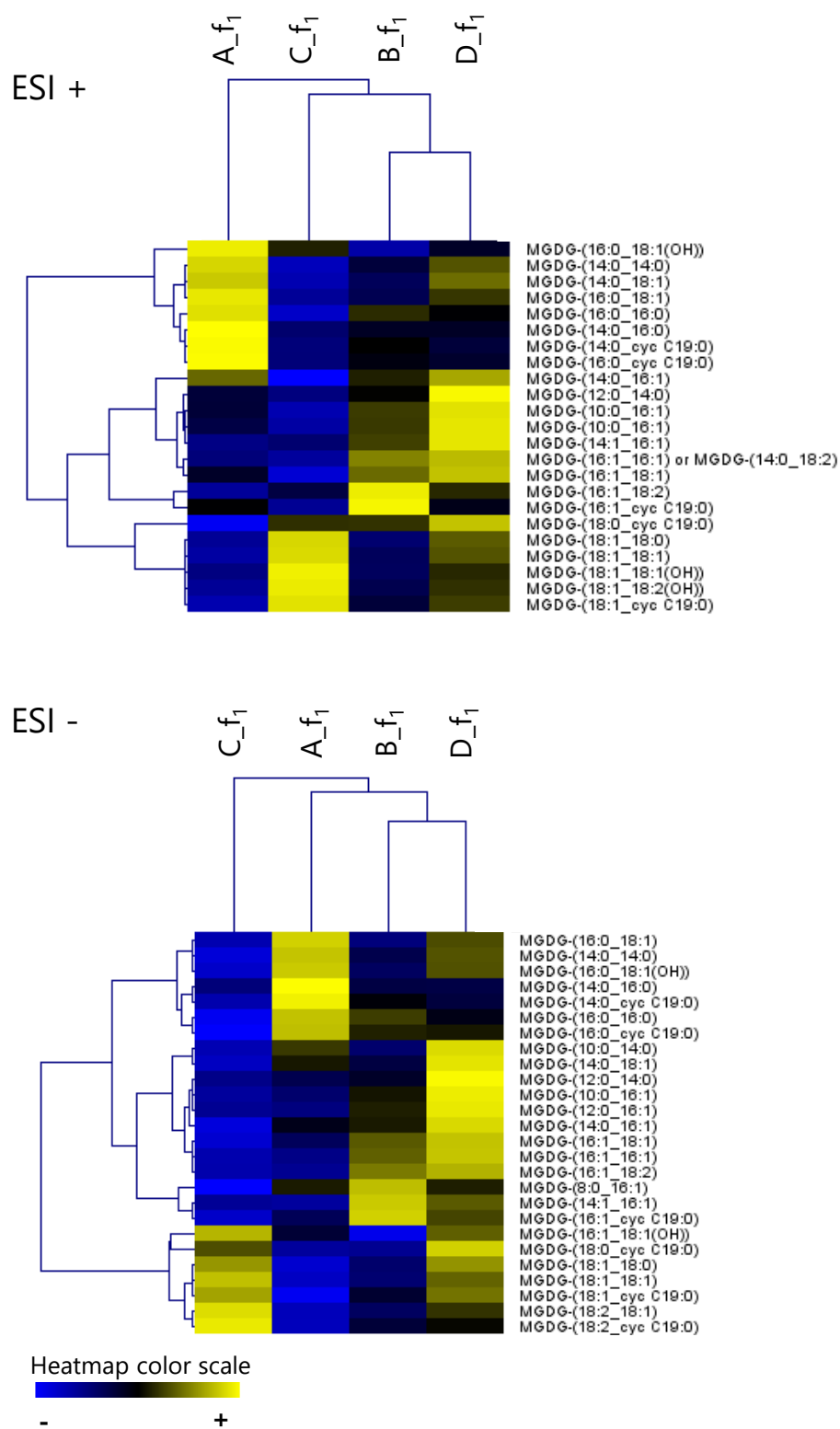


Figure 5.6 Heatmaps of monoglycosyldiacylglycerols (MGDG) found in f₁ for the four fermentation conditions studied. A, [42°C, pH 5.8]; B, [42°C, pH 4.8]; C, [37°C, pH 5.8]; and D, [37°C, pH 4.8]. This fraction was obtained by the elution of chloroform. ESI, electrospray ionization. The Pearson's correlation was used for the hierarchical clustering.

The MGDG in f_2 is shown in Figure 5.7

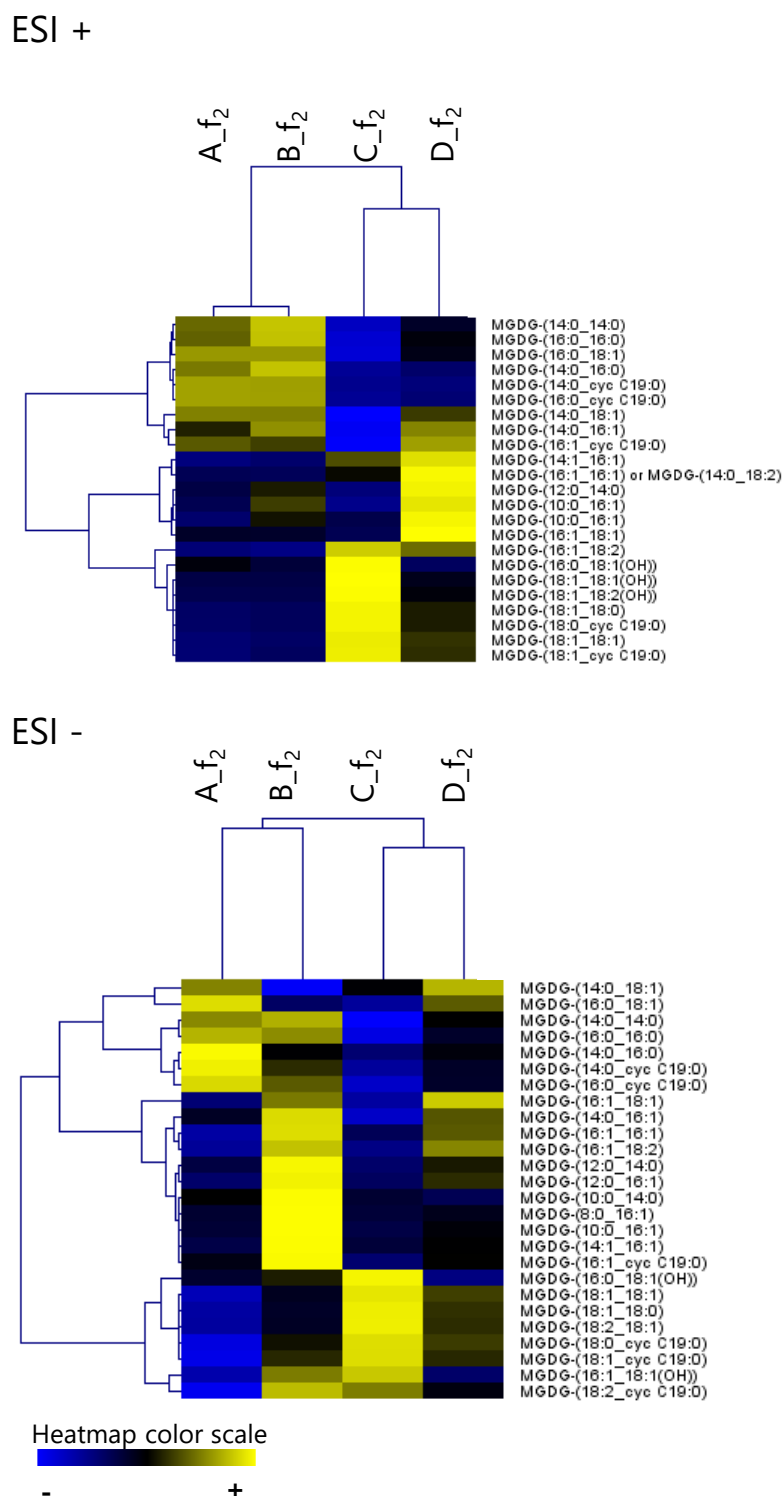


Figure 5.7 Heatmaps of monoglycosyldiacylglycerols (MGDG) found in f_2 for the four fermentation conditions studied. A, [42°C, pH 5.8]; B, [42°C, pH 4.8]; C, [37°C, pH 5.8]; and D, [37°C, pH 4.8]. This fraction was obtained by the elution of chloroform-acetone (50/50). ESI, electrospray ionization. The Pearson's correlation was used for the hierarchical clustering.

In the f_2 , (Figure 5.7) each fermentation condition induced a FA profile previously observed for f_1 . For instance, the fermentation condition [42°C, pH 5.8] (A_{f_1}) induced a membrane containing MGDG with many saturated chains (C14:0 and C16:0), and at [37°C, pH 5.8] (C_{f_1}), MGDG also included FA chains with 18 carbons. The majority were mono or di unsaturated. However, the clustering was different from the f_1 . In both ionization modes, the fermentation conditions were clustered according to the temperature (42°C: A_{f_2} and B_{f_2} and 37°C: C_{f_2} and D_{f_2}).

(2) Glycolipids: Diglycodiacylglycerols, DGDG (Figure 5.8)

The FA composition of DGDG were identical to that of MGDG (C10:0, C12:0, C14:0, C16:0, C18:0, C18:1, and C18:2). Regardless of the ionization mode, the fermentation conditions were clustered by the pH (pH 5.8: C_{f_3} and A_{f_3} ; pH 4.8: B_{f_3} and D_{f_3}). When comparing the four fermentation conditions, DGDG with FA chains with 12, 14, and 16 carbons were more predominant for cells that were cultivated at low pH ([42°C, pH 4.8], B_{f_3} and [37°C, pH 4.8], D_{f_3}). DGDG with fatty acid chains of 18 carbons and one or two unsaturation were mostly presented for cells grown at [37°C, pH 5.8] (C_{f_3}). At [42°C, pH 5.8], the relative abundance of DGDG was the lowest observed among the four fermentation conditions.

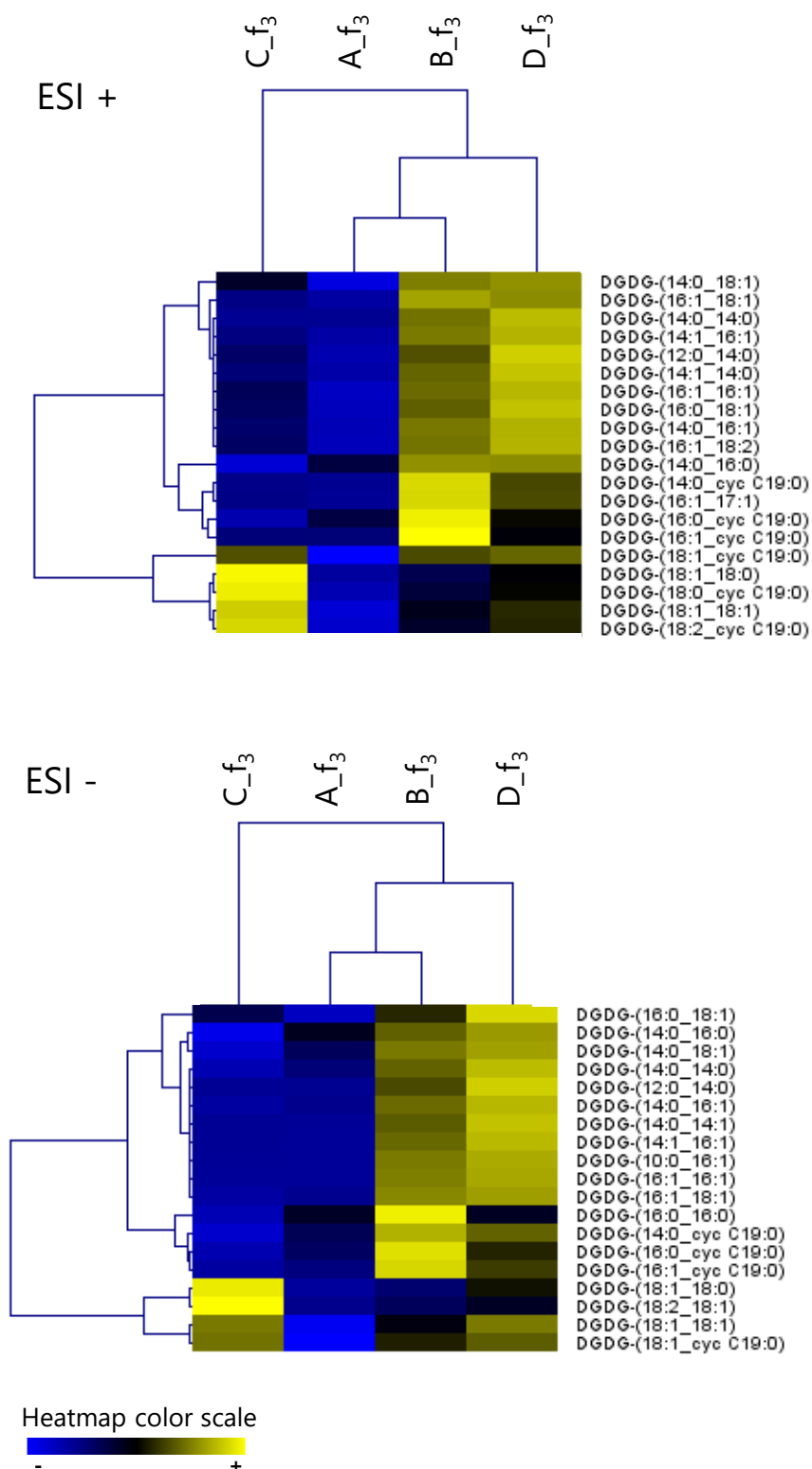


Figure 5.8 Heatmaps of diglycosyldiacylglycerols (DGDG) found in f_3 for the four fermentation conditions studied. A, [42°C, pH 5.8]; B, [42°C, pH 4.8]; C, [37°C, pH 5.8]; and D, [37°C, pH 4.8]. This fraction was obtained by the elution of acetone (f_3). ESI, electrospray ionization. The Pearson's correlation was used for the hierarchical clustering.

(3) Phospholipids: phosphatidylglycerol, PG (Figure 5.9)

The phospholipids identified in *L. bulgaricus* CFL1 were exclusively PG (Figure 5.9). Although CL has been previously observed in LAB membrane (Exterkate et al. 1971; Fernández Murga et al. 2000; Gomez-Zavaglia 2000; Limonet et al. 2004; Machado et al. 2004; Calvano et al. 2011; Hansen et al. 2015a; Kato et al. 2019; Chamberlain et al. 2019), our method did not allow to identify this phospholipid. Further experiments are required to confirm the presence of CL since the HPTLC results suggested the possible presence of CL in *L. bulgaricus* CFL1.

The negative ionization allowed us to identify a larger PG species and discriminate FA chains than positive ionization. The number of carbons in the FA was C14, C16 (with none or one unsaturation), C18 (with one or two unsaturated chains), and cycC19:0. The FA in PG were less diverse than in glycolipids (MGDG and DGDG).

The fermentation condition that led to the highest abundance of Lyso PGs was the one carried out at [42°C, pH 5.8] (A_{f4}). The Lyso-PG's fatty acids match those of PG. This result indicates that Lyso-PG are either lipid mediators to form PGs or are the result of the hydrolysis of PGs (Makide et al. 2009)

At [42°C, pH 4.8] (B_{f4}), PGs with a diversity of FA chains were observed in a high relative abundance (C14:0, C14:1, C16:0, C16:1, C18:1, C18:2). At [37°C, pH 5.8] (C_{f4}), the cell membrane had an abundance of PG with C18:2, C18:1, and cycC19:0 chains, whereas at [37°C, pH 4.8] (D_{f4}) enhanced the FA C14:0, C14:1, C16:1 in the PGs.

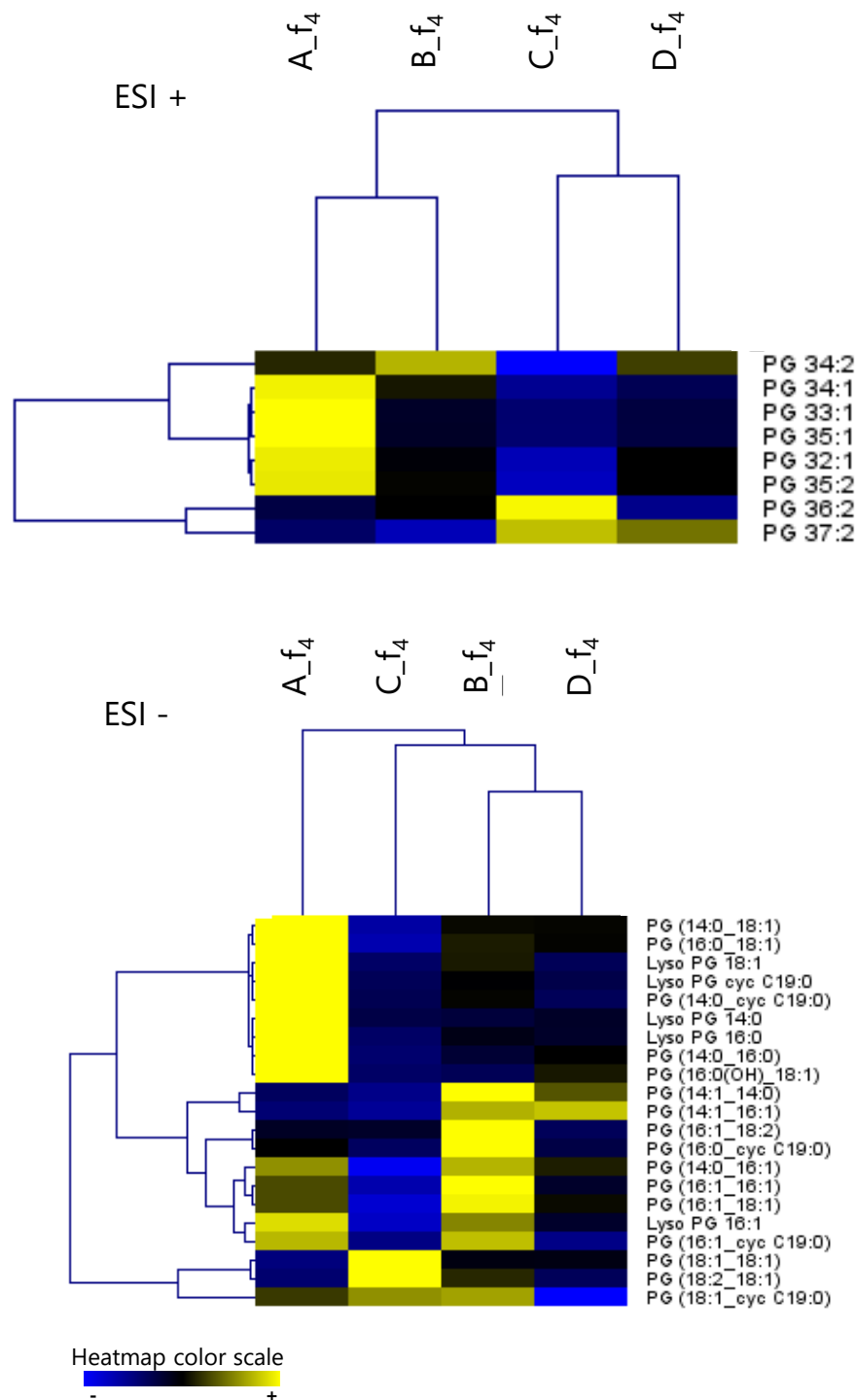


Figure 5.9 Heatmaps of phosphatidylglycerols (PG) found in f_4 for the four fermentation conditions studied. A, [42°C, pH 5.8]; B, [42°C, pH 4.8]; C, [37°C, pH 5.8]; and D, [37°C, pH 4.8]. This fraction was obtained by the elution of methanol. ESI, electrospray ionization.

5.5.2. Lipid phase transitions and membrane fluidity

The lipid phase behavior of *L. bulgaricus* CFL1 cells during cooling and heating was analyzed by FTIR spectroscopy. Monitoring the evolution of symmetric CH₂ stretching band ($\nu_{sym}CH_2$) position around 2850 cm⁻¹ as a function of temperature allows determining when the membrane lipids undergo a phase change from a fluid crystalline phase to a rigid gel phase in a temperature cycle. (Crowe et al. 1989b; Mantsch and McElhaney 1991).

For the four fermentation conditions and harvest times, the temperature decrease resulted in a shift of $\nu_{sym}CH_2$ peak positions to lower wavenumbers (Figure S5.13, fitted blue curves). In contrast, increasing the temperature led to a shift of $\nu_{sym}CH_2$ peak positions to higher wavenumbers (Figure S5.13, fitted red curves).

Regardless of the fermentation condition and harvest time, the $\nu_{sym}CH_2$ curves upon heating (red curves in Figure S5.13) and cooling (blue curves in Figure S5.13) were mostly overlapped. At a certain level, cooling and heating *L. bulgaricus* CFL1 cells appeared not to affect the phase change.

The first derivatives of the fitted curves as a function of temperatures (Figure S5.2) provided the temperatures of the lipid phase transition during cooling (T_s in °C) and heating (T_m in °C)

For all fermentation conditions and harvest times, T_s and T_m values are presented in Figure 5.10. Also, the membrane fluidity determined by fluorescence anisotropy (at 20°C) is displayed. Fluorescence anisotropy measures the membrane fluidity through the mobility of a fluorescent probe within the overall membrane. Fluorescence anisotropy (r) is inversely proportional to membrane fluidity. High anisotropy (r) values suggest a more rigid membrane (Mykytczuk et al. 2007).

For each fermentation condition and harvest time, the difference between T_m and T_s ranged from one degree to nine.

Regardless of the harvest time, *L. bulgaricus* CFL1 cells cultivated at [42°C, pH 5.8] exhibited the highest T_s (19-16°C) and T_m (20-22°C) values. The other three fermentation conditions led to subzero temperatures upon cooling (T_s from -12°C to -1°C) and lower temperatures during heating (T_m from -8°C to 1°C) compared to [42°C, pH 5.8].

Anisotropy values at 20°C were consistent with the temperatures of the lipid phase transition (Figure 5.10). Regardless of when these were harvested, *L. bulgaricus* CFL1 cells grown at [42°C, pH 5.8] showed the highest anisotropy values (0.193-0.209). This result suggests that a rigid membrane was induced under this fermentation condition.

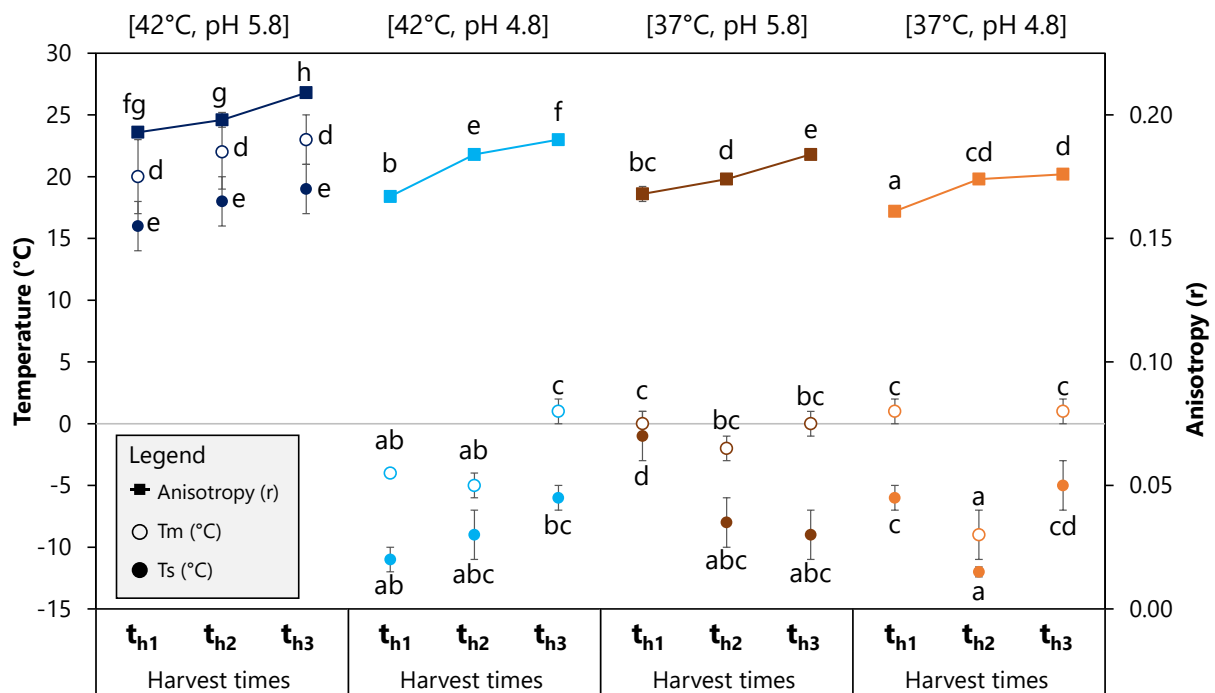


Figure 5.10 Biophysical membrane properties of *L. bulgaricus* CFL1. Lipid phase transition temperatures during cooling (T_s , full circles) and heating (T_m , empty circles), anisotropy values at 20°C (lines with full squares). Cells were grown at different fermentation conditions at increased harvest time: t_{h1} , mid-exponential growth phase; t_{h2} , deceleration growth phase; t_{h3} , stationary growth phase. Values are the mean of at least three independent biological replicates with the corresponding standard deviation values. Superscripts letters represent significant differences among fermentation conditions and harvest times at a 95% confidence level. The error bars that are not visible is because their size is within the symbols size.

For the three remaining fermentation conditions, lower anisotropy values were obtained (≤ 0.190 , a more fluid membrane). When *L. bulgaricus* CFL1 cells were cultivated at 37°C (despite the harvest time and pH), bacteria exhibited lower anisotropy values than at 42°C. For example: t_{h3} at pH 4.8: 0.176 (37°C) vs. 0.190 (42°C) and t_{h3} at pH 5.8: 0.184 (37°C) vs. 0.209 (42°C)

Additionally, for the four fermentation conditions, the later the cells were harvested, the higher the anisotropy values were observed (a membrane rigidification).

5.5.3. Resistance of *L. bulgaricus* CFL1 to freezing and freeze-drying at four different fermentation conditions and harvest times

L. bulgaricus CFL1 cells resistance was represented by the losses of their specific acidifying activity after freezing ($dt_{spe} F$) and freeze-drying ($dt_{spe} FD$). The effects of fermentation parameters on *L. bulgaricus* CFL1 resistance to stabilization processes are presented in Figure 5.11. Low dt_{spe} values indicate an increased resistance to a stabilization process.

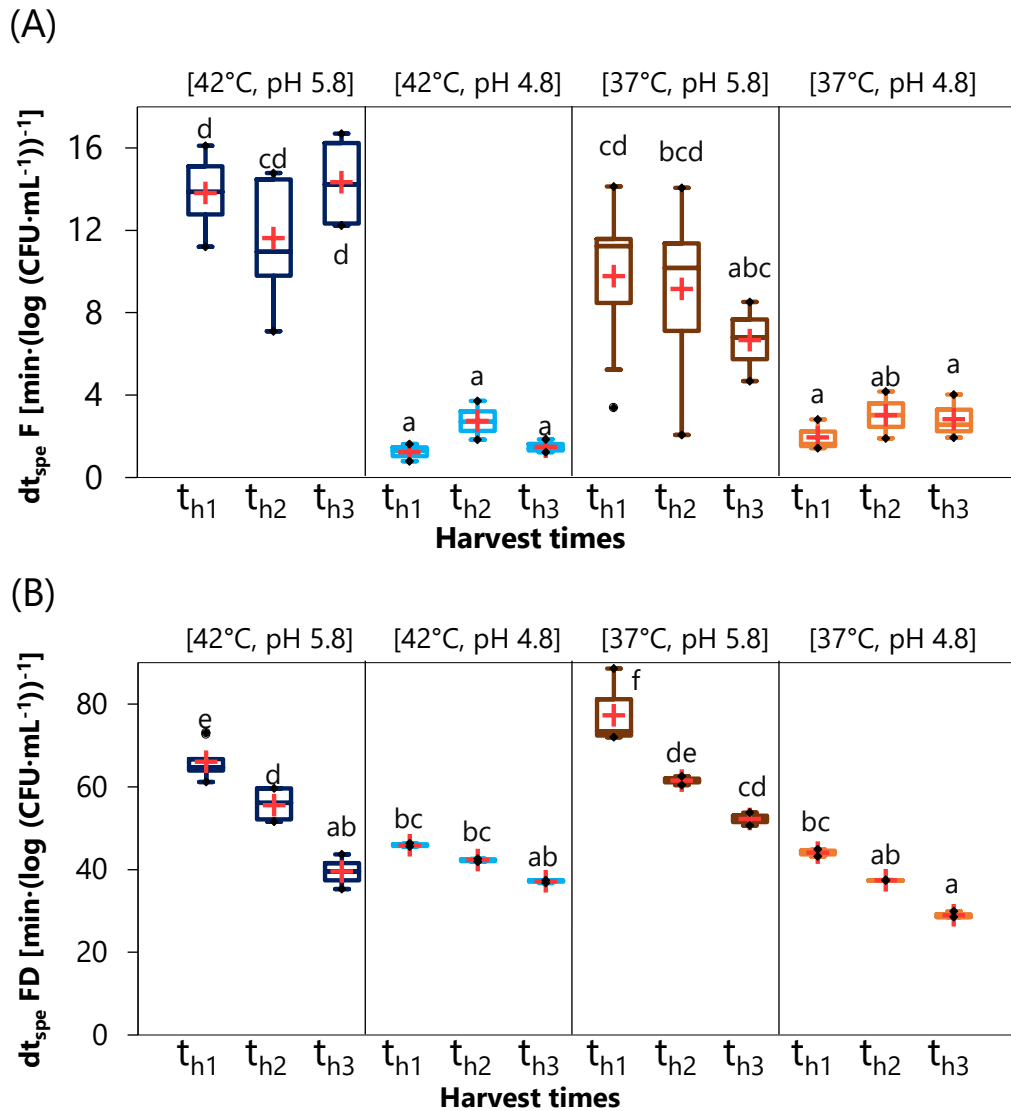


Figure 5.11 Loss of the specific acidifying activity of *L. bulgaricus* CFL1 after (A) freezing ($dt_{spe} F$) and (B) freeze-drying ($dt_{spe} FD$) for the four studied fermentation conditions at different harvest times. t_{h1} : mid-exponential growth phase; t_{h2} : deceleration growth phase; t_{h3} : stationary growth phase. The boxplots (mean = red cross and median = line in the middle of the box) come from at least three independent biological replicates. Superscript letters represent significant differences between samples at a 95% confidence level. The results in this figure were presented in Chapter 4 as response surfaces.

L. bulgaricus CFL1 cells exhibited lower losses (lower dt_{spe} values) after freezing than freeze-drying (1-14 [min·(log (CFU·mL⁻¹))⁻¹] vs. (29-77 [min·(log (CFU·mL⁻¹))⁻¹]). This result was expected since the freeze-drying process involves additional drying steps (sublimation and desorption) that contribute to damaging LAB cells.

For the freezing resistance, the effect of pH was the most significant on *L. bulgaricus* CFL1 resistance (Figure 5.11 (A)). Regardless of the harvest time and temperature, low pH (pH = 4.8) led to the highest freezing resistant cells (low $dt_{spe} F$ values, about 2-3 [min·(log (CFU·mL⁻¹))⁻¹]).

For freeze-drying resistance, the harvest time and pH were the main parameters that affected the resistance of *L. bulgaricus* CFL1. Increasing the harvest time (from t_{h1} to t_{h3}), led to lower dt_{spe} FD values (Figure 5.11 (B)). Thus, for each fermentation condition, bacteria harvested at the stationary growth phase (t_{h3}) presented the highest cell resistance to freeze-drying. Likewise, low pH led to higher resistant cells (lower dt_{spe} FD values). For example, *L. bulgaricus* CFL1 cells cultivated at [42°C, pH 4.8] and harvested at t_{h1} and t_{h2} increased their resistance by 44% and 33 % (respectively) compared to [42°C, pH 5.8] at the exact harvest times. The same trend was observed for cells grown at [37°C, pH4.8] and harvested at t_{h1} , t_{h2} , and t_{h3} . Resistance increased by more than 60% with respect to [37°C, pH 5.8].

5.5.4. Relationships between membrane lipid characteristics and the two stabilization processes

To study the relationships between the physicochemical modulation (biochemical composition and biophysical properties) of the lipid membrane and the cells' resistance to freezing and freeze-drying, we performed the two principal component analyses (PCA) in Figure 5.12 and two Pearson correlation (Table S5.4) for each stabilization process.

For the PCA of freezing resistance (Figure 5.12, upper left side), the first two dimensions accounted for 92% of the data variance. The F1 axis (71% of the total variation) distinguishes *L. bulgaricus* CFL1 cells according to their SFA content, T_s , and T_m values. The CFA content characterizes the F2 axis (21% of the total variation). However, the specific activity $dt_{spe}F$ is not explained by one axis but by the two axes: $dt_{spe}F$ increases when both SFA, T_s , and T_m increase while CFA decreases.

The PCA also allowed us to visualize the four fermentation conditions and the three harvest times into five similar groups (Figure 5.12, upper right side). The first dark blue group (located on the upper and lower right side of the graph) included *L. bulgaricus* CFL1 cells cultivated at [42°C, pH 5.8] and harvested at the three different times (t_{h1} , t_{h2} , and t_{h3}). This first group was identified by high values of anisotropy (low membrane fluidity), high SFA content and values of lipid phase transition temperatures (T_s and T_m), and low resistance to freezing (high values of $dt_{spe}F$). The second light blue and third orange groups (located on the upper left side of the graph) consisted of the bacteria that were grown at pH 4.8, regardless of the fermentation temperature and harvest time ([42°C, pH 4.8] and [37°C, pH 4.8]). It was represented by a high content of CFA and high resistance to freezing (low values of $dt_{spe}F$). The fourth brown group (located on the more down left side of the graph) included bacteria cultivated at [37°C, pH 5.8] and harvested at the three harvest times that displayed high UFA content and low CFA value.

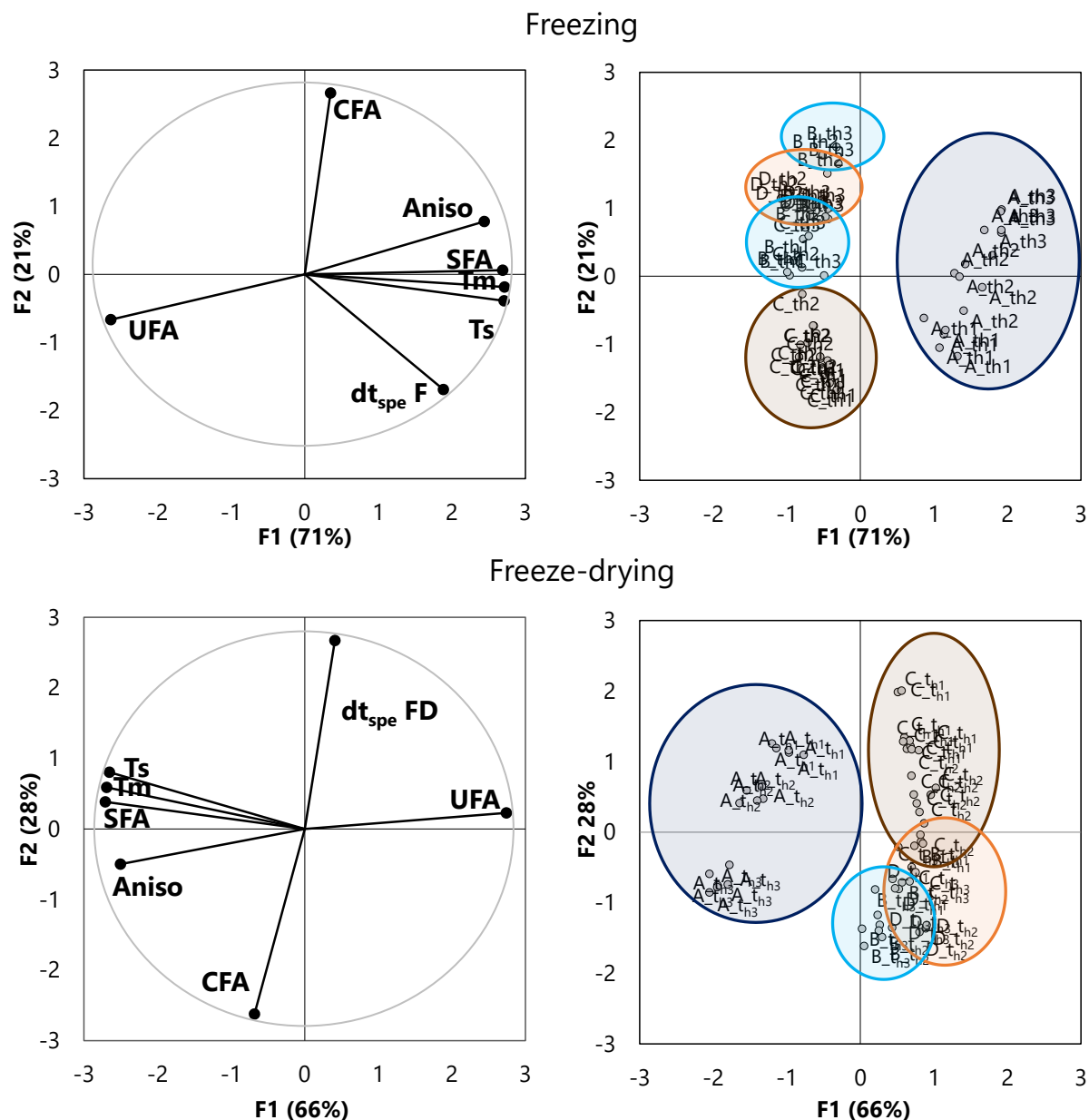


Figure 5.12 Principal component analyses of fatty acid content (SFA, UFA, CFA), lipid transition temperatures, membrane fluidity, and resistance to freezing and freeze-drying of *L. bulgaricus* CFL1 cells. Abbreviations: A, [42°C, pH5.8]; B, [42°C, pH 4.8]; C, [37°C, pH 5.8]; D, [37°C, pH 4.8]; t_{h1}: mid-exponential growth phase; t_{h2}: deceleration growth phase; t_{h3}: stationary growth phase; SFA, Saturated Fatty Acid; UFA, Unsaturated Fatty Acid; CFA, Cyclic Fatty Acid; Ts, lipid transition temperature upon cooling; Tm, lipid transition temperature upon heating; Aniso, Anisotropy values (membrane fluidity); dt_{spe} F, the loss of specific acidifying activity after freezing; and dt_{spe} FD, the loss of specific acidifying activity after freeze-drying.

Concerning the PCA of freeze-drying resistance (Figure 5.12, bottom left side), the first two dimensions accounted for 94% of the data variance. The F1 axis (66% of the total variation) distinguishes *L. bulgaricus* CFL1 cells according to SFA and UFA contents. The F2 axis (28% of the total variation) is characterized by the CFA content and resistance to freeze-drying of *L. bulgaricus* CFL1.

Four groups are observed in Figure 5.12, bottom right side. A first dark blue group consisted of bacteria grown at [42°C, pH 5.8], regardless of the harvest time, with the same membrane characteristics (high SFA content, low membrane fluidity, and high transition temperatures). The second brown group (located on the upper right side of the graph) was characterized by *L. bulgaricus* CFL1 cells cultivated at [37°C, pH 5.8] (regardless of the harvest time) and high UFA content and low resistance to freeze-drying (high values of dt_{spe} FD). The third light blue and fourth orange groups (located on the lower right side of the graph) included bacteria grown at pH 4.8 ([42°C, pH 4.8] and [37°C, pH 4.8]). Under these conditions, bacteria were associated with a high CFA content and low resistance to freeze-drying.

Whatever the stabilization process, the variable vectors SFA, T_s , T_m , and Aniso were mainly parallel in the same direction. Thus, the variation of these variables was independent of the resistance to freezing and freeze-drying.

Interestingly, dt_{spe} FD is well explained by the axis 2 and thus negatively correlated with CFA. In contrast to dt_{spe} F, dt_{spe} FD is not explained by SFA or UFA but only CFA. High content in CFA led to a low dt_{spe} FD corresponding to the desired property. This result hints that the sublimation and dehydration process is strongly related to the properties provided by CFA.

5.6. Discussion

Our study aimed at first deeply characterizing the membrane lipids to better understand lipids' modulation by changing the fermentation conditions from the optimal for growth (42°C, pH 5.8) of a lactic acid bacterium, and second to identify the membrane characteristics that may be related to the resistance of cells to freezing and freeze-drying.

5.6.1. Fermentation conditions affect fatty acid composition at different harvest times

Our findings showed that fatty acid compositions of *L. bulgaricus* CFL1 were modified by cultivating cells at different fermentation conditions and harvesting at distinct growth phases. An increase in the proportion of unsaturated fatty acids (mainly composed of C18:1 cis 9, Table S5.2) was observed for the fermentation conditions carried out at low pH (pH 4.8) or low temperature (37°C). As a response to environmental changes during growth, the LAB membrane is modified, particularly the variations in the composition of fatty acids. This adaptation mechanism has been previously observed for different LAB as an essential biological response to maintain membrane functionalities at low growth temperatures and pHs (De Angelis and Gobbetti 2004; Gao et al. 2021). This adaptation process is referred to bacterial homeoviscous adaptation mechanism (Sinensky 1974; Zhang and Rock 2008).

At low pH, LAB should maintain a pH gradient (Δ pH) where their intracellular pH should be more alkaline than the external low pH. LAB buffering capacity depends on the biophysical state of the membrane (a fluid crystalline phase membrane) because the diffusion of external acid accumulation passes through the membrane into the cytoplasm (Booth 1985; Broadbent et al. 2010). For this purpose, at low growth pH or acid stress, LAB produce specific proteins involved in carbohydrate metabolism (Zhai et al. 2014; Yang et al. 2019), enzymatic activities (e.g., H⁺-ATPases) (Cotter and Hill 2003), and the ability to shift its membrane fatty acid profile, for example, from SFA to mono UFA (Fozo and Quivey 2004).

In this study, the CFA content of *L. bulgaricus* CFL1 was increased by increasing the harvest time. The same behavior has been previously reported for a late harvest time, particularly when LAB had been exposed to stresses such as low pH during growth (Nikkilä et al. 1996; Drici-Cachon et al. 1996; Grandvalet et al. 2008).

The conversion of monounsaturated fatty acids synthesizes CFA. This conversion plays a significant role in adapting bacteria in response to a radical perturbation of the environment (e.g., nutrients depletion during growth) (To et al. 2015). The mechanisms of increased CFA production in LAB at the stationary phase have been explained by the expression of the *cfa* gene regulated at the transcriptional level and the proteolytic degradation of the Cyclopropane-fatty-acyl-phospholipid synthase (Cfa) protein (Budin-Verneuil et al. 2005; Grandvalet et al. 2008).

5.6.2. Fermentation conditions effect on membrane lipids: analysis of lipids fractions

We performed a deep characterization of lipids to gain insights into membrane lipid modulation when fermentation conditions are modified. Although there are some studies applying a complete characterization of LAB lipids (lipid classes and their corresponding fatty acid chains), these have had the sole purpose of characterizing LAB species (Exterkate et al. 1971; Drucker et al. 1995; Gomez-Zavaglia 2000; Calvano et al. 2011; Chamberlain et al. 2019; Kim et al. 2020). Only a few studies have assessed the effect of fermentation conditions on lipids modulation. For instance, the impact of low growth temperature (Fernández Murga et al. 2000) and the supplementation of the culture medium (Hansen et al. 2015a; Walczak-Skierska et al. 2020) on the membrane lipids of LAB have been previously studied.

Here, we expanded the knowledge of lipid modulation by using four different culture conditions. Regardless of the fermentation condition, the fatty acids content remained similar. However, the profile of relative abundance of membrane lipids was different per fermentation condition. This diverse profile was observed for the MGDG glycolipids (one monomer of sugar in the headgroup). For cells cultivated at pH 4.8, the DGDG glycolipids (two monomers of sugars in the headgroups) with fatty acid chains of fourteen, sixteen, and eighteen carbons were the most abundant. At [37°C, pH 5.8], only DGDGs with eighteen-carbon or cyclic FA chains were the most abundant. The optimum fermentation condition for growth, [42°C, pH 5.8], presented the lowest abundance of DGDG. Glycolipids in Gram-positive bacteria have been thought to be in the cytoplasmic membrane covered with the thick cell wall. The central role of glycolipids is anchoring lipoteichoic acid. These molecules play a crucial role in forming lipid domains in the membrane and, thus, may influence the dynamics of the membrane (Caffalette et al. 2020). Under the combinational cold and acid stress, *Lactiplantibacillus plantarum* NMGL2, within several adaptation mechanisms, enhanced the production of glycolipids (Zhang et al. 2021). We could, thus, speculate that *L. bulgaricus* CFL1, under another fermentation condition than the optimal for growth, may induce the presence of these molecules with specific FA to keep proper membrane dynamics.

The PG was the only phospholipid identified in the *L. bulgaricus* CFL1 membrane. PG is one of the most abundant glycolipids in bacteria (Dugail et al. 2017). It has been hypothesized to sort proteins into different regions and regulate processes such as ATP synthesis, chromosomal replication, and DNA repair, among other functions (Strahl and Errington 2017; Dugail et al. 2017). The profile of the relative abundance of PG was different according to the fermentation condition, indicating that *L. bulgaricus* CFL1 favored the production of specific PGs with FA that allowed it to keep its vital membrane functions.

5.6.3. Biophysical properties of membrane lipids

The fatty acids modulation of *L. bulgaricus* CFL1 was linked to the biophysical properties of the membrane. When cells were cultured at low pH (pH 4.8) or temperature (37°C), they exhibited

lower lipid transition temperatures and high membrane fluidity. Both properties were related to high UFA content. These results agreed with the ones observed for *L. bulgaricus* (Gautier et al. 2013; Meneghel et al. 2017) and other LAB species such as *Lacticaseibacillus casei* (Wu et al. 2012) and *Carnobacterium maltaromaticum* (Girardeau et al. 2022). Membrane fluidity is the consequence of the fatty acyl chain conformation. Thus, a membrane composed of UFA, especially cis-UFA, introduce a pronounced kink in the chain. This kink leads to a disorganized bilayer structure, resulting in increased membrane fluidity (Denich et al. 2003). Low lipid phase transition temperature is caused by the low melting points of UFA (Knothe and Dunn 2009).

5.6.4. The resistance to freezing and freeze-drying and the link with the membrane

In this study, different resistance levels to freezing or freeze-drying were observed as a result of cultivating *L. bulgaricus* CFL1 cells under four fermentation conditions and harvested at various growth phases. The membrane characteristics associated with freezing were not the same as with freeze-drying. Improved freezing resistance was correlated to low SFA content, low lipid phase transition temperatures, and high membrane fluidity. A high CFA content was sufficient for improved freeze-drying resistance.

The fatty acid modulation has been widely reported as a LAB mechanism to help bacteria encounter the different stresses during freezing. For an improved freezing resistance, ten out of twelve studies have shown the requirement to increase the UFA/SFA ratio with respect to a control sample (LAB cells exhibiting less resistance to freezing). The increase in UFA/SFA ratio has been observed between 1.2-4.0-fold (Gilliland and Speck 1974; Smittle et al. 1974; Goldberg and Eschar 1977; Béal et al. 2001; Wang et al. 2005a, 2011; Gautier et al. 2013; Louesdon et al. 2015; Girardeau et al. 2022). Additionally, low temperatures of lipid phase transition (close to or more down to 0°C) have been related to a fluid membrane (Gautier et al. 2013; Passot et al. 2014; Girardeau et al. 2022). In the current study, *L. bulgaricus* CFL1 cells grown at 37°C or pH 4.8 exhibited a fluid membrane and sub-zeros lipid phase transition temperatures close to ice nucleation temperature (T_n : from -10°C to -6°C). When ice crystals increase at the external medium, bacteria start dehydrating because of the osmotic imbalance between their external surroundings and internal compartment. This event leads to cell dehydration and shrinkage. If the cell membrane is relatively fluid, it may facilitate the water efflux from the interior compartment to the external medium. Thus, minor damage to cells is expected. In this case, a fluid membrane with low lipid phase transition temperatures is a convenient feature for encountering the osmotic stress during freezing (Gautier et al. 2013).

Concerning the membrane properties linked to an improved freeze-drying resistance, our results agreed with the previous studies relating only to the increase of CFA content and not necessarily to a high UFA/SFA ratio (Li et al. 2009a, 2012; Velly et al. 2015). The authors speculated that CFA might play a crucial role in membrane fluidity.

In this study, the complementary measurements of biophysical membrane properties were not significantly related to freeze-drying resistance. This result suggests that despite a high membrane fluidity of some cells cultivated at low pH or temperature, membrane fluidity did not explain an increased resistance to freeze-drying. When comparing our results to the literature, the only two studies that have associated membrane fluidity with freeze-drying resistance reported contrasting results for the same LAB species (*Lactococcus lactis*). A rigid membrane was related to an improved resistance of *Lactococcus lactis* TOMSC161 (Velly et al. 2015), whereas a fluid membrane to high freeze-drying resistance of two *Lactococcus lactis* (NZ9000 and NCDO 712) (Bodzen et al. 2021a). Our results and the few reported agree with the need to investigate the contribution of CFA to the membrane fluidity.

5.7. Conclusion

This study provided additional insights into the mechanism of *L. bulgaricus* cells to modulate their membrane under different fermentation conditions. *L. bulgaricus* CFL1 cells grown under low pH or temperature led to a membrane with unsaturated fatty acids, high membrane fluidity, and zero or subzero lipid phase transition temperatures. The present results reinforce the assumption that *L. bulgaricus*, like many other LAB, develop mechanisms to grow under different conditions from the one optimal for growth (low temperature and pH).

This study also contributed to new findings in membrane modulation. We observed a high relative abundance of DGDG glycolipids with specific FA chains at low growth pH (pH 4.8) and the lowest abundance of this same glycolipid when cells were cultivated at [42°C, pH 5.8]. The PG was the phospholipid identified in the *L. bulgaricus* CFL1 membrane. The profile of the relative abundance of PG was different per fermentation condition.

The membrane modulation by the fermentation condition was also related to the resistance of cells to freezing and freeze-drying. For freezing resistance, *L. bulgaricus* CFL1 exhibited a membrane with high UFA content, high membrane fluidity, and a low lipid phase transition temperature. In contrast, freeze-drying resistance was only associated with a high CFA content.

So far, the fatty acid composition modulation due to different fermentation conditions has been the most documented in the literature. Our work highlighted the interest in performing a deep characterization of membrane lipids to expand our knowledge on the LAB adaptation. Additionally, it provided relevant results to understand the relationships between membrane lipids properties and cryo-resistance of LAB.

Acknowledgments

This work received funding from the European Union's Horizon 2020 research and innovation program under grant agreement No. 777657. The authors thank Sarrah Ghorbal for her technical support for the fluorescence anisotropy measurements and Ha-Phuong Ta for providing the protocol of glycolipid extraction from a lipid membrane. This work has benefited from the support of IJPB's Plant Observatory technological platforms, and IPS2's metabolomic platform. The authors would like to thank Jean-Christophe Totozafy for the technical supervision for the LC-MS/MS analysis.

Conflicts of interest

The authors declare that they have no competing interests.

Authors contributions

Conceptualization and investigation, MLTC, YG, MHR, FF, SP; experiments, MLTC and ACP; formal analysis MLTC, MHR, YG; data curation and statistical treatment, MLTC, ACP, MHR; writing, review and editing MLTC, MHR, YG; supervision, MHR, YG, FF, SP; funding acquisition SP and FF.

5.8. Supplementary information

5.8.1. Supplementary Tables

Table S5.1 Comparison of extraction methods for fatty acid detection

Fatty acid (% relative)	Folch method			Bigh and Dyer method		
	42C_pH4.8_t _{h3}	42C_pH4.8_t _{h3}	42C_pH4.8_t _{h3}	42C_pH4.8_t _{h3}	42C_pH4.8_t _{h3}	42C_pH4.8_t _{h3}
	Biological replicate 1	Biological replicate 2	Biological replicate 3	Biological replicate 1	Biological replicate 2	Biological replicate 3
C12:0	0.22	0.28	0.29	0.19	0.18	0.24
C14:0	8.07	8.72	8.53	8.04	7.97	7.96
C15:0	NA	NA	NA	NA	NA	NA
C16:0	14.77	14.72	14.48	14.17	14.07	13.83
C16:1 trans 9	1.59	1.79	1.67	1.71	1.70	1.65
C16:1 cis 9	15.99	16.93	16.69	16.73	16.82	16.63
C17:0	0.00	0.00	0.00	0.00	0.00	0.00
C18:0	3.26	3.13	2.77	1.97	1.98	1.77
C18:1 trans 9	0.66	0.74	0.72	0.73	0.79	0.78
C18:1 cis 9	39.55	36.94	38.98	39.62	39.59	39.93
C18:1 cis 11	2.04	2.13	2.00	2.03	2.01	1.88
C18:2 all cis-9,12	0.00	0.00	0.00	0.00	0.00	0.00
cyc C19:0	7.13	7.09	7.10	8.56	8.73	8.67
C18:2 cis 9, trans 11	6.49	7.39	6.68	6.02	6.01	6.56
C22:0	0.23	0.15	0.10	0.23	0.15	0.10
UFA	66.32	65.92	66.74	66.84	66.92	67.43
SFA	26.55	26.99	26.16	24.60	24.35	23.90
UFA/SFA	2.50	2.44	2.55	2.72	2.75	2.82
ng/μL	228.80	252.40	275.10	229.38	255.57	277.80

Table S5.2 Detailed fatty acid composition of *L. bulgaricus* CFL1 for the fermentation conditions at different harvest times. t_{h1} : mid-exponential growth phase; t_{h2} : deceleration growth phase; t_{h3} : stationary growth phase

Fatty acids (%)*	[42°C, pH 5.8]			[42°C, pH 4.8]			[37°C, pH 5.8]			[37°C, pH 4.8]		
	t_{h1}	t_{h2}	t_{h3}	t_{h1}	t_{h2}	t_{h3}	t_{h1}	t_{h2}	t_{h3}	t_{h1}	t_{h2}	t_{h3}
C12:0	0.4±0.1 ^a	0.7±0.1 ^{ab}	0.4±0.1 ^a	2.5±0.05 ^g	2.0±0.2 ^{efg}	1.7±0.4 ^{def}	0.9±0.3 ^b	1.4±0.3 ^{cd}	1.2±0.3 ^{bc}	1.5±0.3 ^{cde}	2.2±0.2 ^{eg}	1.7±0.5 ^{cdef}
C14:0	13.8±0.6 ^e	13.9±1.7 ^e	15±0.3 ^e	5.1±0.3 ^{ab}	5.8±0.4 ^{abc}	7.1±1.3 ^{abc}	10.8±1.3 ^d	7.8±1.4 ^c	6.7±1.6 ^{abc}	6.4±0.5 ^{abc}	4.1±0.9 ^a	7.8±0.7 ^{bc}
C15:0	0.05±0.01 ^a	0.05±0.02 ^a	0.05±0.01 ^a	0.06±0.01 ^{ab}	0.10±0.1 ^c	0.06±0.01 ^{ab}	0.07±0.01 ^{abc}	0.06±0.01 ^{ab}	0.05±0.01 ^a	0.09±0.01 ^{bc}	0.07±0.01 ^{ab}	0.06±0.01 ^{ab}
C16:0	27.7±3.7 ^d	31.8±1.3 ^e	34.7±2.0 ^e	14.0±0.1 ^{bc}	14.6±0.9 ^{bc}	14.6±1.3 ^{bc}	13.4±1.5 ^{bc}	8.7±0.9 ^a	7.3±0.8 ^a	16.6±1.2 ^c	9.9±1.0 ^{ab}	13.5±0.7 ^{bc}
C16:1 trans 9	0.4±0.02 ^{bc}	0.4±0.03 ^{bc}	0.6±0.04 ^{cd}	1.2±0.02 ^f	1.2±0.1 ^f	1.5±0.2 ^g	0.3±0.04 ^{ab}	0.2±0.04 ^a	0.2±0.03 ^a	0.8±0.3 ^{de}	0.4±0.2 ^{abc}	1.2±0.2 ^f
C16:1 cis 9	5.8±0.4 ^{bcd}	6.5±0.1 ^{cd}	7.2±0.4 ^d	11.2±0.2 ^e	16.6±0.5 ^f	16.8±1.4 ^f	5.1±0.7 ^{abc}	4.3±0.5 ^{ab}	3.6±0.5 ^a	11.2±3.1 ^e	6.5±2.3 ^{bcd}	12.9±1.5 ^e
C17:0	0.03 ±0.01 ^a	0.08 ±0.01 ^{abc}	0.03 ±0.01 ^a	0.03 ±0.001 ^a	0.09 ±0.001 ^{cd}	0.08 ±0.01 ^{abc}	0.10±0.02 ^{cd}	0.08±0.01 ^c	0.08±0.02 ^{bc}	0.10±0.01 ^{cd}	0.10±0.01 ^{cd}	0.08±0.01 ^{abc}
C18:0	1.7±0.3 ^{abc}	1.6±0.1 ^{ab}	1.9±0.2 ^{abcd}	3.4±0.8 ^f	2.9±0.3 ^{ef}	2.5±0.2 ^{de}	1.5±0.2 ^a	1.9±0.3 ^{abcd}	1.9±0.2 ^{abcd}	2.7±0.5 ^e	2.2±0.2 ^{bcde}	2.3±0.5 ^{cde}
C18:1 trans 9	0.4±0.1 ^a	0.5±0.2 ^{ab}	0.9±0.2 ^{ab}	0.7±0.04 ^{ab}	0.8±0.02 ^{ab}	0.8±0.02 ^{ab}	0.9±0.3 ^{ab}	1.4±0.1 ^d	1.3±0.2 ^{cd}	0.6±0.2 ^{ab}	0.9±0.1 ^{bc}	0.8±0.1 ^{ab}
C18:1 cis 9	42.4±4.0 ^c	34.5±3.3 ^b	25.2±2.0 ^a	50.9±0.5 ^{de}	39.3±3.5 ^{bc}	37.6±3.8 ^{bc}	59.2±1.4 ^f	59.7±3.4 ^f	58.3±1.6 ^{ef}	45.6±4.9 ^{cd}	56.5±4.8 ^{ef}	43.7± 2.2 ^c
C18:1 cis 11	1.3±0.05 ^a	1.4±0.05 ^{ab}	1.5±0.05 ^{ab}	1.9±0.02 ^{bc}	2.5±0.1 ^d	2.5±0.2 ^d	1.6±0.3 ^{ab}	2.4±0.1 ^{cd}	2.4±0.2 ^{cd}	2.1±0.6 ^{cd}	2.6±0.1 ^d	2.2±0.2 ^{cd}
C18:2 cis 9, cis 12	0.08±0.02 ^a	0.13±0.01 ^a	0.25±0.08 ^a	0.19±0.01 ^a	0.08±0.03 ^a	0.07±0.01 ^a	0.12±0.04 ^a	0.39±0.8 ^a	0.12±0.1 ^a	0.16±0.1 ^a	0.11±0.01 ^a	0.07±0.02 ^a
cyc C19:0 (CFA)	4.0±0.9 ^{ab}	6.0±0.4 ^{bc}	8.7±1.2 ^d	4.8±0.3 ^{ab}	9.4±2.3 ^d	9.3±2.2 ^d	2.3±0.6 ^a	4.5±1.5 ^{ab}	7.5±0.9 ^{cd}	8.8±0.2 ^d	9.5±0.4 ^d	8.6±0.6 ^{cd}
C18:2 cis 9, trans 11	1.9±0.5 ^a	2.4±0.5 ^{ab}	3.5±0.3 ^{bc}	4.0±0.2 ^{bc}	4.6±0.4 ^c	5.3±1.0 ^{cd}	3.8±1.0 ^{bc}	7.1±0.9 ^d	9.4±1.5 ^e	3.3±1.6 ^{abc}	5.0±0.3 ^c	5.3±0.7 ^{cd}
C22:0	0.04±0.01 ^{ab}	0.04±0.01 ^{ab}	0.07±0.01 ^{ab}	0.02±0.02 ^a	0.12±0.04 ^b	0.15±0.1 ^b	0.01±0.01 ^a	0.01±0.01 ^a	0.02±0.01 ^a	0.05± 0.001 ^{ab}	ND	ND

*Values are the mean of at least three independent biological replicates with the corresponding standard deviation. Superscripts letters represent significant differences among fermentation conditions and harvest times at a 95 % confidence level. ND: Not Detected

Table S5.3 (A) Summary of lipid classes and species in *L. bulgaricus* CFL1 by LC-MS/MS in positive mode

		Lipid classes	*m/z			Lipid classes	*m/z
Diacyl glycerols	1	DAG-(4:0_16:0)	418.3527	19	DAG-(16:1_18:1)	610.5404	
	2	DAG-(6:0_16:0)	446.3836	20	DAG-(16:0_18:1)	612.5559	
	3	DAG-(8:0_18:1)	500.4322	21	DAG-(16:1_19:1)	624.556	
	4	DAG-(12:0_14:0)	502.4469	22	DAG-(16:1_18:1)	626.5354	
	5	DAG-(10:0_18:1) or DAG-(14:1_14:0)	528.4621	23	DAG-(16:0_19:1)	626.5717	
	6	DAG-(12:0_16:0)	546.4725	24	DAG-(16:0_18:1)	628.551	
	7	DAG-(14:1_16:1)	554.4781	25	DAG-(18:3_18:1) or DAG-(18:2_18:2)	634.5409	
	8	DAG-(12:0_18:1)	556.4932	26	DAG-(18:2_18:1)	636.5696	
	9	DAG-(14:0_16:0)	558.5093	27	DAG-(18:1_18:1)	638.5717	
	10	DAG-(14:0_18:1) or DAG-(16:1_16:0)	567.498	28	DAG-(18:1_18:0)	640.587	
	11	DAG-(14:0_16:0)	574.5038	29	DAG-(18:0_18:0)	642.6025	
	12	DAG-(14:1_18:2)	580.4937	30	DAG-(18:2_19:1)	650.5713	
	13	DAG-(14:1_18:1)	582.5088	31	DAG-(18:1_19:1)	652.5871	
	14	DAG-(14:0_18:1)	584.525	32	DAG-(18:2_18:1)	654.5665	
	15	DAG-(16:0_16:0)	586.5403	33	DAG-(18:0_19:1)	654.6029	
	16	DAG-(14:1_18:1)	598.5035	34	DAG-(18:2_19:1)	666.5656	
	17	DAG-(14:0_19:1)	598.5403	35	DAG-(19:1_19:1)	666.6022	
	18	DAG-(16:1_18:2)	608.5249	36	DAG-(18:1_19:1)	668.5821	
Triacylglycerols		Lipid classes	*m/z		Lipid classes	*m/z	
	37	TAG-(8:0_8:0_8:0)	488.3946	67	TAG-(14:0_15:0_16:0)	782.7227	
	38	TAG-(8:0_8:0_10:0)	516.4259	68	TAG-(10:0_18:1_18:1)	792.7075	
	39	TAG-(8:0_10:0_10:0)	544.4573	69	TAG-(12:0_16:0_18:1) or TAG-(14:0_14:0_18:1)	794.7225	
	40	TAG-(4:0_10:0_16:0)	572.4885	70	TAG-(14:0_16:0_16:0)	796.7381	
	41	TAG-(6:0_8:0_18:1)	598.5047	71	TAG-(15:0_16:0_16:0)	810.7535	
	42	TAG-(4:0_12:0_16:0) or TAG-(4:0_14:0_14:0)	600.5197	72	TAG-(12:0_18:1_18:1)	820.7381	
	43	TAG-(4:0_12:0_18:1)	626.5357	73	TAG-(16:0_16:0_16:0) or TAG-(14:0_16:0_18:0)	824.7692	
	44	TAG-(4:0_14:0_16:0)	628.5509	74	TAG-(14:0_17:0_18:0)	838.7852	
	45	TAG-(4:0_15:0_16:0)	642.5663	75	TAG-(14:0_18:1_18:1) or TAG-(16:0_16:1_18:1)	848.7691	
	46	TAG-(4:0_14:0_18:1)	654.567	76	TAG-(16:0_16:0_18:1)	850.7848	
	47	TAG-(4:0_16:0_16:0)	656.5821	77	TAG-(16:0_16:0_18:0)	852.8003	
	48	TAG-(4:0_14:0_19:1) or TAG-(4:0_16:0_17:1) or TAG-(4:0_15:0_18:1)	668.582	78	TAG-(15:0_18:2_18:1)	860.7651	
	49	TAG-(6:0_15:0_16:0)	670.5979	79	TAG-(15:0_18:1_18:1)	862.7848	
	50	TAG-(4:0_16:0_18:3)	678.5664	80	TAG-(16:0_18:3_18:2)	870.7528	
	51	TAG-(4:0_16:0_18:2)	680.5821	81	TAG-(16:0_18:2_18:2)	872.7687	
	52	TAG-(4:0_16:0_18:1)	682.5978	82	TAG-(16:0_18:2_18:1)	874.7847	
	53	TAG-(6:0_15:0_18:1)	696.6133	83	TAG-(16:0_18:1_18:1)	876.8001	
	54	TAG-(6:0_15:0_18:0)	698.6284	84	TAG-(16:0_18:1_18:0)	878.8162	
	55	TAG-(4:0_18:1_18:1)	708.6132	85	TAG-(16:0_18:0_18:0)	880.8312	

5. DEEP ANALYSIS OF MEMBRANE LIPIDS

56	TAG-(6:0_16:0_18:1)	710.6288	86	TAG-(16:0_18:1_19:1)	890.8163
57	TAG-(10:0_14:0_16:0)	712.6445	87	TAG-(18:2_18:2_18:1)	898.7836
58	TAG-(10:0_13:0_18:1)	724.6441	88	TAG-(18:2_18:1_18:1)	900.8001
59	TAG-(10:0_15:0_16:0)	726.66	89	TAG-(18:1_18:1_18:1)	902.8157
60	TAG-(6:0_18:1_18:1)	736.6441	90	TAG-(18:1_18:1_18:0)	904.8312
61	TAG-(8:0_16:0_18:1)	738.66	91	TAG-(18:1_18:0_18:0)	906.8478
62	TAG-(10:0_16:0_16:0)	740.6756	92	TAG-(18:1_18:1_20:1)	930.8476
63	TAG-(12:0_15:0_16:0)	754.6912	93	TAG-(18:1_18:1_20:0)	932.8627
64	TAG-(12:0_14:0_18:1) or TAG-(10:0_16:0_18:1)	766.691	94	TAG-(18:2_20:1_20:1)	956.8639
65	TAG-(12:0_14:0_18:0) or TAG-(10:0_16:0_18:0)	768.707	95	TAG-(18:1_18:1_22:0)	960.8942
66	TAG-(12:0_15:0_18:1)	780.7071			
	Lipid classes	*m/z		Lipid classes	*m/z
96	MGDG-(10:0_16:1)	662.4825	108	MGDG-(16:1_18:1)	772.5925
97	MGDG-(10:0_16:1)	662.4837	109	MGDG-(16:0_18:1)	774.6084
98	MGDG-(12:0_14:0)	664.4988	110	MGDG-(16:1_19:1)	786.6083
99	MGDG-(14:0_14:0)	692.5305	111	MGDG-(16:0_19:1)	788.6242
100	MGDG-(14:1_16:1)	716.5307	112	MGDG-(16:0_18:1(OH))	790.6029
101	MGDG-(14:0_16:1)	718.5456	113	MGDG-(18:1_18:1)	800.6241
102	MGDG-(14:0_16:0)	720.5615	114	MGDG-(18:1_18:0)	802.6396
103	MGDG-(16:1_16:1) or MGDG-(14:0_18:2)	744.5614	115	MGDG-(18:1_18:2(OH))	814.6018
104	MGDG-(14:0_18:1)	746.5768	116	MGDG-(18:1_19:1)	814.6395
105	MGDG-(16:0_16:0)	748.5932	117	MGDG-(18:1_18:1(OH))	816.6185
106	MGDG-(14:0_19:1)	760.5925	118	MGDG-(18:0_19:1)	816.6551
107	MGDG-(16:1_18:2)	770.577			
	Lipid classes	*m/z		Lipid classes	*m/z
119	DGDG-(12:0_14:0)	826.5521	129	DGDG-(16:1_18:2)	932.6281
120	DGDG-(14:1_14:0)	852.5673	130	DGDG-(16:1_18:1)	934.6439
121	DGDG-(14:0_14:0)	854.5819	131	DGDG-(16:0_18:1)	936.6594
122	DGDG-(14:1_16:1)	878.5832	132	DGDG-(16:1_19:1)	948.6599
123	DGDG-(14:0_16:1)	880.5981	133	DGDG-(16:0_19:1)	950.6743
124	DGDG-(14:0_16:0)	882.6137	134	DGDG-(18:1_18:1)	962.6752
125	DGDG-(16:1_16:1)	906.6143	135	DGDG-(18:1_18:0)	964.691
126	DGDG-(14:0_18:1)	908.6289	136	DGDG-(18:2_19:1)	974.6762
127	DGDG-(16:1_17:1)	920.6296	137	DGDG-(18:1_19:1)	976.6918
128	DGDG-(14:0_19:1)	922.6446	138	DGDG-(18:0_19:1)	978.7081
	Lipid classes	*m/z		Lipid classes	*m/z
139	PG 32:1	738.5291	143	PG 35:2	778.5583
140	PG 33:1	752.5413	144	PG 35:1	780.5744
141	PG 34:2	764.543	145	PG 36:2	792.5756
142	PG 34:1	766.559	146	PG 37:2	806.5902

*Adduct [M +NH₄]⁺

Table S5.3 (B) Summary of lipid classes and species in *L. bulgaricus* CFL1 by LC-MS/MS in negative mode

Glycolipids	Lipid classes		*m/z	Lipid classes		*m/z
	1	MGDG-(8:0_16:1)	661.4176	14	MGDG-(16:1_18:2)	797.5416
	2	MGDG-(10:0_14:0)	663.4324	15	MGDG-(16:1_18:1)	799.5577
	3	MGDG-(10:0_16:1)	689.4479	16	MGDG-(16:0_18:1)	801.5734
	4	MGDG-(12:0_14:0)	691.4636	17	MGDG-(16:1_19:1)	813.5731
	5	MGDG-(12:0_16:1)	717.4798	18	MGDG-(16:1_18:1(OH))	815.5519
	6	MGDG-(14:0_14:0)	719.4951	19	MGDG-(16:0_19:1)	815.5886
	7	MGDG-(14:1_16:1)	743.495	20	MGDG-(16:0_18:1(OH))	817.5682
	8	MGDG-(14:0_16:1)	745.5106	21	MGDG-(18:2_18:1)	825.5732
	9	MGDG-(14:0_16:0)	747.5266	22	MGDG-(18:1_18:1)	827.5889
	10	MGDG-(16:1_16:1)	771.5262	23	MGDG-(18:1_18:0)	829.6047
	11	MGDG-(14:0_18:1)	773.5421	24	MGDG-(18:2_19:1)	839.5892
	12	MGDG-(16:0_16:0)	775.5556	25	MGDG-(18:1_19:1)	841.6047
	13	MGDG-(14:0_19:1)	787.5571	26	MGDG-(18:0_19:1)	843.6196
	Glycolipids	Lipid classes		*m/z	Lipid classes	
27		DGDG-(18:1_19:1)	1003.6568	37	DGDG-(16:0_16:0)	937.6102
28		DGDG-(10:0_16:1)	851.5009	38	DGDG-(14:0_19:1)	949.6106
29		DGDG-(12:0_14:0)	853.516	39	DGDG-(16:1_18:1)	961.61
30		DGDG-(14:0_14:1)	879.5318	40	DGDG-(16:0_18:1)	963.626
31		DGDG-(14:0_14:0)	881.5473	41	DGDG-(16:1_19:1)	975.6258
32		DGDG-(14:1_16:1)	905.5478	42	DGDG-(16:0_19:1)	977.6412
33		DGDG-(14:0_16:1)	907.5633	43	DGDG-(18:2_18:1)	987.6257
34		DGDG-(14:0_16:0)	909.5791	44	DGDG-(18:1_18:1)	989.6416
35		DGDG-(16:1_16:1)	933.5796	45	DGDG-(18:1_18:0)	991.6579
36	DGDG-(14:0_18:1)	935.5949				
Phospholipids	Lipid classes		**m/z	Lipid classes		**m/z
	46	Lyso PG 14:0	455.2416	57	PG (14:0_19:1)	733.5025
	47	Lyso PG 16:1	481.2567	58	PG (16:1_18:2)	743.4871
	48	Lyso PG 16:0	483.2725	59	PG (16:1_18:1)	745.5025
	49	Lyso PG 18:1	509.2882	60	PG (16:0_18:1)	747.5178
	50	Lyso PG 19:1	523.3048	61	PG (16:1_19:1)	759.5182
	51	PG (14:1_14:0)	663.4247	62	PG (16:0_19:1)	761.5343
	52	PG (14:1_16:1)	689.441	63	PG (16:0(OH)_18:1)	763.5129
	53	PG (14:0_16:1)	691.4551	64	PG (18:2_18:1)	771.5191
	54	PG (14:0_16:0)	693.4714	65	PG (18:1_18:1)	773.5349
55	PG (16:1_16:1)	717.4723	66	PG (18:1_19:1)	787.5492	

*Adduct [M +HCOO]⁻**Adduct [M -H]⁻

Table S5.4 Pearson coefficients of significant relationships between fatty acid composition (UFA, SFA, CFA), lipid phase transition temperatures (Ts and Tm), anisotropy values, and resistance of *L. bulgaricus* CFL1 to freezing (dt_{spe} F) and freeze-drying (dt_{spe} FD).

Variables	dt _{spe} F	UFA	SFA	CFA	Ts	Tm	Anisotropy (r)
dt _{spe} F	1.0	-0.5	0.6	-0.4	0.7	0.7	0.5
UFA		1.0	-1.0	-0.3	-0.9	-0.9	-0.8
SFA			1.0	NS	0.9	0.9	0.8
CFA				1.0	NS	NS	0.4
Ts					1.0	1.0	0.8
Tm						1.0	0.8
Anisotropy (r)							1.0

Variables	dt _{spe} FD	UFA	SFA	CFA	Ts	Tm	Anisotropy (r)
dt _{spe} FD	1.0	NS	NS	-0.9	NS	NS	NS
UFA		1.0	-1.0	-0.3	-0.9	-0.9	-0.8
SFA			1.0	NS	0.9	0.9	0.8
CFA				1.0	NS	NS	0.4
Ts					1.0	1.0	0.8
Tm						1.0	0.8
Anisotropy (r)							1.0

NS: Not Significant; bold values are for the coefficients > 0.5 for dt_{spe} F and dt_{spe} FD.

5.8.2. Supplementary Figures

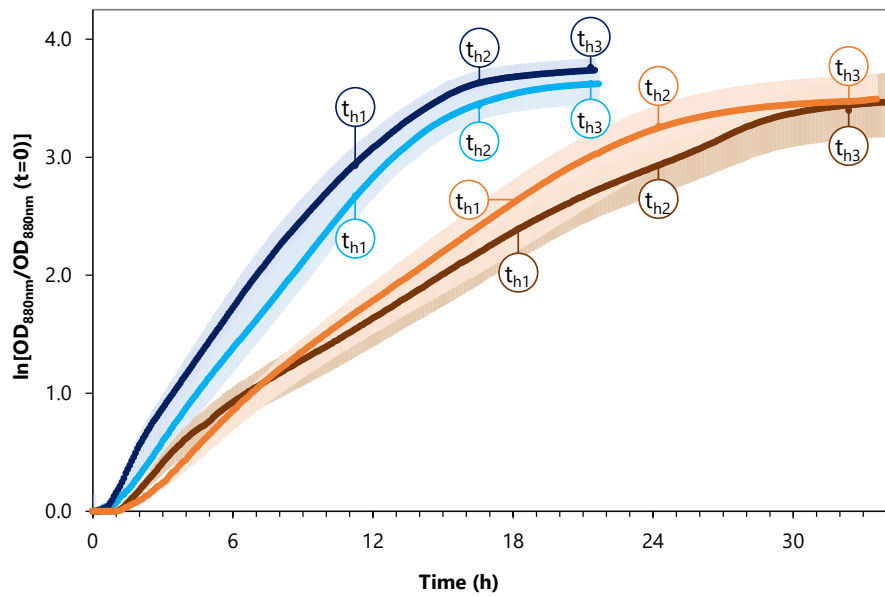


Figure S5.1 Growth curves of *L. bulgaricus* CFL1 at four different fermentation conditions. [42°C, pH 5.8] is represented by a blue curve, [42°C, pH 4.8] by a light blue curve, [37°C, pH 5.8] by a brown curve, and [37°C, pH 4.8] by an orange curve. The three different harvest times are indicated inside circles per fermentation condition. t_{h1} : mid-exponential growth phase; t_{h2} : deceleration growth phase; and t_{h3} : stationary growth phase. Curves correspond to the means of three independent biological replicates and shaded areas to the standard deviations.

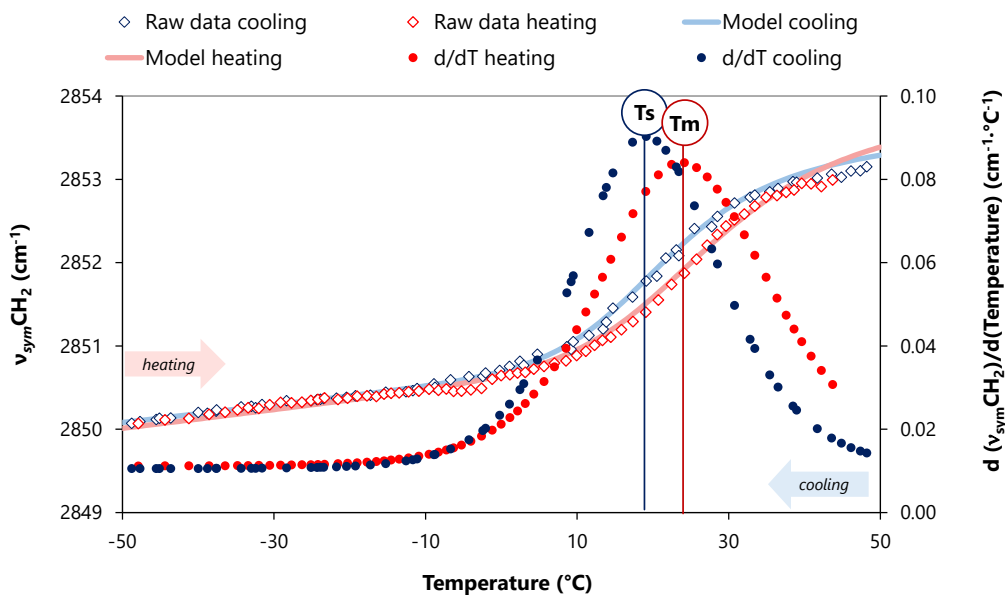


Figure S5.2 Example of wavenumbers of the symmetric CH_2 stretching peak ($\nu_{\text{sym}}\text{CH}_2$) versus temperature upon cooling and heating *L. bulgaricus* CFL1 cells grown at 42°C, pH5.8 and harvested at the stationary growth phase (t_{h3}). Raw data are represented by empty blue and red diamonds and the asymmetric sigmoid transition models by light blue (cooling) and red curves (heating). Full blue and red circles indicate the first derivatives from the model curves and the maximum of each curve corresponds to the lipid phase transition temperatures upon cooling (T_s) and heating (T_m).

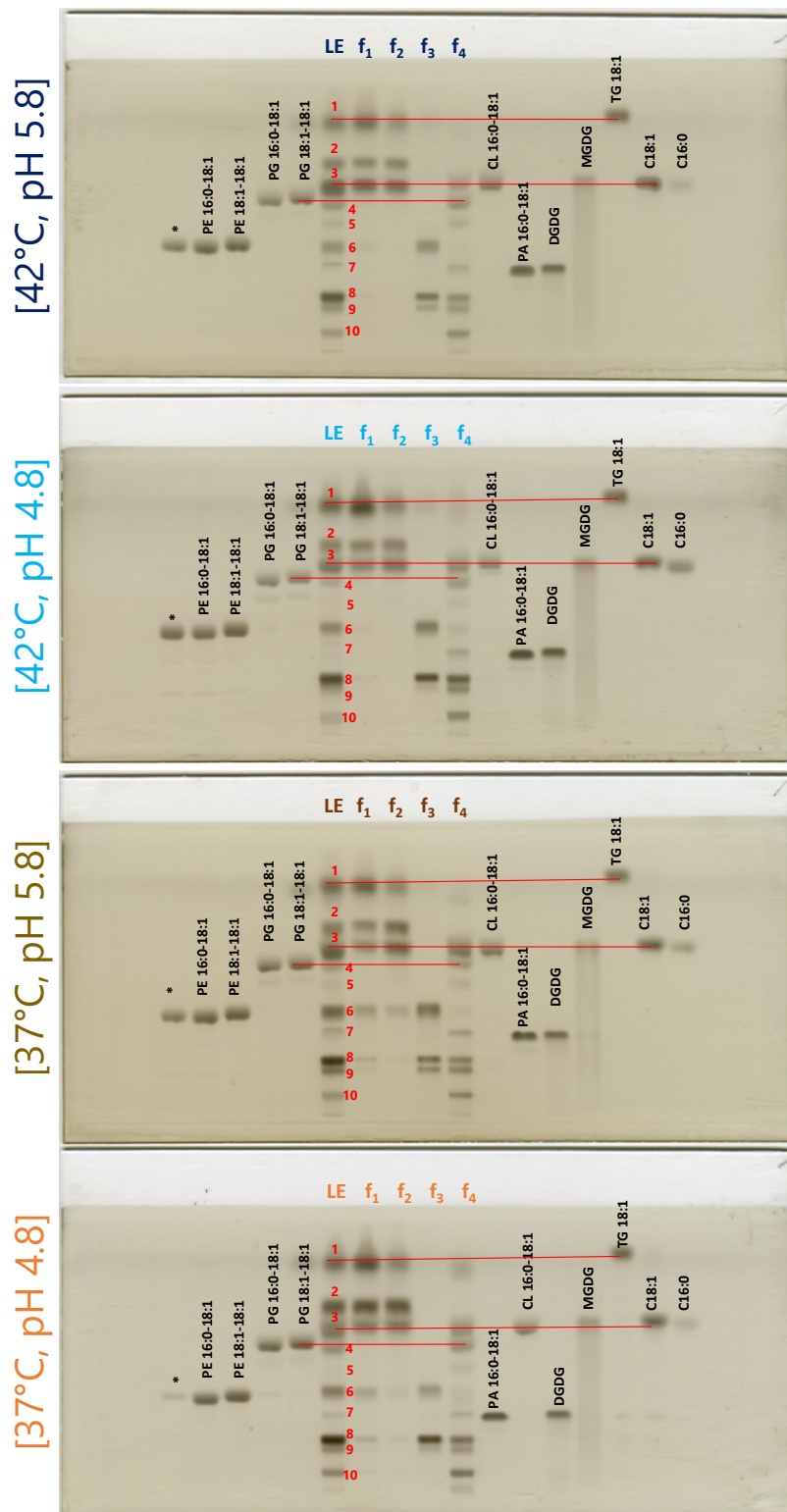


Figure S5.3 Lipid classes distribution of *L. bulgaricus* CFL1 harvested at the stationary growth phase (t_{h3}) for the four fermentation conditions studied: [42°C, pH 5.8], [42°C, pH 4.8], [37°C, pH 5.8], and [37°C, pH 4.8]. Each lipid extract (LE) was fractionated by the elution of different solvents: f₁, chloroform; f₂, chloroform-acetone (50/50); f₃, acetone; and f₄, methanol. Red lines correspond to the phospholipids identified by the retention factor (Rf). The dipping solution used was CuSO₄:H₃PO₄:H₂SO₄ (10/4/4).* in each first track represents PE 16:0-18:1, deposit carried out due to HPTLC equipment configuration.

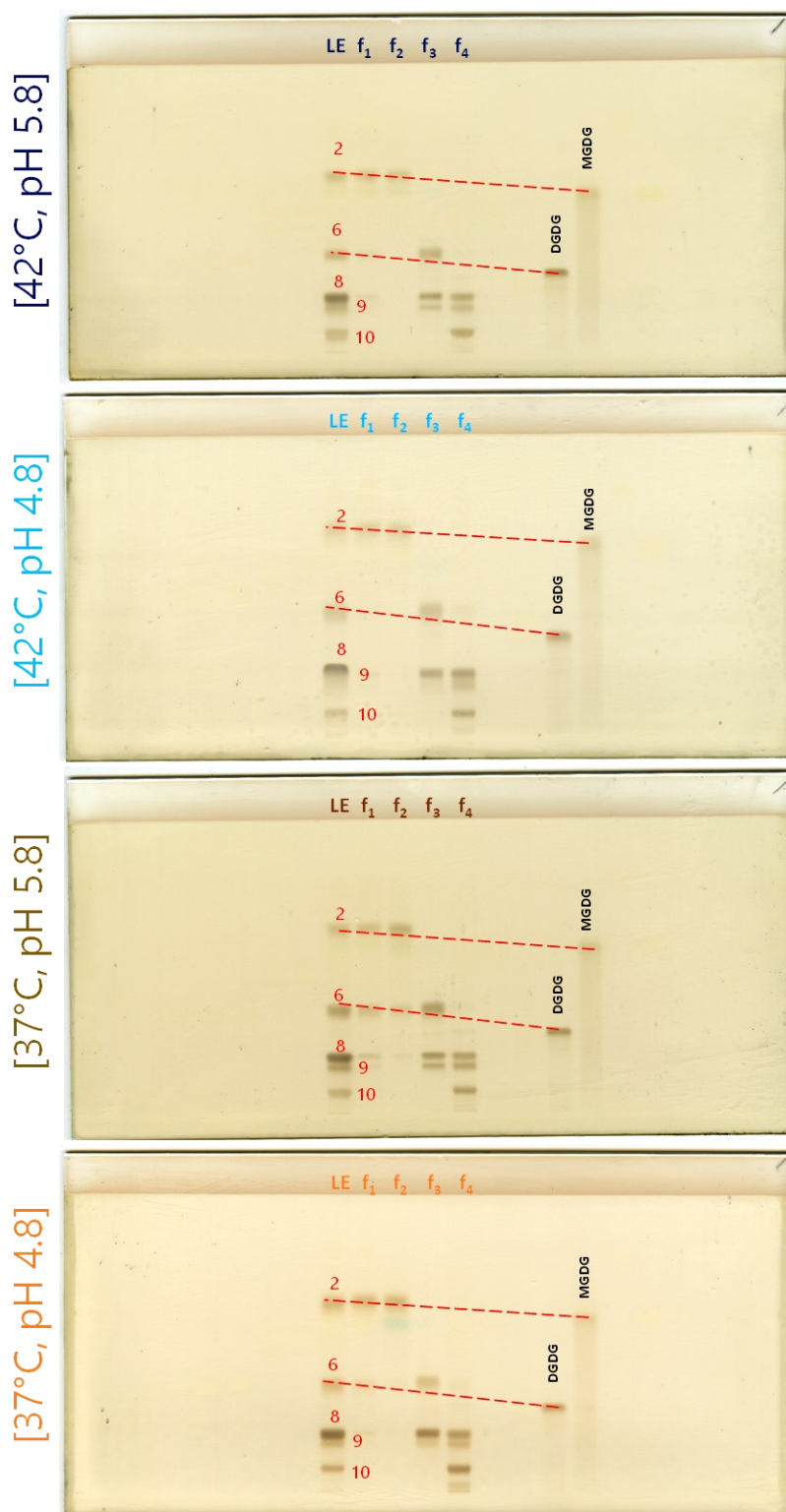


Figure S5.4 Lipid classes distribution of *L. bulgaricus* CFL1 harvested at the stationary growth phase (t_{h3}) for the four fermentation conditions studied: [42°C, pH 5.8], [42°C, pH 4.8], [37°C, pH 5.8], and [37°C, pH 4.8]. Each lipid extract (LE) was fractionated by the elution of different solvents: f₁, chloroform; f₂, chloroform-acetone (50/50); f₃, acetone; and f₄, methanol. Red dashed lines correspond to the possible glycolipids in the samples. The dipping solution used was Naphtol-H₂O-CH₃CH₂OH-H₂SO₄. Less lines per fraction were observed and phospholipids standards were absent since Naphtol only allows the visualization of sugars moieties in lipids.



Figure S5.5 Lipid classes distribution of *L. bulgaricus* CFL1 harvested at the stationary growth phase (t_{h3}) for the four fermentation conditions studied: (a) [42°C, pH 5.8], (b) [42°C, pH 4.8], (c) [37°C, pH 5.8], and (d) [37°C, pH 4.8]. Each lipid extract (LE) was fractionated by the elution of different solvents: f₁, chloroform; f₂, chloroform-acetone (50/50); f₃, acetone; and f₄, methanol. The dipping solution used was Ninhydrin-C₄H₉OH-CH₃COOH. Fractions and phospholipids standards were absent since Ninhydrin only allows the visualization of amino groups in lipids. * in each first track represents PE 16:0-18:1, deposit carried out due to HPTLC equipment configuration.

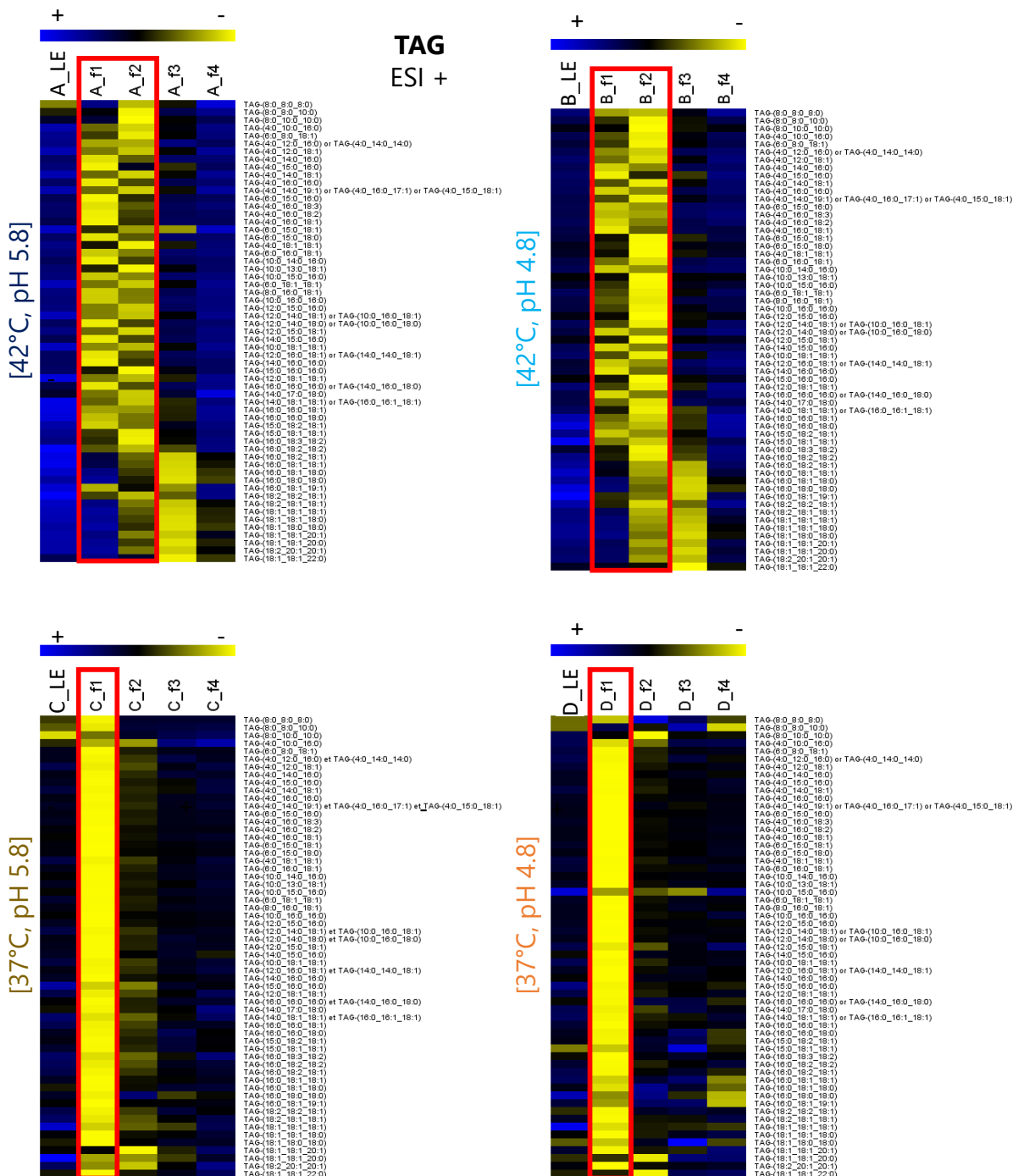


Figure S5.6 Triacylglycerols (TAG) of *L. bulgaricus* CFL1 membrane harvested at the stationary growth phase (t_{h3}) for the four fermentation conditions studied: A, [42°C, pH 5.8]; B, [42°C, pH 4.8]; C, [37°C, pH 5.8]; and D, [37°C, pH 4.8]. Each lipid extract (LE) was fractionated by the elution of different solvents: f₁, chloroform; f₂, chloroform-acetone (50/50); f₃, acetone; and f₄, methanol. Electrospray ionization (ESI) in positive mode. Red boxes indicate the highest relative abundance in the fraction.

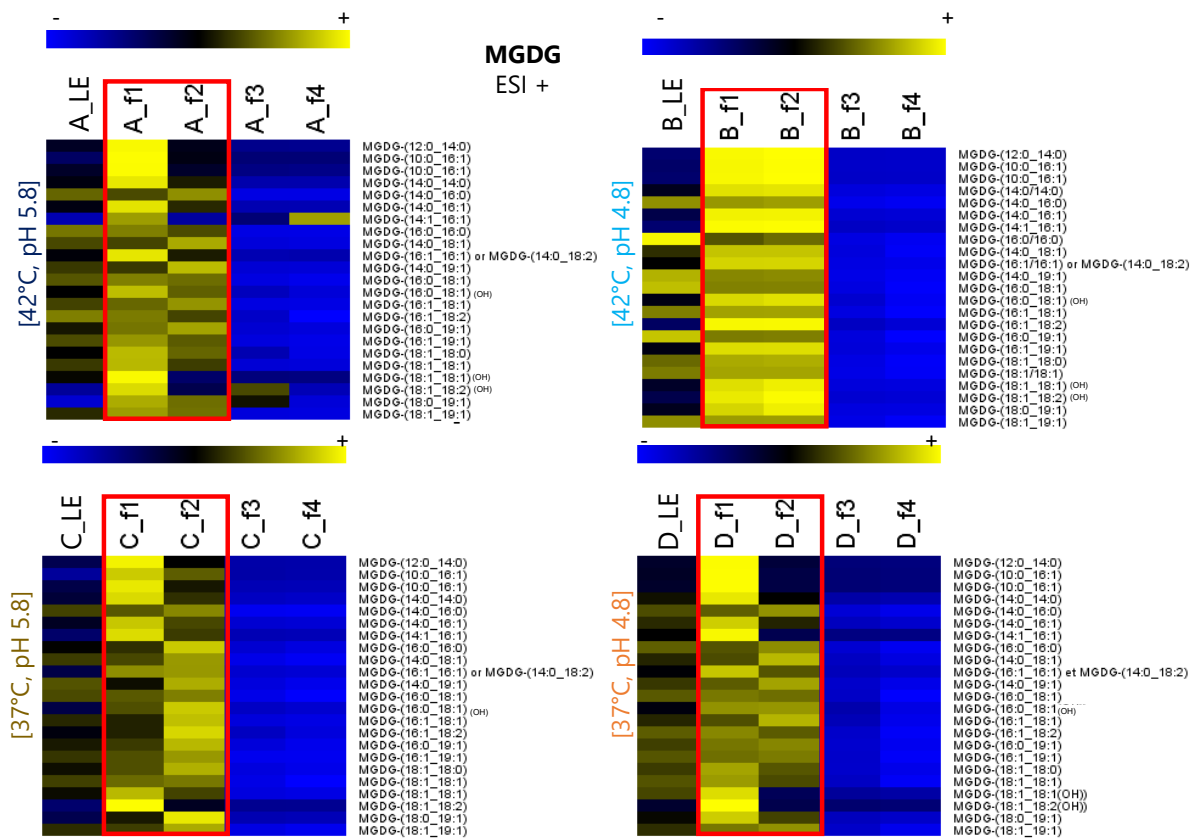


Figure S5.7 Monoglycodiacylglycerols (MGDG) of the *L. bulgaricus* CFL1 membrane harvested at the stationary growth phase (t_{h3}) for the four fermentation conditions studied: A, [42°C, pH 5.8]; B, [42°C, pH 4.8]; C, [37°C, pH 5.8]; and D, [37°C, pH 4.8]. Each lipid extract (LE) was fractionated by the elution of different solvents: f₁, chloroform; f₂, chloroform-acetone (50/50); f₃, acetone; and f₄, methanol. Electrospray ionization (ESI) in positive mode. Red boxes indicate the highest relative abundance in the fraction.

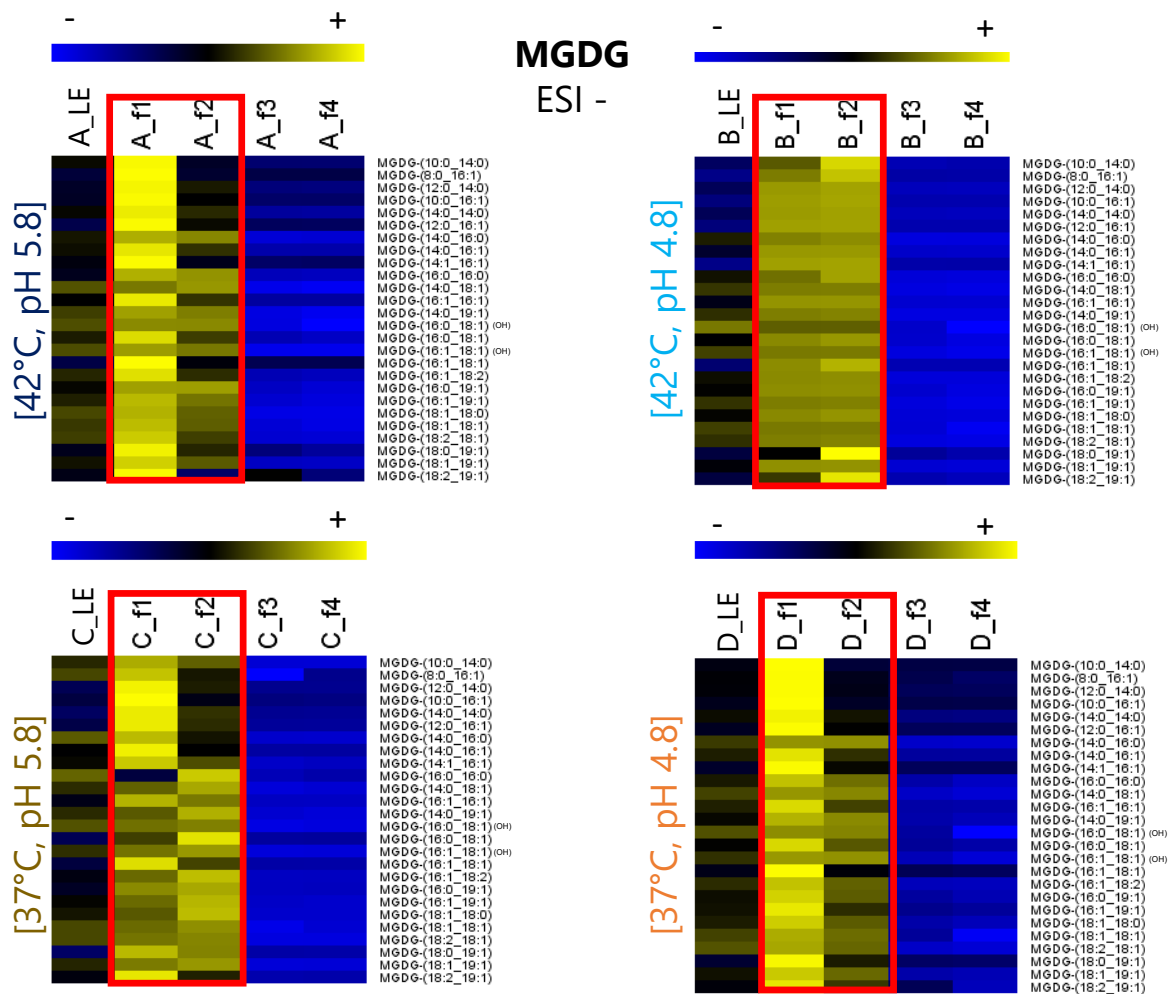


Figure S5.8 Monoglycodiacylglycerols (MGDG) of the *L. bulgaricus* CFL1 membrane harvested at the stationary growth phase (t_{h3}) for the four fermentation conditions studied: A, [42°C, pH 5.8]; B, [42°C, pH 4.8]; C, [37°C, pH 5.8]; and D, [37°C, pH 4.8]. Each lipid extract (LE) was fractionated by the elution of different solvents: f₁, chloroform; f₂, chloroform-acetone (50/50); f₃, acetone; and f₄, methanol. Electrospray ionization (ESI) in negative mode. Red boxes indicate the highest relative abundance in the fraction.

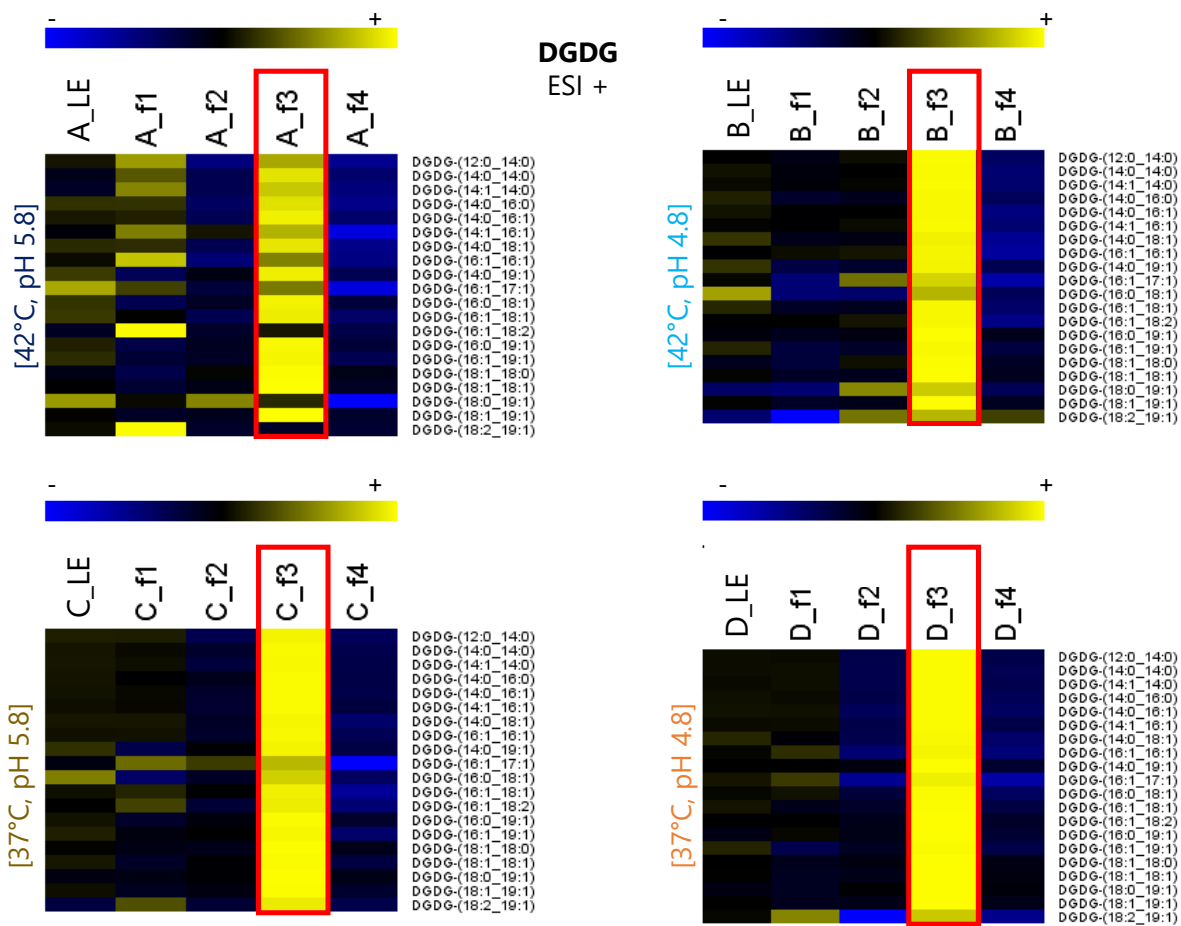


Figure S5.9 Diglycodiacylglycerols (DGDG) of the *L. bulgaricus* CFL1 membrane harvested at the stationary growth phase (t_{h3}) for the four fermentation conditions studied: A, [42°C, pH 5.8]; B, [42°C, pH 4.8]; C, [37°C, pH 5.8]; and D, [37°C, pH 4.8]. Each lipid extract (LE) was fractionated by the elution of different solvents: f₁, chloroform; f₂, chloroform-acetone (50/50); f₃, acetone; and f₄, methanol. Electrospray ionization (ESI) in positive mode. Red boxes indicate the highest relative abundance in the fraction.

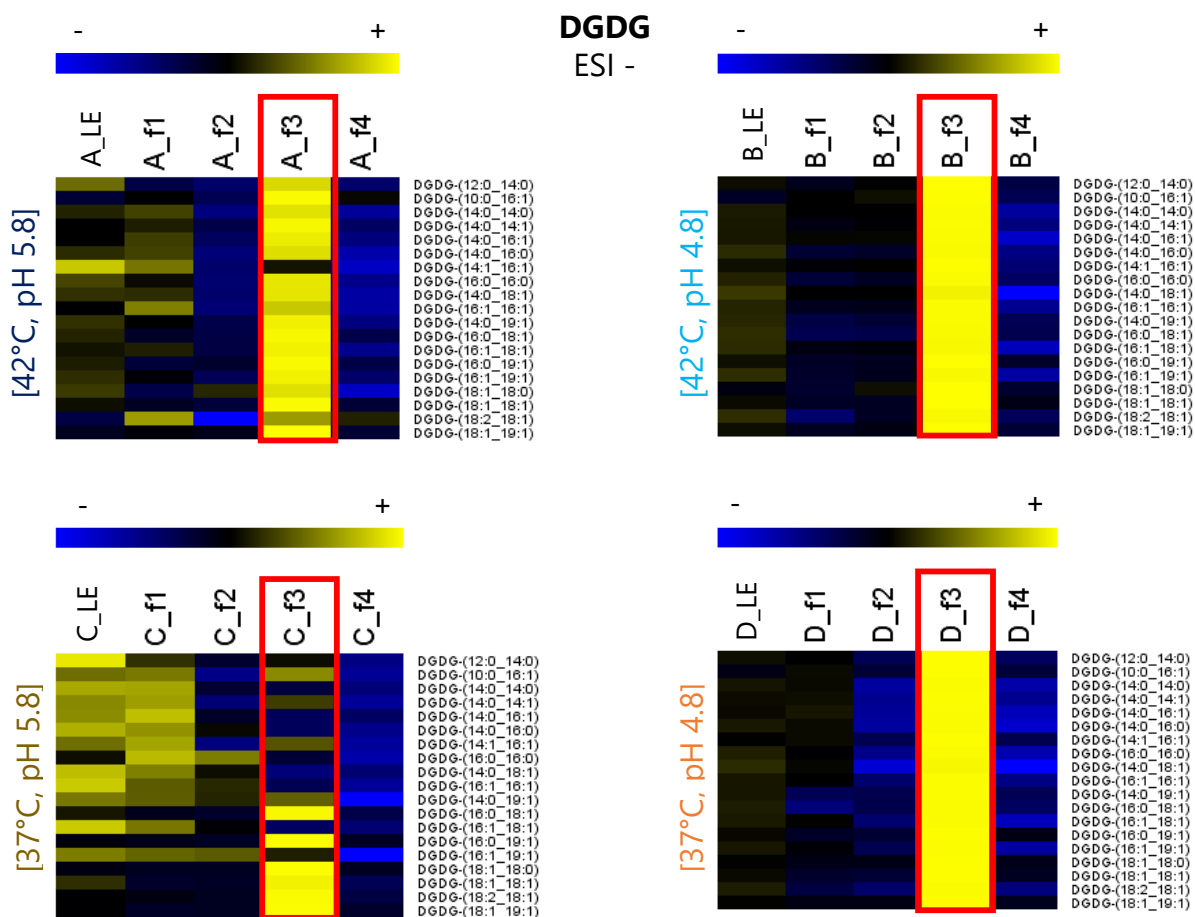


Figure S5.10 Diglycodylacylglycerols (DGDG) of the *L. bulgaricus* CFL1 membrane harvested at the stationary growth phase (t_{h3}) for the four fermentation conditions studied: A, [42°C, pH 5.8], B, [42°C, pH 4.8], C, [37°C, pH 5.8], and D, [37°C, pH 4.8].

Each lipid extract (LE) was fractionated by the elution of different solvents: f₁, chloroform; f₂, chloroform-acetone (50/50); f₃, acetone; and f₄, methanol. Electrospray ionization (ESI) in negative mode. Red boxes indicate the highest relative abundance in the fraction.

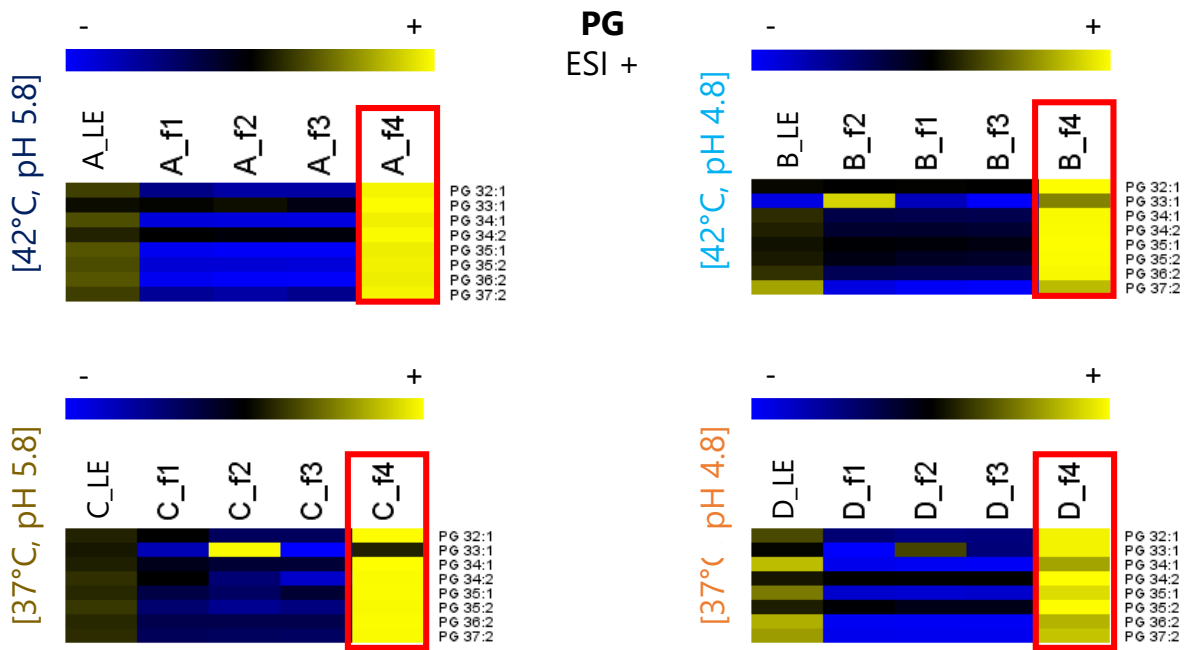


Figure S5.11 Phosphatidylglycerols (PG) of the *L. bulgaricus* CFL1 membrane harvested at the stationary growth phase (t_{h3}) for the four fermentation conditions studied: A, [42°C, pH 5.8]; B, [42°C, pH 4.8]; C, [37°C, pH 5.8], and D, [37°C, pH 4.8]. Each lipid extract (LE) was fractionated by the elution of different solvents: f₁, chloroform; f₂, chloroform-acetone (50/50); f₃, acetone; and f₄, methanol. Electrospray ionization (ESI) in negative mode. Red boxes indicate the highest relative abundance in the fraction.

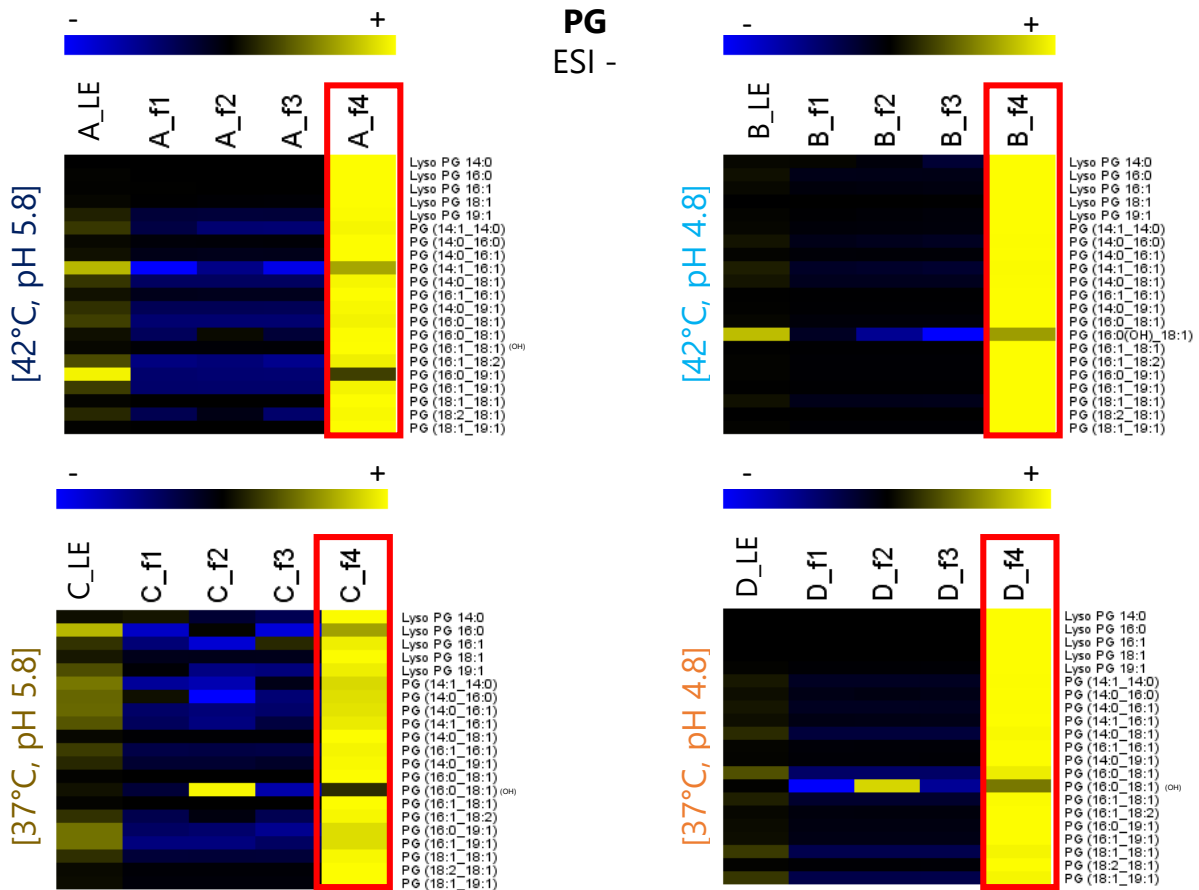


Figure S5.12 Phosphatidylglycerols (PG) of the *L. bulgaricus* CFL1 membrane harvested at the stationary growth phase (t_{h3}) for the four fermentation conditions studied: A, [42°C, pH 5.8]; B, [42°C, pH 4.8]; C, [37°C, pH 5.8], and D, [37°C, pH 4.8].

Each lipid extract (LE) was fractionated by the elution of different solvents: f₁, chloroform; f₂, chloroform-acetone (50/50); f₃, acetone; and f₄, methanol. Electrospray ionization (ESI) in negative mode. Red boxes indicate the highest relative abundance in the fraction.

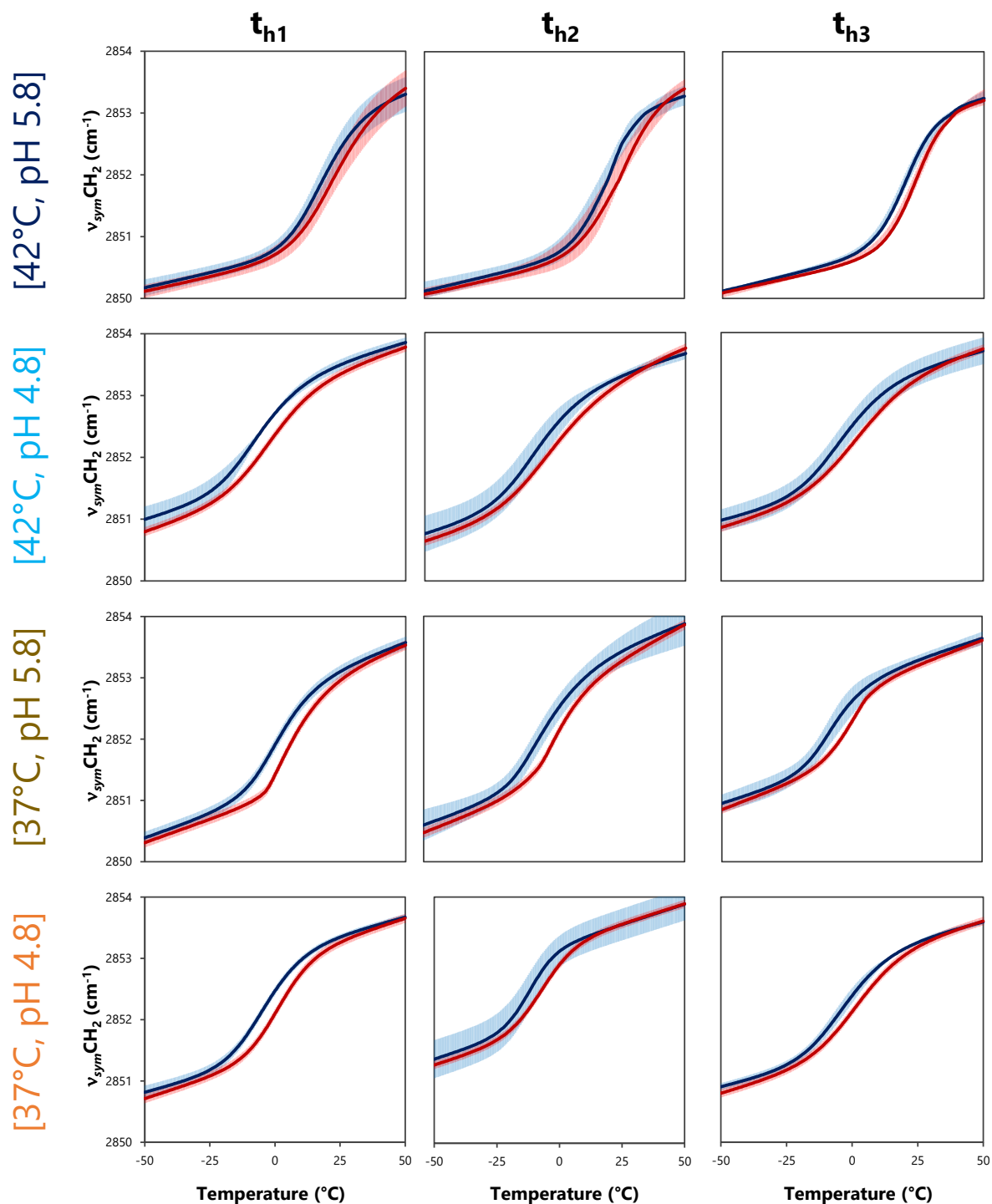


Figure S5.13 Peak positions of the symmetric CH_2 stretching vibration band (ν_{symCH_2}) arising from *L. bulgaricus* CFL1. Upon cooling (blue fitted curves) and heating (red fitted curves) for [42°C, pH 5.8], [42°C, pH 4.8] [37°C, pH 5.8], and [37°C, pH 4.8]. Cells were harvested at different harvest times. t_{h1} : mid-exponential growth phase; t_{h2} : deceleration growth phase; and t_{h3} : stationary growth phase. Curves correspond to the means of three independent biological replicates and shaded areas to the standard deviations.

5.9. Prospects for this study

- Performing a deep analysis of membrane lipids for freeze-dried bacteria

The results in Chapter 5 highlighted that the CFA content was the only parameter linked to the freeze-drying resistance of *L. bulgaricus* CFL1. Castro et al. (1997); Hlaing et al. (2017) showed that the freeze-drying process induces changes in membrane lipids during the drying stage (Castro et al. 1997; Hlaing et al. 2017). Thus, one could speculate that the lipid composition and properties after freeze-drying would differ from the initial (after fermentation and harvest). In that case, the relationships between the changes in membrane lipids during fermentation and the freeze-drying resistance might be subtle. Therefore, it would be necessary to perform a complete characterization of membrane lipids after this stabilization process to understand to which degree the membrane lipids would be associated with the freeze-drying resistance of *L. bulgaricus* CFL1.

- Quantifying the glycolipids and phospholipids identified in the *L. bulgaricus* CFL1 membrane

Our study successfully identified the different lipids in the *L. bulgaricus* CFL1 membrane. It was reported the relative abundance of the lipid was based on the peak areas. Thanks to this information, we could thus perform calibration curves that allowed us to quantify these lipids and correlate the lipid concentration to the resistance data of *L. bulgaricus* CFL1.

Take-home messages**Chapter 5: Deep analysis of membrane lipids and their relationships with *L. bulgaricus* CFL1 resistance to freezing and freeze-drying**

- *L. bulgaricus* CFL1 cultivated at a different condition from the optimal for growth, [42°C, pH 5.8], exhibited different changes in the biochemical composition and biophysical properties of the membrane lipids.
- *L. bulgaricus* CFL1 cultivated at [42°C, pH 5.8] exhibited a membrane with a higher content of SFA, higher lipid phase transition temperatures (Ts and Tm), and a lower membrane fluidity than for cells cultivated in the other three fermentation conditions.
- Low fermentation pH or temperature induced UFA, subzero or zero lipid phase transition temperatures, and a fluid membrane.
- The primary membrane lipids of the *L. bulgaricus* CFL1 are the glycolipids MGDG, DGDG (one and two sugar monomers, respectively), and PG.
- Fermentation carried out at [42°C, pH 5.8] led to cells with the lowest relative abundance of DGDGs and several Lyso-PGs abundances.
- Fermentation at pH 4.8 led to cells with the highest relative abundance of DGDG with specific FA chains (14, 16, and 18 carbon chains).
- The freezing resistance of *L. bulgaricus* CFL1 was related to a high UFA content (low SFA), low lipid membrane phase transition temperatures, and a more fluid membrane.
- The freeze-drying resistance of *L. bulgaricus* CFL1 was only related to a high CFA content.

Chapter 6

6. INFLUENCE OF SUGARS ON RESISTANCE AND THE MEMBRANE OF *L. bulgaricus* CFL1

Of the four fermentation conditions studied in Chapter 4, the fermentation condition that led to the highest biomass production was [42°C, pH 5.8]. This fermentation condition produced *L. bulgaricus* CFL1 cells exhibiting the lowest resistance to freezing and an acceptable resistance to freeze-drying, provided cells were cultivated at t_{h3} .

So far, sucrose was the sugar to protect *L. bulgaricus* CFL1 cells against stabilization stress. In the context of the European project PREMIUM, we tried to understand the effect of the degree of polymerization of sugars on the cryo-resistance.

This chapter, thus, presents the influence of seven sugars with different degrees of polymerization on *L. bulgaricus* CFL1's resistance to freezing and freeze-drying and the membrane lipids of the cells.

SUMMARY OF THE CHAPTER

6. INFLUENCE OF SUGARS ON RESISTANCE AND THE MEMBRANE OF <i>L. bulgaricus</i> CFL1	225
6.1. Preamble	227
6.2. Introduction	227
6.3. Experimental approach	229
6.3.1. Protection of <i>L. bulgaricus</i> CFL1 and physical properties of sugars	229
6.3.1.1. Protection of <i>L. bulgaricus</i> by different sugars	229
6.3.2. The loss of functional properties of protected <i>L. bulgaricus</i> CFL1 cells with different sugars during freezing and freeze-drying	232
6.3.3. Sample preparation for FTIR analysis	232
6.3.4. FTIR spectra acquisition and analysis	232
6.3.5. Statistical analysis	234
6.4. Results and discussion	235
6.4.1. Resistance of <i>L. bulgaricus</i> CFL1 to freezing and freeze-drying using different sugars	235
6.4.1.1. Resistance of <i>L. bulgaricus</i> CFL1 to freezing	235
6.4.1.2. Resistance of <i>L. bulgaricus</i> CFL1 to freeze-drying	238
6.4.2. The influence of sugars with different degrees of polymerization on the membrane of <i>L. bulgaricus</i> CFL1 by FTIR241	
6.4.2.1. Lipid phase transition of hydrated and air-dried cells protected with different sugars upon cooling and heating 242	
i. Hydrated cells	242
ii. Air-dried cells	245
i. Influence of sugars on fatty acyl arrangement	248
6.4.2.2. Effect of sugars on phospholipids' polar head of hydrated and air-dried cells	249
6.5. Conclusion	252
6.6. Prospects for this study	252

6.1. Preamble

This study was conducted as part of a six-month internship for a M1 student under my supervision. The results and analysis of this chapter, unlike Chapters 4 and 5, are not intended for publication. The structure of the current chapter is presented conventionally with the following sections: introduction, experimental approach, results and discussion, and closing with a conclusion.

Supplementary information is available in Chapter 3 materials and methods.

Chapter 6: subsection	Chapter 3: section or subsection
6.3.1. Protection of <i>L. bulgaricus</i> CFL1 and physical properties of sugars	3.1. Production of concentrated <i>L. bulgaricus</i> CFL1
6.3.2. Loss of functional properties of protected <i>L. bulgaricus</i> CFL1 cells with different sugars during freezing and freeze-drying	3.7.3. Protection efficiency of different sugars during freezing and freeze-drying
6.3.3. Sample preparation for FTIR analysis	3.7.4.1. Hydrated cells 3.7.4.2. Air-dried cells
6.3.4. FTIR spectra acquisition and analysis	3.7.4.3. FTIR study
6.3.5. Statistical analysis	3.8.3. ANOVA tests

6.2. Introduction

The essential role of Lactic Acid Bacteria (LAB) in the food and functional food industries emphasizes the requirement of the stabilization process such as freezing and freeze-drying to preserve these bacteria for an extended period. Water removal is the leading cause of damage to bacterial structures during these processes. The cell membrane has been identified as the primary degradation target (Brennan et al. 1986; Tymczynszyn et al. 2007; Bravo-Ferrada et al. 2018). Consequently, losses in the functional activities of LAB (e.g., acidifying activity, viability, culturability, among others) may be encountered. A common prevention strategy is adding a protective solution, such as sugar molecules, after production and concentration (Chapter 1, subsection 1.3.2). The efficiency of sugars as protective molecules to keep LAB's survival and functional properties after freezing or freeze-drying has been demonstrated for different LAB species, including *L. bulgaricus* (Castro et al. 1997; De Giulio et al. 2005; Martos et al. 2007; Romano et al. 2016b).

The mechanisms of protection of sugars are based on two hypotheses involving the lipid membrane: the water replacement and the hydration forces hypothesis. On the one hand, the water replacement hypothesis establishes that the water removal during drying may be replaced by the groups OH of the sugars forming hydrogen bonds with the phosphates in the polar head of the phospholipids (Crowe et al. 1984, 1992; Crowe 2002). On the other hand, the hydration forces (water entrapment) hypothesis states that sugars are preferentially expelled

from the hydration zone of polar heads. Consequently, the sugars help trap the water molecules close to the surrounding phospholipid (Yoon et al. 1998; Demé and Zemb 2000; Dhaliwal et al. 2019).

The European PREMIUM project proposes innovative and efficient protective molecules such as fructo-oligosaccharides (FOS) and galacto-oligosaccharides (GOS). From a chemical point of view, FOS and GOS are mixtures of small chain oligosaccharides with different degrees of polymerization composed of fructose (for FOS) or galactose (for GOS) units. They can be synthesized enzymatically from sucrose (for FOS) or lactose (GOS), or they can be obtained by hydrolysis from bioproducts of vegetal matrices (Romano et al. 2016a; Martins et al. 2019). These processes lead to mixtures of FOS and GOS of different degrees of polymerization (DP) ranging from 2 to 6 (Crittenden and Playne 2008). The degree of polymerization is defined as the number of monomer units in a polymer.

Preliminary studies highlighted the benefit of FOS and GOS in stabilizing LAB during freezing, freeze-drying, and other drying methods (Schwab et al. 2007; Tymczyszyn et al. 2012; Romano et al. 2016b, 2021; Sosa et al. 2016). In this context, we were interested in analyzing if this concept could be extended to another lactic acid bacterium, such as *L. bulgaricus* CFL1. A strain characterized by its high sensitivity to cryo-processes. Also, we aimed at understanding the protection mechanisms of sugars.

Thus, the present work investigates the effect of sugars with different degrees of polymerization (DP), from DP1 to DP>10, on *L. bulgaricus* CFL1 resistance and on the membrane. The selected sugars are part of the basic structures in FOS and GOS. FTIR was used in this work for assessing the effect of sugars on the LAB membrane.

6.3. Experimental approach

The overall experimental approach used for this chapter is summarized in Figure 6.1. Methodological details that are not included in this chapter, please refer to Chapter 3 Materials and Methods.

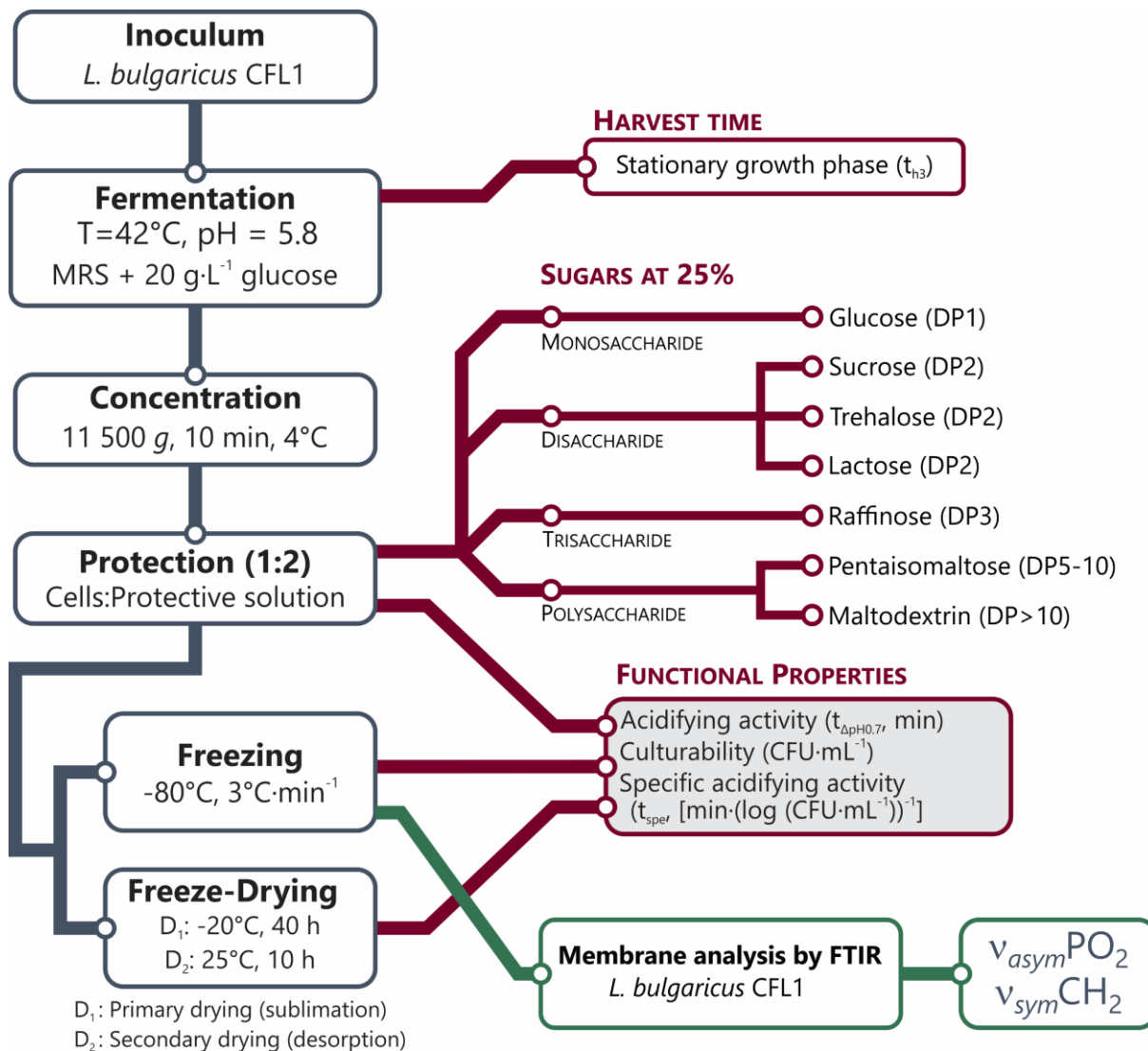


Figure 6.1 Diagram of the experimental approach used in this study and the main investigated parameters. Abbreviations: D₁, primary drying; D₂, secondary drying; DP, degree of polymerization; t_{sper}, specific acidifying activity; v_{asym}PO₂, the asymmetric PO₂ stretching vibration band; v_{sym}CH₂, the symmetric CH₂ stretching vibration band.

6.3.1. Protection of *L. bulgaricus* CFL1 and physical properties of sugars

6.3.1.1. Protection of *L. bulgaricus* by different sugars

L. bulgaricus CFL1 cells were grown at [42°C, pH 5.8], and harvested at the stationary growth phase, t_{h3}. (Chapter 3, subsection 3.1). This fermentation condition was chosen to produce the necessary biomass concentration to protect bacteria with different sugar solutions (>10 g·L⁻¹). Seven different solutions at 25% w/w (in NaCl at 0.9%) were used to protect concentrated bacteria. These were glucose (G), sucrose (S), trehalose (T), lactose (L), raffinose (R),

pentaisomaltose (P), and maltodextrin (M). At a ratio of 1:2 (1 g of concentrated cells for 2 g of the protective solution), *L. bulgaricus* CFL1 suspensions were prepared. The choice of the sugar concentration was adequate to observe the contribution of sugars to the FTIR spectra of bacterial cells (Meneghel et al. 2017).

These seven sugars were selected because of the following reasons:

- (i) Their commercial availability for the seven sugars
- (ii) Their use as standard molecules to protect LAB, such as trehalose
- (iii) Some of them are part of the basic structures in polysaccharides such as FOS and GOS, such as sucrose, lactose, and raffinose.
- (iv) One of them has similar DP to FOS and GOS, such as pentaisomaltose.
- (v) The maltodextrin, a polysaccharide, was chosen to compare its protective efficacy and how this molecule could protect the membrane. The selected maltodextrin has a higher DP (>10) compared to FOS and GOS.

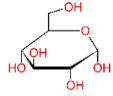
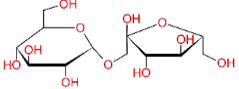
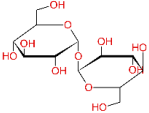
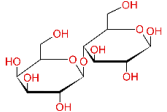
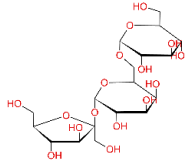
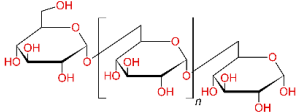
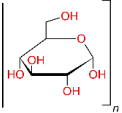
The structure, the degree of polymerization, and the physicochemical properties of the seven sugars are summarized in Table 6.1

The physicochemical properties of each sugar solution were measured as indicated in Chapter 3, subsection 3.6.2. These properties were determined to investigate whether they could be related to bacterial resistance to freezing and freeze-drying. The measurements to characterize each solution included osmolarity, viscosity at two different temperatures, and pH. Osmolarity represents the number of particles per liter of water and remains constant regardless of changes in temperature and pressure (Wapnir and Lifshitz 1985).

The osmolarity of a sugar solution depends on the number of monomers (Koshimoto and Mazur 2002; Sadowska et al. 2020). The more numbers of monomers constituted a sugar, the lower the osmolarity values were observed (Table 6.1).

Concerning the viscosity of the seven sugar solutions, at 20°C and 0°C, the two polysaccharides (pentaisomaltose and maltodextrin) exhibited higher viscosity values than the rest of the sugars (glucose, sucrose, trehalose, lactose, raffinose). The pH remained similar among the seven sugar solutions (about pH = 5.1-5.4).

Table 6.1 Physicochemical properties of different sugar solutions at 25% w/w (NaCl 0.9%)

Sugar Code	Sugar and structure	DP	Monomers glycosidic bond	Molar mass (g·mol ⁻¹)	pH	Osmolarity (mOsm·L ⁻¹)	Viscosity (mPa·s) at 20°C	Viscosity (mPa·s) at 0°C
Glucose G		DP1	NA	180.1	5.1	1925±18	2.7±0.5	5.4±0.4
Sucrose S		DP2	Glc-Fru (α1→β2)	342.3	5.1	1568±16	2.8±0.2	5.4±0.3
Trehalose T		DP2	Glc-Glc (α1→α1)	342.3	5.4	1520±24	2.7±0.5	5.6±0.7
Lactose L		DP2	Gal-Glc (β1→β4)	342.3	5.1	1547±27	2.9±0.4	5.4±0.4
Raffinose R		DP3	Gal-Glc-Fru (α1→α6) -(α1→β2)	504.4	5.1	1187±17	2.6±0.5	5.8±1.4
Pentaisomaltose P		DP5-10	Mainly Glc (α1→α1)	~850-1750	5.4	650±5	3.3±0.2	6.6±0.3
Maltodextrin M		DP~17	Glc α (1→4)	~2700	5.1	578±4	31.3±3.3	85±4.2

Osmolarity and viscosity values are the mean of at least three independent measurements with their corresponding standard deviation. Abbreviations: Glc, glucose, Fru, fructose; Gal, galactose; DP, Degree of Polymerization. These measurements are the mean of three independent sugar solutions.

6.3.2. The loss of functional properties of protected *L. bulgaricus* CFL1 cells with different sugars during freezing and freeze-drying

The functional properties of *L. bulgaricus* CFL1 cells protected by the different sugars in Table 6.1 were measured before, after freezing; and freeze-drying (Figure 6.1). The properties measured were the acidifying activity in minutes by the Cinac system (AMS, Frepillon, France) and the culturability in CFU·mL⁻¹ by the agar plate count method.

To compare our results with the literature, we determined the loss of acidifying activity ($dt_{\Delta pH 0.7}$) and the rate of survival (%) (Chapter 3, Equations 3.9 and 3.10).

Then, the specific acidifying activity was determined, which is defined as the ratio of the acidifying activity to the corresponding log of cell concentration [$\text{min} \cdot (\log(\text{CFU} \cdot \text{mL}^{-1}))^{-1}$] (Chapter 3, subsections 3.3.1-3.3.3). For each sugar, the loss of specific acidifying activity was calculated after freezing ($dt_{\text{spe F}}$) and freeze-drying ($dt_{\text{spe F}}$) (Chapter 3, equations 3.3 and 3.4).

6.3.3. Sample preparation for FTIR analysis

Two states of cells were studied: (i) hydrated bacteria, where the different sugars-cells suspensions were frozen (-80°C) and thawed (42°C, 10 min), and (ii) air-dried cells, where thawed sugars-cells suspensions were dried in a desiccator that was continuously flushed with the dry air of less than 3% RH for 24 hours. More details for sample preparation are given in Chapter 3, subsection 3.6.4.

The air-drying method was applied to understand the effect of sugars on cells when water is removed by drying. The freeze-dried powder of bacteria was not possible to be analyzed because the sample was heterogeneously dispersed on the windows CaF₂ (the sample containers), thus, hampering the direct passage of the IR light into the sample.

Since the samples for FTIR had to be prepared under the above descriptions, the direct correlation between the results of air-dried cells and those from the *L. bulgaricus* CFL1's resistance to freeze-drying should be taken with prudence.

For the hydrated cells, the analysis of the seven sugars (previously shown in Table 6.1) was performed by FTIR. In contrast, air-dried cells were analyzed for only four sugars (trehalose, sucrose, lactose, and raffinose) because of the missing time during the PhD to complete the results.

6.3.4. FTIR spectra acquisition and analysis

The FTIR was used to analyze the influence of the seven sugars on the membrane lipids of frozen-thawed and air-dried cells. For this purpose, two wavelength bands arising from the membrane of *L. bulgaricus* CFL1 were monitored as a function of the temperature.

Bacterial pellets of hydrated cells or air-dried cells were sandwiched at room temperature in two CaF₂ windows (ISP Optics, Riga, Lat-via) to be analyzed in a Nicolet Magna 750 transmission

FT-IR spectrometer (Thermo Fisher Scientific; Madison, WI, USA) equipped with a variable temperature stage (Specac Ltd, Orpington, Kent, UK).

For hydrated bacteria, the starting temperature was room temperature. Upon cooling, the sample was heated until reaching 50°C. The temperature monitoring was, thus, started from 50°C to -50°C (2°C·min⁻¹) by cooling at pouring liquid nitrogen into the cell holder. Upon heating, the temperature monitoring was from -50°C to 50°C by the automatic heating stage.

For air-dried bacteria, the starting temperature was room temperature. Then, the temperature decreased to -50°C. The temperature monitoring was exclusively for heating, thus starting from -50°C to 75°C (2°C·min⁻¹) by the automatic heating stage. In this case, the temperature was higher than for hydrated cells (75°C vs. 50°C) to have a wider temperature range.

For both types of samples (hydrated and air-dried bacteria), the spectral acquisition was performed throughout cooling or heating by the Omnic software (version 7.1, Thermo Fisher Scientific Madison, WI, USA). Peak positions of three different functional groups were determined by analyzing the spectra of samples using a house-developed ASpiR software (Infrared Spectra Acquisition and Processing, INRAE; Thiverval-Grignon, France) (Chapter 3, subsection 3.6.4.3).

The obtained peak frequencies were then plotted against the temperature at which they were measured. Three peak positions were analyzed:

- (i) The symmetric CH₂ stretching vibration band ($\nu_{sym}CH_2$)

$\nu_{sym}CH_2$ is located around 2850 cm⁻¹ arising from lipid acyl chains (Mantsch and McElhaney 1991). The temperature dependence of $\nu_{sym}CH_2$ reveals information about conformational and phase changes for fatty acyl chains. The position of this peak allowed us to determine the membrane lipid phase transition temperatures. The raw $\nu_{sym}CH_2$ plots (without applying any fitted model) arising from the *L. bulgaricus* CFL1 samples (hydrated or air-dried) were used to calculate the first derivative of these plots. The maximums of the first derivative curves were taken as the membrane lipid phase transition temperatures: T_{cooling} (upon cooling, in °C) and T_{heating} (upon heating, in °C).

- (ii) The O-H libration and a bending combination band of water (νH_2O) located around 2200 cm⁻¹

Both were simultaneously monitored to determine ice nucleation temperatures (T_n) (Wolkers et al. 2007).

- (iii) The asymmetric PO₂ stretching vibration band ($\nu_{asym}PO_2$)

This vibration band is located at approximately 1220 cm⁻¹. It represents a sensor for head group hydration (in the membrane), leading to its frequency shift (Fringeli and Günthard 1981).

6.3.5. Statistical analysis

ANOVA and post-hoc tests Tukey HSD were performed using XLSTAT 2020.5 (Addinsoft, Paris, France) to compare data concerning loss of functional properties and the membrane lipid phase transition temperatures upon cooling and heating. A significance level of 95% (*P-value* < 0.05) was considered.

6.4. Results and discussion

6.4.1. Resistance of *L. bulgaricus* CFL1 to freezing and freeze-drying using different sugars

The effect of the seven sugars on the resistance of *L. bulgaricus* CFL1 to freezing and freeze-drying can be observed from the boxplots in Figures 6.2 (freezing) and 6.3 (freeze-drying). In each figure, first, the loss of acidifying activity ($dt_{\Delta pH0.7}$, min) is shown (Figures 6.2 and 6.3 (A)), then the survival rates (Figures 6.2 and 6.3 (B)), and finally, the resistance is expressed in the loss of specific acidifying activity (dt_{spe}) after each stabilization process. dt_{spe} is a descriptor that considers the acidifying activity and culturability of LAB. Low values of dt_{spe} suggest low loss of functional properties after freezing or freeze-drying; thus, high resistance to the stabilization process. As a control sample, *L. bulgaricus* CFL1 was suspended in NaCl at 9% without the addition of any sugar molecule, the survival was less than 5% after freezing, and the CFU were not possible to be quantified after freeze-drying since less than 20 CFU were counted. The loss of acidifying activity exceeded the 500 min after freezing and 800 after freeze-drying. These results confirmed the reported sensitivity to freezing (Fonseca et al. 2000; Meneghel et al. 2017), and now we can also assert its sensitivity to freeze-drying. Therefore, control cells of *L. bulgaricus* CFL1 (without sugars) were not included in Figures 6.2 and 6.3. Both stabilization processes are explained below separately.

6.4.1.1. Resistance of *L. bulgaricus* CFL1 to freezing

For sugars with the same degree of polymerization, sucrose (DP2), lactose (DP2), and trehalose (DP2), as well as similar osmolarity and viscosity values, exhibited different results in $dt_{\Delta pH0.7}$. Sucrose and lactose had the lowest performance in preventing the loss of acidifying activity of *L. bulgaricus* CFL1 (the highest $dt_{\Delta pH0.7}$ values: 80-95 min), whereas trehalose was the most efficient sugar to preserve the acidifying activity of *L. bulgaricus* CFL1 (the lowest $dt_{\Delta pH0.7}$ values: 6 min).

Despite the contrasting osmolarity and viscosity values between a monomer (glucose) and a polymer (pentaisomaltose or maltodextrin), the $dt_{\Delta pH0.7}$ values (Figure 6.2 (A)) were not significantly different for cells protected with glucose (DP1), pentaisomaltose (DP5-10) and maltodextrin (DP~17). Additionally, raffinose (DP3) was also not significantly different from glucose. These four sugars led to $dt_{\Delta pH0.7}$ values about 60-75 min.

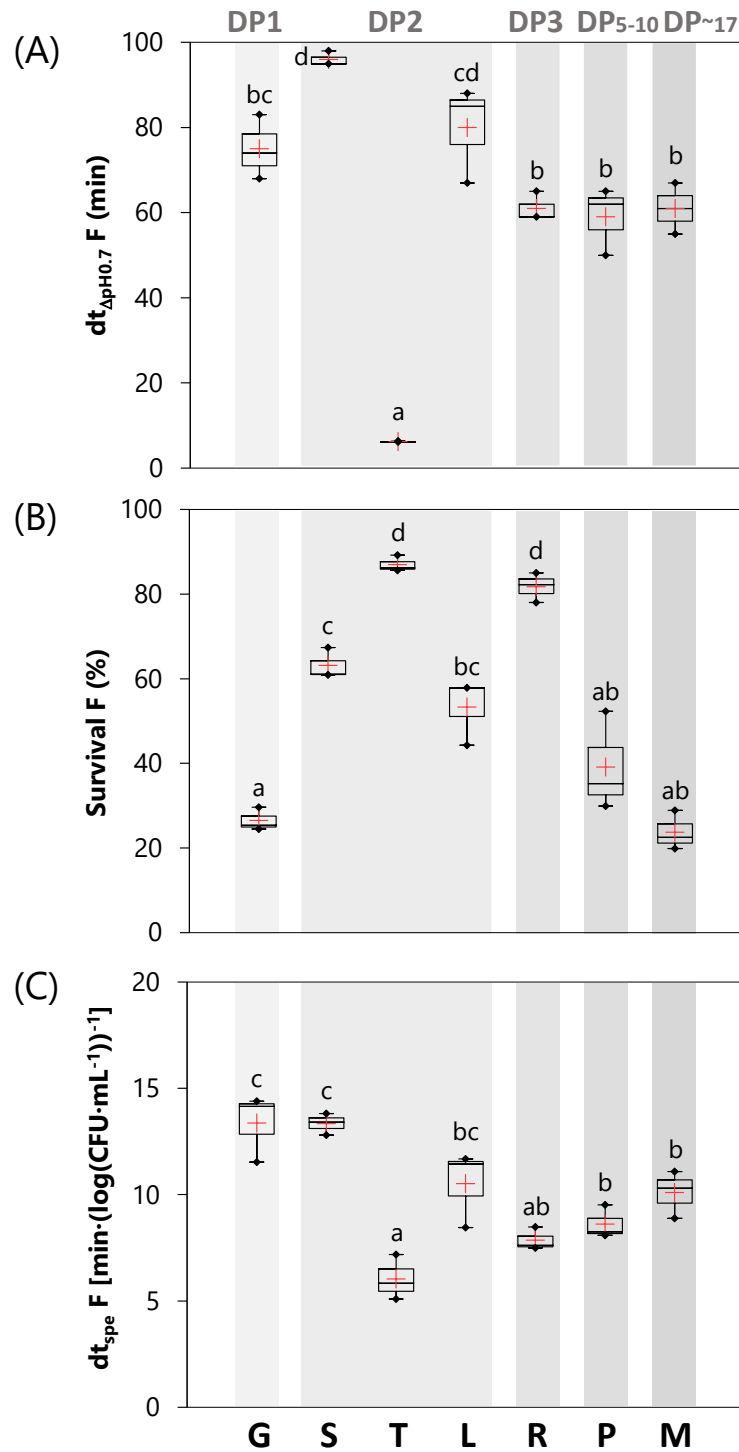


Figure 6.2 Resistance of *L. bulgaricus* CFL1 cells to freezing using different sugars. (A) The loss of acidifying activity ($dt_{\Delta pH 0.7} F$), (B) survival, and (C) the loss of specific acidifying activity ($dt_{spe} F$). Values are the mean of at least three independent measurements. Superscripts letters represent significant differences among sugar solutions at a 95% confidence level. The gray zones correspond to sugars with the same degree of polymerization. Abbreviations: DP, Degree of polymerization; G, Glucose; S, Sucrose; T, Trehalose; L, Lactose; R, Raffinose; P, Pentaismaltose; M, Maltodextrin.

The survival results of *L. bulgaricus* CFL1 had a different behavior than $dt_{\text{ApH}0.7}$ (Figure 6.2 (B)). The survival was reduced (less than 40%) by protecting cells with glucose, pentaisomaltose, and maltodextrin, while *L. bulgaricus* CFL1 protected with sucrose and lactose exhibited an intermediate survival rate (53-60%). This time, the raffinose was as good as trehalose in preserving the CFU deterioration (survival: 81-86%).

When both functional properties were expressed in the $dt_{\text{spe}} F$ descriptor (Figure 6.2 (C)), *L. bulgaricus* CFL1 cells were better protected with sugars in the order T>R>P>M~L>G~S. The variation of the degree of polymerization and the physicochemical sugar solutions (Table 6.1°) seemed to be independent of $dt_{\text{spe}} F$.

L. bulgaricus CFL1 cells protected with trehalose exhibited the highest resistance to freezing (the lowest $dt_{\text{spe}} F$ values: 6 ± 1 [$\text{min} \cdot (\log(\text{CFU} \cdot \text{mL}^{-1}))^{-1}$]). Raffinose also showed great protection for bacteria since there were no significant differences compared to trehalose (same superscript letters). To our knowledge, raffinose has not been used to protect LAB (see Chapter 1, Table 1.7). However, raffinose has provided cryoprotection to eukaryotic cells such as mouse spermatozoa (Tada et al. 1990) and Merino ram sperm (Bucak et al. 2013).

Intermediate freezing protection for *L. bulgaricus* CFL1 was provided by pentaisomaltose, lactose, and maltodextrin. Pentaisomaltose has been proposed for the successful cryopreservation of eukaryotic cells (Svalgaard et al. 2018). No study has been reported so far on its use to protect LAB (see Chapter 1, Table 1.7). Concerning lactose and maltodextrin, these two sugars led to $dt_{\text{spe}} F$ values approximately two times higher than trehalose. Accordingly, the presented data showed that lactose and maltodextrin were less effective than trehalose. These results agreed with previous studies based on survival results. Lower preservation by lactose (compared to trehalose) was previously reported for *Lactobacillus bulgaricus* DSM20081 (De Giulio et al. 2005) and *Lactocaseibacillus rhamnosus* GC. (Miao et al. 2008). Although lactose guaranteed the protection of these two former LAB, trehalose contributed slightly better to their survival (survival: 99.8% vs. 97.1%). Regarding maltodextrin, Castro et al. (1997) also reported the superior capacity of trehalose over maltodextrin to protect *Lactobacillus bulgaricus* NCFB 1489 (survival: 90% vs. 20%).

The effects of glucose and sucrose on $dt_{\text{spe}} F$ were the same (identical superscript letters). *L. bulgaricus* CFL1 cells protected with these two sugars showed the lowest resistance (the highest $dt_{\text{spe}} F$ values: 13 ± 1 [$\text{min} \cdot (\log(\text{CFU} \cdot \text{mL}^{-1}))^{-1}$]). The low glucose protection compared to other sugars was similarly observed for *Lactobacillus acidophilus* DSM20079 (De Giulio et al. 2005). This lactic acid bacterium was protected with different sugars, such as glucose, sucrose, maltose, and lactose. Glucose led to relatively lower cryopreservation than the other sugars (92% vs. 98-95%). In that same study, the capacity of glucose to protect two other LAB was different from *Lactobacillus acidophilus* DSM20079 (De Giulio et al. 2005). For *Lactobacillus bulgaricus* DSM20081 and *Streptococcus thermophilus*, the glucose exhibited similar

cryopreservation compared to other sugars (survival: 97% for glucose, sucrose, maltose, and lactose).

Concerning sucrose for cryoprotection, Figure 6.2 (A) showed that sucrose (similar to glucose) led to the highest loss of acidifying activity freezing and low resistance comparable to glucose (Figure 6.2 (C), highest dt_{spe} F values). This result was unexpected since sucrose has previously been an effective protector for different *Lactiplantibacillus plantarum* strains (Bravo-Ferrada et al. 2015; Wang et al. 2019, 2021). However, for the species of *L. bulgaricus*, no studies have shown the sucrose efficacy over other protectors such as trehalose (De Giulio et al. 2005) or glutamate (Fonseca et al. 2003).

The results in this study for freezing confirm the superiority of protection of trehalose and propose a new alternative of protection (raffinose) as good as trehalose. Raffinose, as FOS and GOS, are non-digestible for humans and has the potential to exert prebiotic properties (Amorim et al. 2020). Also, the results here suggest the efficacy of glucose and sucrose might be LAB species-dependent.

6.4.1.2. Resistance of *L. bulgaricus* CFL1 to freeze-drying

Comparing freeze-drying (Figure 6.3) and freezing (Figure 6.2) resistance, one can observe higher losses of acidifying activity (134-392 vs. 6-95 min), lower survival (8-24 vs. 27-86) and higher dt_{spe} FD values (21-62 [$\text{min} \cdot (\log (\text{CFU} \cdot \text{mL}^{-1}))^{-1}$] vs. 6-13 [$\text{min} \cdot (\log (\text{CFU} \cdot \text{mL}^{-1}))^{-1}$]). Thus, freeze-drying had a greater detrimental effect on cells than freezing, regardless of the sugar used to protect *L. bulgaricus* CFL1 cells.

In Figure 6.3 (A), the minor loss of acidifying activity was observed for cells protected with glucose (DP1) and trehalose (DP2), followed by raffinose (DP3), sucrose, and lactose (DP2). The higher progressive loss was exhibited when pentaisomaltose (DP5-10) and maltodextrin (DP~17) were used as protectors. A moderate pattern could be established in which the higher the DP in the sugar, the higher loss of acidifying activity was obtained.

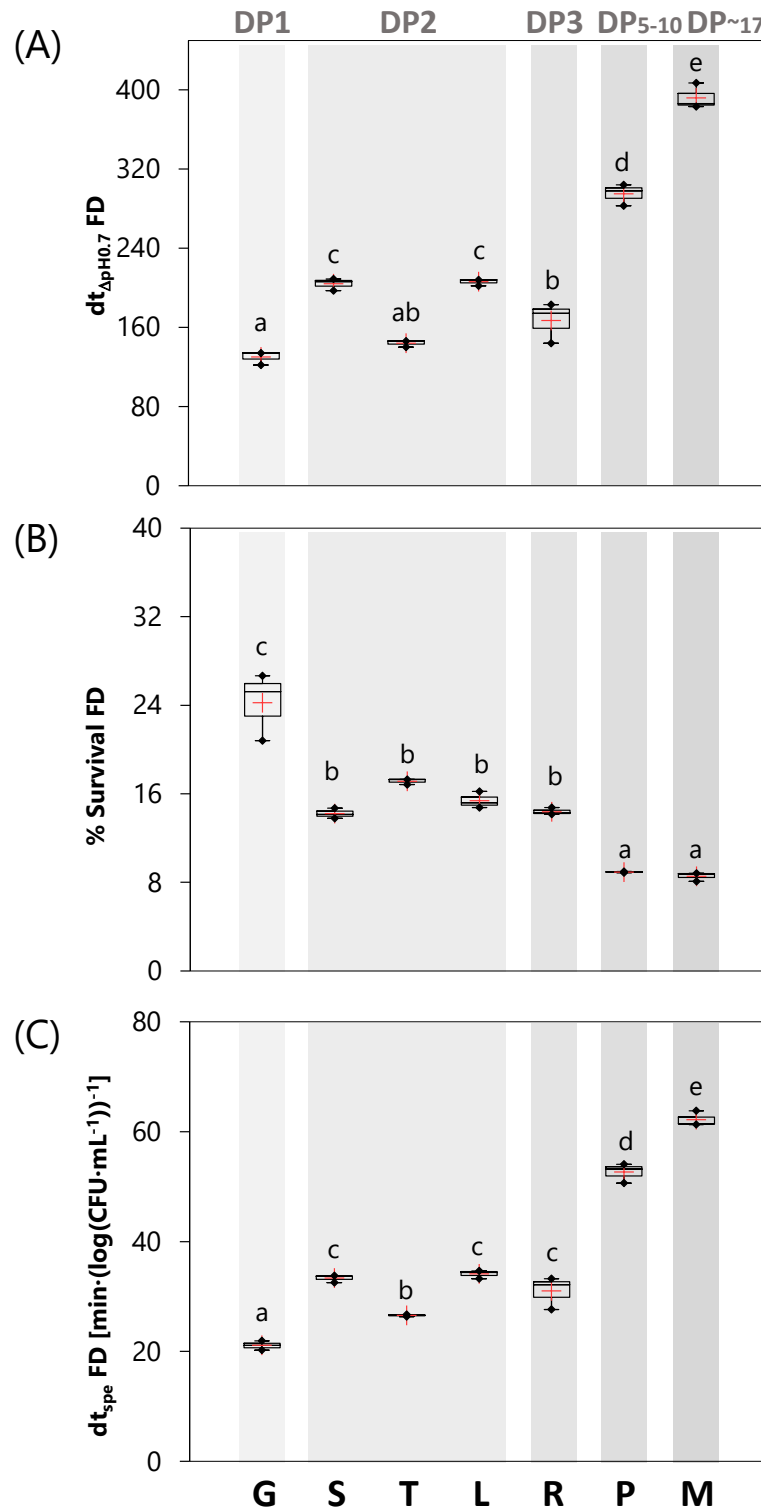


Figure 6.3 Resistance of *L. bulgaricus* CFL1 cells to freeze-drying using different sugars. (A) The loss of acidifying activity ($dt_{\Delta pH 0.7}$ FD), (B) survival, and (C) the loss of specific acidifying activity (dt_{spe} FD). Values are the mean of at least three independent measurements. Superscript letters represent significant differences among sugar solutions at a 95% confidence level. The gray zones correspond to sugars with the same degree of polymerization. Abbreviations: DP, Degree of polymerization; G, Glucose; S, Sucrose; T, Trehalose; L, Lactose; R, Raffinose; P, Pentaisomaltose; M, Maltodextrin.

This pattern was again observed for the survival rate (Figure 6.3 (B)). The survival of *L. bulgaricus* CFL1 decreased with the increase of DP: G>T~S~L~R>P~M.

For dt_{spe} FD values (Figure 6.3 (C)), the order of protection of the sugars was G>T>S~L~R>P>M. In this study, glucose stood out from the other six sugars. *L. bulgaricus* CFL1 cells displayed the highest resistance when it was used as protector (the lowest dt_{spe} FD values: 21 ± 1 [$\text{min} \cdot (\log(\text{CFU} \cdot \text{mL}^{-1}))^{-1}$]).

In detail, according to the DP of sugars, one can observe:

DP1: glucose

In previous studies for different LAB species, glucose had not been identified as a better freeze-drying protector than other sugars, notably not better than trehalose. Based on survival results, this was the case for *Lactobacillus bulgaricus* DSM20081, 86% vs. 95% (De Giulio et al. 2005); *Levilactobacillus brevis*, 19% vs. 57% (Zhao and Zhang 2005); *Lactiplantibacillus plantarum* IFA 278, 10% vs. 40% (Strasser et al. 2009); and *Lacticaseibacillus casei* ATCC 393, 30% vs. 70% (Dimitrellou et al. 2016). Thus, glucose may be a specific protector for freeze-drying *L. bulgaricus* CFL1.

DP2 and DP3: sucrose, lactose and raffinose

The dt_{spe} FD of *L. bulgaricus* CFL1 cells protected with sucrose (DP2) lactose, and raffinose ranged from 31-34 [$\text{min} \cdot (\log(\text{CFU} \cdot \text{mL}^{-1}))^{-1}$]], with no significant differences among them. For different LAB species (*Lactobacillus bulgaricus*, *Lactobacillus acidophilus*, *Lacticaseibacillus casei* and *rhamnosus*, and *Lactiplantibacillus plantarum*), sucrose and lactose have previously proved their potential as suitable protectors during freeze-drying (90-97%), but remaining slightly less efficient than trehalose. When comparing sucrose and lactose versus trehalose, LAB cells protected by either sucrose or lactose exhibited lower survival (about 1.5 times) (De Giulio et al. 2005; Miao et al. 2008; Pehkonen et al. 2008; Dimitrellou et al. 2016). Some exceptions reported in the literature, in which sucrose has led to similar protection as trehalose (Strasser et al. 2009; Bravo-Ferrada et al. 2015; Wang et al. 2020).

As for freezing, raffinose is, for the first time, a good candidate that may protect LAB cells during freeze-drying to the same extent as sucrose.

DP>5: pentaisomaltose and maltodextrin

The lowest resistance of *L. bulgaricus* CFL1 was observed for cells protected with pentaisomaltose and maltodextrin. About two and three times higher dt_{spe} FD values (low resistance) were observed for these polysaccharides than glucose or trehalose. These results agreed with the previous ones in which maltodextrin provided the lowest resistance to *Lactobacillus bulgaricus* NCFB 1489 (8% survival) among three different protectors such as trehalose, glycerol, and skim milk > 18% survival (Castro et al. 1997). This low resistance, when

maltodextrin was used, was also the case for *Lactiplantibacillus plantarum* IFA 278 (19% survival) among two other protectors (trehalose and sucrose, about 40% survival) (Strasser et al. 2009).

For freeze-drying resistance, unlike other *L. bulgaricus* strains, new results were observed here. Glucose, in this study, was more efficient than trehalose. Sucrose, lactose, and raffinose were more modest in protecting *L. bulgaricus* CFL1. The two sugars with a DP>3 used in this study led to the lowest freeze-drying resistance, being the maltodextrin the worst protector. Unlike the freezing process, the protection of the different sugars during freeze-drying could be associated with the extreme values of sugars DP (contrasting viscosity and osmolarity). Glucose (DP1) was suitable to ensure freeze-drying protection, whereas maltodextrin (DP>10) led to less resistant cells to freeze-drying. Based on the water replacement hypothesis, in which the OH of sugars can form hydrogen bonds with the phosphate groups of the phospholipids' membrane, we could speculate that glucose was more accessible access to protect the membrane at the phospholipid surface because of its small size and had a supplementary OH group that is not linked to another monomer. Maltodextrin, as a polymer, might be hindered from diffusing through the cell wall and interacting with the membrane to protect it.

6.4.2. The influence of sugars with different degrees of polymerization on the membrane of *L. bulgaricus* CFL1 by FTIR

To better understanding the exhibited resistance of *L. bulgaricus* CFL1 to freezing and freeze-drying (subsection 6.4.1). An FTIR study was performed to assess the effect of the seven sugars on the membrane of *L. bulgaricus* CFL1. The hypotheses that established the mechanisms of sugars to protect membranes have often been elucidated using lipids models (e.g., liposomes, monolayers) and applying the FTIR method. For example, these were the works of Crowe et al. (1988); Hinchá et al. (2003); Cabela and Hinchá (2006); Díaz et al. (2017). Only three studies reported using this method in LAB cells (Linders et al. 1997; Oldenhof et al. 2005; Santivarangkna et al. 2010).

Based on this background, *L. bulgaricus* CFL1 cells were analyzed by FTIR. Therefore, two bacteria states were considered: (i) hydrated and (ii) air-dried cells. Hydrated cells were used to study the freezing process, whereas air-dried cells were employed to simulate the water removal by desiccation (see subsection 6.3.3).

Two wavelength bands were monitored, $\nu_{sym}CH_2$ and $\nu_{asym}PO_2$. Both are assigned to two different chemical functions of the membrane lipids: the fatty acyl chains ($\nu_{sym}CH_2$) and the polar heads of the phospholipids ($\nu_{asym}PO_2$).

The results and discussion of the $\nu_{sym}CH_2$ variations are first presented for hydrated and air-dried cells and then for the $\nu_{asym}PO_2$ ones.

6.4.2.1. Lipid phase transition of hydrated and air-dried cells protected with different sugars upon cooling and heating

i. Hydrated cells

The consequence of direct interaction between the sugars and the hydrophilic region of the membrane (i.e., head groups) hinders the tight packing of the acyl chains (Crowe 2002). This acyl chain packing can be monitored by the corresponding IR vibration of the $\nu_{sym}CH_2$ (Crowe et al. 1989b; Lewis and McElhaneey 2013).

Figure 6.4 displays the evolution of the $\nu_{sym}CH_2$ peak positions following cooling (blue curves) and heating (red curves) of *L. bulgaricus* CFL1 in the presence of the seven different sugars. In addition, control samples can be observed, in which bacteria were washed with saline water five times to get rid of the sugar molecules in the sample.

Decreasing the temperature resulted in a shift of $\nu_{sym}CH_2$ peak positions to lower wavenumbers (Figure 6.4, blue curves). On the contrary, the temperature increase induced a shift of $\nu_{sym}CH_2$ peak positions to higher wavenumbers (Figure 6.4, red curves).

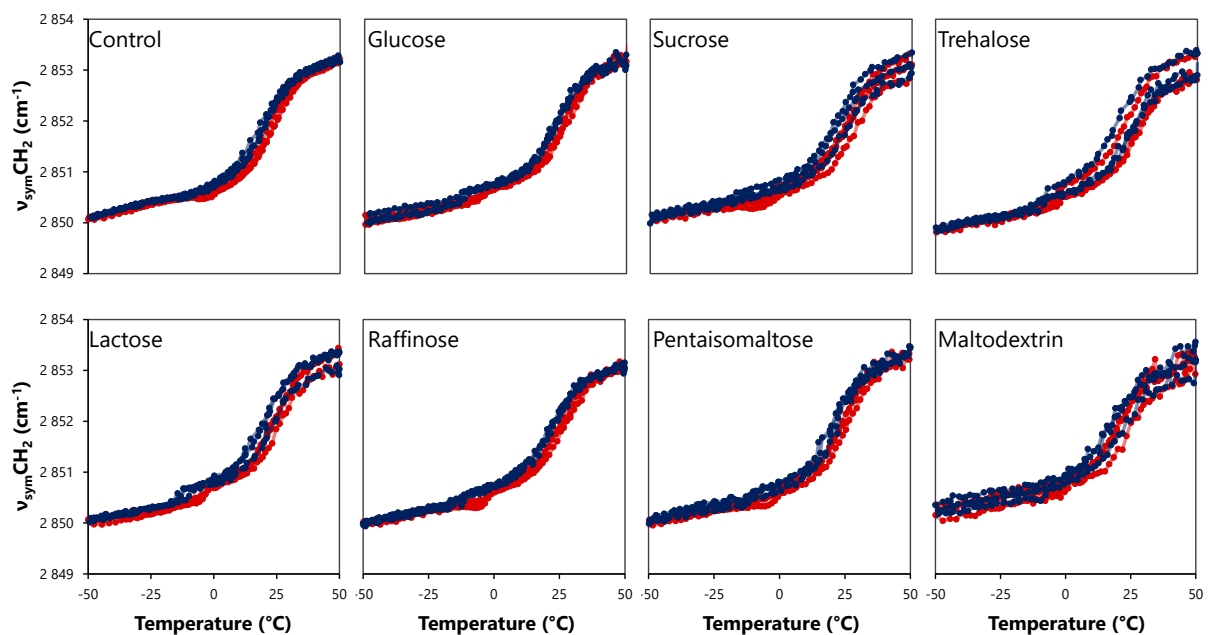


Figure 6.4 Peak positions of the symmetric CH_2 stretching vibration band ($\nu_{sym}CH_2$) arising from hydrated *L. bulgaricus* CFL1 upon cooling (blue curves) and heating (red curves). Washed cells (control) and cells protected with different sugars solution at 25% are presented. Data points correspond to raw data of three independent measurements.

The $\nu_{sym}CH_2$ curves upon cooling and heating were overlapped. A slight shift is observed from $-15^\circ C$ to $30^\circ C$. To determine the lipid phase transition temperatures of cells, the first derivatives of the $\nu_{sym}CH_2$ curves from Figure 6.4 were calculated and shown in Figure 6.5.

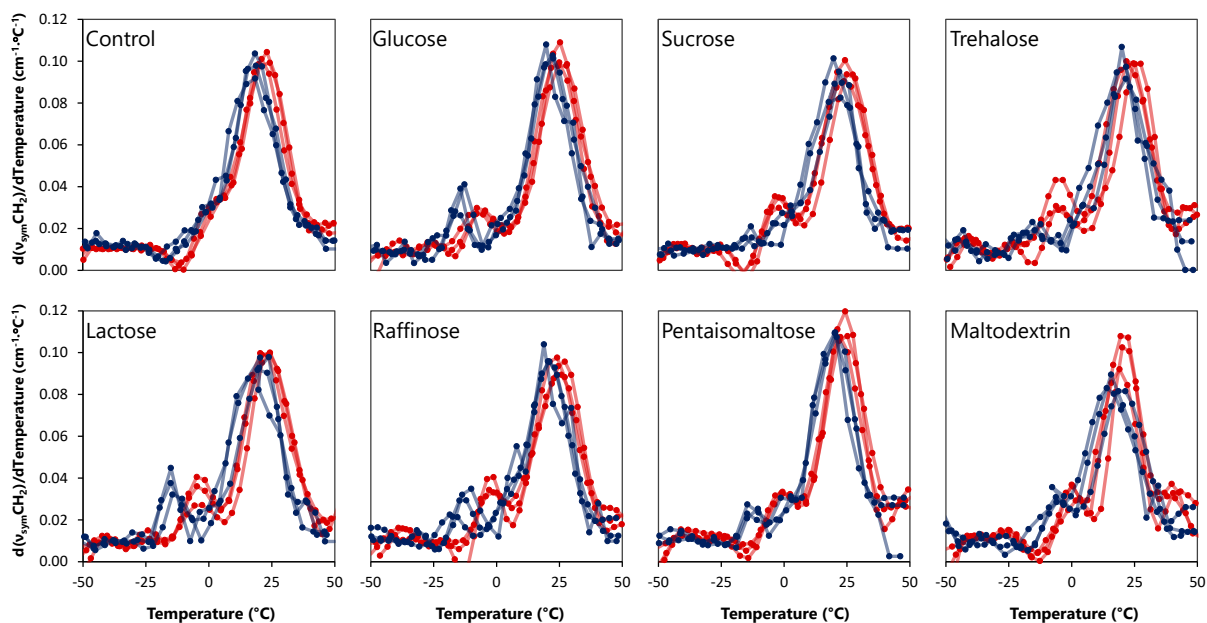


Figure 6.5 The first derivatives of the symmetric CH_2 stretching vibration band ($\nu_{\text{sym}}\text{CH}_2$) of *L. bulgaricus* CFL1 upon cooling (blue curves) and heating (red curves). The maximums of each curve represent the lipid transition temperatures (T_{cooling} and T_{heating}) reported in Table 6.2. Data points correspond to raw data of three independent measurements.

For each sugar in Figure 6.5, the derivative curves upon cooling (blue curves) and heating (red curves) illustrated two maximum peaks. A small peak at subzero temperatures and a big peak around 18-25°C were observed. These peaks suggest two lipid phase transitions.

Our results agreed with previous studies using phosphatidylcholine liposomes showing two transitions, one more pronounced in which the phase change occurred for most of the fatty acyl chains in the membrane (Vereyken et al. 2003a; Cacela and Hinch 2006). For whole cells, Santivarangkna et al. (2010) also reported two lipid transitions of hydrated *Lactobacillus helveticus* cells in the presence of sorbitol.

For the sake of clarity, the small peaks, are assigned to the first lipid phase transition (whatever the temperature variation: cooling or heating). Thus, the major peaks refer to the second lipid phase transitions. The values of these two lipid phase transition temperatures upon cooling (*First and Second* T_{cooling}) and heating (*First and Second* T_{heating}) are shown in Table 6.2.

For the control sample (washed *L. bulgaricus* CFL1 cells), only one maximum peak was observed around 18-25°C. Thus, one temperature is indicated in Table 6.2. The water nucleation temperatures (T_n) occurring during cooling are also included for each sample.

Table 6.2 Lipid phase transitions temperatures of hydrated (T_{cooling} and T_{heating}) *L. bulgaricus* CFL1 in the presence of different sugars. The temperatures are arranged according to the order in which they occur (Figure 6.6)

Lipid phase transition	Control	Glucose	Sucrose	Trehalose	Lactose	Raffinose	Penta-isomaltose	Malto-dextrin	
Cooling	$Second-T_{\text{cooling}}$ (°C)	18±0.2 ^a	22±2 ^a	21±1 ^a	21±1 ^a	21±2 ^a	20±1 ^a	20±0.4 ^a	17±4 ^a
	Tn (°C)	-13±1 ^a	-11±3 ^{ab}	-11±1 ^{ab}	-8±2 ^b	-11±1 ^{ab}	-10±1 ^{ab}	-10±0.3 ^{ab}	-9±2 ^b
	$First-T_{\text{cooling}}$ (°C)	NO	-14±1 ^a	-14±1 ^a	-13±3 ^a	-13±3 ^a	-13±3 ^a	-13±2 ^a	-7±1 ^b
Heating	$First-T_{\text{heating}}$ (°C)	NO	-8±0.1 ^a	-3±1 ^{cd}	-6±1 ^{ab}	-4±1 ^{bc}	-2±1 ^d	-1±0.2 ^{de}	1±1 ^e
	$Second-T_{\text{heating}}$ (°C)	23±2 ^{ab}	26±2 ^b	24±1 ^b	23±1 ^{ab}	23±2 ^{ab}	26±2 ^b	24±1 ^b	20±2 ^a

Water nucleation temperatures (Tn) are presented which corresponds to the upshift of the vibration water band from approx. 2100 cm^{-1} . Values are the mean of at least three independent measurements with their corresponding standard deviation. Superscripts letters represent significant differences among sugar solutions at a 95% confidence level. Abbreviations: NO, Not Observed.

Upon cooling (Figure 6.6), the major peak corresponded was the most predominant for all samples (including the control) and the lipid phase transition at positive temperatures: 17–21°C (Table 6.2: $Second-T_{\text{cooling}}$). This lipid transition corresponds to an entire phase change. Upon cooling, the membrane lipids undergo a disordered liquid crystalline phase (L_{α}) to an ordered rigid gel phase (L_{β}). At decreasing the temperature, the fatty acyl chain rotamers change from *gauche* to *all-trans* conformation, leading to the straightening and packing of acyl chains. Thus, reducing inter-acyl chain distances reinforces inter fatty acyl chain interactions and weakens the C-H bond. At increasing the temperature, the transition of acyl chain rotamers occurs the other way around (Borchman et al. 1991).

Then, ice nucleation took place (Table 6.2, Tn). Finally, the small peak observed only for cells protected with sugars might be attributed to a subphase change from a rigid gel phase (L_{β}) to a subgel phase (L_c) since it occurred at subzero temperatures (Table 6.2: $First-T_{\text{cooling}}$). The subgel phase is characterized by acyl chains that are highly ordered and show a tilt with respect to the bilayer. In contrast, in the rigid gel phase, the acyl chains are parallel and perpendicular to the bilayer (Kranenburg and Smit 2005; Benesch et al. 2015).

Upon heating (Figure 6.6), these lipids' phase and subphase transition occurred in the opposite direction ($L_c \rightarrow L_{\beta} \rightarrow L_{\alpha}$).

Concerning the effect of the degree of polymerization of sugars on $First-T_{\text{cooling}}$ and $First-T_{\text{heating}}$, six of the seven sugars studied were not significantly different. Only *L. bulgaricus* CFL1 protected with maltodextrin contrasted from the other six sugars by showing the highest $First-T_{\text{cooling}}$ ($-7\pm 1^{\circ}\text{C}$) and $First-T_{\text{heating}}$ ($1\pm 1^{\circ}\text{C}$). For $Second-T_{\text{cooling}}$ and $Second-T_{\text{heating}}$ values, no

significant differences were observed among the hydrated cells in the presence of different sugars.

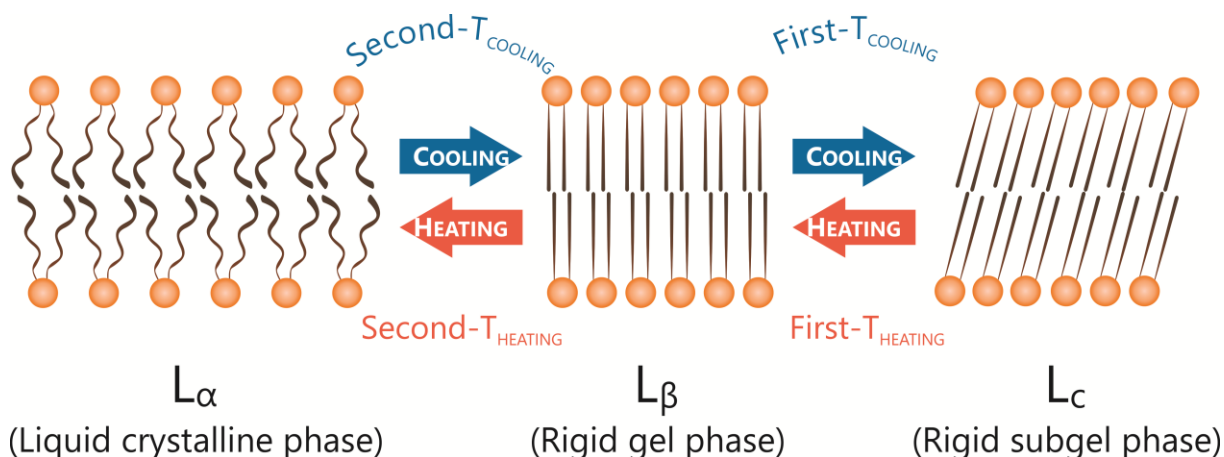


Figure 6.6 Schematic drawings of the various bilayer phases. Adapted from Kranenburg and Smit 2005.

For hydrated LAB, only two studies showed the effect of the absence and presence of sugars on lipid phase transition temperatures upon heating (T_{heating}) (Linders et al. 1997; Kilimann et al. 2006). Linders et al. (1997) reported similar values of T_m for *L. plantarum* P743 in the absence or presence of maltose (4°C). Kilimann et al. (2006) demonstrated that the presence of sucrose on hydrated *L. lactis* MG 1363 induced lower wavelengths of $\nu_{\text{sym}}\text{CH}_2$. However, the lipid phase temperatures were quite similar between the absence and presence of sucrose (rigid gel phase: 7°C vs. 8°C and liquid crystalline phase: 35°C vs. 30°C).

ii. Air-dried cells

As for hydrated cells, the peak positions of $\nu_{\text{sym}}\text{CH}_2$ were plotted as a function of increasing the temperature (Figure 6.7). In this case, only four sugars were analyzed due to the lack of time to finish the study. Here, results are shown when samples were heated because of the water absence. In Figure 6.7, a comparison was made between air-dried (mustard curves) and hydrated (red curves) *L. bulgaricus* cells.

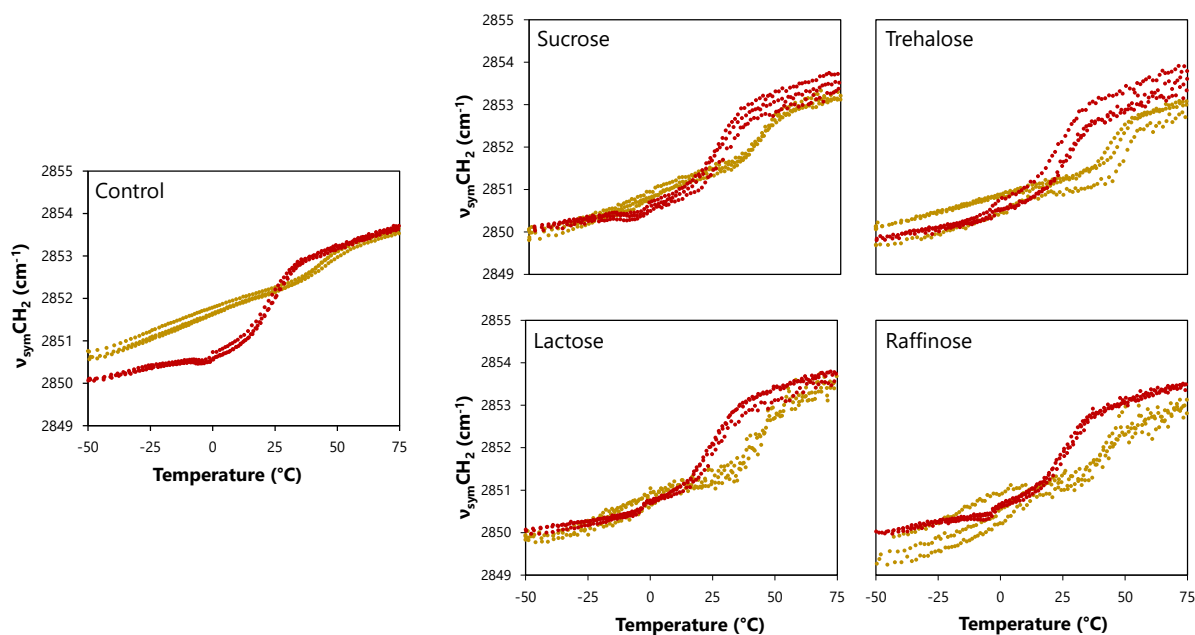


Figure 6.7 Peak positions of the symmetric CH_2 stretching vibration band ($\nu_{\text{sym}}\text{CH}_2$) arising from air-dried *L. bulgaricus* CFL1 upon heating (mustard curves). Washed cells (control) and cells protected with different sugars solution at 25% are presented. Additionally, the peak position $\nu_{\text{sym}}\text{CH}_2$ arising from hydrated *L. bulgaricus* CFL1 are illustrated (red curves). Data points correspond to raw data of three independent measurements.

Regardless of the sample, the variations for air-dried cells extended over a more extensive temperature range than for the hydrated ones. A smaller transition slope (no cooperative) was observed for the air-dried control sample than for the air-dried cells protected with different sugars. The transition slope of the control sample was delimited between the rigid gel phase (from -50°C to 30°C) and the liquid crystalline phase (from 50°C to 75°C).

When comparing hydrated and air-dried *L. bulgaricus* CFL1 cells (Figure 6.6, red curves vs. mustard curves), hydrated cells shifted to higher wavelength bands between 10°C and 30°C . This result indicates that their lipid phase transition occurred earlier than the ones of the air-dried cells. To confirm this information, Figure 6.8 shows the first derivatives of $\nu_{\text{sym}}\text{CH}_2$ curves (hydrated and air-dried bacteria).

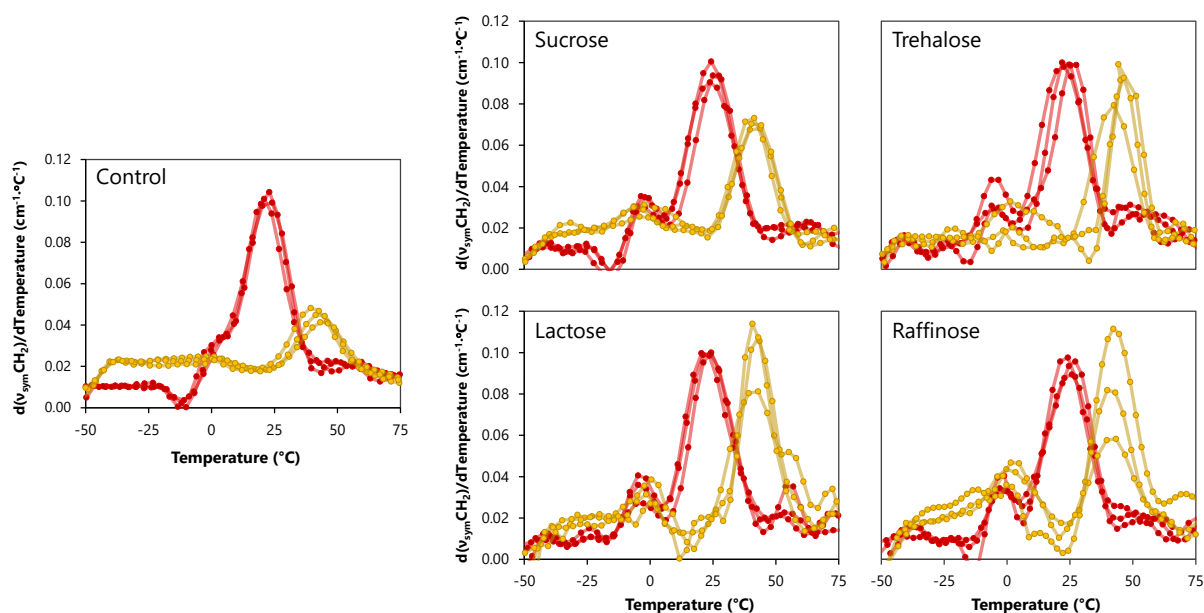


Figure 6.8 The first derivatives of the symmetric CH_2 stretching vibration band ($\nu_{\text{sym}}\text{CH}_2$) arising from air-dried *L. bulgaricus* CFL1 upon heating (mustard curves). Washed cells (control) and cells protected with different sugars solution at 25% are presented. Additionally, the first derivative of $\nu_{\text{sym}}\text{CH}_2$ arising from hydrated *L. bulgaricus* CFL1 are illustrated (red curves). Data points correspond to raw data of three independent measurements. The maximums of each curve represent the lipid transition temperatures (T_{heating}) reported in Table 6.3 for air-dried cells.

In agreement with the previous results of hydrated cells, here (Figure 6.8), two maximum peaks were observed for the air-dried cells protected with the sugars, except for the control sample. The first peaks of protected-hydrated cells and air-dried cells were mostly overlapped. The second peaks of hydrated cells were placed about at 20°C–26°C, whereas the second peaks of air-dried cells were found at 42°C–44°C (Figure 6.8). Therefore, the lipid phase transition occurred before for the hydrated cells. The exact temperature values in which the lipid phase transition took place are summarized in Table 6.3.

Table 6.3 Lipid phase transitions temperatures of Hydrated (H) and Air-Dried (AD) *L. bulgaricus* CFL1 upon heating.

		Control	Sucrose	Trehalose	Lactose	Raffinose
H	First- T_{heating} (°C)	NO	$-3 \pm 1^{\text{cd}}$	$-6 \pm 1^{\text{ab}}$	$-4 \pm 1^{\text{bc}}$	$-2 \pm 1^{\text{d}}$
AD	First- T_{heating} (°C)	NO	$-4 \pm 2^{\text{a}}$	$0 \pm 2^{\text{b}}$	$0 \pm 1^{\text{b}}$	$0 \pm 1^{\text{b}}$
H	Second- T_{heating} (°C)	$23 \pm 2^{\text{ab}}$	$24 \pm 1^{\text{b}}$	$23 \pm 1^{\text{ab}}$	$23 \pm 2^{\text{ab}}$	$26 \pm 2^{\text{b}}$
AD	Second- T_{heating} (°C)	$41 \pm 2^{\text{a}}$	$42 \pm 2^{\text{a}}$	$44 \pm 3^{\text{a}}$	$42 \pm 1^{\text{a}}$	$42 \pm 2^{\text{a}}$

Values are the mean of at least three independent measurements with their corresponding standard deviation. Superscripts letters represent significant differences among sugar solutions at a 95% confidence level. Abbreviations: NO, Not Observed

The *First-T_{heating}* values of protected hydrated cells were lower than those of protected air-dried cells (variations in the range from one to six degrees). The *Second-T_{heating}* values were twice lower for hydrated than those for air-dried cells (23-26°C vs. 42-44°C). A hydration effect was observed on both lipid phase transition temperatures for all the samples analyzed.

The notable difference in *Second-T_{heating}* values between hydrated and air-dried cells agreed with previous studies focusing on *L. plantarum* (Linders et al. 1997), *L. bulgaricus* (Oldenhof et al. 2005), and *L. helveticus* (Santivarangkna et al. 2010).

Phospholipids in the membrane are relatively hydrated. For instance, liposomes made of dipalmitoylphosphatidylcholine (DMPC) revealed that about 18 water molecules hydrogen-bonded to the polar head group (Luzardo et al. 2000). Removal of water results in a decrease in the area occupied by each head group. Consequently, the packing of the polar heads increases, leading to increased van der Waal's interactions among the fatty acyl chains. Thus, the temperature increases when the transition from rigid gel to liquid crystalline phase occurs (Crowe et al. 1998).

In regard to the effect of sugars on *Second-T_{heating}*, no significant differences were observed among the air-dried cells in the presence of sugars (trehalose, sucrose lactose, and raffinose) and the control sample.

i. Influence of sugars on fatty acyl arrangement

Our overall results for hydrated and air-dried cells revealed that the presence of sugars (regardless of their DP) induced a lipid subphase transition in the rigid gel zone (at subzero temperatures). We hypothesize that the presence of sugars changed the lipid chain packing in a particular phase, in this case, the rigid gel phase.

No significant differences between the presence and absence of sugars were observed for the lipid phase transition from liquid crystalline to rigid gel phase upon cooling and vice versa for heating.

The influence of sugars on lipid phase transition temperature has been mainly observed in lipid models. For example, the *T_{heating}* reduction has been observed in air-dried or freeze-dried liposomes prepared with sugars (Tsvetkova et al. 1998; Hinch a et al. 2002, 2003; Vereyken et al. 2003a; Cacula and Hinch a 2006). The water replacement hypothesis bears this assumption. Sugar molecules (particularly disaccharides) may intercalate between the lipid head groups and form hydrogen bonds between -OH groups on the sugars and the phosphate of the membrane phospholipids. The main consequence of these direct interactions is reducing opportunities for van der Waals interactions among the fatty acyl chains, thus, decreasing the lipid phase transition temperatures (Crowe et al. 1998; Wolfe and Bryant 1999; Crowe 2002). The presence of sugars in air-dried *L. bulgaricus* CFL1 cells was also expected to have this effect. However, our results indicated that sugars did not reduce the *Second-T_{cooling}* or *Second-T_{heating}* values

regarding the control. The results are consistent with two previous studies using LAB cells (Linders et al. 1997; Oldenhof et al. 2005), indicating that the influence of sugars in the LAB membrane is more complex than only analyzing the conformation of the fatty acyl chains.

6.4.2.2. Effect of sugars on phospholipids' polar head of hydrated and air-dried cells

FTIR was also used to characterize changes in membrane phospholipids by monitoring the peak position of $\nu_{asym}PO_2$ in the presence of sugars to gain more insights into the influence of sugars on another membrane site. These groups sequester about 80% of the water embedding the phospholipids, forming a sphere of water molecules (Díaz et al. 2003). In the presence of other molecules (such as sugars) in this water sphere, it is expected to affect phosphate groups. $\nu_{asym}PO_2$ has been frequently used to investigate hydrogen bonding between the sugars and the PO_2 groups of the membrane. Downshift $\nu_{asym}PO_2$ is interpreted as hydrogen bonding between the OH-group of sugars and the PO_2 moiety of the membrane (Hübner and Blume 1998).

For hydrated cells, the peak position of $\nu_{asym}PO_2$ as a function of temperature is shown in Figure 6.9. Regardless of cooling and heating *L. bulgaricus* CFL1 cells, bacteria exhibited the highest wavenumbers when protected with maltodextrin, followed by trehalose. The lowest wavenumbers were observed when cells were protected with pentaisomaltose and sucrose. Therefore, the effect of sugars on $\nu_{asym}PO_2$ seemed to be aleatory and different for each sugar (Figure 6.9).

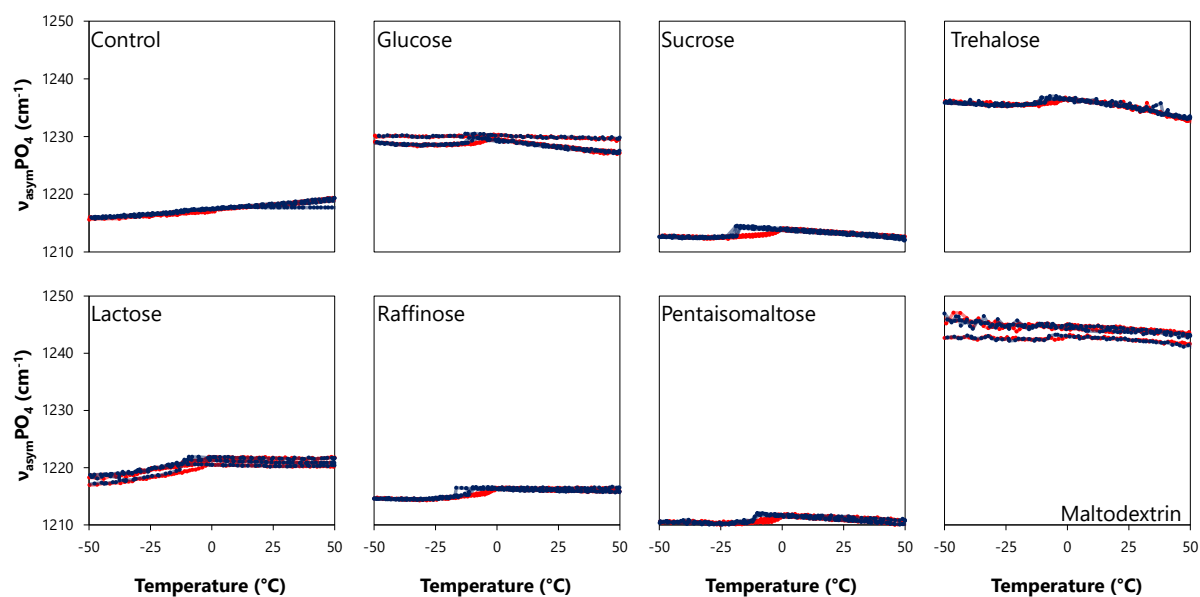


Figure 6.9 Peak position of the asymmetric PO_2 stretching vibration band ($\nu_{\text{asym}}\text{PO}_2$) the asymmetric PO_2 stretching vibration band ($\nu_{\text{asym}}\text{PO}_2$) arising from hydrated *L. bulgaricus* CFL1 upon cooling (blue curves) and heating (red curves).

Washed cells (control) and cells protected with different sugars solution at 25% are presented. Data points correspond to raw data of three independent measurements.

When the air-dried cells were compared to the hydrated ones (Figure 6.10), there was no clear trend of the hydration effect on $\nu_{\text{asym}}\text{PO}_2$. Besides, different behaviors were observed depending on the sample. Air-dried control samples (washed cells) and air-dried cells in the presence of sucrose and raffinose exhibited higher wavelength values than the hydrated ones. In contrast, in the presence of trehalose and lactose, air-dried cells led to lower wavelength values than hydrated ones.

The two studies reported in the literature that analyzed the PO_2 of hydrated LAB were distinguished by two facts. Meneghel et al. (2017) did not focus on the effect of different sugars on bacterium membrane; they only showed a shift in $\nu_{\text{asym}}\text{PO}_2$ wavelength when two *L. bulgaricus* strains were compared. Both strains were protected with sucrose. Santivarangkna et al. (2010) observed no significant variations in the $\nu_{\text{asym}}\text{PO}_2$ wavelength band in the presence or absence of sorbitol. From the above arguments and our results, the interpretation of $\nu_{\text{asym}}\text{PO}_2$ seemed limited when LAB were used as the object of study to elucidate sugars' effect on the phosphate groups.

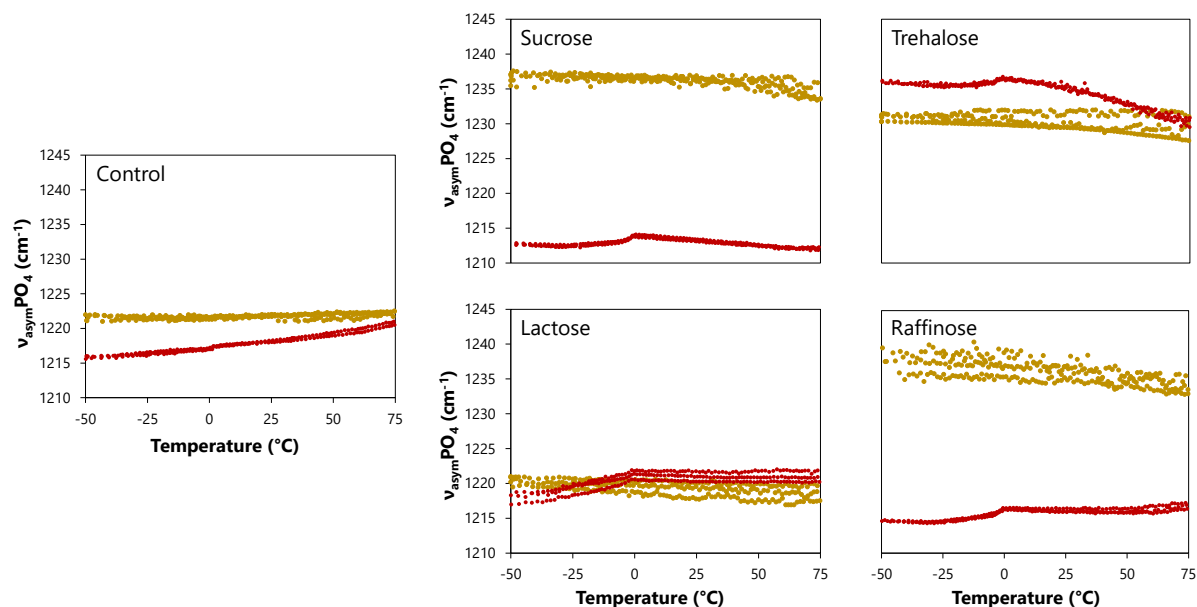


Figure 6.10 Peak position of the asymmetric PO_2 stretching vibration band ($\nu_{\text{asym}}\text{PO}_2$) arising from air-dried *L. bulgaricus* CFL1 upon heating (mustard curves).

Washed cells (control) and cells protected with different sugars solution at 25% are presented. Additionally, the peak position of $\nu_{\text{asym}}\text{PO}_2$ arising from air-dried *L. bulgaricus* CFL1 are presented (red curves). Data points correspond to raw data of three independent measurements.

Based on these results, we questioned whether the $\nu_{\text{asym}}\text{PO}_2$ peak position was well detected in the mid-IR range that has been previously attributed to the phosphate asymmetric stretch region: $1200\text{--}1280\text{ cm}^{-1}$ (Hincha et al. 2003; Cacela and Hincha 2006; Wolkers et al. 2010; Nakata et al. 2015). We hypothesized that there were potentially several peaks in the same region. The localization of the $\nu_{\text{asym}}\text{PO}_2$ might be different from one sample to another.

Moreover, PO_2 groups are not only present in the headgroups of phospholipids but also the phosphodiester functional groups of DNA/RNA polysaccharide backbones and teichoic acids and lipoteichoic acids, charged polymers present in the cell wall of Gram-positive bacteria. Kochan et al. (2018) investigated by atomic force microscopy-infrared (AFM-IR) spectroscopy the cell wall signature of Gram-positive (*Staphylococcus aureus*) and Gram-negative (*Escherichia coli*). Their results showed that changes in the Gram-positive bacteria spectral range of PO_2 group vibrations are mainly ascribed to cell wall components. Therefore, the shifts of $\nu_{\text{asym}}\text{PO}_2$ wavenumbers observed in *L. bulgaricus* CFL1 in the presence of different sugars are not exclusive from the lipid membrane, limiting the interpretation of these results to understand the interaction of sugars with the membrane.

6.5. Conclusion

The present study revealed that the choice of the sugars to protect *L. bulgaricus* CFL1 depended on the stabilization process. For freezing, the best protectors were trehalose and raffinose. For freeze-drying, our data showed that glucose provided the best protection to *L. bulgaricus* CFL1 cells. The extreme degree of polymerization influenced the resistance of freeze-drying since the polysaccharide maltodextrin led to the lowest resistance of *L. bulgaricus* CFL1. These results are a piece of valuable information to guide the production of FOS with a specific degree of polymerization (DP1 or DP2) to protect *L. bulgaricus* CFL1 during freeze-drying.

An FTIR study was used to analyze the effect of sugars on the *L. bulgaricus* CFL1 membrane to understand how sugars act as a protector. Such investigation was applied in whole cells at two physical states (hydrated and air-dried). The sugars affected a subphase transition in the rigid gel zone of the membrane, regardless of their DP. However, sugars' effect on the main lipid phase transition (from liquid crystalline to rigid gel phase) was not significant. This study also revealed the challenges of analyzing the PO₂ from the membrane's phospholipids. It is thus necessary to continue investigating the future development of this method.

6.6. Prospects for this study

- Assessing the resistance of *L. bulgaricus* CFL1 to freeze-dried storage using FOS

Ongoing work by a PREMIUM partner (CONICET, Argentina) is being done to complete this study. It is being assessed the effect of these sugars, including three different FOS (enzymatically produced), on the resistance of *L. bulgaricus* CFL1 to freeze-dried storage. For one month, the storage is carried out at different temperatures (4°C, 25°C, and 37°C). Thus far, results indicate that increased resistance to freeze-drying is guaranteed by one of the FOS (similar results to trehalose were found).

- Developing lipid models from lipid extracts of *L. bulgaricus* CFL1

Due to the limitations identified in this study when analyzing whole cells, efforts are being made to facilitate the elucidation of sugar mechanisms to protect the membrane. For this purpose, the next step in the PREMIUM project is the development of lipid models. Lipid models have been widely used to understand the interactions of some molecules with the membrane because of their less complex structure and constituents.

One partner of the European project PREMIUM (CONICET, Argentina) is currently invested in developing a lipid model from lipid extracts of *L. bulgaricus* CFL1 and elucidating the mechanisms of protection of sucrose and two FOS. In this case, two types of FTIR are being used. The composition of this *L. bulgaricus* CFL1 model considers the lipids identified in Chapter 5 (glycolipids MGDG, DGDG, and PG).

(i) A transmission FTIR spectrometer is being used to monitor the symmetric CH₂ stretching vibration band and determine the lipid phase transition temperature of lipid models in the presence of standard sugars such as sucrose and two different FOS. Measurements are being carried out on the same equipment used to obtain the results of this chapter (Chapter 6). A Nicolet Magna 750 FTIR spectrometer (Thermo Fisher Scientific; Madison, WI, USA).

(ii) An ATR FTIR (Thermo Fisher Scientific, Madison, WI, USA) is also being used to determine the influence of sucrose and FOS on the dehydration kinetics of lipid models. A method developed previously by Wolkers et al. (2010).

Take-home messages

Chapter 6: Influence of sugars on resistance and the membrane of *L. bulgaricus* CFL1

- The sugar used to efficiently protect *L. bulgaricus* CFL1 depended on the stabilization process.
- For freezing, trehalose and raffinose were the best protectors. No correlation was observed between the degree of polymerization and the freezing resistance.
- For freeze-drying, glucose (DP1) was the best protector, whereas maltodextrin (DP>10) led to the lowest resistance of *L. bulgaricus* CFL1.
- The FTIR revealed the influence of sugars on fatty acyl arrangement for hydrated and air-dried cells.
- The presence of sugars (regardless of the DP) induced a subgel phase transition in the gel rigid phase zone (at subzero temperature of lipid phase transitions).

CONCLUSIONS AND PROSPECTS

Conclusions

Lactic acid bacteria are needed to produce various fermented and functional foods. The preservation of these bacteria is a crucial step to warrant their high quality and meet the significant consumer demand for these food products.

This thesis aimed at preserving a sensitive lactic acid bacterium strain and understanding the lipid membrane's role in the cryo-resistance of a lactic acid bacterium.

The first research question investigated in this thesis was:

How to improve the cryo-resistance of a lactic acid bacterium by re-examining the existing strategies?

Two existing strategies to enhance the resistance of LAB were revisited to optimize the production of frozen and freeze-dried *L. bulgaricus* CFL1. Both aimed at minimizing the loss of the main functional properties of *L. bulgaricus* CFL1, using t_{spe} as a descriptor. t_{spe} considered two functional properties, the acidifying activity and culturability of a lactic acid bacterium.

- The first strategy relied on cultivating *L. bulgaricus* CFL1 under three fermentation conditions different from the one for optimal growth.

The fermentation parameters that positively affected the biomass production and the resistance of *L. bulgaricus* CFL1 were identified by multiple regression analysis. This analysis also allowed us to determine the optimum response for producing a high biomass concentration (42°C, pH 5.8, t_{h2}), enhanced resistance to freezing (42°C, pH 4.8, $t_{h1,2,3}$), and freeze-drying (37°C, pH 4.8, t_{h3}) (Figure CP1 ①).

The first strategy improved the resistance of *L. bulgaricus* CFL1, as reported for other LAB strains. The primary drawback is the low biomass concentration produced. This constraint was unlocked in this work using a mathematical tool known as the Pareto front. The Pareto front helped find a compromise between the biomass productivity and resistance of *L. bulgaricus* CFL1 to freezing and freeze-drying. The fermentation condition that allowed a fair biomass production and a good resistance for both stabilization processes was at 42°C, pH 4.8, t_{h2} (Figure CP1 ①).

- The second strategy to stabilize LAB is using protective molecules after the LAB concentration.

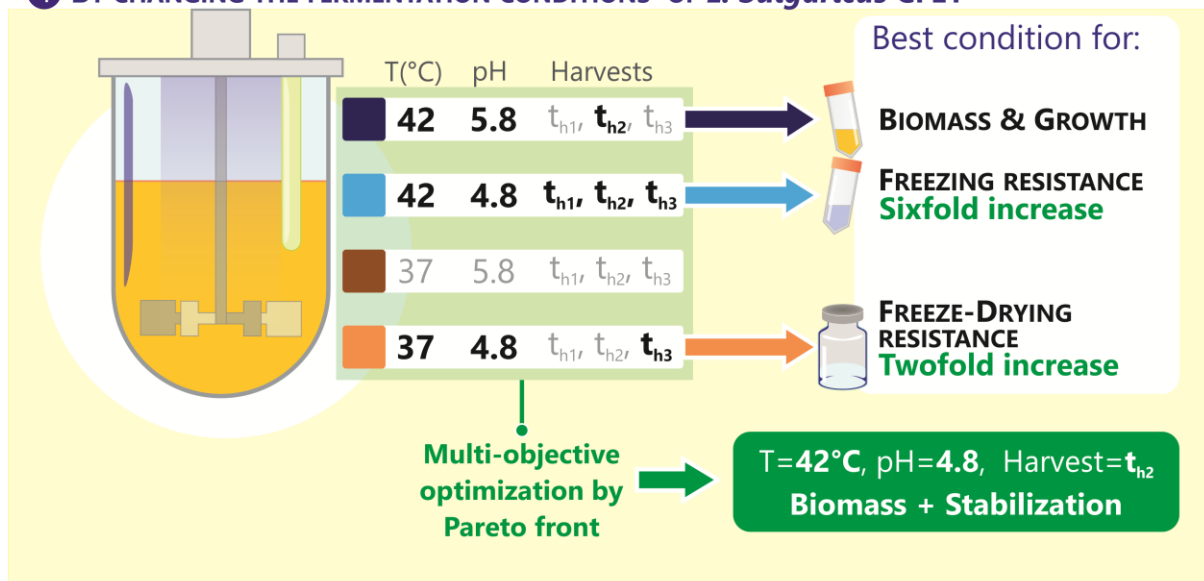
Here, a study was performed to elucidate the influence of sugars on the resistance of *L. bulgaricus* CFL1. The resistance was determined by the survival, the acidifying activity, and the specific acidifying activity of cells (bottom of the Figure CP1 ②).

In the frame of the PREMIUM project, innovative sugar protectors such as FOS and GOS have been proposed. Both are by-products oligosaccharides from food industry (e.g., chicory, banana). FOS and GOS have been reported to have prebiotic properties. For this purpose, seven commercial sugars with different degrees of polymerization (from DP1 to DP>10) were used to protect *L. bulgaricus* CFL1 during freezing and freeze-drying. These sugars represent the monomers that FOS and GOS contain or similar DP (DP3 and DP5-10).

For freezing, *L. bulgaricus* CFL1 cells exhibited high resistance when protected with trehalose (DP2) and raffinose (DP3). The increase in the degree of polymerization was not related to the protection efficiency. For freeze-drying, the glucose (DP1) was the best protector. In this case, extreme DP of sugars led to contrasting protection (Figure CP1 ②). The results in Chapter 6 revealed that the choice of the sugar depended on the stabilization processes selected to preserve *L. bulgaricus* CFL1.

How to improve the cryo-resistance of a lactic acid bacterium?

1 BY CHANGING THE FERMENTATION CONDITIONS OF *L. bulgaricus* CFL1



2 BY SELECTING THE ADEQUATE SUGAR PROTECTOR

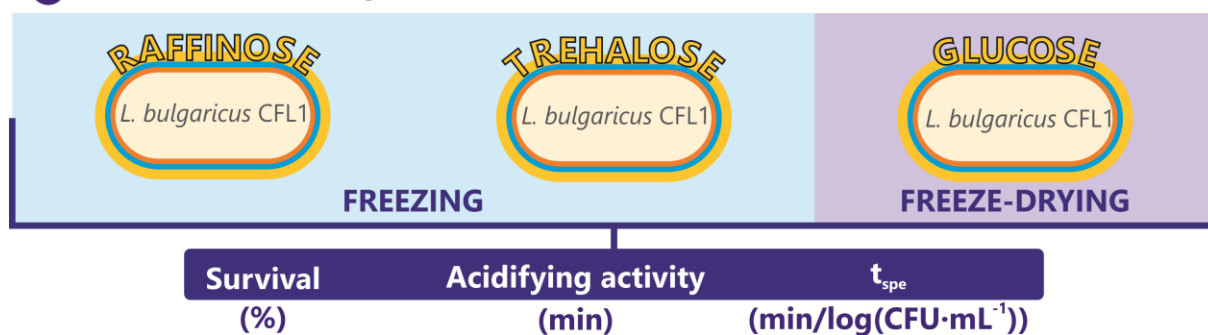


Figure CP1 Schematic overview of the main conclusions obtained after answering the first research question of the thesis.

Re-examining the two strategies to stabilize a cryo-sensitive lactic acid bacterium was successfully performed. From this work, two essential factors should be considered for producing frozen and freeze-dried LAB at the industrial scale:

First, special attention is required to select the fermentation condition to grow LAB since it strongly affects the resistance of bacteria and the quantity of biomass produced. Multi-criteria optimization becomes essential to define the fermentation conditions according to the type of stabilization process and the desired biomass. Second, the adequate choice of the protector is vital and depend on the stabilization process. Therefore, combining the suitable fermentation condition (representing a compromise between enhancing bacterial resistance and biomass production) and the convenient protector will allow a sensitive lactic acid bacterium to be produced at the industrial scale.

From the fundamental point of view, it was also interesting to investigate the impact of the fermentation changes at the lipid membrane scale. Thus, the second research question in this thesis was:

Do the modulation of the membrane lipids and the membrane interaction with sugars explain the cryo-resistance improvement?

Bacteria develop different adaptation mechanisms, for instance, modifying their membrane properties when grown at fermentation conditions other than the optimal for growth. Chapter 5 focused on the modulation of the lipid membrane of *L. bulgaricus* CFL1 by cultivating cells at four fermentation conditions. Here below the main findings:

- Biochemical composition of membrane lipids (Figure CP2 (A))

Phospholipids and glycolipids (namely PG, MGDG, and DGDG) were the membrane lipids identified for the four fermentation conditions. Different lipid classes profile (lipid and fatty acids) were observed per fermentation condition. Low pH (pH 4.8) or temperature (37°C) enhanced the unsaturation of the fatty acids, and a late harvest time induced a high content of CFA in *L. bulgaricus* CFL1.

- Biophysical properties of membrane lipids (Figure CP2 (A))

The fermentation conditions that increased unsaturated fatty acids in the membrane exhibited, as expected, zero or subzero lipid phase transition temperatures (T_s and T_m) and the highest membrane fluidity (lowest anisotropy values) at 20°C.

The observed lipid membrane modulation was related to the resistance of the cells to freezing and freeze-drying (Figure CP2 (B)). The freezing resistance of *L. bulgaricus* CFL1 was associated with a fluid membrane, a high UFA content, and low lipid phase transition temperatures (zero or subzero temperatures). Freeze-drying resistance was only related to an increase in the CFA content. The biophysical properties of the membrane could not be associated with freeze-drying resistance.

Do the modulation of the membrane lipids and the membrane interaction with sugars explain the cryo-resistance improvement?

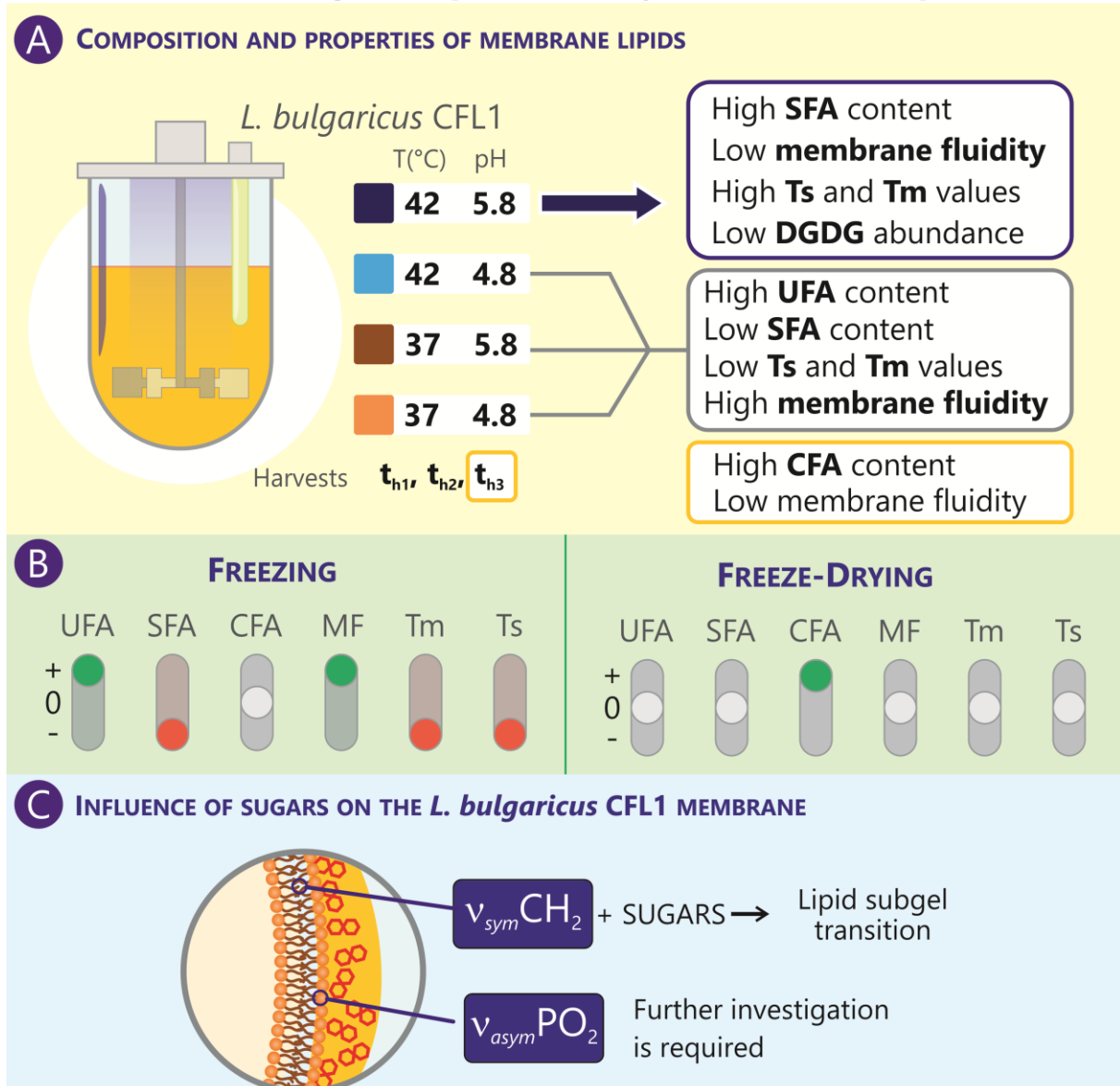


Figure CP2 Schematic overview of the main conclusions obtained after answering the second research question of the thesis. (A) The fermentation parameters that allowed specific modulations on membrane lipids' composition and properties. (B) The relationships between the resistance of *L. bulgaricus* CFL1 to freezing and freeze-drying and the membrane lipids' composition and properties. (C) The influence of sugars on the membrane of *L. bulgaricus* CFL1.

Abbreviations: (+) increase; (-) decrease; (0) no effect; UFA, Unsaturated Fatty Acids; SFA, Saturated Fatty Acids; CFA, Cyclic Fatty Acid, MF, membrane fluidity; Ts and Tm, lipid phase transition temperatures upon cooling and heating, respectively; DGDG, diglycosyldiacylglycerol.

Concerning the interaction of sugars with the membrane (Figure CP2 (C)), an FTIR analysis was proposed considering two absorption bands arising from the main functional groups that constitute the membrane. i.e., the acyl chains group ($v_{sym}CH_2$) and the phosphate groups of the polar heads of the membrane ($v_{asym}PO_2$).

We speculated that the presence of sugars induced a subphase change from a rigid gel phase (L_{β}) to a subgel phase (L_c) upon cooling and vice versa upon heating ($L_c \rightarrow L_{\beta}$). However, there was no effect on the main phase transition, from liquid crystalline (L_{α}) to rigid gel phase (L_{β}). Based on these results, the sugar effect remained modest on the membrane. In Chapter 6, it was also discussed the difficulties of analyzing the $\nu_{asym}PO_2$ wavelength band because we questioned if this peak was well detected or if other adjacent peaks perturbed its position location. Consequently, this study was limited to explaining how sugars affect the hydrophile site of the membrane.

This PhD project provided insights into the modulation of membrane lipids under different fermentation conditions. We now better understand the bacterial adaptation induced by growth conditions at the membrane lipids level.

We observed in this work that the membrane lipids' properties were differently related to freezing and freeze-drying resistance. Moderate influence of the sugars on the hydrophobic site of the membrane was observed. Thus, further investigation is required to elucidate the sugars' interaction with the membrane.

Prospects

- Applying the multi-objective optimization approach to other LAB strains

Using the multi-objective approach proposed in this work will be helpful for the efficient production and stabilization of another lactic acid bacterium of industrial relevance. For instance, the stabilization of LAB that have been identified as producers of exopolysaccharides (Cheirsilp et al. 2018; Ni et al. 2018) and bacteriocins (Costa et al. 2019; Trabelsi et al. 2019). Instead of measuring the acidifying activity after stabilization processes, it would be convenient to determine these functional properties (exopolysaccharides and bacteriocin production).

- Broadening the study of lipid membrane by analyzing other cellular modifications

⇒ Analysis of cell-wall modifications induced by different fermentation conditions

The cell wall is the external constituent in the cell envelope of LAB. LAB wall components such as the peptidoglycan can be altered due to the stabilization of cells by freezing (Girardeau et al. 2022) and freeze-drying (Chen et al. 2022). For example, the increase of peptidoglycan content and the membrane ratio UFA/SFA were related to the enhanced resistance of this bacterium to freeze-drying (Chen et al. 2022). The authors speculated that both adaptation responses might maintain the cell wall and membrane integrity upon freeze-drying.

Thus, it would be convenient to complement the analysis of lipids carried out in this thesis with the characterization of the changes in peptidoglycan that might occur in cultivating *L. bulgaricus* CFL1 in different fermentation conditions.

⇒Proteomic analysis

Proteomics is the large-scale study of proteomes of microorganisms. The proteome refers to the entire set of proteins produced by a particular organism or a cell, including membrane proteins. Some studies have investigated the expression of shock proteins in LAB, produced in response to stressed LAB by heat, cold, and osmotic stresses. These stresses had been applied during growth, specifically after reaching the exponential growth phase (Wouters et al. 2001; Derzelle et al. 2003; Li et al. 2014) or after harvesting and concentrating the cells (Broadbent and Lin 1999; Shao et al. 2014; Song et al. 2014).

Analyzing the proteins expressed after cultivating bacteria in different fermentation conditions would complement the overview already established for lipids as the biological adaptation of *L. bulgaricus* CFL1.

⇒Transcriptomic analysis

The transcriptomic analysis is another omics method that studies the complete set of RNA transcripts produced from the genome. The comparison of transcriptomes allows the identification of genes that are differentially expressed in response to different treatments (Koskenniemi et al. 2011).

This approach has been used to thoroughly comprehend the mechanisms developed by LAB to cope with different stresses such as bile (Lv et al. 2017), ethanol (Yang et al. 2017), cold (freezing for 2 hours) (Lu et al. 2019), and oxidative stress (Cretenet et al. 2014; Zhai et al. 2020).

This method could be coupled with proteomics to study stress-linked gene regulatory networks in *L. bulgaricus* CFL1. Global mRNA and protein level expression changes would provide valuable information about the adaptation mechanisms of *L. bulgaricus* CFL1 growing at different fermentation conditions.

- Optimizing the last step of the production of LAB: storage

This thesis provided some first results about the effect of fermentation conditions on freeze-dried storage. The storage was not affected by the fermentation parameters assessed. Thus, it was not possible to optimize the freeze-dried storage. Further studies are necessary to optimize the storage of frozen or freeze-dried bacteria. A multi-factor optimization would be required to find the best conditions to store LAB. For instance, the crucial factors to consider when storing frozen and freeze-dried storage would be: the storage temperature, the addition of an antioxidant in the protective solution to prevent lipid oxidation in the membrane, the packing material to avoid oxygen entrance among others.

BIBLIOGRAPHY

A

- Abbasalizadeh S, Hejazi MA, Hajiabbas MP (2015) Kinetics of β -galactosidase production by *Lactobacillus bulgaricus* during pH-controlled batch fermentation in three commercial bulk starter media. *Appl Food Biotechnol* 2:39–47. <https://doi.org/10.22037/AFB.V2I4.9512>
- Abedi E, Hashemi SMB (2020) Lactic acid production - producing microorganisms and substrates sources-state of art. *Heliyon* 6 6:1–30
- Adams G (2007) The principles of freeze-drying. In: Day JG, Stacey GN (eds) *Cryopreservation and freeze-drying protocols*, Second edi. *Methods Mol Biol*, pp 15–38
- Aghababaie M, Khanahmadi M, Beheshti M (2015) Developing a kinetic model for co-culture of yogurt starter bacteria growth in pH controlled batch fermentation. *J Food Eng* 166:72–79. <https://doi.org/10.1016/j.jfoodeng.2015.05.013>
- Albrecht RM, Orndorff GR, MacKenzie AP (1973) Survival of certain microorganisms subjected to rapid and very rapid freezing on membrane filters. *Cryobiology* 10:233–239. [https://doi.org/10.1016/0011-2240\(73\)90036-9](https://doi.org/10.1016/0011-2240(73)90036-9)
- Al-Qadiri HM, Al-Alami NI, Al-Holy MA, Rasco BA (2008) Using Fourier Transform Infrared (FTIR) absorbance spectroscopy and multivariate analysis to study the effect of chlorine-induced bacterial injury in water. *J Agric Food Chem* 56:8992–8997. <https://doi.org/10.1021/JF801604P>
- Altaf M, Naveena BJ, Reddy G (2007) Use of inexpensive nitrogen sources and starch for L(+) lactic acid production in anaerobic submerged fermentation. *Bioresour Technol* 98:498–503. <https://doi.org/10.1016/J.BIORTECH.2006.02.013>

- Altermann E, Russell WM, Azcarate-Peril MA, et al (2005) Complete genome sequence of the probiotic lactic acid bacterium *Lactobacillus acidophilus* NCFM. Proc Natl Acad Sci 102:3906–3912. <https://doi.org/10.1073/PNAS.0409188102>
- Alves de Oliveira R, Komesu A, Vaz Rossell CE, Maciel Filho R (2018) Challenges and opportunities in lactic acid bioprocess design-From economic to production aspects. Biochem Eng J 133:219–239. <https://doi.org/10.1016/j.bej.2018.03.003>
- Ambros S, Hofer F, Kulozik U (2018) Protective effect of sugars on storage stability of microwave freeze-dried and freeze-dried *Lactobacillus paracasei* F19. J Appl Microbiol 125:1128–1136. <https://doi.org/10.1111/jam.13935>
- Amorim C, Silvério SC, Cardoso BB, et al (2020) In vitro fermentation of raffinose to unravel its potential as prebiotic ingredient. LWT 126:109322. <https://doi.org/10.1016/j.lwt.2020.109322>
- Ampatzoglou A, Schurr B, Deepika G, et al (2010) Influence of fermentation on the acid tolerance and freeze-drying survival of *Lactobacillus rhamnosus* GG. Biochem Eng J 52:65–70. <https://doi.org/10.1016/J.BEJ.2010.07.005>
- Aragón-Rojas S, Yolanda Ruiz-Pardo R, Javier Hernández-Álvarez A, Ximena Quintanilla-Carvajal M (2019) Sublimation conditions as critical factors during freeze-dried probiotic powder production. <https://doi.org/10.1080/0737393720191570248> 38:333–349. <https://doi.org/10.1080/07373937.2019.1570248>
- Archacka M, Białas W, Dembczyński R, et al (2019) Method of preservation and type of protective agent strongly influence probiotic properties of *Lactococcus lactis*: A complete process of probiotic preparation manufacture and use. Food Chem 274:733–742. <https://doi.org/10.1016/j.foodchem.2018.09.033>
- Arnoux AS, Preziosi-Belloy L, Esteban G, et al (2005) Lactic acid bacteria biomass monitoring in highly conductive media by permittivity measurements. Biotechnol Lett 27:1551–1557. <https://doi.org/10.1007/S10529-005-1781-2>
- Ashaolu TJ, Reale A (2020) A holistic review on Euro-Asian lactic acid bacteria fermented cereals and vegetables. Microorganisms 8:1176. <https://doi.org/10.3390/MICROORGANISMS8081176>

B

- Bâati L, Fabre-Gea C, Auriol D, Blanc PJ (2000) Study of the cryotolerance of *Lactobacillus acidophilus*: Effect of culture and freezing conditions on the viability and cellular protein levels. Int J Food Microbiol 59:241–247. [https://doi.org/10.1016/S0168-1605\(00\)00361-5](https://doi.org/10.1016/S0168-1605(00)00361-5)
- Batt CA (2014) *Lactobacillus* and *Lactococcus*. In: Batt CA, Tortorello M Lou (eds) Encyclopedia of food microbiology, Volume 2, Second edi. Academic press, pp 409–439
- Baumann DP, Reinbold GW (1966) Freezing of lactic cultures. J Dairy Sci 49:259–264. [https://doi.org/10.3168/JDS.S0022-0302\(66\)87846-3](https://doi.org/10.3168/JDS.S0022-0302(66)87846-3)
- Béal C, Corrieu G (1995) On-line indirect measurements of biological variables and their kinetics during pH controlled batch cultures of thermophilic lactic acid bacteria. J Food Eng 26:511–525. [https://doi.org/10.1016/0260-8774\(94\)00071-G](https://doi.org/10.1016/0260-8774(94)00071-G)
- Béal C, Fonseca F (2015) Freezing of Probiotic Bacteria. In: Foerst P, Santivarangkna C (eds) Advances in probiotic technologychnology, First edit. CRC Press, pp 179–212
- Béal C, Fonseca F, Corrieu G (2001) Resistance to freezing and frozen storage of *Streptococcus thermophilus* is related to membrane fatty acid composition. J Dairy Sci 84:2347–2356. [https://doi.org/10.3168/JDS.S0022-0302\(01\)74683-8](https://doi.org/10.3168/JDS.S0022-0302(01)74683-8)

- Béal C, Louvet P, Corrieu G (1989) Influence of controlled pH and temperature on the growth and acidification of pure cultures of *Streptococcus thermophilus* 404 and *Lactobacillus bulgaricus* 398. *Appl Microbiol Biotechnol* 32:148–154. <https://doi.org/10.1007/BF00165879>
- Béal C, Marin M, Fontaine E, et al (2008) Production et conservation des ferments lactiques et probiotiques. In: Corrieu G, Luquet F-M (eds) *Bactéries lactiques, de la génétique aux ferments*, First edit. Lavoisier, pp 661–785
- Benesch MGK, Lewis RNAH, McElhane RN (2015) On the miscibility of cardiolipin with 1,2-diacyl phosphoglycerides: Binary mixtures of dimyristoylphosphatidylglycerol and tetramyristoylcardiolipin. *Biochim Biophys Acta BBA - Biomembr* 1848:2878–2888. <https://doi.org/10.1016/j.bbamem.2015.08.003>
- Beney L, Gervais P (2001) Influence of the fluidity of the membrane on the response of microorganisms to environmental stresses. *Appl Microbiol Biotechnol* 2001 571 57:34–42. <https://doi.org/10.1007/S002530100754>
- Berk Z (2013) Freeze-drying (lyophilization) and freeze concentration. In: Berk Z (ed) *Food process engineering and technology*, Second edi. Academic Press, pp 567–581
- Bernard E, Rolain T, Courtin P, et al (2011) Characterization of O-acetylation of N-acetylglucosamine: a novel structural variation of bacterial peptidoglycan. *J Biol Chem* 286:23950–23958. <https://doi.org/10.1074/JBC.M111.241414/ATTACHMENT/560EB873-DAED-461F-B0E1-A2ABB4800004/MMC1.PDF>
- Bhushani A, Anandharamakrishnan C (2017) Freeze Drying. In: Anandharamakrishnan C (ed) *Handbook of drying for dairy products*, First edit. John Wiley & Sons, pp 95–121
- Bintsis T (2018) Lactic acid bacteria: their applications in foods. *J Bacteriol Mycol Open Access* 6:89–94. <https://doi.org/10.15406/jbmoa.2018.06.00182>
- Bischof JC, Wolkers WF, Tsvetkova NM, et al (2002) Lipid and protein changes due to freezing in dunning AT-1 cells. *Cryobiology* 45:22–32. [https://doi.org/10.1016/S0011-2240\(02\)00103-7](https://doi.org/10.1016/S0011-2240(02)00103-7)
- Blajman JE, Vinderola G, Cuatrin A, et al (2020) Technological variables influencing the growth and stability of a silage inoculant based on spray-dried lactic acid bacteria. *J Appl Microbiol* 14750. <https://doi.org/10.1111/jam.14750>
- Bligh EG, Dyer WJ (1959) A rapid method of total lipid extraction and purification. *Can J Biochem Physiol* 37:911–917. <https://doi.org/10.1139/o59-099>
- Bodzen A, Jossier A, Dupont S, et al (2021a) Increased survival of *Lactococcus lactis* strains subjected to freeze-drying after cultivation in an acid medium: involvement of membrane fluidity. *Food Technol Biotechnol* 59:443–453. <https://doi.org/10.17113/FTB.59.04.21.7076>
- Bodzen A, Jossier A, Dupont S, et al (2021b) Design of a new lyoprotectant increasing freeze-dried *Lactobacillus* strain survival to long-term storage. *BMC Biotechnol* 21:1–10. <https://doi.org/10.1186/S12896-021-00726-2/FIGURES/4>
- Bolotin A, Quinquis B, Renault P, et al (2004) Complete sequence and comparative genome analysis of the dairy bacterium *Streptococcus thermophilus*. *Nat Biotechnol* 22:1554–1558. <https://doi.org/10.1038/nbt1034>
- Booth IR (1985) Regulation of cytoplasmic pH in bacteria. *Microbiol Rev* 49:359–378
- Borchman D, Yappert MC, Herrell P (1991) Structural characterization of human lens membrane lipid by infrared spectroscopy. *Invest Ophthalmol Vis Sci* 32:2404–2416

- Borst JW, Visser NV, Kouptsova O, Visser AJWG (2000) Oxidation of unsaturated phospholipids in membrane bilayer mixtures is accompanied by membrane fluidity changes. *Biochim Biophys Acta BBA - Mol Cell Biol Lipids* 1487:61–73. [https://doi.org/10.1016/S1388-1981\(00\)00084-6](https://doi.org/10.1016/S1388-1981(00)00084-6)
- Bouix M, Ghorbal S (2017) Assessment of bacterial membrane fluidity by flow cytometry. *J Microbiol Methods* 143:50–57. <https://doi.org/10.1016/j.mimet.2017.10.005>
- Bravo-Ferrada BM, Brizuela N, Gerbino E, et al (2015) Effect of protective agents and previous acclimation on ethanol resistance of frozen and freeze-dried *Lactobacillus plantarum* strains. *Cryobiology* 71:522–528. <https://doi.org/10.1016/j.cryobiol.2015.10.154>
- Bravo-Ferrada BM, Gonçalves S, Semorile L, et al (2018) Cell surface damage and morphological changes in *Oenococcus oeni* after freeze-drying and incubation in synthetic wine. *Cryobiology* 82:15–21. <https://doi.org/10.1016/j.cryobiol.2018.04.014>
- Brennan M, Wanismail B, Jhonson MC, Ray B (1986) Cellular damage in dried *Lactobacillus acidophilus*. *J Food Prot* 49:47–53. <https://doi.org/10.4315/0362-028x-49.1.47>
- Briard JG, Poisson JS, Turner TR, et al (2016) Small molecule ice recrystallization inhibitors mitigate red blood cell lysis during freezing, transient warming and thawing. *Sci. Rep.* 6
- Broadbent JR, Larsen RL, Deibel V, Steele JL (2010) Physiological and Transcriptional Response of *Lactobacillus casei* ATCC 334 to Acid Stress. *J Bacteriol* 192:2445–2458. <https://doi.org/10.1128/JB.01618-09>
- Broadbent JR, Lin C (1999) Effect of heat shock or cold shock treatment on the resistance of *Lactococcus lactis* to freezing and lyophilization. *Cryobiology* 39:88–102. <https://doi.org/10.1006/cryo.1999.2190>
- Broeckx G, Vandenheuvel D, Claes IJJ, et al (2016) Drying techniques of probiotic bacteria as an important step towards the development of novel pharmabiotics. *Int. J. Pharm.* 505:303–318
- Bucak MN, Keskin N, Taşpınar M, et al (2013) Raffinose and hypotaurine improve the post-thawed Merino ram sperm parameters. *Cryobiology* 67:34–39. <https://doi.org/10.1016/j.cryobiol.2013.04.007>
- Budin-Verneuil A, Maguin E, Auffray Y, et al (2005) Transcriptional analysis of the cyclopropane fatty acid synthase gene of *Lactococcus lactis* MG1363 at low pH. *FEMS Microbiol Lett* 250:189–194. <https://doi.org/10.1016/j.femsle.2005.07.007>
- Buera MP, Karel M (1995) Effect of physical changes on the rates of nonenzymic browning and related reactions. *Food Chem* 52:167–173. [https://doi.org/10.1016/0308-8146\(94\)P4199-P](https://doi.org/10.1016/0308-8146(94)P4199-P)
- Buera P, Schebor C, Elizalde B (2005) Effects of carbohydrate crystallization on stability of dehydrated foods and ingredient formulations. *J Food Eng* 67:157–165. <https://doi.org/10.1016/J.JFOODENG.2004.05.052>
- Buist G, Ridder ANJA, Kok J, Kuipers OP (2006) Different subcellular locations of secretome components of Gram-positive bacteria. *Microbiol Read Engl* 152:2867–2874. <https://doi.org/10.1099/MIC.0.29113-0>
- Bulatović ML, Rakin MB, Vukašinić-Sekulić MS, et al (2014) Effect of nutrient supplements on growth and viability of *Lactobacillus johnsonii* NRRL B-2178 in whey. *Int Dairy J* 34:109–115. <https://doi.org/10.1016/J.IDAIRYJ.2013.07.014>
- Burgos-Rubio CN, Okos MR, Wankat PC (2000) Kinetic study of the conversion of different substrates to lactic acid using *Lactobacillus bulgaricus*. *Biotechnol Prog* 16:305–314. <https://doi.org/10.1021/BP000022P>

C

- Cacela C, Hinch DK (2006) Monosaccharide composition, chain length and linkage type influence the interactions of oligosaccharides with dry phosphatidylcholine membranes. *Biochim Biophys Acta BBA-Biomembr Biomembr* 1758:680–691. <https://doi.org/10.1016/j.bbamem.2006.04.005>
- Cachon R, Antérieux P, Diviès C (1998) The comparative behavior of *Lactococcus lactis* in free and immobilized culture processes. *J Biotechnol* 63:211–218. [https://doi.org/10.1016/S0168-1656\(98\)00083-2](https://doi.org/10.1016/S0168-1656(98)00083-2)
- Caffalette CA, Kuklewicz J, Spellmon N, Zimmer J (2020) Biosynthesis and export of bacterial glycolipids. *Annu Rev Biochem* 89:741–768. <https://doi.org/10.1146/annurev-biochem-011520-104707>
- Calvano CD, Zambonin CG, Palmisano F (2011) Lipid fingerprinting of Gram-positive lactobacilli by intact cells - Matrix-assisted laser desorption/ionization mass spectrometry using a proton sponge based matrix. *Rapid Commun Mass Spectrom* 25:1757–1764. <https://doi.org/10.1002/rcm.5035>
- Carminati D, Giraffa G, Quiberoni A, et al (2010) Advances and trends in starter cultures for dairy fermentations. In: Mozzi F, Raya RR, Vignolo GM (eds) *Biotechnology of lactic acid bacteria: novel applications*, First edit. Wiley-Blackwell, pp 177–192
- Carvalho AS, Silva J, Ho P, et al (2003a) Impedimetric method for estimating the residual activity of freeze-dried *Lactobacillus delbrueckii* ssp. *bulgaricus*. *Int Dairy J* 13:463–468. [https://doi.org/10.1016/S0958-6946\(03\)00049-9](https://doi.org/10.1016/S0958-6946(03)00049-9)
- Carvalho AS, Silva J, Ho P, et al (2002) Survival of freeze-dried *Lactobacillus plantarum* and *Lactobacillus rhamnosus* during storage in the presence of protectants. *Biotechnol Lett* 24:1587–1591. <https://doi.org/10.1023/A:1020301614728>
- Carvalho AS, Silva J, Ho P, et al (2004a) Relevant factors for the preparation of freeze-dried lactic acid bacteria. *Int Dairy J* 14:835–847. <https://doi.org/10.1016/j.idairyj.2004.02.001>
- Carvalho AS, Silva J, Ho P, et al (2004b) Effects of various sugars added to growth and drying media upon thermotolerance and survival throughout storage of freeze-Dried *Lactobacillus delbrueckii* ssp. *bulgaricus*. *Biotechnol Prog* 20:248–254. <https://doi.org/10.1021/bp034165y>
- Carvalho AS, Silva J, Ho P, et al (2003b) Protective effect of sorbitol and monosodium glutamate during storage of freeze-dried lactic acid bacteria. *Lait* 83:203–210. <https://doi.org/10.1051/lait:2003010>
- Carvalho AS, Silva J, Ho P, et al (2003c) Effects of addition of sucrose and salt, and of starvation upon thermotolerance and survival during storage of freeze-dried *Lactobacillus delbrueckii* ssp *bulgaricus*. *J Food Sci* 68:2538–2541. <https://doi.org/10.1111/j.1365-2621.2003.tb07057.x>
- Carvalho BF, Sales GFC, Schwan RF, Ávila CLS (2021) Criteria for lactic acid bacteria screening to enhance silage quality. *J Appl Microbiol* 130:341–355. <https://doi.org/10.1111/JAM.14833>
- Castro HP, Teixeira PM, Kirby R (1995) Storage of lyophilized cultures of *Lactobacillus bulgaricus* under different relative humidities and atmospheres. *Appl Microbiol Biotechnol* 44:172–176. <https://doi.org/10.1007/BF00164498>
- Castro HP, Teixeira PM, Kirby R (1997) Evidence of membrane damage in *Lactobacillus bulgaricus* following freeze drying. *J Appl Microbiol* 82:87–94. <https://doi.org/10.1111/j.1365-2672.1997.tb03301.x>

- Castro HP, Teixeira PM, Kirby R (1996) Changes in the cell membrane of *Lactobacillus bulgaricus* during storage following freeze-drying. *Biotechnol Lett* 18:99–104. <https://doi.org/10.1007/BF00137819>
- Chamberlain CA, Hatch M, Garrett TJ (2019) Metabolomic profiling of oxalate-degrading probiotic *Lactobacillus acidophilus* and *Lactobacillus gasseri*. *PLOS ONE* 14:e0222393. <https://doi.org/10.1371/journal.pone.0222393>
- Chambers MC, Maclean B, Burke R, et al (2012) A cross-platform toolkit for mass spectrometry and proteomics. *Nat Biotechnol* 30:918–920. <https://doi.org/10.1038/nbt.2377>
- Champagne CP, Detournay H, Hardy MJ (1991) Effect of medium on growth and subsequent survival, after freeze-drying, of *Lactobacillus delbrueckii* subsp. *bulgaricus*. *J Ind Microbiol* 7:147–149. <https://doi.org/10.1007/BF01576077>
- Champagne CP, Gardner NJ, Roy D (2005) Challenges in the addition of probiotic cultures to foods. *Crit Rev Food Sci Nutr* 45:61–84. <https://doi.org/10.1080/10408690590900144>
- Champagne CP, Gomes da Cruz A, Daga M (2018) Strategies to improve the functionality of probiotics in supplements and foods. *Curr Opin Food Sci* 22:160–166. <https://doi.org/10.1016/J.COFS.2018.04.008>
- Chaplin M (2022) Water absorption spectrum. In: Water Absorpt. Spectr. https://water.lsbu.ac.uk/water/water_vibrational_spectrum.html. Accessed 20 Jun 2022
- Chapot-Chartier MP, Kulakauskas S (2014) Cell wall structure and function in lactic acid bacteria. *Microb Cell Factories* 13:1–23. <https://doi.org/10.1186/1475-2859-13-S1-S9/FIGURES/4>
- Chavarri FJ, De Paz M, Nuñez M (1988) Cryoprotective agents for frozen concentrated starters from non-bitter *Streptococcus lactis* strains. *Biotechnol Lett* 1988 101 10:11–16. <https://doi.org/10.1007/BF01030016>
- Cheirsilp B, Suksawang S, Yeesang J, Boonsawang P (2018) Co-production of functional exopolysaccharides and lactic acid by *Lactobacillus kefiranofaciens* originated from fermented milk, kefir. *J Food Sci Technol* 55:331–340. <https://doi.org/10.1007/s13197-017-2943-7>
- Chen W, Hang F (2019) Lactic acid bacteria starter. In: Chen W (ed) *Lactic acid bacteria: bioengineering and industrial applications*. Springer, pp 93–143
- Chen Z, E J, Ma R, et al (2022) The effect of aspartic acid on the freeze-drying survival rate of *Lactobacillus plantarum* LIP-1 and its inherent mechanism. *LWT* 155:1–10. <https://doi.org/10.1016/j.lwt.2021.112929>
- Chikindas ML, Weeks R, Drider D, et al (2018) Functions and emerging applications of bacteriocins. *Curr Opin Biotechnol* 49:23–28. <https://doi.org/10.1016/j.copbio.2017.07.011>
- Claesson MJ, Li Y, Leahy S, et al (2006) Multireplicon genome architecture of *Lactobacillus salivarius*. *Proc Natl Acad Sci U S A* 103:6718–6723. <https://doi.org/10.1073/pnas.0511060103>
- Cohen DPA, Renes J, Bouwman FG, et al (2006) Proteomic analysis of log to stationary growth phase *Lactobacillus plantarum* cells and a 2-DE database. *PROTEOMICS* 6:6485–6493. <https://doi.org/10.1002/PMIC.200600361>
- Corcoran BM, Ross RP, Fitzgerald GF, Stanton C (2004) Comparative survival of probiotic lactobacilli spray-dried in the presence of prebiotic substances. *J Appl Microbiol* 96:1024–1039. <https://doi.org/10.1111/j.1365-2672.2004.02219.x>
- Corveleyn S, Dhaese P, Neiryck S, Steidler L (2010) Cryoprotecteurs pour la lyophilisation de bactéries lactiques Patent EP2424972B1

- Costa JCCP, Bover-Cid S, Bolívar A, et al (2019) Modelling the interaction of the sakacin-producing *Lactobacillus sakei* CTC494 and *Listeria monocytogenes* in filleted gilthead sea bream (*Sparus aurata*) under modified atmosphere packaging at isothermal and non-isothermal conditions. *Int J Food Microbiol* 297:72–84. <https://doi.org/10.1016/j.ijfoodmicro.2019.03.002>
- Cotter PD, Hill C (2003) Surviving the Acid Test: Responses of Gram-Positive Bacteria to Low pH. *Microbiol Mol Biol Rev* 67:429–453. <https://doi.org/10.1128/membr.67.3.429-453.2003>
- Courtin P, Miranda G, Guillot A, et al (2006) Peptidoglycan structure analysis of *Lactococcus lactis* reveals the presence of an L, D-carboxypeptidase involved in peptidoglycan maturation. *J Bacteriol* 188:5293–5298. <https://doi.org/10.1128/JB.00285-06/ASSET/3F4B38CA-33AA-4C6C-B7E9-5E84BBBA453F/ASSETS/GRAPHIC/ZJB0140659130002.JPEG>
- Cretenet M, Le Gall G, Wegmann U, et al (2014) Early adaptation to oxygen is key to the industrially important traits of *Lactococcus lactis* ssp. *cremoris* during milk fermentation. *BMC Genomics* 15:1054. <https://doi.org/10.1186/1471-2164-15-1054>
- Crittenden R, Playne MJ (2008) Prebiotics. In: *Handbook of Probiotics and Prebiotics*, Second edition. John Wiley & Sons, Ltd, pp 533–581
- Crowe JH, Clegg JS, Crowe LM (1998) Anhydrobiosis: the water replacement hypothesis. In: Reid DS (ed) *The properties of water in foods*, First edit. Springer, pp 440–455
- Crowe JH, Crowe LM, Carpenter JF, et al (1988) Interactions of sugars with membranes. *BBA - Rev Biomembr* 947:367–384. [https://doi.org/10.1016/0304-4157\(88\)90015-9](https://doi.org/10.1016/0304-4157(88)90015-9)
- Crowe JH, Crowe LM, Chapman D (1984) Preservation of membranes in anhydrobiotic organisms: the role of trehalose. *Science* 223:701–703. <https://doi.org/10.1126/SCIENCE.223.4637.701>
- Crowe JH, Hoekstra FA, Crowe LM (1992) Anhydrobiosis. *Annu Rev Physiol* 54:579–599
- Crowe JH, Hoekstra FA, Crowe LM (1989a) Membrane phase transitions are responsible for imbibitional damage in dry pollen. *Proc Natl Acad Sci* 86:520–523. <https://doi.org/10.1073/PNAS.86.2.520>
- Crowe JH, Hoekstra FA, Crowe LM, et al (1989b) Lipid phase transitions measured in intact cells with fourier transform infrared spectroscopy. *Cryobiology* 26:76–84. [https://doi.org/10.1016/0011-2240\(89\)90035-7](https://doi.org/10.1016/0011-2240(89)90035-7)
- Crowe JH, Hoekstra FA, Nguyen KHN, Crowe LM (1996) Is vitrification involved in depression of the phase transition temperature in dry phospholipids? *Biochim Biophys Acta BBA - Biomembr* 1280:187–196. [https://doi.org/10.1016/0005-2736\(95\)00287-1](https://doi.org/10.1016/0005-2736(95)00287-1)
- Crowe LM (2002) Lessons from nature: the role of sugars in anhydrobiosis. *Comp Biochem Physiol A Mol Integr Physiol* 131:505–513. [https://doi.org/10.1016/S1095-6433\(01\)00503-7](https://doi.org/10.1016/S1095-6433(01)00503-7)
- da Cruz AG, Faria J de AF, Van Dender AGF (2007) Packaging system and probiotic dairy foods. *Food Res Int* 40:951–956. <https://doi.org/10.1016/J.FOODRES.2007.05.003>

D

- Daba GM, Elkhateeb WA (2020) Bacteriocins of lactic acid bacteria as biotechnological tools in food and pharmaceuticals: current applications and future prospects. *Biocatal Agric Biotechnol* 28:101750. <https://doi.org/10.1016/j.bcab.2020.101750>

- Daba GM, Elnahas MO, Elkhateeb WA (2021) Contributions of exopolysaccharides from lactic acid bacteria as biotechnological tools in food, pharmaceutical, and medical applications. *Int J Biol Macromol* 173:79–89. <https://doi.org/10.1016/j.ijbiomac.2021.01.110>
- Davis SP, Abrams MC, Brault JW (2001) Why choose a Fourier transform spectrometer?. In: Davis SP, Abrams MC, Brault JW, Day JG, Stacey GN (eds) *Fourier transform spectrometry*, First edi. Academic Press, pp 17–25.
- De Angelis M, Gobbetti M (2004) Environmental stress responses in *Lactobacillus*: a review. *PROTEOMICS* 4:106–122. <https://doi.org/10.1002/pmic.200300497>
- De Giulio B, Orlando P, Barba G, et al (2005) Use of alginate and cryo-protective sugars to improve the viability of lactic acid bacteria after freezing and freeze-drying. *World J Microbiol Biotechnol* 21:739–746. <https://doi.org/10.1007/s11274-004-4735-2>
- De Man JC, Rogosa M, Sharpe ME (1960) A medium for the cultivation of *Lactobacilli*. *J Appl Bacteriol* 23:130–135. <https://doi.org/10.1111/J.1365-2672.1960.TB00188.X>
- Delcour J, Ferain T, Deghorain M, et al (1999) The biosynthesis and functionality of the cell-wall of lactic acid bacteria. *Antonie Van Leeuwenhoek* 76:159–184. <https://doi.org/10.1023/A:1002089722581>
- Demé B, Zemb Th (2000) Measurement of sugar depletion from uncharged lamellar phases by SANS contrast variation. *J Appl Crystallogr* 33:569–573. <https://doi.org/10.1107/S0021889899013680>
- Denich TJ, Beaudette LA, Lee H, Trevors JT (2003) Effect of selected environmental and physico-chemical factors on bacterial cytoplasmic membranes. *J Microbiol Methods* 52:149–182. [https://doi.org/10.1016/S0167-7012\(02\)00155-0](https://doi.org/10.1016/S0167-7012(02)00155-0)
- Derzelle S, Hallet B, Ferain T, et al (2003) Improved adaptation to cold-shock, stationary-phase, and freezing stresses in *Lactobacillus plantarum* overproducing cold-shock proteins. *Appl Environ Microbiol* 69:4285–4290. <https://doi.org/10.1128/AEM.69.7.4285-4290.2003>
- Desvaux M, Dumas E, Chafsey I, Hébraud M (2006) Protein cell surface display in Gram-positive bacteria: from single protein to macromolecular protein structure. *FEMS Microbiol Lett* 256:1–15. <https://doi.org/10.1111/J.1574-6968.2006.00122.X>
- Dhaliwal A, Khondker A, Alsop R, Rheinstädter MC (2019) Glucose can protect membranes against dehydration damage by inducing a glassy membrane state at low hydrations. *Membranes* 9:15. <https://doi.org/10.3390/membranes9010015>
- Díaz SB, Ale NM, Ben Altabef A, et al (2017) Interaction of galacto-oligosaccharides and lactulose with dipalmitoylphosphatidylcholine lipid membranes as determined by infrared spectroscopy. *RSC Adv* 7:24298–24304. <https://doi.org/10.1039/c7ra01964e>
- Díaz SB, Biondi de Lopez AC, Disalvo EA (2003) Dehydration of carbonyls and phosphates of phosphatidylcholines determines the lytic action of lysoderivatives. *Chem Phys Lipids* 122:153–157. [https://doi.org/10.1016/S0009-3084\(02\)00186-X](https://doi.org/10.1016/S0009-3084(02)00186-X)
- Diefenbach R, Heipieper HJ, Keweloh H (1992) The conversion of cis into trans unsaturated fatty acids in *Pseudomonas putita* P8: evidence for a role in the regulation of membrane fluidity. *Appl Microbiol Biotechnol* 1992 383 38:382–387. <https://doi.org/10.1007/BF00170090>
- Dimitrellou D, Kandyliis P, Kourkoutas Y (2016) Effect of cooling rate, freeze-drying, and storage on survival of free and immobilized *Lactobacillus casei* ATCC 393. *LWT - Food Sci Technol* 69:468–473. <https://doi.org/10.1016/j.lwt.2016.01.063>

- Dinkçi N, Akdeniz V, Akalin AS (2019) Survival of probiotics in functional foods during shelf life. In: Galanakis CM (ed) Food quality and shelf Life, First edit. Academic Press, pp 201–233
- Dowhan W (1997) Molecular basis for membrane phospholipid: why are there so many lipids? *Annu Rev Biochem* 66:199–232. <https://doi.org/10.1146/ANNUREV.BIOCHEM.66.1.199>
- Drici-Cachon Z, Cavin JF, Diviès C (1996) Effect of pH and age of culture on cellular fatty acid composition of *Leuconostoc oenos*. *Lett Appl Microbiol* 22:331–334. <https://doi.org/10.1111/J.1472-765X.1996.TB01172.X>
- Drucker DB, Megson G, Harty DWS, et al (1995) Phospholipids of *Lactobacillus* spp. *J Bacteriol* 177:6304–6308. <https://doi.org/10.1128/jb.177.21.6304-6308.1995>
- Dugail I, Kayser BD, Lhomme M (2017) Specific roles of phosphatidylglycerols in hosts and microbes. *Biochimie* 141:47–53. <https://doi.org/10.1016/j.biochi.2017.05.005>
- Dührkop K, Fleischauer M, Ludwig M, et al (2019) SIRIUS 4: a rapid tool for turning tandem mass spectra into metabolite structure information. *Nat Methods* 16:299–302. <https://doi.org/10.1038/s41592-019-0344-8>
- Dumont F, Marechal PA, Gervais P (2004) Cell size and water permeability as determining factors for cell viability after freezing at different cooling rates. *Appl Environ Microbiol* 70:268–272. <https://doi.org/10.1128/AEM.70.1.268-272.2004>
- Duwat P, Sourice S, Cesselin B, et al (2001) Respiration capacity of the fermenting bacterium *Lactococcus lactis* and its positive effects on growth and survival. *J Bacteriol* 183:4509–4516. <https://doi.org/10.1128/JB.183.15.4509-4516.2001>

E

- E J, Chen J, Chen Z, et al (2021) Effects of different initial pH values on freeze-drying resistance of *Lactiplantibacillus plantarum* LIP-1 based on transcriptomics and proteomics. *Food Res Int* 149:110694. <https://doi.org/10.1016/j.foodres.2021.110694>
- E J, Ma L, Chen Z, et al (2020) Effects of buffer salts on the freeze-drying survival rate of *Lactobacillus plantarum* LIP-1 based on transcriptome and proteome analyses. *Food Chem* 326:126849. <https://doi.org/10.1016/j.foodchem.2020.126849>
- Emergen Research E 00375 (2020) Fermented Food and Ingredients Market Size USD 875.21 Bn by 2027 | CAGR of 6.0%. <https://www.emergenresearch.com/industry-report/fermented-food-and-ingredients-market>. Accessed 26 May 2022
- Endo A, Dicks LMT (2014) Physiology of the LAB. In: Lactic Acid Bacteria: biodiversity and taxonomy, First edition. John Wiley & Sons, Ltd, pp 13–30
- Endo A, Tanizawa Y, Arita M (2019) Isolation and identification of lactic acid bacteria from environmental samples. In: Kanauchi M (ed) Lactic acid bacteria: methods and protocols, methods in molecular biology. Humana Press, pp 3–13
- Engelman DM (2005) Membranes are more mosaic than fluid. *Nature* 438:578–580. <https://doi.org/10.1038/nature04394>
- Evivie SE, Huo GC, Igene JO, Bian X (2017) Some current applications, limitations and future perspectives of lactic acid bacteria as probiotics. *Food Nutr Res* 61:. <https://doi.org/10.1080/16546628.2017.1318034>
- Exterkate FA, Otten BJ, Wassenberg HW, Veerkamp JH (1971) Comparison of the phospholipid composition of *Bifidobacterium* and *Lactobacillus* strains. *J Bacteriol* 106:824–829. <https://doi.org/10.1128/jb.106.3.824-829.1971>

F

- Fernández Murga ML, Cabrera GM, Font de Valdez G, et al (2000) Influence of growth temperature on cryotolerance and lipid composition of *Lactobacillus acidophilus*. *J Appl Microbiol* 88:342–348. <https://doi.org/10.1046/j.1365-2672.2000.00967.x>
- Fernández Murga ML, Font De Valdez G, Disalvo EA (2001) Effect of lipid composition on the stability of cellular membranes during freeze-thawing of *Lactobacillus acidophilus* grown at different temperatures. *Arch Biochem Biophys* 388:179–184. <https://doi.org/10.1006/abbi.2001.2274>
- Fewster ME, Burns BJ, Mead JF (1969) Quantitative densitometric thin-layer chromatography of lipids using copper acetate reagent. *J Chromatogr A* 43:120–126. [https://doi.org/10.1016/S0021-9673\(00\)99173-8](https://doi.org/10.1016/S0021-9673(00)99173-8)
- Folch J, Lees M, Sloane Stanley GH (1957) A simple method for the isolation and purification of total lipides from animal tissues. *J Biol Chem* 226:497–509. [https://doi.org/10.1016/s0021-9258\(18\)64849-5](https://doi.org/10.1016/s0021-9258(18)64849-5)
- Fonseca F, Béal C, Corrieu G (2000) Method of quantifying the loss of acidification activity of lactic acid starters during freezing and frozen storage. *J Dairy Res* 67:83–90. <https://doi.org/10.1017/S002202999900401X>
- Fonseca F, Béal C, Corrieu G (2001a) Operating conditions that affect the resistance of lactic acid bacteria to freezing and frozen storage. *Cryobiology* 43:189–198. <https://doi.org/10.1006/CRYO.2001.2343>
- Fonseca F, Béal C, Mihoub F, et al (2003) Improvement of cryopreservation of *Lactobacillus delbrueckii* subsp. *bulgaricus* CFL1 with additives displaying different protective effects. *Int Dairy J* 13:917–926. [https://doi.org/10.1016/S0958-6946\(03\)00119-5](https://doi.org/10.1016/S0958-6946(03)00119-5)
- Fonseca F, Cenard S, Passot S (2015) Freeze-drying of lactic acid bacteria. *Methods Mol Biol* 1257:477–488. https://doi.org/10.1007/978-1-4939-2193-5_24
- Fonseca F, Girardeau A, Passot S (2021) Freeze-drying of lactic acid bacteria: a stepwise approach for developing a freeze-drying protocol based on physical properties. In: Wolkers WF, Oldenhof H (eds) *Cryopreservation and freeze-drying protocols, Methods in Molecular Biology*, Fourth edi. Humana Press, pp 703–719
- Fonseca F, Marin M, Morris GJ (2006) Stabilization of frozen *Lactobacillus delbrueckii* subsp. *bulgaricus* in glycerol suspensions: Freezing kinetics and storage temperature effects. *Appl Environ Microbiol* 72:6474–6482. <https://doi.org/10.1128/AEM.00998-06>
- Fonseca F, Meneghel J, Cenard S, et al (2016) Determination of intracellular vitrification temperatures for unicellular micro organisms under conditions relevant for cryopreservation. *PLoS ONE* 11:. <https://doi.org/10.1371/journal.pone.0152939>
- Fonseca F, Obert JP, Béal C, Marin M (2001b) State diagrams and sorption isotherms of bacterial suspensions and fermented medium. *Thermochim Acta* 366:167–182. [https://doi.org/10.1016/S0040-6031\(00\)00725-5](https://doi.org/10.1016/S0040-6031(00)00725-5)
- Fonseca F, Passot S, Cunin O, Marin M (2004) Collapse temperature of freeze-dried *Lactobacillus bulgaricus* suspensions and protective media. *Biotechnol Prog* 20:229–238. <https://doi.org/10.1021/bp034136n>
- Fonseca F, Pénicaud C, Tymczynszyn EE, et al (2019) Factors influencing the membrane fluidity and the impact on production of lactic acid bacteria starters. *Appl Microbiol Biotechnol* 103:6867–6883. <https://doi.org/10.1007/s00253-019-10002-1>

- Food and Health Agricultural Organisation of the United Nations-World Health F (2002) Guidelines for the evaluation of probiotics in food. Working group report. London Ont. 1–11
- Fortune Business insights (2020) Probiotics market trends, share | Global Industry Growth [2020-2027]. In: Probiotics Mark. <https://www.fortunebusinessinsights.com/industry-reports/probiotics-market-100083>. Accessed 26 May 2022
- Foschino R, Fiori E, Galli A (1996) Survival and residual activity of *Lactobacillus acidophilus* frozen cultures under different conditions. *J Dairy Res* 63:295–303. <https://doi.org/10.1017/S0022029900031782>
- Fozo EM, Quivey RG (2004) The fabM gene product of *Streptococcus mutans* is responsible for the synthesis of monounsaturated fatty acids and is necessary for survival at low pH. *J Bacteriol* 186:4152–4158. <https://doi.org/10.1128/JB.186.13.4152-4158.2004>
- Frelet-Barrand A, Boutigny S, Moyet L, et al (2010) *Lactococcus lactis*, an alternative system for functional expression of peripheral and intrinsic arabis membrane proteins. *PLoS ONE* 5:. <https://doi.org/10.1371/journal.pone.0008746>
- Fringeli UP, Günthard HsH (1981) Infrared membrane spectroscopy. In: Grell E (ed) *Molecular biology, biochemistry, and biophysics*, First edit. Springer Verlag, pp 270–332
- Future market insights, Probiotic yogurt market Probiotic Yogurt Market-Market Research Report REP-GB-3259, 2021. <https://www.futuremarketinsights.com/reports/probiotic-yogurt-market>. Accessed 28 Jun 2022

G

- Gao X, Kong J, Zhu H, et al (2021) *Lactobacillus*, *Bifidobacterium* and *Lactococcus* response to environmental stress: Mechanisms and application of cross-protection to improve resistance against freeze-drying. *J Appl Microbiol* 132:802–821. <https://doi.org/10.1111/JAM.15251>
- García-Burgos M, Moreno-Fernández J, Alférez MJM, et al (2020) New perspectives in fermented dairy products and their health relevance. *J Funct Foods* 72:104059. <https://doi.org/10.1016/j.jff.2020.104059>
- Garrison AT, Huigens RW (2017) Eradicating bacterial biofilms with natural products and their inspired analogues that operate through unique mechanisms. *Curr Top Med Chem* 17:1954–1964
- Garvey C, Lenné T, Koster K, et al (2013) Phospholipid membrane protection by sugar molecules during dehydration-insights into molecular mechanisms using scattering techniques. *Int J Mol Sci* 14:8148–8163. <https://doi.org/10.3390/ijms14048148>
- Gautier J, Passot S, Pénicaud C, et al (2013) A low membrane lipid phase transition temperature is associated with a high cryotolerance of *Lactobacillus delbrueckii* subspecies *bulgaricus* CFL1. *J Dairy Sci* 96:5591–5602. <https://doi.org/10.3168/jds.2013-6802>
- Gilliland SE, Speck ML (1974) Relationship of Cellular Components to the Stability of Concentrated Lactic *Streptococcus* Cultures at -17 C. *Appl Environ Microbiol* 27:
- Girardeau A, Passot S, Meneghel J, et al (2022) Insights into lactic acid bacteria cryoresistance using FTIR microspectroscopy. *Anal Bioanal Chem* 414:1425–1443
- Girardeau A, Puentes C, Keravec S, et al (2019) Influence of culture conditions on the technological properties of *Carnobacterium maltaromaticum* CNCM I-3298 starters. *J Appl Microbiol* 126:1468–1479. <https://doi.org/10.1111/jam.14223>
- Goh YJ, Klaenhammer TR (2009) Genomic features of *Lactobacillus* species. *Front Biosci* 14:1362-1386. <https://doi.org/10.2741/3313>

- Goldberg I, Eschar L (1977) Stability of lactic acid bacteria to freezing as related to their fatty acid composition. *Appl Environ Microbiol* 33:489–496. <https://doi.org/10.1128/aem.33.3.489-496.1977>
- Gomez-Zavaglia A (2000) Fatty acid composition and freeze-thaw resistance in *Lactobacilli*. *J Dairy Res* 67:241–247. <https://doi.org/10.1017/S0022029916000029>
- Grandvalet C, Assad-Garcia JS, Chu-Ky S, et al (2008) Changes in membrane lipid composition in ethanol- and acid-adapted *Oenococcus oeni* cells: characterization of the cfa gene by heterologous complementation. *Microbiology* 154:2611–2619. <https://doi.org/10.1099/mic.0.2007/016238-0>
- Granier A, Goulet O, Hoarau C (2013) Fermentation products: immunological effects on human and animal models. *Pediatr Res* 74:238–244. <https://doi.org/10.1038/pr.2013.76>
- Grobben G j., Sikkema J, Smith M r., de Bont J a. m. (1995) Production of extracellular polysaccharides by *Lactobacillus delbrueckii* ssp. *bulgaricus* NCFB 2772 grown in a chemically defined medium. *J Appl Bacteriol* 79:103–107. <https://doi.org/10.1111/j.1365-2672.1995.tb03130.x>
- Grogan DW, Cronan JE (1997) Cyclopropane ring formation in membrane lipids of bacteria. *Microbiol Mol Biol Rev* 61:429–441. <https://doi.org/10.1128/.61.4.429-441.1997>
- Guha D, Banerjee A, Mukherjee R, et al (2019) A probiotic formulation containing *Lactobacillus bulgaricus* DWT1 inhibits tumor growth by activating pro-inflammatory responses in macrophages. *J Funct Foods* 56:232–245. <https://doi.org/10.1016/J.JFF.2019.03.030>
- Gul LB, Con AH, Gul O (2020a) Storage stability and sourdough acidification kinetic of freeze-dried *Lactobacillus curvatus* N19 under optimized cryoprotectant formulation. *Cryobiology* 96:122–129. <https://doi.org/10.1016/J.CRYOBIOL.2020.07.007>
- Gul LB, Gul O, Yilmaz MT, et al (2020b) Optimization of cryoprotectant formulation to enhance the viability of *Lactobacillus brevis* ED25: determination of storage stability and acidification kinetics in sourdough. *J Food Process Preserv* 44:e14400. <https://doi.org/10.1111/jfpp.14400>

H

- Hansen G, Johansen CL, Marten G, et al (2016) Influence of extracellular pH on growth, viability, cell size, acidification activity, and intracellular pH of *Lactococcus lactis* in batch fermentations. *Appl Microbiol Biotechnol* 100:5965–5976. <https://doi.org/10.1007/s00253-016-7454-3>
- Hansen M-LRW, Clausen A, Ejsing CS, Risbo J (2015a) Modulation of the *Lactobacillus acidophilus* La-5 lipidome by different growth conditions. *Microbiology* 161:1990–1998. <https://doi.org/10.1099/mic.0.000145>
- Hansen M-LRW, Petersen MA, Risbo J, et al (2015b) Implications of modifying membrane fatty acid composition on membrane oxidation, integrity, and storage viability of freeze-dried probiotic, *Lactobacillus acidophilus* La-5. *Biotechnol Prog* 31:799–807. <https://doi.org/10.1002/btpr.2074>
- Hatti-Kaul R, Chen L, Dishisha T, Enshasy H El (2018) Lactic acid bacteria: from starter cultures to producers of chemicals. *FEMS Microbiol Lett* 365:1–20. <https://doi.org/10.1093/FEMSLE/FNY213>
- Hayek SA, Gyawali R, Aljaloud SO, et al (2019) Cultivation media for lactic acid bacteria used in dairy products. *J Dairy Res* 86:490–502. <https://doi.org/10.1017/S002202991900075X>

- Hayek SA, Shahbazi A, Awaisheh SS, et al (2013) Sweet potatoes as a basic component in developing a medium for the cultivation of *Lactobacilli*. *Biosci Biotechnol Biochem* 77:2248–2254. <https://doi.org/10.1271/BBB.130508>
- Hecht E (1966) Colour reactions in chromatography. *Clin Chim Acta* 13:506–511. [https://doi.org/10.1016/0009-8981\(66\)90243-9](https://doi.org/10.1016/0009-8981(66)90243-9)
- Heckly RJ, Quay J (1981) A brief review of lyophilization damage and repair in bacterial preparations. *Cryobiology* 18:592–597. [https://doi.org/10.1016/0011-2240\(81\)90127-9](https://doi.org/10.1016/0011-2240(81)90127-9)
- Hernández A, Larsson CU, Sawicki R, et al (2019) Impact of the fermentation parameters pH and temperature on stress resilience of *Lactobacillus reuteri* DSM 17938. *AMB Express* 9:66. <https://doi.org/10.1186/s13568-019-0789-2>
- Hernández-González JC, Martínez-Tapia A, Lazcano-Hernández G, et al (2021) Bacteriocins from lactic acid bacteria. A powerful alternative as antimicrobials, probiotics, and immunomodulators in veterinary medicine. *Animals* 11:1–17. <https://doi.org/10.3390/ani11040979>
- Higl B, Kurtmann L, Carlsen CU, et al (2007) Impact of water activity, temperature, and physical state on the storage stability of *Lactobacillus paracasei* ssp. *paracasei* freeze-dried in a lactose matrix. *Biotechnol Prog* 23:794–800. <https://doi.org/10.1021/bp070089d>
- Hincha DK, Zuther E, Hellwege EM, Heyer AG (2002) Specific effects of fructo- and gluco-oligosaccharides in the preservation of liposomes during drying. *Glycobiology* 12:103–110. <https://doi.org/10.1093/glycob/12.2.103>
- Hincha DK, Zuther E, Heyer AG (2003) The preservation of liposomes by raffinose family oligosaccharides during drying is mediated by effects on fusion and lipid phase transitions. *Biochim Biophys Acta - Biomembr* 1612:172–177. [https://doi.org/10.1016/S0005-2736\(03\)00116-0](https://doi.org/10.1016/S0005-2736(03)00116-0)
- Hlaing MM, Wood BR, McNaughton D, et al (2017) Effect of Drying Methods on Protein and DNA Conformation Changes in *Lactobacillus rhamnosus* GG Cells by Fourier Transform Infrared Spectroscopy. *J Agric Food Chem* 65:1724–1731. <https://doi.org/10.1021/acs.jafc.6b05508>
- Hoekstra FA, Crowe JH, Crowe LM (1992) Germination and ion leakage are linked with phase transitions: of membrane lipids during imbibition of *Typha latifolia* pollen. *Physiol Plant* 84:29–34. <https://doi.org/10.1111/J.1399-3054.1992.TB08760.X>
- Hoffman JIE (2019) Hypothesis testing: sample size, effect size, power, and type II errors. In: Hoffman JIE (ed) *Basic biostatistics for medical and biomedical practitioners*. Academic Press, pp 173–185
- Hollard C, Fett D, Vexoe-Petersen L (2011) Cryoprotective compositions and uses thereof. Patent US20140004083A1
- Holzappel WH, Wood JB (2014) *Lactic Acid Bacteria Biodiversity and Taxonomy*. John Wiley & Sons
- Hölzl G, Dörmann P (2007) Structure and function of glycoglycerolipids in plants and bacteria. *Prog Lipid Res* 46:225–243. <https://doi.org/10.1016/J.PLIPRES.2007.05.001>
- Hongpattarakere T, Patcharawan R, Nirunya B (2013) Improvement of freeze-dried *Lactobacillus plantarum* survival using water extracts and crude fibers from food crops. *Food Bioprocess Technol* 6:1885–1896. <https://doi.org/10.1007/s11947-012-1018-z>
- Hubálek Z (2003) Protectants used in the cryopreservation of microorganisms. *Cryobiology* 46:205–229. [https://doi.org/10.1016/S0011-2240\(03\)00046-4](https://doi.org/10.1016/S0011-2240(03)00046-4)
- Hübner W, Blume A (1998) Interactions at the lipid-water interface. *Chem Phys Lipids* 96:99–123. [https://doi.org/10.1016/S0009-3084\(98\)00083-8](https://doi.org/10.1016/S0009-3084(98)00083-8)

Hutkins RW (2018) Starter cultures. In: Hutkins RW (ed) Microbiology and technology of fermented foods, First edit. Wiley, pp 93–136

I

Iwamori M, Sakai A, Minamimoto N, et al (2011) Characterization of novel glycolipid antigens with an -galactose epitope in *Lactobacilli* detected with rabbit anti-*Lactobacillus antisera* and occurrence of antibodies against them in human sera. J Biochem (Tokyo) 150:515–523. <https://doi.org/10.1093/jb/mvr091>

J

Jain PK, McNaught CE, Anderson ADG, et al (2004) Influence of synbiotic containing *Lactobacillus acidophilus* La5, *Bifidobacterium lactis* Bb 12, *Streptococcus thermophilus*, *Lactobacillus bulgaricus* and oligofructose on gut barrier function and sepsis in critically ill patients: A randomised controlled trial. Clin Nutr 23:467–475. <https://doi.org/10.1016/j.clnu.2003.12.002>

Jalali M, Abedi D, Varshosaz J, et al (2012) Stability evaluation of freeze-dried *Lactobacillus paracasei* subsp. tolerance and *Lactobacillus delbrueckii* subsp. *bulgaricus* in oral capsules. Res Pharm Sci 7:31–36

Jang K-S, Baik JE, Han SH, et al (2011) Multi-spectrometric analyses of lipoteichoic acids isolated from *Lactobacillus plantarum*. Biochem Biophys Res Commun 407:823–830. <https://doi.org/10.1016/j.bbrc.2011.03.107>

Jeong JH, Jang S, Jung BJ, et al (2015) Differential immune-stimulatory effects of LTAs from different lactic acid bacteria via MAPK signaling pathway in RAW 264.7 cells. Immunobiology 220:460–466. <https://doi.org/10.1016/j.imbio.2014.11.002>

John RP, Nampoothiri KM, Pandey A (2007) Fermentative production of lactic acid from biomass: An overview on process developments and future perspectives. Appl Microbiol Biotechnol 74:524–534. <https://doi.org/10.1007/s00253-006-0779-6>

Jouppila K, Roos YH (1994) Glass Transitions and Crystallization in Milk Powders. J Dairy Sci 77:2907–2915. [https://doi.org/10.3168/JDS.S0022-0302\(94\)77231-3](https://doi.org/10.3168/JDS.S0022-0302(94)77231-3)

Juárez-Tomás MS, Bru E, Martos G, Nader-Macías ME (2009) Stability of freeze-dried vaginal *Lactobacillus* strains in the presence of different lyoprotectors. Can J Microbiol 55:544–552. <https://doi.org/10.1139/W08-159>

K

Kapla J, Wohler J, Svensson B, et al (2013) Molecular dynamics simulations of membrane-sugar interactions. J Phys Chem B 117:6667–6673. <https://doi.org/10.1021/jp402385d>

Kates M (2010) Lipid extraction procedures. In: Kates M (ed) Techniques of Lipidology: isolation, analysis, and identification of lipids. Newport Somerville Innovation, Limited, pp 347–353

Kataridis P, Meins L, Kamal SM, et al (2019) ClpG Provides Increased Heat Resistance by Acting as Superior Disaggregase. Biomolecules 9. <https://doi.org/10.3390/BIOM9120815>

Katina K, Maina NH, Juvonen R, et al (2009) In situ production and analysis of *Weissella confusa* dextran in wheat sourdough. Food Microbiol 26:734–743. <https://doi.org/10.1016/J.FM.2009.07.008>

Kato S, Tobe H, Matsubara H, et al (2019) The membrane phospholipid cardiolipin plays a pivotal role in bile acid adaptation by *Lactobacillus gasseri* JCM1131 T. Biochim Biophys Acta - Mol Cell Biol Lipids 1864:403–412. <https://doi.org/10.1016/j.bbalip.2018.06.004>

- Kent B, Hauß T, Demé B, et al (2015) Direct comparison of disaccharide interaction with lipid membranes at reduced hydrations. *Langmuir* 31:9134–9141. <https://doi.org/10.1021/acs.langmuir.5b02127>
- Kets EPW, Teunissen PJM, De Bont JAM (1996) Effect of compatible solutes on survival of lactic acid bacteria subjected to drying. *Appl Environ Microbiol* 62:259–261. <https://doi.org/10.1128/AEM.62.1.259-261.1996>
- Khoramnia A, Abdullah N, Liew SL, et al (2011) Enhancement of viability of a probiotic *Lactobacillus* strain for poultry during freeze-drying and storage using the response surface methodology. *Anim Sci J* 82:127–135. <https://doi.org/10.1111/j.1740-0929.2010.00804.x>
- Khorram E, Khaledian K, Khaledyan M (2014) A numerical method for constructing the Pareto front of multi-objective optimization problems. *J Comput Appl Math* 261:158–171. <https://doi.org/10.1016/j.cam.2013.11.007>
- Kilbride P, Meneghel J (2021) Freezing technology: control of freezing, thawing, and ice nucleation. In: Wolkers WF, Oldenhof H (eds) *Cryopreservation and freeze-drying protocols*, Methods in Molecular Biology, Forth edit. Humana Press, pp 191–201
- Kilimann KV, Doster W, Vogel RF, et al (2006) Protection by sucrose against heat-induced lethal and sublethal injury of *Lactococcus lactis*: an FT-IR study. *Biochim Biophys Acta BBA - Proteins Proteomics* 1764:1188–1197. <https://doi.org/10.1016/J.BBAPAP.2006.04.016>
- Kim H, Kim M, Myoung K, et al (2020) Comparative lipidomic analysis of extracellular vesicles derived from *Lactobacillus plantarum* APsulloc 331261 living in green tea eaves Using Liquid Chromatography-Mass Spectrometry. *Int J Mol Sci* 2020 Vol 21 Page 8076 21:8076. <https://doi.org/10.3390/IJMS21218076>
- Kim WS, Khunajakr N, Dunn NW (1998) Effect of cold shock on protein synthesis and on cryotolerance of cells frozen for long periods in *Lactococcus lactis*. *Cryobiology* 37:86–91. <https://doi.org/10.1006/CRYO.1998.2104>
- Kiviharju K, Salonen K, Moilanen U, Eerikäinen T (2008) Biomass measurement online: the performance of in situ measurements and software sensors. *J Ind Microbiol Biotechnol* 35:657–665. <https://doi.org/10.1007/S10295-008-0346-5>
- Kleerebezem M, Hugenholtz J (2003) Metabolic pathway engineering in lactic acid bacteria. *Curr Opin Biotechnol* 14:232–237. [https://doi.org/10.1016/S0958-1669\(03\)00033-8](https://doi.org/10.1016/S0958-1669(03)00033-8)
- Knothe G, Dunn RO (2009) A comprehensive evaluation of the melting points of fatty acids and esters determined by Differential Scanning Calorimetry. *J Am Oil Chem Soc* 86:843–856. <https://doi.org/10.1007/s11746-009-1423-2>
- Koch S, Eugster-Meier E, Oberson G, et al (2008) Effects of strains and growth conditions on autolytic activity and survival to freezing and lyophilization of *Lactobacillus delbrueckii* ssp. *lactis* isolated from cheese. *Int Dairy J* 18:187–196. <https://doi.org/10.1016/j.idairyj.2007.07.009>
- Koch S, Oberson G, Eugster-Meier E, et al (2007) Osmotic stress induced by salt increases cell yield, autolytic activity, and survival of lyophilization of *Lactobacillus delbrueckii* subsp. *lactis*. *Int J Food Microbiol* 117:36–42. <https://doi.org/10.1016/J.IJFOODMICRO.2007.01.016>
- Kochan K, Perez-Guaita D, Pissang J, et al (2018) In vivo atomic force microscopy-infrared spectroscopy of bacteria. *J R Soc Interface* 15:20180115. <https://doi.org/10.1098/rsif.2018.0115>
- Koistinen KM, Plumed-Ferrer C, Lehesranta SJ, et al (2007) Comparison of growth-phase-dependent cytosolic proteomes of two *Lactobacillus plantarum* strains used in food and

- feed fermentations. *FEMS Microbiol Lett* 273:12–21. <https://doi.org/10.1111/j.1574-6968.2007.00775.x>
- Konings WN (2002) The cell membrane and the struggle for life of lactic acid bacteria. *Antonie Van Leeuwenhoek* 2002 821 82:3–27. <https://doi.org/10.1023/A:1020604203977>
- Konings WN, Lolkema JS, Bolhuis H, et al (1997) The role of transport processes in survival of lactic acid bacteria, Energy transduction and multidrug resistance. *Antonie Van Leeuwenhoek* 71:117–128. <https://doi.org/10.1023/A:1000143525601>
- Koshimoto C, Mazur P (2002) The effect of the osmolality of sugar containing media, the type of sugar, and the mass and molar concentration of sugar on the survival of frozen-thawed mouse sperm. *Cryobiology* 45:80–90. [https://doi.org/10.1016/S0011-2240\(02\)00108-6](https://doi.org/10.1016/S0011-2240(02)00108-6)
- Koskenniemi K, Laakso K, Koponen J, et al (2011) Proteomics and transcriptomics characterization of bile stress response in probiotic *Lactobacillus rhamnosus* GG. *Mol Cell Proteomics MCP* 10:M110.002741. <https://doi.org/10.1074/mcp.M110.002741>
- Koster KL, Webb MS, Bryant G, Lynch D V. (1994) Interactions between soluble sugars and POPC (1-palmitoyl-2-oleoylphosphatidylcholine) during dehydration: vitrification of sugars alters the phase behavior of the phospholipid. *Biochim Biophys Acta BBA - Biomembr* 1193:143–150. [https://doi.org/10.1016/0005-2736\(94\)90343-3](https://doi.org/10.1016/0005-2736(94)90343-3)
- Kranenburg M, Smit B (2005) Phase behavior of model lipid bilayers. *J Phys Chem B* 109:6553–6563. <https://doi.org/10.1021/jp0457646>
- Kurtmann L, Carlsen CU, Risbo J, Skibsted LH (2009) Storage stability of freeze-dried *Lactobacillus acidophilus* (La-5) in relation to water activity and presence of oxygen and ascorbate. *Cryobiology* 58:175–180. <https://doi.org/10.1016/j.cryobiol.2008.12.001>
- L**
- Le Guillou J, Ropers M-H, Gaillard C, et al (2016) Sequestration of bovine seminal plasma proteins by different assemblies of phosphatidylcholine: A new technical approach. *Colloids Surf B Biointerfaces* 140:523–530. <https://doi.org/10.1016/j.colsurfb.2015.11.034>
- Lee BW, Faller R, Sum AK, et al (2005) Structural effects of small molecules on phospholipid bilayers investigated by molecular simulations. *Fluid Phase Equilibria* 228–229:135–140. <https://doi.org/10.1016/j.fluid.2005.03.002>
- Lee SB, Kim DH, Park HD (2016) Effects of protectant and rehydration conditions on the survival rate and malolactic fermentation efficiency of freeze-dried *Lactobacillus plantarum* JH287. *Appl Microbiol Biotechnol* 100:7853–7863. <https://doi.org/10.1007/s00253-016-7509-5>
- Leslie SB, Israeli E, Lighthart B, et al (1995) Trehalose and sucrose protect both membranes and proteins in intact bacteria during drying. *Appl Environ Microbiol* 61:3592
- Leslie SB, Teter SA, Crowe LM, Crowe JH (1994) Trehalose lowers membrane phase transitions in dry yeast cells. *BBA - Biomembr* 1192:7–13. [https://doi.org/10.1016/0005-2736\(94\)90136-8](https://doi.org/10.1016/0005-2736(94)90136-8)
- Lewis RNAH, McElhane RN (2013) Membrane lipid phase transitions and phase organization studied by Fourier transform infrared spectroscopy. *Biochim Biophys Acta - Biomembr.* <https://doi.org/10.1016/j.bbamem.2012.10.018>
- Li B, Tian F, Liu X, et al (2011) Effects of cryoprotectants on viability of *Lactobacillus reuteri* CICC6226. *Appl Microbiol Biotechnol* 92:609–616. <https://doi.org/10.1007/s00253-011-3269-4>

- Li C, Li PZ, Sun JW, et al (2014) Proteomic analysis of the response to NaCl stress of *Lactobacillus bulgaricus*. *Biotechnol Lett* 36:2263–2269. <https://doi.org/10.1007/s10529-014-1601-7>
- Li C, Liu LB, Liu N (2012) Effects of carbon sources and lipids on freeze-drying survival of *Lactobacillus bulgaricus* in growth media. *Ann Microbiol* 62:949–956. <https://doi.org/10.1007/s13213-011-0332-4>
- Li C, Sun J, Qi X, Liu L (2015) NaCl stress impact on the key enzymes in glycolysis from *Lactobacillus bulgaricus* during freeze-drying. *Braz J Microbiol* 46:1193–1199. <https://doi.org/10.1590/S1517-838246420140595>
- Li C, Zhao J-L, Wang Y-T, et al (2009a) Synthesis of cyclopropane fatty acid and its effect on freeze-drying survival of *Lactobacillus bulgaricus* L2 at different growth conditions. *World J Microbiol Biotechnol* 25:1659–1665. <https://doi.org/10.1007/s11274-009-0060-0>
- Li H, Zhao W, Wang H, et al (2009b) Influence of culture pH on freeze-drying viability of *Oenococcus oeni* and its relationship with fatty acid composition. *Food Bioprod Process* 87:56–61. <https://doi.org/10.1016/j.fbp.2008.06.001>
- Lievonen SM, Laaksonen TJ, Roos Y (1998) Glass transition and reaction rates: Nonenzymatic Browning in Glassy and Liquid Systems. *J Agric Food Chem* 46:2778–2784. <https://doi.org/10.1021/JF980064H>
- Limonet M, Cailliez-Grimal C, Linder M, et al (2004) Cell envelope analysis of insensitive, susceptible or resistant strains of *Leuconostoc* and *Weissella* genus to *Leuconostoc mesenteroides* FR 52 bacteriocins. <https://doi.org/10.1016/j.femsle.2004.10.002>
- Linders LJM, Wolkers WF, Hoekstra FA, Van 'T Riet K (1997) Effect of added carbohydrates on membrane phase behavior and survival of dried *Lactobacillus plantarum*. *Cryobiology* 35:31–40. <https://doi.org/10.1006/cryo.1997.2021>
- Liu M, Zeng X, He Y, et al (2021) iTRAQ-based quantitative proteomic analysis of the effect of heat shock on freeze-drying of *Lactobacillus acidophilus* ATCC4356. *Int J Food Sci Technol* 56:5569–5580. <https://doi.org/10.1111/ijfs.15101>
- Liu S, Ma Y, Zheng Y, et al (2020) Cold-Stress response of probiotic *Lactobacillus plantarum* K25 by iTRAQ proteomic analysis. *J Microbiol Biotechnol* 30:187–195. <https://doi.org/10.4014/jmb.1909.09021>
- Liu XT, Hou CL, Zhang J, et al (2014) Fermentation conditions influence the fatty acid composition of the membranes of *Lactobacillus reuteri* I5007 and its survival following freeze-drying. *Lett Appl Microbiol* 59:398–403. <https://doi.org/10.1111/lam.12292>
- Loffhagen N, Härtig C, Babel W (2001) Suitability of the trans/cis Ratio of Unsaturated Fatty Acids in *Pseudomonas putida* NCTC 10936 as an Indicator of the Acute Toxicity of Chemicals. *Ecotoxicol Environ Saf* 50:65–71. <https://doi.org/10.1006/EESA.2001.2089>
- Lopez-Quiroga E, Antelo LT, Alonso AA (2012) Time-scale modeling and optimal control of freeze-drying. *J Food Eng* 111:655–666. <https://doi.org/10.1016/J.JFOODENG.2012.03.001>
- Lorca GL, Font de Valdez GF (2001) A low-pH-inducible, stationary-phase acid tolerance response in *Lactobacillus acidophilus* CRL 639. *Curr Microbiol* 42:21–25. <https://doi.org/10.1007/s002840010172>
- Lorca GL, Font de Valdez GF (1999) The effect of suboptimal growth temperature and growth phase on resistance of *Lactobacillus acidophilus* to environmental stress. *Cryobiology* 39:144–149. <https://doi.org/10.1006/CRYO.1999.2193>

- Lorusso A, Coda R, Montemurro M, Rizzello CG (2018) Use of delected lactic acid bacteria and quinoa flour for manufacturing novel yogurt-like beverages. *Foods* 2018 Vol 7 Page 51 7:51. <https://doi.org/10.3390/FOODS7040051>
- Louesdon S, Charlot-Rougé S, Juillard V, et al (2014) Osmotic stress affects the stability of freeze-dried *Lactobacillus buchneri* R1102 as a result of intracellular betaine accumulation and membrane characteristics. *J Appl Microbiol* 117:196–207. <https://doi.org/10.1111/jam.12501>
- Louesdon S, Charlot-Rougé S, Tourdot-Maréchal R, et al (2015) Membrane fatty acid composition and fluidity are involved in the resistance to freezing of *Lactobacillus buchneri* R1102 and *Bifidobacterium longum* R0175. *Microb Biotechnol* 8:311–318. <https://doi.org/10.1111/1751-7915.12132>
- Lu J, Cui L, Lin S, et al (2019) Short communication: Global transcriptome analysis of *Lactococcus lactis* ssp. *lactis* in response to gradient freezing. *J Dairy Sci* 102:3933–3938. <https://doi.org/10.3168/jds.2018-15972>
- Luzardo M del C, Amalfa F, Nuñez AM, et al (2000) Effect of trehalose and sucrose on the hydration and dipole potential of lipid bilayers. *Biophys J* 78:2452–2458. [https://doi.org/10.1016/S0006-3495\(00\)76789-0](https://doi.org/10.1016/S0006-3495(00)76789-0)
- Lv LX, Yan R, Shi HY, et al (2017) Integrated transcriptomic and proteomic analysis of the bile stress response in probiotic *Lactobacillus salivarius* LI01. *J Proteomics* 150:216–229. <https://doi.org/10.1016/j.jprot.2016.08.021>

M

- Macedo MG, Lacroix C, Gardner NJ, Champagne CP (2002) Effect of medium supplementation on exopolysaccharide production by *Lactobacillus rhamnosus* RW-9595M in whey permeate. *Int Dairy J* 12:419–426. [https://doi.org/10.1016/S0958-6946\(01\)00173-X](https://doi.org/10.1016/S0958-6946(01)00173-X)
- Machado MC, López CS, Heras H, Rivas EA (2004) Osmotic response in *Lactobacillus casei* ATCC 393: Biochemical and biophysical characteristics of membrane. *Arch Biochem Biophys* 422:61–70. <https://doi.org/10.1016/j.abb.2003.11.001>
- Madureira AR, Amorim M, Gomes AM, et al (2011) Protective effect of whey cheese matrix on probiotic strains exposed to simulated gastrointestinal conditions. *Food Res Int* 44:465–470. <https://doi.org/10.1016/J.FOODRES.2010.09.010>
- Mainville I, Arcand Y, Farnworth ER (2005) A dynamic model that simulates the human upper gastrointestinal tract for the study of probiotics. *Int J Food Microbiol* 99:287–296. <https://doi.org/10.1016/J.IJFOODMICRO.2004.08.020>
- Makarova K, Slesarev A, Wolf Y, et al (2006) Comparative genomics of the lactic acid bacteria. *Proc Natl Acad Sci* 103:15611–15616. <https://doi.org/10.1073/pnas.0607117103>
- Mantsch HH, McElhaney RN (1991) Phospholipid phase transitions in model and biological membranes as studied by infrared spectroscopy. *Chem Phys Lipids* 57:213–226. [https://doi.org/10.1016/0009-3084\(91\)90077-O](https://doi.org/10.1016/0009-3084(91)90077-O)
- Marceau A, Zagorec M, Chaillou S, et al (2004) Evidence for involvement of at least six proteins in adaptation of *Lactobacillus sakei* to cold temperatures and addition of NaCl. *Appl Environ Microbiol* 70:7260–7268. <https://doi.org/10.1128/AEM.70.12.7260-7268.2004>
- Markets and Markets, Polylactic Acid market Polylactic Acid (PLA) Market, 2022-2026, Markets and Markets CH 8047 Report. <https://www.marketsandmarkets.com/Market-Reports/polylactic-acid-pla-market-29418964.html>. Accessed 28 Jun 2022

- Markets and Markets, Probiotics market RRF 2269 2021 Probiotics Market - Global Forecast to 2026-. <https://www.asdreports.com/market-research-report-586044/probiotics-market-global-forecast>. Accessed 28 Jun 2022
- Mårtensson O, Andersson C, Andersson K, et al (2001) Formulation of an oat-based fermented product and its comparison with yoghurt. *J Sci Food Agric* 81:1314–1321. <https://doi.org/10.1002/JSFA.947>
- Martinez B, Rodriguez A, Kulakauskas S, Chapot-Chartier MP (2020) Cell wall homeostasis in lactic acid bacteria: threats and defences. *FEMS Microbiol Rev* 44:538–564. <https://doi.org/10.1093/femsre/fuaa021>
- Martins GN, Ureta MM, Tymczynsyn EE, et al (2019) Technological aspects of the production of fructo and galacto-oligosaccharides. Enzymatic synthesis and hydrolysis. *Front Nutr* 6:
- Martos GI, Minahk CJ, Font de Valdez G, Morero R (2007) Effects of protective agents on membrane fluidity of freeze-dried *Lactobacillus delbrueckii* ssp. *bulgaricus*. *Lett Appl Microbiol* 45:282–288. <https://doi.org/10.1111/j.1472-765X.2007.02188.x>
- Makide K, Kitamura H, Sato Y, et al (2009) Emerging lysophospholipid mediators, lysophosphatidylserine, lysophosphatidylthreonine, lysophosphatidylethanolamine and lysophosphatidylglycerol. *Prostaglandins Other Lipid Mediat* 89:135–139. <https://doi.org/10.1016/j.prostaglandins.2009.04.009>
- Marty-Teyssset C, De La Torre F, Garel JR (2000) Increased production of hydrogen peroxide by *Lactobacillus delbrueckii* subsp. *bulgaricus* upon aeration: involvement of an NADH oxidase in oxidative stress. *Appl Environ Microbiol* 66:262. <https://doi.org/10.1128/AEM.66.1.262-267.2000>
- Mayo B, Aleksandrzyk-Piekarczyk T, Fernández M, et al (2010) Updates in the metabolism of lactic acid bacteria. In: *Biotechnology of lactic acid bacteria*, First edition. John Wiley & Sons, Ltd, pp 3–33
- Mäyrä-Mäkinen A, Bigret M (2004) Industrial use and production of lactic acid bacteria. In: Salminen S, Wright A Von, Ouwehand A (eds) *Lactic acid bacteria microbiological and functional aspects*, Third edit. CRC Press, pp 175–198
- Mazur P (1977) The role of intracellular freezing in the death of cells cooled at supraoptimal rates. *Cryobiology* 14:251–272. [https://doi.org/10.1016/0011-2240\(77\)90175-4](https://doi.org/10.1016/0011-2240(77)90175-4)
- Mazur P (1966) Theoretical and experimental effects of cooling and warming velocity on the survival of frozen and thawed cells. *Cryobiology* 2:181–192. [https://doi.org/10.1016/S0011-2240\(66\)80165-7](https://doi.org/10.1016/S0011-2240(66)80165-7)
- Mazur P, Leibo SP, Chu EHY (1972) A two-factor hypothesis of freezing injury. Evidence from Chinese hamster tissue-culture cells. *Exp Cell Res* 71:345–355. [https://doi.org/10.1016/0014-4827\(72\)90303-5](https://doi.org/10.1016/0014-4827(72)90303-5)
- Medina-Pradas E, Pérez-Díaz IM, Garrido-Fernández A, Arroyo-López FN (2017) Review of vegetable fermentations with particular emphasis on processing modifications, microbial ecology, and spoilage. In: Bevilacqua A, Corbo MR, Sinigaglia M (eds) *The Microbiological quality of food*, First edit. Woodhead Publishing, pp 211–236
- Meneghel J, Dugat-Bony E, Irlinger F, et al (2016) Draft genome sequence of *Lactobacillus delbrueckii* subsp. *bulgaricus* CFL1, a lactic acid bacterium isolated from French handcrafted fermented milk. *Genome Announc* 4:2–3. <https://doi.org/10.1128/genomeA.00052-16>
- Meneghel J, Passot S, Dupont S, Fonseca F (2017) Biophysical characterization of the *Lactobacillus delbrueckii* subsp. *bulgaricus* membrane during cold and osmotic stress

- and its relevance for cryopreservation. *Appl Microbiol Biotechnol* 101:1427–1441. <https://doi.org/10.1007/s00253-016-7935-4>
- Meng XC, Stanton C, Fitzgerald GF, et al (2008) Anhydrobiotics: The challenges of drying probiotic cultures. *Food Chem* 106:1406–1416. <https://doi.org/10.1016/j.foodchem.2007.04.076>
- Merivaara A, Zini J, Koivunotko E, et al (2021) Preservation of biomaterials and cells by freeze-drying: Change of paradigm. *J Controlled Release* 336:480–498. <https://doi.org/10.1016/j.jconrel.2021.06.042>
- Meyrand M, Guillot A, Goin M, et al (2013) Surface proteome analysis of a natural isolate of *Lactococcus lactis* reveals the presence of pili able to bind human intestinal epithelial cells. *Mol Cell Proteomics MCP* 12:3935–3947. <https://doi.org/10.1074/MCP.M113.029066>
- Miao S, Mills S, Stanton C, et al (2008) Effect of disaccharides on survival during storage of freeze-dried probiotics. *Dairy Sci Technol* 88:19–30. <https://doi.org/10.1051/dst:2007003>
- Mika JT, Poolman B (2011) Macromolecule diffusion and confinement in prokaryotic cells. *Curr Opin Biotechnol* 22:117–126. <https://doi.org/10.1016/J.COPBIO.2010.09.009>
- Mika JT, Van Den Bogaart G, Veenhoff L, et al (2010) Molecular sieving properties of the cytoplasm of *Escherichia coli* and consequences of osmotic stress. *Mol Microbiol* 77:200–207. <https://doi.org/10.1111/J.1365-2958.2010.07201.X>
- Mikajiri S, Sogabe T, Cao R, et al (2021) Glass transition behavior of carnosine and its impact as a protectant on freeze-dried lactic acid bacteria. *Food Biophys* 1:1–9. <https://doi.org/10.1007/S11483-021-09694-8/FIGURES/6>
- Miller CW, Nguyen MH, Rooney M, Kailasapathy K (2003a) The control of dissolved oxygen content in probiotic yoghurts by alternative packaging materials. *Packag Technol Sci* 16:61–67. <https://doi.org/10.1002/PTS.612>
- Miller LM, Smith GD, Carr GL (2003b) Synchrotron-based biological microspectroscopy: from the mid-infrared through the far-infrared regimes. *J Biol Phys* 29:219–230. <https://doi.org/10.1023/A:1024401027599>
- Moiset G, López CA, Bartelds R, et al (2014) Disaccharides impact the lateral organization of lipid membranes. *J Am Chem Soc* 136:16167–16175. <https://doi.org/10.1021/ja505476c>
- Mordor intelligence, Yogurt market report Yogurt Market Analysis | 2022 - 27 | Industry Share, Trends, Size. <https://www.mordorintelligence.com/industry-reports/yogurt-market>. Accessed 28 Jun 2022
- Morgan C, Vesey G (2009) Freeze-drying of microorganisms. In: Schaechter M (ed) *Encyclopedia of Microbiology*. Academic Press, pp 162–173
- Morice M, Bracquart P, Linden G (1992) Colonial Variation and Freeze-Thaw Resistance of *Streptococcus thermophilus*. *J Dairy Sci* 75:1197–1203. [https://doi.org/10.3168/JDS.S0022-0302\(92\)77867-9](https://doi.org/10.3168/JDS.S0022-0302(92)77867-9)
- Morris GJ, Goodrich M, Acton E, Fonseca F (2006) The high viscosity encountered during freezing in glycerol solutions: effects on cryopreservation. *Cryobiology* 52:323–334. <https://doi.org/10.1016/J.CRYOBIOL.2006.01.003>
- Mourão MA, Hakim JB, Schnell S (2014) Connecting the Dots: The Effects of Macromolecular Crowding on Cell Physiology. *Biophys J* 107:2761–2766. <https://doi.org/10.1016/J.BPJ.2014.10.051>

- Murzyn K, Róg T, Pasenkiewicz-Gierula M (2005) Phosphatidylethanolamine-phosphatidylglycerol bilayer as a model of the inner bacterial membrane. *Biophys J* 88:1091–1103. <https://doi.org/10.1529/biophysj.104.048835>
- Mussatto SI, Fernandes M, Mancilha IM, Roberto IC (2008) Effects of medium supplementation and pH control on lactic acid production from brewer's spent grain. *Biochem Eng J* 40:437–444. <https://doi.org/10.1016/j.bej.2008.01.013>
- Myers OD, Sumner SJ, Li S, et al (2017) One step forward for reducing false positive and false negative compound identifications from mass spectrometry metabolomics data: new algorithms for constructing extracted ion chromatograms and detecting chromatographic peaks. *Anal Chem* 89:8696–8703. <https://doi.org/10.1021/acs.analchem.7b00947>
- Mykytczuk NCS, Trevors JT, Leduc LG, Ferroni GD (2007) Fluorescence polarization in studies of bacterial cytoplasmic membrane fluidity under environmental stress. *Prog. Biophys. Mol. Biol.* 95:60–82

N

- Nagaoka S (2019) Yogurt production. In: Walker JM (ed) *Lactic acid bacteria*. Springer, New York, pp 45–54
- Nakano M, Fischer W (1978) Trihexosyldiacylglycerol and acyltrihexosyldiacylglycerol as lipid anchors of the lipoteichoic acid of *Lactobacillus casei* DSM 20021. *Hoppe Seylers Z Physiol Chem* 359:1–11. <https://doi.org/10.1515/bchm.1978.359.1.1>
- Nakata S, Deguchi A, Seki Y, et al (2015) Characteristic responses of a phospholipid molecular layer to polyols. *Colloids Surf B Biointerfaces* 136:594–599. <https://doi.org/10.1016/J.COLSURFB.2015.09.035>
- Ni D, Xu W, Bai Y, et al (2018) Biosynthesis of levan from sucrose using a thermostable levansucrase from *Lactobacillus reuteri* LTH5448. *Int J Biol Macromol* 113:29–37. <https://doi.org/10.1016/j.ijbiomac.2018.01.187>
- Nicolson GL (2014) The Fluid—Mosaic Model of Membrane Structure: Still relevant to understanding the structure, function and dynamics of biological membranes after more than 40 years. *Biochim Biophys Acta BBA - Biomembr* 1838:1451–1466. <https://doi.org/10.1016/J.BBAMEM.2013.10.019>
- Nikkilä P, Johnsson T, Rosenqvist H, Toivonen L (1996) Effect of pH on growth and fatty acid composition of *Lactobacillus büchneri* and *Lactobacillus fermentum*. *Appl Biochem Biotechnol* 1996 593 59:245–257. <https://doi.org/10.1007/BF02783568>
- Noda S, Koyama F, Aihara C, et al (2020) *Lactococcus insecticola* sp. Nov. and *Lactococcus hodotermopsisidis* sp. nov., isolated from the gut of the wood-feeding lower termite *hodotermopsisis sjostedti*. *Int J Syst Evol Microbiol* 70:4515–4522. <https://doi.org/10.1099/IJSEM.0.004309/CITE/REFWORKS>

O

- Ojha KS, Kerry JP, Duffy G, et al (2015) Technological advances for enhancing quality and safety of fermented meat products. *Trends Food Sci Technol* 44:105–116. <https://doi.org/10.1016/J.TIFS.2015.03.010>
- Oldenhof H, Wolkers WF, Fonseca F, et al (2005) Effect of sucrose and maltodextrin on the physical properties and survival of air-dried *Lactobacillus bulgaricus*: An in situ fourier transform infrared spectroscopy study. *Biotechnol Prog* 21:885–892. <https://doi.org/10.1021/bp049559j>

- Olivon F, Elie N, Grelier G, et al (2018) MetGem software for the generation of molecular networks based on the t-SNE algorithm. *Anal Chem* 90:13900–13908. <https://doi.org/10.1021/acs.analchem.8b03099>
- Otero MC, Espeche MC, Nader-Macías ME (2007) Optimization of the freeze-drying media and survival throughout storage of freeze-dried *Lactobacillus gasseri* and *Lactobacillus delbrueckii* subsp. *delbrueckii* for veterinarian probiotic applications. *Process Biochem* 42:1406–1411. <https://doi.org/10.1016/j.procbio.2007.07.008>
- Ouwehand AC (2019) Gastrointestinal benefits of probiotics: clinical evidence. In: *Lactic Acid Bacteria: microbiological and functional aspects*, 5th edition. CRC Press, pp 409–417

P

- Palmfeldt J, Hahn-Hägerdal B (2000) Influence of culture pH on survival of *Lactobacillus reuteri* subjected to freeze-drying. In: *International Journal of Food Microbiology*. pp 235–238
- Papadimitriou K, Alegría Á, Bron PA, et al (2016) Stress physiology of lactic acid bacteria. *Microbiol Mol Biol Rev* 80:837–890. <https://doi.org/10.1128/mmlbr.00076-15>
- Passot S, Cenard S, Douania I, et al (2012) Critical water activity and amorphous state for optimal preservation of lyophilised lactic acid bacteria. In: *Food Chemistry*. Elsevier, pp 1699–1705
- Passot S, Jamme F, Réfrégiers M, et al (2014) Synchrotron UV fluorescence microscopy for determining membrane fluidity modification of single bacteria with temperatures. *Biomed Spectrosc Imaging* 3:203–210. <https://doi.org/10.3233/BSI-140062>
- Passot S, Tréléa IC, Marin M, et al (2009) Effect of Controlled Ice Nucleation on Primary Drying Stage and Protein Recovery in Vials Cooled in a Modified Freeze-Dryer. *J Biomech Eng* 131:. <https://doi.org/10.1115/1.3143034>
- Pehkonen KS, Roos YH, Miao S, et al (2008) State transitions and physicochemical aspects of cryoprotection and stabilization in freeze-drying of *Lactobacillus rhamnosus* GG (LGG). *J Appl Microbiol* 104:1732–1743. <https://doi.org/10.1111/j.1365-2672.2007.03719.x>
- Pénicaud C, Monclus V, Perret B, et al (2018) Life cycle assessment of the production of stabilized lactic acid bacteria for the environmentally-friendly preservation of living cells. *J Clean Prod* 184:847–858. <https://doi.org/10.1016/j.jclepro.2018.02.191>
- Péter G, Reichart O (2001) The effect of growth phase, cryoprotectants and freezing rates on the survival of selected micro-organisms during freezing and thawing. *Acta Aliment* 30:89–97. <https://doi.org/10.1556/AAlim.30.2001.1.10>
- Pflaster EL, Schwabe MJ, Becker J, et al (2014) A high-throughput fatty acid profiling screen reveals novel variations in fatty acid biosynthesis in *Chlamydomonas reinhardtii* and related algae. *Eukaryot Cell* 13:1431–1438. <https://doi.org/10.1128/EC.00128-14>
- Piatkiewicz A, Mokrosinska K (1995) Effect of thawing rate on survival and activity of lactic acid bacteria. *Pol J Food Nutr Sci* 04:33–46
- Pikal MJ, Shah S (1990) The collapse temperature in freeze drying: Dependence on measurement methodology and rate of water removal from the glassy phase. *Int J Pharm* 62:165–186. [https://doi.org/10.1016/0378-5173\(90\)90231-R](https://doi.org/10.1016/0378-5173(90)90231-R)
- Pluskal T, Castillo S, Villar-Briones A, Oresic M (2010) MZmine 2: modular framework for processing, visualizing, and analyzing mass spectrometry-based molecular profile data. *BMC Bioinformatics* 11:395. <https://doi.org/10.1186/1471-2105-11-395>
- Poger D, Mark AE (2015) A ring to rule them all: The effect of cyclopropane fatty acids on the fluidity of lipid bilayers. *J Phys Chem B* 119:5487–5495. https://doi.org/10.1021/ACS.JPCB.5B00958/SUPPL_FILE/JP5B00958_SI_001.PDF

- Polo L, Mañes-Lázaro R, Olmeda I, et al (2017) Influence of freezing temperatures prior to freeze-drying on viability of yeasts and lactic acid bacteria isolated from wine. *J Appl Microbiol* 122:1603–1614. <https://doi.org/10.1111/jam.13465>
- Pot B, Ludwig W, Kersters K, Schleifer K (1994) Taxonomy of lactic acid bacteria. In: De Vuyst L, Vandamme EJ (eds) *Bacteriocins of lactic acid bacteria: microbiology, genetics and applications*, First edit. Springer Science and business media, pp 13–90
- Potts M (1994) Desiccation tolerance of prokaryotes. *Microbiol Rev* 58:755–805. <https://doi.org/10.1128/MR.58.4.755-805.1994>
- Prasad J, McJarrow P, Gopal P (2003) Heat and osmotic stress responses of probiotic *Lactobacillus rhamnosus* HN001 (DR20) in relation to viability after drying. *Appl Environ Microbiol* 69:917–925. <https://doi.org/10.1128/AEM.69.2.917-925.2003>
- Pridmore RD, Berger B, Desiere F, et al (2004) The genome sequence of the probiotic intestinal bacterium *Lactobacillus johnsonii* NCC 533. *Proc Natl Acad Sci* 101:2512–2517. <https://doi.org/10.1073/PNAS.0307327101>
- Pyar H, Peh KK (2011) Effect of cryoprotective agents on survival and stability of *Lactobacillus acidophilus* cultured in food-grade medium. *Int J Dairy Technol* 64:578–584. <https://doi.org/10.1111/j.1471-0307.2011.00715.x>

R

- Räisänen L, Draing C, Pfitzenmaier M, et al (2007) Molecular Interaction between lipoteichoic acids and *Lactobacillus delbrueckii* phages depends on d-Alanyl and α -Glucose Substitution of Poly(Glycerophosphate) backbones. *J Bacteriol* 189:4135–4140. <https://doi.org/10.1128/JB.00078-07>
- Rault A, Béal C, Ghorbal S, et al (2007) Multiparametric flow cytometry allows rapid assessment and comparison of lactic acid bacteria viability after freezing and during frozen storage. *Cryobiology* 55:35–43. <https://doi.org/10.1016/J.CRYOBIOL.2007.04.005>
- Rault A, Bouix M, Béal C (2010) Cryotolerance of *Lactobacillus delbrueckii* subsp. *bulgaricus* CFL1 is influenced by the physiological state during fermentation. *Int Dairy J* 20:792–799. <https://doi.org/10.1016/j.idairyj.2010.05.002>
- Rault A, Bouix M, Béal C (2008) Dynamic analysis of *Lactobacillus delbrueckii* subsp. *bulgaricus* CFL1 physiological characteristics during fermentation. *Appl Microbiol Biotechnol* 81:559–570. <https://doi.org/10.1007/s00253-008-1699-4>
- Rault A, Bouix M, Béal C (2009) Fermentation pH influences the physiological-state dynamics of *Lactobacillus bulgaricus* CFL1 during pH-controlled culture. *Appl Environ Microbiol* 75:4374–4381. <https://doi.org/10.1128/AEM.02725-08>
- Reddy KBPK, Awasthi SP, Madhu AN, Prapulla SG (2009) Role of cryoprotectants on the viability and functional properties of probiotic lactic acid bacteria during freeze-drying. *Food Biotechnol* 23:243–265. <https://doi.org/10.1080/08905430903106811>
- Regulski K, Courtin P, Meyrand M, et al (2012) Analysis of the peptidoglycan hydrolase complement of *Lactobacillus casei* and characterization of the major γ -D-Glutamyl-L-Lysyl-endopeptidase. *PLOS ONE* 7:1–11. <https://doi.org/10.1371/JOURNAL.PONE.0032301>
- Ren, Zentek, Vahjen (2019) Optimization of production parameters for probiotic *Lactobacillus* strains as feed additive. *Molecules* 24:1–17. <https://doi.org/10.3390/molecules24183286>
- Reuter G (1985) Elective and selective media for lactic acid bacteria. *Int J Food Microbiol* 2:55–68. [https://doi.org/10.1016/0168-1605\(85\)90057-1](https://doi.org/10.1016/0168-1605(85)90057-1)

- Romano N, Marro M, Marsal M, et al (2021) Fructose derived oligosaccharides prevent lipid membrane destabilization and DNA conformational alterations during vacuum-drying of *Lactobacillus delbrueckii* subsp. *bulgaricus*. *Food Res Int* 143:110235. <https://doi.org/10.1016/j.foodres.2021.110235>
- Romano N, Santos M, Mobili P, et al (2016a) Effect of sucrose concentration on the composition of enzymatically synthesized short-chain fructo-oligosaccharides as determined by FTIR and multivariate analysis. *Food Chem* 202:467–475. <https://doi.org/10.1016/j.foodchem.2016.02.002>
- Romano N, Schebor C, Mobili P, Gómez-Zavaglia A (2016b) Role of mono- and oligosaccharides from FOS as stabilizing agents during freeze-drying and storage of *Lactobacillus delbrueckii* subsp. *bulgaricus*. *Food Res Int* 90:251–258. <https://doi.org/10.1016/j.foodres.2016.11.003>
- Roos YH (2004) Phase and state transitions in dehydration of biomaterials and foods. *Dehydration Prod Biol Orig* 3–22
- Roos YH (2010) Glass transition temperature and its relevance in food processing. *Annu Rev Food Sci Technol* 1:469–496. <https://doi.org/10.1146/annurev.food.102308.124139>
- Roos YH, Karel M (1991) Applying state diagrams to food processing and development. *Food Technol* 45:66–68
- Roos, Y. H (1997) Frozen state transitions in relation to freeze drying. *Journal of Thermal analysis*, 48, 535–544.
- Roy A, Dutta R, Kundu N, et al (2016) A comparative study of the influence of sugars sucrose, trehalose, and maltose on the hydration and diffusion of DMPC lipid bilayer at complete hydration: investigation of structural and spectroscopic aspect of lipid–sugar interaction. *Langmuir* 32:5124–5134. <https://doi.org/10.1021/acs.langmuir.6b01115>

S

- Sadowska A, Świdorski F, Laskowski W (2020) Osmolality of components and their application in the design of functional recovery drinks. *Appl Sci* 10:7663. <https://doi.org/10.3390/app10217663>
- Santivarangkna C, Higl B, Foerst P (2008) Protection mechanisms of sugars during different stages of preparation process of dried lactic acid starter cultures. *Food Microbiol* 25:429–441. <https://doi.org/10.1016/j.fm.2007.12.004>
- Santivarangkna C, Kulozik U, Foerst P (2011) Storing lactic acid bacteria: current methodologies and physiological implications. In: Tsakalidou E, Papadimitriou K (eds) *Stress responses of lactic acid bacteria*, First edit. Springer, pp 479–504
- Santivarangkna C, Naumann D, Kulozik U, Foerst P (2010) Protective effects of sorbitol during the vacuum drying of *Lactobacillus helveticus*: an FT-IR study. *Ann Microbiol* 60:235–242. <https://doi.org/10.1007/s13213-010-0032-5>
- Santivarangkna C, Wenning M, Foerst P, Kulozik U (2007) Damage of cell envelope of *Lactobacillus helveticus* during vacuum drying. *J Appl Microbiol* 102:748–756. <https://doi.org/10.1111/j.1365-2672.2006.03123.x>
- Santoni V, Molloy M, Rabilloud T (2000) Membrane proteins and proteomics: Un amour impossible? *Electrophoresis* 21:1054–1070. [https://doi.org/10.1002/\(SICI\)1522-2683\(20000401\)21:6](https://doi.org/10.1002/(SICI)1522-2683(20000401)21:6)
- Santos MI, Araujo-Andrade C, Esparza-Ibarra E, et al (2014) Galacto-oligosaccharides and lactulose as protectants against desiccation of *Lactobacillus delbrueckii* subsp. *bulgaricus*. *Biotechnol Prog* 30:1231–1238. <https://doi.org/10.1002/btpr.1969>

- Sauvageau J, Ryan J, Lagutin K, et al (2012) Isolation and structural characterisation of the major glycolipids from *Lactobacillus plantarum*. *Carbohydr Res* 357:151–156. <https://doi.org/10.1016/J.CARRES.2012.05.011>
- Savedboworn W, Teawsomboonkit K, Surichay S, et al (2019) Impact of protectants on the storage stability of freeze-dried probiotic *Lactobacillus plantarum*. *Food Sci Biotechnol* 28:795–805. <https://doi.org/10.1007/s10068-018-0523-x>
- Savijoki K, Ingmer H, Varmanen P (2006) Proteolytic systems of lactic acid bacteria. *Appl Microbiol Biotechnol* 71:394–406. <https://doi.org/10.1007/S00253-006-0427-1>
- Savini M, Cecchini C, Verdenelli MC, et al (2010) Pilot-scale production and viability analysis of freeze-dried probiotic bacteria using different protective agents. *Nutrients* 2:330–339. <https://doi.org/10.3390/nu2030330>
- Savoie S, Champagne CP, Chiasson S, Audet P (2007) Media and process parameters affecting the growth, strain ratios and specific acidifying activities of a mixed lactic starter containing aroma-producing and probiotic strains. *J Appl Microbiol* 103:163–174. <https://doi.org/10.1111/j.1365-2672.2006.03219.x>
- Schiller J, Süß R, Arnhold J, et al (2004) Matrix-assisted laser desorption and ionization time-of-flight (MALDI-TOF) mass spectrometry in lipid and phospholipid research. *Prog Lipid Res* 43:449–488. <https://doi.org/10.1016/j.plipres.2004.08.001>
- Schleifer KH, Kandler O (1972) Peptidoglycan types of bacterial cell walls and their taxonomic implications. *Bacteriol Rev* 36:407–477. <https://doi.org/10.1128/BR.36.4.407-477.1972>
- Schoug Å, Fischer J, Heipieper HJ, et al (2008) Impact of fermentation pH and temperature on freeze-drying survival and membrane lipid composition of *Lactobacillus coryniformis* Si3. *J Ind Microbiol Biotechnol* 35:175–181. <https://doi.org/10.1007/s10295-007-0281-x>
- Schoug Å, Olsson J, Carlfors J, et al (2006) Freeze-drying of *Lactobacillus coryniformis* Si3-effects of sucrose concentration, cell density, and freezing rate on cell survival and thermophysical properties. *Cryobiology* 53:119–127. <https://doi.org/10.1016/j.cryobiol.2006.04.003>
- Schwab C, Vogel R, Gänzle MG (2007) Influence of oligosaccharides on the viability and membrane properties of *Lactobacillus reuteri* TMW1.106 during freeze-drying. *Cryobiology* 55:108–114. <https://doi.org/10.1016/j.cryobiol.2007.06.004>
- Senz M, Keil C, Schmach M, et al (2019) Influence of media heat sterilization process on growth performance of representative strains of the genus *Lactobacillus*. *Fermentation* 5:1–11. <https://doi.org/10.3390/fermentation5010020>
- Shao Y, Gao S, Guo H, Zhang H (2014) Influence of culture conditions and preconditioning on survival of *Lactobacillus delbrueckii* subspecies *bulgaricus* ND02 during lyophilization. *J Dairy Sci* 97:1270–1280. <https://doi.org/10.3168/JDS.2013-7536>
- Sharma R, Garg P, Kumar P, et al (2020) Microbial Fermentation and Its Role in Quality Improvement of Fermented Foods. *Fermentation* 6:106. <https://doi.org/10.3390/fermentation6040106>
- Shiraishi T, Yokota S, Fukiya S, Yokota A (2016) Structural diversity and biological significance of lipoteichoic acid in Gram-positive bacteria: focusing on beneficial probiotic lactic acid bacteria. *Biosci Microbiota Food Health* 35:147–161. <https://doi.org/10.12938/bmfh.2016-006>
- Shu G, Wang Z, Chen L, et al (2018) Characterization of freeze-dried *Lactobacillus acidophilus* in goat milk powder and tablet: Optimization of the composite cryoprotectants and

- evaluation of storage stability at different temperature. *LWT - Food Sci Technol.* <https://doi.org/10.1016/j.lwt.2017.12.013>
- Siaterlis A, Deepika G, Charalampopoulos D (2009) Effect of culture medium and cryoprotectants on the growth and survival of probiotic lactobacilli during freeze drying. *Lett Appl Microbiol* 48:295–301. <https://doi.org/10.1111/j.1472-765X.2008.02529.x>
- Sinensky M (1974) Homeoviscous adaptation: a homeostatic process that regulates the viscosity of membrane lipids in *Escherichia coli*. *Proc Natl Acad Sci U S A* 71:522–525. <https://doi.org/10.1073/pnas.71.2.522>
- Sinha RN, Shukla AK, Lal M, Ranganathan B (1982) Rehydration of freeze-dried cultures of lactic *Streptococci*. *J Food Sci* 47:668–669. <https://doi.org/10.1111/J.1365-2621.1982.TB10148.X>
- Slade L, Levine H (1994) Water and the glass transition, dependence of the glass transition on composition and chemical structure: special implications for flour functionality in cookie baking. In: Fito P, Mulet A (eds) *Water in Foods Fundamental Aspects and their significance in relation to processing of foods*, First edit. Elsevier, pp 143–188
- Smittle RB, Gilliland SE, Speck ML, Walter WM (1974) Relationship of cellular fatty acid composition to survival of *Lactobacillus bulgaricus* in liquid Nitrogen. *Appl Microbiol* 27:738–743. <https://doi.org/10.1128/aem.27.4.738-743.1974>
- Snell EE (1945) The nutritional requirements of the lactic acid bacteria and their application to biochemical research. *J Bacteriol* 50:373–382. <https://doi.org/10.1128/jb.50.4.373-382.1945>
- Sochacki KA, Shkel IA, Record MT, Weisshaar JC (2011) Protein diffusion in the periplasm of *E. coli* under Osmotic Stress. *Biophys J* 100:22–31. <https://doi.org/10.1016/J.BPJ.2010.11.044>
- Song S, Bae DW, Lim K, et al (2014) Cold stress improves the ability of *Lactobacillus plantarum* L67 to survive freezing. *Int J Food Microbiol* 191:135–143. <https://doi.org/10.1016/j.ijfoodmicro.2014.09.017>
- Sosa N, Gerbino E, Golowczyc MA, et al (2016) Effect of galacto-oligosaccharides: Maltodextrin matrices on the recovery of *Lactobacillus plantarum* after spray-drying. *Front Microbiol* 7:1–8. <https://doi.org/10.3389/fmicb.2016.00584>
- Soumya MP, Nampoothiri KM (2021) An overview of functional genomics and relevance of glycosyltransferases in exopolysaccharide production by lactic acid bacteria. *Int J Biol Macromol* 184:1014–1025. <https://doi.org/10.1016/j.ijbiomac.2021.06.131>
- Spinnler HE, Corrieu G (1989) Automatic method to quantify starter activity based on pH measurement. *J Dairy Res* 56:755–764. <https://doi.org/10.1017/S0022029900029332>
- Stachura SS, Malajczuk CJ, Mancera RL (2019) Does sucrose change its mechanism of stabilization of lipid bilayers during desiccation? influences of hydration and concentration. *Langmuir* 35:15389–15400. <https://doi.org/10.1021/acs.langmuir.9b03086>
- Stefanello RF, Nabeshima EH, Iamanaka BT, et al (2019) Survival and stability of *Lactobacillus fermentum* and *Wickerhamomyces anomalus* strains upon lyophilisation with different cryoprotectant agents. *Food Res Int* 115:90–94. <https://doi.org/10.1016/j.foodres.2018.07.044>
- Stein AJ, Rodríguez-Cerezo E (2008) Functional foods in the European union. Seville
- Stillwell W (2016) Membrane polar lipids. In: Stillwell W (ed) *An introduction to biological membranes: composition, structure and function*, Second edi. Elsevier, pp 63–87

- Strahl H, Errington J (2017) Bacterial Membranes: Structure, Domains, and Function. *Annu Rev Microbiol* 71:519–538. <https://doi.org/10.1146/annurev-micro-102215-095630>
- Strasser S, Neureiter M, Gepl M, et al (2009) Influence of lyophilization, fluidized bed drying, addition of protectants, and storage on the viability of lactic acid bacteria. *J Appl Microbiol* 107:167–177. <https://doi.org/10.1111/j.1365-2672.2009.04192.x>
- Strauss G, Schurtenberger P, Hauser H (1986) The interaction of saccharides with lipid bilayer vesicles: stabilization during freeze-thawing and freeze-drying. *Biochim Biophys Acta BBA - Biomembr* 858:169–180. [https://doi.org/10.1016/0005-2736\(86\)90303-2](https://doi.org/10.1016/0005-2736(86)90303-2)
- Streit F, Corrieu G, Béal C (2007) Acidification improves cryotolerance of *Lactobacillus delbrueckii* subsp. *bulgaricus* CFL1. *J Biotechnol* 128:659–667. <https://doi.org/10.1016/J.JBIOTECH.2006.11.012>
- Streit F, Delettre J, Corrieu G, Béal C (2008) Acid adaptation of *Lactobacillus delbrueckii* subsp. *bulgaricus* induces physiological responses at membrane and cytosolic levels that improves cryotolerance. *J Appl Microbiol* 105:1071–1080. <https://doi.org/10.1111/j.1365-2672.2008.03848.x>
- Succi M, Tremonte P, Reale A, et al (2007) Preservation by freezing of potentially probiotic strains of *Lactobacillus rhamnosus*. *Ann Microbiol* 57:537–544. <https://doi.org/10.1007/BF03175352>
- Sulabo ASL, Villasanta MEL, Lascano KG, et al (2020) Storage stability of freeze-dried *Lactobacillus plantarum* S20 starter culture as affected by various formulations of drying medium, and its fermentation characteristics in mung bean (*Vigna radiata* L.) slurry. *Food Reseach* 4:964–975. [https://doi.org/10.26656/fr.2017.4\(4\).361](https://doi.org/10.26656/fr.2017.4(4).361)
- Sumeri I, Arike L, Stekolštšikova J, et al (2010) Effect of stress pretreatment on survival of probiotic bacteria in gastrointestinal tract simulator. *Appl Microbiol Biotechnol* 86:1925–1931. <https://doi.org/10.1007/S00253-009-2429-2/FIGURES/2>
- Svalgaard JD, Talkhonchek MS, Hastrup EK, et al (2018) Pentaisomaltose, an alternative to DMSO. Engraftment of cryopreserved human CD34+ cells in immunodeficient NSG mice. *Cell Transplant* 27:1407–1412. <https://doi.org/10.1177/0963689718786226>

T

- Tablin F, Wolkers WF, Walker NJ, et al (2001) Membrane reorganization during chilling: implications for long-term stabilization of platelets. *Cryobiology* 43:114–123. <https://doi.org/10.1006/CRYO.2001.2355>
- Tada N, Sato M, Yamanoi J, et al (1990) Cryopreservation of mouse spermatozoa in the presence of raffinose and glycerol. *Reproduction* 89:511–516. <https://doi.org/10.1530/jrf.0.0890511>
- Tang HW, Abbasiliasi S, Murugan P, et al (2020) Influence of freeze-drying and spray-drying preservation methods on survivability rate of different types of protectants encapsulated *Lactobacillus acidophilus* FTDC 3081. *Biosci Biotechnol Biochem* 84:1913–1920. <https://doi.org/10.1080/09168451.2020.1770572>
- Tavera-Quiroz MJ, Romano N, Mobili P, et al (2015) Green apple baked snacks functionalized with edible coatings of methylcellulose containing *Lactobacillus plantarum*. *J Funct Foods* 16:164–173. <https://doi.org/10.1016/J.JFF.2015.04.024>
- Teixeira H, Gonçalves MG, Rozès N, et al (2002) Lactobacillic acid accumulation in the plasma membrane of *Oenococcus oeni*: a response to ethanol stress? *Microb Ecol* 43:146–153. <https://doi.org/10.1007/s00248-001-0036-6>

- Teixeira P, Castro H, Kirby R (1996) Evidence of membrane lipid oxidation of spray-dried *Lactobacillus bulgaricus* during storage. *Lett Appl Microbiol* 22:34–38. <https://doi.org/10.1111/j.1472-765X.1996.tb01103.x>
- Terpou A, Papadaki A, Lappa IK, et al (2019) Probiotics in food systems: significance and emerging strategies towards improved viability and delivery of enhanced beneficial value. *Nutr* 2019 Vol 11 Page 1591 11:1591. <https://doi.org/10.3390/NU11071591>
- Terzaghi BE, Sandine WE (1975) Improved Medium for lactic *Streptococci* and their bacteriophages. *Appl Microbiol* 29:807. <https://doi.org/10.1128/am.29.6.807-813.1975>
- To TMH, Grandvalet C, Alexandre H, Tourdou-Maréchal R (2015) Cyclopropane fatty acid synthase from *Oenococcus oeni*: expression in *Lactococcus lactis* subsp. *cremoris* and biochemical characterization. *Arch Microbiol* 2015 197:1063–1074. <https://doi.org/10.1007/S00203-015-1143-Y>
- Trabelsi I, Ben Slima S, Ktari N, et al (2019) Incorporation of probiotic strain in raw minced beef meat: Study of textural modification, lipid and protein oxidation and color parameters during refrigerated storage. *Meat Sci* 154:29–36. <https://doi.org/10.1016/j.meatsci.2019.04.005>
- Tripathi MK, Giri SK (2014) Probiotic functional foods: survival of probiotics during processing and storage. *J Funct Foods* 9:225–241. <https://doi.org/10.1016/J.JFF.2014.04.030>
- Tripathi P, Dupres V, Beaussart A, et al (2012) Deciphering the nanometer-scale organization and assembly of *Lactobacillus rhamnosus* GG pili using atomic force microscopy. *Langmuir ACS J Surf Colloids* 28:2211–2216. <https://doi.org/10.1021/LA203834D>
- Tsvetkov T, Brankova R (1983) Viability of *micrococci* and *lactobacilli* upon freezing and freeze-drying in the presence of different cryoprotectants. *Cryobiology* 20:318–323. [https://doi.org/10.1016/0011-2240\(83\)90020-2](https://doi.org/10.1016/0011-2240(83)90020-2)
- Tsvetkov T, Shishkova I (1982) Studies on the effects of low temperatures on lactic acid bacteria. *Cryobiology* 19:211–214. [https://doi.org/10.1016/0011-2240\(82\)90143-2](https://doi.org/10.1016/0011-2240(82)90143-2)
- Tsvetkova NM, Phillips BL, Crowe LM, et al (1998) Effect of sugars on headgroup mobility in freeze-dried dipalmitoylphosphatidylcholine bilayers: Solid-state ³¹P NMR and FTIR studies. *Biophys J* 75:2947–2955. [https://doi.org/10.1016/S0006-3495\(98\)77736-7](https://doi.org/10.1016/S0006-3495(98)77736-7)
- Turuvekere Sadguruprasad L, Basavaraj M (2018) Statistical modelling for optimized lyophilization of *Lactobacillus acidophilus* strains for improved viability and stability using response surface methodology. *AMB Express* 8:1–11. <https://doi.org/10.1186/s13568-018-0659-3>
- Tymcyszyn E, Gerbino E, Illanes A, Gómez-Zavaglia A (2011) Galacto-oligosaccharides as protective molecules in the preservation of *Lactobacillus delbrueckii* subsp. *bulgaricus*. *Cryobiology* 62:123–129. <https://doi.org/10.1016/J.CRYOBIOL.2011.01.013>
- Tymcyszyn EE, Del Rosario Díaz M, Gómez-Zavaglia A, Disalvo EA (2007) Volume recovery, surface properties and membrane integrity of *Lactobacillus delbrueckii* subsp. *bulgaricus* dehydrated in the presence of trehalose or sucrose. *J Appl Microbiol* 103:2410–2419. <https://doi.org/10.1111/j.1365-2672.2007.03482.x>
- Tymcyszyn EE, Sosa N, Gerbino E, et al (2012) Effect of physical properties on the stability of *Lactobacillus bulgaricus* in a freeze-dried galacto-oligosaccharides matrix. *Int J Food Microbiol* 155:217–221. <https://doi.org/10.1016/j.ijfoodmicro.2012.02.008>

U

- Unsay JD, Cosentino K, Subburaj Y, García-Sáez AJ (2013) Cardiolipin effects on membrane structure and dynamics. *Langmuir* 29:15878–15887. <https://doi.org/10.1021/la402669z>

V

- Vadyvaloo V, Hastings JW, van der Merwe MJ, Rautenbach M (2002) Membranes of class IIa bacteriocin-resistant *Listeria monocytogenes* cells contain increased levels of desaturated and short-acyl-chain phosphatidylglycerols. *Appl Environ Microbiol* 68:5223–5230. <https://doi.org/10.1128/AEM.68.11.5223-5230.2002>
- Van De Guchte M, Penaud S, Grimaldi C, et al (2006) The complete genome sequence of *Lactobacillus bulgaricus* reveals extensive and ongoing reductive evolution. *Proc Natl Acad Sci U S A* 103:9274–9279. <https://doi.org/10.1073/pnas.0603024103>
- Van Den Bogaart G, Hermans N, Krasnikov V, et al (2007) On the decrease in lateral mobility of phospholipids by sugars. *Biophys J* 92:1598–1605. <https://doi.org/10.1529/biophysj.106.096461>
- Vandamme P, De Bruyne K, Pot B (2014) Phylogenetics and systematics. In: Holzappel WH, Wood JB (eds) *Lactic acid bacteria: biodiversity and taxonomy*, First edit. John Wiley & Sons, pp 31–44
- Velly H, Bouix M, Passot S, et al (2015) Cyclopropanation of unsaturated fatty acids and membrane rigidification improve the freeze-drying resistance of *Lactococcus lactis* subsp. *lactis* TOMSC161. *Appl Microbiol Biotechnol* 99:907–918. <https://doi.org/10.1007/s00253-014-6152-2>
- Velly H, Fonseca F, Passot S, et al (2014) Cell growth and resistance of *Lactococcus lactis* subsp. *lactis* TOMSC161 following freezing, drying and freeze-dried storage are differentially affected by fermentation conditions. *J Appl Microbiol* 117:729–740. <https://doi.org/10.1111/jam.12577>
- Vereyken IJ, Chupin V, Hoekstra FA, et al (2003a) The effect of fructan on membrane lipid organization and dynamics in the dry state. *Biophys J* 84:3759–3766. [https://doi.org/10.1016/S0006-3495\(03\)75104-2](https://doi.org/10.1016/S0006-3495(03)75104-2)
- Vereyken IJ, Van Kuik JA, Evers TH, et al (2003b) Structural requirements of the fructan-lipid interaction. *Biophys J* 84:3147–3154. [https://doi.org/10.1016/S0006-3495\(03\)70039-3](https://doi.org/10.1016/S0006-3495(03)70039-3)
- Verlhac P, Vessot-Crastes S, Degobert G, et al (2020) Experimental study and optimization of freeze-drying cycles of a model Casei type probiotic bacteria. *Dry Technol* 38:2120–2133. <https://doi.org/10.1080/07373937.2019.1683859>
- Vinderola G, Champagne CP, Desfossés-Foucault É (2019) The production of lactic acid bacteria starters and probiotic cultures: an industrial perspective. In: Vinderola G, Ouwehand AC, Seppo S, Wright von A (eds) *Lactic acid bacteria: microbiological and functional aspects*, Fifth edit. CRC Press, pp 317–336
- Vinogradov E, Sadovskaya I, Grard T, et al (2018) Structural studies of the cell wall polysaccharide from *Lactococcus lactis* UC509.9. *Carbohydr Res* 461:25–31. <https://doi.org/10.1016/J.CARRES.2018.03.011>
- Vogel RF, Pavlovic M, Ehrmann MA, et al (2011) Genomic analysis reveals *Lactobacillus sanfranciscensis* as stable element in traditional sourdoughs. *Microb Cell Factories* 10:1–11. <https://doi.org/10.1186/1475-2859-10-S1-S6/TABLES/2>
- Volkert M, Ananta E, Luscher C, Knorr D (2008) Effect of air freezing, spray freezing, and pressure shift freezing on membrane integrity and viability of *Lactobacillus rhamnosus* GG. *J Food Eng* 87:532–540. <https://doi.org/10.1016/J.JFOODENG.2008.01.008>
- Vorhauer-Huget N, Mannes D, Hilmer M, et al (2020) Freeze-drying with structured sublimation fronts-visualization with neutron imaging. *Process* 2020 Vol 8 Page 1091 8:1091. <https://doi.org/10.3390/PR8091091>

W

- Waako A, Polak-Berecka M, Gustaw W (2013) Increased viability of probiotic *Lactobacillus rhamnosus* after osmotic stress. *Acta Aliment* 42:520–528. <https://doi.org/10.1556/AALIM.42.2013.4.7>
- Walczak-Skierska J, Złoch M, Pauter K, et al (2020) Lipidomic analysis of lactic acid bacteria strains by matrix-assisted laser desorption/ionization time-of-flight mass spectrometry. *J Dairy Sci* 103:11062–11078. <https://doi.org/10.3168/jds.2020-18753>
- Walker GM (2014) Fermentation (industrial): media for industrial fermentations. In: Batt CA, Tortorello M Lou (eds) *Encyclopedia of Food Microbiology*, Volume 1, Second edi. Academic Press, pp 769–777
- Wang G, Luo L, Dong C, et al (2021) Polysaccharides can improve the survival of *Lactiplantibacillus plantarum* subjected to freeze-drying. *J Dairy Sci* 104:2606–2614. <https://doi.org/10.3168/jds.2020-19110>
- Wang G, Yu X, Lu Z, et al (2019) Optimal combination of multiple cryoprotectants and freezing-thawing conditions for high *lactobacilli* survival rate during freezing and frozen storage. *LWT - Food Sci Technol* 99:217–223. <https://doi.org/10.1016/j.lwt.2018.09.065>
- Wang GQ, Pu J, Yu XQ, et al (2020) Influence of freezing temperature before freeze-drying on the viability of various *Lactobacillus plantarum* strains. *J Dairy Sci* 103:3066–3075. <https://doi.org/10.3168/jds.2019-17685>
- Wang Y, Corrieu G, Béal C (2005a) Fermentation pH and Temperature Influence the Cryotolerance of *Lactobacillus acidophilus* RD758. *J Dairy Sci* 88:21–29. [https://doi.org/10.3168/jds.S0022-0302\(05\)72658-8](https://doi.org/10.3168/jds.S0022-0302(05)72658-8)
- Wang Y, Delettre J, Corrieu G, Béal C (2011) Starvation induces physiological changes that act on the cryotolerance of *Lactobacillus acidophilus* RD758. *Biotechnol Prog* 27:342–350. <https://doi.org/10.1002/btpr.566>
- Wang Y, Delettre J, Guillot A, et al (2005b) Influence of cooling temperature and duration on cold adaptation of *Lactobacillus acidophilus* RD758. *Cryobiology* 50:294–307. <https://doi.org/10.1016/J.CRYOBIOL.2005.03.001>
- Wang Y, Tashiro Y, Sonomoto K (2015) Fermentative production of lactic acid from renewable materials: Recent achievements, prospects, and limits. *J Biosci Bioeng* 119:10–18. <https://doi.org/10.1016/j.jbiosc.2014.06.003>
- Wang YC, Yu RC, Chou CC (2004) Viability of lactic acid bacteria and bifidobacteria in fermented soymilk after drying, subsequent rehydration and storage. *Int J Food Microbiol* 93:209–217. <https://doi.org/10.1016/j.ijfoodmicro.2003.12.001>
- Wang Z, Benning C (2011) *Arabidopsis thaliana* polar glycerolipid profiling by thin layer chromatography (TLC) coupled with gas-liquid chromatography (GLC). *J Vis Exp* 2–7. <https://doi.org/10.3791/2518>
- Wapnir RA, Lifshitz F (1985) Osmolality and solute concentration their relationship with oral hydration solution effectiveness: an experimental assessment. *Pediatr Res* 19:894–898. <https://doi.org/10.1203/00006450-198509000-00004>
- Wassenaar TM, Lukjancenko O (2014) Comparative genomics of *Lactobacillus* and other LAB. In: Holzappel WH, Wood BJB (eds) *Lactic acid bacteria: biodiversity and taxonomy*, First edit. John Wiley & Sons, Ltd, pp 55–69
- Whitehead WE, Ayres JW, Sandine WE (1993) A review of starter media for cheese making. *J Dairy Sci* 76:2344–2353. [https://doi.org/10.3168/JDS.S0022-0302\(93\)77572-4](https://doi.org/10.3168/JDS.S0022-0302(93)77572-4)

- Wilkinson MG, LaPointe G (2020) Invited review: Starter lactic acid bacteria survival in cheese: New perspectives on cheese microbiology. *J Dairy Sci* 103:10963–10985. <https://doi.org/10.3168/JDS.2020-18960>
- Wolfe J, Bryant G (1999) Freezing, drying, and/or vitrification of membrane-solute-water systems. *Cryobiology* 39:103–129. <https://doi.org/10.1006/cryo.1999.2195>
- Wolkers WF, Balasubramanian SK, Ongstad EL, et al (2007) Effects of freezing on membranes and proteins in LNCaP prostate tumor cells. *Biochim Biophys Acta BBA - Biomembr* 1768:728–736. <https://doi.org/10.1016/j.bbamem.2006.12.007>
- Wolkers WF, Oldenhof H (2021) Use of in situ Fourier Transform Infrared Spectroscopy in cryobiological research. In: Wolkers WF, Oldenhof H (eds) *Cryopreservation and freeze-drying protocols. Methods in Molecular Biology*. Humana Press, pp 331–349
- Wolkers WF, Oldenhof H, Glasmacher B (2010) Dehydrating phospholipid vesicles measured in real-time using ATR Fourier transform infrared spectroscopy. *Cryobiology* 61:108–114. <https://doi.org/10.1016/j.cryobiol.2010.06.001>
- Wouters JA, Frenkiel H, de Vos WM, et al (2001) Cold shock proteins of *Lactococcus lactis* MG1363 are involved in cryoprotection and in the production of cold-induced proteins. *Appl Environ Microbiol* 67:5171–5178. <https://doi.org/10.1128/AEM.67.11.5171-5178.2001>
- Wright CT, Klaenhammer TR (1983) Survival of *Lactobacillus bulgaricus* during freezing and freeze-drying after growth in the presence of calcium. *J Food Sci* 48:773–777. <https://doi.org/10.1111/j.1365-2621.1983.tb14896.x>
- Wu C, Huang J, Zhou R (2014) Progress in engineering acid stress resistance of lactic acid bacteria. *Appl Microbiol Biotechnol* 98:1055–1063. <https://doi.org/10.1007/s00253-013-5435-3>
- Wu C, Zhang J, Wang M, et al (2012) *Lactobacillus casei* combats acid stress by maintaining cell membrane functionality. *J Ind Microbiol Biotechnol* 39:1031–1039. <https://doi.org/10.1007/s10295-012-1104-2>

Y

- Yang K, Zhu Y, Qi Y, et al (2019) Analysis of proteomic responses of freeze-dried *Oenococcus oeni* to access the molecular mechanism of acid acclimation on cell freeze-drying resistance. *Food Chem* 285:441–449. <https://doi.org/10.1016/J.FOODCHEM.2019.01.120>
- Yang X, Teng K, Zhang J, et al (2017) Transcriptome responses of *Lactobacillus acetotolerans* F28 to a short- and long-term ethanol stress. *Sci Rep* 7:2650. <https://doi.org/10.1038/s41598-017-02975-8>
- Yasuda E, Tatenno H, Hirabarashi J, et al (2011) Lectin microarray reveals binding profiles of *Lactobacillus casei* strains in a comprehensive analysis of bacterial cell wall polysaccharides. *Appl Environ Microbiol* 77:4539–4546. <https://doi.org/10.1128/AEM.00240-11>
- Ying D, Sanguansri L, Weerakkody R, et al (2011) Tocopherol and ascorbate have contrasting effects on the viability of microencapsulated *Lactobacillus rhamnosus* GG. *J Agric Food Chem* 59:10556–10563. <https://doi.org/10.1021/JF202358M>
- Yoon YH, Pope JM, Wolfe J (1998) The effects of solutes on the freezing properties of and hydration forces in lipid lamellar phases. *Biophys J* 74:1949–1965. [https://doi.org/10.1016/S0006-3495\(98\)77903-2](https://doi.org/10.1016/S0006-3495(98)77903-2)

Yu KC, Chen CC, Wu PC (2011) Research on application and rehydration rate of vacuum freeze drying of rice. *J Appl Sci* 11:535–541. <https://doi.org/10.3923/JAS.2011.535.541>

Z

Zayed G, Roos YH (2004) Influence of trehalose and moisture content on survival of *Lactobacillus salivarius* subjected to freeze-drying and storage. *Process Biochem* 39:1081–1086. [https://doi.org/10.1016/S0032-9592\(03\)00222-X](https://doi.org/10.1016/S0032-9592(03)00222-X)

Zhai Z, Douillard FP, An H, et al (2014) Proteomic characterization of the acid tolerance response in *Lactobacillus delbrueckii* subsp. *bulgaricus* CAUH1 and functional identification of a novel acid stress-related transcriptional regulator Ldb0677. *Environ Microbiol* 16:1524–1537. <https://doi.org/10.1111/1462-2920.12280>

Zhai Z, Yang Y, Wang H, et al (2020) Global transcriptomic analysis of *Lactobacillus plantarum* CAUH2 in response to hydrogen peroxide stress. *Food Microbiol* 87:103389. <https://doi.org/10.1016/j.fm.2019.103389>

Zhang G, Fan M, Li Y, et al (2012) Effect of growth phase, protective agents, rehydration media and stress pretreatments on viability of *Oenococcus oeni* subjected to freeze-drying. *Afr J Microbiol Res* 6:1478–1484. <https://doi.org/10.5897/AJMR11.1336>

Zhang M, Yao M, Lai T, et al (2021) Response of *Lactiplantibacillus plantarum* NMGL2 to combinational cold and acid stresses during storage of fermented milk as analyzed by data-independent acquisition proteomics. *Foods* 10:1514. <https://doi.org/10.3390/foods10071514>

Zhang YM, Rock CO (2008) Membrane lipid homeostasis in bacteria. *Nat Rev Microbiol* 6:222–233. <https://doi.org/10.1038/nrmicro1839>

Zhang, J., & Zografi, G (2000) The relationship between “BET” and “free volume”-derived parameters for water vapor absorption into amorphous solids. *Journal of Pharmaceutical Sciences*, 89(8), 1063–1072.

Zhao G, Zhang G (2005) Effect of protective agents, freezing temperature, rehydration media on viability of malolactic bacteria subjected to freeze-drying. *J Appl Microbiol* 99:333–338. <https://doi.org/10.1111/j.1365-2672.2005.02587.x>

Zhao G, Zhang G (2009) Influence of freeze-drying conditions on survival of *Oenococcus oeni* for malolactic fermentation. *Int J Food Microbiol* 135:64–67. <https://doi.org/10.1016/J.IJFOODMICRO.2009.07.021>

Zhao W, Li H, Wang H, et al (2009) The effect of acid stress treatment on viability and membrane fatty acid composition of *Oenococcus oeni* SD-2a. *Agric Sci China* 8:311–316. [https://doi.org/10.1016/S1671-2927\(08\)60214-X](https://doi.org/10.1016/S1671-2927(08)60214-X)

Zhen N, Zeng X, Wang H, et al (2020) Effects of heat shock treatment on the survival rate of *Lactobacillus acidophilus* after freeze-drying. *Food Res Int* 136:109507. <https://doi.org/10.1016/j.foodres.2020.109507>

Zheng J, Wittouck S, Salvetti E, et al (2020) A taxonomic note on the genus *Lactobacillus*: Description of 23 novel genera, emended description of the genus *Lactobacillus* Beijerinck 1901, and union of Lactobacillaceae and Leuconostocaceae. <https://doi.org/10.7939/R3-EGNZ-M294>

Zhou M, Theunissen D, Wels M, Siezen RJ (2010) LAB-Secretome: a genome-scale comparative analysis of the predicted extracellular and surface-associated proteins of lactic acid bacteria. *BMC Genomics* 11:651. <https://doi.org/10.1186/1471-2164-11-651>

Zhou X, Li Y (2015) Basic biology of oral microbes. In: Zhou X, Li Y (eds) *Atlas of oral microbiology*, First edit. Academic Press, pp 1–14

- Zhu Y, Zhang Y, Li Y (2009) Understanding the industrial application potential of lactic acid bacteria through genomics. *Appl Microbiol Biotechnol* 83:597–610. <https://doi.org/10.1007/S00253-009-2034-4>
- Ziadi M, Touhami Y, Achour M, et al (2005) The effect of heat stress on freeze-drying and conservation of *Lactococcus*. *Biochem Eng J* 24:141–145. <https://doi.org/10.1016/J.BEJ.2005.02.001>
- Zotta T, Guidone A, Ianniello RG, et al (2013) Temperature and respiration affect the growth and stress resistance of *Lactobacillus plantarum* C17. *J Appl Microbiol* 115:848–858. <https://doi.org/10.1111/jam.12285>
- Zwietering MH, Jongenburger I, Rombouts FM, Van't Riet K (1990) Modeling of the bacterial growth curve. *Appl Environ Microbiol* 56:1875–1881. <https://doi.org/10.1128/aem.56.6.1875-1881.1990>

Annexes

A. ANNEXES

SUMMARY OF THE CHAPTER

A. ANNEXES	297
A.1. The updated list of the new genera in the family Lactobacillaceae	298
A.2. Overview of the two LAB examples shown in Table 1.1 from family to species	299
A.3. Media composition for the growth of lactic acid bacteria	300
A.4. Glass transition temperature (T_g) of different freeze-dried protective suspensions	301
A.5. Glass transition temperature of the maximally freeze-concentrated phase (T_g') and collapse temperature (T_{coll}) of different sugar solutions used to freeze-dry lactic acid bacteria*	302
A.6. Induced proteins description after applying the different stresses shown in Table 1.5	303

A1. The updated list of the new genera in the family *Lactobacillaceae*

Former name	New name*
<i>Lactobacillus algidus</i>	<i>Dellaglioia algidus</i>
<i>Lactobacillus alimentarius</i>	<i>Companilactobacillus alimentarius</i>
<i>Lactobacillus amylophilus</i>	<i>Amylolactobacillus amylophilus</i>
<i>Lactobacillus brevis</i>	<i>Levilactobacillus brevis</i>
<i>Lactobacillus buchneri</i>	<i>Lentilactobacillus buchneri</i>
<i>Lactobacillus casei</i>	<i>Lacticaseibacillus casei</i>
<i>Lactobacillus composti</i>	<i>Agrilactobacillus composti</i>
<i>Lactobacillus concavus</i>	<i>Lapidilactobacillus concavus</i>
<i>Lactobacillus coryniformis</i>	<i>Loigolactobacillus coryniformis</i>
<i>Lactobacillus mellifer</i>	<i>Bombilactobacillus mellifer</i>
<i>Lactobacillus fermentum</i>	<i>Limosilactobacillus fermentum</i>
<i>Lactobacillus floricola</i>	<i>Holzapfelia floricola</i>
<i>Lactobacillus fructivorans</i>	<i>Fructilactobacillus fructivorans</i>
<i>Lactobacillus jinshanensis</i>	<i>Acetilactobacillus jinshanensis</i>
<i>Lactobacillus kunkeei</i>	<i>Apilactobacillus kunkeei</i>
<i>Lactobacillus malefermentans</i>	<i>Secundilactobacillus malefermentans</i>
<i>Lactobacillus mali</i>	<i>Liquorilactobacillus mali</i>
<i>Lactobacillus paracasei</i>	<i>Lacticaseibacillus paracasei</i>
<i>Lactobacillus perolens</i>	<i>Schleiferilactobacillus perolens</i>
<i>Lactobacillus plantarum</i>	<i>Lactiplantibacillus plantarum</i>
<i>Lactobacillus rossiae</i>	<i>Furfurilactobacillus rossiae</i>
<i>Lactobacillus salivarius</i>	<i>Ligalactobacillus salivarius</i>
<i>Lactobacillus sakei</i>	<i>Latilactobacillus sakei</i>
<i>Lactobacillus selangorensis</i>	<i>Paralactobacillus selangorensis</i>
<i>Lactobacillus reuteri</i>	<i>Limosilactobacillus reuteri</i>
<i>Lactobacillus vaccinoferus</i>	<i>Paucilactobacillus vaccinoferus</i>

*(Zheng et al. 2020)

A2. Overview of the two LAB examples shown in Table 1.1 from family to species

Family	Some examples of genus ^δ	Some examples of species ^δ
Aerococcaceae	<i>Abiotrophia</i>	<i>defectiva</i>
	<i>Aerococcus</i>	<i>viridans</i>
	<i>Dolosicoccus</i>	<i>paucivorans</i>
	<i>Eremococcus</i>	<i>coleocola</i>
	<i>Facklamia</i>	<i>hominis</i>
	<i>Globicatella</i>	<i>sanguinis</i>
	<i>Ignavigranum</i>	<i>ruoffiae</i>
Carnobacteriaceae	<i>Alkalibacterium</i>	<i>olivapovliticus</i>
	<i>Allofustis</i>	<i>seminis</i>
	<i>Alloiococcus</i>	<i>otitis</i>
	<i>Atopobacter</i>	<i>phocae</i>
	<i>Atopococcus</i>	<i>tabaci</i>
	<i>Atopostipes</i>	<i>suicloacalis</i>
	<i>Bavariococcus</i>	<i>seileri</i>
	<i>Carnobacterium</i>	<i>divergens</i>
	<i>Desemzia</i>	<i>incerta</i>
	<i>Dolosigranalum</i>	<i>pigrum</i>
	<i>Granulicatella</i>	<i>adiacens</i>
	<i>Isobaculum</i>	<i>melis</i>
	<i>Lacticigenium</i>	<i>naphtae</i>
<i>Marinilactibacillus</i>	<i>psychrotolerans</i>	
<i>Trichococcus</i>	<i>flocculiformis</i>	
Enterococcaceae	<i>Catelicoccus</i>	<i>marimammalum</i>
	<i>Enterococcus</i>	<i>faecalis</i>
	<i>Melissococcus</i>	<i>plutonius</i>
	<i>Pilibacter</i>	<i>termitis</i>
	<i>Tetragenococcus</i>	<i>halophilus</i>
	<i>Vagococcus</i>	<i>fluvialis</i>
Lactobacillaceae	<i>Lactobacillus</i>	<i>delbrueckii</i>
	<i>Pediococcus</i>	<i>damnosus</i>
	<i>Fructobacillus</i>	<i>fructosis</i>
	<i>Leuconostoc</i>	<i>mesenteroides</i>
	<i>Oenococcus</i>	<i>oeni</i>
	<i>Weissella</i>	<i>viridescens</i>
Streptococcaceae	<i>Streptococcus</i>	<i>salivarius</i>
	<i>Lactococcus</i>	<i>lactis</i>
	<i>Lactovum</i>	<i>miscens</i>

^δHolzapfel and Wood, 2014

A3. Media composition for the growth of lactic acid bacteria

Culture medium	Ingredients and chemical structure (if applicable)	Concentration	References
Man, Rogosa, and Sharpe (MRS)	Glucose C ₆ H ₁₂ O ₆	20 g·L ⁻¹	(De Man et al. 1960)
	Peptone C ₁₃ H ₂₄ O ₄	10 g·L ⁻¹	
	Yeast extract C ₁₉ H ₁₄ O ₂	4 g·L ⁻¹	
	Meat extract	8 g·L ⁻¹	
	Polysorbate 80 (Tween 80)	0.1 g·L ⁻¹	
	Sodium acetate trihydrate C ₂ H ₃ NaO ₂ ·3H ₂ O	5 g·L ⁻¹	
	Triammonium citrate C ₆ H ₁₇ N ₃ O ₇	2 g·L ⁻¹	
	Dipotassium hydrogen phosphate K ₂ HPO ₄	2 g·L ⁻¹	
	Magnesium sulfate heptahydrate MgSO ₄ ·7H ₂ O	0.2 g·L ⁻¹	
Manganous sulfate tetrahydrate MnSO ₄ ·4H ₂ O	0.05 g·L ⁻¹		
M17	Lactose C ₁₂ H ₂₂ O ₁₁	5 g·L ⁻¹	(Terzaghi and Sandine 1975)
	Soya peptone	5 g·L ⁻¹	
	Yeast extract C ₁₉ H ₁₄ O ₂	2.5 g·L ⁻¹	
	Meat extract	5 g·L ⁻¹	
	Meat peptone	2.5 g·L ⁻¹	
	Tryptone	2.5 g·L ⁻¹	
	Ascorbic acid C ₆ H ₈ O ₆	0.5 g·L ⁻¹	
	β-disodium glycerophosphate (GP)	19 g·L ⁻¹	
	Magnesium sulfate MgSO ₄	0.25 g·L ⁻¹	

A4. Glass transition temperature (T_g) of different freeze-dried protective suspensions

Freeze-dried sugar suspension	T _g (°C) from Gordon and Taylor*	References
Glucose	31-36	(Zhang and Zografis, 2000)
Sucrose	62	(Roos, 1997)
Trehalose	115	(Zhang and Zografis, 2000)
Lactose	97	(Jouppila and Roos, 1994)
Dextran	200	(Zhang and Zografis, 2000)
Starch	225	(Zhang and Zografis, 2000)
Skim milk	97	(Jouppila and Roos, 1994)
Isolated soy	92	(Jouppila and Roos, 1994)

*Gordon *et al.* 1977

A5. Glass transition temperature of the maximally freeze-concentrated phase (T_g') and collapse temperature (T_{coll}) of different sugar solutions used to freeze-dry lactic acid bacteria*

Sugar	Concentration (%, w/w)	T_g' (°C) measured by DSC	T_{coll} (°C) measured by FDM
Glucose	20	-44	-42
Fructose	20	-44	-43
Galactose	10	-42	-41
Sucrose	20	-33	-31
Trehalose	20	-29	-26
Lactose	10	-28	-27
Maltose	20	-29	-27
Raffinose	20	-26	-24
Inulin (from chicory)	10	-17	-15
Fructooligosaccharide (from chicory)	10	-17	-15
Pentaisomaltose	20	-19	-18
Maltodextrin (Glucidex 6)	20	-7	-3

*Fonseca et al. 2021; DSC: Differential Scanning Calorimetry; FDM: Freeze-drying Microscopy

A6. Induced proteins description after applying the different stresses shown in Table 1.5

Protein	Protein family or name*	Function	References
DnaK	Heat shock proteins Hsp70	These proteins fold newly synthesized proteins, facilitate the transport of proteins across membranes, reactivate the misfolded proteins, disaggregate the aggregated proteins, and control the activity of regulatory proteins.	(Broadbent and Lin 1999; Prasad et al. 2003; Waako et al. 2013)
GroEL	Heat shock proteins Hsp60		(Broadbent and Lin 1999; Prasad et al. 2003; Waako et al. 2013)
GroES	Heat shock proteins Hsp10		(Shao et al. 2014)
Lo18	Heat shock proteins	Lo18 prevents the thermal aggregation of proteins and plays a crucial role in membrane quality control.	(Zhen et al. 2020)
CspE	Cold shock proteins	Csps function as RNA chaperones by destabilizing secondary structures in target RNA at low temperature so that the single-stranded state of target RNA is maintained.	(Wouters et al. 2001)
CspL			(Song et al. 2014)
CspP			(Derzelle et al. 2003; Song et al. 2014)
ClpB	Chaperon protein	ClpB is involved in the recovery of the cell from heat-induced damage, in cooperation with DnaK. It acts before DnaK, in the processing of protein aggregates.	(Waako et al. 2013)
TF	Transcription factor	TF regulates genes in order to make sure that they are expressed in the desired cells at the right time and amount throughout the cell growth.	
TS	Thymidylate synthase	TS participates in the amino acid biosynthesis of bacteria	
EF-G	Elongation factor G	EF-G participates in the protein synthesis of bacteria	
IMPDH	Inosine-5'-monophosphate dehydrogenase	These proteins participate in the nucleotide synthesis of bacteria	(Li et al. 2014)
UMPK	Uridylate kinase		
LDH	L-lactate dehydrogenase		
SlrB	Component of phosphatetransferase system (sugar PTS)	SlrB is involved in the transport system of molecules	
Piridoxine 5	Piridoxine 5'-phosphate oxidase	Piridoxine 5 participates in the vitamin biosynthesis of bacteria	

*Protein base from <http://www.unitprot.org>

RÉSUMÉ EN FRANÇAIS

1. Introduction

Les Bactéries Lactiques (BL) sont un groupe de bactéries à l'origine de nombreux produits alimentaires fermentés tels que les yaourts, les fromages, les viandes et les légumes fermentés et à l'origine de plusieurs probiotiques. Ces bactéries donnent aux aliments fermentés des arômes uniques et des textures caractéristiques grâce à leur capacité métabolique à produire des acides organiques (par exemple, de l'acide lactique), des composés organoleptiques et des gélifiants (par exemple, des exopolysaccharides). Parmi les aliments fermentés, le yaourt est l'un des produits les plus consommés et issu de la fermentation du lait par proto-coopération de deux espèces de BL (*Lactobacillus bulgaricus* et *Streptococcus thermophilus*).

L'adoption mondiale des aliments laitiers fermentés dans l'alimentation quotidienne et la prise de conscience de maintenir un mode de vie sain et de bien-être ont conduit à l'essor des marchés des aliments fermentés et des probiotiques. Le marché mondial, devrait encore augmenter de 54% pour les produits laitiers fermentés d'ici 2027 (Emergen Research 2020) et même de 93% pour les probiotiques d'ici 2027 (Fortune Business insights 2020). La qualité des

cultures bactériennes, autrement appelées starters, est donc un point clé pour les industriels de ces secteurs.

Les BL sont produites par une succession de 5 étapes : 1-la fermentation, 2-la récolte, 3-la concentration, 4-la protection et la stabilisation comme la congélation et la lyophilisation, et finalement 5-le stockage. Les procédés de stabilisation soumettent les cellules à différents stressés (e.g. thermique, osmotique, mécanique) dans lesquels la membrane cellulaire des BL a été identifiée comme la principale cible de dégradation (Brennan et al. 1986 ; Castro et al., 1997 ; Girardeau et al. 2022 ; Chen et al. 2022). Même si les procédés de stabilisation permettent de préserver la culture bactérienne, ceux-ci ne permettent de préserver à 100% les propriétés fonctionnelles des BL (viabilité, activité acidifiante, entre autres). La perte en propriétés fonctionnelles peut toutefois être réduite de façon significative par quatre stratégies différentes : (i) la modification des paramètres opérationnels des processus de stabilisation, comme par exemple la cinétique de congélation, les conditions de sublimation pendant la lyophilisation ; (ii) l'induction d'un stress léger pendant la croissance ou après la récolte (par des traitements thermiques, froids et osmotiques) ; (iii) l'usage de conditions de fermentation optimales pour la croissance ; et (iv) l'introduction d'une solution protectrice adéquate dans les BL concentrées. La conservation des BL peut être généralement maximisée lorsque toutes les stratégies mentionnées sont bien maîtrisées. Cependant, il a été observé que l'optimisation de la résistance par la modification des conditions de fermentation faisait perdre en biomasse, ce qui n'est pas industriellement acceptable. Dans ce contexte, nous nous sommes demandés si un compromis acceptable pouvait être trouvé entre une bonne biomasse et une bonne résistance aux procédés de stabilisation. Lorsque les conditions de fermentation changent, les BL développent des mécanismes d'adaptation, ce qui engendre une modulation de la composition de la membrane lipidique, généralement étudiée par la composition en acides gras. Ce descripteur est réducteur quand on connaît la diversité des lipides dans le monde vivant. Nous nous sommes donc demandés comment la composition lipidique globale de la membrane des BL variaient avec la modification des conditions de fermentation, en relation avec les propriétés fonctionnelles. Un autre inconvénient des stratégies de préservation des BL concerne la solution de sucre comme agent cryoprotecteur car ceux-ci ne sont pas produits de façon durable. Des sources de sucre issues de la valorisation de co-produits pourraient être de bons candidats. Dans la mesure où ils sont produits avec des degrés de polymérisation différents, nous nous sommes demandés si le degré de polymérisation des sucres pouvait avoir un rôle dans la préservation des BL.

Pour répondre à ces enjeux, ce travail de thèse a été mené avec les objectifs suivants :

- Identifier les paramètres de fermentation qui assurent une production efficace de biomasse et la résistance d'une bactérie lactique à la congélation et à la lyophilisation.

- Comprendre la modulation des propriétés des lipides membranaires selon différentes conditions de fermentation et l'implication de ces propriétés dans la résistance des bactéries lactique.
- Évaluer l'influence des sucres de différents degrés de polymérisation sur la résistance et la membrane des bactéries lactiques.

2. Revue de la littérature

Les BL constituent un groupe hétérogène de bactéries à Gram positif, qui peuvent être homofermentaires ou hétérofermentaires. Les BL sont constituées d'un cytoplasme où se trouve le matériel génétique, d'une membrane cytoplasmique et d'une paroi cellulaire. La membrane cytoplasmique des BL est constituée principalement par des phospholipides et des glycolipides. Les phospholipides les plus courants dans les BL sont le phosphatidylglycérol (PG) et la cardiolipine (CL) (Exterkate et al. 1971; Fernández Murga et al. 2000; Gomez-Zavaglia 2000; Limonet et al. 2004; Machado et al. 2004; Calvano et al. 2011; Hansen et al. 2015a; Kato et al. 2019; Chamberlain et al. 2019). Les principales structures glycolipidiques présentes dans les BL sont le diacylglycérol (DG) lié au galactose (Gal) ou au glucose (Glc) (Drucker et al. 1995; Fernández Murga et al. 2000; Calvano et al. 2011; Iwamori et al. 2011; Kato et al. 2019).

Les acides gras dans les phospholipides et glycolipides sont souvent des chaînes aliphatiques de 12 à 22 carbones, comprenant des carbones saturés et insaturés. La structure et la géométrie de la chaîne d'acyle gras régissent la forme du lipide et le degré de compactation des lipides dans la bicouche. Certaines LAB contiennent des acides gras cycliques, appelés cycCx:y (CFA) (Goldberg et Eschar 1977 ; Gomez-Zavaglia 2000 ; Girardeau et al. 2022). Les CFA sont formés in situ par modification post-synthétique, qui implique le transfert d'un groupe méthyle de la S-adénosyl-L-méthionine (AdoMet) à la double liaison des acides gras insaturés dans une molécule de phospholipide (Grogan et Cronan 1997). La membrane cytoplasmique contient également des protéines membranaires. Elles sont liées à la membrane ou ancrées via plusieurs domaines transmembranaires et sont impliquées dans plusieurs fonctions cellulaires, comme par exemple, la croissance, la division et le maintien de l'intégrité des cellules, entre autres.

La paroi cellulaire des BL est caractérisée par une couche de peptidoglycane, qui sert d'échafaudage pour la fixation d'autres composants tels que les acides téichoïques, les polysaccharides et les protéines.

Les BL sont essentiellement utilisées dans l'industrie des aliments fermentés (produits laitiers, légumes, viande et additifs alimentaires), l'industrie des aliments fonctionnels (probiotiques) et l'industrie chimique (production d'acide lactique et d'acide polylactique). Par conséquent, des progrès significatifs ont été réalisés dans la production de BL. Les efforts de recherche sont actuellement plutôt consacrés à la conservation à long terme de ces micro-organismes, à l'aide de procédés de stabilisation, tels que la congélation et la lyophilisation.

Les processus de stabilisation visent à éliminer la majeure partie de l'eau disponible sous forme liquide afin de stabiliser les structures cellulaires et de limiter les réactions biologiques. Le processus de congélation consiste à abaisser la température à des valeurs inférieures à zéro (-80°C ou -196°C). Les BL peuvent ensuite être stockées à -50°C (congélateurs industriels) ou -80°C (congélateurs de laboratoire). Le processus de lyophilisation comporte trois étapes : 1-la congélation, 2-le séchage primaire (sublimation) et 3-le séchage secondaire (désorption).

Ces procédés génèrent différents stressés qui conduisent à la dégradation plus ou moins des BL et à la perte plus ou moins importante de leurs propriétés fonctionnelles. Pour les BL, la membrane cellulaire a été identifiée comme la principale cible de dégradation.

Diverses stratégies ont été proposées pour améliorer la résistance des BL à la congélation ou à la lyophilisation. L'une d'entre elles consiste à modifier les conditions de fermentation pour induire un stress léger afin que les BL puissent développer des mécanismes d'adaptation qui les aideront à faire face aux stressés survenant au cours des processus de stabilisation. Le milieu de culture, la température, le pH et le temps de récolte ont été ainsi identifiés comme les paramètres cruciaux à modifier pour améliorer la résistance des BL. En général, les conditions de fermentation qui entraînent cet effet bénéfique sur la résistance des BL diffèrent des conditions de croissance optimales. Par conséquent, une optimisation complète semble nécessaire pour trouver un compromis entre les deux objectifs (résistance et concentration cellulaire).

Suite à la modification des conditions de fermentation des BL, une modulation de la composition en acides gras des lipides membranaires a été observée et liée à la résistance des BL. Quelques études ont également effectué des mesures de la fluidité de la membrane et de la température de transition de phase des lipides. Néanmoins, la caractérisation des lipides ne tient pas compte de la contribution des différentes classes de lipides présentes dans la membrane des BL. Une analyse multiple des lipides membranaires des BL pourrait élargir la connaissance des informations actuelles sur la contribution des lipides membranaires à la résistance des BL.

Le dernier procédé de stabilisation consiste à ajouter une solution de différentes molécules protectrices, notamment des sucres, largement utilisés sous forme de disaccharides et polysaccharides, qui limitent les effets néfastes des processus de stabilisation. Aujourd'hui, la recherche des molécules protectrices innovantes sont nécessaires, notamment dans un contexte de réduction de notre empreinte environnementale. Dans le cadre du projet européen PREMIUM (H2020-MSCA-RISE-2017, projet n°777657), de nouvelles alternatives de protecteurs ont été proposées pour stabiliser les bactéries lactiques : les fructo-oligosaccharides (FOS) et les galacto-oligosaccharides (GOS). Les FOS et GOS ont démontré leur activité prébiotique (composés qui induisent la croissance des probiotiques) (Tavera-Quiroz et al. 2015 ; Romano et al. 2016a ; Sosa et al. 2016). Par ailleurs, les FOS et GOS peuvent être produits à partir de

l'hydrolyse des déchets d'agri-ressources dans un contexte écologique. Ces molécules sont des mélanges d'oligosaccharides de différents degrés de polymérisation. Certains sucres avec différents degrés de polymérisation sont fréquemment utilisés dans la stabilisation des BL sans réelle compréhension de l'effet du degré de polymérisation.

La revue de la littérature apporte plusieurs éléments concernant les bactéries lactiques : maîtriser leurs propriétés fonctionnelles est un enjeu pour la qualité des produits, notamment alimentaire, dont le marché est toujours en pleine expansion. Cela passe par la maîtrise de leur production et leur stabilisation. L'un des enjeux actuels est de maîtriser le processus de stabilisation qui peut faire perdre beaucoup des propriétés d'une bactérie et donc son intérêt industriel.

3. L'approche expérimentale de la these

Certaines bactéries lactiques aux propriétés fonctionnelles intéressantes ne sont pas utilisées à l'échelle industrielle car elles ne sont pas assez robustes pour résister aux processus de stabilisation. Dans le but de revisiter les stratégies de production et de stabilisation des BL, la présente thèse s'est concentrée sur un modèle de bactéries lactique cryosensible : *Lactobacillus delbrueckii* subsp. *bulgaricus* CFL1 (appelée *L. bulgaricus* CFL1 dans les parties suivantes). *L. bulgaricus* CFL1 appartient à la sous-espèce largement utilisée dans les produits laitiers fermentés, notamment pour la production de yaourt, mais qui a une forte sensibilité à la congélation, comme l'ont rapporté des études antérieures (Fonseca et al. 2000 ; Rault et al. 2007 ; Meneghel et al. 2017). L'approche expérimentale globale est illustrée dans la Figure RF1.

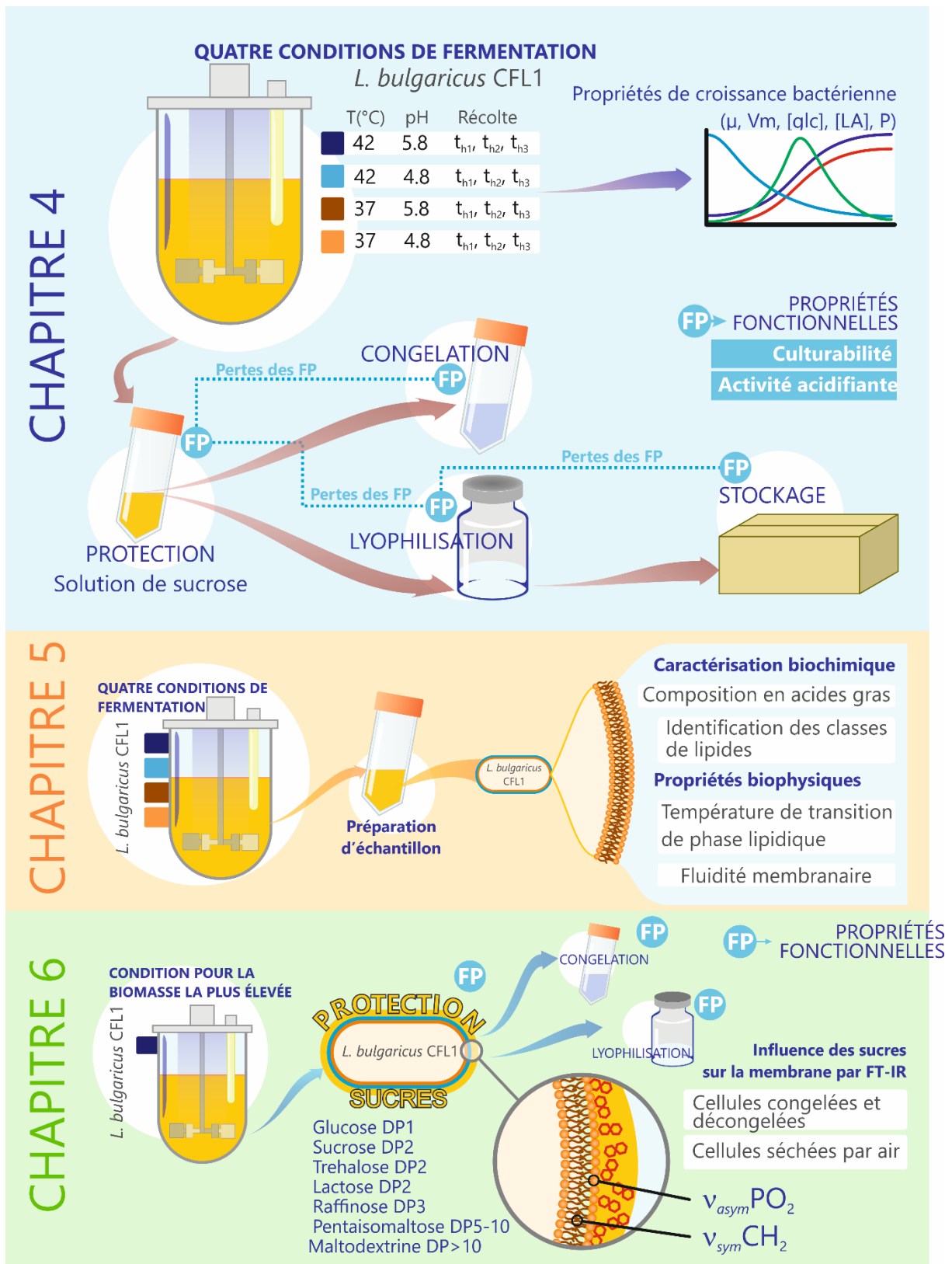


Figure RF1 Représentation schématique de l'approche expérimentale globale mise en œuvre dans la présente thèse. Abréviations : t_h , temps de récolte ; μ , taux de croissance ; V_m , taux d'acidification maximal ; [glc], glucose ; [LA], acide lactique ; P, productivité de la biomasse ; DP, degré de polymérisation ; FTIR, spectroscopie infrarouge à transformée de Fourier ; $v_{asym}PO_2$, bande de vibration d'étirement asymétrique PO_2 ; $v_{sym}CH_2$, bande de vibration d'étirement symétrique CH_2 . Les molécules de sucres sont représentées par des hexagones au contour rouge.

3.1 Optimisation multi-objectifs de la croissance de *L. bulgaricus* CFL1

La bactérie *L. bulgaricus* CFL1 a été cultivée dans un bioréacteur de laboratoire dans le milieu de culture MRS. Ce milieu a été identifié précédemment pour améliorer la résistance de cette souche à la congélation (Gautier et al. 2013). Suite à l'analyse de la littérature, quatre conditions de fermentation différentes ont été choisies, dont deux niveaux de température (42°C et 37°C) et de pH (pH 5,8 et pH 4,8). Le niveau élevé de température et de pH (42°C et pH 5,8) a été choisi pour améliorer la croissance de cette souche (Streit et al. 2007 ; Rault et al. 2007). Le faible niveau de température et de pH (37°C et pH 4,8) a été choisi pour induire un stress léger, tout en permettant une production suffisante de biomasse ($>1 \text{ g}\cdot\text{L}^{-1}$).

Les cellules bactériennes ont été récoltées en fonction du taux d'acidification du milieu de culture (déterminé en ajoutant une solution de base pour contrôler le pH). Les propriétés de croissance des cellules primaires telles que le taux de croissance (μ), le taux d'acidification maximal (V_m), la consommation de substrat ($[glc]$), la production d'acide lactique ($[LA]$) et la productivité de la biomasse (P) ont été mesurées. V_m a permis une normalisation du temps de récolte (Rault et al. 2009), qui correspond à différentes phases de croissance : la phase de croissance exponentielle (t_{h1}), la phase de croissance de décélération (t_{h2}), et la phase de croissance stationnaire (t_{h3}).

La résistance de *L. bulgaricus* CFL1 a été déterminée par la perte de leurs principales propriétés fonctionnelles : activité acidifiante et cultivabilité. La résistance à la congélation et à la lyophilisation a été déterminée par condition de fermentation et par temps de récolte. Une analyse de régression multiple couplé à une méthode de surface de réponse a été utilisée pour évaluer l'effet de ces trois paramètres de fermentation (température, pH et temps de récolte) et de leurs interactions sur la production de biomasse et la résistance de *L. bulgaricus* CFL1. De plus, une optimisation multi-objectifs a été mise en œuvre pour prédire les conditions de fermentation conduisant à une résistance accrue à la congélation et à la lyophilisation avec une production de biomasse acceptable.

3.2 Analyse approfondie des lipides membranaires et de leurs relations avec la résistance de *L. bulgaricus* CFL1 à la congélation et à la lyophilisation

Les modifications de conditions de fermentation étaient attendues induire des variations de la composition et des propriétés des membranes plasmiques des BL. Ainsi, une étude comprenant une analyse complète des propriétés de la membrane a été engagée. Pour chaque condition de fermentation et temps de récolte, une analyse approfondie des lipides membranaires de *L. bulgaricus* CFL1 a été conduite. Elle a consisté à caractériser la composition en acides gras et l'identification des différentes classes de lipides. La composition et quantification des acides gras ont été déterminés par la chromatographie en phase gazeuse. Pour l'identification des classes des lipides, une purification en utilisant différents solvants a été nécessaire pour analyser les échantillons par chromatographie en couche mince et

chromatographie liquide haute performance couplée à la spectrométrie de masse en tandem. En parallèle, différentes propriétés biophysiques ont été déterminées (Figure RF1), comme les températures de transition de phase des lipides et la fluidité de la membrane, à l'aide de la spectroscopie infrarouge et des mesures d'anisotropie de fluorescence.

3.3 Analyse du rôle du degré de polymérisation des sucres sur la résistance et la membrane de *L. bulgaricus* CFL1

La dernière partie expérimentale de la thèse a visé à étudier l'influence de sept sucres avec différents Degrés de Polymérisation (DP) sur la résistance de *L. bulgaricus* CFL1 à la congélation et à la lyophilisation et sur la membrane de *L. bulgaricus* CFL1.

Une condition de fermentation a été sélectionnée parmi les quatre conditions précédemment évaluées au chapitre 4 (42°C, pH 5,8, t_{h3}) car cette condition de fermentation a produit une concentration de biomasse suffisante. Les sucres sélectionnés représentent les monomères que contiennent les FOS et les GOS avec des DP similaires (DP3 et DP5-10).

L'efficacité de chaque sucre pour protéger les cellules de *L. bulgaricus* CFL1 a été déterminée en mesurant la perte de leurs propriétés fonctionnelles pendant la congélation et la lyophilisation de la même manière que précédemment.

La spectroscopie infrarouge à transformée de Fourier (IRTF) a été choisie dans cette partie de la thèse pour élucider l'effet des sucres sur la membrane de *L. bulgaricus* CFL1, à deux niveaux : la chaîne grasse via les bandes vibrationnelles des acides gras ($\nu_{sym}CH_2$) et la tête polaire via les vibrations d'élongation des phosphates du groupe phosphate ($\nu_{asym}PO_2$). Cette technique a été utilisée sur des cellules entières intactes dans des cellules entières intactes de *L. bulgaricus* CFL1 congelées et séchées à l'air.

4. Résultats et conclusions des chapitres 4, 5 et 6

4.1 Conditions de fermentation, biomasse et cryo-résistance : quel meilleur compromis ?

La première partie de cette thèse (chapitre 4) a conduit à l'élaboration de modèles prédictifs pour la production et la stabilisation de *L. bulgaricus* CFL1. La croissance de cette souche CFL1 a été améliorée lorsque les cellules ont été cultivées à [42°C, pH 5,8] et récoltées dans la phase de décélération (t_{h2}). Ce résultat (point rouge) peut être observé par des surfaces de réponses à différents pH dans la Figure RF2 (A).

L'amélioration de la résistance à la congélation de *L. bulgaricus* CFL1 a été obtenue lorsque les cellules ont été cultivées à un pH de 4,8, indépendamment du temps de récolte (Figure RF2 (D)). La résistance à la lyophilisation de *L. bulgaricus* CFL1 était accrue lorsque les cellules étaient cultivées à un pH de 4,8 et récoltées à la phase de croissance stationnaire (t_{h3}) (Figure RF2 (F)).

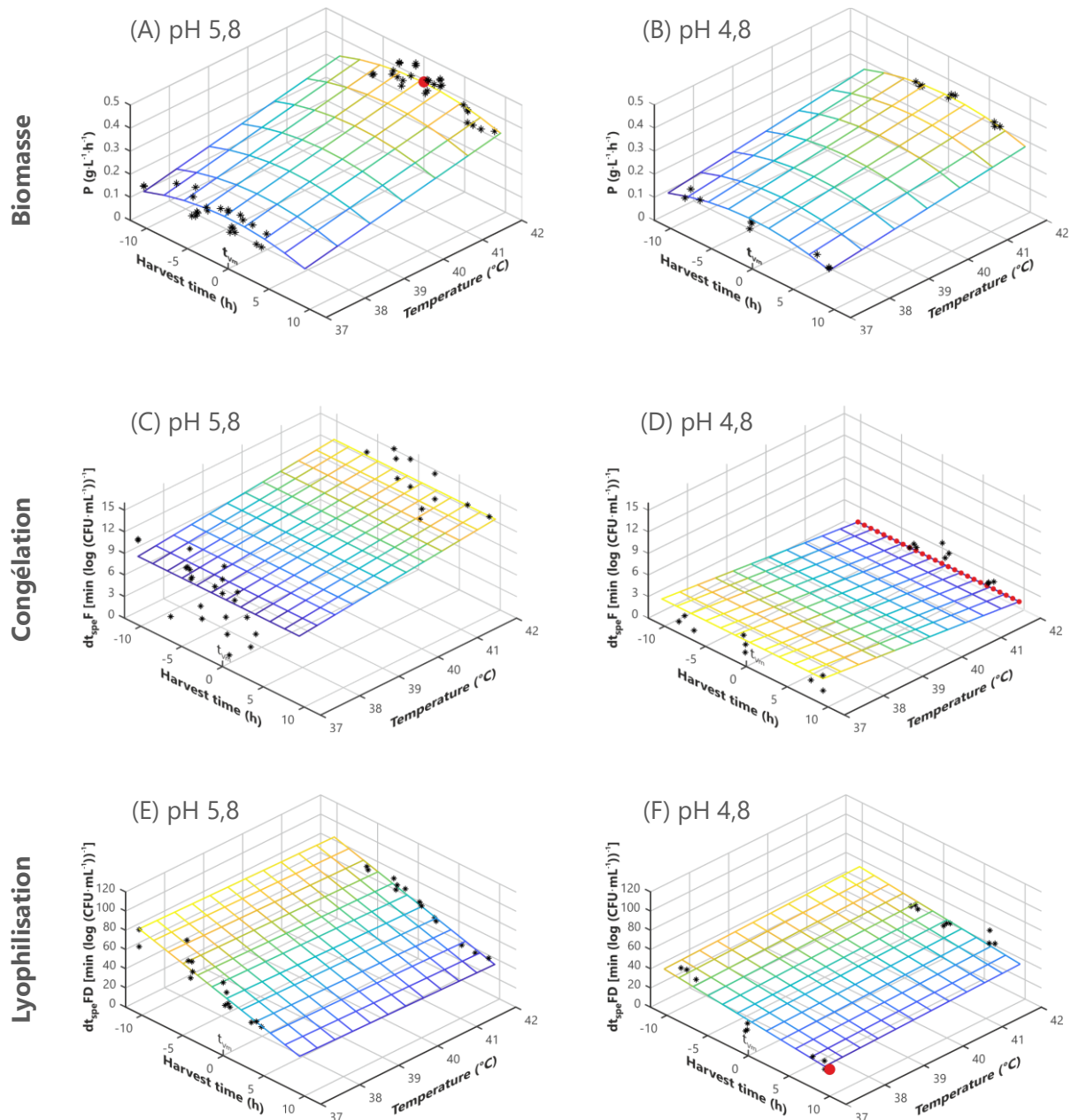


Figure RF2 Représentations de la surface de réponse de l'effet du temps de récolte et de la température de la fermentation sur (A et B) la productivité de la biomasse (P , en $g \cdot L^{-1} \cdot h^{-1}$); (C et D) la résistance à la congélation ($dt_{spe} F$, [$min \cdot \log(CFU \cdot mL^{-1})^{-1}$]); et résistance à la (E et F) lyophilisation ($dt_{spe} FD$, [$min \cdot \log(CFU \cdot mL^{-1})^{-1}$]) de *L. bulgaricus* CFL1 produite à pH 5,8 et pH 4,8. Les astérisques représentent les points de données expérimentales utilisés dans le modèle au pH donné. Le point rouge sur chaque maille représente la réponse optimale prédite par le modèle de régression multiple. t_{vm} : le temps nécessaire pour atteindre le taux maximal de la consommation de NaOH.

D'après ces résultats, les conditions qui induisent la croissance optimale de *L. bulgaricus* CFL1 sont différentes de celles qui améliorent sa résistance de cette souche à la congélation et à la lyophilisation.

Le principal inconvénient des conditions de fermentation qui favorisent la résistance à la congélation et lyophilisation est la faible concentration de la biomasse produite. Cette contrainte a été débloquée dans ce travail grâce à un outil mathématique connu sous le nom

de front de Pareto. Le front de Pareto a permis de trouver un compromis entre la productivité de la biomasse et la résistance de *L. bulgaricus* CFL1 aux deux procédés de stabilisation. Parmi les 12 conditions testées (2 températures, 2 pH, 3 temps de récolte), la condition de fermentation qui a permis une bonne production de biomasse et une bonne résistance pour les deux processus de stabilisation était à 42°C, pH 4.8, t_{h2} (Figure RF3).

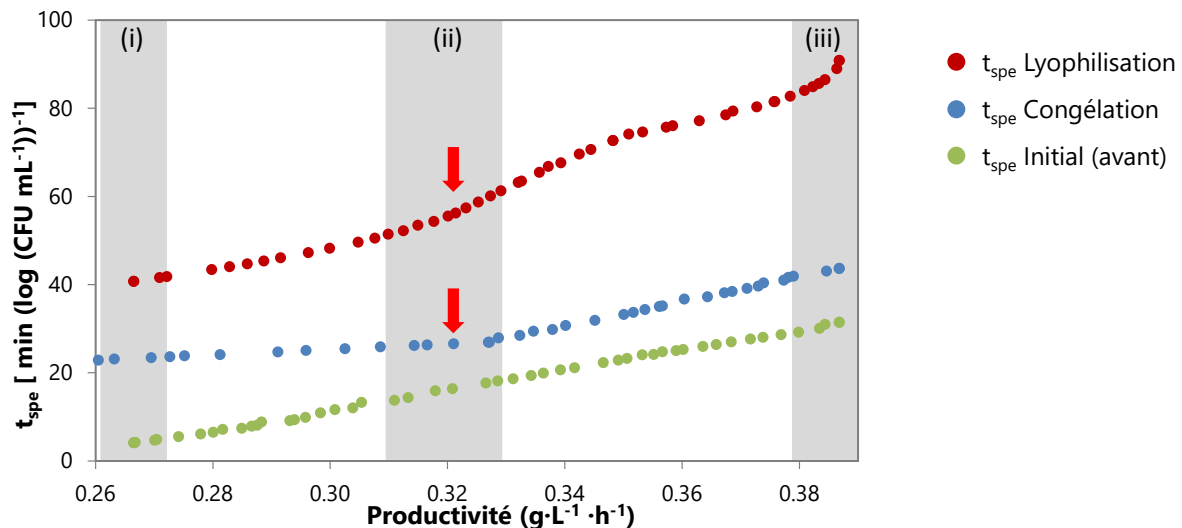


Figure RF3 Une optimisation multi-objectifs Pareto en maximisant la productivité de la biomasse (valeurs élevées de productivité, axe x) et en minimisant les valeurs de t_{spe} ont été obtenues après congélation ou lyophilisation (axe y, correspondant à la maximisation de la t_{spe}) de *L. bulgaricus* CFL1. La section (i) représente la productivité minimale de la biomasse et les valeurs de t_{spe} les plus faibles (42°C, pH 4,8, t_{h1}). La section (ii) est délimitée par des lignes pointillées, représentant le compromis entre la productivité de la biomasse et la t_{spe} . La condition de fermentation (42°C, pH 4,8, t_{h2}) conduisant à ce compromis est indiquée par des flèches rouges pour les courbes après congélation et lyophilisation. La section (iii) représente la productivité maximale de la biomasse et les valeurs de t_{spe} les plus élevées (42°C, pH 5,8, t_{h3}).

4.2 Adaptation de la membrane aux conditions de fermentation : quels lipides impliqués ?

En subissant un stress léger, *L. bulgaricus* CFL1 pourrait avoir développé des mécanismes d'adaptation pour promouvoir des réponses biologiques actives dans des conditions autres que les conditions optimales de croissance. La modification des lipides membranaires, l'expression des protéines de stress et les changements dans la morphologie ont été rapportés comme des réponses biologiques pour aider BL à résister à l'environnement stressant qui se produit pendant la congélation et la lyophilisation (Papadimitriou et al. 2016 ; Fonseca et al. 2019 ; Gao et al. 2021). Dans une deuxième partie, cette thèse s'est concentrée sur la modulation de la membrane lipidique de *L. bulgaricus* CFL1 en utilisant les cellules dans les quatre conditions de fermentation précédentes. Les principaux résultats sont présentés ci-dessous :

4.2.1 Composition biochimique des lipides membranaires

Un pH faible (pH 4,8) ou une température faible (37°C) de fermentation a augmenté l'insaturation des acides gras, et une récolte tardive a induit une teneur élevée en CFA dans la membrane de *L. bulgaricus* CFL1 (Figure RF4).

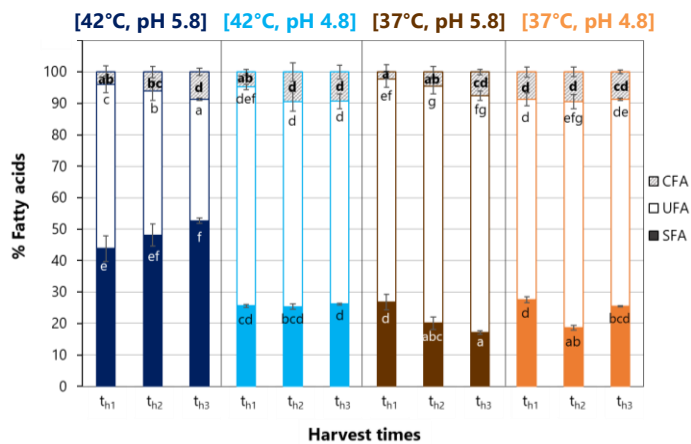


Figure RF4 Distribution en pourcentage relatif des acides gras saturés (SFA), des acides gras insaturés (UFA) et des acides gras cycliques, cycC19:0 (CFA) des lipides totaux extraits de *L. bulgaricus* CFL1. Les cellules ont été cultivées dans quatre conditions de fermentation et récoltées à différents moments. t_{h1} : phase de croissance mi-exponentielle ; t_{h2} : phase de croissance décélérée ; t_{h3} : phase de croissance stationnaire. Les valeurs sont la moyenne d'au moins trois répliques biologiques indépendantes. Les lettres représentent les différences significatives entre les conditions de fermentation et les temps de récolte à un niveau de confiance de 95 %.

En utilisant la chromatographie en couche mince et la chromatographie liquide haute performance couplée à la spectrométrie de masse en tandem, c'était possible identifier les phospholipides et les glycolipides, à savoir phosphatidylglycerol (PG), monoacyldiacylglycerol (MGDG) et diacylglycerol (DGDG) ont été les lipides membranaires identifiés pour les quatre conditions de fermentation. En raison de la trop forte quantité de biomasse nécessaire à la quantification des lipides par classe, seule l'analyse de la structure des lipides de chaque classe a été déterminée. On sait néanmoins que la quantité de lipide est indépendante des conditions de fermentation. L'abondance relative des chaînes grasses pour le DGDG le PG est présentée sur la Figure RF5.

4.2.2 Propriétés biophysiques des lipides membranaires

Les conditions de fermentation qui ont induit une augmentation des acides gras insaturés dans la membrane ont entraîné des températures de transition de phase lipidique (T_s et T_m) à zéro ou inférieures à zéro (RF6 (A)). Ces conditions ont également généré une membrane plus fluide (valeurs d'anisotropie les plus faibles) à 20°C (Figure RF6 (B)).

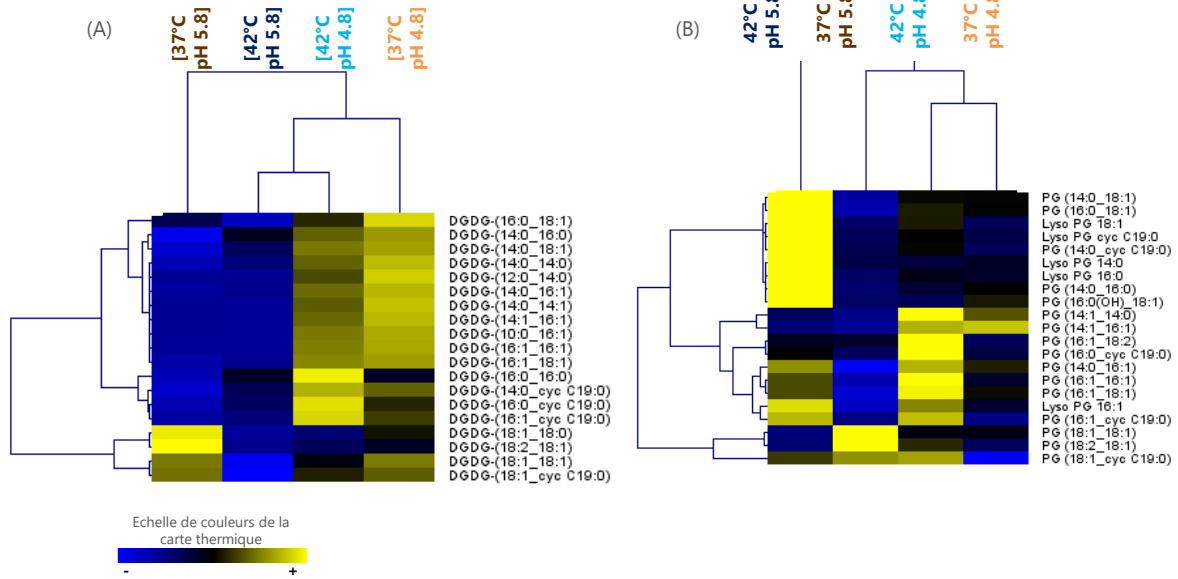


Figure RF5 Cartes thermiques des (A) diglycosyldiacylglycérols (DGDG) et (B) phosphatidylglycerol trouvés dans la membrane de *L. bulgaricus* CFL1. Les cellules ont été cultivées dans quatre conditions de fermentation différentes : [42°C, pH 5,8] ; [42°C, pH 4,8] ; [37°C, pH 5,8] ; et [37°C, pH 4,8]. La corrélation de Pearson a été utilisée pour le regroupement hiérarchique.

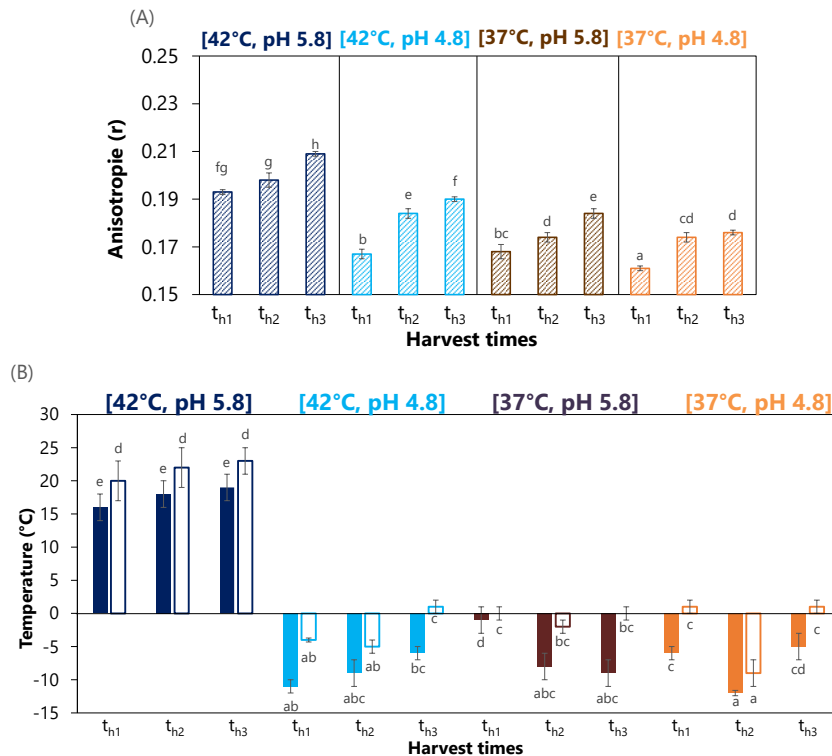


Figure RF6 Propriétés biophysiques de la membrane de *L. bulgaricus* CFL1. (A) Valeurs d'anisotropie à 20°C. (B) Températures de transition de phase des lipides pendant le refroidissement (T_s , barres pleines) et le chauffage (T_m , barres vides). Les cellules ont été cultivées dans différentes conditions de fermentation à des temps de récolte accrus : t_{h1} , phase de croissance mi-exponentielle ; t_{h2} , phase de croissance de décélération ; t_{h3} , phase de croissance stationnaire. Les valeurs sont la moyenne d'au moins trois répliques biologiques indépendantes avec les valeurs d'écart type correspondantes. Les lettres en exposant représentent des différences significatives entre les conditions de fermentation et les temps de récolte à un niveau de confiance de 95 %.

4.3 Quel rôle du degré de polymérisation du sucre dans la protection des bactéries ?

L'étude développée pour élucider l'influence des sucres sur la résistance de *L. bulgaricus* CFL1 a été réalisée au cours des 2 procédés de stabilisation (congélation et lyophilisation) via la mesure de l'activité acidifiante spécifique des cellules.

Pour la congélation, les cellules de *L. bulgaricus* CFL1 ont présenté une résistance élevée lorsqu'elles étaient protégées par du tréhalose (DP2) et du raffinose (DP3). L'augmentation du degré de polymérisation ne semble pas liée à l'efficacité de la protection (Figure RF7 (A)). Pour la lyophilisation, le glucose (DP1) était le meilleur protecteur (Figure RF7 (B)). Ici le degré de polymérisation agit négativement sur la résistance à la lyophilisation. Ces résultats ont révélé que le choix du sucre dépendait des procédés de stabilisation sélectionnés pour préserver *L. bulgaricus* CFL1.

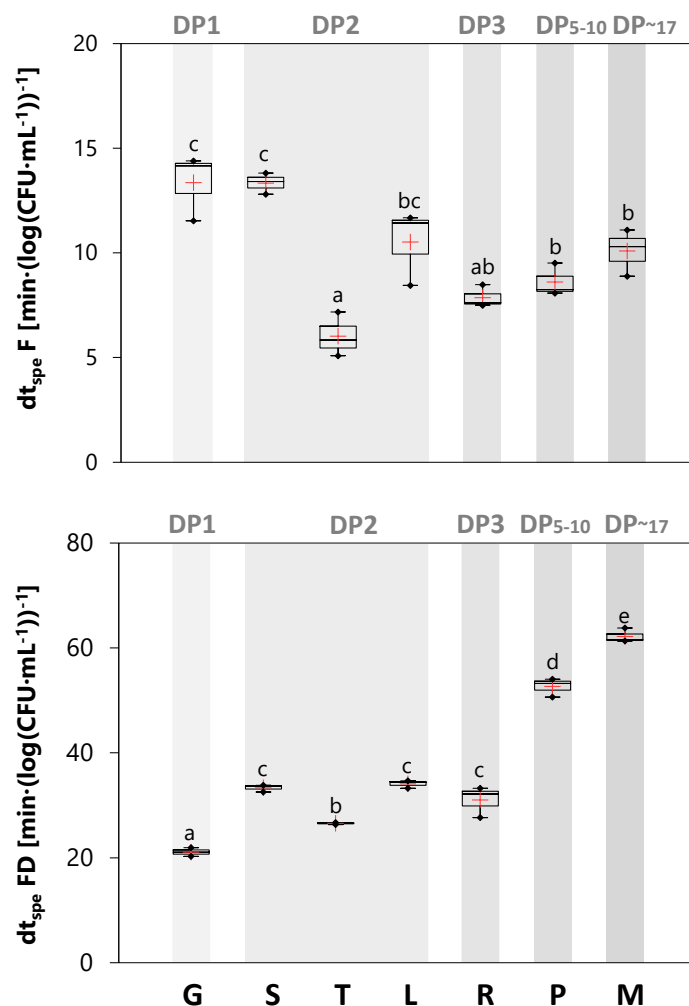


Figure RF7 Résistance de *L. bulgaricus* CFL1 à la (A) congélation et à (B) la lyophilisation en utilisant différents sucres par la perte de l'activité acidifiante spécifique (dt_{spe} F and FD). Les valeurs sont la moyenne d'au moins trois mesures indépendantes. Les lettres en exposant représentent les différences significatives entre les solutions de sucre à un niveau de confiance de 95 %. Les zones grises correspondent aux sucres ayant le même degré de polymérisation. Abréviations : DP, Degré de polymérisation ; G, Glucose ; S, Saccharose ; T, Tréhalose ; L, Lactose ; R, Raffinose ; P, Pentaisomaltose ; M, Maltodextrine.

Concernant l'interaction des sucres avec la membrane, une analyse FTIR a été réalisée en considérant deux bandes d'absorption provenant des principaux groupes fonctionnels qui constituent les lipides de la membrane, c'est-à-dire le groupe des chaînes acyles ($\nu_{sym}CH_2$) et les groupes phosphates des têtes polaires ($\nu_{asym}PO_2$).

Nous avons observé que la présence de sucres ne modifie pas la température de transition principale, correspondant au passage des chaînes grasses de l'état cristallisé à l'état liquide. En revanche, la transition de phase entre les deux phases liquides cristallines (probablement L_β à P_β) se produisait à plus basse température en présence de sucres, permettant de conclure que le sucre introduit un certain désordre dans la membrane. Face aux difficultés d'analyse de la bande de longueur d'onde de $\nu_{asym}PO_2$, il n'a pas été possible de conclure à l'effet du sucre sur le phosphate et à une éventuelle interaction directe avec la membrane.

5. Conclusions

D'après ce travail, deux facteurs essentiels doivent être pris en compte pour produire des BL congelées et lyophilisées à l'échelle industrielle. Premièrement, une attention particulière doit être portée à la sélection des conditions de fermentation pour cultiver les BL, car elles affectent fortement la résistance des bactéries et la quantité de biomasse produite. L'optimisation multicritères devient essentielle pour définir les conditions de fermentation en fonction du type de processus de stabilisation et de la biomasse souhaitée. Ensuite, le choix adéquat du protecteur est vital et dépend du procédé de stabilisation. Par conséquent, la combinaison des conditions de fermentation appropriées (représentant un compromis entre l'amélioration de la résistance bactérienne et la production de biomasse) et du protecteur adéquat permettra de produire une bactérie lactique sensible à l'échelle industrielle. Une fois encore, nous avons mis en évidence des adaptations de la composition de la membrane aux conditions de fermentation et nous avons pu aller plus loin : la présence d'acides gras conjugués est favorable pour le procédé de lyophilisation tandis que les acides gras insaturés sont favorables à la congélation.